

The Early Middle Palaeolithic Blade Industry from Hummal, Central Syria

Inauguraldissertation

ZUR
Erlangung der Würde eines Doktors der Philosophie
vorgelegt der
Philosophisch-Naturwissenschaftlichen Fakultät
der Universität Basel
von

Dorota

Wojtczak

(Vorname)

(Familiename)

aus Jastrzebie-Zdroj

Polen

(Heimat)

(Kanton oder Land)

Basel 2014

Original document stored on the publication server of the University of Basel
edoc.unibas.ch



This work is licenced under the agreement
„Attribution Non-Commercial No Derivatives – 3.0 Switzerland“ (CC BY-NC-ND 3.0
CH). The complete text may be reviewed here:
creativecommons.org/licenses/by-nc-nd/3.0/ch/deed.en

Genehmigt von der Philosophisch-Naturwissenschaftlichen Fakultät
auf Antrag von

Prof. Dr. Jean-Marie Le Tensorer und Prof. Dr. Liliane Meignen

(Mitglieder des Dissertationskomitees)

Basel, den 27.03.2012

(Datum der Genehmigung durch die Fakultät)

Prof. Dr. Martin Spiess

Dekanin/Dekan
(Name der/des amtierenden
Dekanin/Dekans ansetzen)



Attribution-NonCommercial-NoDerivatives 3.0 Switzerland
(CC BY-NC-ND 3.0 CH)

You are free: to **Share** — to copy, distribute and transmit the work

Under the following conditions:



Attribution — You must attribute the work in the manner specified by the author or licensor (but not in any way that suggests that they endorse you or your use of the work).



Noncommercial — You may not use this work for commercial purposes.



No Derivative Works — You may not alter, transform, or build upon this work.

With the understanding that:

Waiver — Any of the above conditions can be **waived** if you get permission from the copyright holder.

Public Domain — Where the work or any of its elements is in the **public domain** under applicable law, that status is in no way affected by the license.

Other Rights — In no way are any of the following rights affected by the license:

- Your fair dealing or **fair use** rights, or other applicable copyright exceptions and limitations;
- The author's **moral** rights;
- Rights other persons may have either in the work itself or in how the work is used, such as **publicity** or privacy rights.

Notice — For any reuse or distribution, you must make clear to others the license terms of this work. The best way to do this is with a link to this web page.

Acknowledgements

Firstly, I would like to acknowledge gratefully the contributions of the Swiss National Science Foundation, the Freiwillige Akademische Gesellschaft and the Tell Arida Foundation for financial support that made this doctoral work possible.

I am indebted to Prof. Jean-Marie Le Tensorer for giving me the opportunity to work in such an important and stimulating field, and also for his patience and friendship. I hope that I was a help during those years and that he will be happy with this work. I would also like to thank Liliane Meignen, not only for her willingness to join the dissertation committee, but also for allowing me to study part of the Hayonim Cave collection in Valbonne, and for her kindness in sharing opinions and offering various manuscripts and papers.

My thanks should go to Eric Boëda for his interesting comments on lithic technology and for showing me part of the laminar-industry collection from Umm el Tlel. My thanks also go to the Institut de Paléontologie Humaine in Paris for allowing me to study the collection from Abu Sif; to Jürgen Richter of the Institut für Vor- und Frühgeschichte der Universität zu Köln for allowing me to study the collections from Yabrud; and to the staff of the Archaeological Museum of Cambridge University for letting me see assemblages from Tabun, Hazar Merd and Haua Fteh. I am additionally grateful to Reto Jagher for making available the laminar assemblages from Nadaouiyeh Ain Askar and for sharing his knowledge of the El-Kowm area and his library. I am indebted to Daniel Schuhmann for providing invaluable computer support and for drawing plans of Hummal and artefact distributions, and to Philippe Rentzel and Kristin Ismail-Meyer for their geomorphological analysis and their interesting discussions on the related results. Special thanks go to Ruth Minert for her editorial help in a final stage of the present manuscript. Many thanks go to Daniel Richter (Max Planck Institute for Evolutionary Anthropology, Leipzig) for TL dating of Hummal.

I would like to show my appreciation to all the colleagues, students and co-workers who assisted me in the field work. Without their cooperation, this work would have been impossible. I wish to express my special thanks to all members of the El-Kowm

Archaeological Project: Sultan Muhesen, H  l  ne Le Tensorer, Vera von Falkenstein, Peter Schmid, Thomas Hauck, Fabio Wegm  ller, Daniel Schuhmann, Hani El Sued, Manar Kerdy, Mustafa Al Najjar, and H  ba Al Sakhel.

I would like to show my warm gratitude to all my Syrian friends for their help and hospitality. I say thank you to Mahmud Taha, Taha Taha, Sultan Sukhne, Ammar Anusi, Waleed Asa'ad and all the people of El-Kowm. I am exceptionally grateful to Ahmed Taha, not only for making an effort to speak in my mother tongue, but especially for his help during all the years of excavations and my lonely stays in Palmyra, when I was studying the lithic material. He and his family were always ready to help and made sure that I was safe and not hungry.

For their inspiring discussions I would like to thank Yuri Demidenko, Gilbert Tostevin, Steven L. Kuhn, St  phanie Bonilauri and Christine P  mpin.

I am indebted to my brother, Jacek, for the wonderful artwork and design of the cover pages. I would also like to show my appreciation to my parents without whose continued support I would not be in the position I am today.

Last but not least I would like to thank my husband, Richard Frosdick, for help in correcting my English, for archaeozoological analysis, and for lasting patience and support. I thank our children Mathilda and Joakim for keeping me sane and for making me laugh when I need it.

Reasoning behind the project

The earliest work on the stratigraphical and sedimentological sequences of the Hummal site at El-Kowm (Le Tensorer 2004) showed that the previous studies of the lithic material from the Ia layer were carried out on assemblages that were not *in situ* and were highly selected (oral communication Le Tensorer). A new series of studies carried out on the Hummal sequence during the 1999-2005 and 2009 seasons' shows that the materials from these new excavations are, unlike the previous work, considered to have been *in situ* and that all the lithic specimens were gathered. This means that a far greater understanding of the lithic industries is now possible.

The main goal of this work is to present the new Hummalian sequence established from the recent excavations, and the detailed studies on the Hummalian industries uncovered from the new stratified layers. The proposed aim is to define the Hummalian industry based on these results and to compare them to those from other Early Middle Palaeolithic industries in the Near East.

This study will form part of interdisciplinary work undertaken in Hummal over many years, with numerous people contributing to the research on the site. It is worth mentioning them here, because all have contributed in different ways to this study.

- J.-M. Le Tensorer and S. Muhesen, directors of the mission since 1999, assured the scientific and financial sides.
- H. Le Tensorer and V. von Falkenstein have assisted in archaeological investigations since 1997.
- Ph. Rentzel, assisted by K. Ismail-Meyer and Ch. Pümpin, is responsible for the geoarcheological research.
- J. Renault-Miskovsky is responsible for pollen analyses.
- P. Schmid started the anthropological study (Le Tensorer *et al.* 1997; Schmid 2004, 2005) and after the sad death of Ph. Morel in 1999 also became responsible for the palaeontological and archeozoological research with the contributions of N. Reynauld-Savioz (Reynauld 2001, 2004, 2011) and R. Frosdick (Frosdick 2009).

- In 1999 D. Richter from the Max Plank Institute in Leipzig started the dating programme of archaeological sequences in Hummal using the TL and ESR method. This programme has continued until today (Richter *et al.* 2011).
- In 2001 T. Tonner and Ph. Drechsler from Tübingen University started to study the topography of the Hummal site and its immediate vicinity (an area of 55m x 90m). In 2002 R. Jagher undertook the topographical investigation of Hummal's surrounding area. The current topographic models include the Hummal site, an area covering the immediate vicinity, and the principal adjoining topographic formations in a limited locality (Jagher 2003/04).
- In 2004 Ch. Pümpin und R. Jagher carried out geological evaluations of the area (Ch. Pümpin & R. Jagher 2004).
- Since 2007 A.-S. Martineau has undertaken a geological study of Hummal (Martineau 2008, 2009, 2010).
- In 2009 J.J. Villalain from the University of Burgos started a dating programme for Hummal, using the principles of paleomagnetism.

An important part of the research undertaken in Hummal has been completed within Master's and PhD programmes.

- In 2001 K. Meyer presented her Master's research on micromorphological analyses undertaken on layers 13 to 5 of the Hummal stratigraphy (profiles P.3 and P.7) visible at that time.
- In 2003 the present author started the systematic excavation of the Upper Hummalian (layers 6-7) as part of her PhD project centred on the Hummalian culture.
- In 2004 Th. Hauck began PhD research into the systematic investigation of the Mousterian complex and in 2010 presented the results in his thesis 'The Mousterian Sequence of Hummal (Syria)'.
- In 2007 D. Schuhmann established a 3D model of the Hummal site using the topographical data recorded within the Master's research *Digitale Modellierung und Schichtrekonstruktionen der paläolithischen Fundstelle*

Hummal, Syrien, and started his PhD under the title: ‘El-Kowm GIS: A New Program for the Documentation of Archaeological Sites’.

- In 2008 D. Hager presented her investigation on the possible use of fire in Hummal within her Master’s project *Frühe menschliche Nutzung von Feuer. Nachweismöglichkeiten und ausgewählte Ergebnisse für die Fundstelle Hummal, El Kowm, Syrien*.
- In 2008 A. Al-Qadi presented his Master’s work: *Le Yabroudien et la transition entre le Paléolithique inférieure et moyen au Proche-Orient, l’exemple d’El Kowm (Syrie Centrale)*.
- In 2008 F. Wegmüller completed his Master’s research centred on the Lower Palaeolithic, *Die Stenartefakte aus den frühpaläolithischen Schichten 15-18 der Fundstelle Hummal in Syrien*. He continued his research on this early period in a PhD with the preliminary title *Die Frühpaläolithischen Funde aus El Kowm, Syrien*.
- In 2008 H. El Sued concluded his paleontological research into Equidae with a Master’s thesis entitled *Etude d’un crâne d’Equidé Yabroudien du site de Hummal*. He is persevering with the paleontological study in his PhD project.
- In 2010 Pietro Martini from Zurich University began paleontological study of Camelidae. In 2011 he presented his results in the Master’s thesis, ‘A metric analysis of the morphological variation in recent and fossil camels’.

Contents

| | |
|--|-----------|
| Abstract | 9 |
| 1. Introduction | 15 |
| 1.1. History of the term ‘Levallois’ and the problem with blades | 15 |
| 1.2. The appearance of the blade industries | 27 |
| 2. History of research in El-Kowm | 32 |
| 2.1 First evidence of settlement in the region and discovery of Hummal | 32 |
| 2.2 Systematic investigations | 33 |
| 2.3 The beginning of the Syrian-Swiss research program | 39 |
| 2.4 The investigation of Hummal | 40 |
| 2.5 Excavation of Hummalian complexes: 2000-2005 and 2009 | 43 |
| 3. Presentation of the area | 45 |
| 3.1 The site and its surroundings | 45 |
| 3.2 Climate and hydrology | 46 |
| 3.3 Paleoecology | 48 |
| 3.4 Geological aspect of Hummal | 49 |
| 3.5 Raw material and procurement strategies in Hummal | 50 |
| 3.6 Date estimations of the Hummalian occupations | 52 |
| 3.7 The stratigraphical sequences | 53 |
| 3.7.1 The western and eastern sequences | 53 |
| 3.7.2 The southern sequence | 55 |
| 4. Archaeological Samples and their taphonomy | 57 |
| 4.1 Introduction | 57 |
| 4.2 State of preservation | 58 |
| 4.3 Burnt flints | 62 |
| 4.4 Quantification of layers 6a and 6b | 63 |

| | |
|---|-----------|
| 5. Methodology of the lithic analysis | 72 |
| 5.1. Raw material procurement | 72 |
| 5.2. Reduction strategies | 74 |
| 5.3 Core orientation | 76 |
| 5.4 Core management | 77 |
| 5.5 Platform maintenance | 78 |
| 5.6 Dorsal surface | 79 |
| 5.7. Shape of lateral edges | 82 |
| 5.8 Flake profile | 83 |
| 5.9 Proximal end modification of flakes | 83 |
| 5.10 Distal terminus of flakes | 83 |
| 5.11 Morphology of flake ventral surface | 84 |
| 5.12 Manufacturing of retouched specimens, curation and discard | 85 |
| 5.13 Recycling | 86 |
| | |
| 6. Presentation of lithic material | 90 |
| 6.1 Introduction | 90 |
| 6.2 Raw material procurement strategies | 90 |
| 6.3 The goal of the reduction strategy | 94 |
| 6.4 Core Trimming Elements | 95 |
| 6.5 Non-retouched blank blades | 108 |
| 6.5.1 Introduction | 108 |
| 6.5.2 Lithic analysis | 109 |
| 6.6 Non-retouched blank flakes | 125 |
| 6.6.1 Levallois flakes | 128 |
| 6.6.2 Non-Levallois flakes | 131 |
| 6.7 Retouched blanks | 132 |
| 6.7.1 Introduction | 132 |
| 6.7.2 Retouched blades | 133 |
| 6.7.3 Retouched flakes | 143 |
| 6.8 Core reduction strategies | 146 |

| | |
|---|------------|
| 6.8.1 Introduction | 146 |
| 6.8.2 Laminar method | 148 |
| 6.8.3 Levallois method | 152 |
| 6.8.4 The Nahr Ibrahim Technique (NI) | 154 |
| 6.8.5 Bladelet production | 156 |
| 6.9 Summary | 159 |
| 7. Comparison | 163 |
| 7.1 Introduction | 163 |
| 7.2 Comparison with Abu Sif B and C | 164 |
| 7.3 Comparison with the blade industry from Nadaouyieh Ain Askar | 165 |
| 7.4 Metrical analysis of assemblages from Hummal, Nadaouiyeh and Abu Sif | 167 |
| 7.5 Conclusions | 170 |
| References | 174 |

Abstract

The Hummal site, situated in the El-Kowm area of central Syria, is characterised by the presence of many artesian springs related to faults in the substratum, and by high-quality Lower Eocene flint outcrops. The El-Kowm oasis is located 450m above sea level in the Syrian steppe between Rasafa, Palmyra, and Deir ez Zor. A 20-km depression inside the mountain chains that extend across Syria from the Anti-Lebanon Mountains in the west to the Euphrates River in the east, it separates the northern fertile zones from the Arabian Desert in the south. The area attracted humans to return to the same places over long periods, and so accumulated cultural remains from many occupations. Currently, 206 locations and 142 places containing Palaeolithic stone artefacts have been found in the region of El-Kowm. The Hummal site is in direct contact with the old artesian spring that supplied water to a pool of variable size. As a result, the sediment formation of the site and the conservation of archaeological layers are highly influenced not only by aeolian processes (the wind is a constant erosional agent in this region), but also by the degree of spring activity. Attracted by the water, animals and raw material, humans settled continuously in the immediate vicinity of the source from the Lower to the Upper Palaeolithic, as attested by an archaeological record more than 20 metres deep.

Systematic excavations in Hummal began in 1999 under the direction of J.-M. Le Tensorer and S. Muhesen (Le Tensorer 2000). More than 20 archaeological layers from Upper to Lower Paleolithic were recognised and thousands of artefacts gathered. This *in situ* sequence, containing layers 6a, 6b, 6c and 7a, 7c, integrated the Hummalian. A blade industry was additionally discovered in a massive sand deposit, subsequently labelled α h. This deposit was several metres thick and had collapsed from between layers 7 and 10 into the centre of the doline.

The sand is geologically perfectly *in situ*. It does not present any mixing with other layers, is homogenous, shows all the features identified in other Hummalian layers, and is considered to be of the same technological tradition.

From 2001 to 2005, systematic excavation of the upper sequence of the Hummalian (layers 7c, 7a, and 6c-2, 6c-1, 6b, 6a) was undertaken under the direction of the author. Up to 2005, the excavation area reached 26m², and more than 7000 lithic objects and more than a hundred faunal remains were collected. The excavated area was divided into two distinct parts: West and East. In 2009 the new Sondage S1 was opened in the southern part of the site and a surface of about 2m² was excavated.

The stratigraphical sequences recorded in the eastern, western and southern sectors are similar in the main, but there are some differences: Complex 6c appears only in the eastern zone and Layer 6a is more complex in the southern sector. The Hummalian blade industry excavated in all three sectors is subdivided into stratified archaeological layers and is clearly positioned between the Yabrudian and Mousterian complexes.

Taphonomic factors such as erosion, diagenesis and trampling, alongside the probable lack of sedimentation, had a destructive effect on a significant number of the archaeological remains from the stratified layers 6a and 6b. This makes some of the archaeological and archaeozoological analysis problematic. The faunal remains were very poorly preserved and it is difficult to draw conclusions owing to the small size of the samples. Post-depositional forces were the major influence on the destruction of the bones. Stone artefacts were the most numerous in the excavated samples and lithic analyses were undertaken accordingly, despite the fragmentation of and damage to a portion of the sample from layers 6a and 6b.

The site was occupied repeatedly, but the density of the archaeological remains between layers is variable. This is connected to the limited extent of the excavation and possibly also to differing intensities of occupation. The high concentration of artefacts in layers 6b and 6a seems to be related to successive occupation episodes without clear intermediate layers. In the case of layers 7a, 7c and 6c-2, the lower density of artefacts and the position and conservation of lithic specimens, together with micromorphological observations and some refittings of lithic material, correspond most to short-term occupation. The lithic assemblages from all the Hummalian layers seem to represent similar technological and typological features.

The common flaking technique is direct percussion with a hard hammer, as demonstrated by a circular and well-detectable impact point, bowed bulb and abundant radial flake. The presence of a few products with a lipped butt and diffuse bulb suggests the use of a soft hammer, but it seems that it was used only marginally. The unidirectional flaking system dominates in all layers, but bidirectional is also well represented, especially in Sand *ah* and layers 6c-2 and 7c.

The goal of production was elongated blanks regardless of their size, with the greatest lengths between 2 and 16cm and a mean length/width from 2.7 to 3. The blank blades encompass a number of specimens with different morphologies. They can present high triangular or trapezoidal cross-sections or be flat, narrow or broad, thick or thin. The majority are bowed in longitudinal profile, but a number of pieces are also rectilinear. Most butts are slightly faceted or plain, but several present a cautiously faceted platform. These blanks, although looking morphologically different – either prismatic or Levallois-like – seem to be the result of a single reduction strategy involving different kinds of core volume management. These can be structured into two principal types: semi-rotating and frontal. The flaking surface of such cores, usually arranged to the length of the nodule, onto the convex, elongated and narrow face, could be expanded on its lateral sides during flaking. Faceting was used for rejuvenation of the core platform. Additionally, management of the flaking surface was regularly attained by the removal of a flake edge along a natural or cortical ridge, and occasionally by secondary crested blades. The first face, working on the thickness of the core, resulted in blades of a rather high cross-section and a plain butt. As flaking progressed and expanded onto the wider and flatter side of the core (with the volume of the core decreasing), the morphology of the obtained blanks changed. They became flatter in cross-section and often present a prepared butt, because the flint knapper started to facet the core striking platform, aiming to better control the flaking process and the morphology of the desired blank blades. The morphology of such a core changed simultaneously as well. In many cases, the flint knapper started to treat the available volume differently and began to prepare intensively the distal and lateral portions of the cores. The core upper surface, exhibiting the recurrent method of debitage –

guaranteed by the regular removal of *éclats débordants*, or alternatively the extraction of the small flakes around the periphery of the exploitation surface – could be used to the same effect. The large platform was established on the proximal or proximal and distal (bidirectional) part of the core. They are in the main faceted, and occasionally plain. The blanks were struck from one or two parallel platforms, and a typical product of this reduction *enlèvement* II was detached. The sequence of detachment of a few blanks was repetitive, resulting in the decreasing size of the core and the products.

It seems that the flint knapper moved from Laminar debitage to Levallois-like debitage when the volume of cores decreased, with the core becoming flatter and requiring more preparations to control the manufacture of blanks. But many times the morphology of cores seems to have remained constant despite the diminishing size, showing that the core volume management was maintained from the early stage through to exhaustion.

As blank production was carried out until exhaustion of the core, the assemblage includes blanks with a size scale ranging from elongated blades to small bladelets. But there was also a separate production of bladelets from burin-cores, and of bladelet cores and small flakes from truncated-faceted pieces. All these elements indicate a level of complexity in blank production. Although blade reduction was certainly dominant in the Hummalian industry primary flaking processes, the two additional reductions, directed towards production of different small-sized debitage items, are also clearly identifiable.

In all layers, the majority of products present the preparation of the proximal part using a series of small removals coming from the edge of the butt into the proximal part of their upper surface. It appears that this “abrasion-like thinning” with the faceting of the platform was undertaken to correct the flaking angle, at once allowing the production of long supports and prolonging the flaking.

The retouched tools made on flakes and blades seem to be quite standardised in their metrical and non-metrical attributes, both between the assemblages and the tools categories. The most numerous categories of retouched items are the elongated end-

point items fashioned by a rather heavy retouch (typologically regarded as points and convergent side-scrapers) and the parallel blades retouched regularly on one or both sides (typologically regarded as single or double side-scrapers on blades). The retouched blades are usually longer and broader than the unmodified blades. This signifies a preference for bigger supports for shaping these implements, particularly if the original size has been reduced during repeated use and retouching. The thick blades with a high-cross section are often retouched, but the elongated, rather flat-in-cross-section products, which often resemble Levallois-like products, are not modified. This may indicate a different use of the blades.

The importance of recycling in the Hummalian is demonstrated by the abundant cores on flake, double patinated tools, the reuse of broken items, debris for bladelet manufacturing, and Yabrudian scrapers as cores. In Hummalian layers, it seems that the bulk of cores on flakes and burin-cores with their corresponding end-products can be interpreted as the result of a recycling process in which the stone specimens manufactured during the main reduction strategy were reused for completing new cores and tools. They may be an indication of an economic strategy aimed at raising the proficiency of raw material exploitation. At the same time, the significant presence of burin-cores and cores on flakes cannot in the author's opinion be solely interpreted as being aimed at maximising the productivity of the flint. The end-products obtained during their flaking must have represented a desired supplementary element next to implements manufactured by the main reduction strategy.

The estimated TL age for Hummalian is approximately 200 ka (Richter 2006, Richter et al. 2011) and is comparable to those of the Laminar phenomenon highlighted at Hayonim layer 'F top' and 'F base', which have mean TL-dates on heated flint of 210 ± 28 ka and 221 ± 21 ka, respectively (Mercier *et al.*, 2007), or with Tabun's unit IX (Tabun D-type), with its mean TL dates of 256 ± 26 ka, and Rosh Ein Mor, dated 200 ka (Rink *et al.* 2003). These assemblages were discovered at different site types that varied in their use of Laminar and Levallois reduction strategies and in their production of diverse tools. The collections from Tabun and Rosh Ein Mor, in contrast to the Hummalian, seem to be dominated by the Levallois method (Meignen 1994,

143, Hauck 2010, 200). They comprise a considerable number of Upper Palaeolithic tools and a small percentage of elongated, slightly modified blades. At present it seems that the lithic industries from Hayonim layers F and E (Meignen 1998, 2000) and the undated Abu Sif layers B and C (Neuville 1951, and personal studies on part of collection at the Institut de Paléontologie Humaine, Paris) show the greatest resemblance to the Hummalian industry. Just like the Hummalian ones, these assemblages show a tendency to produce an elongated blank of different morphology. The tool-kit comprises numerous retouched blades and, less frequently, Mousterian and Upper Palaeolithic tools. Furthermore, the production of bladelets from core-burin was also documented in blade assemblages from both Hummal and Hayonim.

“No retrospective law authorises us to limit the field of freedom of action of Palaeolithic people any more than of ourselves.” (M. Otte, 1995:123)

1. Introduction

1.1 History of the term ‘Levallois’ and the problem with blades

The term ‘Levallois’, first employed after finds made in 1861 by the geologist Rebourg, referred to large and flat flakes discovered in Levallois-Perret, a suburb of Paris.

Before Breuil (1926) introduced the term ‘Levalloisian’, Mortillet gave a first morphological description of the finds: *“ce sont des éclats très grands et très larges, de forme oval, belles pieces à arêtes vives, ce sont les plus grandes de cette époque”* (1883:255).

In 1909 Victor Commont proposed the first reconstruction of this flaking method based on combined study of cores, flakes and some refitting, and described it as a Mousterian flaking technique. Attention was paid to the shaping out of the core, to the special preparation of a striking platform and to the traces of the platform on flakes.

Commont’s description was followed by an international debate over what typological aspects might be employed to recognise Levallois flakes and how Levallois flakes seemed to result from a special production strategy. There was a long international polemic concerning the use of the faceted platform as a criterion for recognition of Levallois debitage.

In 1945, van Riet Lowe presented a development diagram of flaking technologies in South Africa, showing a movement from prehistoric pre-Levallois to a later proto-Levallois *“à plan de frappe facetté”* (1955:338) towards the Levallois technique.

In 1947, participants in a Pan-African Congress of Prehistory proposed to discard the use of the word ‘Levallois’ in the description of industries from Africa and to replace it with the term “faceted platform technique” (Pan-African Congress of Prehistory 1947:8, as quoted in Bordes 1961:14).

In the same year, Bordes referred to ‘Levalloisian’ as a *technique du plan de frappe à facettes* (Bordes 1961b:24). He explained why those *facettes* were important: “*ces facettes peuvent être disposées de telle sorte que le plan de frappe devienne convexe, ce qui permet de déterminer plus exactement le point où le percuteur rencontrera le nucléus*” (Bordes 1947:8). But at the same time, he indicated that Levallois flakes may sometimes also present plain platforms.

At this point Bordes began his collaboration with Maurice Bourgon, and his ideas about Levallois developed (Bourgon 1957, preface). It seems that the fruit of this partnership was the paper published in 1950, in which he stated: “*plusieurs études des techniques de débitage dans le Paléolithique inférieur et moyen ont déjà été faites, mais on y a confondu à plaisir deux choses qui peuvent être liées ou n’avoir aucun rapport entre elles, la préparation du plan de frappe et le débitage ‘levalloisien.’*” Thus Bordes reduced the importance of the platform preparation within the definition of the Levallois technology and stressed the importance of the upper surface preparation, which usually forms “*une surface rappelant grossièrement le dos d’une tortue et ses écailles*” – although he has also shown the presence of cores with upper surfaces with parallel negatives (Bordes 1950:21), which may sometimes result in blades that share similarities in morphology to Upper Palaeolithic blades. For comparative purposes, he also integrated a Levallois index into the typological studies (Bordes 1950 and 1953).

Bordes’s ideas were very similar to those developed long before by Maurice Bourgon (unfortunately, Bourgon’s ideas were only published in 1957). Bourgon had described Levallois (Levalloisian) as a flaking system which had as its goal: “*la fabrication d’éclats préfigurés... dont la forme a été préparée, déterminée par l’épannelage du nucléus. Les arêtes d’intersection des faces d’épannelage dessinent sur le nucléus les arêtes directrices du future éclat*” (Bourgon 1957:28). He retained in his definition the importance of scar negatives visible on the upper surface of the core that had shaped the potential flakes.

Today, it is important that we recognise Bourgon's work in developing the idea of what constitutes 'Levalloisian', because many researchers have forgotten the significance of his labour and his major influence on the progress of his field, which was visible in the work of Bordes around this time.

In 1951, Breuil and Lantier proposed a definition of 'Levalloisian' that was almost identical, but still indicated the importance of the faceted platform: "*Lorsqu'on examine le plan de frappe d'éclat obtenus par cette technique, on observe la présence de facettes éclatées de haut en bas, mais segmentées par l'éclatement de sorte que la seconde moitié de leur trajectoire est restée sur le nucléus*" (1951:74).

In 1954 Breuil and Kelley suggested that Levalloisian was an independent 'culture', like Mousterian or Acheulian. Once again this definition was very similar to the ones presented above, but some more observations concerning the angle of the striking platform were made:

La face supérieure (d'un nucléus) a subi des enlèvements bien plus plats, convergeant vers le centre et destinés à préparer sur cette face le dos du future éclat. Ensuite un point du bord a été réduit à un angle droit par le facettage. Il semble que cet angle ait été nécessaire pour l'enlèvement de l'éclat-outil, on constate en effet un certain nombre des éclats levalloisiens, soigneusement préparés sur nucléus, mais à plan de frappe sans facettes.

Furthermore, Kelley employed refitting as a tool to decipher the Levallois strategy (1954:100) and demonstrated that a multipart preparation of cores is visible, not just a faceted platform, and that the method aimed to produce one or several flakes or blades: "*c'est l'ensemble de la préparation du bloc destiné à livrer un ou plusieurs éclats ou lames qui caractérise l'industrie levalloisienne*" (1954: 150, see also pp. 168-169). "*Lorsque la taille levalloisienne a été perfectionnée, cette méthode a permis la fabrication en série d'éclats symétriques*" (1954:151).

For Leroi-Gourhan, the Levallois technique was present from the "third technical stage":

La fabrication... aboutit à la confection d'une sorte de biface dissymétrique en épaisseur, de la forme d'une carapace de tortue de jardin. Pour obtenir cette dissymétrie deux séries de gestes sont successivement mises en jeu: la série... qui donne la face la plus abrupte et la série... qui conduit au profil de la face aplatie. A partir de ce point une troisième série de gestes est destinée à traiter le biface, non comme un outil à façonner, mais comme un nucléus dont on va extraire des éclats plats et larges qui seront eux-mêmes les outils (1962:15).

Most Anglo-Saxon scholars seemed to agree completely with the definition of Levallois technology proposed by French academics: “Palaeolithic industries consisting principally of flake-tools produced by the tortoise-technique are usually classed as Levalloisian. The technique was sometimes modified so that, instead of oval flakes, long, narrow flakes or flake-blades were produced” (Oakley 1945:51).

Although some Anglo-Saxon scholars still insisted on the importance of faceted butts visible on Levallois flakes (McBurney and Hey 1955), and although the definition proposed by Bourgon and Bordes was often reformulated, it appeared to be broadly accepted (de Heinzelin de Braucourt 1962, Tixier 1967, Hours 1973) by both French and Anglo-Saxon academics. In all the definitions mentioned, three essential ideas were always present:

- the method was mainly concerned with the morphology of its end products,
- the method was capable of producing a single flake per reduction (ignoring the observations made previously by Kelley), and
- the notion of predetermination in the production of Levallois flake.

Slowly, however, difficulties in the recognition of Levallois supports in archaeological assemblages began to arise, and even Bordes had to admit:

Sera classé comme éclat Levallois tout éclat dont on peut penser que sa forme a été prédéterminée par préparation spéciale du nucléus, avant son détachement. C'est là évidemment la difficulté majeure, et l'appréciation

du caractère Levallois ou non-Levallois d'un éclat, facile pour les cas typiques, demande parfois, pour les cas atypiques, une certaine expérience.

But the problem did not lie in the lack of experience in typology, but rather in an incomplete definition of the Levallois flake and its comparison to the other products of the reduction sequence.

To overcome this problem and to try to remain objective, de Heinzelin (1960) proposed the use of metrical attributes to recognise Levallois flakes. His method had little success, being judged as too time-consuming and in any case inadequate to resolve such a problem (see Bordes 1961:17).

In 1975, Crew examined the variability of the Levalloisian method for the Levantine Mousterian and argued that: “The definition accepted for the Levallois flakes is that presented by Bordes... Many workers believe that the term Levallois flake should be confined to those flakes with radial or centripetally-directed preparation. However, for the Levantine Mousterian, this restrictiveness would disqualify many Levallois flakes which are ‘typical’ in most other respects.”

Crew also admitted that there were major difficulties in deciding which blades were Levallois and which were not. He decided to overlook the distinction altogether in his study.

To study the variability of the direction of preparation visible on lithic artefacts, Crew used analysis of their dorsal scar patterns (1975:13, p. 12, Fig. 2:1). This procedure was later used by many other scholars and was developed by Boëda in his *lecture des schémas diacritiques* (analysis of distinctive patterns) (1986:16).

The problems that Crew had observed with blades were also visible in Jelinek's study of Tabun material. Originally, he divided blades with parallel scars into two categories: Levallois with a faceted butt, and ‘normal’ with a plain butt (Jelinek 1975: 304). But a few years later, he decided to put all blades with parallel scars into a special category of prismatic blades (Jelinek 1982:75).

With the introduction of experiments and development of reconstruction (refitting), perceptions of Levallois began to adjust. Archaeologists began to pay more attention to the dynamic reduction processes, moving out from the particular importance of Levallois flakes to the whole range of flaking products manufactured during the Levallois reduction sequence.

In 1975, Bradley proposed to use experiment and replication to better understand the Levallois reduction sequence and its products. His goal was to generate the classical, centripetal Levallois flake and to replicate the Levallois reduction strategy. The ensuing experimental assemblage would be then useful to compare with archaeological collections.

In 1980, Tixier, Inizan and Roche reformulated the Bordesian definition of Levallois, but once again the end-products were used to describe the Levallois flaking system and the notion of predetermination in the production of the Levallois flake was stressed:

- broad oval Levallois flake production,
- triangular Levallois points production throughout the unipolar or Nubian method,
- Levallois blade production: in which a series of blades can be obtained from one flaking surface using two platforms. Blades are struck off alternately from each platform and the scars of the preceding removals act as guides for the following blades, though re-preparation of the flaking surface is not needed.

The problem with Levallois arose once again after the publication describing the production strategy of the Levallois point observed in lithic assemblages from layers 1 and 2 at Boker Tachtit in the Negev (Marks and Volkmann 1983, 1987), based on refitting. The presented reduction strategy started from the side of a flat core (thus making it entirely different from the classical Levallois reduction) and ended with the removal of a typical Levallois point. But it was shown that the same authors had not classified as Levallois points products of the same morphology discovered in Level 4

at the same site because they came from a different reduction strategy, the objective of which was not to produce such supports.

For Copeland, this point of view was too rigid and also incompatible with Bordes and Tixier's classical definition of Levallois, which was allied to the notion of the end-product (1983:17). She stated that the lack of well-developed new approaches to the study of lithic material made the use of Bordes method inevitable, but she also confessed that: "Today, a divergence of views has developed as to what are the criteria for these [Levallois/not Levallois] attributes, and this affects interpretations" (1983:15). She also questioned the validity of the Levallois index, as in her opinion no agreement had been reached on what represented Levallois. She admitted that the definition of Levallois had expanded and needed serious reassessment and that there existed a real problem with elongated Levallois products. Concerning the latter, she concluded: "If Levalloisness resides in the additional stage of preparation, then series blades do not qualify" (1983:19). As a solution, she suggested creating a third 'intermediate' category in artefact classifications (Levallois or not Levallois). This group would include all unclear series-blades and series-points and might help researchers to recognise special features in an assemblage.

The Levallois method for blades with two platforms on opposite ends struck alternately had to obtain at least two blades per reduction from the same flaking surface, and thus it was from the beginning totally disconnected from the classical Levallois method which was supposed to be capable of producing only single flake per reduction. Bordes' definition of Levallois for a blade stated:

la préparation de la face supérieure se fait par une série d'enlèvements de long éclat étroits, ou des lames, parallèles au lieu d'être centripètes, et souvent le débitage qui suit est du type à deux plans de frappe opposés, le nucléus étant frappé alternativement sur les deux bouts (Bordes 196:72).

Another approach to the Levallois, by Genest (1985), was based on reading the scar patterns of the core and flake to replicate flake characteristics according to the stage in the reduction process to which the flake belonged. Such a procedure would help to

identify the reduction sequence according to the orientation and temporal emergence of removals. Genest elaborated the model of *chaîne opératoire* (Leroi-Gourhan 1971, 1973) for Levallois flake production.

Despite all this polemic on the Levallois, the problems continued ostensibly without conclusion.

In 1986, Perpère undertook an interesting experiment to compare an intuitive typological classification with a classification based on measurements. This study showed clearly that the problem lay with the definition of Levallois.

Three experienced archaeologists – Perpère herself, Tuffreau and Boëda – were asked to classify 198 flakes from the French site of Ault (Somme) into two categories: Levallois and non-Levallois. Additionally, the two last scholars introduced a third category, ‘*douteux*’. The result was startling: of 137 specimens, only 69% of the flakes were classified in the same category by all three scholars. As one possible means of avoiding such problems, Perpère proposed studying flakes with a ratio known as *enlèvement-tranchant* (E.T.), which would be capable of showing typo-metrical differences between Levallois and non-Levallois. But at the same time, she confessed that the “*indice E.T. est plutôt adapté à la détermination des éclats Levallois souvent décrits comme ‘classiques’*” (1986:117).

In the same year Boëda proposed an innovative definition of Levallois, which he later developed (Boëda 1986, 1988, Boëda *et al.* 1990) into a full-blown theory. Based on his *lecture de schémas diacritiques* and on experiment, it used three basic ideas: concept, method and technique.

- The description of concept originated from experimental work and resided in the volumetric perception of the core: “*Le nucléus est conçu comme ayant deux surfaces sécantes de convexités opposées délimitant un plan unique, dans lequel se fera le débitage des enlèvements prédéterminés. Une surface assumera la mise en place des convexités latérales et distales tandis que l’autre assumera le rôle de plan de frappe*” (1986: 26).

- “Method” referred to a stage of production and consisted in setting up the technical criteria of Levallois predetermination. The *lecture de schémas diacritiques* was employed to expose the variability demonstrated in individual reductions by analysis of scars left on artefacts manufactured during Levallois reduction. It focused on the temporal succession and the orientation of scars. Two methods were proposed, each with different modalities of the flaking surface:
 - the *méthode linéalle*, generating one Levallois flake for every prepared upper core surface, and
 - the *méthode récurrente*, capable of producing a series of Levallois flakes from the same upper core surface. Such flakes would be both predetermined and predetermining.
- “Technique” in the case of Levallois was limited to direct percussion with a hard hammer, representing an act of detachment from all predetermined and predetermining flakes.

A very different definition of Levallois, in which the concept of predetermination was rejected, was put forward by Dibble in 1988. He investigated the predetermined nature of the Levallois flake through analysis of the metrical attributes of three groups of products – Levallois flakes, biface trimming flakes and ordinary flakes – for which no particular production technique was identified, and found that these three categories actually displayed no significant variation in length, width or surface area. He therefore concluded that Levallois should be regarded as a method of continuous fabrication of flakes, a particular system of core reduction, and not as a method for production of a single flake predetermined in its size and shape.

In 1992 another scholar, Van Peer, joined the Levallois debate by presenting a study of five Middle Palaeolithic assemblages from Upper Egypt. This work was extremely important because a high proportion of the material could be refitted, and as a result it was able to present completely reconstructed sequences and a dynamic variability in the assemblages studied.

This study agreed with Boëda in two respects. It found that there was a unified Levallois concept which included the notion of predetermined blank production, and also that a strategy could be characterised as Levallois if certain criteria were met. However, Van Peer did not agree with extending the predetermination notion to “making use of pre-existing ridges”, and he retained “a rather strict notion of predetermined products and morphological control and the way in which such products are exploited from the upper surface of a Levallois core” (Van Peer 1995:3). In his opinion, a Levallois flaking surface was intended to generate a restricted number of large end-products. He argued that these specimens were exceptional compared to other reduction products.

Van Peer also stressed the importance of refitting as a methodological tool for accurate reconstruction of the order of events, arguing that: “the only means to recognise a Levallois strategy is through physical reconstruction of reduction sequence” (1995:8). Using refitted material from Taramsa-1 (Van Peer 1995:6), he showed that the occurrence of the Levallois criteria on a core and on end-products did not always signify the Levallois character of the reduction.

Another important outcome from this example was the finding that classical Levallois reduction was not capable of systematic production of series-blades. Nonetheless, occasional blades could be removed, owing to the construction of the upper core surface and the platform thickness at the moment of flake propagation. During propagation, the flake is guided by the exterior ridges of the core; these determine its shape, as well as the convexity of flaking surface, the degree of which establishes its size. To produce elongated specimens from a Levallois core we would have to decrease blank width, which involves positioning the fracture plane of the flake at a higher level, resulting in a very thin blank. The solution for this would be to transform the flaking surface and its correlation with the lower surface in such a way as to make possible the tangential exploitation of upper surface. The blank would then retain a significant thickness.

This finding meant, however, that the principle of one-plane exploitation in Levallois strategy had to be abandoned. Van Peer indicated that such a treatment of the flaking surface additionally showed that “other strategies may be closely related to Levallois or even be adaptations of it” (Van Peer 1995: 8). Moreover, he criticised the use of detailed analysis of the upper surface of cores and blanks as a feasible means for the description of surface exploitation, arguing that it was not clear how the order of appearance of scar negatives could be determined. If this could not be judged, it followed that the presence of a *récurrent* method could not be determined either.

It seemed to Van Peer that information collected from blanks and cores throughout such analysis remained disconnected and was not capable of documenting possible changes from one method to another within one reduction strategy. It could therefore not be employed to illustrate the possible dynamics of reduction development. Basing his case on outcomes from refitting, he argued that the Levallois recurrent method had not been used for the production of Levallois blades (Van Peer 1992, p. 89, 111). Subsequently, his conclusion appeared to be confirmed by the refitting of classical Levallois points from Europe (Demidenko and Usik 1995) and the Near East (Demidenko and Usik 2003), where the Levallois reduction was found to be classical but not recurrent. The blades produced through the unidirectional-convergent reduction for points were seen as waste.

Dibble (1995), after reviewing the assemblage from Level II of Biache-Saint-Vaast, a French Mousterian site, made a similar criticism. Tuffreau (1988) and Boëda had previously studied this material typologically and had used it as an example of the so-called *modalité récurrente* of the Levallois method. However, Dibble’s analysis, based on qualitative examination of the discarded cores and debitage of the assemblage, and essentially using the visible scar patterns on them, identified two categories that for him were clearly separate: *modalité récurrente unipolaire* and *modalité récurrente bipolaire*. Moreover, in contrast to Boëda, Dibble investigated almost entire elements from this assemblage, including non-Levallois items, and conducted a detailed quantitative attribute analysis. His conclusions varied considerably from Boëda’s. Dibble showed that scar patterns changed as reduction went on. Uni-directional, bi-

directional, sub-radial and radial methods were interchangeable and were performed on the same core, probably in reaction to the changing topography of the flaking surface. Dibble was able to show that relying solely on scar pattern analysis of cores and some Levallois products was not suitable for studying the dynamics of a reduction strategy.

A diverging hypothesis was presented by Meignen (1995). After examination of material from Kebara IX-X, Meignen concluded that this assemblage was primary and had indeed been obtained using the recurrent unidirectional-convergent method.

Alongside Boëda's and Van Peer's hypothesis that there was a unified and uniform Levallois concept, another approach to the definition of Levallois appeared. Otte (1995:123) argued that the high variability visible in Levallois and its universality indicated "its value as evidence of a spirit, not of a context". Otte saw Levallois as:

... a phenomenon of convergence produced by the conjunction of three factors: the mechanical properties of raw material, the conceptual capacities of the knapper, and the functional needs of the group. This phenomenon can thus appear independently countless times and in different places in the course of human evolution. So its particular ethnic significance must be determined in each situation where it is discovered.
(1995:117)

Baumler (1995) presented a similar definition of Levallois, proposing a model of core reduction appropriated to all reduction sequences, without bifacial reduction. It suggested that investigations in a particular archaeological assemblage should consider the reduction strategy used as a whole. This approach could integrate numerous inter-related subsystems that were reliant on the site-specific conditions. In such a perspective, the Levallois would be perceived as just a particular core reduction, or one part of a general technological system.

1.2. The appearance of the blade industries

The latest chronological and geographical data suggest the appearance of the laminar phenomenon in the heart of Palaeolithic in different places: the Near East, Central Asia, Europe and Africa. This activity seems to have developed over a long period and reflects different production strategies that always led to the production of an elongated support.

Five sites of the Kapthurin Formation in East Africa (Johnson and McBrearty 2010, Port *et al.* 2010) and the Kathu Pan 1 site in South Africa (Wilkins and Chazan 2012) contained blade-like components that have been dated to about 500 ka. The first group appears to be not related to the Levallois methods, since blades in series were manufactured using a unidirectional or centripetal method from a convex flaking surface. This surface was created by the intersection of two or more planes and appears to be similar to the Hummalian technique, as described by Boëda (1995). The first blade was detached from either the long natural edge or from an edge of a core that was only lightly prepared; the next few blades were then removed continuously. On the South African site, blades were struck from a single platform, or more often two platforms; the cores appear to have been prepared and maintained by employing centripetal flaking. The assemblage seems to be related to Levallois, as defined by Boëda (Wilkins and Chazan 2012:11).

These descriptions indicate the diversity of blade production in eastern and southern Africa. The various kinds seem to have been clearly distinct in a technological sense but related in their chronology.

Another African site showing blade elements, Haua Fteah in Libya, was characterised as “an archaic leptolithic industry with virtual absence of Levalloisian traits” (McBurney 1967:325-326) and as belonging to the Pre-Aurignacian of the Near East. Found under the Levallois-Mousterian levels and separated from the latter by a 0.5m sterile horizon, this set remains undated.

On the other hand, Grigoriev's analysis of the published lithic materials displayed the possible use of the Levallois method and the Mousterian character of the tool-kit. Therefore the character of the industry remains uncertain.

In Asia, Early Middle Palaeolithic blade industries had already been identified in Tajikistan (Schäfer, J. u. Ranov, V.A. 1998) and Georgia on both slopes of the Central Caucasus in the 1980s. For example, Weasel Cave in North Ossetia and Kudaro I, Kudaro III, Tsona, Djrchula, and Hviraty in South Ossetia (Liubin 1977; Liubin and Beliaeva 2006, Meignen and Tushabramishvili 2006, Tushabramishvili *et al.* 2007). These sites have been conglomerated under the name of the Kudaro-Djrchula group and are associated with the Tabun D-type industries, as they contain a large quantity of blades. The dating obtained from two occupation spans in Djrchula Cave, with assemblages presenting clear technological affinities with the blade industries of the Near East, has put their estimated age at between 260 ka and 140 ka (Mercier *et al.* in press). The Khonako III site in Tajikistan is estimated to date from 200-240 ka (Meignen and Vandermeersch 1999:13).

In Europe, the production of blades in the Middle Palaeolithic context was first recognised in the Somme Valley terraces of northern France at the beginning of the last century (Commont 1912). At that time blade production was supposed to be associated exclusively with the Upper Palaeolithic, and so for a long time this evidence was ignored. Only in the 1960s (Bosinski 1966), after the well-dated discoveries at Rheindahlen in Germany and later in Seclin in France (Tuffreau 1983), was the presence of blades industries in the heart of the Middle Palaeolithic recognised.

After this recognition, numerous sites containing blade components were located in the western part of the North European plain (Révillon 1989, 1993, 1995; Conard 1990, 1992; Otte *et al.* 1990; Otte 1994, 1995; Révillon and Tuffreau 1994; Delagne and Kuntzmann 1996; Conard and Adler 1997). Chronologically, this phenomenon covered a rather short period, appearing during the course of the penultimate glaciation. It seems to have been well established during the first part of the Glacial and then disappeared at 60,000 BP (Oxygen isotope stage 5) (Van Vliet-Lanoe *et al.*

1993; Deloze *et al.* 1994, Delagnes 1996). In almost all the sites with blade industries, the method and the core volume management were similar. Blades were removed from either one or two platforms using the same hard hammer percussion. The reduction seems to have been ruled by four main observed principles: rotating, semi-rotating, facial and frontal debitage (Delagne 2000). The majority of blades were not retouched, but some present a marginal retouch and some were selected as blanks for particular tools (Beyries 1993, Otte *et al.* 1990). The important point here is that this blade production was never exclusive (except Rocour) and is always found alongside a generally predominant manufacture of flakes using Levallois technology.

In the Near East, the laminar phenomenon appears at the end of the Lower Palaeolithic immediately following the Acheulo-Yabrudian (Pre-Aurignacian and Amudian) and is then seen systematically in the early Middle Palaeolithic (Hayonim layers F and E, Abu Sif, Tabun D, Tabun E, Rosh Ein Mor, Ain Difla, Hummal layers 6 and 7, Nadaouyieh, Umm el Tlel) and later in the heart of the Middle Palaeolithic (Nahal Aqev, Douara IV (Akazawa 1979), Jerf Ajla Unit E (Schroeder 1969), and Hummal (Hauck 2010).

The early Middle Palaeolithic group shows non-Levallois debitage and contains two industries: the Pre-Aurignacian and the Amudian. The first was identified in levels 13 and 15 at Yabrud I in Syria (Rust 1950; Bakdach 1982) and the second in a few sites: in Tabun (Garrod 1956, 1970, Jelinek 1975, Vishnyatsky 2000), Abri Zumoffen/Adlun (Garrod and Kirkbride 1961; Copeland 1975), Masloukh (Skinner 1970), Zuttiyeh (Gisis and Bar-Yosef 1974) and Qesem Cave (Barkai *et al.* 2003, 2005). The Amudian from Tabun unit XI (Tabun E) has been dated to 264 +/-28 ka (Mercier and Valladas 2003) and those from Qesem Cave may possibly have started more than 380 ka and persisted to up to 200 ka (Barkai, *et al.* 2003; Barkai, *et al.* 2005). Both industries are often assembled together, although they differ in their core reduction strategies and tool-kits.

The Amudian from Tabun unit XI is characterised by the appearance of blades that are often backed. Unfortunately there is a lack of published data for this site; there is no

inventory of the assemblage or any other information which would give the number or the exact percentage of the elements in Amudian. The only reference is the doctoral thesis of Dibble (1981:47), which gives the inventory of Amudian Bed 75I1. In this inventory the Bordes type 36-37-38, displaying the presence of backed elongated items, was well represented and comprised 52% of the set. The collected blades were detached from unidirectional cores using the hard hammer technique (Jelinek 1990; Meignen 1994). Cores were rarely shaped; the flint knapper used the natural convexities of the block of raw material to start flaking. The lateral convexities of the core were maintained by regular subtraction of *lames débordantes* (Marks and Monigal 1995: 254). Blades were detached in series from a single flaking surface. The elongated specimens seem to have been regularly modified, with abrupt or semi-abrupt retouching forming a precise tool with a retouched back opposite the long cutting edge (Marks and Monigal 200; Barkai, *et al.* 2005; Lemorini *et al.* 2006). Other Upper Paleolithic tool types, such as end scrapers and burins, are rare in Tabun unit XI (Meignen 1994) and in Qesem (Barkai *et al.* 2005). In almost all Amudian assemblages from Tabun unit XI, as well as those from Abri Zumoffen/Adlun, the existence of flake production alongside blade production has been documented, with the sole exception of Qesem Cave, where the manufacture of blades seems to have been exclusive (Barkai *et al.* 2003, 2005).

The Pre-Aurignacian at Yabrud I showed important blade production with an ILam of about 40 (Bakdach 1982). The cores are semi-prismatic and usually unidirectional, and they were not initially prepared or decorticated. The negative left by the subtraction of a large specimen from one end of the block of raw material generated a core striking platform. There is evidence for the occasional use of crested blades. The cores were often made on flake and were often exhausted, in contrast to Amudian cores from Tabun, which are not exhausted. The resultant blades present parallel edges and large, plain butts, and are triangular or trapezoidal in cross-section. The production of flakes from a separate reduction strategy using discoidal cores has been documented (Bakdach 1982). However, Vishnyatsky (2000:148) argues that the majority of these are waste and by-products of blade manufacture. Flakes make up 52% of the

assemblage whilst blades constitute 48%, with the latter seeming to be retouched most often (Bakdach 1982). The tool-kit of the Pre-Aurignacian is characterised by burins and end scrapers, with no bifaces (Garrod and Kirkbride 1961), and backed blades are rare.

The more recent Early Middle Palaeolithic blade assemblages are positioned in the stratigraphy between the Acheulo-Yabrudian and the Middle Palaeolithic complex (e.g. Tabun IX, Hayonim lower E and F and Hummalian) or above the Acheulo-Yabrudian (e.g. Abu Sif C-D), with other sites, such as Rosh ein Mor, Nahal Aqev and Ain Difla, presenting full and short stratigraphical sequences. These assemblages display the use of the Laminar and Levallois reduction strategies simultaneously and contain a high percentage of blades. They differ not only in the use of both reduction strategies, but also in the production of various tools; site type and site use; and chronology (between 260 to 160 ka). The goal was to produce elongated blanks, although not exclusively so. Short specimens are always recorded and seem to have been manufactured through a distinct core reduction strategy, generally Levallois in nature.

The estimated age of blade industries of the Hayonim cave shows that this phenomenon persisted there from 230 to 160 ka (Mercier *et al.* 2006). This is more recent than the assemblages from Tabun IX, dated 256 ± 26 ka (Mercier and Valladas 2003), and possibly more recent than those dated 200 ka (Rink *et al.* 2003) from Rosh Ein Mor, which also have a dominant Levallois component.

Many of the Levallois industries from the Middle Palaeolithic period show high proportions of Levallois blades, indicating that the tendency to produce elongated blanks had not been completely abandoned. This can be observed in the assemblages discovered from Levallois-Mousterian levels in Hummal, where the Levallois blade percentage ranges between 30 and 50% (Hauck 2011); in Kebara unit XI, where Levallois blades represent more than 30% (Meignen and Bar-Yosef 1991); with 35.8% in Amud (Hovers 1998) and 37.1% in Tor Sabiha (Henry 1995).

In next period, the Initial Upper Palaeolithic, systematic blade production appeared (Kuhn 2004; Meignen 2006, 2007). Blades seem to develop in the Near East between 47 and 45 ka. This date is obtained from the oldest level, Level 1, of Boker Tachtit (Goldberg and Brimer 1983). Blades production persisted until 36 ka, as recorded in the Umm el-Tlel site (Boëda *et al.* 1996).

2. History of research

2.1 First evidence of settlement in the region and discovery of Hummal

The El-Kowm area (Fig.1) was archaeologically investigated for the first time in 1965 by an Oriental Institute of Chicago expedition led by M. Van Loon. The investigation of the main tells, under the responsibility of R.H. Dornemann (Dornemann 1969) revealed a preceramic occupation, although there was no mention of the Palaeolithic.

In August 1966, G. and M.K. Buccellati (Buccellati G. & Buccellati M.K. 1967) from the University of California, Los Angeles surveyed the northern part of the Syrian Desert for the first time with the aim of finding evidence of the Bronze Age people who had lived in the region. The results of the survey produced nothing in terms of Bronze Age evidence, but there were signs from Palaeolithic period in the El-Kowm area and a few sites were reported where the “flints of the type already known from Jarf Ajla near Palmyra were found.” The results also referred to Tell Hummal, where the finds were “very rich and well preserved”.

In May 1967, a Japanese expedition directed by H. Suzuki and known as the Tokyo University Scientific Expedition to Western Asia conducted a series of surveys around Lebanon and Syria (Suzuki and Kobori 1970). This expedition included the region of El-Kowm and noted two Palaeolithic sites already found by the Buccellatis: Tell el-Madar (Tell Umm el-Madar), Tell Oumn Teil (Tell Umm el-Tlel). It also mentioned a third site under the name Tell Hassan Unozi (Fig. 2). This last tell was most likely the ‘Tell Hummal’ reported by the Buccellatis. The flints found on these sites presented abraded edges and were strongly lustrous.

In February 1969, the Russian geologist I.S. Chumakov, who produced the geological map of the desert part of Syria, found dozens of Mousterian flakes and cores (78 pieces) in El Qdeir. He published this assemblage with archaeologist N.O. Bader and assigned it to the “developed Levallois-Mousterian”, noting that it contained a high proportion of points and noticing the analogy with the assemblages from Jerf Ajla and Yabrud (Bader and Tchumakov 1970).

2.2 Systematic investigations

In September 1978, a French mission led by J. Cauvin started the investigation of El-Kowm by digging a sondage in Tell El-Kowm and the Caracol tell. In parallel with this, a systematic survey of the region was undertaken with the aim of estimating its archaeological potential (Cauvin *et al.*, 1979). From this date onwards, prospecting and studies of the various sites continued annually. The presence of numerous Palaeolithic sites was indicated, including Hummal, a site described as being without bifaces, but with high laminar and Levallois indexes. The rich assemblage was collected from the back dirt of a well constructed in 1951, which had itself been dug into an ancient Roman well. The assemblage contains numerous elongated Mousterian points and scrapers and a few burins and end-scrapers. The artefacts were made of a black, glossy flint, and some pieces presented rounded edges. During the same investigation, a similar industry with elongated points was also identified in Umm el-Tlel. The site comprises a spring surrounded by tells.

In 1980, a first study campaign was conducted by P. Salanville, J. Besançon, L. Copeland, F. Hours and S. Muhesen at the invitation of J. Cauvin, who at the time was the director of the French Permanent Mission in El-Kowm. The project, devoted to the geomorphology and the Palaeolithic of El-Kowm (Cauvin *et al.* 1979), identified 51 sites occupied from the final Acheulean to the end of the Middle Palaeolithic (Besançon *et al.* 1981, Hours 1982). The region was characterised by the abundant spring mounds that resulted from the constant amassing of aeolian and travertine deposits around the vent of an artesian spring. As the farmers of El-Kowm dug shafts through the midpoint of these mounds to reach the water table, their infill could be

observed in section. One such site, number 7, was Hummal, a spring mound in which a well had been dug and exploited until the 1970s. The well was abandoned by the time archaeological prospecting started. The bottom was 20m below the current ground surface and was crowned with 5m of back earth, giving a total depth of 25m. Supporting walls were partially built, and the section view was not complete. The survey team collected six samples of artefacts from the seven layers that were evident in section. In the lowest layer (Hummal Ia), a new culture was identified and labelled “Hummalian”. On the other side of the well, 75cm above Layer Ia, there were typical Yabrudian artefacts (Hummal Ib). At the point of discovery it seemed that the Hummalian had to precede the Yabrudian level. Above them were found a sequence of Mousterian assemblages in succession (Hummal II, III, IV and V) (Besançon and Sanlaville 1991) (Fig. 4).

A sample of 419 artefacts was collected from Layer Ia. They were elongated and seemed to be a result of Levallois technology, in which unidirectional cores were used without radial preparation. Three-quarters of the striking platforms were plain. The most typical tools included pointed blades shaped on distal parts on one or both sides by a flat or oblique retouch. Burins and end-scrapers were rare. The flint was covered in a glazed coating.

The same assemblage was further studied in detail and used by Francis Hours to describe this new industry (Hours 1982). It was characterised by:

- High laminar index (ILam 65.85).
- Intentional production of elongated blanks struck off cores with one or two opposite platforms; they were very often produced in succession whereby the negative left by the detached blade formed the guide-ridge for the next blade to be knapped; there was no centripetal preparation.
- The large majority of striking platforms were plain, broad and thick; the remainder were faceted, dihedral, punctiform and cortical (IF 37.61).
- Cores were not frequent (1%), usually smaller than blanks. One Levallois core was documented.

- The retouched tool-kit comprises numerous scrapers; blades pointed by abrupt retouch, notches and denticulate; continuously and lightly retouched (nibbled) blades; and a small number of burins. Inverse retouch had been applied, but infrequently.

In 1982 and 1983 a sample of 6600 objects were gathered from Layer Ia and partially studied by L. Copeland (1985). 132 pieces from the same collection were studied by Bergman and Ohnuma (1983). Their analyses completed the previous study and characterised the objects as follows:

- The collection is dominated by blades (ILam 52.67). The majority of blades have a plain or faceted striking platform (IF 37.95) and the point of percussion is positioned directly behind or to the side of a central ridge.
- The majority of the blanks were detached using a hard hammer; the point of percussion was positioned well onto the butt.
- The blanks were produced on cores with a single platform or two opposed platforms. The cores have long parallel ridges which served as guides for the force of the blow, or the ridges were prepared using a crested blade.
- The majority of cores are exhausted; when compared with the length of the blanks, it confirms that they were significantly reduced in size throughout flaking.
- The Levallois index is difficult to count, as it is difficult to tell how much Levallois technology was used; IL without the blades amounts to 6.3%.
- The industry includes several pointed and backed tools, nibbled and variously retouched blades, few notches and denticulate, infrequent end-scrapers and borers. IL^{ty} (Indice Levallois typologique) equal to 17.4.
- The presence of cores on flake and the Nahr Ibrahim technique were identified.

In 1982, J.M. Le Tensorer joined the French team. After F. Hours' death, he was given responsibility (in collaboration with S. Muhesen) for Palaeolithic research in the region of El-Kowm (Le Tensorer and Hours 1989).

From 1982 to 1985 a new series of stratigraphic and sedimentological studies of the Hummal infill by J.M. Le Tensorer led to previous observations being revised and a recognition that none of the previously collected material, except for that of the Yabrudian industry, had been *in situ* (Le Tensorer, Hours 1989). The blade industry (Ia), for example, had not been collected *in situ* but in a secondary position at the bottom of the well. As a result, and in direct opposition to the preceding publications (Besançon et al. 1981; Hours 1982), it was recognised that the Yabrudian layers preceded the Hummalian.

The basic travertine which contains the Yabrudian was dated between 138 and 179 ka (Henning and Hours 1982); three analyses by thermoluminescence confirmed this age of approximately 150ka.

The stratigraphy of the lower sequence of Hummal was extremely complex and was made more complicated due to a large section being either concreted or covered with dry-stone retaining walls (Fig. 5). Six Loci were raised around the centre of the well, and two profiles – P.1 and P.2 – were documented (Fig. 5 and 6). The upper sequence was investigated in Locus VII. The following sedimentary complexes were recognised from the base to the top (Le Tensorer 1994, 2004):

- Yabrudian travertine: archaeological complex Ib.
- A level composed of a conglomerate of abraded travertine blocks with a thickness greater than 1m was found at the bottom of the well. Several Yabrudian levels were recognised at the base of the deposit. 703 artefacts were collected and studied by L. Copeland and F. Hours (1983). The most frequently recognised elements of this assemblage were the numerous scrapers with Quina or semi-Quina retouching (IR ess: 68.93), but important numbers of Upper Palaeolithic tool types, as well as notches and denticulate and hand-axes, were also identified.
- Sand deposits with Hummalian and Mousterian elements: archaeological complex Ia and partly II.

The levels, which were of variable thickness from 0.50 m to 1m, were composed of cemented quartz rich sands at the base and loose sand at the top. The surface of this sand was deeply eroded. At the base and in the middle section of these sands, several archaeological levels containing Hummalian artefacts were recognised. At the top, one sandy level demonstrated a Mousterian assemblage of Levallois debitage with very laminar emergence (IIb).

Above these sands, all the central part of the stratigraphy was composed of levels with Mousterian assemblages (complexes II, III and IV) containing commonly elongated items (Ilam: 48-25).

- Detrital Composite-Complex II/III: breccia with abundant Mousterian flint and bones fragments. This deposit occurred in a secondary position. Above it, the stratigraphy was no longer visible because of a concrete wall approximately 3m in height.
- The detritic series terminate with sand and cemented gravel (Complex III) consisting of profuse archaeological material with Levallois debitage.
- Sandy Complex IV: these sands have been identified only in the north-western part of Hummal at the same depth as complexes II and III. These quartzitic sands supplemented by clay elements contained numerous elongated Levallois artefacts (including Levallois points).
- Clay sandy loam intersected by an organic clayey level (*'niveau tourbeux V'*), sterile.
- The above-mentioned clayey level on the south was eroded and replaced by sterile upper sands *'sables supérieurs B'*.
- Clayey loam with aeolian and evaporated components – Complex VI: above the organic clayey levels appeared a 1m-thick loamy and clayey formation with two archaeological levels, VIa and VIb. They contained principally thick blades, occasionally retouched. The preliminary observations suggest a transitional culture between Middle and Upper Palaeolithic.

- A top deposit of sandy loam with isolated artefacts: over Complex VI, the 8m Holocene deposit covering the site.

The stratigraphical situation at this point showed the Yabrudian complex (Ib) with its characteristic scrapers at the base, followed by the Hummalian (Ia) with regular blade production, and above this a Mousterian complex (V) with an overlying but as yet unidentified culture with non-Levallois blades (VIb).

In the winter of 1987, major surface erosion of ancient excavated material occurred and filled the well, covering nearly the whole lower part of the stratigraphy presented above, so that it is unfortunately no longer available.

In 1988, at the request of F. Hours, the burnt flints from layers Ib and VIb were dated at the Oxford Laboratory (Ancient TL Supplement 1988, Oxford Laboratory, Entry 22). The reported results give a context age of 160 ± 22 ka for layer Ib and 104 ± 9 ka for layer VIb. These results for Layer VIb did not correspond to the previous idea of a transitional industry between the Mousterian and Upper Palaeolithic, as they suggested that the layer was too old.

At the end of 1985, after J. Cauvin's team had led the last survey campaign in the El-Kowm region, the number of Lower and Middle Paleolithic sites discovered amounted to sixty, and almost 12,000 artefacts had been collected from them (Le Tensorer and Hours, 1989). Unluckily, after the death of F. Hours in 1987, his personal documents were lost and a large part of the information concerning the sites surveyed by the French team was also lost. Nevertheless, an inventory of Palaeolithic sites in the area has continued until the present under the direction of J.M. Le Tensorer (Le Tensorer *et al.* 2001). In the following years, new sites were discovered during the geological surveys of Swiss and French teams working in the area with *ad hoc* topographical investigations (Ploux and Soriano 2003). At present, 142 points and 206 Palaeolithic sites (from Lower Palaeolithic to Natufian) have been recorded (R. Jagher in preparation) (Fig. 6).

In 1987, at the initiative of J. Cauvin and J.-M. Le Tensorer, E. Boëda joined the team in order to apply his technological analyses to a number of lithic series. Later he became the leader in excavations of two important Palaeolithic sites in the region: Umm el-Tlel and El Meirah.

2.3 The beginning of the Syrian-Swiss research program

From 1989, the IPAS and the Department of History and Archaeology of Damascus University, under the joint direction of J.-M. Tensorer and S. Muhsen, undertook an interdisciplinary research program focusing on the Palaeolithic period in the El-Kowm area. This work resulted from a close cooperation with the French Permanent Mission in El-Kowm, whose general director at this time was Jacques Cauvin.

The research began with the systematic excavation at Nadaouiyeh Ain Askar, an Acheulian site already mentioned by Jacques and Marie-Claire Cauvin in 1978 and investigated in 1980 and in 1983 by F. Hours, J.-M. Le Tensorer, S. Muhsen and I. Yalçinkaya (Hours *at al.*1983). There had also been a one-season exploration at Juwal B (Ain Zarka), an Acheulian site already discovered in 1980. There were annual excavations at the former site until 2003, and these exposed more than 32m of stratigraphy, mostly covering the Acheulean period (Jagher 2000, 2011; Reynaud-Savioz 2011; Pümpin 2003). Nevertheless, evidence was also found of the presence of earlier occupations, namely Yabrudian, Hummalian and Mousterian. In 1992 a Hummalian industry was discovered in a dislocated sandy level between the Yabrudian and Moustarian layers. Several hundred flints were gathered and partially studied by R. Jagher (Jagher 1993).

In 1990 Inge Diethelm from Basel University started geological surveys using mineralogical and petrographical methods with the aim of establishing the origins of the raw material exploited at Palaeolithic sites of the El-Kowm area. In 1994 a one-season exploration took place at Qdeir 23 (Aïn Wajbeh), a site that had been discovered in 1980, and 431 hand axes and thousands of flakes were collected (Le Tensorer 1991).

In the same year, within the framework of the French Permanent Mission in El-Kowm, systematic excavation began at Umm el-Tlel (and, in 1996, at El Meirah) under the direction of E. Boëda and S. Muhesen.

In 1998, with the support of Basel University and the Directorate General of Antiquities and Museums of Syria, a research station in the area of El-Kowm was constructed. Thanks to private funds and the preparatory work of Reto Jagher, under the control of A. Taha, the construction was completed in the same year. From 1999 to the present, the team working in Nadaouyieh and Hummal have had a suitable location to continue their research in the region and to store the excavated material (Fig. 164).

Parallel to the construction of the Research Centre of Tell Arida, geophysical surveys started in Nadaouiyeh Ain Askar. These surveys, led by Pascal Turberg from the University of Neuchâtel, were aimed at future exploration of the other sites in the El-Kowm area. Despite promising results, these surveys were not continued (Turberg 1999).

2.4 The Investigation of Hummal

In 1997 J.-M. Le Tensorer and S. Muhesen decided to investigate Hummal, firstly to add to the results already obtained with the stratigraphic observation of the upper sequence (Layer VI and above) from 1982 to 1985, and secondly to identify the nature of the archaeological complex VI (Fig. 7). As a result, the 1997 field work in Hummal was limited to a simple cleaning of old, still-available profiles. A small sondage in Layer VI was started and Profile P.3 was raised. More than 500 flint artefacts were gathered, and sampling for analyses was undertaken. The differences in the stratigraphy from that outlined by F. Hours in 1981, which started at the base, meant that a decision was taken to describe the organisation of the archaeological layers, starting from the top of the sequence, by numbering the levels in Arabic numerals from 1 to infinity.

The new stratigraphy (from top to bottom) was constructed from Profile P.3 (Fig. 8). Only the archaeological layers received a number.

Layer 1: Holocene deposits, with fragments of ceramics and isolated flints documented.

Layer 2: a fine sub-horizontal continuous level rich in mollusc shells but poor in archaeological material, Epipaleolithic;

Layer 3: containing some blades, Epipaleolithic or Upper Paleolithic.

Layer 4: a fine, diffuse but continuous level containing rare artefacts (blades), Upper Paleolithic;

Layer 5: several thin levels (5a, 5b, etc.) presenting a dip in the direction of the centre of the well. These levels contained rare artefacts, including one beautiful typical Mousterian scraper, a Levallois flake and some blades and laminar flakes.

Layer 6: (former VIb), a rich, continuous layer a few cm thick. It presents a light depression towards the centre of the well. The numerous artefacts portray traces of weathering corresponding to a prolonged presence lying uncovered on the ground. Excavated on a small area during the rectification of Profile P.3 (8m long and only a few centimetres wide), this layer produced nearly 500 flint items. The laminar supports that predominated included thick, prismatic blades. This industry seemed to be a part of the Hummalian industry.

Layer 7 (old layer VIa): a thick level (up to 30cm) of black clays containing several sublevels; poor in archaeological material. 45 artefacts were gathered from an excavated surface of approximately half a square metre.

Layer 8: a diffuse level of yellowish clayey sediment, contained weathered bones and rare artefacts (16); one typical chopping-tool was also found;

Layer 9: black, clayey, corresponds to the former '*niveau tourbeux V*'.

To this point it was recognised that the previously documented Mousterian layers were not found in a primary stratigraphic position and that Layer VIb (the current Layer 6) corresponded to an *in situ* Hummalian assemblage positioned below the Mousterian complex.

In September 1997, a series of samples for pollen analysis were extracted from Profile P.3 at layers 5a, 5b, 6b, 7 and 8. Even though the sediment was uniformly sterile or very poor in pollen material, it was noted that the majority of recognised pollen taxa

belonged to steppe vegetation (Renault-Miskovsky, 1998). The level between Hummalian and Mousterian delivered the greatest number of grains (73), distributed between two pollen taxa that were particularly resistant: *Anthemideae* and *Cichoriae*.

Systematic excavations in Hummal began in 1999 under the direction of J.-M. Le Tensorer and S. Muhesen (Fig. 9). At the beginning, a major clean-up of ancient back dirt was undertaken: more than 100m³ of sediments were removed and 100m² of stratigraphical profiles of the long trenches on a North-South axis parallel to the northern irrigation collected from squares C/D contained two well-distinguished partitions:

- Layers of back dirt occupy the centre of the site and correspond to the historical works, with a last date of 1951.
 - These layers, often well stratified, contain a notable quantity of flint and bones coming from the Pleistocene levels which were crossed during digging.
 - Levels which collapsed in to the heart of the doline. These layers, annotated in Greek letters (αh and αm), result from random collapses, and because of this are usually difficult to place in the stratigraphical sequence. They primarily consist of sand containing abundant artefacts.
- Around these disturbed levels, the archaeological layers that remained in place were present. More than 20 archaeological layers from Upper Palaeolithic to the Acheulian were recognised and a few hundred artefacts were gathered.

This *in situ* sequence integrated the following:

Complex A: layers 1 to 4, including the Holocene sequence, the Epipalaeolithic and the Upper Palaeolithic.

Complex B: layers 5a to 5h, the Levallois-Mousterian.

Complex C: layers 6 to 9 and Sand αh. The Hummalian sequence contains layers 6a, 6b, 7 and αh (the former “upper sand IV” 1983). Layers 8 and 9 were almost sterile and at the moment it is difficult to precisely gauge their cultural relation.

- Layer 6a furnished 32 flints, often broken, and dozens of debris fragments.
- Layer 6b appears as a thin, continuous level, a few centimetres thick and filled with small pebbles, limestone gravels and artefacts. It was easily placed in the stratigraphy and thus was a precious level of reference for the rest of the sequence. During rectification and cleaning of Profile P. 7, a small surface (about a third of a square metre) of Layer 6b was excavated for the first time and 148 flint objects and hundreds of pieces of debris were gathered. From Profile P. 7 itself, 218 artefacts were collected. The lithic artefacts belong without doubt to the Hummalian, but they often present altered edges.
- Clayey layer 7, with a thickness varying from 0 to 40cm, delivered well-conserved bone and 37 flint items, the latter typically Hummalian.
- Sand αh was located in complete separation from the other layers. This sandy unit, several metres thick, occupied the centre of the doline between levels 8 and 21. Thus it is a later sediment and yet seems to have originated from the between layers 7 and 8. More than 600 collected artefacts confirmed its relationship to the Hummalian industry.

Complex D: Layers 10 to 21, Yabrudian and Old Palaeolithic sequences.

In 2000 the profile from the area D/E 29 to 31 had to be moved back in an attempt to clarify the stratigraphical position of Sand αh (the former “upper sand IV” of the stratigraphy from 1983). Excavation of the central zone of the site at Layer 13, including ‘Tayacian’, was undertaken.

2.5 Excavation of Hummalian complexes: 2000-2005 and 2009

- Between 2000 and 2004, Hélène Le Tensorer directed the excavation of Hummalian Sand αh, and more than 3000 lithic items and hundreds of faunal remains were gathered.
- From 2001 to 2005 the systematic excavation of the Hummalian upper sequence (layers 7 and 6) was undertaken under the direction of the author (Fig. 10, 11, 163). Up to 2005 the excavation area reached 39.5 m² and more

than 8000 lithic objects and 105 faunal remains were collected. The excavated area was bisected by a drainage channel and hence was divided into two distinct parts: West and East. The western part covered a surface of 18.4m² but only 10m² could be excavated, due to further disturbances caused by earlier channel digging. This problem also affected the eastern part, where of 21.1m² only 16 m² could be excavated.

- The lithic artefacts bigger than 2cm were measured three-dimensionally (x, y and z axes), and items equal to or smaller than 2cm were collected for each square, per 3cm thick units. The faunal remains bigger than 2cm or of a characteristic type (e.g. a tooth) were measured using the 3D system, and items smaller than 2cm were gathered employing the same method as for small lithic artefacts.
- Thanks to the cleaning that took place in 2000, it was possible to excavate the upper Hummalian on the squares M/N 34-37 in an area of about 4m². More than one thousand artefacts were collected in Layer 6b. Alongside this, another sample of Hummalian artefacts was recovered from unit α h, with more than 1200 artefacts collected from 1m². This assemblage delivered not only the typical Hummalian industry, but also rich faunal remains (Le Tensorer, 2003).
- In 2002, the excavation area of the upper Hummalian sequence continued not only in squares M/N (the East part), but also in area H/I 36-40 (the West part) and on squares C/D 31. Later it was recognised that the lithic material collected from squares C/D in Layer 6b was mixed with that from the Mousterian levels. Therefore this collection was excluded from further technological and typological study of the Hummalian industry. At the end of the season, Layer 7c and part of Layer 8 had been reached in both the eastern and western parts of the excavation.
- 2003 saw the continuation of excavations from 2002, with Layer 10 being reached in the West part and layer 8b in the East part of the excavation.
- A year later, the western part of the excavation was expanded northwards on the line of Profile P.34. Approximately 10m² were surveyed in squares

H/I 41-45. In the eastern part, new areas of 8m² southward in squares M/N 30-33 and to the north in M/N/O 37-39 were also excavated.

- In 2005 a large investigation was undertaken in the northeast part of the excavation in an area of 10m² at the upper edge of the well. The goal was to increase the excavation area and to follow the Mousterian layers to where there was contact with the Hummalian.
- The lower part of this survey – about 3m², including Hummalian layers 6a to 7c – was excavated. Parallel to this, investigation of the squares M/N 30-33 was continued, with hundreds of artefacts collected.
- In 2009, under the direction of J.-M. and H. Le Tensorer, the new Sondage S1 was opened in the southern part of the site and layers 6A, 6B and 7A, as well as 7B, 7C and 7D, were excavated on a surface of about 2m². The stratigraphical position of Hummalian between the Yabrudian and Mousterian was yet again confirmed.

3. Presentation of the area

3.1 The site and its surroundings

The El-Kowm oasis is located 450m above sea level in the Syrian steppe between Rasafa, Palmyra, and Deir ez Zor. The region took its name from the remarkable 20m-high hill called Tell El-Kowm that looms over the surrounding area. The region is a 20km depression inside the mountainous chains which extend across Syria from the Anti-Lebanon Mountains in the west to the Euphrates River in the east and separates the northern fertile zones from the Arabian Desert in the south. The southern limit of the El-Kowm area is covered by the northern Palmyrides (Jebel Minshar and Jebel Mqabra), with its core of Upper Cretaceous limestone. In the north emerges the Jabal Bishri with an altitude of more than 850m, whose upper layers date to the Lower Eocene. In the past, the open landscape between the mountain ranges offered an ideal path for passing herds, as can be confirmed by the still well-worn path in the desert and abundant ambush sites exploited for hunting gazelles. The area is characterised by the presence of many artesian springs related to faults in the substratum and by high-

quality Lower Eocene flint outcrops. The springs in the El-Kowm area attracted humans to return to the same places over long periods, accumulating cultural remains of occupations as they did so. 20% of the sites known in the area of El-Kowm are spring sites showing excellent preservation for Palaeolithic open-air sites. This is due to the rapid build-up of fine sediments. Other regional sites are mainly surface scatters of flint tools and provide little information on the settlement structure. The action of springs combined with wind action and human activity frequently caused the formation of a hillock around the spring. The current inhabitants of El-Kowm often dig new wells on these raised points, which helped to identify several archaeological sites of thick stratigraphy, such as Hummal, Nadaouiyeh Ain Askar, Umm el-Tlel, and Juval A (Besançons *et al.* 1982). Currently 220 Palaeolithic sites have been found in the region of El-Kowm. Three major kinds of sites are recognised: flint knapping workshops related to natural outcrops of flint; open-air settlements in the hills or on the slopes of valleys; and sites related to the waterholes, which may conserve thick stratigraphies (Le Tensorer *et al.* 2001).

3.2 Climate and hydrology

Palaeoclimatic information on the Pleistocene is still lacking for interior areas like El-Kowm. The data from central Mediterranean lacustrine and marine sequences indicate important climate oscillations causing the formation of submarine sapropel for the period of higher rainfall (Kroon *et al.*, 1998, Aritztegui *et al.* 2000).

Twelve humid periods have been recognised from marine cores during the last 500,000 years. The deviation of precipitation and of temperature is also indicated by an isotopic record from cave deposits (speleothems) (Bar-Matthews *et al.*, 2000; Bar-Matthews *et al.*, 2003; A. Almogi-Labin *et al.* 2004) from the Mediterranean coastal region.

The climate of the Levant and northeastern Africa is influenced by the Atlantic/Mediterranean frontal system and the African/west Asian monsoonal systems, which interact. The recorded data show that during warm interglacial periods when the Mediterranean frontal and monsoonal systems became more powerful and almost

overlapped, the area became particularly humid and wet. For the period of glacial maxima, the whole area turns out to have been cool and dry. In between these extremes, either the dry and warm interglacial phase or the cool and humid glacial intervals of local extent occurred (A. Almogi-Labin, M. Bar-Matthews and A. Aylon 2004).

It is unknown how strongly the paleoclimate in the area of El-Kowm was influenced by those climatic fluctuations, but it seems that the fresher temperatures and increased precipitation slowed evaporation and led to a thicker vegetation cover, and possibly had an effect on the karsts system. Geological evaluation of the region (Pümpin and Jagher 2004) and geophysical investigation of Nadaouiyeh Ain Askar (Turberg, 1999) have exposed the existence of a significant faulting of the bedrock, which suggests that the regional tectonic system may control the appearance of artesian springs in this small area.

Today, the Syrian steppe is characterised by a Mediterranean climate, with two main seasons: rainy and dry. The former lasts from October to April, with the maximum rainfall occurring in December, January and February. The dry period is long, very hot, and severe (Sanlaville 2000). It has been noted that Palmyra may have around 150 to 186 consecutive days without rainfall, and that such rainfall as it did have was concentrated, occurring on only a few days between mid-October and late May (Besançon *et al.* 1982). The annual rainfall is irregular and unpredictable, with precipitation in this area varying strongly from one year to another. It can be less than 100mm or relatively high, at more than 300mm. Alongside the irregular rainfall, the increased evaporation caused by the sun, the extreme dryness of the air and the effect of almost endless wind must also be taken into consideration. In addition, the soils of this arid zone are thin and do not readily hold water. Most of the water that appears during the rainfall is drained off by the wadis to the southeast and then disappears into the alluvial plain of Qsar al Hair or salt pans (*sebkhas*). Drinkable water is only available in the wadis for a few days after heavy rain. This shows the importance that the numerous natural springs had in enabling permanent settlement in the arid steppe. The majority of the recognised natural springs in El-Kowm were epithermal artesian

wells, highly saturated with mineral salts, with the water flowing out at temperatures around 27-28°C (Margueron 1998). Many of them were semi-permanent and must have flowed for a very long period. Nowadays, the water reserves are highly exploited for irrigation. The water table has fallen from subsurface to a depth between 40 and 75 metres, and all the natural springs have dried out.

3.3 Paleoecology

The paleoecological data for the Paleolithic in the El-Kowm area are relatively meagre and come essentially from three sites: Hummal, Nadaouiyeh Ain Askar and Umm el-Tlel. The record from the geoarcheological (Le Tensorer *et al.* 2007), paleobotanical (Emery-Barbiès 2005:74-91; Renault-Miskovsky 1998:26) and paleontological analysis of animal bones (Griggo 2005, Reynaud-Savioz and Morel 2005) indicates a dry climate with steppe vegetation during the Lower and Upper Pleistocene. The humidity and pedological conditions were unfavourable for woodland cover, but a few short periods with increasing precipitation were noted. The soil formation in Hummal shows indications of dry periods without water cover, as evidenced by the presence of calcified root cells of plants containing calcium carbonate, the accumulation of aeolian sands, traces of iron oxides, mud cracks and layers of debris (Le Tensorer *et al.* 2007, Ismail-Meyer 2009).

The fauna recognised in El-Kowm are unusual for the Middle East. The most abundant were the dromedary (*Camelus dromedarius*); equids, including zebra (*Equus quagga*), the ass (*Equus assinus*), and onager (the Asiatic wild ass, *Equus hemionus*); and gazelle (*Gazella subgutturosa*). Some sites indicate the presence of aurochs (*Bos primigenius*), the steppe rhinoceros (*Dicerorhinus hemitoechus*), oryx (*Oryx leucoryx*) and ostriches (*Struthio camelus*). The different fauna associations reflect significant climate fluctuations from arid to semi-arid conditions. Dromedary, oryx, gazelle, ass, onager and ostrich represent a dry steppe; zebra, aurochs and steppe rhinoceros are related to a wooded steppe. Remarkably, in the Acheulian site of El-Meirah, two fragments of canines from hippopotami (*Hippotamus amphibius*) were found (Boëda *et al.* 2004). The occurrence of this large mammal may suggest a much more humid

climate with lush plant life available, but this interesting find still needs to be evaluated.

From the earliest periods, humans exploited the different species of animals – the big game like camels, equids and antelopes, but also gazelles, ostrich (Bonilauri *at al.* 2007) and small birds and rodents (Reynaud 2011, Frosdick 2010). The presence of carnivores like hyenas (*Crocuta crocuta*) and lions (*Panthera leo*) adds weight to the probability that significant numbers of grazing animals existed at certain points.

It seems that the hunting of big mammals such as aurochs or the rhinoceros was random and sporadic, as it is reflected in only a small number of remains. It could be also possible that the remnants of those large animals were the results of scavenging.

The significant numbers of tortoise carapaces (Reynaud 2011) and ostrich shells (Frosdick 2010) seems to indicate gathering activities throughout the Paleolithic.

3.4 Geological aspect of Hummal

The artesian spring site of Hummal, also called Bir Onusi, is a prominent mound of sediments which built up during the Quaternary. Tectonic faults in the bedrock enabled the underlying water in a karstic system to flow out into a doline which trapped lacustrine, limnic and aeolian sediments from the Early Pleistocene onwards. The site is in direct contact with the old artesian spring, which was active for more than 780,000 years (the geological sequence investigated paleomagnetically by J.J. Villalain indicates the horizon of Brunhes-Matuyama for the Lower Palaeolithic) until the early 1980s (oral communication J.M. Le Tensorer). It supplied water to a pool of variable size. The water level varied according to the periods (wet and arid) and played a big role in the sediment formation of the site and the conservation of its archaeological levels. The majority of the sediment contains micritic loam directly precipitated from the water. The sediment built up not only during times of high water levels, but also while water levels were decreasing, when the depression of the dried pool and the remaining plant cover around it caught loose wind-driven sand, creating considerable accumulations of aeolian sand that was later displaced into the centre of

the water (Le Tensorer *et al.* 2007). It seems that from the Holocene on, the spring was much less active than previously, and that due to the deflation, aeolian deposits of silt and gypsum sand covered the previous Pleistocene delineation of the site (Pümpin and Jagher 2004).

From the Lower to the Upper Palaeolithic, the water, animals and raw material attracted humans to settle continuously in the immediate vicinity of the source, as attested by an archaeological record that is more than twenty metres deep.

3.5 Raw material and procurement strategies in Hummal

Two main geological flint types have been identified in the El-Kowm area. In the south appears an Upper Cretaceous (campanian) flint type that can be recognised in the Cretaceous formation of the Palmyrides range (the north side of the Jebel Mqabra). In the north, a Paleocene and Lower Eocene flint type is documented in the Paleogene formation of Jebel Bishri (Fig. 12). These two horizons of flint were formed on the same open marine carbonate shelf and have a parallel geological genesis (Julig *et al.* 2006, Julig and Long 2001). Except in the eastern part, the deposits of the Paleogene are rich in high-quality flint and emerge around the El-Kowm area at a maximum distance of 15km from the identified prehistoric sites. Microfossil analyses indicate two types of supply to the Paleogene: flint nodules that were in a primary deposit, and flint nodules weathered and transferred onto lower terraces by the wadis. This type of flint is very fine-grained and excellent for knapping. Its colour varies from black to light brown, with a white or sometimes red cortex. The nodule size fluctuates from a few centimetres up to tens of centimetres, and the flint is highly heterogeneous, forming both nodules and plates.

The Cretaceous flint deposits appear in the form of bands, lenses and nodules, which can be exposed by erosion in the parent rock. The bands of reddish-grey coloured flint, without cortex, are usually tectonically deformed, veined, by numerous breaks. They are of low quality for knapping tools. They are positioned within 10-15 km of the prehistoric sites.

It appears that both sources of flint were easily available, but the humans preferred the high-quality Lower Eocene flint for tool making. This type of flint seems to have been exploited consistently throughout the Paleolithic.

The survey of the primary flint outcrops of the region and their surroundings demonstrates that all varieties of nodule types and colours occur in all major outcrops. The mineralogical and microfossils composition of Eocene flint is very similar between the outcrops and thus it is not possible to define the local groups of diverse flint and set any precise place where the prehistoric people collected their raw material. As a consequence, it is difficult to prove a possible provisioning strategy in the region (Diethelm 1990, Julig and Long 2001).

The other possible material for tool making is limestone, which can be found with Eocene flint outcrops. It can be well silicified and its rather big blocks are appropriate for knapping.

The origin of the limestone used in Hummal is unknown, although one possible source is the alluvial deposits uncovered from some wells in the area of Hummal.

The raw material used in Hummal is mainly local Lower Eocene flint, which occurs in the alluvial deposits. The rest is Cretaceous flint and limestone. Campanian flint was rarely employed, but there are a few examples of it being used from the Lower to the Middle Paleolithic. Interestingly, this type of flint was preferentially employed in the oldest horizon in Hummal (layers 16-18) for chopper and chopping tools production, and Paleogene flint was used for debitage (cores and flakes). The majority of the Cretaceous raw material was collected in secondary positions, as shown by the weathered cortex and neocortex covering artifacts (Wegmüller 2008). The small quantity of artifacts made of limestone appears in Middle Paleolithic contexts (Hauck 2010, Wojtczak 2011); however, it was the most frequently used raw material in chopper and chopping tool production in the Lower Paleolithic horizon (Wegmüller 2008).

3.6 Date estimations of the Hummalian occupations

The first chronometric age estimation for the Hummalian was made using thermoluminescence (TL) on heated flints from Layer 6b, situated between the Yabrudian and Mousterian occupation (see Profile P.3 in Fig. 8). The context age of 104 ± 9 ka (Ancient TL date list, 1988) of the three heated flint samples from this layer seems to underestimate the age (for more details, see Richter *et al.* 2011) and therefore has to be regarded as a minimum age.

The next attempts to estimate the Hummalian's age were carried out by Daniel Richter from the Max Planck Institute for Evolutionary Anthropology, also using the thermoluminescence method on heated flint. Richter analysed several heated specimens from layers 6b and αh (Tab.1) (Richter 2006, Richter *et al.* 2011). The results gathered from samples of Layer 6b displayed large inconsistencies in model ages and indicated that the employed dose rate models were not suitable for all samples from this layer. The estimated dates probably overestimate the actual age. On the other hand, if using a similar external γ -dose rate model from the results for the sediment of the Hummalian layer αh , comparable results would be obtained. Looking at the stratigraphical situation, it is supposed that the deposition of the artefacts from Layer 6b took place later than those in αh (Richter *et al.* 2010).

The estimated TL age for sandy Layer αh is of approximately 200 ka (minimum model 190 ± 35 ka and maximum model 210 ± 40 ka) and seems to compare favourably with age estimations for similar Early Middle Palaeolithic blade industries. One such example is the Hayonim layer 'F top' and 'F base', with mean TL dates on heated flint of 210 ± 28 ka and 221 ± 21 ka, respectively (Mercier *et al.*, 2007). Another example is Tabun unit IX (Tabun D-type), where the same method yields 256 ± 26 ka (Mercier and Valladas 2003), with compatible Early Uptake ESR dates on animal teeth (Grün and Stringer 2000). This similarity in TL ages indirectly confirms the hypothesis that the time interval between the original deposit and re-deposition of the artefacts in ' αh ' was relatively short.

3.7 The stratigraphical sequences

The stratigraphy of Hummal is composed of micritic loam precipitated directly in the water supplied by the well. The surface water level fluctuated in accordance with climatic changes and tectonic processes. Soil formation took place during times of reduced water levels (Le Tensorer *at al.* 2007).

The sequence also contains a massive sand deposit of several metres in the heart of the doline (Fig. 13). These ‘ah’ sands contain a vast quantity of lithic and faunal artefacts. Archaeologically, these artefacts are not *in situ*; however, the geological observations made on the ground show that it intercalates between the Yabrudian Layer 8 and Hummalian Layer 7 (Le Tensorer 2004: 229) and that geologically it is perfectly *in situ* – that is, it does not present any mixing with other layers.

The stratigraphical sequences were recorded in the East, West and South sectors. In the main they are similar, but there are also some differences. The levels with a blade component were always found between the Levallois-Mousterian Complex 5 and Yabrudian complexes 7d and 8. Complex 6c appears only in the eastern zone. The stratigraphical description and interpretations presented here result from micromorphological studies and on-site field work observations. The geological studies are still on going and will in the near future allow a fuller and, it is hoped, a clearer picture of the sedimentological formation of layers.

3.7.1 The western and eastern sequences (Fig. 14, 15 and 16.)

Layer 6a

This layer consists of Carbonatic silt sediment with an average thickness of 15cm. It eroded part of Layer 6b. On Profile 33, it is not distinguishable from Layer 5h. The depositional context of this layer is as yet undetermined. It is possible that the archaeological remnants were redeposited within a repeated debris flow, but it is just as likely that humans arrived on the site after the accumulation of debris and settled on colluviated material. In the South sector, this layer is subdivided into three sub-levels: 6A1a, 6A2, 6A3.

Layer 6b

This layer consists of a thin detritic carbonatic deposit with a maximum thickness of 14cm. The layer seems to have formed over a long period of varying water levels, so intermittently the surface was relatively dry, and it was during these dry phases that the soil formation took place. The surface of the layer during the deposition of the artefacts was relatively dry and seems to be well conserved, as suggested by the presence of small bone fragments and a carnivore coprolite observed in the micromorphological analysis (Rentzel 2011, Ismail-Meyer n.d). It seems that the artefacts in this layer lay uncovered on the surface for a long time and formed a thick layer of flints without clear intermediate sub-levels. One small zone of approximately 4m² represents the physical deformation and erosion of Layer 7c (western sequence).

Layer 6c

A change to damper conditions led to the precipitation of Layer 6c. Its compact, carbonate silt, of approximately 30cm thickness, partially eroded by the deposition of Layer 6b, is currently limited to one surface on the eastern profile. The partial erosion of Layer 6c happened before the formation of the following layer, 6b. Minute remains of Layer 6c were perceptible throughout the East profile, but were not identified on the West and South part of the excavation. The soil formation is indicated by the presence of mud cracks and calcified root remains. It is subdivided into two sub-levels: 6c1 and 6c2.

Layer 6c-1 is compact, white carbonate loam. It is nearly sterile. Only a few lithic items were collected in the upper part of this layer, which was in contact with Layer 6b above it. The upper part of Layer 6c-1 could possibly be part of Layer 6b, as they also present the same patination.

Layer 6c-2 consists of brown-grey carbonatic silt. The lithic material and a number of small bones (including a felid bone), three fragments of ostrich shell and also equid teeth, were collected from an area of two square metres.

Layer 7

Situated on Yabrudian Layer 8, this layer is a complex series of clay mineral deposits and erosions of thickness varying from five to 40cm. It was established in a swampy environment in a hot climate and is intersected throughout with red sand (Layer 7b). Layer 7 is divided into four sub-levels (a, b, c, d).

Layer 7a: a greenish clay containing a small number of lithic and faunal artefacts;

Layer 7b: a reddish, sterile sand which sometimes forms accumulations up to 20cm thick (Fig. 162);

Layer 7c: a black clay containing organic levels, which developed due to a change in the deposition conditions. The occurrence of a calcified horizon composed of calcified and silicified roots; fragments of carnivore coprolites; many bones, some of which are burnt; and lithic artefacts, indicate soil formation without water coverage. However, the presence of algae spores and gastropod shells testify to the existence of water in close proximity. After a change to *sebkha* conditions interrupted soil formation, the green-black clay started to accumulate and formed Level 7a. It is the richest of sublevels in terms of artefacts.

Layer 7d: up to 20cm thick with carbonatic silt, rich in greenish clay, this layer appeared on a limited surface. It was rich in bones. A few broken lithic items and dozens of items of debris were also found.

3.7.2 The southern sequence (Fig. 17)

Layer 6AI

This layer is a succession of levels of carbonatic silt crossed with small lenses of sand and loam. It has a thickness of 15-20cm and encompasses three different levels: 6AIa, 6AIb, 6AIc. The first is in contact with the Mousterian layer 5FVII. The layer is poor in lithic and faunal artefacts. Rapid sedimentation took place at a time when the water level was low and the water was clean and still.

Layer 6A2

Detritic carbonatic silt with intercalations of sand accumulations. It has a thickness of about ten centimetres. The presence of fragments of molluscs and other biomineralisation phenomena were also observed. The layer is rich in artefacts and faunal remains. The lithic artefacts collected from this horizon, unlike those gathered from the West and East sectors, were fresh and unbroken.

Aeolian processes appear to have played an important role in the sedimentation, as the layer was established at a time of low water levels or perhaps even an absence of water.

Layer 6AIII

Carbonatic silt 20cm thick comprises three sub-levels: 6AIIIa, 6AIIIb, 6AIIIc. The layer is sterile and was established under middle or high water levels in contact with the air. The water formed a shallow lake.

Layer 6B

Detritic carbonatic silt of two to five centimetres in thickness. The occurrence of fragments of molluscs and others biomineralisations (*Characeae* stems) was also observed. The layer is rich in lithic and faunal remains, and seems to have formed during a period without water coverage; the action of erosion is also highly visible. Through this period, the site could have been continuously occupied. However, if there were multiple occupations, there would also have been brief interludes.

Layer 7

This is a complex series of clay mineral deposits and erosions intersected throughout with red sand (Layer 7b). It has a variable thickness up to 90cm. It lies on Yabrudian Layer 8. It seems to have been formed under the low and very low water levels in contact with the air. Short sedimentation phases were noted. Layer 7 is divided into four sub-levels (A, B, C, D), as in the East and West sectors. The levels are not very rich in artefacts. Remarkably, in Layer 7D typical Yabrudian scrapers were discovered

in 2010. This discovery indicated that this level was part of the Yabrudian complex and not Hummalian, as had been supposed previously, the lithic material found earlier in other sectors not being distinctive.

4. Archaeological Samples and their taphonomy

4.1 Introduction

In 2002 R. Jagher undertook a topographical investigation of the surrounding area of Hummal. Thanks to this study, the current topographic models include the Hummal site, an area immediately adjacent to the site, and the principal adjoining topographic formations within a limited locality. It also became possible to better describe the position of the archaeological levels, which are covered by several metres of deposit, and to appreciate the dimensions and the real extent of the site. It is estimated that the Mousterian occupation may possibly have covered a surface area of about 2.5 hectares, the Hummalian and Yabrudian about 10 hectares, and the Lower Palaeolithic about 30 hectares (Fig. 19) (Jagher 2003/04). There were repeated occupations of the site during the Hummalian, but the density of the artefacts in the layers remains variable (Tab. 4). This may be owing to the fact that the excavated area is limited, but differing occupation strategies must also be considered as a possible factor. The assemblage from an individual layer represents a temporal sample, the duration of which is very difficult if not impossible to calculate. The time interval between the deposition of the first and last items in the lithic assemblages is seldom precise and rarely defines a single phase of occupation.

The high concentration of items in layers 6b and 6a could be related to successive occupation episodes without clear intermediate layers, or it could be due to palimpsest. In the case of layers 7a, 7c and 6c, the lower density of artefacts may well correspond to short-term occupation, during which blanks were at least partially produced and maintained on-site.

4.2 State of preservation

Taphonomic factors such as erosion, diagenesis and trampling, alongside the probable lack of sedimentation, had a destructive effect on a significant number of the archaeological remains. This makes some of the archaeological and archaeozoological analysis problematic. The faunal remains are very poorly preserved and it is difficult to draw conclusions because the samples are small. Post-depositional forces were the major influence on the destruction of the bones. High proportions of shaft fragments and teeth attest to this (Frosdick 2009).

As the Nadaouiyeh Ain Askar and Hummal sequences demonstrate, three main types of weathering usually occur in semi-arid milieus: physical, chemical and biogenic (Pümpin 2003).

Mechanical weathering consists of the failure of rocks and soils through direct interaction with atmospheric conditions, such as heat, water, ice and pressure (<http://facstaff.gpc.edu>). It is usually related to dry environments where strong heating leads to strong evaporation and thus to salt crystallisation. In Hummal, possible cryoturbation phenomena were identified at the sediment Complex V1 in the western Mousterian sequence (Hauck 2010: 48). However, this phenomenon was not observed in any of the Hummalian sectors.

Chemical weathering is the direct result of atmospheric chemicals interacting with rocks, soils and minerals to cause degradation and breakdown. It changes the structure of rocks, frequently transforming them by the interaction of water with minerals to cause various chemical reactions. The diagenetic processes in the sediments can lead to a solution phenomenon and the growth of authigenic quartz crystals and a secondary deposition of SiO₂ around mineral grains (Le Tensorer *et al.* 2007: 634). The accretion of secondary silica was recognised in the massive quartzitic sand deposits discovered at the bottom of the wells *ah* and *am*, where the numerous artefacts show a glossy patina.

Another example of such weathering is the dissolution of dolomite minerals within heavily corroded flint, which was primarily recognised in Nadaouiyeh (Pümpin

2003:75-76). Pieces displaying this kind of corrosion were also discovered in the Mousterian context (Hauck 2010: 49), but they are extremely rare – just two examples were found within the Hummalian sequence.

Biogenic weathering is often due to paedogenesis and animal activity. Bioturbation refers to the irregular disturbance of sediment by plants and animals that can come into contact with sediment. Burrowing by rodents was identified in the Holocene deposit of Hummal. The bioturbation caused by plant roots was identified all over the Mousterian sequence and in the upper part of the Hummalian.

4.2.1 Layers 6a and 6b

The state of preservation of the artefacts from layers 6a and 6b indicates that the taphonomic alteration of these layers was important, and also explains the small number of preserved bones, the majority of which are teeth. The majority of artefacts from layers 6a and 6b are broken. At the same time, nearly all the objects were found in a sub-horizontal position in accordance with the layer inclination. The white-grey patination of the lithic objects in both layers is homogenous. Some animal bones and two fragments of ostrich shell were also collected (Fig. 20, 21, 22, 23).

In Layer 6a, 90% of blades are broken and several artefacts show signs of edge damage. The lithic collection of Layer 6b as a whole is characterised by the same state of alteration. Its patina is rather strong, homogeneous and of a white-grey colour. 65% of blades and 3% of flakes have undergone mechanical breakage. 18% of all artefacts show crushing or a series of pseudo-retouch removals (Fig. 24). These three phenomena – erosion, mechanical breakage and crushing – are related to the post-depositional conditions of preservation within the assemblage. The presence of the broken blanks observed at the time of the excavation, the fragments of which were easily refitted, also suggests mechanical disturbances to the artefacts. In the same way, some refitting of the broken elements made on 4m² of the excavation testifies to a displacement of less than 1m, and thus an *in situ* breakage, probably mechanical in nature. However, time constraints meant that a systematic refitting of all broken artefacts was not possible.

The bad preservation of the artefacts could be due to the effect of long-term exposure on the surface (erosion and diagenesis) in addition to their being trampled. Several experiments (Behrensmayer *et al.* 1986; Mcbrearty *et al.* 1998; Thiébaud 2007; Villa and Courtin 1983) have shown that trampling can cause severe damage to artefacts. It can cause breakage, crushing, pseudo-retouch and vertical and horizontal displacement. In the case of the artefacts from layers 6a and 6b, breakage, crushing and pseudo-retouch are evident. Cryoturbation could cause similar damage, but this process has never been identified within the Hummalian sequences. The occurrence of a high degree of fragmentation in the faunal remains also lends weight to the trampling hypothesis (Frosdick, n.d).

Layer 6b appears identical in all the sectors excavated and is easy to locate due to the regular presence of pebbles and blocks of limestone and travertine. These blocks although eroded were certainly brought into the site by hominids, as the type (limestone) and size of rock are not found naturally at this location. The blocks form something of an imitation manuport living floor (Fig. 25). It is difficult to reveal whether the assemblages from layers 6a and 6b are a result of a single or successive human occupations, but the lithic material seems to represent a single technological tradition.

4.2.2 Layers 6c1 and 6c2

Layer 6c1 contains only a few lithic pieces that present an identical patination to that visible in Layer 6b.

In Layer 6c2 nearly all the artefacts were found in a sub-horizontal position, which is in accordance with the inclination of the layer. 20% of the lithic items present a grey patina. All are well preserved; their sharp edges remain and thus seem to have been covered by sediment soon after deposition (Fig. 26).

4.2.3 Layers 7a and 7c

The lithic artefacts from layers 7a and 7c are well preserved. Nearly all were found in a sub-horizontal position in accordance with the inclination of layer (Figs. 27, 28 and

21). They do not show any edge damage, but at the same time a number of blades are fragmented. Several pieces demonstrate an orange patination, probably originating from the iron oxide deposits. Additionally, in Level 7c a small debitage workshop was also discovered (Fig. 29). All uncovered pieces were collected within numerous Kombewa flakes. They are slightly patinated, but still present sharp edges. It was possible to make a major refitting which showed that the flint knapper had been flaking a core on flake with Nahr Ibrahim preparation there. It confirms also that the surface on which the flint knapper was working was quickly covered; we can thus speak of an *in situ* situation.

In Layer 7c, the majority of faunal material came from the western part and unfortunately is highly fragmented. As a result, the number of identified fragments is low. Among the identified fauna are camelids (which predominate), equids and a few large bovids. The surface preservation and edge sharpness of bones suggest that the burial probably took place relatively rapidly and that post-depositional forces were responsible for the destruction of the bones. It is possible that this organic layer became highly compressed over time owing to sediment overload. This would account for the high degree of bone fragmentation and also the fragmentation of several blades.

4.2.4 Layers 6A and 6B

The lithic material from Layer 6A was well preserved, with fresh edges, although covered by a grey-white patina. The artifacts from Layer 6B present the same grey patina and edge damage as those from Layer 6b, uncovered in the western and eastern sectors.

4.2.5 Sand ah

The lithic artifacts from sandy Layer ah are well preserved. Some are broken but they do not present any edge crushing. 40% of them present blunt edges, while the edges of the rest are fresh and sharp. Some of them are covered by a faint white veil and 40% by secondary glossy silica, making them look like they have been varnished or glazed (Fig. 30).

Similar glossy flints have been noted on several spring mound sites in North Africa and the Levant and have been the subject of a number of studies. Masson (1982), who reported a similar phenomenon in other complexes from El-Kowm, describes it as a patina formed through either wind or water action. However, Meeks (Meeks *et al.* 1982) and Shackley (1988) contradict these results and argue that such a glaze is a true chemical deposit associated with exceptional circumstances existing in artesian spring mounds.

Similar conclusions were reached by Jagher (1990) in his examination of the glossy flint from Hummal. It was proposed that the agent causing the chemical destruction of the surface was warm, strongly sulphated groundwater. It was also put forward that the transition between patina and fresh break shows clearly that the gloss does not consist of a mineral base but most likely was generated by an erosion of the surface and then mechanical formation.

4.3 Burnt flints

The Hummalian layers contained about 200 burnt flints. The majority of these were collected from Layer 6b. There, the overheated flints were found in three main concentrations, around which other flints, burnt and unburnt, were distributed. Natural fires appeared frequently (Alperson-Afil *et al.*, 2007). But because the heat infiltration of natural fire into sediment seems to be low (Bellomo, 1993), the lithic material covered by sediment could not have been heated to a degree that would permit TL dating (Richter 2007). Taking into consideration the geomorphological position of Hummal and the fact that only some of the flints show traces of heating, the fire seems more likely to have been a result of human activity than a natural agent. Some archaeological and experimental evidence (Sergent *et al.* 2006) shows that severely overheated flints are the best marker of non-structured surface hearths. In addition, the micromorphological analysis shows the presence of charcoal in layers 6a and 6b (2001 Meyer, n.d.). This could point to the existence of hearths, which might easily have been destroyed by intensive trampling.

4.4 Quantification of layers 6a and 6b

4.4.1 Introduction

The high fragmentation of artefacts due to the post-depositional taphonomy of the collections from layers 6a and 6b makes them difficult to quantify. In both cases, blades were the worst affected by fracturing; they seem to have broken consistently into two or more pieces. Using simple counts as a measure of relative abundance overlooks the fact that the sum total is significantly influenced by this degree and pattern of fragmentation.

Lithic assemblages frequently exhibit a variable rate of breakage, and the problem of accounting for these fragments seems to be unresolved. Different researchers produce different fragment counts, and different accounts of their size and nature. Comparison between assemblages is often extremely difficult.

When the specimens retain their platforms, their original size can be estimated following the method advocated by Dibble and Pelcin (1995; Dibble 1998, Pelcin 1996, 1998). But then, additional studies have questioned this method, arguing that it is still not an accurate original flake mass predictor (Davis and Shea 1998, Shott *et al.* 2000). Further studies are needed.

Attempts to adopt the method of Dibble and Pelcin (1995) have encountered two fundamental problems which show that the method is not adapted for all lithic items.

The measuring of the exterior platform angle (EPA) seems in theory to be non-problematic, but in practice this is not the case. The theoretical EPA is formed by the intersection of two projected lines: one normal from the platform and another normal or tangential line from the exterior surface (Dibble and Pelcin 1995, Fig.1). If the specimen has an irregular and arched surface, the question arises of which point the tangent should be drawn from – which raises the subsequent questions of which platform angle and which platform thickness is being measured. Each point gives a different EPA result, and *ergo* a different platform thickness and final mass, so which one is valid? Should the mean of them all be considered?

One more unresolved problem needs to be mentioned: how to calculate the mass for items whose EPA equals or exceeds 90° and whose tangent is negative? These obstacles would have had to be resolved before employing the method of Dibble and Pelcin (1995). Thus, it was decided to not work with this method, as it was not appropriate for specimens treated in this study. The EPA of most specimens treated here was equal to or surpassed 90°, and their tangent was negative.

Shott (2000) showed that some possibilities exist for evaluating the quantification problem, even if there are still many unresolved problems with the calculations of fragments: “otherwise, differences may owe as much to how we count as to what” (Shott 2000:737). For an estimation of the number of specimens in Hummalian assemblages, the quantification of blades using three formulas proposed by Shott (2000 and references therein) were applied to assemblages from layers 6a and 6b.

1. Tool information equivalent (TIE) by means of estimated tool equivalent (ETE) (Baxter and Cool 1996: 92). The method was used originally for pottery quantification.

Methodology:

ETE equals 100 for intact specimens which possess three elements (proximal, mesial and distal); fragments possessing one element are thus ETE=33, and those with two elements ETE=66.

ETEn: ETE multiplied by the number of items

ETE²: ETE squared

ETE²n: ETE² multiplied by the number of items

$TIE = ((n-1)/n) * (\sum ETE * n^2 / \sum ETE^2)$

2. Minimum number of intact tool (MNIT) is calculated by summing the number of entire items with proximal, medial and distal fragments; the most numerous is then considered the MNIT (Portnoy 1987). In cases where an item retains two elements, for example distal-medial or proximal-medial, the most frequent element is counted.
3. Estimated tool equivalent using Tool Length Value (TLV):

- TLV 1 discarded: the total length of intact tools added to the total length of fragments that are greater than 2cm and divided by the mean length of the intact tool at discard. This value approximates the minimum number of discarded tools.
- TLV 2 maximum: total length of intact tools added to the total length of fragments that are greater than 2cm and divided by the minimum length of intact specimens at discard. This value estimates the maximum number of discarded items.

To quantify the number of blades in both Hummalian layers, all fragments bigger than 2cm were used when morphology (narrow, thick cross-section) assigns them to the blade category.

The blades group includes both blade-blanks and core trimming blades. The quantification of different groups of retouched blades was made separately, as was that for bladelets, which come at least partly from a reduction strategy distinct from that of blades.

4.4.2 Layer 6b

4.4.2.1 Blades (Tab. 5)

Blades seem to break into five portions: proximal, proximal-medial, medial, distal-medial and distal parts.

A calculation using the three above-mentioned formulae gives the following results:

| | |
|-------------------------|------|
| TIE | 2492 |
| MNIT | 2043 |
| TLV 1 discarded | 1819 |
| TLV 2 maximum | 3148 |
| Actual Total items (n.) | 3082 |

The TLV 2 surpasses the number of the recovered items, since the minimum length is just 4cm but the mean length of the intact blades is 6.7 and seems to be exaggerated. The length of intact specimens (TLV1) estimates the minimum number of discarded tools and is significantly smaller than MNIT and TIE. This value is underestimated because a large proportion of the measured fragments only slightly exceed 2cm. This results in the items having a small total length, even while the mean length of intact specimens is quite high (6.7cm).

Some blades probably broke into four portions, because the number of medial fragments is very high – more than twice the number of proximal fragments. In this case, the MNIT would be strongly influenced by the aggregation effect (Grayson 1984:29) and probably overestimated.

However, if the blade blanks and core trimming blades (CT) are counted separately, the results change as follows (Tab. 6 and Tab. 7):

| | Blade blanks | CT Blades |
|-------------------------|--------------|-----------|
| TIE | 2263 | 292 |
| MNIT | 1770 | 278 |
| TLV 1 discarded | 1411 | 316 |
| TLV 2 maximum | 2681 | 649 |
| Actual Total items (n.) | 2739 | 348 |

Adding the number of blade blanks and CT blades for TVL 1 now equals 1727. Compared to the previously combined count of 1819, this result is slightly smaller, but this is probably not significant. It must be remembered that the results are approximate.

4.4.2.2 Bladelets (Tab. 8)

Uncovered bladelets retain the proximal-medial, medial or distal-medial part.

| | |
|-------------------------|-------|
| TIE | 122.2 |
| MNIT | 99 |
| TLV 1 discarded | 120.6 |
| TLV 2 maximum | 178.3 |
| Actual Total items (n.) | 153 |

TLV 2 is greater than the total number of items, suggesting that a proportion of bladelets exceed the minimum length of 2.6cm. Quantification of TVL1 is problematic due to there being just 14 intact items. However, the measure of negatives left by the bladelet removal from core burins shows a mean length of 2.6cm, exactly that of the measurements of the intact bladelets. This suggests that the TVL1 is not exaggerated by the small sample of intact items.

4.4.2.3 Retouched blades

The largest proportion of retouched specimens is represented by groups of blades that are retouched on one or two sides. These make up 90% of all retouched tools. They were separated into the three different groups below and the ETE was calculated for each:

- Blades retouched on one side (typologically single scrapers)
- Blades retouched on two sides (typologically double scrapers)
- End-pointed blades retouched on one or two sides (including typologically Mousterian points and converging scrapers).

Furthermore, the rest of the retouched tools – 28 items representing 10 different tool types – were counted as another distinct group.

In addition to calculating the distinct groups, the retouched blades were also thrown together as a single sample in order to see whether the whole sample would approximate the results of the split groups.

Lame retouched on one side (Tab. 9)

These seem to break into five elements: proximal, proximal-medial, medial, distal and distal-medial. The items retaining the distal part are the most abundant and are used for the calculation of MNIT.

| | |
|-------------------------|-------|
| TIE | 103.6 |
| MNIT | 86 |
| TLV 1 discarded | 93.6 |
| TLV 2 maximum | 172 |
| Actual Total items (n.) | 118 |

TLV 2 exceeds the total number of discovered elements. The TLV1 places between TIE and MNIT.

Lame retouched on two sides (Tab. 10)

These also break into the five elements, as above. Again, the distal parts are the most numerous and will be employed to calculate the MNIT.

| | |
|-------------------------|------|
| TIE | 32.4 |
| MNIT | 24 |
| TLV 1 discarded | 28.1 |
| TLV 2 maximum | 41.8 |
| Actual Total items (n.) | 38 |

The TLV2 only slightly exceeds the total number of uncovered items. The TLV1 falls between TIE and MNIT, but just nine intact tools were discovered.

Lame retouched on one or two converging sides (Tab. 11)

This assemblage seems to be the least affected by fragmentation effects, probably because they are the thickest retouched tools. The most frequent specimens are those retaining distal-medial parts and, to a lesser degree, proximal-medial parts.

| | |
|-------------------------|-------|
| TIE | 84.3 |
| MNIT | 87 |
| TLV 1 discarded | 69 |
| TLV 2 maximum | 125.7 |
| Actual Total items (n.) | 89 |

The TLV2 is considerably greater than the actual number of recovered items. The TLV1 is smaller than both MNIT and TIE, because the mean length at discard is quite high: 8.2cm. Taking into consideration the fact that 37 items were intact, and that 50 retain distal and medial parts and just two are proximal-medial fragments, the MNIT seems a reliable result.

The total number of retouched tools is reached by summing the estimated value for each group:

| | MNIT | TVL1 | TIE |
|-------------------------------------|------|------|-----|
| For blades retouched on one side | 86 | 94 | 104 |
| For blades retouched on two sides | 24 | 28 | 32 |
| For end-pointed blades | 87 | 69 | 84 |
| Rest of retouched items | 28 | 28 | 28 |
| Pooled retouched tool groups | 197 | 191 | 220 |
| Total number of retouched specimens | 225 | 219 | 248 |

The quantification of the retouched blades as a single sample gives the value of 222, 221 and 243 for MNIT, TLV 1 and TIE respectively, and approximates the numbers calculated using the values from each group (Tab. 12).

4.4.3. Layer 6a

4.4.3.1 *Blades* (Tab. 13)

Blades broke into five elements: proximal, proximal-medial, medial, distal and distal-medial parts. The calculations give the following results:

| | |
|-------------------------|-------|
| TIE | 286 |
| MNIT | 237 |
| TLV 1 discarded | 197 |
| TLV 2 maximum | 248.6 |
| Actual Total items (n.) | 3228 |

The TLV2 is smaller than the total number of uncovered specimens, indicating that the number of blades was bigger than the minimum length at discard. The TLV1 fits between the MNIT and the TIE. However, only seven intact blades were discovered and the use of length value as an estimate seems to be unreliable.

4.4.3.2 *Bladelets* (Tab.14)

Bladelets seem to break in three parts: proximal, medial and distal. The medial elements are the most numerous and are used to calculate the MNIT.

| | |
|-------------------------|------|
| TIE | 16.9 |
| MNIT | 17 |
| TLV 1 discarded | 13.2 |
| TLV 2 maximum | 15.4 |
| Actual Total items (n.) | 22 |

Just two complete specimens were found, and the use of TLV seems to be inappropriate. The TIE and MNIT are approximately equal.

4.4.3.3 *Retouched blades* (Tab. 15)

The tools from this layer are not numerous and represent blades retouched on one or

two sides (typologically single scrapers and Mousterian points); they are therefore quantified together. They retain two elements: proximal-medial and distal-medial.

| | |
|-------------------------|-----|
| TIE | 9.7 |
| MNIT | 11 |
| TLV 1 discarded | 7.2 |
| TLV 2 maximum | 7.8 |
| Actual Total items (n.) | 11 |

Only two intact items were found, so using TLV 1 and 2 appears problematic. The TIE and MNIT are reasonably close.

The three calculated formulas show that in almost all cases the estimate of quantification is fairly accurate and that the value of MNIT falls between TIE and TLV1. It also seems that the TLV1 value is a good predictor of the number of discarded tools if the assemblage retains statistically suitable samples of intact items; it can certainly be used for unifacial specimens that are reduced in length through the reduction process, as is shown by the retouched blades from Layer 6b. The value of TIE is always greater than that from TLV1 and often greater than that from MNIT, giving the highest number of tools every time.

In the case of Layer 6a, the MNIT value will be useful for calculation of blade quantities (Tab. 13). Likewise, in the case of Layer 6b, the TLV1 value of blade blanks summarised with TLV1 of CT blades will provide useful information on the blade quantities. However, in Layer 6a the intact specimens are scarce and the metrical value of these specimens is not appropriate for such analysis. Yet at the same time the value of TIE and MNIT offer good approximations.

The TIE was calculated with the assumption that each item retains only one element, proximal, medial or distal. The TIE results from these single-element items were always smaller than those calculated from those with finer divisions, showing that the methodology of quantification is significant.

Quantification of an assemblage should use different measurements, depending on the conservation condition of assemblage and the questions posed. ETE and TIE can help to recognise the significance of fragmentation and may possibly aid in the reconstruction of the

taphonomic history of assemblages, but the most important profit from using these estimation formulae is the fact that uniformity in quantification procedures makes comparisons between assemblages possible.

5. Methodology of the lithic analysis

The reconstruction of the reduction sequence in the Hummalian layers depends on the combined attribute analysis of both the cores and the debitage, using the methods outlined in Tables 2 and 3.

Techno-typological analysis of this lithic material centres on:

- the raw material procurement and transport;
- identification of reduction strategies, including core modification and blank production;
- retouching, tool curation, recycling and discard.

5.1. Raw material procurement

In the procurement strategies of raw material, there are only a few variables – for example, availability, quantity and quality. But each of these variables must be considered, since they helped shape the lithic technology and appear to have affected the actions of the prehistoric people who used it (Edmonds 1987; Hayden 1989).

Quite a few researchers (Andrefsky 1983, 1991; Torrence 1983, 1989; Bamforth 1986, 1990; Kelly 1988; Morrow and Jefferies 1989 and Shackley 1990) have demonstrated a clear relationship between stone-tool making efforts and prehistoric mobility. Furthermore, in discussing the ethnographic example of flint knappers in Australia, as well as archaeological examples from the western United States, Andrefsky (1994) points out that the accessibility of lithic raw material is a crucial factor in influencing stone-tool production technology. When high-quality raw material is scarce, it tends to be manufactured into ‘formal’ tools (Andrefsky 1994, 22), while poor-quality raw material is used for informal tools. But as soon as high-quality raw material becomes abundant, that material is used for both formal and informal tools.

Formal tools, such as bifaces, prepared cores and retouched specimens, have been described as implements that have a potential to be rejuvenated or remodelled for use in different activities. Informal tools can be described as ‘situational kit’ (Binford 1979), produced, employed and discarded over a relatively short time period.

Other archaeologists have shown that the choice of a particular type of raw material may depend on the planned purpose of the tool (Perlès 1984).

Good-quality raw material facilitates knapping and thus offers increased tool productivity (Edmonds 1987), but sometimes it does not seem to offer the required functional quality for the intended use. An example can be taken from Hummal layers 16-18, where bad-quality Cretaceous flint and limestone were used for manufacturing choppers and chopping tools, and all cores and flakes were made in good-quality Paleogene flint (Wegmüller 2008).

The selection of high-quality raw material may be further determined by the technical requirements of a specific production system. Some flaking techniques, such as pressure, can only be undertaken if the stone-tool maker has a high quality, homogeneous material to hand (Pelegrin 1984).

Strategies of raw material procurement are essential in understanding the organisation of hunter-gatherer land use. There is an extensive body of published literature on this subject.

Many archaeologists are convinced by the theories proposed by Binford (1979, 1980) and Torrence (1983, 1989). The former developed the concepts of embeddedness and logistical versus residential mobility, whilst the latter argues that time pressure depends partly on the mobility pattern that governs the setting of the group in relation to lithic resources, where the time spent and the reliability of the raw material are critical to tool production. Many other authors (Gamble 1986, 1999; Geneste 1988, 1989; Morala and Turq 1990; Féblot-Augustins 1993, 1997a, 1997b, 1997c; Potts 1994; Kuhn 1995 and Mellars 1996) have developed a model for the organization of adaptive strategies in Palaeolithic times based on the abundance of different types of stone raw materials in archaeological assemblages, their transport over the

geographical distances, and the forms in which they were transported. The conclusions of these scholars point towards possible consideration and planning in land use, risk minimisation, and optimisation of mobility and technological strategies.

Other researchers (Grayson 1984; Shott 1989; Hayek and Buzas 1997) concentrate on differences in the exploitation of raw material. Some archaeological assemblages show the use of relatively few types of raw material, whilst in others there is a vast array of raw material types. Furthermore, Brantingham (2003) has developed an interesting neutral model in which raw material procurement is governed only by the accidental discovery of stone sources and by the volume of accessible space in the mobile toolkit. These scholars reject the theories of adaptive variability based on the pattern of raw material richness and transport.

5.2. Reduction strategies

The majority of cores found at archaeological sites present the last stages of their reduction sequence or sequences. They very rarely provide us with information about the sequence of reduction itself. They are the by-product of debitage and frequently are unable to produce further blanks. The reduction sequence is accomplished at the time when most cores are exhausted. However, their dorsal scar patterns, size, shape, cross-section and platforms can yield information about the number of core reduction sequences represented at a site. Their size in relation to blank size can help to determine which specimens were manufactured in either the early or the later stages of reduction.

Nevertheless, there are occasionally some cores that were prematurely discarded, whether because of imperfections in the raw material, knapping errors which prohibited further flaking, or simply a lack of interest in further blank production. These cores supply important information about the conditions that did not lend themselves to further core reduction.

Cores are therefore an important point of reference in lithic analysis, but to gain more information about the whole reduction sequence it is essential to pay similar detailed

attention to debitage pieces. Flakes gathered on site can represent the different points of reduction and can convey important information about the major part of the sequence. Their dorsal surface can reveal the appearance of the core at various stages of the reduction sequence.

The main goal of this part of lithic analysis was to identify the kinds of core reduction strategies that were employed in the manufacturing of the Hummalian lithic industry. Initially, the cores made on flake were detached from other cores and analysed as two distinct groups: 'on flake' and 'on flake with NI preparation.' Later, the cores on flake presenting a particular reduction strategy were put together with the cores on block that presented the same reduction strategy. They were then analysed collectively.

Five coexistent production systems are recognised:

- The Laminar system of debitage (Meignen 1998 p. 176) presents a particular core volume management and can be allied to a rotating system of debitage (Wojtczak 2011);
- The Levallois system of debitage (Genest 1985, Boëda 1986, 1988a, b, 1990, 1995, Boëda *et al.* 1990, Van Peer 1992). The criteria of the Levallois concept proposed by E. Boëda were used to find out if this system of flaking was present in Hummalian assemblages. The use of this method was visible in layers 6b, 7c and ah either by the presence of cores or through typical Levallois products. However, typical Levallois cores are very rare.
- Debitage from cores on flake. Some present an opportunistic debitage and usually delivered small flakes. Others present a particular reduction strategy, usually following Laminar debitage observed on cores made on block. They usually provided blades and bladelets.
- The Nahr Ibrahim technique (Solecki & Solecki 1979), recognised at the site by the presence of pieces that are truncated-faceted (Schroeder 1969) either on one end or at both ends, or sometimes on one of their sides, and are flaked as cores on flakes.

- The manufacturing of bladelets from core-burins and bladelet cores has also been documented. This seems to be an important feature of Hummalian industry, demonstrating a systematic bladelet production.

In all the presented lithic samples, cores, core trimming elements (CTE) and blanks obtained from different reduction strategies were separated if possible and analysed independently, following the same scheme, although there are a number of lithic blanks and CTE which were impossible to associate with just one reduction strategy.

5.3 Core orientation

In the early stage of analysis, it is important to identify the different surfaces of the core and which one in particular acted as the flaking surface. A surface with a higher number of flake negatives ($\geq 1\text{cm}$) is expected to be a debitage surface. Consequently, the core platform surface can be described as having fewer scars and possibly a lower percentage of negatives from the percussion bulbs (Van Peer 1992:23).

The orientation of raw material is the preliminary choice of the stone-tool maker in shaping this future core. Multiple locations of flaking surface on the block of raw material can indicate an adaptation to the shape of the raw block or differing technological purposes.

Assemblages studied in this investigation revealed five options for flaking surface orientation:

- On a narrow face: the narrowest and longest part of the nodule serves as the flaking surface.
- On a narrow face followed by a broad face: the narrow surface is firstly exploited and exhausted and subsequently the widest face is subtracted.
- On a broad face: the debitage is carried out on the broadest surface of the block.
- On a broad and narrow face (semi-rotating debitage): the wider and narrower surfaces are exploited simultaneously.
- On a broad face followed by a narrow face: the widest surface is exploited and exhausted first and subsequently the narrow face is subtracted.

Differences in morphology were recognised for different flaking surfaces, which vary in shape and convexity. The convexity was estimated by eye and noted as flat or convex.

5.4 Core management

The cores and core trimming elements were analysed to identify the means of core management, and a number of core management options were recognised. The most important of these relate to the perpetuation of flaking surface convexity, the management of lateral convexity, the initiation of core exploitation, and the cleaning of the debitage surface. The following types of core management were recognised in the material and form the basis of the quantitative and qualitative analysis of the lithic material:

- Removing the edge-flakes (*éclats débordants*) to re-establish the convexity of the flaking surface.
- Extraction of small flakes around the periphery of the exploitation surface, also to recreate the necessary convexity.
- Employing frontal crests to start the core exploitation, or otherwise to mend the longitudinal convexity during a reduction.
- Removing a secondary crested blade to repair the longitudinal convexity of a reduction in progress.
- Extracting backed items from the core lateral edge to expand the flaking surface on the sides of a core.
- Frequent use of ‘cleaning flakes’ to maintain the flaking surface and clean it, especially from the negatives of step and hinge terminations.
- Extracting the minute blades from the edge of the striking platform onto the proximal part of core, when it needed reparation after the debitage of a few specimens. It would be abrasion-like, as well as involving regulation of the edge by the extraction of tiny flakes. Many lithic items, mainly blades, show such a dorsal reduction and “thinning” of the proximal part. Therefore it may be that its purpose was not only a simple regulation of the edge and proximal part of the core, but that the knapper planned to adjust this part of the specimen

for different purposes, such as, for example, hafting. However, the lack of use-wear analysis makes this hypothesis only tentative.

5.5 Platform maintenance

5.5.1 Platform aspect

Different treatments of the striking platform can cause changes between the exterior angle and the flaking surface that influence the final flake mass (Dibble and Pelcin 1995). In analysing the Hummalian assemblages, various aspects of platform treatment were observed on cores and flakes, including:

- Cortical: showing no modification, all or the majority of the platform surface is covered by cortex.
- Plain: a single scar is left on the platform surface.
- Faceted: three or more scars debited from the top of the platform, establishing a butt surface.
- *Chapeau de gendarme* (Bordes 1947, Inizan *et al.* 1999).
- Dihedral: two removals separated by a crest.
- Punctiform: a point of a few millimetres in thickness which represents the butt.
- Broken: the platform is shattered through flaking or by post-depositional phenomena.
- Crushed: the platform surface is damaged during debitage or affected by post-depositional phenomena.

The upper edge of striking platforms in the Hummalian material shows different shapes: straight, triangular, double triangle, convex, biconvex, concave and sinusoidal.

5.5.2 Flaking angle

The angle between the platform and the flaking surface is measured on cores and the exterior platform angle is measured behind the point of percussion onto the debitage (Dibble and Pelcin 1995). In the present study, both angles were taken using a goniometer.

5.5.3. Platform thickness

This is calculated as width of butt/thickness of butt.

5.5.4. Point of percussion relative to the dorsal scar patterns.

This point is very often punctiform and highly noticeable. Two morphological types were observed:

- Axial to the central ridge or between two ridges.
- Lateral to the central ridge or two ridges.

5.6 Dorsal surface

5.6.1 Direction of exploitation visible on cores and flakes

The number and the direction of dorsal flake negatives give information about the direction of flake detachment and possibly the chronological sequence of flake removal. Flakes removed from core earlier usually present fewer negatives of previous flakes than those detached later. However, these negatives are not always an absolute pointer to the flake's place in the reduction sequence. They can indicate the relative position of the flake and be beneficial in the comparison between different flake categories.

Furthermore, the direction of flake scars may define the number of core platforms and their relationship at the moment of flake detachment.

To describe the dorsal scar pattern, the technique proposed by Crew (1975, p. 13, Fig. 2:1) of dividing the whole flake into four quadrants of 90° each was employed here. The number of negatives visible on each of the four sectors was documented.

The records of the direction and number of scars by sector determined the scar pattern for whole flake. These could be:

- Unidirectional: all scars recorded on the proximal part of lithic artefact.
- Unidirectional convergent: all scars converge from the intersection of sectors B and D with Sector C in the direction of the distal part of flake (Tostevin 2003, 85).

- Bidirectional: scars originate from both proximal and distal ends of specimen.
- Crossed: at least one scar recorded from a lateral direction.
- Subcentripetal: scars found in three sectors.
- Centripetal: scars noted in four sectors.
- Unidentified: it is not possible to detect the direction of a scar.

It should be kept in mind that a reduction strategy is a dynamic process and therefore the direct typology of dorsal scar patterns of cores and/or debitage may be erroneous. Here a reminder is needed that the results of analyses by Boëda (1988) and Dibble (1995) of the Middle Palaeolithic assembly from Level IIA at Biache Saint-Vaast were inconsistent and contradictory.

5.6.2 The amount of cortex

The occurrence of cortex on a dorsal surface offers further important information about the core reduction sequence. Estimation of the percentage of cortex visible on the upper surface of flakes is also one variable that is often used to define the stage of core reduction (Genest 1985, Ahler 1989). Flakes presenting various cortical covers on their dorsal surface were organised into classes of primary, secondary and tertiary removals, on the assumption that the amount of cortex is related to their place in the reduction sequence. It should be noted that Sullivan and Rosen (1985) warned against sole use of the proportion of cortex on the dorsal flake surface to describe the stage of reduction, because of the lack of standardised measurement techniques and terminology. It should also be noted that studies have shown that different factors – such as raw material properties and availability (Rosen 1981), nodule size (Fish 1981), the reduction system and its intensity (Keller and Wilson 1976, Doelle 1980) and function (Gould *et.al* 1971, Shimelmitz *et al.* 2010) – can all have an impact on cortical variation. But regardless of the criticism this method has attracted, the utility of this relationship in principle seems convincing and several studies have proved that the quantity of dorsal cortex can be reliably measured (Magne and Pokotylo 1981; Mauldin and Amick 1989:70).

It can be expected that the primary flakes will be removed at an early stage of core reduction where the outer surface of core is still covered by cortex. Further detachment of cortical flakes depends on the particular method of reduction employed. In some cases, the proportion of cortex observed can actually increase when a new part of the core becomes the subject of reduction.

In this study, the flakes with visible cortex were classified into five categories:

- 1: 1-25% of cortex on the dorsal surface
- 2: 26-50 of cortex on the dorsal surface
- 3: 51-75% of cortex on the dorsal surface
- 4: 76-99% of cortex on the dorsal surface
- 5: first flake: 100% of cortex on the dorsal surface

The position of cortex on a flake's dorsal surface can help in reconstructing the method of initial core reduction (Baumler 1988, p. 54, Fig.1).

The cortex pattern description of the flake dorsal surface was set out using six sectors (Fig. 18).

In Hummalian assemblages, primarily, flakes bearing more than 50% of cortex on their upper surface (classes 3-4) are observed.

The estimation of cortex on broken blades was undertaken only on the items that retained two parts, either proximal and medial or distal and medial, and these were split into two classes:

- Items showing any cortex coverage: cx 1-25%
- Specimens totally covered: cx 26-50%

Only intact specimens were assigned as first flakes. In any case, all metrical analysis was completed only on unbroken items.

5.6.3 Convexity of dorsal surface

The convexity of the dorsal surface of lithic artefacts can be measured in the longitudinal, lateral and vertical planes.

3.6.3.1 Longitudinal convexity

High laminarity in lithic specimens indicates a choice by the flint knapper for a ridge pattern in which the convexity of the core concerns the longitudinal axis. Low laminarity indicates a choice for a ridge arrangement in which the convexity is distributed along the lateral axis.

3.6.3.2 Lateral convexity

This category can be defined by flake cross-section, which indicates utilisation of one, two or more ridges during flaking. The cross-sections of proximal, medial and distal parts of lithic specimens were noted as either:

- Triangular flat: one ridge is present on the dorsal surface.
- Triangular thick: one ridge is vertical.
- Trapezoidal: two ridges are visible on the dorsal surface.
- Domed: three or more ridges are present; usually this cross-section is strongly curved.
- Ovoid: no dorsal ridges exist; in the majority of cases such a cross-section also shows a pronounced thinning of the proximal end.
- Irregular: the piece is broken or very asymmetrical.

3.6.3.3 Vertical convexity

The ratio of width to thickness can help to specify trends in using curved or flat convexities during debitage, and accordingly these properties were recorded during analysis.

5.7. Shape of lateral edges

Five types of lateral edge were recognised and recorded in the Hummalian material:

- Parallel: the edges are parallel.
- Converging: the edges meet at the distal part.
- Expanding: the edges diverge toward the distal end.
- Ovoid: the edges diverge from the proximal toward the middle part of flake in the main and then converge toward the distal end.
- Unidentified: the specimen is broken or very irregular.

5.8 Flake profile

This category was defined ‘by eye’ and indicates the longitudinal convexity on core surfaces during the flakes detachment. These have been split into four categories:

- Flat: the flake profile is almost straight.
- Incurvate:
 - a whole piece.
 - the distal-medial part is bowed.
 - the proximal-medial part is bowed.
- Twisted: the distal end is twisted.
- Irregular: broken or irregular items.

5.9 Proximal end modification of flakes

Five types of proximal part modification are recognised in the Hummal material:

- Abrasion: detachment of small flakes from the edge of the platform toward the dorsal surface.
- Dorsal reduction: detachment of elongated flakes from the edge of the platform into the proximal-medial part of the flake.
- Truncation.
- Tang: only a few specimens show this kind of preparation.

5.10 Distal terminus of flakes

Some researchers (Crabtree 1968; Hiscock 1988) have advocated that a thick knapping platform and an inward directed force are very often responsible for the manufacturing

of overpassed endings of flakes. Pelcin (1997:1111) demonstrated that if all other variables are held constant, an increasing platform thickness will create systematic changes in flake termination type, because the force of the blow becomes insufficient to follow the length of the upper surface. Thus the distal terminus of flake has been recorded in six categories:

- Feathering: the flake that does not reach the core end and its termination is thin. This happens frequently if the core flaking surface is convex and the blow is accurately applied.
- Blunt: the flake reaches the end of the core but does not overpass it.
- Hinge and step: knapping accidents which appear when the applied force rolls away from the core, producing a rounded (hinge) or sharp (step fracture) at the distal end.
- Overpassed: the force of blow is so powerful that the fracture path turns noticeably away from the core surface edge, removing a part of the core base.
- Retouched: the distal end of flake is modified by retouch after its removal from the core surface.
- Broken: the distal part is missing.

5.11 Morphology of flake ventral surface

The ventral surface is created when a flake is removed. Beneath the point of percussion on the ventral surface, there may appear an undulation known as the “bulb of percussion”. Some researchers believe that the size of the bulb of percussion depends on the type of hammer used for flaking and the angle of the applied force.

The bulb has been recorded as either:

- prominent: large and highly visible.
- diffuse: flat.

The bulb of percussion is also associated with:

- ripple marks or fissures radiating away from the point of percussion.
- erailure scars produced during the original impact of the flake removal appearing below the point of percussion on the bulb.
- compression waves.

These have also been recorded where they appear.

5.12 Manufacturing of retouched specimens, curation and discard

Retouched items can be analysed for almost all of the attributes mentioned above. The set of supplementary attributes in this group concerning retouch consists of:

- its extent
- its angle
- its morphology
- position and localisation are also noted.

The aim is to detect the main approaches to retouched tool production and maintenance using the specific attributes listed above.

Binford (1978) was acquainted with the curation concept in 1973. He used the term ‘curated’ vs. ‘expedient’ to define the different behaviours of Nunamiut hunters. They would treat implements in their various tool-kits in two different ways. ‘Curated’ would correspond to ‘personal gear’ or ‘site furniture’.

Binford’s concept received both widespread acceptance and severe criticism in the archaeological world (Hayden 1979; Bamforth 1986, 1991; Shott 1989, 1996; Andrefsky 1994; Odell 1996). Lack of precision in the original description of the concept meant that researchers have used it in their own ways, and as a result ‘curation’ now has many different definitions in the published literature. In 1996 Shott proposed a new definition of curation, seeing it as a continuous variable and property of tools, not entire assemblages. In 2009 Binford called curation “the degree to which technology is maintained, the amount of labour investment in the design and production of tools so as to ensure them a long use life” (Debating Archaeology

2009:465). In the present study, curation is viewed as a concept including both maintenance and re-sharpening of tools.

5.13 Recycling

Following analysis of stone material from all the Hummalian layers, it can be argued that on-site recycling was an important part of the procurement of raw materials. For instance, the tendency to recycle on-site raw material can be supported by:

- Recycling of blanks for shaping new tools, which is perceptible in double-patinated items.
- Scavenging lithic material from older occupations or different cultural horizons.
- Retouching of exhausted cores for tool use.
- Reuse of exhausted cores for blade and bladelets production.
- Reuse of broken blanks and debris, as well as blades for bladelet production.
- The presence of numerous cores on flake, including those with Nahr Ibrahim preparation.
- Heavily retouched pieces (curated tools) as a possible example of short term recycling.

5.13.1 The double patina

Double patinated items, in which the secondary modification can be distinguished from the older patinated surface, seem to be the most consistent element in identifying recycling in Palaeolithic assemblages, even though it is usually not possible to calculate the time span between the creations of the first, second or even third generations of patina. We can only see the chronology of the patina and the episodes of use (Fig. 151 and 152). The reuse of older items for shaping new tools was recognised in four of six Hummalian layers: 6b, 6c2, 7b and α h. It occurs only sporadically in layers 6b, 6c and 7b, but it is notable in the rich and well-conserved sandy Layer α h (Fig. 8). In this deposit, 10% of all retouched tools were accomplished

on already patinated specimens. Several cores-burin and truncated faceted pieces (six from 19) were also made on items chemically altered, within the few with previous retouching. In layers 6a and 6b such observations were very limited, as all artefacts from both assemblages were covered by a similar white-grey patina.

5.13.2 Scavenging from a different cultural horizon

Three examples of cores made on Yabrudian scrapers and coming from layers 6b, 6c, and 7c (as well as one edge-flake in Layer 6b and three in Sand *oh* which were clearly struck from the edge of Yabrudian scrapers, Fig. 148:2 and 153) show that lithic material was procured from older occupations as well. The lower face of Yabrudian scrapers becomes the flaking surface, and the upper face, still covered by stepped retouch, becomes the ventral face of the core.

5.13.3 Retouching of cores for secondary utilisation

Only a couple of cores have been transformed for probable tool use. Two exhausted cores from Layer 6b and one from *oh* were modified on their side by invasive, abrupt retouching and could possibly have been used as scrapers (Fig. 148:1, 3).

5.13.4 Reuse of exhausted cores for bladelet manufacturing

The reuse of exhausted cores for additional flaking of smaller supports can be visible when one flaking event working on the broader face of the core has finished and a second flaking episode has been performed on the side or the dorsal face of the same item. This usually involves a supplementary preparation, principally setting a new striking platform. The items are covered by the same patination but the second episode is clearly performed after the first has finished, as can be understood using the chronology of the surface scars pattern.

There are a few cores which were primarily unidirectional, and when they became flat in cross-section, a second striking platform offset to the axis of the first one was set on the opposite end or on the side of the core. If arranged on the opposite end, this additional platform was exploiting the core on its thickness. The negatives coming

from the second striking platform clearly crossed the negatives obtained from first platform. When new platform was arranged on the side, this supplementary platform was exploiting the dorsal face of the core.

Several cores were clearly reused for blade/bladelet production (Fig. 136:3, 5) and were exploited on their sides.

Occasionally, cores were fragmented and, if the partition formed by the old platform and the broken surface (a perpendicular flaking plane) created an apt angle, were struck again. The flint knapper would obtain only one or two blanks.

5.13.5 Cores for bladelet production

There are two types of core for bladelet production: one that resembles typical bladelet cores (Fig. 139: 6 and 12) and another that is similar to typologically identifiable burins (2, 7-10, 13). The latter present removal negatives that are frequently multifaceted and relatively wide (starting from ca. 5mm and larger). Additionally, there is sometimes a combination of a bladelet core and a burin-core arising together on the same core.

In all the analysed layers, bladelets and/or core-burin and bladelet cores were present.

5.13.6 Cores on flakes

Cores made on flakes can be set in three groups: those in which the reduction strategy follows the one observed on cores made on block; those presenting a rather opportunistic flaking method; and those with Nahr Ibrahim preparation.

6. Presentation of lithic material

6.1 Introduction

The earliest work on the stratigraphical and sedimentological sequences (Le Tensorer 2004) of the Hummal site at El-Kowm showed that the previous studies of the lithic material from the Ia layer were carried out on assemblages that were not *in situ*. A new series of studies carried out on the Hummal sequence during the 1997-2005 and 2009 season's shows that the materials from these new excavations can, unlike the materials found in the previous work, be considered to have been *in situ*. This means that a far greater understanding of the lithic Hummalian industries is now possible, and this chapter focuses on this new material. Attention is also turned toward artefacts from sandy Layer ah, which contained pure sand and numerous well-conserved lithic artefacts. This layer seems to be homogenous and presents all the technological features observed in the *in situ* layers. It therefore appears to be from the same technological tradition.

The lithic analysis studied 10,275 artefacts of which 7,414 came from *in situ* layers and 2,899 from the sandy layer (Tab. 16 and 17). Blades, core trimming elements (CTE) and small items of debris are the most abundant categories, with their number varying between the layers. Unfortunately, many blades from layers 6a and 6b were broken, leading to problems with quantification (see Section 4.4, above), and others present crushed edges, making them of limited value for this study. In most layers, the chips category (very thin flakes) and debris are also well represented. The percentage of retouched items is not very high and varies in all layers (from 1 to 14%). Cores are the least represented. In any case, the abundance of small and large items of debris, chips, flake and cores indicates that the sample contains material from all stages of core reduction, tool production, recycling and re-sharpening.

Statistical analysis was also performed alongside the attribute analysis. Where necessary, appropriate statistical testing – including t-tests and analysis of variance (ANOVA) – was conducted. The plotting of means with 95% Confidence Intervals allowed the description of central tendencies in samples.

6.2 Raw material procurement strategies

The raw material used in Hummalian layers is approximately 99% local Lower Eocene flint from the El-Kowm area (Tab. 18). The rest of the raw material is composed of Cretaceous flint and limestone (Fig. 31).

The original form of the raw material may significantly affect the shape of cores and consequently the debitage, but it is difficult to appreciate its importance without refitting. Experiments carried out in El-Kowm on Eocene flint show that even an inexperienced flint knapper starting with an elongated and convex nodule (such nodules are largely present in the outcrops of the region) may be capable of striking some elongated flakes but will not succeed in producing a regular series and will even make the same knapping errors as those observed in the Hummalian material. On the other hand, because the flint is of such good quality, the smallest mistake – such as an imprecise, badly controlled, over-forceful or weak blow – will cause a mistake, generally producing an overshoot or fracturing of the proximal part, which often requires mending for the flaking to continue. The systematic debitage of a great number of elongated supports requires experience, but it is also facilitated by the quality of the flint. The laminar debitage noted here may in fact appear rather opportunistic due to the use of the natural shape of the block and the lack of extensive core shaping, but it was also effective.

The occurrence of lithic items which bear a weathered cortex or neocortex gives evidence of the use of flint gathered in secondary contexts. This strategy is represented in differing proportions in all layers (Tab. 19). In rich assemblages, the amount of neocortex does not exceed 30% of all cortical items; in the case of small collections, such as those from layers 7a, 6A1 and 6B, the high percentage of items with neocortex is certainly due to sample errors.

Flint found on site was an additional source of raw material. This is noticeable in the reuse of exhausted cores, broken blanks and debris for bladelet production. The tendency to recycle the raw material is visible in, amongst other things, the occurrence of cores on flake and core-burins. The large flakes were struck on their dorsal (or

occasionally ventral) surface, following the different reduction strategies. Their final stage of reduction shows that the aim was to obtain as many elongated supports as possible.

The recycling of blanks for shaping new tools, which is evinced by double patinated items, occurred sporadically in layers 6a and 6c but is not noteworthy in assemblages from layers 7 and αh. In Layer 6b, recycled material makes up 5% of all retouched tools, and this figure increases to 8% in αh. Occasionally the exhausted cores were retouched, probably for tool use (Fig. 148: 1, 3). Three examples of cores made on Yabrudian scrapers coming from layers 6b, 6c, and 7c show that the procuring of lithic material from older occupations took place as well (Fig. 148: 2; 153, 161). Additionally, one edge-flake in Layer 6b and three in Sand αh were clearly struck from the edge of Yabrudian scrapers suggesting the reuse of lithic specimens from an earlier period as well.

There were no blocks of raw material or pre-cores found in any of the *in situ* Hummalian layers. In sandy Layer αh, one small block of Cretaceous flint measuring 10cm x 10cm x 4cm was collected. The nodule does not present any traces of treatment.

Primary flakes with cortex coverage exceeding 50% on their dorsal face are considered as originating from the early stage of core reduction. They are numerous in layers 6a, 6b, and αh. First flakes (*entame*) result from the opening of the flint nodule, and thus create a link to the initial core reduction stage. Their dorsal face is completely covered by cortex. They are infrequent in the presented assemblages: only ten such flakes were found, comprising six in Layer 6b and four in Layer αh. They are rather large, with a mean thickness of 1.5cm, length from 5 to 11cm and width from 3 to 8cm. Just as common as the fresh nodule of Eocene flint are flakes entirely covered by cortex, so the striking platform of such items is also cortical.

In Layer 6b, 12% of the total debitage and shaped items are flakes having from 51-99% cortex on their dorsal surface. 35% of these have lost their platform either totally or in part, probably at the moment of the debitage. A further 59% present cortical

butts; the remainder are plain, punctiform, and rarely dihedral or faceted. They show a large variation in size, with the proportion of cortical specimens decreasing with length (Fig. 32). A single ridge is observed on the majority of cortical items. The cortex is present in most cases on the distal part, followed by the middle portion and then less frequently on the proximal part of the specimens. The most numerous of these are flakes carrying from 51 to 75% of cortex with a length from 2 to 4cm. 66% of items from this group are small and thin (mean thickness 0.5cm, mean length 3.2cm), and the rest are thicker and larger (mean thickness 1.4cm, mean length 5.1), with a few of them presenting a cortical back. The size, length and thickness, as well as the cortical platform, suggest that flakes with lengths ranging from 2 to 4cm may result from the stage of core maintenance or enlarging the flaking surface, when the non-treated surface was still covered by cortex. The paucity of flakes with the cortex coverage bigger than 75% in Layer 6b suggests that the nodules of raw material were slightly trimmed elsewhere before being transported to the site. Only six of these can be called first flakes (*entames*), detached from the rough block. These have a dorsal surface and striking platform that are totally covered by cortex. There are also numbers of items that are thick, triangular in section and totally covered by cortex. They could possibly be the natural crests detached from the edge of raw material. Unfortunately, most of them are broken.

The ratio of CTE to blanks is quite high (Tab. 20). The CTE appear to be a bit shorter, broader and thicker than the blanks from layers 6b and αh (Tab. 21), but they seem to have been produced in turn.

In sandy Layer αh , primary flakes make up 10% of total debitage and shaped items. Four first flakes and 166 primary specimens were recorded. 67% of items are thin (mean thickness 0.6cm, mean length 5.5cm) and the remaining 33% are thicker (mean thickness 1.4cm, mean length 8.7cm). The majority of flakes also present cortical butts and a single ridge on the upper surface. In Layer αh , the items with cortex from 76 to 99% are well represented alongside those having from 51 to 75% of cortex on their dorsal face. The most numerous are those from 3 to 6cm in length. The lack of smaller cortical flakes is probably due to sample error.

The marked presence of flakes bearing from 51 to 100% of cortex on their surface, several of which are *entames* that present the initial stages of raw material acquisition (Tixier 1963:33), core trimming elements and cores shows that the debitage was at least partially carried out on site in both layers.

In other layers the first, cortical removals from a natural platform (the *entames*) were not recorded, but CTEs that belong to the stage of maintaining the cores existed alongside cores.

In Layer 6a just four cores were found, three made on flakes and one on debris. CTE consisted 15% of debitage and shaped items, suggesting that debitage was at least partially undertaken at the site. The primary flakes have cortical platforms and are small, with a mean thickness of 0.6cm and a mean length of 3.7cm. The high degree of small debris in Layer 6a may be related to post-depositional disturbances rather than to knapping activities.

It can be supposed that in the cases of layers 6a, 6c and 7c, already partially decorticated nodules were transported to the site, where they were shaped and blanks were produced. The abundance of small debris, chips and cores indicates that those samples contain material from the different stages of core and tool production. The relatively frequent use of overhang removal from blanks in all levels could also be responsible for producing small debris.

22% of debitage and shaped items in Layer 7c are primary elements. The size of CTEs in Layer 7c is related to blank size (Tab. 22). Additionally, in Level 7c a small debitage workshop was also discovered. A partial refitting shows that the flaking was performed on a small convex nodule that is a few centimetres in length and displays traces of cortex removal. A few items were removed from the nodule; of these, two elongated items were broken and left with the waste. The presence of abundant small, characteristic chips could indicate the stage of core or tool re-sharpening, plausibly related to the Nahr Ibrahim technique.

In the case of Layer 6c, 24% of debitage and shaped items are primary flakes but the blanks are significantly longer than the CTEs, indicating that the blanks were probably

manufactured elsewhere and transported to the site, where they were possibly retouched or modified and then later abandoned (Tab. 21). Therefore the numerous small debris and chips would come principally from tool production or alternatively from tool re-sharpening.

The small sample sizes gathered at present from layers 7a, 6A1-2 and 6B make any interpretation difficult. Further excavation should uncover more archaeological material. In layers 6A1-2 and 6B, primary elements are not present; CTEs make up 14% of debitage and shaped items in both layers.

Although Layer 7a was excavated on 14m², just 182 lithic specimens and 13 bone fragments were discovered. Besides a few blanks, just two cores on flake and five CTEs were discovered in this layer. Chips make 82% of the total assemblage, indicating knapping activities. Undoubtedly some blank production took place here, but the extent of the excavation uncovered only a small part of the activity zone.

6.3 The goal of the reduction strategy

The identification of intentional products is crucial to defining the probable guidelines which reduction followed. To obtain, repeatedly, the particular morphology of these specimens, the flint knapper had to replicate that sequence of reduction which had yielded the intended product previously. It follows that recognition of the desired product is an important point of reference for the reconstruction of the reduction sequence. In core reduction, these intentional products are the tool blanks. In the past, only retouched objects, or those lithic objects presenting secondary modification, were regarded as tools. Yet ethnographic observations (White 1968) and numerous use-wear analyses (e.g. Hayden 1979, Keeley 1980, Beyries and Boëda 1983, Lemorini *et al.* 2006) have shown that many flakes were used without ever being retouched. Consequently, the desired flake blanks are not necessarily limited to the retouched tool assemblage. Therefore it seems that the study of use-wear should be a principal method for describing the desired products of core reduction. Often the evidence of use is preserved on retouched and non-retouched edges and surfaces of flakes, if the

extensive post-depositional phenomena have not damaged the lithic assemblage. These can then be studied macroscopically and microscopically. However, the determination of intended products from their use is not always straightforward. Low and high power microscopic studies of lithic objects are extremely time-consuming and unfortunately have not as yet been undertaken on any of the presented assemblages, so that identification of desired product must proceed on a different tack. The following analysis attempts to determine different types of blanks and the existence of some form of patterning. By-products of reduction, such as CTEs and cores and all of the ‘remainder’, are analysed separately. The initial working hypothesis is that the ‘remainder’ group constitutes the desired end products.

Cores, CTEs and blanks of different morphologies were recognised in all the investigated layers. Therefore the lithic specimens from all assemblages were studied by technological category to discover parallels between them, and *ergo* whether different reduction strategies were carried out simultaneously within the layers.

6.4 Core Trimming Elements

6.4.1 Introduction

Since different core reduction strategies were used in all the analysed assemblages, it is important to recognise which types of core trimming elements (CTE) are linked to which particular reduction strategy.

The primary flakes, backed specimens, *lames débordantes*, cleaning blades, crested elements, semi-crested elements, abrasion flakes, rejuvenation flakes, preparation flakes *sensu lato*, and the plunging and hinged items are all considered representative of this group.

Some of the CTE – for example, the *éclats débordants* with prepared or cortical backing – are clearly related to Levallois core reduction. Others, such as crests, semi-crests, backing elements and rejuvenation flakes, are related to the Laminar method. Altogether, 1225 identified CTE were found in layers 6a, 6b, 6c2, 7a, 7c, 6A2-1 and 6B, while 484 were found in sandy Layer α h. All are listed in Table 23.

36% of core trimming blades in Layer 6b and ah display the preparation of their proximal part by a series of small removals, a hinge fracture of 0.5 to 1.5cm in length, or a small triangular removal of less than 0.5cm in length. It seems to serve to regulate the edge of the platform and the proximal part of the core. First flakes and cortical flakes were described in the chapter 3.5 and preparation flakes *sensu lato* in the chapter 6.6.

6.4.2 Backed elements

Technologically, backed items are preparation flakes which can be obtained during all stages of blank production. They follow the principal axis of debitage and can extract the lateral side of the flaking surface to uphold the necessary convexity and/or to increase the flaking surface, in the case of Laminar cores. Altogether 250 of these backed items were found in *in situ* layers, with 69 in sandy Layer ah.

In the presented assemblages three different backed flakes were recognised:

- With cortical back.
- With plain back.
- With prepared back.

6.4.2.1 Cortical backed elements

A total of 90 flakes, including 56 intact with cortical backs, were discovered in *in situ* layers, together with 35 in ah (Tab. 24; Fig. 160). They present a regular cutting edge and a marked cortical back. They seem to fit into the typological criteria of Bordes' *couteau à dos* (196:32-33) or Tixier's *couteau à dos cortical* (1960:201). Typologically, these specimens are perceived as tools. Two examples of use-wear analyses made on the cortically backed items confirm that they were indeed tools. In the French Mousterian site of Corbehem they appeared to have been used for working four different materials: bone, flesh, cervidae antlers, and wood (e.g. Beyries and Boëda 1983:278). Interestingly, the micro-wear traces were documented only on the cutting edge and none of them appeared on the cortical back or edges of the striking

platform. In the Palaeolithic site of Qesem Cave (Israel), analogous pieces were mainly employed for the cutting of soft materials (Lemorini *et al.* 2006).

In technological analysis these flakes are seen as pieces having a particular function in preparation of the flaking surface. In the Levallois concept, they are seen as preparation flakes (Beyries and Boëda 1983, 275-277) which track the principal flaking axis and remove the lateral side of the flaking surface of the core to maintain the necessary longitudinal and transverse convexities. Often the lateral side of the preparation surface was not peeled; such edge-flake presents a cortical back. These are supposed to have been produced during the advanced stages of preparation of the Levallois surface, before the flaking of the first series started, or during repair of this surface after the removal of a series of flakes (Bar-Yosef and Meignen 1992: 175).

In the studied assemblages, a number of edge-flakes present asymmetrical, triangular cross-sections and their upper surface shows the negatives of previous radial preparation of the Levallois surface. They can be described as the cortical edge-flakes produced throughout the Levallois core reduction. They are curved in profile, few are overshots and some are twisted. They appear to be less elongated and larger and thicker than the other edge-flakes with cortical backs (Tab. 25). The cortex usually covers almost the whole surface of the backing.

However, the upper surface of a large majority of the analysed edge-flakes presents unidirectional or bidirectional former negatives. They show from one to three ridges on their upper face. Sometimes the backing is partial and appears only on the proximal-medial part of the edge-flakes. The profile of these edge-flakes is bowed along the whole length of the piece; less frequently, only the distal-medial part of specimen is incurved. A few are plunging and removed a distal part of the core. They are mainly unidirectional, but bidirectional examples are also well represented. The cortical back can cover from 20 to 75% of the upper surface, but in the main it covers from 30 to 50%. The striking platforms are mainly cortical or plain, and sometimes punctiform or faceted; just one is dihedral (Tab. 26). They are variable in size, but generally elongated. Their length ranges from 3cm to 13cm, showing that they were

employed throughout the core reduction. It seems that the majority of them are more likely allied to Laminar reduction strategies. Comparison of the length of backed specimens recorded as Laminar with those of Levallois in Layer 6b shows that the former are longer, with a median length of 6cm, and more than 50% of them are longer than the median, reaching up to 10cm in length. The latter present a median length of 5cm; 50% of them are longer than 6cm, even reaching up to 8cm (Fig. 33). Looking at their volumes, it can be seen that the median volume of Levallois-like pieces is 30cm³, with 50% having greater volume, up to 53cm³. The median volume of the Laminar is smaller at 20cm³, but about 35% of them have a volume greater than 30cm³ and they can reach up to 70cm³ (Fig. 34). The situation is similar in Layer ah; there the median length of Levallois-like and Laminar-backed elements is almost identical, but the former are never as long as the latter (Fig. 34). Still, they present a greater median volume, similar to the specimens from Layer 6b (Fig. 35). From this it can be concluded that the Laminar-backed elements were generally detached from longer cores and removed relatively less raw material from the core than the Levallois-like elements. The great volume of some pieces assigned to the Laminar method is caused by their greater elongation and not by their width or thickness (as in the case of Levallois-like items).

6.4.2.2 Elements with prepared backs

This specimen type is associated with the Levallois concept. The classical *éclat débordant* was recognised in two layers: 6b and ah. *Eclat débordant* was documented by Tixier (1960:201) under the name *couteau à dos préparé*. Like the *couteau à dos cortical*, these pieces are perceived as a tool in a typological sense, as traceological analysis carried out on the lithic material from French site of Corbehem confirmed (Beyries and Boëda 1983, 277-278). Their distal and proximal edges as well as the striking platform served to scrape, and provided a sharp edge to cut or saw, a single raw material: cervidae antlers. Unlike the *couteau à dos naturel*, where only the sharp edge carries the traces of use, all edges of these specimens were active.

The technological function of these pieces in the Levallois reduction strategy was recognised by Boëda (Beyries and Boëda 1983, 275-277). They were used in the same way as cortical-backed items: their role was to re-establish the lateral and distal convexities of the flaking surface.

In the present study, 24 such edge-flakes were gathered from Layer 6b and 10 from Layer ah (Tab. 27). They make 2% of all CTE in layers 6b and ah. Their backs present a number of scars whose axis is perpendicular to the ventral surface of the flake and which were produced before the extraction of edge-flake. In other words, those pieces removed a part of the prepared, lateral side of the Levallois core. On the ventral face of half of these are the negatives of small removals from the lateral edges onto the flaking surface of the core. These were produced on the flaking surface of the core before the removal of such a specimen. It shows that the transversal convexity of the flaking surface was often achieved not only by removing edge-flake, but by radial removals of small flakes from the periphery platform as well. These two methods seem to be complementary.

Some edge-flakes also present hinge negatives on their upper surface and illustrate the problems met by flint knappers during a flaking. Such flakes were documented by Boëda (Beyries and Boëda 1983, 277) during his experimental work and replication of the place of the *éclat débordant* in the Levallois reduction sequence. Occasionally, if the transverse convexity could not be re-established by radial removals from the periphery platform, the *éclat débordant* seemed to be the last remedy for flaking perpetuation. In this case, the edge-flake can repair the convexity of the flaking surface without the necessity of modifying the core shape.

These edge-flakes are mostly unidirectional, but bidirectional debitage is also present (Tab. 28). Their platform can be punctiform, faceted, plain or cortical (Tab. 29). 50% show a small amount of cortex coverage on their back, indicating that the lower surface of cores, despite preparation, still preserves a small amount of cortex. All specimens are bowed in profile and a few are twisted. More than half can be described as overshots and remove a distal part of the core. These pieces appear to have allowed

the instantaneous repair of both lateral and distal convexities, thus perpetuating the flaking (Bar-Yosef and Meignen 1992, 175). In Layer 6b their median length is 5.5cm and about 60% present a greater length, ranging up to almost 10cm, whilst the smaller reach down to 3cm. In Sand *ah* they are longer, with a median length of 8cm ranging between 7.5 and 9.5cm. It shows that removing of such specimens was possibly used during the whole reduction in the case of assemblage 6b and was limited – only on the same point of reduction – in sandy Layer *ah*.

6.4.2.3 Elements with plain backs

The backs of such items are plain and perpendicular to the flaking surface. They usually correspond to the core maintenance stage.

This category of backed elements is the most abundant in the presented assemblages. In total, 134 from *in situ* layers and 27 from *ah* were found. In Layer 6b they constitute 11% of CTE; in the sand, they are 6%. They seemed to be detached to enlarge the flaking surface onto the flanks and recreate the longitudinal and transversal convexities of the flaking surface. Simultaneously, they also create a new guide-ridge for following blades. All these elements facilitate the maintaining of the core, perpetuating the flaking and allowing expansion onto the core sides. The plain back can appear along the whole length of the piece or only partially, on the proximal-medial part of the specimen. Sometimes the perpendicular, plain backing has a negative clearly produced from the opposite direction, showing that flaking was undertaken alongside on the other flank of the core from the second platform. They are triangular and symmetrical or trapezoidal in cross-section and bowed in profile along the whole length or on the distal-medial part of specimen. A few are plunging and lack a distal part of the core. Sometimes on this distal part a second offset platform of the core and/or offset (to the axis of edge-flake) negatives of earlier detached flakes are visible. The length of edge-flakes with plain backs ranges between 3.4cm and 12cm, indicating that the extraction of such edge-flakes was used throughout the flaking (Tab. 30). They are mostly unidirectional, but bidirectional debitage is also visible (Tab.31).

A large proportion show one or two ridges on their upper surface, and several exhibit three ridges. The majority of the striking platforms are faceted, plain or punctiform, but rarely dihedral (Tab. 32). Less than half show small cortex patches on the proximal, medial or distal part of their upper surface. In layers 6b and α h, their median length is approximately 6cm, and about 60% of specimens no longer approach 12cm. The remainder are smaller, down to less than 4cm. In Layer 6b their size, which incorporates length, width and thickness, seems to be comparable to the size of the edge-flakes with a cortical back associated with Laminar debitage.

6.4.3 Crests

This kind of flake is related to the shaping out of a core in prismatic debitage. It is accomplished by detaching bifacial small flakes which are perpendicular to the length axis of the core. This generates a ridge made of two series of scars, directed transversely to the lateral edges on the upper surface of the core, which serves as a guide for the removal of the first blade, thus opening the flaking surface. A first blade produced thus will have a symmetrical, triangular cross-section and lateral flake scars on the dorsal surface (Crabtree 1982, 41, Inizan *et al.* 1999, 137). Altogether, twelve crested specimens were found in Hummalian layers: five in Layer 6b, two in 6c and one each in 6a and 6A2-1. Alongside these were three in sandy Layer α h. Unfortunately, all the crested elements from Layer 6b lost their proximal portions and so their length cannot be calculated. Even though they are broken, their mean length/width ratio equals 2.5, suggesting that they had to be very elongated. The crested items from other layers are also long; their thickness ranges from 1cm to 1.4cm (Tab. 33) and the platforms are cortical or punctiform (Tab. 34).

Only one intact example of a natural crest was found in Layer 6b. This piece is totally covered by thick cortex, triangular in cross-section, and seems to be peeled from a slightly rounded edge of the raw material. A few broken blades from the same layer show identical morphology and could possibly stem from a cortical ridge of raw material, showing that the flint knapper sometimes used the natural shape of the raw material block to start the flaking.

6.4.4 Semi-crested elements

If the shape of raw material is appropriate or the negative of an earlier detached specimen can be used, the removal of a semi-crested item can be undertaken, showing perpendicular small flakes present on only one side of the blade. The resultant piece shows one prepared and one flat side. Such a situation may often occur when the flaking surface needs to be repaired during a flaking stage. Without refitting, however, it is difficult to recognise which semi-crested specimens were opening crests and which ones shaped out the flaking surface during the debitage.

There are a few semi-crested items in Layer 6b for which the preparation was more elaborate than that of the others. These could possibly represent the first generation of crested blades. If we separate them from the others, it seems that they are longer, thicker, and detached more volume from the core than the secondary crests (Tab. 35). Nonetheless, semi-crested elements were collected mainly from layers 6b and αh , with one specimen each from layers 7c, 6A1-2 and 6B. Altogether, there were 40 from *in situ* layers and seven from sandy Layer αh . They are triangular in cross-section; their butts are cortical, plain, punctiform or faceted (Tab. 36). They are generally quite thick and their width varies from 1.4 to 5cm. Their length ranges between 3.9cm and 11.6cm, indicating that they were produced throughout the reduction (Tab. 37), but they seem to have been produced more rarely than other edge-flakes with plain or cortical backing.

6.4.5 Rejuvenation flakes

A rejuvenation flake is removed if the core platform needs restoration to continue the flaking (Inizan *et al.* 1999:153). Removal of such a flake seems to be rarely undertaken in the presented assemblages. Altogether, six rejuvenation flakes were recognised, with four from Layer 6b and two from αh . They present the scars of preparation of the striking platform and their butts comprise a part of the flaking surface. They are round in shape, with a mean length of 3cm and a mean thickness of 0.8cm.

6.4.6 Abrasion and dorsal reduction flakes

These kinds of flakes are products of the preparation of the proximal part of the core, and are removed to facilitate the further debitage. These are supposed to eliminate the overhangs left by earlier blank removals to improve the manufacture of controlled blanks. The identification of such flakes is problematic because their production accompanied the production of blanks. Looking at blanks present in the Hummalian layers, it appears that the preparation of the proximal part of the core was often undertaken. It could be achieved by removing a series of minute flakes or a couple of bigger flakes, generally 1-2cm in length, which usually leaves a negative of the hinge fracture or a small triangular removal on the proximal part of the specimen. Such traces are visible on the greater part of core trimming blades and blank blades (Tab. 38).

Often a narrow (up to 5cm) and converging negative of bladelets along one or two ridges at the proximal end of the upper surface of a blank is visible, and it could be a part of the maintenance of the proximal end of the core as well. The point of percussion was placed behind a main ridge of the lithic item; the removal followed the ridge from the upper surface and could even reach its midpoint. Such negatives are flat and the resultant bladelets, very thin. In five Hummalian layers, 138 very thin bladelets were found in layers 6b, 6c2, 7a and 7c, with 37 in total in Layer *ah*. Their sides always converge, just like the negatives visible on the upper face of the blank; they match those flat negatives perfectly. The length ranges between 2 and 5cm and the thickness from 0.2 to 0.3cm. The majority still show a tiny punctiform butt. They were produced before the blank was detached from the core; the proximal part of their scar is often cut by the negatives of small removals stemming from the edge of the proximal end of cores. These tiny, elongated, converging subtractions prepared the proximal part of flaking surface of the core and at the same time thinned a proximal-medial part of the blank as well, and could possibly be related to the specific mode of hafting. Yet the resultant bladelets can represent the researched end-products as well.

The similar production of tiny bladelets was recognised in Mousterian levels III2a and II based on the site of Umm el-Tlel. The bladelets were detached from the proximal

part of elongated Levallois points (Boëda and Bonilauri 2006:77-81). The micro-wear analysis showed that they were used for working meat, bone and vegetal matter. Furthermore, they show hafting traces (Boëda and Bonilauri 2006:86-91).

It may be supposed that these minute bladelets detached from blades in Hummalian layers were produced not for maintaining of the core or thinning the proximal part of lithic items, but for planned activities, or maybe for all these reasons.

6.4.7 Cleaning flakes

These specimens were found in all presented layers and seem to have been produced for the purpose of cleaning the flaking surface from deep hinge and step fractures. On their upper surface, between two to four negatives of earlier removals are visible and at least one presents a deep hinge fracture. They are usually irregular in shape and can be quite broad and thick. Their length ranges from 3 to 13cm; this shows that they were manufactured throughout the whole reduction process (Tab. 39). They seemed to remove a large volume of the raw material from the core; in Layer 6b they removed as much volume as the *éclat débordant* (Fig. 33, 35). Their dorsal scar patterns indicate the preferential use of unidirectional debitage, but bidirectional is also quite often employed (Tab. 40). Their striking platforms are plain, faceted, punctiform and sometimes dihedral (Tab. 41). Half of them present small patches of cortex on the upper surface.

6.4.8 Hinges

Hinges occur when the angle between the platform and the flaking surface of the core is not adjusted (Crabtree 1982, 37). The plane of the fracture turns abruptly towards the outside and produces a flake with blunt and smoothly rounded edges. To continue flaking, an intentional correction of the flaking angle is required. Numerous hinged flakes were discovered in layers 6b and 6h, and only a few in layers 6a and 7c (Tab. 42). They are mostly unidirectional but bidirectional examples are also present, especially in sandy Layer 6h (Tab. 43). Their butts are faceted, plain, and punctiform, but only rarely dihedral (Tab. 44). Their length ranges between 3 and 9cm in Layer 6b

and 4 and 12cm in Layer α h, showing that this kind of error happened frequently throughout the reduction progression. In Layer 6b the median length of hinges is only 4.5cm, and only a small volume of raw material, with a median size of 10cm³ and a range of 1.3 to 30cm³ (Fig. 32, 33), appears to have been removed. However, in Layer α h these pieces are quite long, with a median length of 7cm, and would have involved removing a significant amount of raw material (Fig. 35). More than 50% have a volume larger than 20cm³, ranging up to 50cm³ (Fig. 36).

Once again the metrical data show clearly that the flint knappers from sandy Layer α h disposed of, or chose to use, longer blocks of raw material than those from Layer 6b. The metrical data also show that they stopped the debitage when the core length approached 4cm.

5.4.9 Plunging

Plunging happens when the fracture plane turns abruptly in the direction of the centre of the lithic specimen and the removed part of the core. This occurs when the flaking angle is too acute and the flaking surface is too bowed (Cotterell and Kamminga 1987, 701). The negative of such a removal – and the removal itself, with its thick distal end – is very characteristic. A plunging termination is more likely if the point of impact is located further away from the edge of the core on the striking platform (Cotterell and Kamminga 1987, 701). Plunging is usually defined as a knapping error, but sometimes it can be undertaken intentionally, similar to the intentionally overshot *éclats débordants* of the Levallois reduction strategy, for example (Meignen 1995).

Plunging is well represented in the group of CTE in layers 6b and α h. They can be as long as 14cm and as short as 3cm (Tab. 45). They are not very thick, but their distal end with the removed part of the core can be important, so such flakes can remove a big portion of the raw material from the core. Their dorsal scar patterns show that unidirectional debitage was employed most often, but that bidirectional was also in use (Tab. 46). Their striking platforms can be faceted, cortical, plain or punctiform (Tab. 47). In Layer 6b, half of the plungings show cortex coverage of 25 to 75% on their

upper surface; the cortex appears on the distal or medial-distal part of the specimen. The items covered by cortex are longer, broader and thicker than those without cortex coverage, indicating that the decortication of the distal part of the cores did not matter. The cortex was removed as the reduction progressed.

6.4.10 Summary

Comparing now the two elements associated with the Levallois technique – specimens with cortical backs and classical *lames débordantes* – it appears that in Layer 6b the latter are slightly longer, with a median length of 5.7cm, and about 60% are considerably longer, up to 9.7cm. The rest, starting from 3cm, are shorter. Those with cortical backs have a median length of 5cm; more than 50% rise to 8cm (equalling or exceeding the median of specimens with prepared backs, or *éclats débordants*); and the remainder are smaller, going down to 2.5cm. Specimens with cortical backs show a median volume of 30cm³, while the median volume of *éclats débordants* is 22cm³ (Fig. 33). It seems that the cortical elements were generally removed from smaller blocks than the *éclats débordants* and that even some of very small cores were then still covered by cortex, since about 20% of cortical-backed items are smaller than 4cm. Consequently, the *éclats débordants* were detached from longer blocks of raw material, as their length ranges between 4cm and 12cm, or they were simply not created on cores smaller than 4cm. But 50% of those which show cortex coverage of 10 to 30% are shorter and thicker than those without cortex coverage and have a median length of 5cm exactly, the same as is observed in specimens with cortical backs. It appears that pieces with cortical backing and those with prepared backing with cortex coverage were often detached from smaller cores than the *éclats débordants* without cortex coverage and that the flint knapper clearly used different block sizes to manufacture Levallois-like products.

In Layer 6a the specimens with cortical backing are longer, with a median length of 8.4cm; about 60% are longer, reaching up to 10.6cm. The *éclats débordants* with prepared backs are shorter, with a mean length of 7.6cm, and only 35% of them are longer than the median length of 8.4cm. But taking into account *éclats débordants*

with cortex coverage (and these are always less than 25% of the total), their median length equates to 8.6cm, with more than 50% of these elements being longer. In both cases the median volume approaches 40cm³ (Fig. 35). This shows that, in contrast to the first assemblage, these two backed elements could be removed from blocks presenting roughly the same size.

For the Laminar CTE, three types were considered: Laminar edge-flakes with cortical backs, those with plain backs, and semi-crested. In Layer 6b the median length of all three is approximately 6cm, with semi-crested being the longest at 6.3cm, and specimens with cortical and plain backs the shortest at 6.1cm. 50% of these are longer than this median, ranging up to 12cm for semi-crests and 10cm for the cortical backed. The rest can be as small as 3cm for cortical and 4cm for semi-crests (Fig. 32). They all present the same median volume of approximately 20cm³ (Fig. 33). These three types seem to be similar in respect to their metrical attributes, especially the elements with cortical and plain backs, since they show the same median length and thickness, and vary only slightly in width (2.8cm plain; 3cm cortical back). The semi-crested seem to be slightly longer (6.3cm), narrower (2.5cm) and thicker (1.4cm). These metrical differences between the semi-crested and backed elements become more pronounced with in-depth investigation into unilateral and secondary crests. The former are significantly longer, with a median length of 7.6cm, compared to 6.3cm, and also thicker; the median thickness is 1.7cm against 1.4cm.

To conclude, it seems that it was correct to separate the unilateral crested from the secondary crested. The latter, although thicker and slightly narrower, present the same length as the backed items, confirming that they were used simultaneously with other backing elements to shape out the flaking surface during debitage, rather than as an opening crest.

In sand Layer αh, semi-crested edge-flakes are the longest Laminar items, with a median length of 9.4cm. However, only 30% are longer than the median, after the specimens with cortical backs with a median of 8.2, with also only 30% being longer than the median of the semi-crested. Finally, those with a plain back have a median of

6.2cm, and only approximately 16% have a median greater than that of the semi-crested. The remainder can be as small as 3.8cm for plain-back specimens, 4.8cm for semi-crested, and 5.5cm for cortical back pieces. It seems that the longest edge-flakes have the important cortical back covering between 25% and 75% of the upper surface. Semi-crested edge-flakes were employed as opening flakes, using the natural shape of the block of raw material. They were further employed for shaping the convexity of the flaking surface. The ones with cortical backs were probably used to some extent in spreading the flaking surface onto the flanks. The items with plain backs were produced once the flaking surface was deprived of cortex.

In both layers, the large majority of specimens featuring greater than 25% cortical coverage of the upper surface are longer, wider and, most significantly of all, thicker than pieces with little or no cortex coverage, showing again that cortex was removed step by step as the reduction advanced.

Comparison of all CTE from both layers shows that the items from Sand α h are significantly longer. It seems that the flint knappers who left their products in the sands had available or chose to use longer blocks of raw material than the flint knappers from Layer 6b, and did not maintain cores smaller than 4cm in length.

6.5 Non-retouched blank blades

6.5.1 Introduction

Blades are the best-represented category of debitage in the analysed assemblages. The large majority of CTEs are elongated, and the scar patterns visible on the discarded cores confirm that the blade morphology was the most desired.

As in all the present collections, different core reduction strategies seem to have been employed, and it is often difficult to determine which products stem from which reduction. The negatives on discarded cores suggest that the analysed Laminar cores had to produce a number of blades with a thick cross-section and parallel or convergent ridges. However, the flaking surface often became flatter as the reduction advanced, so that specimens with a rather flat section might also be obtained.

Additionally, if the flaking surface moved from the narrow side of the core (working on the thickness of the block) onto the wide side, blanks with a rather flatter cross-section could be also produced.

The core shape for blade reduction seems to affect blade width and thickness: a wide-faced core will produce broad, thin blades, while a narrower-faced core will produce narrow, thicker blades (Pelegrin 1984).

The Levallois method could also produce blades with parallel edges (Meignen and Bar-Yosef 1991:56) and points of different morphologies. Furthermore, the Levallois point can be a result of different operational schemas (Marks and Volkmann 1983, 1987, Boëda 1995:45). Finally, some blades could also be by-products of Levallois point production.

All blade-blanks in all layers were analysed together and, where possible, separated into three groups: prismatic, Levallois and indeterminate. They were then analysed independently. The bladelets were also studied individually.

6.5.2 Lithic analysis

The metrical properties of blades vary between the layers (Tab. 48). For blank blades from layers 6b, 6c2, 7c and Sand α h, the relationship between the length and the layer is only marginally significant ($F=3.115$, $p=0.026$), at the 92.5% confidence level. The group of means are very similar between layers 6b and α h, whilst in layers 6c2 and 7c they are more variable. This is probably due to the small sample sizes. 35% of blades from Layer 6c2 are related to 6b and α h in their length, whilst those from Layer 7c are more separate but related in more than 30% of cases to Layer 6c2 (Fig. 37). In *in situ* layers the length of blades varies between 4 and 11cm, with several specimens from Layer 6b reaching 16cm (Fig. 38). In layers 6b and 6c2, the bulk of blades present a length between 6 and 8.5cm and in Layer α h they are very similar, whilst reaching 9cm. The coefficient of variation (CV) of length means for layers 6b, 6c2, and 7c and α h is 0.3 and reflects the same variability in length measurements in all these layers (Tab. 49).

For blank blades from layers 6b, 6c2, 7c and Sand αh, the relationship between the width and the layer has significance ($F=4.711$, $p=0.0027$). Their widths range between 1.2 and 4.5cm, with a few exceptions that reach 6.5cm in layers 6b and αh (Fig. 38). However, in all layers the majority of blades have a breadth between 2 and 3.3cm, with some small discrepancies between layers. Plotting the group means, it becomes clear that the widths of blades from Layer 6b are disassociated from those of Sand αh, whilst the three other layers seem to be more closely related (Fig. 40). The CV of width means for layers 6c2, 7c and αh is 0.3, indicating that these three samples have the same variability in width measurements. The CV for Layer 6b is 0.2, showing that the distribution in width in this assemblage is marginally different from that of other layers.

The dissimilarity perceived in L/W ratio of blank blades from all four layers is highly significant ($F=10.22$, $p=0.0001$). The L/W ratio ranges between 2.4 and 3.3, indicating that the analysed blades are considerably elongated. The most elongated are the specimens from layers 6c2 and αh; 50% of them have an elongation ratio of approximately 3 (Fig. 40). The less elongated are blades from Layer 6b, with only 20% of blades having a ratio of 3 or above. Layer 7c, where 15% present an elongation equal to or greater than 3, has the least elongated blank blades. The plot of mean groups shows that the major portion of blades from Layer 7c have an elongation smaller than 2.6, whilst all other layers have a higher elongation ratio (Fig. 42).

For blank blades from layers 6b, 6c2, 7c and Sand αh, the relationship between thickness and layer is highly significant ($F=27.19$, $p=0.0001$). The thickness of blank blades ranges between 0.4 and 2.6cm in all layers (Fig. 43). However, the greater part of specimens from Layer 6b present a thickness between 0.8 and 1.2cm, and the blades from layers 6c2, 7c and Sand αh seem to be thinner. Approximately 10% of blades from Layer 6c2 and Sand αh have a thickness smaller than 0.4cm. The CV of mean thickness for layers 6b, 7c and αh is 0.4 and specifies the same variability in breadth in these three samples. The CV for Layer 6c2 is 0.3 and again displays a slightly different variability in thickness. The plot of group means illustrates those differences more clearly (Fig. 44). Layer 6b is noticeably isolated from other layers, which are

characterised by significantly thinner blades. Sand αh is connected to Layer 7c and disconnected from Layer 6c2. These last two layers are the most closely related; more than 50% of their blank blades are similar in their breadth.

The difference observed in the width/thickness (W/T) ratio in blank blades from all four layers is also significant ($F=15.60$, $p=0.0001$). The W/T ratio shows that the blades from layers 6c2 and 7c are thinner than those from layers αh and 6b. The blades from 6b appear to be the largest (Fig. 45). It is even more evident if we plot the group means with 95% confidence intervals (Fig. 46). Layer 6b is clearly different from the other layers, whilst layers 7c and αh as well 6c2 and 7c seem to be partially related. The length/thickness ratio confirms that the blades from Layer 6c2 are the most slender, and those from Layer 6b, the most robust (Fig. 47).

The large distribution in length, width and thickness in blank blades in layers 6b, 6c2, 7c and αh shows that they had to be produced during the whole reduction process and that while a particular dimension was not important, the overall morphology of the blade was important. In layers with a small number of lithic artefacts, the lack of patterning with respect to the dimensions is also visible.

The artefacts from Layer 6b seem to be the most robust. They are the thickest and the broadest. On the other hand, it is believed that this is linked to the taphonomic history of the layer. Only intact items were measured for this metrical analysis, and it seems that the more robust specimens did not undergo the breakage that the thinner items did. Analysis of intact items, and of broken items which encompass two parts together, suggests that their thickness, mean and median of 0.9cm, as well as their width, mean and median 2.6cm, are smaller. These results, alongside the statistical analysis (which this time also took into consideration the broken pieces), confirm that the difference observed in the width of blank blades from all four layers is not significantly different ($F=0.2342$, $p=0.87$). But there are still significant differences in their thickness ($F=12.4$, $p=0.0001$). The blades from αh are slightly longer, but also thinner. The coefficient of variation of length in all layers is the same; the CV of mean width and thickness is similar for three layers and varies slightly in the case of layers 6b and 6c2,

respectively. From a metrical perspective, the blank blades from layers 6b, 6c2, 7c and αh appear to be comparable in respect to their length and width; only their thickness differs.

Excluding those that are broken, the butts are in the main faceted or plain; less often they are dihedral or punctiform. They are rarely cortical; a few from layers 6b and αh are lipped (Tab. 50). Nonetheless, the faceting of large numbers of butts suggests that it was not used judiciously. It seems to be an after-effect of the elimination of overhangs left by previous removals and adjustment of the flaking angle (ex. Tixier 1972, 136). This idea can be reinforced by results taken from analysis of the flaking angles of blades: plain vs. faceted butts. The former have a flaking angle approaching 110° , with a mean of 98° , whilst in the latter group the flaking angles lean towards 90° , with a mean of 93° (Tab. 51). The difference observed in the W/T ratio of butts of blank blades from layers 6b, 6c2, 7c and αh has high significance ($F=6.448$, $p=0.0003$).

The mean width and thickness of striking platforms varies slightly between layers and can range from 1.5 to 2cm and from 0.4 to 0.7cm respectively. The W/T ratio of intact blank blades from layers 6b, 6c2, and 7c and αh ranges between 0.8 and 9 and varies significantly among layers. Only a small number of items present a narrow and thick striking platform – a ratio of less than 1 in layers 6b and αh . 50% of Layer 6b and 25% in layers 6c2, 7c and αh show a value of around 2, signifying that the butt is twice as wide as it is thick. 50% from Layer 6b and 75% from layers 6c2, 7c and αh exhibit values bigger than 2.5, indicating that those platforms are thin relative to platform breadth (Fig. 47). The CV for butt W/T ratio shows a similarity between layers 7c and αh , and a different variability in mean ratio between other layers (Tab. 49). The plot of means of butts W/T shows the central tendencies in the sets with 95% confidence intervals. Layer 6c2 presents similarities in this ratio with all three other layers and is the best connected to layers 7c and Sand αh . The blades from Layer 6b have the lowest W/T ratio of butts, so distinguishing this layer from Layer 7c and the sand layer, whilst only 10% of butts in Layer 6c2 present similar dimensions (Fig. 48).

In all layers, the shortest and the longest blank blades present a faceted or dihedral butt, and the mean length of blank blades with a faceted or dihedral striking platform is higher than those of blades with plain butts. This indicates that control was exercised continuously over the platform angle of a core.

In Layer 6b, 16% of blades present small cortex coverage (from 10 to 30%) on their upper surface. In layers 6c2 and ah, the figure is 29%. The cortex appears on the distal part in the main, but in a few it appears on the medial and proximal ends of the blades. In all three layers the blades with cortex coverage are longer, broader and thicker than those lacking cortex (Tab. 52). This suggests that the decortication of a core's flaking surface was not undertaken and that the length of the flaking surface decreases during a reduction. This conclusion can be reinforced with the results obtained from the plunging elements, where the longest, broadest and thickest pieces are covered by cortex, while the shorter and less robust specimens present no cortex at all on their upper surface.

In all layers, the majority of blades are bowed in longitudinal section along their whole length, sometimes partially on the medial-distal portion, or (rarely) on the proximal-medial part of the specimen. 16% of blades are non-curved in layers 6b and ah, and the remainder are bowed. Just a few are twisted. Their medial cross-section is mainly 60% trapezoidal and 40% triangular in all layers. The broadest part of the specimen is usually located in the middle section, after which comes the proximal part. Only rarely is the distal part thickest (Tab. 53).

More than 50% of blades from layers 6a and 6b present parallel lateral edges, 40% are converging, and only a few are expanding. In other layers, the blades with converging lateral edges are the best represented, followed by those with parallel edges, and finishing with several with expanding edges (Tab. 54).

The dorsal scar patterns show that unidirectional parallel debitage was most frequently employed, followed by bidirectional and then (rarely) unidirectional convergent. The frequency of use of uni- and bidirectional flaking varies between layers, but both are always used simultaneously. Bidirectional debitage seems to become very important in

layer 6c2 and especially in αh . The use of crossed debitage is extremely rare: just one item from Layer 6b and three from Layer αh exhibit such a flaking method (Tab. 55).

The majority of blades show three or more previous scars on their upper surface (Tab. 56).

Preparation of the proximal part of the blank seems to have been undertaken often, although the frequency of this technique varies between layers, encompassing from 40 to 70% of non-retouched blades (Tab. 57). Dorsal reduction is also visible in all layers and appears to have been used most often in layers 6c2, 7c and αh .

Points of percussion were usually placed well back on the platform. They were often punctiform and were placed in most cases behind the central ridge or to the side of one ridge. In a few cases, it was between two central ridges (Tab. 58).

Bulbs are usually pronounced, although sometimes diffuse. The conchoidal fracture marks are generally well visible, and the point and cone of percussion is in most cases clear. All this evidence indicates the use of hard hammer direct percussion. A few examples of lipped butts, always accompanied by a diffuse bulb, suggest the use of soft hammer percussion (ex. Ohnuma and Bergman 1983, 169; Pelegrin 2000, 77-80,) but this mode seems to have been employed only marginally.

The blank blades from all analysed layers encompass a number of specimens with different morphologies. A portion of them show features which could be associated with Levallois technology (Fig. 136, 154, 155). They are relatively thin in comparison to Laminar, slightly convex in section, and have a well-prepared, often long and thin butt. The others show larger variability in their widths, and are thick, triangular or trapezoidal in cross-section; they are often bowed, with plain or slightly faceted butts, and can be related to Laminar debitage. Blanks presenting either of these characteristics were separated, but between these groups there are a significant number of blanks that, because of their ambiguous morphology and with respect to their metrical attributes, are somewhat problematic. They may have been struck from either Levallois-like cores or from Laminar cores as their volume reduced and as they became flatter.

6.5.2.1 Prismatic blank blades

These blades were categorised as prismatic because they present a high, triangular or trapezoidal cross-section in their midpoint, and plain or slightly faceted striking platforms. They are frequently bowed, and sometimes have a rectilinear longitudinal section.

Prismatic pieces present in most cases the unidirectional scar pattern, but bidirectional is also represented, especially in Layer αh , where it represents 47% of items (Tab. 63). On the upper surfaces there are usually three or more previous scars. Those with two scars are less well represented, showing that the pieces were detached throughout the reduction.

The lateral edges converge or are parallel, but are rarely expanding (Tab. 64). In profile they are frequently bowed on the whole length or on the proximal-medial or medial-distal end, and less often rectilinear, indicating that the flaking surface of the core from which they were produced must also have been convex. The broadest part of the specimen is regularly found in the middle portion, less often in the proximal portion, and only occasionally in the distal portion (Tab. 65). The preparation of the proximal part of blades and dorsal reduction seems to have been undertaken quite often, especially in layers 6c2 and αh (Tab. 66)

The striking platforms of the most prismatic blank blades are plain or slightly faceted by just two or three blows (Tab. 67).

The cortex usually appears in small patches, sometimes covering more than 25% of the upper surface of items and was observable in 20% of prismatic blades in Layer 6b, and in 38% in layers 6c and αh . It covers the most frequently the distal, followed by the proximal and least frequently the medial part of specimens. The mean length and width of cortical pieces in all layers is significantly greater than those of items without cortex coverage. This indicates that cortex was not peeled from the ends and the flaking surface of the core before the reduction started, and also that the cortex was removed as reduction advanced.

Next to attribute analysis, the metrical features of the prismatic blanks across the three layers 6b, 6c2 and α h are also studied (Tab. 59, 60, 61).

The differences observed in length and width of prismatic blades from all three layers were not significant ($F=0.7100$, $p=0.49$; $F=1.958$, $p=0.14$ respectively). The length of these blades ranges between 4 and 14cm and the median approximates to 8cm (Fig. 49). Although the specimens from Sand α h are slightly longer, they present a very similar length pattern to those from Layer 6b, and the CV in both layers equals 0.3. In Layer 6c2 the maximal length is smaller and the minimum length is higher than in the two former layers, and the CV is dissimilar, =0.2 (Tab. 62). The central tendencies in the presented group show that 95% of blades from Layer 6b, and more than 80% from 6c and α h, are of similar length (Fig. 51a).

The widths vary from 1 to 4.6cm, the median values of layers 6b and α h are similar at 2.9cm and 2.7cm respectively, and the median from Layer 6c2 seems to be smaller, 2.3cm (Fig. 52). But the CV in all layers is 0.3, indicating the same intra-layer variability. The plot of the group means indicates the connection in thickness between all layers. Approximately 70% of blades from Layer 6b and 30% from 6c2 and α h display similarities in length, but 65% from layers 6c2 and α h are narrower than those from Layer 6b (Fig. 51b).

The variation perceived in the thickness of prismatic blank blades from layers 6b and α h is highly significant ($F=26.28$, $p=0.0001$). The thickness ranges between 0.4 and 1.8cm, the medians of which are very similar to those from layers 6b and α h (1.1 and 1cm respectively). In Layer 6c the median is considerably smaller, at 0.7 (Fig. 53). The CV of thickness in all layers is 0.3. Observing the dominant tendencies in all sets, it can be recognised that all are separated from each other (Fig. 54). The bulk of blades from Layer 6b appear to be the thickest, and those from Layer 6c, the thinnest, with blades from Sand α h coming in between.

The W/T ratio of butts of prismatic items varies between 0.6 and 6 with a median of 2.3 for Layer 6b, 2.8 for Layer 6c2 and 2.5 for Layer α h (Fig. 55). The CV for the W/T ratio of butts is 0.4 in the case of layers 6c2 and α h and differs from Layer 6b, giving a

value of 0.3. The butts from Layer 6b are the most robust, and those from Layer 6c2, the narrowest.

The L/W ratio diverges from 2 to 5.3, and the medians of blanks from all three layers are similar, with values of 2.7 for layers 6b, 2.8 for 6c2 and 2.9 for αh (Fig. 56). The W/T ratio ranges between 1 and 5.3 (Fig. 57). The median of layers 6b and αh approaches 2.6 and 2.8 respectively, while the high median of 4.1 from Layer 6c2 indicates the presence of very thin specimens.

To summarise, it seems that prismatic blades from all three layers are fairly similar from the statistical perspective. Only their thickness separates them. Their non-metrical attributes also appear to be highly analogous in all the analysed layers.

6.5.2.2 Levallois-like blank blades

Specimens are considered as Levallois if they show a rather plane trapezoidal cross-section, although a number of pieces present fairly concave cross-sections. They are seldom triangular, the platforms are usually well faceted, and they have a faintly curved or rectilinear longitudinal section. Specimens from three layers – 6b, 7c and αh – were examined. Unfortunately, the sample from Layer 7c is very small, so care must be taken with any interpretation.

The dorsal scar pattern of Levallois blank blades shows that unidirectional reduction predominates in layers 6b and 7c; but in αh , bidirectional is slightly higher, being visible on 51% of specimens (Tab. 63). In all layers, three or four negatives of former detachments are visible on the upper surface of blades, and their lateral edges in most cases converge; few are parallel (Tab. 64). They are usually faintly bowed in profile along the whole length or on the distal-medial part of the specimen (Tab. 68). They are largest in their proximal or medial part (Tab. 65) and often present the preparation of the proximal end and the reduction of the dorsal surface (Tab. 66). The striking platforms of these blank blades are mostly faceted, and sometimes plain, cortical or punctiform. The faceting is cautiously completed through numerous small removals.

Cortex seldom appears on the Levallois-like blank blades. Only four pieces from the layers and eleven from the sand layer, which is 13% of assemblages in both layers, have small patches of cortex (less than 25%) on their proximal and sometimes distal ends. None of the pieces from Layer 7c presents cortex coverage. This indicates that the flaking surface was regularly cleaned of cortex or that the block selected for such flaking was already deprived of cortex, but that occasionally the cortex was left on the proximal and distal part of the cores. This can also be seen from the very small number of cortical butts. 50% of *lames débordantes* from layers 6b and α h carry small patches of cortex on their medial, proximal and distal parts; these specimens were the longest and the widest among the *lames débordantes*, indicating that only a small amount of cortex was present on the surface, and suggesting as well the use of already decorticated cores (Fig. 113: 7, 8). 2

The variation perceived in the length of all three sets of Levallois blank blades from layers 6b, 7c and α h is not very significant ($F=2.676$, $p=0.073$) at the 92% confidence level. The plot of group means shows that all sets are, to different extents, overlapping each other (Fig. 58). The length varies from 4 to 11cm with a median of 6.8cm for layers 6b, 6.2cm for 7c and 7.4cm for α h (Fig. 59). The CV for length is the same in the case of layers 7c and α h and gives a value of 0.3, whilst for Layer 6b it is 0.2.

The difference observed in width and thickness of Levallois-like blank blades from all three layers has no statistical importance ($F=1.622$, $p=0.20$; $F=2.325$, $p=0.10$ respectively). The widths range between 1.4 and 4.7cm; the medians of layers 6b and α h are similar, with values of 3cm and 2.8cm respectively; and the smallest, 2.4cm, derive from Layer 7c (Fig. 60). About 30% of blades from Sand α h and 60% from Layer 7c are narrower than those from Layer 6b. 47% of blades from the latter layer are wider than the blades from 7c and the sand (Fig. 61). The CV for width is 0.2 in layers 6b and 7c and 0.3 in Layer α h.

The thickness varies from 0.4 to 1.1cm, with the same median (0.7cm) for layers 6b and α h, with 0.6cm for Layer 7c (Fig. 62). The plot of group means illustrates that 48% of blades from Layer 6b are thicker than those from other layers and that 47%

from Layer 6b and 95% from Sand α h are very similar in their thickness (Fig. 63). The CV for thickness in layers 6b and 7c is the same (0.2), varying slightly to 0.3 in Layer α h.

The W/T ratio of butts ranges from 1.3 to 9, and the medians in all layers are comparable with the values of 3.7 for layers 7c and α h and 3.8 for Layer 6b (Fig. 64). The CV for W/T ratio of butts is 0.5 for both layers 6b and 7c, differing slightly to 0.4 in Layer α h.

The index of elongation (the L/W ratio) varies from 2 to 4.2, with an approximating median for layers 6b and 7c of 2.3 and 2.4 respectively, and a higher value of 2.6 for α h (Fig. 65).

The W/T ratio ranges between 2 and 6.8 with the same median (4.2) for layers 6b and α h and a slightly lower median for 7c, equalling 4. In all layers, more than 50% of blades have a W/T ratio greater than 4, indicating rather thin lithic items (Fig. 66).

The Levallois-like blank blades from the three analysed layers give the impression of being closely related to each other in respect to their metrical and non-metrical features. The pieces from Layer α h appear slightly more elongated and those from 6b slightly wider, but these differences are not significant.

6.5.2.3 Indeterminate blank blades

The remaining blades, which fitted neither the Levallois nor the prismatic group, were categorised as indeterminate, and were examined separately to observe their features compared to those of other reduction strategies. The analyses were made on unbroken specimens uncovered from layers 6b and α h. In other layers, the number of items categorised as indeterminate was too small to undertake metrical analysis.

In both layers the indeterminate blank blades are generally unidirectional, but the bidirectional reduction is also present and is better represented in Sand α h. As before, the upper surface of specimens shows three or more negatives of previously detached items, with their lateral edges converging or, less often, parallel. They are usually curved along the whole length, and are sometimes rectilinear in profile. The broadest

part of the lithic specimens is the proximal or medial part. They show large numbers of specimens with prepared proximal ends and with dorsal reduction.

The platforms in both layers are frequently plain and slightly faceted, and sometimes cortical and dihedral. Only six pieces, or 10% of this set, carry a small patch of cortex on their proximal, medial or distal end. As with the former two categories, those exhibiting cortex are longer than those without.

Statistical analysis shows that length ($t=1.85$, $p<.05$), width ($t=-3.21$, $p<.05$) and thickness ($t=-8.04$, $p<.05$) differ significantly between blades coming from both layers. The length ranges between 3.4 and 13cm in Layer αh and between 5 and 10cm in 6b. The median in the former layer is 6.9cm, and in the latter, 7.4cm (Fig. 67). The CV for length is dissimilar, giving a value of 0.2 in Layer 6b and 0.3 in αh , reflecting the different length distributions within the layer.

Twenty percent of blades from Sand αh have a width smaller than 2cm, and the rest range up to 4cm with a median of 2.6cm. In Layer 6b the width varies from 1.9 to 3.9cm. Only 5% of blades have a width smaller than 2cm. The median is higher than in the former layer, giving a value of 2.9cm (Fig. 68). The CV for width varies, with 0.1 for Layer 6b and 0.3 for Sand αh .

The thickness in Layer 6b ranges between 0.6 and 1.1cm, with a median of 0.9cm. Only 25% of blades have a thickness greater than 1cm, and in 12% it is less than 0.7cm. In Sand αh the breadth varies from 0.3 to 1cm, with a median of 0.7cm. In 50% of specimens a thickness less than 0.7cm was documented, with 50% being greater than 0.7cm (Fig. 69). The CV for thickness gives values of 0.2 in Layer 6b and 0.3 in αh . The pieces from the sand seem to be significantly thinner.

The W/T ratio of platforms in this category ranges between 0.7 and 4.6, with a median of 2.7 in Sand αh , and between 0.8 and 3.6 with a median of 2.2 in Layer 6b. 60% of blank blades from Layer 6b have a ratio around 2, indicating that the butts were roughly rectangular in shape. Only 25% present a higher ratio than 2.5; 11% are

between 2.5 and 1, and 4% are smaller than 1, indicating narrow and thick platforms respectively (Fig. 70).

In Layer αh 55% of items have a ratio greater than 2.5cm, showing that the majority of pieces have a rather thin platform relative to platform breadth, 30% have a ratio around 2, and only 4% – like those in Layer 6b – less than 1. The CV for this ratio varies in both layers, giving a value of 0.3 for Layer 6b and 0.4 for sand. The L/W ratio varies from 2 to 3.7 in Layer 6b, and from 2 to 4.7 in sand Layer αh . The median in 6b is 2.4, with 50% of specimens presenting a greater ratio and 50% a smaller one. Sand Layer αh has a median of 2.9 and only 25% of pieces have a ratio smaller than 2.4, the median of the previous layer, indicating that the items from sand Layer αh are significantly narrower than those from Layer 6b (Fig. 71).

The W/T ratio ranges between 2.3 and 4.6 in Layer 6b and between 1.5 and 6.3 in sand Layer αh . The median of Layer 6b is 3.3, with 55% of items having a lesser ratio, and 45%, a higher ratio. In the sand the median is 3.6, with 30% of pieces presenting a ratio smaller than 3.3, the median of 6b. The remainder have a greater ratio, signifying that more specimens in this layer are gracile than those from 6b (Fig. 72).

Unlike the two previous categories of blank blades, the indeterminate blades seem to be considerably different in their metrical constructions, although the non-metrical attributes unite them again.

6.5.2.4 Comparison between Prismatic, Levallois and Indeterminate blank blades from layers 6b and αh

6.5.2.4.1 Metrical analysis

The differences observed in the length of prismatic, Levallois and indeterminate blank blades from layers 6b and αh have high significance ($F=8.868$, $p=0.0002$; $F=11.28$, $p=0.0001$ respectively). But then, in both layers the median length is similar in the Levallois and indeterminate blank groups, whilst the prismatic blades appear to be considerably longer (Fig. 73, Fig. 74). This is better expressed if the group means are

plotted with 95% confidence intervals (Fig. 75, 76). The mean length of the prismatic group in 6b and αh seems to be separate from that of the two other groups, which are not significantly different ($t=0.04$, $0.1 > p > .05$; $t=-0.07$, $0.1 > p > .005$ respectively). Their CV for length is also the same, at 0.2.

In layers 6b and αh , the relationship between the width and the category of blank blade is not important ($F=0.6757$, $p=0.51$; $F=3.63$, $p=0.032$ respectively). In both layers the median widths are similar (Fig. 77, 78), but in Layer 6b the CV for width is slightly dissimilar in all three categories of blank (Tab. 62), whilst αh gives the same value.

The variation perceived in the thickness of all three sets of blank blades from layers 6b and αh is highly significant ($F=52.16$, $p=0.0001$; $F=88.61$, $p=0.0001$ respectively). In Layer 6b, the median as well the mean thickness of prismatic blades is greater than those from the Levallois and indeterminate groups (Fig. 79). But the thicknesses between the two latter groups are also unrelated. About 70% of indeterminate blank blades have a mean thickness higher than that from the Levallois. The CV for length varies in all three categories of blank (Tab. 62). In Sand αh , the prismatic blades are similar to those in Layer 6b, the thickest (Fig. 80), whereas the median and the mean thickness of Levallois and indeterminate blades are the same. The CV for thickness is identical in all three categories of blank blades.

In layers 6b and αh , the relationship between the LW ratio and the blank blade type is highly significant ($F=7.279$, $p=0.0009$; $F=7.950$, $p=0.0004$ respectively). The median and mean of the L/W ratio for all three groups in Layer αh are higher than in Layer 6b, indicating that the blades from the previous group are more elongated. In Layer 6b the median ratio of Levallois and indeterminate blades is comparable (Fig. 81). The ratio of prismatic blades is considerably higher, and they are separated from the two previous categories. The situation in Layer αh appears to be slightly different; the L/W ratio of prismatic and indeterminate blank blades seems to be similar, whilst those from Levallois are smaller (Fig. 82). Now, considering the plot of the group means with 95% confidence intervals, it can be shown that the blades from the indeterminate

group share the ratio value of about 20% with prismatic and Levallois blades, whilst the prismatic blades seem to be totally disassociated from the Levallois (Fig. 83, 84).

The difference detected in the W/T ratio in prismatic, Levallois and indeterminate blades is highly significant in both layers ($F=80.89$, $p=0.0001$; $F=76.94$, $p=0.0001$ respectively). The median and mean of this ratio are dissimilar in all three types of blank blades from layers 6b and αh . The highest ratio observed was in the Levallois blades, and the lowest, in the prismatic blades (Fig. 85, 86). The plot of the group means with 95% confidence intervals in Layer 6b clearly shows the separation of the ratio between groups, whilst in Sand αh the indeterminate blades seem to be more connected with the Levallois than with the prismatic blades (Fig. 87, 88).

In layers 6b and αh the relationship between the W/T ratio of platform and the blank blades type is highly significant ($F=30.71$, $p=0.0001$; $F=25.66$, $p=0.0001$ respectively). In layers 6b and αh , the medians of this ratio in prismatic and indeterminate blades are similar and their CV for W/T of butts is the same (Fig. 89, 90). The median and mean of the W/T butts ratio from the Levallois group is in both layers appreciably higher and seems to be totally detached from the two previous types of blank blades (Fig. 91, 92). It appears that in both layers the width of the three categories of blank blades is an unimportant feature.

Conclusions from metrical analysis

The length and thickness of the prismatic blades separates them from the Levallois and the indeterminate blades, which are rather similar in length, and also from the thickness of blades found in Sand αh . The ratio of elongation shows similarities between the indeterminate and Levallois blades in Layer 6b and between all three types in Sand αh . The W/T ratio is generally dissimilar in both layers. The W/T of striking platforms is comparable between the prismatic and indeterminate categories in both layers, showing the highest values for the Levallois type and the smallest for the prismatic. It appears that all categories of blank blades in both layers share certain metrical features. In Layer 6b the thickness seems to be the most dissimilar value between three types of blades. The Levallois and indeterminate blades are similar in

length and width and consequently in LW ratio; the prismatic specimens are less related to the Levallois group (other than in width), whilst sharing some similarities with the indeterminate group with respect to the W/T ratio of butts. Similarly, the prismatic blades from Sand oh appear to be separate from the Levallois and show certain parallels to the indeterminate blades in respect to the W/T of striking platforms and the LW ratio. The Levallois and indeterminate blades present resemblances in length, width, and thickness and consequently in the LW and W/T ratios, but they have a dissimilar W/T ratio to butts. Seen in this perspective, the Levallois and indeterminate blades from Sand oh may be fairly closely related, even if the mean and median of W/T of their butts are quite different. Only 10% of blades from the indeterminate group present a W/T of butts smaller than the minimal W/T of butts in the Levallois collection. In Layer 6b, things are different: 30% of indeterminate blades have a W/T ratio of butts smaller than the minimum in the Levallois category, and a high connection between those two categories appears less likely than in the previous case.

6.5.2.4.1 Attributes analysis

This section considers the non-metrical characters of three types of blank blades in 6b and the sandy layer. In Sand oh the dorsal scar patterns visible on the upper surfaces of blank blades show that bidirectional reduction was very important in this set. 51% of Levallois blades present this kind of reduction, with the remainder (43%) being unidirectional parallel or convergent. 38% of indeterminate specimens document bidirectional debitage, and 61%, unidirectional parallel. 47% of prismatic blades show bidirectional negatives, and the rest, unidirectional parallel. In Layer 6b unidirectional debitage prevails in all categories, but bidirectional is also well represented in the prismatic and Levallois groups, giving values of 25% and 23% respectively. Bidirectional is less noteworthy in the indeterminate group, with only 14%. The specimens from the three groups in layers 6b and oh present the smallest number of pieces with only two previous negatives; the rest have three or more scars on their upper surface, but the Levallois group has the smallest percentage of items, with only

two former scars. The pieces with converging edges are in all categories and in both layers the most current, after those with parallel edges. In both layers the indeterminate blades show mostly plain and slightly faceted striking platforms, whilst in the Levallois set well-faceted butts predominate, with a very small number of plain butts. The pieces from the prismatic group have slightly faceted or plain platforms, with a few that are cortical or dihedral. The cross-section of indeterminate blank blades in both layers is relatively plane, trapezoidal or triangular, and in this respect approaches rather the Levallois specimens than the prismatic.

6.5.2.4.2 Summary

Altogether, the metrical and non-metrical characteristics give the impression that the Levallois and indeterminate blades from Layer αh are closely related and that at least the major part of the indeterminate blade specimens are related to the Levallois group. In Layer 6b, the relationship between these two categories is not so convincing. Nonetheless, here too the indeterminate blank blades seem to be more likely linked to the Levallois than to the prismatic group; otherwise, the biggest portion of indeterminate blades is possibly associated with the Levallois-like group and less with the prismatic. They seem to be so closely related because both groups were flaked from broad and rather flat core surfaces. This means that they could actually form one set and might have been manufactured during the same reduction.

6.6 Non-retouched blank flakes

Flakes without cortex coverage, or with cortex coverage on less than 50% of their upper surface, are grouped under this heading, even though this set is not homogenous and the specimens contrast in their morphology. In layers 6b and αh , two main groups were perceptible. The first group consisted of irregularly shaped, thin, short (mean $L=3.5\text{cm}$ and $T=0.5\text{cm}$ for both layers) and wide continuously unidirectional items with cortex coverage from 10 to 50% spread irregularly on their upper surface. The second group contained flakes that were more regular in shape, with thicker and longer pieces. Small cortex patches of from 1 to 25% appeared in 35% of them on their

proximal, distal and (rarely) medial parts. As with the blades, their proximal part was often prepared and platform faceted, whilst in the previous group these features were not apparent. As a result it was decided to consider the first set as representative of the preparation flakes *sensu lato*, or more probably as waste created during flaking. Even if a part of them were to be considered preparation flakes, it would be very difficult to precisely place their point in the production chain, as the analysed assemblies encompass different reduction strategies. The items from the latter group may then be seen as blank flakes. Attribute analysis was undertaken in all layers, but the metrical analysis was done for only three layers – 6a, 6b and αh – since their sample size was statistically significant (Tab. 69).

The differences observed in length, width and thickness of blank flakes from those layers are highly significant ($F=74.81$, $p=0.0001$; $F=31.73$, $p=0.0001$; $F=5.783$, $p=0.0034$ respectively).

The specimens from Layer 6a are the shortest: 35% of them have a length smaller than 3cm, and the remainder are only 1cm longer. About 90% of items from Layer 6b, and 100% from αh , are longer than 3cm, but only 25% of specimens from Layer 6ba and 50% from Sand αh are longer than 6cm; they range up to 9cm. It seems that these last two layers are more closely related to each other than to 6a (Fig. 93). The scatter plot of length and width of blank flakes from the three layers confirms this as well, showing that the main group of flakes from the sand and 6b are very similar with respect to their length and width (Fig. 94). But then, the principal tendencies in the length group of means visible in each layer separate them all considerably (Fig. 95).

The pieces from 6a are the narrowest, with a median of 3cm; only 25% of them are wider, reaching 4cm. 30% of specimens from Layer 6b and 10% from Layer αh have a width smaller than 3cm; the rest have a greater width, ranging up to 7cm (Fig. 96). This time it seems that all three layers are better related to each other, even if their median varies, but again 6b and αh seem to be more closely connected. This is also confirmed by the CV for width, which is the same in layers 6b and αh , while differing

for 6a (Tab.70). Then, if we plot the group means for all three layers, it can be seen that they are totally separated in their trend, as was the case for length (Fig. 97).

The items from 6b and Sand α h present almost the same elongation ratio – an LW of 1.5 and 1.6 respectively – whilst 6a has a smaller ratio, 1.3. A ratio smaller than 1, indicating items where the width was equal to or higher than their length, was documented in only about 25% of flakes from Layer 6a, 20% from 6b and 17% from α h. The remainder show a ratio from 1 to almost 2. Approximately 50% in Layer 6b and Sand α h have a ratio bigger than 1.5, demonstrating elongated items (Fig.98).

The thickness seems to be the most similar metrical attribute across all three layers. The median of 6a and Sand α h makes 0.7cm; for 6b, it is 0.8cm (Fig.99). Nonetheless, the majority of pieces from 6a present the same thickness, whilst those from other layers are more variable, ranging from 0.3 to 1.6cm. The bulk of flakes from layers 6b and α h have a thickness greater than 0.7cm. While the CV for thickness varies in all three layers, the plot of group means confirms the relationship between layers 6b and α h, and also relates some similarities between 6a and α h (Fig. 100). 75% of flakes from layers 6a and α h and about 55% from 6b have a W/T ratio higher than 4, reflecting thin specimens (Fig. 101).

The median W/T ratios of striking platforms are similar in all three layers (Fig. 102).

Values of 3.2 for 6a, 3.0 for 6b and 3.3 for the sand are recorded. Only 5% from 6a and less than 20% from layers 6b and α h show a W/T of butts smaller than 2, indicating that they are roughly rectangular in shape, and twice as wide as they are thick. The remainder exceed this value, reflecting the thin butts relative to their breadth.

The majority of striking platforms of blank flakes are, in all layers, mostly faceted plain, while some are cortical, dihedral and punctiform (Tab. 71). The pieces with faceted butts are similar to those of blank blades, i.e., longer than those with plain butts. It also seems here that the faceting of butts was used to adjust the flaking angle. The flaking angles of flakes with plain butts are more open than those with faceted butts (Tab. 72).

The dorsal scar patterns of these flakes show that they were produced mostly throughout unidirectional reduction. Bidirectional was also often undertaken, but lineal only rarely (Tab. 73). The point of percussion was often punctiform and was placed in most cases behind the central ridge or to the side of one ridge (Tab. 74). In almost all layers, the preparation of the proximal part of the specimen was frequently undertaken, including blank blades (Tab. 75).

The group of blank flakes is also not standardised. Some items are thick, with mostly plain, roughly rectangular-shaped striking platforms, while on the other hand some are thinner, with thin, well-faceted butts, and appear to be the result of the Levallois reduction strategy. This dichotomy was visible in all layers. Furthermore, the presence of a few flakes with subcentipetal dorsal scar patterns, the *enlevements II* and Levallois points, was documented. However, connections made between all these elements are not always free of doubt. Currently, the *enlevement II* is perceived by some scholars as the blank characteristic of the recurrent Levallois method (Meignen 1995:365), but by some others as “non-Levallois” (Usik 2006:152 and references therein). Further, Levallois points can be manufactured during different reduction strategies which are unconnected to the Levallois method of flaking (Boëda 1995:45). Since the analysed assemblages show not only those specimens which were identified, but also the typical Levallois cores and CTE characterised for this reduction strategy, it was decided to consider them as a part of the Levallois set.

For finer division within sets, only the samples from 6b and Sand α h were big enough to undertake the metrical analysis of Levallois-like and non-Levallois flakes (Fig. 155 and 154:2).

6.6.1 Levallois flakes

The Levallois group makes up 39% of blank flakes in Layer 6b and 38% in Sand α h (Tab. 76).

In both layers, the Levallois specimens have the same median length; about 50% of items have a length equal to or greater than 5cm, ranging up to 8cm in Layer 6b. The remainder have shorter lengths, reaching up to 3.5cm (Fig. 103).

Their median widths differ significantly, featuring 3.8cm in Layer 6b and 5.0cm in α h. 50% from Layer 6b and 75% from Sand α h are wider than 3.8cm, with the smaller ones falling to 2cm (Fig. 104).

The LW ratio differs slightly, with the median at 1.4 for Layer 6b and 1.5 for sand α h. About 20% in 6b and 14% in α h have a ratio smaller than 1, indicating specimens whose width is equal to or greater than their length. 38% from 6b and 45% from α h have a ratio bigger than 1.5, reflecting slightly elongated pieces (Fig. 105). The scatter plot of the length and width of artefacts from both layers shows that there are differences between both groups, but in the main they seem to be parallel (Fig. 106).

In both layers, the median thickness is 0.7cm. However, only 25% in Sand α h, and approximately 60% from 6b, are thicker. The remainder are thinner, ranging down to 0.4cm (Fig. 107). The median W/T ratio is small (it is just 2 in Sand α h), and reflects the rather massive specimens in 6b whose thickness approaches their width and height, giving a value of 5, indicating thinner items (Fig. 108). But then this ratio is greater in about 40% of specimens from Sand α h and around 55% from 6b; these range up to 10.5.

In 6b, 60% of specimens present well-faceted platforms, 14% are plain, and the remainder are dihedral or cortical. In Sand α h, the striking platforms are 70% faceted, 10% plain and the rest are dihedral or cortical. The median of W/T of butts varies significantly in both layers: it is 4.3 for 6b, but 5.7 for sand α h. More than 50% of items in 6b and around 70% in the sand have a ratio higher than 4, indicating thin, elongated butts (Fig. 109). In both layers, the use of unidirectional, bidirectional and subcentripetal debitage is confirmed. 63% of flakes in the sand and 74% in 6b present unidirectional dorsal scar patterns, with 12% and 8% respectively being convergent. 9% in Sand α h and 13% of flakes in 6b present the subcentripetal debitage. The less perceptible in Layer 6b is the bidirectional debitage being recognised only on 10% of

flakes, but in sand it makes 28%. The tendency to use bidirectional flaking more frequently in Sand αh than in 6b is again noticeable (Fig. 157: 4 and 5).

In both layers, Levallois points represent 9% of Levallois blank flakes. They are classical Y-shaped Levallois points, or 'constructed points' (Boëda 1990), exhibiting four or five previous removals. Their mean length is greater than that of the assemblage as a whole, i.e. 6.4 compared to 5cm in 6b, and 6.1 vs. 5.2cm in sand. Their L/W ratio equals 1.6, signifying rather elongated specimens. Their platforms are well faceted, thin and elongated, but only a couple can be described as *chapeaux de gendarmes*. They are mostly unidirectional, but in each layer one bidirectional point is also present.

The *enlèvement II* specimens are relatively long, with a mean of 6.2cm in 6b and 5.7cm in Sand αh . They represent 10% of Levallois blank flakes in 6b and 9% in αh . They are unidirectional and show faceted or plain, rather thin platforms (W/T butt=4.1 and 4.5 respectively).

The flakes demonstrating subcentripetal dorsal scar patterns are more numerous in Layer 6b than in αh . They make up 12% of the Levallois flakes in 6b and only 5% in αh . Their striking platforms are usually well faceted and in both layers their median length is equal to 5.0. Their L/W ratio is 1.1 and the W/T ratio is 5.7 in 6b and 6.1 in αh , demonstrating thin items with a width approaching their length. There are only two examples of preferential flakes.

In layers 6b and αh , 26% and 20% respectively bear a small amount of cortex (1-25%) on their dorsal face on the proximal, distal or medial parts. The points have no cortex coverage, but a few of the longest *enlèvement II* specimens have cortex coverage greater than 25% on their distal end. This indicates that at the beginning of the reduction, part of flaking surface was covered by cortex, which was peeled as reduction advanced.

It appears that Levallois blank flakes from both layers are fairly similar in their non-metrical attributes, except that bidirectional flaking seems to be more often employed in αh than in 6b. However, there are differences in size between flakes from both sets,

and the difference observed in length, width and thickness between the specimens from both layers is significant ($t=0.76$, $0.1 > p > .05$; $t=4.88$, $0.1 > p > .005$; $t=-2.83$, $0.1 > p > .005$ respectively). The pieces from Sand αh are thinner and wider than those from 6b. The scatter plot of length and width of Levallois blank flakes from both layers shows one central group with longer and narrower pieces and a smaller second one where items are shorter and broader.

6.6.2 Non-Levallois flakes

The remaining blank flakes from both layers are usually longer, narrower and thicker than those from the Levallois group (Tab. 76). The scatter plot of length and width shows that the majority are between 3.5 and 8.5cm in length and between 2 and 5cm in width (Fig. 110). In both layers, these blank flakes are mainly unidirectional (85% in Layer 6b and 77% in sand αh), and the rest are bidirectional. Their platform is plain or faceted, and sometimes cortical or dihedral. They are also narrower than in the Levallois group, with a median W/T ratio of 2.3 for 6b and 2.7 for sand, indicating that they are roughly rectangular in shape. 53% in Layer 6b and 58% of flakes in Sand αh carry a cortex covering from 5 to 50% of their upper surface on the distal, proximal and (rarely) medial portions. These specimens present a mean length, width and thickness greater than the items without cortex; this suggests that when the flaking started, the cores were partially covered by cortex, which was then removed as the debitage advanced. The pieces with prepared butts are longer than those with plain ones, and the flaking angle of the first one is more acute. It appears that, as in the case of blades, the faceting of the platform was undertaken to correct the flaking angle and at the same time to allow longer manufacture periods.

In both layers, more than 30% of the specimens from the Levallois and non-Levallois groups present the preparation of the proximal part using a series of small removals coming from the edge of the butt into the proximal part of their upper surface, and also dorsal reduction. The flakes from both layers seem to be related in respect to their length and width: the majority are between 3.5 and 8cm in length and between 2 and 4cm in width, but it also appears that there is a small number of specimens which are longer and broader, and some which are shorter.

Simplifying, it can be seen that, as for the blank blades, there are two strategies for the production of blanks: one through the Levallois-like reduction method and another through the other reduction strategy. Plotting the length and width of all non-retouched blank flakes and blades from *in situ* layers, it appears that both form a rather coherent set in which the large majority of lithic specimens tend to be elongated, with a length ranging from 2 to 12cm and a width from 1.5 to 5cm (Fig. 111). Adding non-retouched blank items from Sand α h to the same plot makes the plotting denser but does not alter the results (Fig. 112).

6.7 Retouched blanks

6.7.1 Introduction

The percentage of retouched artefacts varies between the assemblages (6b, 6c2, 7c, α h) from 21% of debitage in Sand α h, to 14% in 6c2, 11% in 6b and 8% in Layer 7c. They were shaped mostly on thick blades and, less often, on flakes or debris (Tab. 77). The large majority are elongated; their average L/W ratio is greater than 2 (Tab. 78).

As with the non-retouched blanks, the use of hard hammer direct percussion seems to be evidenced. Points of percussion were frequently prominent and were positioned in most cases behind the central ridge, between two central ridges or to the side of one ridge. Bulbs are usually marked, sometimes diffuse. The conchoidal fracture marks are clearly visible and in most cases the point and cone of percussion are also clear.

The retouched tool assortment consists of a high percentage of elongated end-point products fashioned by intense retouching. Typologically, these are considered points and convergent scrapers and parallel or convergent blades retouched continuously on one or both sides, typologically classified as single or double scrapers on blade (Tab. 79). Nevertheless, Mousterian tool types such as scrapers fashioned on flake, denticulate/notches, truncations, and such Upper Palaeolithic-style tools as end-scrapers are also present (Fig. 113: 5, 6; 144: 1-5, 7; 157:1). There are also a few items presenting intensive thinning of the proximal end and a genuine tang (Fig. 114). The majority of blades are covered from the proximal to the distal part by invading, semi-abrupt retouching. Abrupt retouching is also present but is rare and essentially

involves the distal part of the blank. The retouched pointed blades are symmetrical or asymmetrical (*'pointes incurvées'*, according to Neuville, 1951), with the semi-abrupt retouch mostly covering both sides and abrupt retouch concerning the distal parts (*'Hummalian point'*, according to Copeland, 1985). The retouch applied on the rest of the blanks is also often continuous, sometimes partial and usually invading (Fig. 157: 2, 3, 6-8 and Fig. 145). An occasionally invasive retouch covering almost the whole of the dorsal surface is also observed (Fig. 145: 10).

Following the idea of the “Frison effect” (Jelinek 1976) and the suggestion of scraper transformation through re-sharpening and reduction put forward by Dibble (1987), the simple lateral scrapers exhibit the least reduction, whereas the converging scrapers exhibit the most. The heavily retouched specimens could be considered in the maintained tool category, indicating numerous re-sharpening events and thus a longer use-life. The assemblages here present some variability in their composition, and the high rate of heavily retouched specimens relative to the total number of artefacts may possibly indicate controlled use of the lithic resources, perhaps a more intense occupation, and thus less mobility (Shott 1989). The majority of the elongated Levallois products were not retouched (Fig. 113:1-4).

6.7.2 Retouched blades

The metrical data of retouched blades differ between the layers (Tab. 80). For retouched blades from layers 6b, 6c2 and α h, the relationship between the length and the layer is highly significant ($F=14.7$, $p=0.001$). The group means vary between layers 6b and α h, whilst 6c shares certain similarities with 6b and α h. There is a strong tendency for the longest blades (8.6 to 9cm) to be found in Layer α h. The blades from Layer 6b are significantly shorter (7.4 to 8.1cm), whilst in Layer 6c2 they are more variable, probably because of the small sample size (Fig. 116).

The median length of blades from layers 6c2 and α h is the same: 8.5cm. 45% of blades from Layer 6c2 and 60% from Sand α h are longer than the median, ranging up to 13cm. The median in Layer 6b is smaller, at 7.8cm, and only 25% of retouched blades are longer than the median of 6c2 and α h. However, in Layer 6c2 the blades are not

shorter than 6cm, whereas in layers 6b and αh they are as short as 4.2cm. This shows that in the latter two layers the blades were produced throughout the whole reduction sequence, whilst in Layer 6c2 there are no small elements (Fig. 117).

For retouched blades from layers 6b, 6c2 and Sand αh , the relationship between the width and layer has no significance ($F=0.1016$, $p=0.90$). This seems to be confirmed by the median width of 2.9cm in all three layers. 50% of retouched blades in three layers are broader than the median, going up to 4.5cm; the rest are narrower, ranging down to 1.3cm in Sand αh (Fig. 118). Looking at general trends, it can be seen that blades in Layer αh tend to be more uniform in their width than those from the other two layers, which are more disparate (Fig. 119).

The dissimilarity perceived in the L/W ratio of blank blades from all three layers has a high significance ($F=13.10$, $p=0.0001$). The plotted group means show the clear separation between layers 6b and αh , whilst Layer 6c2 again shows a much wider variability, although sharing more in common with the sand layer than with 6b (Fig. 120a). The median L/W ratio of 2.8 is the same for Layer 6c2 and the sand, with more than 50% of blades having a greater ratio, ranging up to 4.5. The median L/W ratio of retouched blades in Layer 6b is 2.5, and only about 30% have a ratio exceeding the median of two previous layers (Fig. 121a). This indicates a greater majority of elongated specimens in layers 6c2 and Sand αh and fewer in Layer 6b.

For retouched blades from layers 6b, 6c2 and sand α , the relationship between their thickness and their layer has a high significance ($F=12.55$, $p=0.0001$). The median thickness of blades from Layer 6c2 and the sand is the same in both, 0.7cm, with about 45% showing a smaller thickness than the median. The median thickness for Layer 6b is 1cm, and around 85% of its blades are thicker than the median of the two former layers. Only 25% of retouched blades from Layer 6c2 and 35% from the sand equal or exceed the median of Layer 6b. Consequently, the majority of retouched blades from this layer are significantly thicker than those from layers 6c2 and αh (Fig. 122). The plotted group means confirm the clear separation in thickness between retouched blades from Layer 6b and the other two layers (Fig. 123).

The difference observed in the W/T ratio of retouched blades from the three layers is marginally significant ($F=2.433$, $p=0.089$). The W/T ratio of 3.5 shows that the specimens from Layer 6c2 are the most slender, followed by those from the sand at 3.3, with the most robust being those from Layer 6b, with a ratio of 3 (Fig. 121b). The plotted means demonstrate that about 20% of blades from Layer 6b are situated in the lower range of blades from the sand. They also show that 30% of blades from 6c2 are more slender than those from the two other layers, confirming the results calculated from the median and ANOVA (Fig. 120b).

The bulk of striking platforms are plain or faceted or – less often – cortical, punctiform or dihedral (Tab. 81). As with the non-retouched blades, the majority of the faceting is not very carefully carried out.

For retouched blades from layers 6b, 6c2 and Sand α h, the relationship between their W/T ratio of butts and their layer has no significance ($F=0.759$, $p=0.47$). The plot of means of W/T butts shows that the striking platforms of retouched blades from the Sand α h are more standardised than those from layers 6b and 6c2 but are still closely related to each other (Fig. 120c). The median ratio is 2.6 for Layer 6b and the sand, where half of them have a greater ratio, ranging up to 4.6, and the other half are smaller and spread down to 1. The median ratio for Layer 6c2 is 3, but more than 60% of items have this ratio or greater than the median of two previous layers. The remainder have a smaller ratio, but never smaller than 2 (Fig. 121c).

The dorsal scar patterns show that unidirectional parallel debitage was used most often, followed by bi-directional debitage. The regularity of use of these flaking methods differs between sets, but bidirectional debitage seems to be more frequent in α h and Layer 6c2 than in 6b (Tab. 82).

The majority of retouched blades show three or more previous scars on their upper surface, indicating that the blades used for retouching came mainly from the more advanced stages of reduction.

In layers 6b and α h, 26% of retouched blades present cortex coverage, even though such coverage is usually small – from 10 to 30% on the upper surface. The cortex

appears in the main on the distal part, but often also on the medial and proximal ends of blades. Cortical backs are observed in only 7% of blades in Layer 6b and 3% in the sand. In layers 6b and Sand α h, the blades are often bowed in longitudinal section along their whole length or along part of it, on the medial-distal or less often proximal-medial fragment of the item (Tab. 83). Their medial cross-section is 60% trapezoidal and 35% triangular. The widest portion of pieces are mainly placed in the midsection, followed by the proximal part, and only rarely the distal part. About 70% of blades from layers 6b and Sand α h and 90% in 6c2 present converging lateral edges, often accomplished through retouching. In all layers, preparation of proximal parts and dorsal reduction of retouched blades seem to have been undertaken often (Tab. 84).

Comparing the length and width of retouched and non-retouched blades in Layer 6b, 6c2 and the sand, it can be seen that they form a corresponding set (Fig. 124, 125). From Layer 6b the median width (2.9cm) and thickness (1cm) of blades are the same, but the majority of retouched blades have a greater median length (7.8cm), compared to 7.2cm for non-retouched. In Layer Sand α h, the retouched blades are significantly longer and wider, with the appropriate thickness. The median length in the first layer is 6.9cm for non-retouched blades and 8.7cm for retouched; the median width is 2.3cm against 2.9cm respectively. In the second layer, the median length is 7.7cm for non-retouched specimens and 8.4cm for retouched, with the median width being 2.7cm vs. 2.9cm. This indicates a choice of longer and broader supports for shaping the retouched tools, especially if the original size of many of them was reduced through repeated use and retouching.

6.7.2.1 Single scrapers on blade

This is the best-represented group of tools in all layers, with 34% of retouched specimens in 6b, 41% in the sand and 50% in 6c2. Sets from these three layers are analysed here (the other layers have too small a sample size to be representative). Layer 6c2 had only eleven single scrapers and it will be used just in terms of general trends (Tab. 85). The majority of single scrapers present unidirectional dorsal scar patterns, followed by bi-directional, in all layers. But in Sand α h the bidirectional

method is visible on 40% of blades (Tab. 86). The bulk of them present two or more previous scars on their upper surface (Tab. 87). The majority have convergent lateral edges and the rest are parallel, or sometimes expanding (Tab. 88). They are retouched unifacially along their whole length, or on a portion of one edge. The retouch is regularly semi-abrupt but occasionally abrupt, scaled, rarely stepped, invading, sometimes marginal but in the main convex, sometimes concave or straight in form. About 40% of single scrapers in layers 6b and the sand are pointed. They were formed from one-sided retouching along the whole length or just on the medial-distal or distal part, usually convex in form, which joins another non-retouched side to create the pointed end. The majority of single scrapers in Layer 6c2 present such an arrangement as well. The remainder is constituted of specimens with converging or parallel lateral sides, retouched on the whole length or on the medial-distal part of one edge. 30% of single scrapers on blades present cortex coverage from 5 to 50% on the proximal, medial and distal end on their upper surface. 10% of single scrapers in Layer 6b and the sand layer present the backing opposed to the retouched edge, more than half show a cortical back, and the rest are plain and rarely prepared.

The striking platforms of single scrapers on blades are frequently plain or faceted, and sometimes cortical, punctiform or dihedral. The median ratio of butts is similar in all layers: it is 2.5 in layers 6b and 6c2, and 2.6 in the sandy layer. 50% of specimens from Layer 6b, and 60% from the other two layers, have a ratio that is larger, ranging up to 4.6 in the sandy layer but only up to 3.4 in Layer 6b. 25% of specimens from Layer 6b and about 40% in the other two layers present thin platforms relative to width. This ratio seems to be most diverse in the sand and less variable in Layer 6b, ranging from 1 to 4.6 in the former case and 1.6 to 3.4 in the latter (Fig. 127c).

The median length of pieces from Sand α h is 8.3cm and about 55% of them are longer, ranging up to 13cm. In Layer 6b the median length is 7.9cm, and about 40% of specimens range up to 11cm, equalling or exceeding the median of Sand α h. 60% of specimens from Layer 6b and 45% from Sand α h are smaller than 8.3cm, reaching down to 4.5cm. Blades from Layer 6c2 present the longest median length: 8.7cm. 60%

of them are longer than the median of Sand α h, and the rest are smaller, ranging down to 6.1cm. Some small elements are missing (Fig. 126a).

The median width of single scrapers on blades is similar in all layers, with values of 2.9cm for 6b and 6c2, and 3cm for Sand α h. About 50% of them are broader, ranging up to 4.7cm in Sand α h and 4cm in Layer 6b. The remainder of the pieces are narrower, reaching 1.3cm in Sand α h and 1.7cm in Layer 6b. The width of pieces from 6c2 seems to be less disparate, with ranges between 2.2 and 3.7cm (Fig. 126b).

The median L/W ratios in Sand α h and Layer 6c2 are comparable, giving values of 2.8 and 2.9 respectively. About 60% of pieces from both layers have a greater ratio, reaching 4.5. The median of this ratio for Layer 6b is 2.6 and only 30% of specimens have a greater ratio than those from previous layers, ranging up to 4. This indicates that the majority of single scrapers from Layer 6b are less elongated than those from Sand α h and 6c2 (Fig. 127a).

The median thickness of single scrapers from Sand α h and Layer 6c2 is the same: 0.8cm. More than 50% are thicker, ranging up to 1.4cm. In Layer 6b a median thickness of 1cm is observed; more than half of these are thicker, reaching up to 1.8cm. Only 25% of items are thinner than the median of 0.8 from two previous layers (Fig. 126c).

Consequently, the median W/T ratio in Layer 6b is the smallest, with a value of 3; approximately 55% of the scrapers have a greater value, ranging up to 4.5. The W/T ratio of specimens from Layer 6c2 seems to correlate well with that from Sand α h: in both layers it is approximately 3.5, with 75% presenting a ratio greater than that from Layer 6b, reaching up to 6. This shows that the majority of items from layers 6c2 and Sand α h are relatively thin compared to those from Layer 6b (Fig. 127b).

The single scrapers made on blades from layers 6b, 6c2 and Sand α h present different lengths, although in the last two layers the thickness is the same, and in all three layers the width is similar. The specimens from layers 6c2 and Sand α h seem to be more closely related in respect to their metrical attributes, and they are more elongated and thinner than those from Layer 6b. The non-metrical features show a greater similarity

between layers, with one exception: a large proportion of items from Sand αh were produced using the bidirectional flaking method.

6.7.2.2 Pointed blades

After single scrapers, the next best-represented group of blades is pointed blades, which make up 26% of the retouched specimens in Layer 6b, and 28% in Sand αh (Tab. 89). The retouch can cover the whole length on either edge of the specimen, or the medial-proximal part of one side and the entire length on the other side. It is semi-abrupt, long or invasive on the sides and usually covering or invasive on the distal-pointed part. 50% in Sand αh and 30% in Layer 6b have an asymmetrical distal end going towards the left or right. This asymmetry was also observed in other layers. About 20% in Layer 6b and 13% in Sand αh show small patches of cortex on the proximal or distal portion of their upper surface.

The majority of these items in Layer 6b and Sand αh present a unidirectional flaking method – 74% and 80% respectively. The rest show a bidirectional dorsal scar pattern (Tab. 90). In both layers a preponderance of specimens show more than three negatives from previously detached items, indicating that the majority come from advanced stages of reduction.

The platforms are usually plain or faceted. The W/T ratio of butts is the same in both layers, giving a value of 2.6. More than half of the butts in both layers have a greater ratio, ranging up to 4.6 and indicating rather thin platforms (Fig. 129c). The rest have a smaller ratio, representing butts twice as wide as they are thick, and those whose width equals their thickness (Tab. 91).

The median length of pointed blades from layers 6b and Sand αh are similar, giving values of 8.3 and 8.4 respectively. Around 40% of items in 6b and about 60% in Sand αh are longer, ranging up to 11cm in 6b and 13.5cm in Sand αh. The remainder are shorter, going down to 5.3cm in Sand αh and 6.1cm in Layer 6b (Fig. 128a)

The median width of pointed blades varies between layers 6b and Sand αh: it is 3.2cm and 2.7cm respectively. About 65% of items in both layers exceed the median width of

specimens from the sand, ranging up to 4.4cm in Layer 6b and up to 4cm in Sand αh. The rest of the blades are narrower, with widths as low as 1.5cm (Tab.128b). As a comparison, the pointed blades from Layer 6c2 present a median width of 3.2cm.

The L/W ratio is similar in both layers, giving values of 2.7 in Layer 6b and 3 in Sand αh. 35% of blades from Layer 6b and more than 55% in Sand αh have a greater elongation, ranging up to 4.5 in Layer 6b and up to 5 in Sand αh (Fig. 129a). This indicates that more items from Sand αh are more elongated than those from Layer 6b. The median thickness varies significantly between both layers: it is 1.1cm in Layer 6b and 0.8cm in sand αh. 87% of items from Layer 6b are thicker than the median of the sand and only 20% of items from the sand show a thickness greater than the median thickness of blades from 6b. The remaining blades are thinner, going down to 0.4cm in Sand αh and 0.6cm in Layer 6b (Fig. 128c).

The median W/T ratio of pointed blades is comparable between layers, with values of 3.1 for Layer 6b and 3.2 for Sand αh. 35% of specimens in 6b and 50% in Sand αh have this ratio or higher, ranging up to 4.0 in 6b and 5.0 in Sand αh (129b). This indicates that more pointed items in Sand αh are more gracile, while the majority of those from Layer 6b are more robust.

It seems that pointed blades from 6b and Sand αh are rather standardised and close to each other in respect of their median length. They differ mainly in their width and thickness. The specimens from Layer 6b are thicker and wider than those from Sand αh, but if comparing the L/W and W/T ratios, these two sets seem to be correlated. Evidently the flint knappers in both layers used similar blocks of raw material and were looking for analogous modules. Furthermore, re-sharpening and reduction seem to affect these pieces equally, suggesting that they were used for similar purposes (Fig. 145).

6.7.2.3 Double scrapers on blades

Double scrapers made on blades make up 11% of retouched tools in Layer 6b, and 12% in Sand αh. Unfortunately, only nine items from Layer 6b are intact and their

metrical analysis does not hold weight with respect to sample error (Tab. 92). Therefore, attribute analysis was also undertaken on the broken pieces, which contain at least two partitions. The retouch can cover almost the whole length on both edges of the specimen, or the medial-proximal part of one side and nearly the entire length on the other side. The majority of them were made on blades with converging lateral sides, often having an asymmetrical distal end that does not show retouching. Retouch is semi-abrupt, long or invasive, convex, sometimes concave and rarely straight in form.

The items in Layer 6b are usually unidirectional; only 11% show bidirectional dorsal scar patterns. In Sand α h the bidirectional method prevails, being visible on 55% of blades (Tab. 93). The majority of specimens from Sand α h and Layer 6b have four or more previous negatives on their upper surface – almost 70% in the former and 60% in latter. This indicates that they originate from an advanced stage of reduction. Their striking platforms are plain or faceted (Tab. 94). The median W/T ratio of butts is 2.6 in Sand α h, with about 60% having a greater ratio, reaching a value of 4.7. The median ratio in 6b is slightly higher at 2.9, and nearly 70% have a larger value than the median in Sand α h, ranging up to 5.3 (Fig. 129c). This shows that more specimens in Layer 6b have a thinner butt than those from Sand α h.

The median length in Sand α h is 8.7cm and nearly 60% of items are longer, ranging up to 12.5cm. In Layer 6b, the median length is 7.9cm and nearly 40% of blades are longer than the median in Sand α h. The remainder are shorter, going down to 5.3cm (Fig. 130a).

The median width in Sand α h is 3cm, with about 60% of blades being broader and reaching up to 5cm. In Layer 6b, this median is smaller at 2.7cm (Fig. 130b). The median L/W ratio is similar in both layers, with values of 2.8 in Sand α h and 2.9 in Layer 6b. About half in both layers have a higher ratio, ranging up to 4.3 (Fig. 129a).

The median thickness is 0.8cm in Sand α h and 1cm in Layer 6b. Only about 35% of items in sandy Layer α h are thicker than 1cm; these range up to 1.4cm. The remainder are thinner, going down to 0.5cm (Fig. 130c). The median W/T ratio of double

scrapers in Sand α h has a value of 3.5, with nearly 50% exceeding this ratio. In Layer 6b this ratio is smaller, just 2.8 (Fig. 129b).

Because of the smallness of the sample from Layer 6b, it is difficult to draw conclusions concerning the metrical attributes of double scrapers across both layers. Generalising, it seems that the specimens from Sand α h are longer, but not more elongated, and they are wider and thinner than those from Layer 6b. As the items from Layer 6b are shorter and narrower, it can be considered hypothetically that they are more reduced, *ergo* that they were employed for longer or more intensively.

6.7.2.4 Evaluation between tools on blades and conclusions

Retouched pointed blades, with a median length of 8.3cm, seem to be the longest of the three analysed tool categories. However, more than 40% of blades from each category are longer, showing that they are closely related (Fig. 131a). Similar observations can be made for Sand α h; here, the greater median length of 8.7cm is assigned to double scrapers, but almost 50% of blades from other categories are even longer (Fig. 132a).

In Layer 6b, the width differs slightly. Points are the broadest, with a median of 3.0cm, and double scrapers are the narrowest, with a median of 2.7cm. But then again, about 40% in each layer are broader than the 3cm median, and nearly 35% of points and double scrapers, and 25% of single scrapers, are narrower than the median of 2.7cm (Fig. 131b). In Sand α h the median width of single and double scrapers is the same at 3cm, and the median width of points is 2.7cm. 40% of single scrapers and points and 60% of double scrapers are broader than 3cm (Fig. 132b). In Layer 6b, the single and double scrapers have the same median thickness of 0.9cm, and that of points is greater, 1.1cm. However, in all categories 50% exceed the median of 1.1cm, showing that about 20% of single scrapers are the thickest, ranging up to 1.9cm (Fig. 131c).

In Sand α h, all three categories of tools present the same median thickness of 0.8cm and about 60% surpass this median, but only 25% surpass the median of 1.1cm from points in Layer 6b (Fig. 132c). It seems that in both layers these three categories of

tools are highly related in their metrical attributes. It seems that the flint knapper typically used the same size of blank to produce these tools. Additionally, the majority of all retouched blank blades seem to converge at the distal end and to present three or more scars on their upper surface, indicating that they come from an advanced stage of reduction. But the majority of single scrapers carry cortex coverage, and sometimes cortical backs opposed to the retouched edge. The points and double scrapers meanwhile commonly show no cortex coverage. If size seems to have been unimportant in choosing a blank for shaping these tools, the knapper seems to have taken the presence of a cortex back or cortical surface into consideration.

There are some differences between tools on blades from Sand α h and those from Layer 6b. The first are longer and thinner than those from 6b and were more often produced through bidirectional reduction. Additionally, their butts are more often faceted than those from 6b. Taphonomical problems aside, it could be this faceting that causes the tools to be longer and thinner than those from 6b. It has been shown in previous analyses, including studies of non-retouched blades, that the blades with a prepared butt are always longer and thinner than those with a plain butt. It is clear that the knappers from Sand α h had better control of their products through monitoring and mending the angle between the platform and the flaking surface of the core, more often than in 6b.

The other attributes – such as retouch, its location and intensity on blanks, as well as the cross-section, profile, preparation of proximal part, and the number of previous scars on the upper surface – all seem to be very similar, including between different tool assemblages.

6.7.3 Retouched flakes (Tab. 95)

6.7.3.1 Introduction

Only 12% of retouched tools in Layer α h, and 21% in Layer 6b, were produced on flakes. This group comprises mainly the single scrapers, notches and denticulate, truncations, a few points, a couple of pieces thinned on their proximal end and some

unstandardised tools. The majority – 86% in Layer 6b and 56% in Sand αh – show a unidirectional dorsal scar pattern. A bidirectional pattern is seen in only 9% of flakes in first layer and 36% in Sand αh (Tab. 96). Almost 50% of those from Layer 6b and more than 40% from Sand αh present cortex coverage ranging from 5 to 50% on their upper surface, but the majority have small cortex patches covering less than 25%. The platforms are mostly faceted, followed by plain (Tab. 97), and give the same median and mean ratio of 3.0 for the W/T of butts in both layers.

With a median of 6.5cm compared to 4.5cm, the retouched flakes from Sand αh are longer than those from Layer 6b. More than 50% of the flakes from Sand αh are larger than the median, and range up to 10cm. Only 20% of flakes from Layer 6b are longer, reaching up to 8.3cm. The remainder are shorter, ranging down to 3.0cm (Fig. 117). The median width of flakes in both layers gives similar values, 3.8cm in 6b and 3.9cm in Sand αh. More than half are wider in both layers, ranging up to 7.4cm in Layer 6b and up to 5.7cm in αh. The rest are narrower, with a lower boundary of 2cm (Fig. 118). The median thickness is 1.1cm in Layer 6b and 0.9cm in Sand αh. About 35% of retouched flakes from Sand αh and 50% from 6b are thicker than 1.1cm: they range up to 2.3cm in 6b and up to 1.7cm in Sand αh (Fig. 122). The remainder range down to 0.5cm.

The retouched flakes from Layer αh are longer and thinner than those from Layer 6b, but their width is equivalent. The large majority from Layer αh were produced using bidirectional flaking, whilst those from Layer 6b are generally unidirectional.

6.7.3.2 Single scrapers made on flakes

There were thirteen single scrapers made on flakes in layers 6b, and 17 in Sand αh; in other layers, there is usually only a single specimen. The scrapers from the first two layers were analysed in detail. The majority of single scrapers present unidirectional dorsal scar patterns (70% from 6b and 60% in Sand αh) and the rest are bidirectional. Only two pieces present subcentripetal scars on their upper surface.

The semi-abrupt, sometimes abrupt, scalar-form and long retouch usually covers the whole length of one edge or its medial-proximal part. It is usually convex, and rarely straight in form. The majority in both layers present small patches of cortex covering from 5 to 25% of their upper surface. A few items have important cortical or plain backs opposite a retouched edge. The majority have a well-faceted striking platform, with a few that are plain or cortical.

The median W/T ratio of butts is similar in both layers, with values of 3.3 in layers 6b and 3.1 in sand α h. 60% of single scrapers from both layers have this ratio or higher than 3.0, ranging up to 4.0 in the former layer and up to 5.0 in the latter. The rest have smaller ratios, with the lower limit being 2.4 in 6b and 1.5 in Sand α h (Fig. 127c). This indicates that the large majority of tools have a relatively thin platform. As with single scrapers made on blades, this ratio seems to be less variable in Layer 6b than in Sand α h.

These tools are the longest among tools on flake. Their median length in Sand α h is 6.5cm and nearly 55% of them are longer, ranging up to 9.6cm. In Layer 6b, the median length is 6.2cm, and 50% of them range up to 9.3cm, equalling or exceeding the median of the Sand α h group. The rest are smaller, but in neither layer are they shorter than 4.5cm (Fig. 126a). The median width of single scrapers on flake is also similar in both layers, with values of 4.2cm in 6b and 4.1cm for Sand α h. About 45% in the former layer are broader, ranging up to 6.5cm, although in Sand α h only 20% are broader, ranging up to 4.5cm. The rest are narrower, with the narrowest being 2.6cm in Layer 6b and 3.2cm in Sand α h (Fig. 126b). The scrapers made on flake from both layers are significantly larger than those made on blades. The median L/W ratio is similar in both layers, with a value of 1.6. About 60% of pieces from Layer 6b and 75% in Layer α h have a ratio greater than 1.5, but they do not exceed 1.8 in the former layer or 2.0 in the latter. The remainder have smaller ratios, ranging down to 1 (Fig. 127a). This indicates that the majority are elongated, being approximately one-and-a-half times longer than they are wide.

The median thickness of the single scrapers from Sand α h and Layer 6b differs slightly, with values of 0.9cm in the latter layer and 1.1cm in the first. 50% in both layers range up to 1.5cm, making them thicker than the median. The rest are thinner, but no thinner than 0.8cm in Layer 6b and 0.5cm in Sand α h (Fig. 126c). Therefore, just as the median width and thickness of these specimens in both layers are quite similar, the median W/T ratio is analogous as well, with values of 4.5 in Layer 6b and 4.4 in Sand α h. About 40% of scrapers in Layer 6b and more than 60% in Sand α h have a greater value than the median, ranging up to 8.6 in the latter and 6.1 in the former. The rest have smaller ratios – 1.9 in Sand α h, and 1.4 in 6b. This shows that the bulk of items from Sand α h are relatively thin in relation to those from Layer 6b, where specimens are typically more robust (Fig. 127b).

The single scrapers made on flakes from layers 6b and Sand α h seem to be highly correlated in respect to their metrical and non-metrical attributes. As with other products, more items from Sand α h are more elongated and more gracile than those from 6b, and the larger part of the items from Sand α h were detached using the bidirectional flaking method. It appears that the knappers chose similar blanks for shaping single scrapers on flakes in both layers.

In Layer 6b, the retouched flakes are not noticeably longer than the non-retouched, but the blanks chosen for scraper shaping were significantly longer: 6.5cm in the former group, and 4.9cm in the latter. They were also longer in Sand α h: 6.5cm compared to 6.0cm. They do not differ significantly in their width in either layer but the retouched blanks are thicker in both assemblages: 1.1cm against 0.8cm in 6b, and 0.9cm compared to 0.7cm in Sand α h. This shows that thicker and longer blanks were used to complete the retouch, especially in the case of scrapers.

6.8 Core reduction strategies

6.8.1 Introduction

In total, 228 cores were discovered from *in situ* layers 6a, 6b, 6c2, 7a, 7c, 6A1-2 and 6B, and 82 from sandy Layer α h (Tab. 98). The former group contains 104 cores

which were made on block and plate, with 67 on flake, and a further 58 items that can be described as bladelets cores and core-burins for bladelet production. In the latter, 33 were completed on block, 35 on flake and 14 are core-burins. The sample of 310 cores was subject to analysis based on the approach proposed in Chapter 5.

290 of the cores were intact and have been used for metrical analysis. 17 were partially broken but it is still possible to recognise their association with the reduction strategy at the end of their exploitation. This section presents a study of core morphology, management, reduction and discard, followed by an attempt to interpret these data with the results from debitage.

A large proportion of the cores from all layers are exhausted, and many were discarded due to knapping mistakes and raw material failures. Since most of the cores in the Hummalian samples are considered exhausted, it can be supposed that their final shape bears little resemblance to their former stages of reduction. Nevertheless, a constant morphology is evident in many of the cores, in spite of their variations in size from three to twelve centimetres. The state of exhaustion of most of cores indicates that the aim of core reduction was to extract the maximum possible number of operative blanks from a given nodule.

The blanks produced were of differing size, including small blades from two to sixteen centimetres in length. The maximal exploitation of cores was attained by decreasing core size until the convexity of the upper surface could no longer be re-established; the exterior platform angle overpassed 90° and the flaking surface became covered by hinge fractures. The mean core exterior platform angle, from all layers, at abandonment ranged between 65 and 77° . These angles are supposed to be suitable for further direct, stone-hammer flaking (Pelegrin 2000, 75) so they most likely did not influence the decision to discard a core. The flint knapper was certainly limited by the size and volume of cores but it seems that sometimes the upper surface was not able to be mended if it was marked by step and hinge fractures, and this is the reason some of the cores were discarded.

Fig. 133 shows that the length of blanks and CTE is in agreement with the length of cores. Several blanks are the longest in sequence, whilst the length of blanks follows perfectly the length of CTE and cores. The cores with lengths between three and eight centimetres are the most numerous; likewise with the debitage. This supposition can be reinforced by the presence on the site, unfortunately not *in situ*, of several cores that are typically Hummalian and reach up to 20cm in length.

In this context, both the mean length of cores, which is always smaller than the mean length of blanks (Tab. 99), and the presence of blanks, whose length noticeably surpasses the size of all cores and trimming elements (Tab. 21), indicates the prolonged exploitation of cores, rather than off-site production (Binford 1979).

The different orientations of the flaking surface on the Hummalian cores leads to a production of morphologically different blanks and probably at the same time an adaptation relating to the shape of the raw material block.

6.8.2 Laminar Method

The use of the Laminar method for blank production was recognised in all investigated layers by the presence of cores, the products of their maintenance, and elongated, thick blanks. The Laminar cores were found in almost all layers, except Layer 7a, and in the rich layers 6b and αh they constituted 65% and 70% of all cores respectively. Cores were made either on blocks or on flakes (Tab. 101) and measure from three to twelve centimetres. Some examples show that they can present a consistent morphology, allowing the manufacture of thick elongated blanks of differing size, including small blades and flakes (Fig. 146, 147, 158). Thanks to the natural form of the block or flake, the first blade was struck directly from a single plain or cortical platform, initialising the debitage. The setting up of a crest for a flaking surface opening was rarely observed. Only six blades in Layer 6b, two in Layer 6c and three in αh attest to this mode (Fig. 156).

The flaking surface of the Laminar cores, usually arranged to the length of the nodule, onto the convex, elongated and narrow face, could be expanded on its lateral sides

during flaking (Fig. 134). Faceting was used for rejuvenation of the core platform; the removal of a core tablet was hardly ever employed. Additionally, the management of the flaking surface was regularly attained by the removal of a flake edge along a natural or cortical ridge and occasionally by a secondary crested blade. The constant removals of ‘cleaning flake’ during the reduction helped to maintain the flaking surface when convexity was lost or hinge marks appeared. Most of the ‘cleaning flakes’ usually corrected the middle part of flaking surface; however, a few occur on the distal part of flaking surface, and occasionally being plungings. They are also non-cortical: few show 1 to 25% cortex on their dorsal face. They are rather substantial, with a median thickness of 1.3cm and a length of four to ten centimetres, which indicates that this practice was used throughout the core reduction. To eliminate the overhangs after striking a few blanks from the proximal part, the tool-maker frequently struck thin flakes from the border of the core platform onto the flaking surface.

The blanks were usually removed from either one striking platform or two opposing, offset platforms. Three platforms were seldom used.

Those cores with two opposed, offset platforms indicate that the flaking was carried out independently on the narrowest and broadest faces of the core, with the intersection between them forming the necessary convexity to continue the production (Fig. 148, 167). The core volume management is structured into two principal types of flaking system (Fig. 135a):

- semi-rotating
- frontal.

6.8.2.1 Semi-Rotating Debitage (Tab. 102)

In this reduction strategy, the flaking surface covers the broadest face of the nucleus and its sides, and opposes a plain or cortical surface. However, if produced on flake it opposes the ventral face of the flake. Thedebitage is generally organised according to the vertical axis (length) of the block. The block of raw material or large flake was

firstly exploited on its thickness (the narrow face), and with time the flaking surface expanded on its sides. Consequently, with the development of the striking surface, new striking platforms were completed on the core.

The cores are rectangular to triangular in shape, and usually elongated; the mean ratio of L/W is 1.4. As a rule they present a longitudinal convexity and a semi-prismatic transversal cross-section (Fig. 135b). Their initial flaking surface could be expanded onto the adjoining side (flank) during the debitage. They were made mostly on block, followed by flake (Tab. 103). Their dorsal scar patterns in Layer 6b show that they are unidirectional in 56% of cases, bidirectional in 44%, while in Layer αh they are 50% unidirectional and 50% bidirectional (Tab. 104). A few cores which had two opposite and offset striking platforms lost one of them at the end of flaking through the knapping of a plunging flake. The cores with two opposed faintly twisted platforms demonstrate that the flaking was undertaken independently along the narrow and broad faces of the core (Fig. 30-1, 2, 4) at the same time. Each flaking face has a parallel striking platform which works on a different level surface, and as a result the intersection between these two surfaces created the required convexity for perpetuation of the debitage. There are also a few cores which were primarily unidirectional; when they became flat in cross-section, a second striking platform offset to the axis of the first one was set on the opposite end of, or on the side of, the core. If arranged on the opposite end, this additional platform was exploiting the core on its thickness (Fig. 30:5). The negatives coming from the second striking platform clearly crossed the negatives obtained from the first platform. When the new platform was arranged on the side, this supplementary platform was exploiting the dorsal face of the core (Fig. 30:3). A few semi-rotating cores were also made on edge-flakes or other flakes presenting a triangular cross-section (3 or 4) with a convex ventral face. The flint knapper set a platform with one or two blows on one or two ends of the flake and used the natural convexity of this item to start the debitage.

Many semi-rotating cores present a preparation of the flaking surface by small flakes coming usually from one periphery, often looking similar to the subcentripetal preparation of the *surface Levallois*. Additionally, the core platform on the proximal

part of the core is well faceted. Often, one lateral side of the core shows the typical *surface Levallois*: the platform is faceted and another lateral side is perpendicular, reminding us that the core volume management was initially different. But if the flint knapper had carried out the same preparation on both lateral sides of cores, we would be in the presence of the typical Levallois core *sensu* Boëda. Consequently, cores, exactly like blanks, present a mixed morphology.

The semi-rotating cores are the most numerous among the Laminar cores, representing 95% in Layer 6b and 97% in sandy Layer αh. All cores provided blades of various sizes.

The platforms of the majority of the semi-rotating cores are slightly faceted or plain (Tab. 105). Several present a platform prepared by one or two blows from the lateral sides. These removals from the core sides have a role in refreshing the intersection between the platform and the flaking surface and allow the exploitation of the lateral sides of the core. Six pieces exhibiting the removal of the rejuvenation core flake from the platform are observed in Layer 6b, and one such a flake was found in Layer αh. Cortex occurs on the majority of cores: on 83 (69% of semi-rotating cores) in Layer 6b and on 38 (66% of semi-rotating cores) in Layer αh. In the case of Layer 6b, the cortex appears on 54 items on their dorsal face and the remainder in the main are on the proximal part, and then on the distal and mesial part of the ventral surface of the core. 21 cores in layers 6b and 8 in αh are 50% covered by cortex. The rest carry cortical patches covering from 1 to 49% of their upper surface.

6.8.2.2 Frontal Debitage

Frontal debitage is less represented among Laminar cores and was recognisable on only nine cores, four complete on block (Fig. 134:4) and five on flake. They have in most cases one striking platform and the flaking concerns the narrowest face of the core (Tab. 106). Just two bidirectional cores were collected (Tab. 107, 108). Their platforms seem to be used successively, thus representing two adjacent unidirectional reductions carried out on the same core, rather than a real bidirectional reduction. The

cores are rectangular or triangular in shape and convex in cross-section. They are among the most elongated Laminar cores. The platform is prepared by one or two removals, and debitage starts on the natural edge of the block; in the case of core on flake, the edge of the flake serves as a guide-ridge. All present cortex cover of from 1 to 50% on their ventral or dorsal faces. They provide three or four blades at the end of their exploitation.

6.8.3 Levallois method

A notion of Levallois developed by Boëda (1986, 1988a, b, 1990, 1995, Boëda *et al.* 1990) was used to find out whether this system of flaking was present in the studied assemblages. Levallois cores, as defined by Boëda (1986), are composed of two opposed surfaces, of which one is conceived as the preparation of the Levallois surface for blank production, and the other, often cortical, is a surface of the striking platform. The intersection of these surfaces defines a plane.

The use of the Levallois method as defined by Boëda was visible in layers 6b, 7c and αh , either by the presence of a few cores or in typical Levallois products (Fig. 136, 165). It should be mentioned that in other layers, Levallois cores and CTE characteristic of this reduction strategy were not discovered (Tab. 23).

The attributes analysis of the core and CTE indicates that two Levallois methods for blank production were applied (Tab. 109):

- **Recurrent**, which aims to obtain several blanks from a single flaking surface and
- **Preferential**, the objective of which is to receive just a single blank from a single flaking surface.

Six Levallois-like cores were collected from three Hummalian layers: 6b, 7c and αh (Tab. 110). Four were made on block and two on flake. These cores have a cautiously accomplished faceted platform. The dorsal scar patterning shows evidence of debitage of flakes and elongated flakes.

Usually the Levallois cores result mainly in large blanks of varying sizes, and occasionally in narrow and thin ones. As was shown earlier, in analysed collections it can be difficult to determine which products were removed through Levallois reduction. There are a number of flakes with well-faceted butts, sometimes triangular in shape, which might result from this reduction. There are only a few specimens showing the *chapeau de gendarme* butt, but many blanks present a cautiously prepared platform. Finally, a few blanks with centripetal negatives on their upper surface, a couple of *enlèvements II* (Fig. 136:11) and a few *éclats débordants* seem to be characteristic blanks of the recurrent method *sensu* Boëda.

6.8.3.1 Recurrent debitage

This method was observed on three cores: one core each from layers 6b and ah, and 7c. They are unidirectional (Fig. 136:3) or centripetal. The convexity of the distal and lateral portions of the cores exhibiting the recurrent method of debitage is guaranteed by the regular removal of edge-flake. This removal recreates the hinges or guides and follows the exploitation of the Levallois surface (Boëda 1988). The *éclats débordants* (Fig. 136: 5, 7-10) with prepared or cortical backs aid the continued flaking by systematically reducing the plane of intersection and allow a better use of the block volume (Boëda 1995). The distal convexity is also assured by small removals from the latero-distal part of the core. The large platform is established on the proximal or proximal-and-distal (bidirectional) part of the core. They are in the main faceted. The blanks were struck from one or two parallel platforms, and a typical product of this reduction *enlèvement II* was detached. The lateral and distal convexities are achieved in the centripetal Levallois method by the removal of *éclat débordants* – often overshoot (Fig. 136: 9) – which maintains the rest of the Levallois preparation. Alternatively, the extraction of small flakes around the periphery of the exploitation surface could be used to the same affect. The striking platform is organised around the whole core periphery.

The sequence of detachment of a few blanks is repetitive, possibly provoking the decrease in size of the core and the products. It can be seen in the length, where the

blanks can be as small as 2cm and cores as small as 4cm. The distal and lateral convexity was guaranteed by the systematic subtraction of cortical or prepared edge-flakes during the reduction when the flaking surface became too flat. It can be seen by the length of the edge-flakes, which ranges between three and ten centimetres. The majority of cores are exhausted.

6.8.3.2 Preferential method

Two cores from Layer 6b and one from Layer 7c show the negative of preferential flakes, covering the main part of the exploitation surface (Fig. 136: 3). The preferential flake method was not used regularly, probably only at the end of the core reduction. This can be further evidenced by the fact that the median length of blanks surpasses the length of this type of core, the mean length of the cores is 4.2cm, and the mean length of the blank-flakes is 5.1cm. There are hardly any well-centred flakes in layers 6b, 7c or ah.

6.8.4 The Nahr Ibrahim Technique (NI)

There are three hypotheses to consider with truncated-faceted pieces.

The first perceives the retouch on the ventral face as having been made for a functional purpose. Semenov (1964, 63, fig. 65) proposed such an interpretation after analysing Kostienki knives. Dibble (1984 p. 29), who studied the Mousterian industry of Bistun Cave, drew similar conclusions.

The second assumption is that the NI technique was used to thin the lithic specimen intended for hafting (Schroeder 1969, 29). Use-wear analysis of some truncated pieces from the Umm El-Tlel site in Syria was undertaken, and it appears that they showed traces of hafting (Boëda *et al.* 2001, 24, fig.17). Unfortunately, too few details have been presented to permit further discussion.

The last hypothesis is that such a modification was used for core preparation and that these specimens are in fact cores for flake production (cf. Newcomer and Hivernel-Guerre 1974, Goren-Inbar 1988, Dibble and McPherron 2007).

Rose and Ralph Solecki proposed a typological list of NI pieces and suggested that this kind of technique could be used for various purposes: for hafting and for core preparation when the flint knapper wanted to strike a flake from another flake. Hence, this piece became a core on flake (Solecki and Solecki 1979).

The use of the NI technique is visible in seven of the eight Hummalian layers and is seen in 43 specimens (Tab. 111). These are made in the main on non-cortical flakes, with a few showing only small patches of cortex covering less than 25% of their ventral face (Fig. 115, 150, 166). Six were made on a retouched specimen. They were truncated and then faceted on either the proximal or distal ends or both. The prepared edge serves as a platform. In all pieces, the faceted platform is situated on the dorsal face; if applied to the proximal end, the faceting removed the bulbs. The angle between the prepared platform and the dorsal face varies between 105 and 130 degrees. There are 23 bidirectional pieces, and 20 unidirectional (Tab. 112). Rectangular to triangular in shape and mainly convex in cross-section, they are thicker than retouched or non-retouched blanks (Fig. 137).

Comparing the metrical data of NI cores with the cores on flake, it is noticeable that the former are longer and thinner than the latter. The mean number of negatives visible on the upper face of NI cores is slightly smaller than that from cores on flake: 2.9 and 3.3 respectively. Yet by comparison of the unidirectional and bidirectional items among the NI cores, it is evident that the former are longer and thinner, their L/W ratio equals 1.9, and towards the end of reduction they produced small blades. The bidirectional are broader; the end part of reduction manufactured blades and flakes, and on average more negatives are present on their ventral face; and their mean is 3.9, versus 2.4 for unidirectional. The mean thickness of truncated-faceted pieces is also greater than that of the retouched and non-retouched blanks. It means that the knapper wanted relatively large items with a thick cross-section to set up the truncation and start the flaking.

There is one interesting piece from sandy Layer oh. Originally, it was a finely retouched pointed tool with a thick triangular cross-section, but the distal portion

broke and so the item was discarded. Over time, the piece developed a slight patina. At some later point, the piece was picked up once more and prepared with the NI technique on the proximal end in an attempt to flake on the ventral face of the item. The dorsal face is marked by just one small subtraction. The piece was once more discarded, with the fracture not repaired. Evidently the flint knapper had been trying to recycle the broken specimen for flaking purposes, but did not want to invest the time in maintaining it, which would have been rather difficult anyway because of the decreased thickness of the item.

A lack of traceological studies of truncated-faceted pieces from Hummal does not help in their interpretation. In the present study, these truncated-faceted specimens were classified as core on flake with NI preparation.

6.8.5 Bladelet Production

6.8.5.1 Introduction

Burins have long been discussed as engraving tools, and their types were renowned on the basis of either manufacturing technique (Bordes 1947, LaPlace 1956) or morphology (Pradell 1948). The results of use-wear analysis show that the burin was an object employed for different purposes. In addition, some of them display the traces of use, while others do not (Beyries 1993, 60, de Araujo-Igreya and Pesses 2006). It is supposed that the burins that do not demonstrate evidence of use could have served as cores for bladelet production.

6.8.5.2 Core-burins

Core-burins were documented in all Hummalian layers. Unfortunately, no traceological analyses on the Hummalian burins were undertaken, but because of the significant number of bladelets next to burins in all the analysed layers, it is supposed that burins were used for bladelet production. Thus, all items which would be typologically described as a 'burin' may be considered a bladelet core.

In all the analysed layers, bladelets and/or core-burins are present. Comparing the width of bladelets with the width of the last negatives visible on the core-burin, it

appears that the majority seem to have been produced from the last few (Fig. 138, Fig. 159). It can also be observed that the flint knapper produced bladelets from the core-burins with widths ranging between 0.3-0.5 mm; however, the collected bladelets do not show comparable measurements, since all of them are wider. This mismatch is probably due to sample error. Furthermore, the graph shows that a number of bladelets with a breadth wider than 1.2cm were probably not manufactured from the collected core-burins, at least not at the end of their reduction. It seems that they were obtained from different Laminar cores at the end of their reduction, sometimes from the side of exhausted Levallois cores or cores with NI preparation.

In the case of Layer 6b, core-burins represent 25% of all cores (Tab. 113).

The bladelets (width \leq 1.4cm, length \leq 5cm) were produced from core-burins made on intact or broken thick flakes and blades, or on debris (Fig. 139), and were achieved by three different methods:

- ‘Burin-flaking’, working on the thickness of the support, is the best represented. The flint knapper used the natural shape of the support and started to detach the blank from its natural edge. In a few cases, the flaking started on one edge of the support and expanded onto the other, not unlike semi-rotating debitage. This resulted in one to five bladelets, of two to four centimetres in length. Three items were also removed from the dorsal face from the same platform. They were completed on flake and debris.
- Transversal debitage employed on flakes: the bladelets were knapped on the proximal or distal part of the flake transversally to the axis of flake debitage. Two were made on the distal part of a large plunging flake. A plain striking platform was arranged on the side of the distal part of the flake by one blow from the distal edge, parallel to the axis of the flake but transversally to the flaking axis of knapped bladelets. From one to three negatives were visible on the flaking surface of such core-burins.
- Flaking on the front of the lithic support, similar to ‘end-scraper debitage’. It is the least represented; just two items were noted (Fig. 139:6). The edge of the

front of such cores is very irregular and five negatives were visible on their ventral face. The widest negative shows 1cm.

Comparing the metrical data of core-burins made on flake and on debris, it can be seen that they are fairly similar: those made on flake are slightly longer, and those made on debris are thicker (Tab. 114). Both present between one to seven bladelet negatives on their ventral face.

The majority of core-burins are unidirectional (Tab. 114, 115). The bidirectional cores do not represent a genuine bidirectional reduction, but rather two juxtaposed unidirectional reductions realised on the same core. Anyway, just a few bladelets present bidirectional scars on their ventral face. They are thicker than retouched and non-retouched blanks, and the thickness is comparable to the thickness of cores on flake, including those with NI preparation. This shows that the knapper was looking for relatively thick lithic items to carry out the debitage of bladelets.

6.8.5.3 Bladelets

Bladelets are described in the analysed assemblages as small blades whose width is equal to or less than 1.4cm and whose length is no more than 5cm. They were uncovered in seven of the eight studied layers. Bladelets were not discovered in Layer 6B, but cores and core-burins which show the negatives of small bladelets on their flaking surfaces were found. Their percentage varies between layers; considering just the large assemblages 6a, 6b, 6c2, 7c and α h, values of between 4% and 10% of debitage are recorded. They are frequently broken, with only a few remaining intact; therefore, the measurements of width and thickness and the W/T ratio of the platform were considered from the broken pieces as well. The length, ratios, surface and volume were calculated only for intact items (Tab. 117). Their length ranges from 2.3 to 4.8cm, their width from 0.6 to 1.4cm, and their thickness from 0.2 to 1.2cm. Layer 6a had the highest proportion, with 6b and 7c having 37%, and 6c2 having 50%. Only 25% of bladelets in α h equalled or exceeded the 1cm width level; the remainder were narrower. The CoV for the mean width is the same in layers 6a, 6c2 and Sand α h, with

a value of 0.1; layers 6b and 7c showed a CoV of 0.2. The thickness of most bladelets from Layer 7c surpasses 0.5cm, as is the case with 25% of bladelets from layers 6a and 6b. The bladelets from layers 6c2 and 6h present the same thickness pattern, and 75% of them are thinner than those from the previous layers. 25% of bladelets from the two latter layers are very thin (only 0.2 to 0.3cm), and it is possible that they were produced from the upper surface of blank blades. The CoV for thickness is different in each layer (Tab. 118). The large majority of bladelets are unidirectional, but in every layer one or two pieces also present bidirectional reduction. Two or three, and occasionally four, previous scars can be observed on their upper surfaces. Their edges are mostly parallel, followed by those that are convergent. About 80% of them have a high (oblique) triangular cross-section (or, less often, a trapezoidal cross-section) in the middle point. Half of them show a relatively bowed profile, and the rest are rectilinear. When not broken, their striking platforms are frequently plain; less frequently slightly faceted; and sometimes dihedral and cortical. The W/T of butts as well as the CoV for this ratio varies in all layers. Around 10% of items from each layer show a slight preparation of the proximal end of the item by tiny removals from the platform, extending into the proximal part of the upper surface. Only a few carry a small patch of cortex on their upper surface.

6.9 Summary

The assemblages presented here seem to be part of the same lithic tradition in which the aim was to produce blades, regardless of their size. As the statistical studies have shown, there is a high variability within non-retouched blades from different collections, as well as within categories of blank blades with respect to their metrical attributes. The most consistent element between blades from different assemblages seems to be their width, whilst the length and thickness vary. They can present high triangular or trapezoidal cross-sections or be flat, narrow or broad, thick or thin. The majority are bowed in longitudinal profile, but a number are also rectilinear. Mostly the butts are slightly faceted or plain, but a number present a cautiously faceted platform. The majority presenting a high cross-section, bowed profiles, and a plain or

slightly faceted platform seem to be associated with the Laminar reduction strategy. A minority with carefully prepared butts and a plane cross-section can possibly be associated with Levallois. However, there are a number of blades that are difficult to place within either of these reduction strategies, due to their non-distinctive morphology. They seem to present a fusion of metrical and non-metrical features from both the Laminar and the Levallois groups. The metrical analyses show that in Sand 6a they seem to share more similarities with Levallois specimens than with Laminar, whilst in Layer 6b this is not so clear-cut.

Boëda (1997:53-54) proposed that both reduction strategies could take place within the same sequence, and in this case these undetermined blades could possibly have been obtained when the flint knapper passed from Laminar-pyramidal reduction to Levallois. Unfortunately, Boëda did not present any evidence or facts as to how this conclusion was reached, whether through experimental work or observations, and consequently the information about products and CTE which would be vital in identifying and recording this phenomenon has been missed.

Nonetheless, this study seems partly to confirm Boëda's assumption. In our opinion also (and *contra* Wojtczak 2011), the Hummalian industry presents only one reduction strategy which results in blanks of different morphology. The system of debitage is associated with the characteristic CTEs and so-called 'Hummal-type of Volumetric Construction' as defined by Boëda (1995:63), and with simple frontal debitage. The flint knapper used the natural shape of the block or large flake to begin debitage. He started to chip on its narrow, convex and elongated side (usually its thickness), and as flaking progressed, the flaking surface was expanded onto one of the lateral sides of the core and semi-rotating debitage was achieved.

Faceting was used for rejuvenation of the core platform. Additionally, management of the flaking surface was regularly attained by the removal of a flake edge along a natural or cortical ridge, and occasionally by secondary crested blades. The first face, working on the thickness of the core, resulted in blanks with high cross-sections and plain butts. As flaking proceeded (with the volume of the core decreasing) and

expanded onto the wider and flatter side of core, the morphology of the obtained blanks transformed. They became flatter in cross-section, often with a prepared butt, because the flint knapper started to prepare the core striking platform in order to achieve better control of the flaking process and of the morphology of the desired blank blades. The morphology of many such cores was simultaneously changed as well. In numerous cases, the flint knapper started to treat the available volume differently and started to prepare the distal and lateral portions of the cores intensively. The upper surface of such cores exhibiting the recurrent method of debitage – guaranteed by the regular removal of *éclats débordants*, or alternatively the extraction of small flakes around the periphery of the exploitation surface – could be used to the same effect. The large platform was established on the proximal or proximal and distal (bidirectional) part of the core. They were in the main faceted. The blanks were struck from one or two parallel platforms and a typical product of this reduction *enlèvement II* was removed. The sequence of detachment of a few blanks was repetitive, provoking the decrease in size of the core and the products.

It seems that the flint knapper often moved from Laminar debitage to Levallois-like debitage when the volume of cores decreased, since cores became flatter and needed more preparations to control the manufacture of blanks. The use of the Levallois recurrent method *sensu* Boëda with characteristic CTEs (*éclats débordants*) and products (*enlèvement II*) is the most prevalent in the studied assemblages. The linear method is also seen, although only sporadically and mainly in the presence of cores, and involving only two layers, 6b and 7c. Only a few blanks can be associated with this reduction system.

The existence of bidirectional cores with two opposite platforms that are slightly offset seems to be an important and characteristic trait. Crested blades were rarely used to initialise the flaking. Management of the laminar flaking surface was achieved by the removal of a flake edge along a natural ridge or by secondary crested blades. The maintenance of the flaking surface was assured by the regular removal of ‘cleaning flakes’ throughout the reduction.

It appears also that the faceting of the platform was undertaken to correct the flaking angle, at once allowing the production of longer supports and prolonging the flaking. The products obtained throughout this method are mainly blades with plain or faceted, but rarely cortical, striking platforms of different sizes.

The retouched tools made on flake and on blade seem to be quite standardised in their metrical and non-metrical attributes, in both the assemblages and the tools categories. The tool-kit from all layers (except for Layer 7a) comprises of elongated retouched blades, often converging in the distal part and also frequently pointed by retouch; that is, Mousterian tool-type scrapers and notches/denticulate, and also Upper Palaeolithic types such as end scrapers.

Interestingly, the thick prismatic blades are often retouched, but the elongated Levallois products are not modified. This may indicate different uses of the blades. This assumption appears to be confirmed by the use-wear analysis undertaken recently by Beyries (in Meignen 2011) on a series of elongated tools from Hayonim Layer F. This work revealed that the thick items were mainly used in hide and bone processing activities, while the Levallois tools were often implicated in butchery activities.

The presence of short blanks, although less numerous, is also confirmed. Similarly, as with non-retouched blades, some of them present Levallois morphology; a number of them are triangular in shape with thin, well-faceted platforms; and others are relatively rectangular in shape and thicker, with a significantly lower value of W/T butts, namely 2.3, compared to 4.3 in 6b, and 2.8 against 5.7 in Sand ah. They are elongated, presenting a median L/W ratio of 1.5 in Layer 6b and 1.6 in Sand ah.

The unidirectional flaking system dominates in all layers, but bidirectional is also well represented, especially in Sand ah and layers 6c2 and 7c.

In all the analysed assemblages, the Hummalian production strategies characterised by passing from Laminar (rotating) to Levallois-like debitage were practised, as shown by the presence of cores and their characteristic CTEs and blanks. The aim of production was converging or parallel elongated blanks of different sizes. But the production of

blades was not exclusive and is associated with short blanks of Levallois and non-Levallois morphology.

The debitage of cores on flakes, with or without NI preparation, is also documented. The negatives left on these cores indicate the production of flakes, blades and bladelets. The obtained product had to be relatively thin and of small size. As blank production was carried out until the core was exhausted, the assemblage includes blanks with a size scale ranging from elongated blades to small bladelets, but there was also a separate production of bladelets from core-burins and bladelet cores manufactured on a thick support.

It can be concluded that all these elements indicate some complexity in blank production and, as shown through the traceological analysis made on the supports from Hayonim F, the products of different morphology were used for diverse activities.

In all layers, the majority of products present the preparation of the proximal part, using a series of small removals coming from the edge of the butt into the proximal part of the upper surface, and also dorsal reduction.

It appears also that faceting of the platform was undertaken to correct the flaking angle, at once allowing the production of longer supports and prolonging the flaking.

The significance of recycling is indicated. It is documented by the appearance of numerous cores on flake, the reuse of patinated blanks for shaping new tools, the production of bladelets on broken blanks and debris, the recycling of Yabrudian scrapers as cores (Fig. 148:2, 153, 161), and the shaping of exhausted cores for tool use (Fig. 148: 1, 3).

In all layers, the technique of percussion using the hard hammer mode was identified. The presence of a few products with a lipped butt and diffuse bulb suggests the use of a soft hammer, but it seems that it was used only marginally. Bergman and Ohnuma also reported the presence of soft hammer technique in Assemblage Ia from Hummal (Bergman, Ohnuma 1983:173).

7. Comparison

7.1 Introduction

The Early Middle Palaeolithic blade industries from Hummal are clearly intercalated between the Yabrudian and Mousterian levels. The estimated TL age for sandy Layer α h is approximately 200 ka, and is comparable with those of the Laminar phenomenon highlighted at Hayonim Layer 'F top' and 'F base' with mean TL dates on heated flint of 210 ± 28 ka and 221 ± 21 ka, respectively (Mercier *et al.*, 2007), or at Tabun for unit IX (Tabun D-type) from 256 ± 26 ka and Rosh Ein Mor, dated 200 ka (Rink *et al.* 2003). These assemblages were discovered at different site types that varied in the use of Laminar and Levallois reduction strategies and in the production of diverse tools. In contrast to the Hummalian, the collections from Tabun and Rosh Ein Mor seem to be dominated by the Levallois method (Meignen 1994:143, Hauck 2010; 200). They are comprised of a considerable number of Upper Palaeolithic tools and a small percentage of elongated, slightly modified blades. At present, it seems that the lithic industries from Hayonim layers F and E (Meignen 1998, 2000) and the undated Abu Sif layers B and C (Neuville 1951, and personal studies on part of collection at IPH, Paris) show the greatest resemblance to the Hummalian industries presented above. These assemblages, precisely like the Hummalian, seem to contain the predominating Laminar and Levallois elements, whilst showing a tendency to produce elongated blanks. The tool-kit comprises numerous retouched blades and, less frequently, Mousterian and Upper Palaeolithic tools. Furthermore, in blade assemblages from Hummal and Hayonim, the production of bladelets from core-burins has also been documented (Meignen 2011).

7.2 Comparison with Abu Sif B and C

This study analysed collections from the Abu Sif B and C sites that are housed in the IPH in Paris, but these collections are incomplete. The comparison and interpretation that follow are limited to general observed tendencies.

80% of the blanks show unidirectional reduction, and the remainder are bidirectional. Non-retouched blades were scarce in both layers; only four in Layer C and 13 in Layer B were documented. A couple of typical Levallois points with well-faceted, thin platforms were acknowledged. Retouched blades are better represented: there were 43 in Layer B and 30 in Layer 6. They are mainly unidirectional, with three or more previous scars on their upper surface. All blades, with one exception, converge at their distal end. In the main they are asymmetrical towards the left or right, sometimes inclining to the right and sometimes to the left. Their proximal part was often prepared by minor triangular removal, but this was not as intensive as in blades from Hummal.

Their butts are faceted but some cautiously so, and others only slightly, being plain, sometimes cortical or dihedral. Their cross-sections can be triangular or trapezoidal, plane or high. They are usually broadest in the midsection, followed by the proximal part.

The tool-kits from both layers contain mainly blades retouched on one or both sides. Typologically, they are seen as single scrapers and retouched Mousterian points, and only rarely double scrapers. A few single scrapers present a cortical back on the side opposing the retouched edge. But there are a number of tools, ten in Layer B and three in Layer C, usually single scrapers that were made on short Levallois-like supports as well. They are large with a well-faceted platform. The applied retouch is usually long or invasive, semi-abrupt, and covers one or both sides of specimen along the whole length or medial-distal part, but only rarely on the distal part.

7.3 Comparison with the blade industry from Nadaouiyeh Ain Askar

The surveys carried out in the region of El-Kowm exposed only five sites with Hummalian layers: Hummal, Arida A, Ain Juwal, Umm el-Tlel, and Nadaouiyeh Ain Askar. These sites are all related to the water sources where archaeological material was gathered in stratigraphy. By comparison, eleven Yabrudian sites and 64 Levallois-Mousterian sites were discovered in the same area (Jagher, in preparation). This shows the scarcity of Hummalian sites (Fig. 165).

Analyses of blade assemblage from Nadaouiyeh Ain Askar (or, for short, Nadaouiyeh) were undertaken for comparative purposes (for stratigraphical details, see Jagher 1993). It has to be mentioned that the analysed assemblage is not complete and that the results obtained are to be revised in the future. Only whole pieces were taken into account in this study. Altogether, 315 items were studied (Tab. 122).

The similarity of patinas and of the raw material argues in favour of the homogeneity of this assembly. Many artefacts also show a gloss that has already been observed in collections from Sand α h at Hummal. The artefacts are well preserved and very fresh, and present no traces of crushing.

Compared to the lithic series from Hummal, which represents all the stages of *chaîne opératoire*, Nadaouiyeh appears to be very incomplete. Initialisation of flaking is difficult to determine, as only a single crest was recorded. CTE is 13% of the assemblage and is represented mainly by edge-flakes with plain, cortical and prepared backs. There are a couple of semi crests which, with edge-flakes, can probably be associated with the Laminar method of debitage, and two *lames débordantes* and a couple of pseudo-Levallois points, which are a link to the Levallois method. 30% of artefacts present small cortex patches (from 1 to 25%) on the proximal, distal or medial part. Dorsal scar patterns indicate unidirectional flaking in 60% of items and bidirectional in the rest. It shows a similarity with Sand α h, where the bidirectional method is also well represented, giving a similar value of 40%. The centripetal method is visible on only two items. In assemblages from Hummal, centripetal dorsal scar patterns are also visible on only a few blanks. The majority of blades present the preparation of their proximal part, and frequently dorsal reduction, exactly as seen in Hummal.

Half of the blades are bowed in their profile, and half are rectilinear. Their cross-section is triangular or trapezoidal, plane or high. The majority present converging followed by subparallel lateral sides, rarely expanding. They usually have three or more previous scars on their upper surface, indicating provenance from the advanced stage of reduction. Their butts are usually slightly faceted, plain and sometimes

cortical. But there are also a number of blades with well-faceted platforms and plane cross-sections, with several presenting *chapeaux de gendarmes*. They are long, with a L/W ratio median of 2.6 for non-retouched and 2.7 for retouched.

The greater part of the flakes presents a well-faceted platform, rarely plain or cortical, with a W/T ratio for butts of 4.3, indicating thin butts. Flakes are elongated with an L/W ratio median of 1.6, and half are triangular in shape.

7.4 Metrical analysis of assemblages from Hummal, Nadaouiyeh and Abu Sif

This section compares the metrical attributes of the assemblages from Hummal, Nadaouiyeh and Abu Sif. For non-retouched blades, the comparison was made using assemblages from Hummal 6b and Sand α h, Nadaouiyeh and Abu Sif B. It has to be said that the last collection is very small and statistically the sample sizes are prone to error. However, it is possible to discern general trends and a fit with the other, larger assemblages.

The longest non-retouched blades appear in Nadaouiyeh and Abu Sif B with a median of 8.0cm. Blades from Sand α h are similar, with a median of 7.7cm, and those from 6b are the shortest, with a median of 7.2cm. About 50% of blades from the first three of these assemblages, and more than 35% from 6b, exceed the 8.0cm median. In Nadaouiyeh, they range up to 14cm. The rest are smaller, ranging down to 3.5cm. The length of more than 70% of blades in each collection is between 5 and 11cm, indicating the largest similarity between them (Fig. 140a). The largest blades are the specimens from Layer 6b and Nadaouiyeh, with a median width of 2.8cm; the Sand α h blades are slightly less, at approximately 2.6cm, and the narrowest are those from Abu Sif B, at 2.4cm. More than 80% of blades from every assemblage have a width between 1.4cm and 4cm, indicating high variability within the set and showing the similarities between them. Nevertheless, sets from El-Kowm seem to be quite consistent with those from these three groups (Fig. 140b). Their L/W ratios are similar to those from El-Kowm, with 2.7 in Sand α h, 2.6 in Nadaouiyeh and 2.5 in 6b. The

ratio is very high in Abu Sif B, which is probably due to the sample size but still fits into the trend displayed by the other sites (Fig. 141a).

The thickest blades, with a median 1.0cm, are definitely those from 6b, and the thinnest (0.6cm) are from Abu Sif B. The collections from Nadaouiyeh and Sand α h present the same median thickness of 0.8cm and the same variability. The bulk of blades from Nadaouiyeh and Sand α h have a thickness between 0.7 and 1cm (Fig. 140c).

The W/T ratio is smallest in 6b as a consequence of the great thickness of blades, with a value of 2.7 indicating relatively massive specimens. The highest ratio, 3.7, is found in the collection from Nadaouiyeh. The ratios of Sand α h and Abu Sif B are similar, at 3.4 for the former and 3.5 for the latter. It appears that more than half of the blades from Nadaouiyeh, and about 40% from Sand α h and Abu Sif, have a ratio higher than the median 3.7, indicating that a large proportion of those blades were gracile. Only 20% of the blades in 6b were as thin (Fig. 141b).

The median W/T ratio of butts is highest in the Nadaouiyeh collection, with a value of 3.5, and smallest in 6b and Abu Sif, with 2.3. But more than 50% of butts from 6b and Abu Sif have a higher ratio, ranging in Abu Sif B up to 5.5. The box plot shows clearly that the majority of blades from Nadaouiyeh have a rather thin platform. The variability in respect to this ratio is greater in this collection than in 6b or Sand α h (Fig. 141c).

The metrical analysis for retouched blades was undertaken for Sand α h, 6b, Nadaouiyeh and Abu Sif B and C. This time, collections from the last site seem to be statistically sound.

The retouched blades from Nadaouiyeh have the largest median length of 9.0cm. The specimens from Abu Sif C are similar at 8.6cm and Sand α h and Abu Sif B are also similar, with medians of 8.3cm and 8.2cm respectively. The median length for 6b is the smallest, with 7.7cm. Nearly 50% of items from Sand α h and Nadaouiyeh present a greater length than the median of 0.9cm, indicating that they are related. Only 20% of blades from 6b have a length greater than this median (Fig. 142a).

Blades from all assemblages are similar in their median L/W ratios, ranging from 2.9 for Sand αh and 2.5 for 6b. More than half of the specimens from Abu Sif B and C, Nadaouiye h and Sand αh have a greater ratio, but only 25% of those from 6b do. This shows that the first four collections are very similar with respect to this ratio.

The assemblages from Sand αh, 6b and Abu Sif B all have a median width approximating 2.9cm. The median for Abu Sif B is slightly smaller at 2.7cm and for Nadaouiye h it is slightly greater, 3.3cm. More than half of the blades from Nadaouiye h, 35% from Abu Sif B, but only 25% from Abu Sif C, Sand αh and 6b, have a width greater than the median of 2.9cm. There is a larger proportion of larger blades in the collection from Nadaouiye h than in the others (Fig. 142b).

Blades from Nadaouiye h and Abu Sif B and C present the same median thickness of 0.6cm. Those from Sand αh are thicker, with a median of 0.8cm, and those from 6b are the thickest, with a median of 1.0cm (Fig. 142c).

The median W/T ratio of specimens from Sand αh and Abu Sif B and C are similar at 3.4. From Nadaouiye h it is greater with a value of 4.0, and from 6b, smaller, with 3.0. The W/T ratio of butts is similar in Nadaouiye h and Abu Sif B and C, with a value of 3.3. This ratio is smaller in layer 6bs and Sand αh with a value of 2.5, indicating a relatively thick platform in comparison to the others (Fig. 143).

In conclusion, the major part of the retouched and non-retouched blades from Nadaouiye h seems to be the longest and widest among blades from all the analysed sites. The width and length of the blades from other collections are similar, but those from 6b are the shortest. The thickness of blades in all layers is comparable, except for those from 6b, which are the thickest. The L/T ratio for retouched and non-retouched blades seems to be analogous in all layers, and the same is true for the W/T ratio, with the exception of Layer 6b. The W/T ratio of butts is clearly shared in two groups from the analysed assemblages. In one group, that of retouched tools from Nadaouiye h and Abu Sif B and C, the majority of the blades have a relatively thin platform; while the second group, from 6b and Sand αh, has a significantly smaller ratio. Rephrasing, the large proportion of blades from Sand αh are as long, wide and thick as the others, other

than 6b, but their striking platforms are thicker. Those from 6b are the shortest and thickest, with a thick platform.

Comparing the assemblages from El-Kowm, it seems that those from Nadaouiyeh and Sand ah from Hummal are highly correlated with respect to their length, width, thickness, and L/W ratios. The metrical feature that separates them is the W/T ratio of butts. Those from 6b are shorter and thicker, perhaps because of taphonomic phenomena, as only the more robust specimens would not be affected by such phenomena, and only measurements of intact items were used for this statistical and metrical analysis. On the other hand, the measurements of width and thickness taken from broken pieces confirm their massiveness in comparison to those from other assemblages.

7.5. Conclusions

Generalising, the assemblages from Nadaouiyeh and Abu Sif seem not to differ from those of Hummal. The support in both cases contains a majority of blade components, but also short blanks. Direct percussion with a hard hammer is attested at all these sites. The majority of blades are convergent or subparallel. In Nadaouiyeh, the presence of the production of small blades 4cm in length is also confirmed. The composition of their tool-kits appears very similar. All assemblages are dominated by retouched blades, often converging, but the retouch observed on tools from Hummal and Abu Sif seems to be more important than those from Nadaouiyeh. This may indicate that they were rejuvenated more often, *ergo* more intensively used. The presence of blanks coming from Laminar and Levallois reduction strategies appears well documented at all sites.

It seems that all these blade assemblages are closely related. Both blade production and metrical variation were quite standardised. One feature well represented in assemblages from Hummal that seems to be lacking in the collections from Nadaouiyeh and Abu Sif is the clear production of bladelets. There is one edge-flake in Abu Sif with a clear negative of a bladelet which was detached by frontal debitage,

but it is the only one, and there are no bladelets as such. In Nadaouyieh small blades of 4cm in length exist, but they are not as narrow as those from Hummal.

There are many similarities between the presented collections, but there are also some differences. Abu Sif is a cave site and the settlement dynamic and subsistence strategy would most likely have been distinct from those of open-air sites such as Hummal and Nadaouyieh. However, it is difficult to show whether the differences observed here were due to subsistence strategies or to technical traditions.

Surveys carried out in the region of El-Kowm uncovered only five sites with Hummalian layers: Hummal, Arida A, Ain Juwal, Umm el-Tlel, and Nadaouyieh Ain Askar. These sites are all related to the water sources where archaeological material was gathered in the stratigraphy. For comparative purposes, eleven Yabrudian sites and 64 Levallois-Mousterian sites were discovered in the same area (Jagher, in preparation). This clearly shows the scarcity of the Hummalian sites.

It seems that the occupation in Hummal's Layer 6b was relatively long and intensive. It is attested by the high density of artefacts; the presence of almost all stages of lithic production; their maintenance on the site, with the presence of many highly retouched specimens; and the frequency of recycling, with the majority of cores being exhausted and discarded at the site. This suggests a strategy related to provisioning places (Kuhn 1995). Contrary to this, in layers 6c2, 7a and 7c the occupation seems to have been short, as shown by the low artefact density and the low percentage of debitage by-products, suggesting that the main knapping activity took place elsewhere. Additionally, in Layer 6c2 the high percentage of retouched pointed blades may suggest a task-specific location. The high percentage of CTE in this layer is linked to the presence of numerous thin bladelets, probably detached from the upper surface of blades, which could also suggest specific activities. This then leads to a suggestion of a 'provisioning for individuals' strategy (Kuhn 1995) with 'personal gear' (Binford 1979). But, as the Hummal site is very large and only a small proportion of it has been excavated, these observations are only a first step in understanding the site. In all layers, the lack of artefacts made on exotic raw material suggests that the Hummalian

people identified in advance that there was ready access to high-quality raw material from local sources.

In Nadaouiyeh, any interpretation can only be potential, as the assemblages were not found in a clear stratigraphical position. However, the low proportion of such debitage by-products as CTEs and cores, together with a high proportion of retouched and non-retouched convergent blanks, may suggest a task-specific location and the provisioning of individuals. This scarce information from the region suggests a high residential mobility, with the people relocating through the landscape, which in turn leads to possibility that Layer 6c2 and Nadaouiyeh had a restricted tool-kit. However, Layer 6b shows signs of long-term occupation, with the strategy of provisioning a place rather than individuals.

Prospection carried out in the area of the Negev highlands – abundant in good-quality raw material and water sources – as well as the excavation of sites at Avdat Aqev and Rosh Ein Mor, has returned interesting results (Munday 1977, 1979; Marks and Friedel 1977). It appears that the wet seasons were characterised by a stable settlement dynamic when the base camps were intensively and long occupied and provisioned logistically by ‘radiating mobility’ from short-term camps (Henry 1995). The region of El-Kowm is comparable, with high-quality flint and numerous waterholes, so a similar pattern of settlements would be possible. The data even suggest it.

The Abu Sif site, with its low artefact density, was interpreted by Neuville as a short-term occupation: *le site ne fut peut-être jamais habité très longtemps* (1951:54). The low number of debitage by-products, and the high proportion of non-retouched and especially retouched blanks, suggests that the flaking took place away from the cave and that previously prepared blanks were introduced to the site. This implies the provisioning of individuals. Furthermore, the homogeneity of tool-kits, with their pointed blades and short blanks, could indicate that particular activities were undertaken at the cave. The Hayonim cave has been interpreted as a residential camp of short duration within a strategy of high mobility (Meignen 2006:155). The results

from Abu Sif are comparable to those at Hayonim and add further weight to the idea that Abu Sif was more likely a temporary settlement.

In any case, the sophistication visible in all the studied assemblages seems quite startling in comparison to the succeeding Middle Palaeolithic complexes, governed as they were by the Levallois reduction strategy.

References

Ancient TL date list 2, 1988. Ancimt TL Supplement, 26.

Ahler, S. A., 1989. Mass analysis of flaking debris: studying the forest rather than the tree. In: Henry, D. O., Odell, G. H., Ahler, S. A. (Eds.), *Alternative approaches to lithic analysis*. American Anthropological Association, Boulder, 86-118.

Al-Qadi, A, 2008. Le Yabroudien et la transition entre le Paléolithique inférieure et moyen au Proche-Orient, l'exemple d'El Kowm (Syrie Centrale). Unpublished Master thesis, University of Basel.

Akazawa, T., 1979. Middle Paleolithic assemblages from Douara Cave. *Bulletin of the Museum of the University of Tokyo* 16, 1-30.

Alimen, H., 1955. *Préhistoire de l'Afrique*. Boubée, Paris.

Almogi-Labin, A., Bar-Matthews, M. & Aylon, A., 2004. In: Goren-Inbar, N. and Speth, J.D. (eds.) *Human Paleoecology in the Levantine Corridor*. Oxford: Oxbow Books.

Alperson-Afil, N., Richter, D., Goren-Inbar, N., 2007. Phantom Hearths and the Use of Fire at Gesher Benot Ya'aqov, Israel. *PalaeoAnthropology*, 1-15.

Amick, D. S., Mauldin, R. P., 1989. Experiments in lithic technology. *British Archaeological Reports* 528, Oxford.

Andrefsky, W., 1994. Raw-material availability and the organization of technology. *American Antiquity* 59, 21-34.

Aritzegui, D., Asioli, A., Lowe, J.J., Trincardi, F., Bigliotti, L., Tamnurini, F., Chondrogianni, C., Accorsi, C.A., Bandini Mazzanti, M., Mercui, A.M., Van Der Kaars, S., McKenzie, J.A. & Oldfield, F., 2000. Palaeoclimate and the formation of Sapropel S1: inferences from Late Quaternary lacustrine and marine sequences in the central Mediterranean region. *Palaeogeography, Palaeoclimatology, Palaeoecology* 158, 2000, 215-240.

Bader, N.O. & Tschoumakov, I.S. 1977. Le site moustérien d'El Kdeyra dans le désert de la Syrie. *Sovietskaja Archologija* (2), 1977, 135-141.

Bakdach, J., 1982. Das Jungpaläolithikum von Jabrud in Syrien. Ph. D. Dissertation, Universität Köln.

Bamforth, D. B., 1986. Technological efficiency and tool curation. *American Antiquity* 51(1), 38-50.

Barkai R., Gopher A., Shimelmitz R., 2005. Middle Pleistocene blade production in the Levant: an Amudian assemblage from Qesem cave, Israel. *Eurasian Prehistory* 3(2):39-74

Barkai R., Gopher A., Lauritzen S., Frumkin A., 2003. Uranium series dates from Qesem Cave, Israel, and the end of the Lower Palaeolithic. *Nature* 423:977-979.

Bar-Matthews, M. Ayalon, A., Gilmour, M., Matthews, A. & Hawkesworth, C.J., 2003. Sea-land oxygen isotopic relationship from planktonic foraminifera and speleothems in the Eastern Mediterranean and their implication for paleorainfall during interglacial intervals. *Geochimica et Cosmochimica Acta* 67 (17), 2003, 3181-3199.

- Bar-Matthews, M., Ayalon, A., Kauffman, A., 2000.** Timing hydrological conditions of Sapropel events in the Eastern Mediterranean, as evidence from speleothems, Soreq cave, Israel. *Chemical Geology* 169, 145-156.
- Bar-Yosef, O., Meignen, L., 1992.** Insights into Levantine Middle Paleolithic cultural variability. In: Dibble, H. L., Mellars, P. (Eds.), *The Middle Paleolithic: adaptation, behavior, and variability*. The University Museum, Philadelphia, 163-182.
- Bar-Yosef, O. and S. L. Kuhn. 1999.** The big deal about blades: laminar technologies and human evolution. *American Anthropologist* 101(2):322-338.
- Binford, L. R. 1978.** *Nunamiut ethnoarchaeology*. New York: Academic Press.
- Bellomo, R.V., 1993.** A methodological approach for identifying archaeological evidence of fire resulting from human activities. *Journal of Archaeological Science* 20 : 525-553.
- Behrensmeyer A.K., Gordon K., Yanagi G., 1986.** Trampling as a cause of bone surface damage and pseudo-cutmarks. *Nature* 319: 768-771.
- Bergman C.A., Ohnuma K., 1983.** Technological notes on some blades from Hummal Ia, El-Kowm, Syria. *Quärtar* 33/34:171-180
- Besançon, J., Copeland, L., Hours, F., Muhesen, S., Sanlaville, P., 1981.** Le paléolithique d'El Kowm. Rapport préliminaire. *Paléorient* 7(1), 33-55.
- Besançon L., Copeland L., Hours F., Muhesen S., Sanlaville P., 1982. Prospection géographique et préhistorique dans le bassin d'El Kowm (Syrie); rapport préliminaire. *Cahiers de l'Euphrate* 3:9-26.
- Besançon, J. & Sanlaville, P. 1991.** Une oasis dans la steppe aride syrienne: la cuvette d'El Kowm au Quaternaire. *Cahier de l'Euphrat* 5, 6: 47-92.

Baumler, M. F. 1988. Core reduction, flake production, and the Middle Palaeolithic industry of Zobiste (Yugoslavia). In *Upper Pleistocene prehistory of Western Eurasia*, edited by H. L. Dibble and A. Montet-White. Philadelphia: The University Museum, University of Pennsylvania, 255-274.

Baumler, M., F., 1995. Principles and Proprieties of Lithic Core Reduction : Implications for Levallois technology. In: Dibble, H.L. & Bar-Yosef, O. (eds), *The Definition and Interpretation of Levallois Technology*. Monograph in World Archaeology 23. Madison: 11-23.

Beyries, S. & Boëda, E. 1983. Etude technologique et traces d'utilisation des «éclats débordants» de Corbehem (Pas-de-Calais). *Bulletin de la Société Préhistorique Française* 80, 275-279.

Beyries S., 1993. Analyse fonctionnelle de l'industrie lithique du niveau CA : rapport préliminaire et directions de recherche. In A. Tuffreau (ed.) : *Riencourt-lès-Bapaume, Pas-de-Calais : un gisement du Paléolithique moyen*, Paris, Maison de sciences de l'Homme, p. 53-61.

Binford, L. R., 1979. Organization and formation processes: Looking at curated technologies. *Journal of Anthropological Research* 35(3), 255-273.

Binford, L. R., 1980. Willow smoke and dogs' tails: hunter-gatherer settlement systems and archaeological site formation. *American Antiquity* 45(1), 4-20.

Binford, L. R., 1986. An Alyawara Day: Making men's knives and beyond. *American Antiquity* 51(3), 547-562.

Binford, L. R., 2001. Constructing frames of reference: An analytical method for archaeological theory building using hunter-gatherer and environmental data sets. University of California Press, Berkeley.

Boëda E., 1986. Approche technologique du concept Levallois et évaluation de son champ d'application. Thèse Doctorat Université Paris X- Nanterre.

Boëda E., 1988. Le concept laminaire : rupture et filiation avec le concept Levallois. In: M. Otte (ed), *L'homme de Néandertal- La mutation*, ERAUL, 35, Liège, pp 41-59.

Boëda, E., 1990. De la surface au volume: analyse des conceptions des débitages Levallois et laminaire. In: Farizy, C. (Ed.), *Paléolithique moyen récent et paléolithique supérieur ancien en Europe. Ruptures et transitions: Examen critique des documents archéologiques*. CNRS, Nemours, 63-68.

Boëda, E., 1995. Levallois: A volumetric construction, methods, a technique. In: Dibble, H. L. Bar-Yosef, O. (Eds.), *The definition and interpretation of Levallois technology*. Prehistory Press, Madison (Wis.), pp 41-68.

Boëda, E., 1997. Technogénese de systèmes de production lithique au Paléolithique inférieure et moyen en Europe occidentale et au Proche-Orient. Habilitation à diriger des recherches. Université de Paris-X-Nanterre (unpublished).

Boëda, E., Connan, J., Dessort, D., Muhesen, S., Mercier, N., Valladas, H., Tisnerat, N., 1996. Bitumen as a hafting material on Middle Palaeolithic artefacts. *Nature* 380(6572), 336-338.

Boëda, E., Courty, M.-A., Fedoroff, N., Griggo, C., Hedley, I. G., Muhesen, S., 2004. Le site Acheuléen d'El Meirah, Syrie. In: Aurenche, O., Le Mière, M., Sanlaville, P. (eds) From the river to the sea. The Palaeolithic and the Neolithic on the Euphrates and in the Northern Levant, Studies in honour of Lorraine Copeland, British Archaeological Reports, Oxford, 165-201.

Boëda, E., Geneste, J.-M., Meignen, L., 1990. Identification de chaînes opératoires lithiques du Paléolithique ancien et moyen. *Paléo* 2, 43-80.

Boëda, E., Griggo, C., Noël-Soriano, S., 2001. Différents modes d'occupation du site d'Umm El Tlel au cours du Paléolithique moyen (El Kowm, Syrie Centrale). *Paléorient* 27(2), 13-28.

Bonilauri, S., Boëda, E., Griggo, C., Al Sakhel, H., Muhesen, S., 2007. Un éclat de silex moustérien coincé dans un bassin d'autruche (*struthio camelus*) à Umm El Tlel (Syrie Centrale). *Paléorient* 33(2), 39-46.

Boëda E., Bonilauri S., 2006. The Intermediate Paleolithic: the first bladelet production 40,000 years ago. *Anthropologie* XLIV/1, p.75-92.

Bordes, F., 1947. Etude comparative des différentes techniques de taille du silex et des roches dures. *L'Anthropologie* 51, 1-29.

Bordes, F., 1950. Principes d'une méthode d'étude des techniques de débitage et de la typologie du Paléolithique ancien et moyen. *L'Anthropologie* 54, 19-34.

Bordes, F., 1953. Notules de typologie paléolithique II: Pointes levalloisiennes et pointes pseudo-levalloisiennes. *Bulletin de la Société Préhistorique Française* 50, 311-313.

Bordes, F., 1961. Typologie du Paléolithique ancien et moyen. CNRS, Paris.

Bosinski G. 1966. Der Palaölitische Fundplatz Rheindalen, Ziegelei Dreesen-Westwand. *Bonner Jahrbuch*, 166: 318-343.

Bourgon, M., 1957. Les industries moustériennes et pré-moustériennes du Périgord. *Archives de l'Institut Paléontologie humaine*, mémoire 27.

Brantingham, J. P., 2003. A neutral model of stone raw material procurement. *American Antiquity* 68(3), 487-509.

Breuil, H., 1926. Palaeolithic industries from the beginning of the Wurmian glaciation. *Man*, 26, 116.

Breuil, H. & Lantier, R., 1951. Les hommes de la pierre ancienne. Payot, Paris.

Buccellati, G., Buccellati, M., 1967. Archaeological survey of the Palmyrene and the Jebel Bishri. *Archaeology* 20, 305.

Cauvin, J., Cauvin, M.-C., Stordeur, D., 1979. Recherches préhistoriques à El Kowm (Syrie). Première campagne 1978. *Cahiers de l'Euphrate* 2, 80-117.

Comment V. 1912. Moustérien à faune chaude dans la vallée de la Somme à Montieres- les Amiens. Geneve : Congrès international d'Archéologie et d'Anthropologie préhistorique, 1912 : 291-300.

Conard, N.J. 1990. Laminar lithic assemblages from the Last Interglacial Complex in Northwestern Europe. *Journal of Anthropological Research* 46: 243-262.

Conard, N.J. 1992. Tönchesberg and its position in the Paleolithic prehistory of northern Europe. *Römisch-Germanisches Zentralmuseum Mainz Monograph* 20. Bonn.

Conard, N., J. & Adler, D., S., 1997. Lithic reduction and hominid behavior in the Middle Paleolithic of the Rhineland. *Journal of Anthropological Research* 53: 147-176.

Copeland, L., 1975. The Middle and Upper Paleolithic of Lebanon and Syria in the light of recent research. In: Wendorf, F., Marks, A. E. (Eds.), *Problems in prehistory: North Africa and the Levant*. SMU Press, Dallas, 317-350.

Copeland, L., 1983. Levallois / Non-Levallois determinations in the early Levant Mousterian. Problems and questions for 1983. *Paléorient* 9, 15-27.

Copeland, L., 1985. The pointed tools of Hummal Ia (El Kowm, Syria). *Cahiers de l'Euphrate* 4, 177-189.

Copeland, L., Hours, F., 1983. Le Yabroudien d'El Kowm (Syrie) et sa place dans le Paléolithique du Levant. *Paléorient* 9(1), 21-37.

Crabtree, D. E., 1982. An Introduction to flintworking. Occasional Papers of the Idaho State University Museum, No. 28. Pocatello: Idaho State University Museum, 98.

Cotterell, B., Kammiga, J., 1987. The formation of flakes. *American Antiquity*, 52/4 : 675-708.

Crew, H. L., 1975. An examination of the variability of the Levalloisian method: its implications for the internal and external relationships of the Levantine Mousterian. Ph.D. dissertation, University of California.

Crew H.L., 1976. The Mousterian site of Rosh Ein Mor. In: A.E. Marks (ed), *Prehistory and Paleoenvironment in the Central Neguev (Israël)*. Southern Methodist University Press, Dallas, 75-112.

Davis, Z. J., Shea, J. J., 1998. Quantifying lithic curation: An experimental test of Dibble and Pelcin's original flake-tool mass predictor. *Journal of Archaeological Science* 25(7), 603-610.

D'Araujo-Igreya, M., Pesesse, D., 2006. Entre modalités techniques et objectives fonctionnelles: le burin de l'unité OP10 de La Vigne Brun (Villerest, Loire, France), 165-196. Burin préhistorique : formes, fonctionnements, fonctiona, *Archéologique* 2, Luxembourg.

De Heinzelin de Braucourt, J., 1960. Principes de diagnose numérique en typologie. Académie royale de Belgique, Brussel.

De Heinzelin de Braucourt, J., 1962. Manuel de typologie des industries lithiques. Patrimoine de l'Institut royal des sciences naturelles de Belgique, Brussel.

Delagne A., Kuntzmann F., 1996. L'organisation technique et spatiale de la production laminaire à Etoutteville. In Delagne A., Ropars A. eds. Paleolithic Moyen en Pays de Caux (Haute Normandie) : Le Puceuil, Etoutteville : Deux gisements de plein air en Milieux loessique. Paris: Maison de Science de l'Homme. ed. A. Ronen and M. Weinstein-Evron.

Delagne, A., 2000. Blade production during the Middle Paleolithic in Northwestern Europe, *Acta Anthropologica Sinica*, supplement to vol. 19 181-188.

Deloze, V., Depaepe, P. Gouedo J.M., et al. 1994. Le Paléolithique dans le Nord du Senonais (Yonne): contexte géomorphologique, industrie lithique et chronostratigraphie. Paris: Maison de Science de l'Homme.

Demidenko, Y. E., Usik, V. I., 1995. Establishing the potential evolutionary technological possibilities of the "Point" Levallois-Mousterian: Korolevo I sitecomplex 2B in the Ukrainian Transcarpathians. In: Dibble, H. L., Bar-Yosef, O. (eds), *The definition and interpretation of Levallois technology*. Prehistory Press, Madison (Wis.), 439-454.

Demidenko, Y. E., Usik, V., 2003. Into the mind of the maker: refitting study and technological reconstructions. In: Henry, D. O. (Ed.), *Neanderthals in the Levant. Behavioral organization and the beginnings of human modernity*. Continuum, London, 107-155.

Dibble, H., L., 1981. *Technological Strategies of Stone Tool Production at Tabun Cave (Israel)*. Ph.D. Dissertation, University of Arizona, 1981.

Dibble, H., L., 1984. The Mousterian industry from Bisitun Cave (Iran). *Paléorient* 10(2), 23-34.

Dibble, H., L., 1987. The interpretation of Middle Paleolithic scraper morphology. *American Antiquity* 52(1), 109-117.

Dibble, H., L., 1988. The interpretation of middle palaeolithic scraper reduction patterns. In: *L'Homme de Néandertal, volume 4. La Technique*. ERAUL 31, 49-58.

Dibble, H., L., 1995. Middle paleolithic scraper reduction: Background, clarification, and review of the evidence to date. *Journal of Archaeological Method and Theory* 2(4), 299-368.

Dibble, H., L., 1997. Platform variability and flake morphology: a comparison of experimental and archaeological data and implications for interpreting prehistoric lithic technological strategies. *Lithic Technology* 22(2):150-170

Dibble, H., L., McPherron, S., P., 2007. Truncated-faceted pieces: Hafting modification, retouch, or cores? In: McPherron, S. P. (Ed.), *Tools versus cores: Alternative approaches to stone tool analysis*. Cambridge Scholars Publishing, Newcastle, 75-90.

Dibble, H., L., Pelcin, A., 1995. The effect of hammer mass and velocity on flake mass. *Journal of Archaeological Science* 22(3), 429-439.

Diethelm, I., 1996. The silex raw material of the Acheulean site Nadaouiyeh Aïn Askar in the El Kowm Basin, Syria - Mineralogical preliminary report. *Travaux de la Mission Archéologique Syro-Suisse d'El Kowm*, 1, 82-84.

Dornemann, R.H., 1969. An Early Village. *Archaeology* 22 (1), 1969, 68-70.

Edmonds M., 1987. Rock and risk : problems with lithic procurement strategies. In *Lithic analysis in Later British prehistory: some problems and approaches*, edited by A.G. Brown and M.R.Edmonds. Oxford: BAR British Series no.162.p155-179.

El Sued, H., 2008. Etude d'un crâne d'Equidé Yabroudien du site de Hummal. Unpublished Master thesis, University of Basel.

Emery-Barbier, A., 2005. Rapport Palynologie. Mission Archéologique d' Umm el-Tlel/ El Meirah, Bassin d'El Kowm, Syrie, p. 74-81.

Féblot-Augustins, J., 1997. *La circulation des matières premières au Paléolithique*. Liège: Université de Liège (ERAUL 75).

Féblot-Augustins, J., 1999. Raw material transport patterns and settlement systems in the European Lower and Middle Palaeolithic : continuity, change and variability. In ROEBROEKS W. and GAMBLE C. (eds), *The Middle Palaeolithic occupation of Europe*: 193-214. Leiden: University of Le

Fish, P., 1981. Beyond tools: Middle Paleolithic debitage analysis and cultural inference. *Journal of Anthropological Research* 37 (4), 374-386.

Frosdick, R. 2010. Hummal, Syria 2009: A study of the taphonomic processes occurring in the faunal assemblages. *Travaux de la Mission Archéologique Syro-Suisse d'El Kowm*, 15.

Garrod, D., 1956. Acheuléo-Jabroudien et "Pré-Aurignacien" de la grotte du Taboun (Mont Carmel); étude stratigraphique et chronologique. *Quaternaria* 3:39-59.

Garrod, D. & Kirkbride, D., 1961. Excavation of Abri Zumoffen. A Paleolithic Roc Schelter near Adlun, South Lebanon 1958. *Bulletin de Musée de Beyrouth* 16: 7-47.

Garrod, D., 1970. Pre-Aurignacian and Amudian: a comparative study of the earliest blade industries of the Near East. In: K. Gripp, R. Schüttrumpf, H.R. Schwabedissen (eds), *Frühe Menschheit und Umwelt*. Fundamenta A2, Köln-Wein, p 224-229.

Geneste, J.-M., 1985. Analyse lithique d'industries moustériennes du Périgord: Une approche technologique du comportement de groupes humains au Paléolithique moyen. Ph.D. dissertation, University of Bordeaux.

Geneste, J.-M., 1988. Systèmes d'approvisionnement en matières premières au Paléolithique moyen et au Paléolithique supérieur en Aquitaine. In : L'Homme de Néandertal, volume 8 : La Mutation. ERAUL 35, 61-70.

Geneste, J.-M., 1989. Economie des ressources lithiques dans le Moustérien du Sud-Ouest de la France. In: Otte, M. (Ed.), *L'Homme de Neandertal: La subsistance*. ERAUL, Liège, 75-98.

Gisis L., Bar-Yosef O. 1974. New Excavation in Zuttiyeh cave, Wadi Amud, Israel, *Paléorient* 5: 175-180.

Griggo, Ch., 2005. Rapport Pléontologie, Étude la faune d'Umm el Tlel Mission Archéologique d' Umm el-Tlel/ El Meirah, Bassin d'El Kowm, Syrie, p. 82-91.

Grigoriev, G.P., 1977. The Palaeolithic of Africa. In: The Old Stone Age of the World. Studies in the Palaeolithic Cultures. Nauka, Leningrad, pp. 44–208 (in Russian).

Goren-Inbar, N., 1988. Too small to be true? Reevaluation of cores-on-flakes in Levantine Mousterian assemblages. *Lithic Technology* 17, 7-28. préliminaire. Fouilles 1991-1993. *Cahiers de l'Euphrate* 8, 11-25.

Gould, A., Koster D. A., Sontz, A. H. L, 1971. The lithic assmblages of the Western Desert Aborigines of Australia. Society for American Archaeology, 149-169.

Grün, R., Stringer, C., 2000. Tabun revisited: Revised ESR chronology and new ESR and U-series analyses of dental material from Tabun C1. *Journal of Human Evolution* 39, 601-612.

Hager, D., 2008. Frühe menschliche Nutzung von Feuer. Nachweismöglichkeiten und ausgewählte Ergebnisse für die Fundstelle Hummal, El Kowm, Syrien. Unpublished Master thesis, University of Basel.

Hauck, T.C., 2010. The Mousterian Sequence of Hummal (Syria). PhD-Thesis, Basel University.

Hauck, T.C., 2011. The Mousterian Sequence of Hummal and its tentative placement in the Levantine Middle Palaeolithic. *The Lower and Middle Palaeolithic in the Middle East and Neighbouring Regions*, ERAUL 126, 309-324.

Hayden, B., 1979. Lithic Use-Wear Analysis. New-York: Academic Press.

Henning G.J., Hours F. 1982. Dates pour le passage entre l'Acheuléen et le Paléolithique moyen à El-Kowm (Syrie). *Paléorient* 8, 1: 81-83.

Henry, D. O., 1995. The influence of mobility levels on Levallois point production, Late Levantine Mousterian, Southern Jordan. In: Dibble, H. L., Bar-Yosef, O. (Eds), *The definition and interpretation of Levallois technology*. Prehistory Press, Madison (Wis.), 185-200.

Hours, F., Copeland, L., Aurenche, O., 1973. Les industries paléolithiques du Proche Orient, essai de corrélation, *L'Anthropologie* 77 : 229-280, 437-496.

Hours, F., 1982. Une nouvelle industrie en Syrie entre l'Acheuléen supérieur et le Levalloiso-Moustérien. In: *Maison de l'Orient* (Ed.), *Archéologie du Levant Recueil Roger Saidah*. Maison de l'Orient, Lyon, 33-46.

Hours, F., Le Tensorer, J.-M. & Yalçinkaya, I., 1983. Premiers travaux sur le site acheuléen de Nadaouiyeh I (El Kowm, Syrie). *Paléorient* 9 (2), 1983, 5-13.

Hovers, E., 1998. The lithic assemblages of Amud Cave. Implications for understanding the end of the Mousterian in the Levant. In: Akazawa, T., Aoki, K., Bar-Yosef, O. (Eds.), *Neandertals and Modern Humans in Western Asia*. Plenum Press, New York, 143-163.

Ismail-Meyer, K., 2009. Reconstrucion of some site Formation Processes of Hummal (Syria). *Frankfurter geowiss. Arbeiten*, 30, 45-58.

Jagher, R. ., 1990. Nadaouiyeh Aïn Askar Grabung 1989. Vorbericht.

Jagher, R. 1993. Nadaouiyeh Aïn Askar : un nouveau site hummalien dans le bassin d'El Kowm (Syrie). *Cahiers de l'Euphrate* 7 : 37-46, (éd.) *Recherche sur les Civilisations*, Paris.

Jagher, R., 2000. Nadaouiyeh Aïn Askar, Entwicklung der Faustkeiltraditionen und der Stratigraphie an einer Quelle in der syrischen Wüstensteppe. Ph.D. dissertation, University of Basel.

Jagher, R., 2011. Nadaouiyeh Aïn Askar – Acheulean variability in the Central Syrian Desert. *The Lower and Middle Palaeolithic in the Middle East and Neighbouring Regions*, ERAUL 126, 209-224.

Jelinek A. J., 1975. A preliminary report on some Lower and Middle Paleolithic industries from the Tabun Cave, Mount Carmel (Israel). In: F. Wendorf F., A.E. Marks (eds), *Problems in Prehistory: North Africa and the Levant*. Southern Methodist University Press, Dallas, 297-315.

Jelinek, A., 1981. The Middle Paleolithic in the Southern Levant from the perspective of the Tabun Cave. In: Cauvin, J., Sanlaville, P. (Eds.), *Préhistoire du Levant*. Maison de l'Orient. Editions du C.N.R.S., Lyon, 265-280.

Jelinek, A., 1982. The Middle Palaeolithic in the Southern Levant, with comments on the appearance of modern Homo Sapiens. In: Ronen, A. (Ed.), *The transition from Lower to Middle Palaeolithic and the origin of modern man*. British Archaeological Reports, Oxford, 57-104.

Jelinek, A., 1990. The Amudien in the context of the Mugharian Tradition at the Tabun Cave, in: *The Human Revolution - Behavioural and Biological perspectives on the origins of Modern Humans*, Edinburgh University Press, 81-90.

Julig, P. & Long, G.F., 2001. Flint sourcing in Central Steppe Desert Region, Syria. In: *Canadian Research on Ancient Syria*, edited by M. Fortin, 19-31. Québec: Musée de la Civilisation, 2001.

Johnson, C., McBrearty, S., 2010. 500, 000 year old blades from the Kapthurin Formation, Kenya. *Journal of Human Evolution* 58: 193-200.

Kelley, H., 1954. Contribution à l'étude de la technique de taille Levalloisienne. *Bulletin de la Société préhistorique française* 51, 149-169.

Keeley, L.H., 1980. Experimental determination of stone tools uses, a microwear analysis. University of Chicago Press, Chicago

Kelly, R. L., 1988. The three sides of a biface. *American Antiquity* 53(4), 717-734.

Kroon, D., Alexander, I., Little, M., Lourens, L.J., Matthewson, A., Robertson, A.H.F. & Sakamoto, T., 1998. Oxygene Isotope and Sapropel Stratigraphy in the Eastern Mediterranean During the Last 3.2 Million Years. *Proceedings of the Ocean Drilling Program, Scientific Results* 160, 1998, 181-189.

Kuhn S.L., 1992. On planning and curated technologies in the Middle Paleolithic. *Journal of Anthropological Research* 48: 185-213.

Kuhn, S. L., 1995. Mousterian lithic technology: An ecological perspective.

Laplace-Jauretche, G., 1957. Typologie analytique. Application d'une nouvelle méthode d'étude des formes et des structures aux industries à lames et lamelles. *Quaternaria* IV: 133-164. Princeton University Press, Princeton (N.J.).

Lindly, J., Clark, G., 1987. A Preliminary Lithic Analysis of the Mousterian Site of 'Ain Difla (WHS Site 634) in the Wadi Ali, West-Central Jordan. *Proceedings of the Prehistoric Society* 53:279-292

Leroi-Gourhan, A., 1971. *Evolution et techniques I—L'Homme et la matière*, 2nd edn., Albin Michel, Paris.

Leroi-Gourhan, A., 1973. *Evolution et techniques II—Milieu et techniques*, 2nd edn., Albin Michel, Paris.

Le Tensorer, J.-M. et Hours, F., 1989. L'occupation d'un territoire à la fin du Paléolithique ancien et au Paléolithique moyen à partir de l'exemple d'El Kowm (Syrie). In : Freeman L. and PATOU M. (éds), *L'Homme de Néandertal 6* : 107-114. Liège, ERAUL 33.

Le Tensorer, J.-M., 1991. Le Paléolithique d'El-Kowm, premier bilan : 1989-1991. *Travaux de la Mission Archéologique Syro-Suisse d'El Kowm* (unpublished).

Le Tensorer, J.-M. 1994. Le passage du Paléolithique ancien au Paléolithique moyen en Syrie: l'exemple d'El Kowm (unpublished manuscript).

Le Tensorer, J.-M., 2000. Hummal. *Travaux de la Mission Archéologique Syro-Suisse d'El Kowm*, 5, 14-23.

Le Tensorer, J.-M., 2003. Principaux résultats concernant Hummal. *Travaux de la Mission Archéologique Syro-Suisse d'El Kowm*, 8, 7-21.

Le Tensorer, J.-M., Jagher, R. Muhsen, S., 2001. Paleolithic settlement dynamics in the El Kowm area (Central Syria). In: Conard, N. (Ed.), *Settlement dynamics of the Middle Paleolithic and Middle Stone Age*. Kerns Verlag, Tübingen, 101-122.

Le Tensorer, J.-M., 2004. Nouvelles fouilles à Hummal (El Kowm, Syrie Centrale). Premiers résultats (1997-2001). In: Aurenche, O., Le Mière, M., Sanlaville, P. (eds) *From the river to the sea. The Palaeolithic and the Neolithic on the Euphrates and in the Northern Levant, Studies in honour of Lorraine Copeland*, British Archaeological Reports, Oxford, 223-239.

Le Tensorer, J.-M., Jagher, R., Rentzel, P., Hauck, T., Ismail-Meyer, K., Pümpin, C., Wojtczak, D., 2007. Long-term site formation processes at the natural springs Nadaouiyeh and Hummal in the El Kowm Oasis, Central Syria. *Geoarchaeology* 22(6), 621-640.

Lioubin V.P., Beliaeva E. V., 2006. Early prehistory of the Caucasus. Ed. St. Petersburg, 107.

Lemorini, C., Stiner, M. C., Gopher, A., Shimelmitz, R., Barkai, R., 2006. Usewear analysis of an Amudian laminar assemblage from the Acheuleo-Yabrudian of Qesem Cave, Israel. *Journal of Archaeological Science* 33(7), 921-934.

Lindly, J. M., Clark, G. A., 1987. A preliminary lithic analysis of the Mousterian site of Ain Difla (WHS Site 634) in the Wadi Ali (West Central Jordan). *Proceedings of the Prehistoric Society* 53, 279-292.

Magne, M. P. & Pokotylo, D., 1981. A pilot study in bifacial lithic reduction sequences. *Lithic Technology* 10(2-3):34-47.

Margueron, T., 1998. Fonctionnement hydrogéologique de la dépression d'El Kowm (Syrie) données préliminaires pour une interprétation paléohydrologique. D.E.A., Université d'Avignon et Pays de Vaucluse.

Marks, A.E. & Crew, H.L., 1972. Rosh Ein Mor, an Open-Air Mousterian Site in the Central Negev, Israël. *Current Anthropology* 13(5):591-593

Marks, A.E., 1983. Changing core reduction strategies: a technological shift from the Middle to the Upper paleolithic in the Southern Levant. In: *The Mousterian legacy: human biocultural change in the Upper Pleistocene*. BAR International Series 164, 13-34.

Marks, A.E., 1987. Technological Variability and Change seen through core reconstruction. In: Sieveking, G. & Newcomer, M.H. (eds.) *The human uses flint and chert.* Cambridge University Press, Cambridge, 11-20.

Marks A.E., Monigal K., 1995. Modeling the production of elongated blanks from the early Levantine Mousterian at Rosh Ein More, *The Definition and Interpretation of Levallois Technology*, ed. H. Dibble and O.Bar-Yosef, Madison: Prehistory Press.

Masson, A., 1982. Les pièces lustrées des sources d'El-Kowm (Syrie). *Cahiers de l'Euphrate* 3.

Martini, P., 2010. A metric analysis of the morphological variation in recent and fossil camels. Unpublished Master Thesis, Zurich University.

McBrearty S., Bishop L., Plummer Th., Dewar R., Conard N., 1998. Human trampling as an Agent of Lithic Artefact Edge Modification. *American Antiquity*, Vol. 63, No.1, 108-129.

McBurney, C.B.M., 1955. Prehistory and Pleistocene geology in Cyrenaican Libya: a record of two seasons' geological and archaeological fieldwork in the Gebel Akhdar Hills: With a summary of prehistoric finds from neighbouring territories. University Press Cambridge, Cambridge.

McBurney C.B.M., 1967. *The Haua Fteah (Cyrenaica) and the Stone Age of the South-East Mediterranean.*

Meeks, N.D., Sieveking G. de G., Tite, M.S., Cook, J. 1982. Gloss and use-wear traces on flint sickles and similar phenomena. *Journal of Archaeological Science* 9 :317-340.

Meignen L. 1994. Paléolithique moyen au Proche-Orient : le phénomène laminaire. In: S. Révillion, A. Tuffreau (eds), Les industries laminaires au Paléolithique moyen. Dossier de Documentation Archéologique, 18, CNRS Editions, Paris, p 125-159

Meignen, L., 1995. Levallois lithic production systems in the Middle Paleolithic of the Near East: The case of the unidirectional method. In: Dibble, H. L., Bar-Yosef, O. (Eds.). The definition and interpretation of Levallois technology. Prehistory Press, Madison (Wis.), 361-379.

Meignen, L., 1998. Hayonim Cave lithic assemblages in the context of the Near Eastern Middle Paleolithic: A preliminary report. In: Akazawa, T., Kenichi, A., Bar-Yosef, O. (Eds.), Neandertals and modern humans in Western Asia. Plenum Press, New York, 165-180.

Meignen, L., 2007. Néandertaliens et Hommes modernes au Proche-Orient: Connaissances techniques, stratégies de subsistance et mobilité. In: Vandermeersch, B. (Ed.), Les Néandertaliens: biologie et cultures, Ed. du CTHS, Paris, 231-261.

Meignen, L., Bar-Yosef, O., 1991. Les outillages lithiques Moustériens de Kébara (fouilles 1982-1985). Premiers résultats. In: Bar-Yosef, O., Vandermeersch, B. (Eds.), Le squelette moustérien de Kébara 2. CNRS, Paris, 49-76.

Meignen L., 2000. Early Middle Palaeolithic Blade Technology in Southwestern Asia, p.158-168. Acta Anthropologica Sinica. Supplement to vol.19.

Meignen, L. and N. Tushabramishvili, 2006. Paléolithique moyen Laminaire sur les flancs Sud du Caucase : productions lithiques et fonctionnement du site de Djruchula (Géorgie). Paléorient 2006 : 82-104.

Meignen, L., Bar-Yosef, O., Speth, J., Stiner, M., 2006. Changes in settlement patterns during the Near Eastern Middle Paleolithic, in Transitions before the Transition : Evolution and stability in the Middle Paleolithic and Middle Stone Age,

eds E. Hovers et S. Kuhn, New York, Boston, Dordrecht, London, Moscow : Springer, 149-170.

Meignen, L., 2011. The contribution of Hayonim cave assemblages to the understanding of the so-called Early Levantine Mousterian. *The Lower and Middle Palaeolithic in the Middle East and Neighbouring Regions*, ERAUL 126, 85-100.

Mercier N., Valladas H., 1994. Thermoluminescence dates for the Paleolithic Levant. In: O. Bar-Yosef, R.S. Kra (Eds), *Late Quaternary Chronology and Paleoclimates of the Eastern Mediterranean*, 13-20.

Mercier, N., Valladas, H., 2003. Reassessment of TL age estimates of burnt flints from the Paleolithic site of Tabun Cave, Israel. *Journal of Human Evolution* 45(5), 401-409.

Mercier, N., Valladas, H., Valladas, G., Reyss, J. L., Jelinek, A., Meignen, L., Joron, J. L., 1995. TL dates of burnt flints from Jelinek's excavations at Tabun and their implications. *Journal of Archaeological Science* 22(4), 495-509.

Mercier, N., Valladas, H., Froget, L., Joron, J. L., Reyss, J. L., Weiner, S., Goldberg, P., Meignen, L., Bar-Yosef, O., Belfer-Cohen, A., Chech, M., Kuhn, S. L., Stiner, M. C., Tillier, A. M., Arensburg, B., Vandermeersch, B., 2007. Hayonim Cave: A TL-based chronology for this Levantine Mousterian sequence. *Journal of Archaeological Science* 34(7), 1064-1077.

Mercier, N. H. Valladas, H., Meignen, L., Joron, J-L., Tushabramishvili, N., Adler, D. S., Bar-Yosef, O., Dating the Early Middle Palaeolithic Laminar Industry from Djrchula Cave, Republic of Georgia (in press).

Meyer, K., 2001. Mikromorphologische Untersuchungen an Ablagerungen der artesischen Quelle Hummal, Syrien. Master thesis, University of Basel, Basel.

Mortillet G. de, 1883. Le préhistorique. Antiquité de l'homme. Paris, Reinwald (Bibl. de Sciences Contemporaines), 642.

Munday F.C., 1977. Nahal Aqev (D.35): a stratified open-air mousterian occupation in the Avdat/Aqev area. In: A. Marks (ed), Prehistory and Paleoenvironment in Central Negev, Israel. Southern Methodist University Press, Dallas, 35-60

Munday F.C., 1979. Levantine Mousterian Technological Variability: A Perspective from the Negev, Paléorient, Vol. 5, 87-104.

Neuville R., 1951. *Le Paléolithique et le Mésolithique du désert de Judée.* Masson et Cie, Paris.

Newcomer, M. H., Hivernel-Guerre, F., 1974. Nucléus sur éclat: Technologie et utilisation par différentes cultures préhistoriques. *Bulletin de la Société Préhistorique Française* 71, 119-128.

Oakley, K., P., 1956. Man the tool-maker. British Museum, London, 98.

Odell, G. H., 1996. Stone tools: Theoretical insights into human prehistory. Plenum Press, New York.

Ohnuma, K. & Bergman, C., 1983. Experimental Studies in the Determination of Flaking Mode. *Bulletin of the Institute of Archaeology*, Number 19, 1982, 161-170, London.

Otte, M., 1994. Rocourt (Liège, Belgique): industrie laminaire ancienne. In: Révillion, S. & Tuffreau, A. (eds), Les industries laminaires au Paléolithique moyen. Dossier de Documentation Archéologique 18: 179-186.

Otte, M., 1995. The nature of Levallois. In: Dibble, H.L. & Bar-Yosef, O. (eds), The Definition and Interpretation of Levallois Technology. Mon. in World Archaeology 23. Madison: 117-124.

Otte, M., Boëda, E. & Haesaerts, P., 1990. Rocourt: industrie laminaire archaïque. Hel. 29: 3-13.

Payson, D. Sheets & Guy R. Muto., 1972. Pressure blades and tool cutting edge: an experiment in lithic technology. American Association for the Advancement of Science, 632-634.

Pelcin, A. W. 1996. Controlled experiments in the production of flake attributes. Ph.D. Dissertation, University of Pennsylvania.

Pelcin, A. W. 1997. The formation of flakes: the role of platform thickness and exterior platform angle in the production of flake initiations and terminations. Journal of Archaeological Science 24:1107-1113.

Pelcin, A. W., 1998. The threshold effect of platform width: a reply to Davis and Shea. Journal of Archaeological Science 25:615-620.

Pelegrin, J. 1984. Approche technologique expérimentale de la mise en forme de nucléus pour le débitage systématique par pression. In Préhistoire de la pierre taillée. Volume 2: Economie du débitage laminaire: technologie et expérimentation, edited by J. Tixier. Paris: CERP., 93-10.

Pelegrin J., 2000. Les techniques de débitage laminaire au Tardiglaciaire : critères de diagnose et quelques réflexions. L'Europe Centrale et Septentrionale au Tardiglaciaire, Table-rond de Namour, 13-16 mai 1997. *Mémoires du Musée de Préhistoire d'Ile de France*, 7, 73-86.

Perlès, C., 1984. Débitage laminaire de l'obsidienne dans le néolithique de Franchthi (Grèce): technique et place dans l'économie de l'industrie lithique. In *Préhistoire de la pierre taillée. Volume 2: économie du débitage laminaire: technologie et expérimentation*, edited by J. Tixier. Paris: CERP, 129-138.

Perpère, M., 1986. Apport de la typométrie à la définition des éclats Levallois: L'exemple d'Ault. *Bulletin de la Société Préhistorique Française* 83(4), 115-118.

Perrot J., 1968. La préhistoire palestinienne. (Supplément au *Dictionnaire de la Bible*), 8 (43), Letouzey et Ané, Paris:286-446.

Ploux, S., Soriano, S., 2003. Umm El Tlel, une séquence du Paléolithique supérieur en Syrie centrale. Industries lithiques et chronologie culturelle. *Paléorient* 29(2), 5-34.

Port, N., Chazan, M., Grün, R., Aubert, M., Eisenmann, V., 2010. New radiometric ages from the Fauresmith industry from Kathu Pan, southern Africa: implications from the Earlier Stone Age Transition. *Journal of Archaeological Science* 37: 269-283.

Portonoy, A. W., 1987. A formula for estimating the minimum number of individual lithic tools. Paper presented at the 52d Annual Meeting of Society for American Archaeology, Toronto.

Pümpin, C., 2003. Geoarchäologische Untersuchungen an der pleistozänen Fundstelle von Nadaouiyeh Aïn Askar (Syrien). Master thesis, University of Basel.

Pümpin, C., Jagher, R., 2005. Révision géologique. *Travaux de la Mission Archéologique Syro-Suisse d'El Kowm*, 10, 46-59.

Renault-Miskovsky, J., 1998. Etude pollinique du site de Nadaouiyeh Aïn Askar (Nad. 1, El Kowm, Syrie) – Premiers résultats. *Travaux de la Mission Archéologique Syro-Suisse d'El Kowm*, 3, 28-35.

Rentzel Ph., Ismail-Meyer K. n.d.- Aktennotiz zur mikromorphologischen Analyse der Schichten 6a bis 6c. *Travaux de la Mission Archéologique Syro-Suisse d'El Kowm*, 13.

Révillion, S. 1989. Le débitage du gisement Paléolithique moyen de Seclin (Nord). Paléolithique et Mésolithique du Nord de la France: nouvelles recherches. Publications du CERP 1: 79-89.

Révillion, S. 1993. Question typologique à propos des industries laminaires du Paléolithique moyen de Seclin (Nord) et de Saint-Germain-des-Vaux/Port-Racine (Manche): lames Levallois ou lames non-Levallois? *Bulletin de la Société Préhistorique Française* 90: 269-273.

Révillion, S., 1995. Technologie du débitage laminaire au Paléolithique moyen en Europe septentrionale: état de la question. *Bulletin de la Société Préhistorique Française* 92, 4: 425-441.

Révillion, S. & Tuffreau, A., 1994. Valeur et signification du débitage laminaire du gisement Paléolithique moyen de Seclin (Nord). In: Révillion, S. & Tuffreau, A. (eds), *Les Industries Laminaires au Paléolithique Moyen. Dossier de Documentation Archéologique* 18: 19-44.

Reynaud Savioz, N. & Morel, Ph., 2005. La faune de Nadaouiyeh Aïn Askar (Syrie central, Pléistocène moyen): aperçu et perspectives. *Revue de Paléobiologie*, Vol. spec. 10, 31-35.

Reynaud-Savioz, N., 2011. The faunal remains from nadaouiyeh Aïn Askar (Syria). Preliminary indications of animal acquisition in an Acheulean site. *The Lower and Middle Palaeolithic in the Middle East and Neighbouring Regions*, ERAUL 126, 225-234.

Richter D. 2006. Erste Ergebnisse der Thermoluminiszenz-Datierung für die Fundstelle Ain Hummal. *Travaux de la Mission Archéologique Syro-Suisse d'El Kowm*, 11, 45.

Richter, D., 2007. Advantages and limitations of thermoluminescence dating of heated flint from Paleolithic sites. *Geoarchaeology* 22, 671-683.

Richter, D., Hauck, T.C., Wojtczak, D., Le Tensorer, J.-M. & Muhesen, S. , 2011. Chronometric age estimates for the site of Hummal (El Kowm, Syria). *The Lower and Middle Palaeolithic in the Middle East and Neighbouring Regions*, ERAUL 126, 249-262.

Rink, W. J., Richter, D., Schwarcz, H. P., Marks, A. E., Monigal, K., Kaufman, D., 2003. Age of the Middle Palaeolithic site of Rosh Ein Mor, Central Negev, Israel: Implications for the age range of the Early Levantine Mousterian of the Levantine corridor. *Journal of Archaeological Science* 30(2), 195-204 Neumünster.

Sanlaville, P., 2000. Environment and developments. In Mundy. M., and Mussalam., M. (Ed). *The transformation of nomadic Society in the Arab East*. Cambridge University Press, 6-16.

Schumman, D., 2007. Digitale Modellierung und Schichtrekonstruktionen der paläolithischen Fundstelle Hummal, Syrien. Unpublished Master thesis, University of Basel.

Semenow, S. 1964. *Prehistoric technology: an experimental study of the oldest tools and artifacts from traces of manufacture and wear*, Moonrakerpress edition. London: Cory: Adams and Mackay.

Sergent, J., Crombé, Ph., Perdaen, Y., 2006. The invisible hearths: a contribution to the discernment of Mesolithic non-structured surface hearths. *Journal of Archaeological Science* 33: 999-1007.

Schäfer, J. u. Ranov, V.A. 1998. Middle Paleolithic blade industries and the Upper Paleolithic of Central Asia. In: *Préhistoire d'Anatolie, Genèse de deux mondes. Actes du colloque international Liège, 28 avril-3 mai 1997.* ERAUL 85/2, 785-814.

Shakley, M., 1988. Hot spring and 'glazed' flints: a controversial phenomenon observed on spring-mound artefacts in the Near East. *Levant*, Vol. XX, 119-126.

Schroeder, H. B., 1969. The lithic industries from Jerf al-Ajla and their bearing on the problem of a Middle to Upper Paleolithic transition. Ph.D. dissertation, University of Columbia, Columbia.

Shott, M. J., 1996. An exegesis of the curation concept. *Journal of Anthropological Research* 52(3), 259-280.

Shott, M. J., 1989. On tool-class use lives and the formation of archaeological assemblages. *American Antiquity* 54(1), 9-30.

Shott, M. J., 2000. The quantification Problem in Stone-Tool Assemblages. *AmericanAntiquity* 65(4):725-738.

Shot M. J., 2000. Flake size form platform attributes: predictive and empirical approaches. *Journal of Arcaheological Science* 27, 877-894.

Skinner J.H., 1965. The flake industries of southwest Asia: a typological study. Columbia University, Ph.D.

Skinner, J.H., 1970. El Masloukh: A Yabroudian Site in Lebanon. *Bulletin du Musée de Beyrouth* 23, 1970, 143-172.

Solecki, R. L., Solecki, R. S., 1979. A new secondary flaking technique at the Nahr Ibrahim cave site, Lebanon. *Bulletin du Musée de Beyrouth* 23, 137-140.

Sullivan, A. P., Rozen, K. C., 1985. Debitage analysis and archaeological interpretation. *American Antiquity* 50(4), 755-779

Suzuki, H., Kobori, I., 1970. Report of the reconnaissance survey on Palaeolithic sites in Lebanon and Syria. *Bulletin of the Museum of the University of Tokyo* 1. Archaeological Reports, Oxford, 137-161.

Thiébaud C., 2007. Les pieces enochées au Paléolithique moyen et les pseudo-outils : peut-on les distinguer ? Congrès du Centenaire Un siècle de construction du discours scientifique en Préhistoire. Vol.3 "... Aux conceptions d'aujourd'hui".

Tixier, J. 1967. Procédés d'analyse et questions de terminologie concernant l'étude des ensembles industriels du Paléolithique récent et de l'Épipaléolithique dans l'Afrique du Nord-Ouest. In Bishop, W. W., and Clark, J. D. (eds.), *Background to Evolution in Africa*, University of Chicago Press, Chicago, 771–820. J. Evin dir., 201-216.

Tixier, J., Inizan, M.-L. & Roche, H., 1980. Préhistoire de la pierre taillée: terminologie et technologie. Cercle de recherche et d'études préhistoriques, Antibes.

Torrence, R., 1983. Time budgeting and hunter-gatherer technology. In: Bailey, G. (Ed.), *Hunter-gatherer economy in prehistory*. Cambridge University Press, Cambridge, 11-22.

Torrence, R., 1989. Time, energy and stone tools. Cambridge University Press, Cambridge.

Tostevin, G. B., 2003. Attribute analysis of the lithic technologies of Stranska Skala IIIc and IIIId. In: Svoboda, Jiri, A., Bar-Yosef, O. (Eds.), Stranska Skala. Origins of the Upper Paleolithic in the Brno Basin, Moravia, Czech Republic. Peabody Museum of Archaeology and Ethnology, Cambridge, 77-117.

Tuffreau, A., 1983. Les industries lithiques à débitage laminaire dans le Paléolithique moyen de la France septentrionale. *Studia Praehistorica Belgica* 3: 135-141.

Tuffreau, A., Somme, J., 1988. Le gisement paléolithique moyen de Biache-Saint-Vaast. Vol.1: Stratigraphie, environnement et études archéologiques. Paris, *Mémoires de la Société Préhistorique Française*, 21, 9-29.

Tuffreau, A., 1993 (ed.). Rencourt-lès-Bapaume, Pas-de-Calais: un gisement du Paléolithique moyen, Paris, Maison de sciences de l'Homme.

Turberg, P., 1999. Cartographie électromagnétique du site de Nadaouiyeh Aïn Askar. *Travaux de la Mission Archéologique Syro-Suisse d'El Kowm*, 4, 16-25.

Tushabramishvili N., Pleurdeau D., Marie-Hélène M., Mgeladze A., 2007. Le complexe Djrchula-Koudaro au sud Caucase (Géorgie). Remarques sur les assemblages lithiques pléistocènes de Koudaro I, Tsona et Djrchula. *Anthropolgie XLV/1*, 1-18.

Van Peer, P., 1995. Current Issues in the Levallois problem. In *The definition and interpretation of Levallois technology*. (Ed.) H. L. Dibble and O. Bar-Yosef, 1–10. Madison: Prehistory Press.

Van Vliet-Lanoe, B, Tuffreau, A, Cliquet D, 1993. Position stratigraphique des industries à lame du Paléolithique moyen en Europe occidentale in Tuffreau A. ed Riencourt-les Baume (Pas de Calais), un gisement du Paléolithique M. Paris Maison de sciences de l'homme,

Villa, P., Courtin, J., 1983. The interpretation of stratified sites: A view from underground. *Journal of Archaeological Science* 10(3), 267-281.

Vishnyatsky, L.B., 2000. The Pre-Aurignacian and Amudian as an intra-Yabroudian episode, BAR S850; Toward modern humans: yabroudian and miquoquian, 400-50 kyears ago.

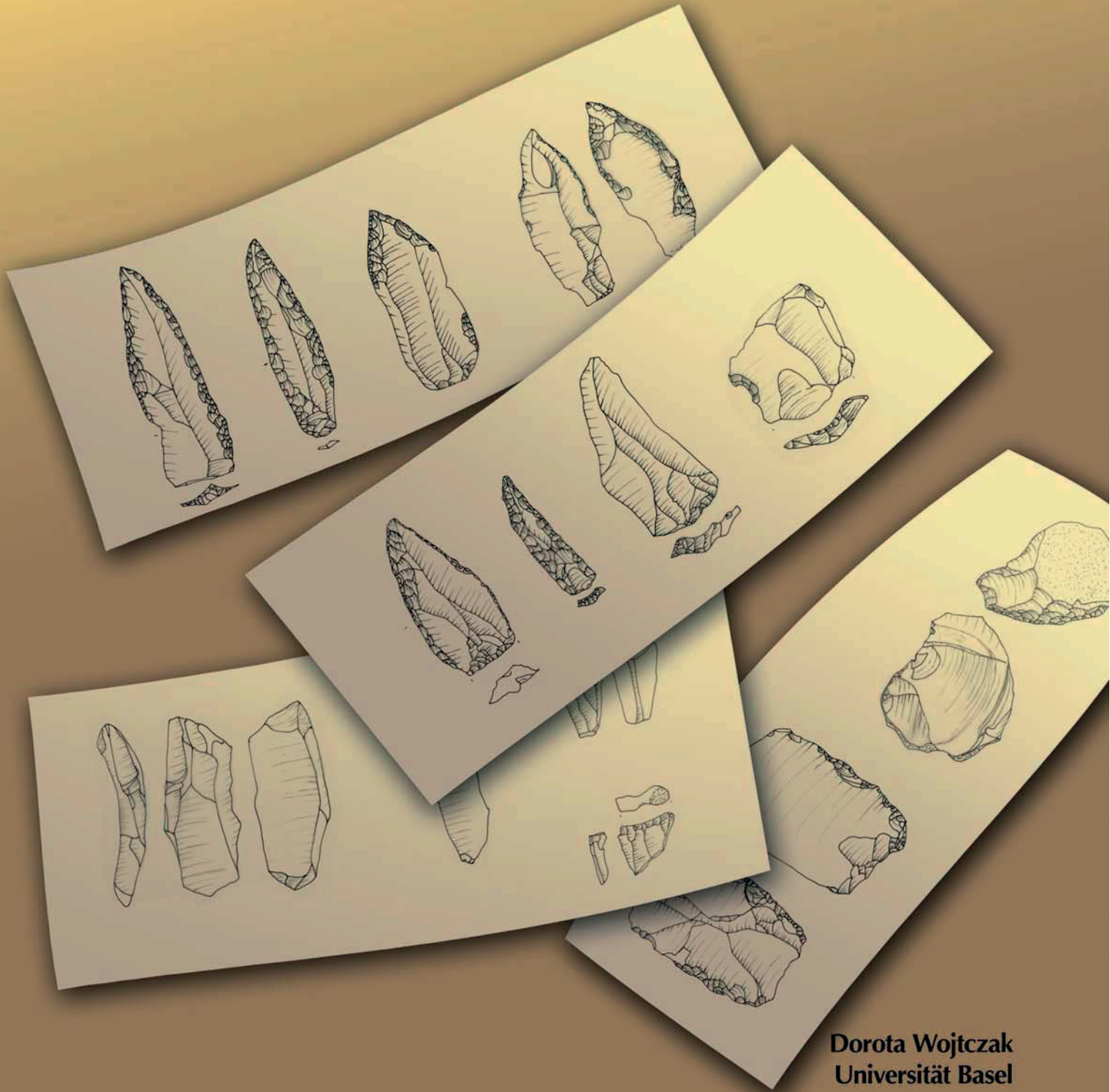
Wegmüller, F. 2008. Die Steinartefakte aus den frühpaläolithischen Schichten 15-18 der Fundstelle Hummal in Syrien. Unpublished Diploma-Thesis.

Wilkins J., Chazan M., 2012. Blade production ab. 500 thousand years ago at Kathu Pan 1, South Africa: support for a multiple origins hypothesis for early Middle Pleistocene blade technologies. *Journal of Archaeological Science* XXX: 1-18.

Wojtczak, D., 2011. Hummal (Central Syria) and its Eponymous Industry. *The Lower and Middle Palaeolithic in the Middle East and Neighbouring Regions*, ERAUL 126, 289-308.

Tables and Figures

The Early Middle Palaeolithic Blade Industry
from Hummal, Central Syria.



Dorota Wojtczak
Universität Basel

| layer of sample | min. age | max. age |
|-----------------|----------|----------|
| 6b East | 255±22 | 410±29 |
| 6b East | 135±11 | 201±14 |
| 6b East | 365±29 | 507±34 |
| 6b East | 492±40 | 773±52 |
| 6b East | 1221±88 | 1221±88 |
| 6b East | 518±46 | 916±69 |
| 6b East | 461±38 | 715±49 |
| 6b East | 588±47 | 901±60 |
| α-h | 180±18 | 199±19 |
| α-h | 234±25 | 263±13 |
| α-h | 193±20 | 216±22 |
| α-h | 151±15 | 170±17 |

Tab.1: The dating results for layers 6b and ah (after Richter et al.2010) obtained using TL dating on heated flints.

Tab. 1

Tab.2

| Attribute | Features |
|--|--|
| Signature / year | HU... |
| Level | E.g. "6b" |
| Raw materia | Paleocene flint, Cretacious flint, limestone |
| Category | Flake; blade; point, debris |
| Type | Blank, CTE, undetermined |
| Fragmentation | Intact, broken: proximal, medial or distal part |
| Cortex <ol style="list-style-type: none"> 1. Type 2. Amount 3. Location | <ol style="list-style-type: none"> 1. none; fresh; weathered; neocortex 2. 0-25%, 26-50%, 51-75%, 76-99%, 100% 3. Proximal, distal, left or righth lateral |
| Patination | Color, double patination |
| Dorsal scar pattern | Unidirectional convergent or parallel, bidirectional parallel, bidirectional shifted, centripetal, lineal |
| Length (L) in mm | Measured along the technological axis from the point of percussion to the most distal point of the flake |
| Width (W) in mm | The maximum width was measured |
| Thickness (Th) in mm | The measure of maximum thickness; excluding the bulb area |
| Weight | in g |
| Cross section of proximal, medial and distal part | Triangular thick, triangular flat; trapezoidal thick, trapezoidal flat; pentagonal thick and flat, oval |
| Profile | <ol style="list-style-type: none"> 1. Flat 2. Incurvate strong or light : dist-med part, prox-med part, whole piece; 3. twisted, 4. concorde 5. irregular |
| Presence of back | No or yes: brute de debitage, cortical, prepared, siret, abrupt retouch |
| Use wear possibility | Yes / no |
| Damage traces | Yes / No: location |
| Proximal end modification | Abrasion, tang, thinned, truncated |
| Dorsal reduction | <ol style="list-style-type: none"> 1. 1 or more longitudinal removals, 2. 1 or more short removals |
| Flaking angle | Measured using a goniometer |
| Striking platform : <ol style="list-style-type: none"> 1. category 2. shape | <ol style="list-style-type: none"> 1. Cortical, plain, facated, dihedral, broken, damaged, 2. Punctiforme or linear: chapeau de gendarme, |

| | |
|--|--|
| | rectangular, triangular, trapezoidale, straight, conave, convexe, double triangle, biconvex, sinusoidale |
| Platform width in mm | Measure taken on the distance between the two lateral edges of butt |
| Platform thickness in mm | Measure taken from the point of percussion to the intersection of butt and flaking surface |
| Point of percussion | Axial, lateral, punctiforme, removed |
| Shape of distal part | Sub-ovale, sub-triangular, sub-rectangular, retouched, symmetrical, asymmetrical: on right , on left; inclination of distal profile: on right, on left |
| Distal termination | Absent, feathering, blunt, hinge, overpassed, retouched |
| The broadest part of flake | Proximal, medial or distal part |
| Lateral edges | Parallel, expanding, converging |
| Organisation of dorsal ridges | <ol style="list-style-type: none"> 1. Around one longitudinal ridge 2. Around two longitudinal and parallel ridges 3. Around two longitudinal and converging on 1/2 or 2/3 of piece 4. Around three or more longitudinal and parallel ridges 5. Around three or more longitudinal and converging ridges |
| Number of flake negatives | 2, 3... |
| Bulb | Flat; pronounced; missing |
| Stigmata visible on bulb | Radial defaults, micro ripples |
| Broken tool or tool made on blank fragment | |
| Retouch | <ol style="list-style-type: none"> 1. Extent (short, long, invasive, covering) 2. Distribution (continuous, discontinuous, partial) 3. Angle of retouch (abrupt, semi-abrupt) , 4. Delineation, morphology (scaled, stepped, pralel), Position (direct, inverse, alternate, alternating, bifacial, crossed), 5. Localisation (right or left side: proximal, medial, distal parts) |

Tab.2: Attributes recorded for flakes..

Tab.2

| Attribute | Features |
|---|--|
| Signature / year | HU.... |
| Level | E.g. "6b" |
| Raw material | Paleocene flint, Cretaceous flint, limestone |
| Category | Core; core fragment; tested pebble; indeterminable |
| Morphology | Block, tablet, polyhedral, flake, debris, irregular |
| Maximum length | in mm |
| Maximum width | in mm |
| Maximum thickness | in mm |
| Weight | in g |
| Patination | Color; double patination |
| Cortex; 1. Type 2. Amount 3. Location | 1. none; fresh; weathered; neocortex 2. 0-25%; 26-50%; 51-75%; 76-99%; 100% 3. Proximal, distal, lateral part |
| n° of surfaces | 1, 2, 3, volumetric |
| Cross section | 1, 2, 3a, 3b, 4a, 4b, see fig. |
| Dorsal scar pattern | Determination for each surface: unidirectional parallel, unidirectional convergent, bidirectional parallel, bidirectional shifted, centripetal, lineal |
| Flaking surface morphology: 1. Shape 2. Condition | 1. Rectangular; triangular; round; cylindrical 2. Flat or convex |
| Orientation of flaking surface on core | On narrow face; broad face; both narrow and broad face |
| Face inferieur | Natural, cortical, Levallois preparation, brute de débitage |
| Exploitation | On dorsal, ventral or both |
| n° of striking platforms | 1; 2; 3 |
| Platform width | in mm |
| Platform thickness | in mm |
| Exterior platform angle | Angle between flaking surface and striking platform |
| Preparation of striking platform | Determination for each striking platform: faceted; plain; cortical, damaged, broken, indeterminable |
| Reduction strategy | Levallois; Laminar; semi-rotating; rotating; core on flake; core-burin |
| Reduction stage | Early; exhausted core; unclear |
| Surface scar pattern | Blade; flake; both |
| Maximum last scar dimension | in mm |

Tab. 3: Attributes recorded for cores.

| layer | 6a | 6b | 6c2 | 7a | 7c |
|--------------------------------|-----|------|-----|----|-----|
| excavated surface (m2) | 10 | 14 | 2 | 14 | 18 |
| density (item per m3) | 241 | 2682 | 137 | 19 | 50 |
| fauna (artefacts \geq 2cm) | 6 | 51 | 6 | 13 | 29 |
| lithics (artefacts \geq 2cm) | 476 | 3704 | 186 | 41 | 332 |

Tab.4: Density of the artefacts in the Hummalian layers.

Tab. 4

| Blades : 5 element | n | ETE | ETE*n | ETE ² | ETE ² *n | TIE | TLV 1 | TLV 2 |
|---------------------------|-------------|-----|---------------|------------------|---------------------|---------------|---------------|---------------|
| intact | 356 | 100 | 35600 | 10000 | 3560000.0 | | | |
| proximal | 366 | 33 | 12078 | 1089 | 398574.0 | | | |
| proximal-medial | 375 | 66 | 24750 | 4356 | 1633500.0 | | | |
| medial | 1687 | 33 | 55671 | 1089 | 1837143.0 | | | |
| distal | 49 | 33 | 1617 | 1089 | 53361.0 | | | |
| distal-medial | 249 | 66 | 16434 | 4356 | 1084644.0 | | | |
| Σ | 3082 | | 146150 | | 8567222.0 | 2492.4 | 1819.3 | 3183.9 |

| element | n | total length | mean L at discard | min. L at discard |
|------------------|-------------|----------------|-------------------|-------------------|
| intact specimens | 356 | 2510.0 | 7.0 | 4.0 |
| fragments > 2cm | 2726 | 10225.4 | 4.6 | |
| Σ | 3082 | 12735.4 | | |

| Blades: three elements | n | ETE | ETE*n | ETE ² | ETE ² *n | MNIT |
|-------------------------------|-------------|-----|---------------|------------------|---------------------|---------------|
| intact | 356 | 100 | 35600 | 10000 | 3560000.0 | |
| prox | 741 | 33 | 24453 | 1089 | 806949.0 | |
| medial | 1687 | 33 | 55671 | 1089 | 1837143.0 | |
| distal | 298 | 33 | 9834 | 1089 | 324522.0 | |
| Σ | 3082 | | 125558 | | 6528614.0 | 2043.0 |

ETE: estimated tool equivalent 100= intact specimen which retain three parts; one retained element ETE= 33 and those which retain 2, ETE=66

TIE : Tool Information Equivalent $((n-1)/n)*(\sum ETE*n^2/\sum ETE^2)$

MNIT : Minimum Number of Intact T number of entire items + the biggest value among proximal, medial and distal fragments

TLV: Tool Length Value

TLV 1: total length of intact tools added to the total length of fragments divided by the mean length of intact tool at discard

TLV 2: total length of intact tools added to the total length of fragments divided by the minimum length at discard

Tab.5: Quantification of blades from Layer 6b.

| Blades : 5 element | n | ETE | ETE*n | ETE ² | ETE ² *n | TIE | TLV 1 | TLV 2 |
|---------------------------|-------------|-----|---------------|------------------|---------------------|---------------|---------------|---------------|
| intact | 204 | 100 | 20400 | 10000 | 2040000.0 | | | |
| proximal | 366 | 33 | 12078 | 1089 | 398574.0 | | | |
| proximal-medial | 346 | 66 | 22836 | 4356 | 1507176.0 | | | |
| medial | 1566 | 33 | 51678 | 1089 | 1705374.0 | | | |
| distal | 49 | 33 | 1617 | 1089 | 53361.0 | | | |
| distal-medial | 208 | 66 | 13728 | 4356 | 906048.0 | | | |
| Σ | 2739 | | 122337 | | 6610533.0 | 2263.2 | 1411.1 | 2681.1 |

| element | n | ETE | ETE*n | ETE ² | ETE ² *n | TIE | TLV 1 | TLV 2 |
|------------------|-------------|----------------|-------|------------------|---------------------|-----|-------|-------|
| intact specimens | 204 | 1554.7 | 7.6 | 4.0 | | | | |
| fragments >2cm | 2535 | 9169.5 | 4.5 | | | | | |
| Σ | 2739 | 10724.2 | | | | | | |

| Blank blades element | n | ETE | ETE*n | ETE ² | ETE ² *n | TIE | MNIT |
|-----------------------------|-------------|-----|---------------|------------------|---------------------|---------------|---------------|
| intact | 204 | 100 | 20400 | 10000 | 2040000.0 | | |
| prox | 712 | 33 | 23496 | 1089 | 775368.0 | | |
| medial | 1566 | 33 | 51678 | 1089 | 1705374.0 | | |
| distal | 257 | 33 | 8481 | 1089 | 279873.0 | | |
| Σ | 2739 | | 104055 | | 4800615.0 | 2254.6 | 1770.0 |

ETE: estimated tool equivalent 100= intact specimen which retain three parts; one retained element ETE= 33 and those which retain 2, ETE=66

TIE : Tool Information Equivalent $((n-1)/n)*(\sum ETE*n^2/\sum ETE^2)$

MNIT : Minimum Number of Intact T number of entire items + the biggest value among proximal, medial and distal fragments

TLV: Tool Length Value

TLV 1:

total length of intact tools added to the total length of fragments divided by the mean length of intact tool at discard

TLV 2:

total length of intact tools added to the total length of fragments divided by the minimum length at discard

Tab.6: Quantification of blank-blades from Layer 6b

| CTBlades | n | ETE | ETE*n | ETE ² | ETE ² *n | TIE | MNIT | TLV 1 | TLV 2 |
|-----------------|------------|-----|--------------|------------------|---------------------|--------------|--------------|--------------|--------------|
| intact | 152 | 100 | 15200 | 10000 | 1520000.0 | | | | |
| proximal-medial | 29 | 66 | 1914 | 4356 | 126324.0 | | | | |
| medial | 126 | 33 | 4158 | 1089 | 137214.0 | | | | |
| distal-medial | 41 | 66 | 2706 | 4356 | 178596.0 | | | | |
| Σ | 348 | | 23978 | | 1962134.0 | 292.2 | 278.0 | 315.9 | 648.8 |

| element | n | total length | mean length | min. length at discard |
|------------------|------------|---------------|-------------|------------------------|
| intact specimens | 152 | 955.3 | 6.4 | 3.1 |
| fragments >3cm | 196 | 1055.9 | 5.3 | |
| Σ | 348 | 2011.2 | | |

ETE: estimated tool equivalent 100= intact specimen which retain three parts; one retained element ETE= 33 and those which retain 2, ETE=66

TIE : Tool Information Equivalent $((n-1)/n)*(\sum ETE*n^2/\sum ETE^2)$

MNIT : Minimum Number of Intact T number of entire items + the biggest value among proximal, medial and distal fragments

TLV: Tool Length Value

TLV 1:

TLV 2:

total length of intact tools added to the total length of fragments divided by the mean length of intact tool at discard
total length of intact tools added to the total length of fragments divided by the minimum length at discard

Tab. 7: Quantification of Core trimming blades from Layer 6b

| Bladelets 3 elements | n | ETE | ETE*n | ETE ² | ETE ² *n | TIE | MNIT | TLV 1 | TLV 2 |
|----------------------|------------|-----|-------------|------------------|---------------------|--------------|-------------|--------------|--------------|
| intact | 14 | 100 | 1400 | 10000 | 140000 | | | | |
| prox | 28 | 33 | 924 | 1089 | 30492 | | | | |
| medial | 85 | 33 | 2805 | 1089 | 92565 | | | | |
| distal | 26 | 33 | 858 | 1089 | 28314 | | | | |
| Σ | 153 | | 5987 | | 291371 | 122.2 | 99.0 | 120.6 | 178.3 |

| elements | n | total length | mean length at discard | min. length at discard |
|------------------|------------|--------------|------------------------|------------------------|
| intact specimens | 14 | 47.5 | 3.4 | 2.3 |
| fragments >1.5cm | 139 | 362.6 | 2.6 | |
| Σ | 153 | 410.1 | | |

ETE: estimated tool equivalent 100= intact specimen which retain three parts; one retained element ETE= 33 and those which retain 2, ETE=66

TIE : Tool Information Equivalent $((n-1)/n)*(\sum ETE*n^2/\sum ETE^2)$

MNIT : Minimum Number of Intact T number of entire items + the biggest value among proximal, medial and distal fragments

TLV: Tool Length Value

TLV 1: total length of intact tools added to the total length of fragments divided by the mean length of intact tool at discard

TLV 2: total length of intact tools added to the total length of fragments divided by the minimum length at discard

Tab. 8: Quantification of bladelets from Layer 6b

| Blades :5 element | n | ETE | ETE*n | ETE ² | ETE ² *n | TIE | TLV 1 | TLV 2 |
|--------------------------|------------|-----|-------------|------------------|---------------------|--------------|-------------|--------------|
| intact | 37 | 100 | 3700 | 10000 | 370000.0 | | | |
| proximal | 2 | 33 | 66 | 1089 | 2178.0 | | | |
| proximal-medial | 23 | 66 | 1518 | 4356 | 100188.0 | | | |
| medial | 7 | 33 | 231 | 1089 | 7623.0 | | | |
| distal | 18 | 33 | 594 | 1089 | 19602.0 | | | |
| distal-medial | 31 | 66 | 2046 | 4356 | 135036.0 | | | |
| Σ | 118 | | 8155 | | 634627.0 | 103.9 | 93.6 | 172.0 |

| elements | c | total length | mean L. at discard | min. L at discard |
|------------------|------------|--------------|--------------------|-------------------|
| intact specimens | 37 | 291.0 | 7.9 | 4.3 |
| fragments > 2cm | 81 | 448.6 | 5.6 | |
| Σ | 118 | 739.6 | | |

| Blades: three elements | n | ETE | ETE*n | ETE ² | ETE ² *n | TIE | MNIT |
|-------------------------------|------------|-----|-------------|------------------|---------------------|-------------|-------------|
| intact | 37 | 100 | 3700 | 10000 | 370000.0 | | |
| prox | 25 | 33 | 825 | 1089 | 27225.0 | | |
| medial | 7 | 33 | 231 | 1089 | 7623.0 | | |
| distal | 49 | 33 | 1617 | 1089 | 53361.0 | | |
| Σ | 118 | | 6373 | | 458209.0 | 87.9 | 86.0 |

ETE: estimated tool equivalent 100= intact specimen which retain three parts; one retained element ETE= 33 and those which retain 2, ETE=66

TIE : Tool Information Equivalent $((n-1)/n)*(\sum ETE*n^2/\sum ETE^2)$

MNIT : Minimum Number of Intact T number of entire items + the biggest value among proximal, medial and distal fragments

TLV: Tool Length Value

TLV 1:

TLV 2:

total length of intact tools added to the total length of fragments divided by the mean length of intact tool at discard
total length of intact tools added to the total length of fragments divided by the minimum length at discard

Tab. 9: Quantification of blades with one retouched borde from Layer 6b

| Blades 2 ret. bordes:5 elements | | | | | | | | |
|--|-----------|-----|-------------|------------------|---------------------|-------------|-------------|-------------|
| | n | ETE | ETE*n | ETE ² | ETE ² *n | TIE | TLV 1 | TLV 2 |
| intact | 9 | 100 | 900 | 10000 | 90000.0 | | | |
| proximal | 1 | 33 | 33 | 1089 | 1089.0 | | | |
| proximal-medial | 10 | 66 | 660 | 4356 | 43560.0 | | | |
| medial | 3 | 33 | 99 | 1089 | 3267.0 | | | |
| distal | 7 | 33 | 231 | 1089 | 7623.0 | | | |
| distal-medial | 8 | 66 | 528 | 4356 | 34848.0 | | | |
| Σ | 38 | | 2451 | | 180387.0 | 32.4 | 28.1 | 41.8 |

| elements | Σ | total length | mean L at discard | min. L at discard |
|------------------|-----------|--------------|-------------------|-------------------|
| intact specimens | 9 | 71.0 | 7.9 | 5.3 |
| fragments > 2cm | 29 | 150.7 | 5.2 | |
| Σ | 38 | 221.7 | | |

| Blades: three elements | | | | | | | |
|-------------------------------|-----------|-----|-------------|------------------|---------------------|-------------|-------------|
| | n | ETE | ETE*n | ETE ² | ETE ² *n | TIE | MNIT |
| intact | 9 | 100 | 900 | 10000 | 90000.0 | | |
| prox | 11 | 33 | 363 | 1089 | 11979.0 | | |
| medial | 3 | 33 | 99 | 1089 | 3267.0 | | |
| distal | 15 | 33 | 495 | 1089 | 16335.0 | | |
| Σ | 38 | | 1857 | | 121581.0 | 27.6 | 24.0 |

ETE: estimated tool equivalent 100= intact specimen which retain three parts; one retained element ETE= 33 and those which retain 2, ETE=66

TIE : Tool Information Equivalent $((n-1)/n)*(\sum ETE*n^2/\sum ETE^2)$

MNIT : Minimum Number of Intact T number of entire items + the biggest value among proximal, medial and distal fragments

TLV: Tool Length Value

TLV 1:

TLV 2:

total length of intact tools added to the total length of fragments divided by the mean length of intact tool at discard

total length of intact tools added to the total length of fragments divided by the minimum length at discard

Tab. 10: Quantification of blades with two retouched borders from Layer 6b

| Blades :2 element | n | ETE | ETE*n | ETE ² | ETE ² *n | TIE | MNIT | TLV 1 | TLV 2 |
|-------------------|-----------|-----|-------------|------------------|---------------------|-------------|-------------|-------------|--------------|
| intact | 37 | 100 | 3700 | 10000 | 370000.0 | | | | |
| proximal-medial | 2 | 66 | 132 | 4356 | 8712.0 | | | | |
| distal-medial | 50 | 66 | 3300 | 4356 | 217800.0 | | | | |
| Σ | 89 | | 7132 | | 596512.0 | 84.3 | 87.0 | 69.0 | 125.7 |

| elements | n | total length | mean length at discard | min. length at discard |
|------------------|-----------|--------------|------------------------|------------------------|
| intact specimens | 37 | 301.7 | 8.2 | 4.5 |
| fragments > 2cm | 52 | 263.9 | 5.1 | |
| Σ | 89 | 565.6 | | |

ETE: estimated tool equivalent 100= intact specimen which retain three parts; one retained element ETE= 33 and those which retain 2, ETE=66

TIE : Tool Information Equivalent $((n-1)/n)*(\sum ETE*n^2/\sum ETE^2)$

MNIT: Minimum Number of Intact T number of entire items + the biggest value among proximal, medial and distal fragments

TLV: Tool Length Value

TLV 1: total length of intact tools added to the total length of fragments divided by the mean length of intact tool at discard

TLV 2: total length of intact tools added to the total length of fragments divided by the minimum length at discard

Tab. 11: Quantification of blades with retouched and converging borders from Layer 6b

| Blades :5 element | n | ETE | ETE*n | ETE ² | ETE*n | TIE | MNIT | TLV 1 | TLV 2 |
|--------------------------|------------|-----|--------------|------------------|------------------|--------------|--------------|--------------|--------------|
| intact | 105 | 100 | 10500 | 10000 | 1050000.0 | | | | |
| proximal | 4 | 33 | 132 | 1089 | 4356.0 | | | | |
| proximal-medial | 38 | 66 | 2508 | 4356 | 165528.0 | | | | |
| medial | 10 | 33 | 330 | 1089 | 10890.0 | | | | |
| distal | 46 | 33 | 1518 | 1089 | 50094.0 | | | | |
| distal-medial | 71 | 66 | 4686 | 4356 | 309276.0 | | | | |
| Σ | 274 | | 19674 | | 1590144.0 | 242.5 | 222.0 | 220.5 | 394.8 |

| elements | Σ | total length | mean L at discard | min. length at discard |
|------------------|------------|---------------|-------------------|------------------------|
| intact specimens | 105 | 806.0 | 7.7 | 4.3 |
| fragments > 2cm | 169 | 891.6 | 5.3 | |
| Σ | 274 | 1697.6 | | |

ETE: estimated tool equivalent 100= intact specimen which retain three parts; one retained element ETE= 33 and those which retain 2, ETE=66
TIE : Tool Information Equivalent $((n-1)/n)*(\sum ETE*n^2/\sum ETE^2)$
MNIT : Minimum Number of Intact T number of entire items + the biggest value among proximal, medial and distal fragments
TLV: Tool Length Value
TLV 1: total length of intact tools added to the total length of fragments divided by the mean length of intact tool at discard
TLV 2: total length of intact tools added to the total length of fragments divided by the minimum length at discard

Tab. 12: Quantification of retouched blades from Layer 6b.

| Blades : 5 element | n | ETE | ETE*n | ETE ² | ETE*n | TIE | MNIT | TLV 1 | TLV 2 |
|---------------------------|------------|-----|--------------|------------------|-----------------|--------------|--------------|--------------|--------------|
| intact | 3 | 100 | 300 | 10000 | 30000.0 | | | | |
| proximal | 44 | 33 | 1452 | 1089 | 47916.0 | | | | |
| proximal-medial | 21 | 66 | 1386 | 4356 | 91476.0 | | | | |
| medial | 216 | 33 | 7128 | 1089 | 235224.0 | | | | |
| distal | 15 | 33 | 495 | 1089 | 16335.0 | | | | |
| distal-medial | 5 | 66 | 330 | 4356 | 21780.0 | | | | |
| Σ | 304 | | 11091 | | 442731.0 | 276.9 | 219.0 | 179.3 | 220.0 |

| element | n | total length | mean length | minimum length |
|------------------|------------|--------------|-------------|----------------|
| intact specimens | 3 | 16.3 | 5.4 | 4.4 |
| fragments > 2cm | 301 | 951.7 | 4.0 | |
| Σ | 304 | 968.0 | | |

ETE: estimated tool equivalent 100 for intact specimen which retain three parts; element retain one ETE= 33 and those which retain 2 elements ETE=66

TIE : Tool Information Equivalent $((n-1)/n)*(\sum ETE*n^2/\sum ETE^2)$

MNIT : Minimum Number of Intact T number of entire items + the biggest value among proximal, medial and distal fragments

TLV: Tool Length Value

TLV 1: total length of intact tools added to the total length of fragments divided by the mean length of intact tool at discard

TLV 2: total length of intact tools added to the total length of fragments divided by the minimum length at discard

Tab. 13: Quantification of blades from Layer 6a

| Bladelets: three elements | | | | | | | | | |
|----------------------------------|-----------|-----|------------|------------------|---------------------|-------------|-------------|-------------|-------------|
| | n | ETE | ETE*n | ETE ² | ETE ² *n | TIE | MNIT | TLV 1 | TLV 2 |
| intact | 2 | 100 | 200 | 10000 | 20000.0 | | | | |
| prox | 3 | 33 | 99 | 1089 | 3267.0 | | | | |
| medial | 15 | 33 | 495 | 1089 | 16335.0 | | | | |
| distal | 2 | 33 | 66 | 1089 | 2178.0 | | | | |
| Σ | 22 | | 860 | | 41780.0 | 16.9 | 17.0 | 13.2 | 15.4 |

| element | n | total length | mean length at discard | min. length at discard |
|------------------|-----------|--------------|------------------------|------------------------|
| intact specimens | 2 | 8.4 | 4.2 | 3.6 |
| fragments > 2cm | 20 | 47.0 | | |
| Σ | 22 | 55.4 | | |

ETE: estimated tool equivalent 100= intact specimen which retain three parts; one retained element ETE= 33 and those which retain 2, ETE=66

TIE : Tool Information Equivalent $((n-1)/n)*(\sum ETE*n^2/\sum ETE^2)$

MNIT : Minimum Number of Intact T number of entire items + the biggest value among proximal, medial and distal fragments

TLV: Tool Length Value

TLV 1: total length of intact tools added to the total length of fragments divided by the mean length of intact tool at discard

TLV 2: total length of intact tools added to the total length of fragments divided by the minimum length at discard

Tab. 14: Quantification of bladelets from Layer 6a

| Retouched Blades :2 element | | | | | | | | | | |
|------------------------------------|-----------|-----|------------|------------------|---------------------|------------|------------|------------|------------|--|
| | n | ETE | ETE*n | ETE ² | ETE ² *n | TIE | MNIT | TLV 1 | TLV 2 | |
| intact | 2 | 100 | 200 | 10000 | 20000.0 | | | | | |
| proximal-medial | 3 | 66 | 198 | 4356 | 13068.0 | | | | | |
| distal-medial | 6 | 66 | 396 | 4356 | 26136.0 | | | | | |
| Σ | 11 | | 794 | | 59204.0 | 9.7 | 8.0 | 7.2 | 7.8 | |

| elements | Σ | total length | mean length at disgard | min. length at disgard |
|------------------|-----------|--------------|------------------------|------------------------|
| intact specimens | 2 | 14.0 | 7.5 | 6.9 |
| fragments > 2cm | 9 | 39.7 | | |
| Σ | 11 | 53.7 | | |

ETE: estimated tool equivalent 100= intact specimen which retain three parts; one retained element ETE= 33 and those which retain 2, ETE=66

TIE : Tool Information Equivalent $((n-1)/n)*(\sum ETE*n^2/\sum ETE^2)$

MNIT : Minimum Number of Intact T number of entire items + the biggest value among proximal, medial and distal fragments

TLV: Tool Length Value

TLV 1: total length of intact tools added to the total length of fragments divided by the mean length of intact tool at discard

TLV 2: total length of intact tools added to the total length of fragments divided by the minimum length at discard

Tab. 15: Quantification of retouched blades from Layer 6a

| Layers | 6a | | 6b | | 6c2 | | 7a | | 7c | | 6A1-2 | | 6B | | ah | | Total | |
|---------------------|------|--------|------|--------|-----|--------|-----|--------|-----|--------|-------|--------|-----|--------|------|--------|-------|--------|
| | No. | % | No. | % | No. | % | No. | % | No. | % | No. | % | No. | % | No. | % | No. | % |
| Flakes | 63 | 4.9% | 252 | 5.2% | 9 | 3.0% | 4 | 2.2% | 35 | 5.8% | 6 | 7.6% | 5 | 6.3% | 153 | 5.3% | 527 | 5.1% |
| Retouched flakes | | | 73 | 1.5% | 2 | 0.7% | 1 | 0.5% | 4 | 0.7% | 3 | 3.8% | 2 | 2.5% | 44 | 1.5% | 129 | 1.3% |
| Unretouched blades* | 221 | 17.1% | 1411 | 28.9% | 44 | 14.7% | 12 | 6.6% | 49 | 8.1% | 16 | 20.3% | 10 | 12.7% | 545 | 18.8% | 2268 | 22.1% |
| Retouched blades | 11 | 0.9% | 275 | 5.6% | 19 | 6.3% | 1 | 0.5% | 9 | 1.5% | 6 | 7.6% | 11 | 13.9% | 323 | 11.1% | 655 | 6.4% |
| Bladelets | 17 | 1.3% | 121 | 2.5% | 11 | 3.7% | 1 | 0.5% | 16 | 2.6% | 2 | 2.5% | | | 111 | 3.8% | 279 | 2.7% |
| CTE | 54 | 4.2% | 1021 | 20.9% | 70 | 23.3% | 12 | 6.6% | 52 | 8.6% | 10 | 12.7% | 6 | 7.6% | 484 | 16.7% | 1709 | 16.6% |
| Cores | 4 | 0.3% | 195 | 4.0% | 7 | 2.3% | 2 | 1.1% | 5 | 0.8% | 5 | 6.3% | 7 | 8.9% | 83 | 2.9% | 308 | 3.0% |
| débris >2cm | 106 | 8.2% | 342 | 7.0% | 4 | 1.3% | 6 | 3.3% | 84 | 13.9% | | | | | 215 | 7.4% | 757 | 7.4% |
| chipss≤2cm | | | 13 | 0.3% | 20 | 6.7% | 143 | 78.6% | 84 | 13.9% | 30 | 38.0% | 13 | 16.5% | 462 | 15.9% | 765 | 7.4% |
| débris <2 cm | 816 | 63.2% | 1165 | 23.9% | 114 | 38.0% | | | 263 | 43.4% | 25 | 31.6% | | | 474 | 16.4% | 2857 | 27.8% |
| hammerstone | | | 7 | 0.1% | | | | | 5 | 0.8% | 1 | 1.3% | | | 5 | 0.2% | 18 | 0.2% |
| Total | 1292 | 100.0% | 4875 | 100.0% | 300 | 100.0% | 182 | 100.0% | 606 | 100.0% | 79 | 100.0% | 79 | 100.0% | 2899 | 100.0% | 10272 | 100.0% |

Tab.16: Inventory of analysed assemblages.

* for layers 6a and 6b the number of artefacts was calculated using TLV (see chapter Quantification)

| Layers | 6a | | 6b | | 6c2 | | 7a | | 7c | | 6A1-2 | | 6B | | ah | | Total | |
|---------------------|-----|--------|------|--------|-----|--------|-----|--------|-----|--------|-------|--------|-----|--------|------|--------|-------|--------|
| | No. | % | No. | % | No. | % | No. | % | No. | % | No. | % | No. | % | No. | % | No. | % |
| Flakes | 63 | 17.0% | 252 | 7.5% | 9 | 5.6% | 4 | 12.1% | 35 | 20.6% | 6 | 12.5% | 5 | 12.2% | 153 | 8.8% | 527 | 8.9% |
| Retouched flakes | | | 73 | 2.2% | 2 | 1.2% | 1 | 3.0% | 4 | 2.4% | 3 | 6.3% | 2 | 4.9% | 44 | 2.5% | 129 | 2.2% |
| Unretouched blades* | 221 | 59.7% | 1411 | 42.1% | 44 | 27.2% | 12 | 36.4% | 49 | 28.8% | 16 | 33.3% | 10 | 24.4% | 545 | 31.3% | 2268 | 38.3% |
| Retouched blades | 11 | 3.0% | 275 | 8.2% | 19 | 11.7% | 1 | 3.0% | 9 | 5.3% | 6 | 12.5% | 11 | 26.8% | 323 | 18.5% | 655 | 11.1% |
| Bladelets | 17 | 4.6% | 121 | 3.6% | 11 | 6.8% | 1 | 3.0% | 16 | 9.4% | 2 | 4.2% | | | 111 | 6.4% | 279 | 4.7% |
| CTE | 54 | 14.6% | 1021 | 30.5% | 70 | 43.2% | 12 | 36.4% | 52 | 30.6% | 10 | 20.8% | 6 | 14.6% | 484 | 27.8% | 1709 | 28.9% |
| Cores | 4 | 1.1% | 195 | 5.8% | 7 | 4.3% | 2 | 6.1% | 5 | 2.9% | 5 | 10.4% | 7 | 17.1% | 83 | 4.8% | 308 | 5.2% |
| Total | 370 | 100.0% | 3348 | 100.0% | 162 | 100.0% | 33 | 100.0% | 170 | 100.0% | 48 | 100.0% | 41 | 100.0% | 1743 | 100.0% | 5915 | 100.0% |

Tab. 17: Frequency of debitage elements and cores in analysed layers.

* for layers 6a and 6b the number of artefacts was calculated using TLV (see chapter Quantification)

| Layer | Paleogene | Cretaceous | Limestone |
|-------|-----------|------------|-----------|
| 6a | 99.0% | 1.0% | |
| 6b | 98.9% | 0.8% | 0.3% |
| 6c2 | 98.4% | 1.6% | |
| 7a | 100.0% | | |
| 7c | 99.0% | 1.0% | |
| 6A1 | 100.0% | | |
| 6B | 99.1% | 0.6% | 0.3% |
| ah | 99.1% | 0.6% | 0.3% |

| layer | llam* | Ratio blank to CTE |
|-------|-------|--------------------|
| 6a | 68.6 | 5.0 |
| 6b | 66.0 | 3.0 |
| 6c2 | 72.8 | 3.1 |
| 7a | 75.0 | 4.0 |
| 7c | 52.8 | 3.4 |
| 6A1 | 70.0 | 5.7 |
| 6B | 42.9 | 5.8 |
| ah | 62.0 | 4.7 |

Tab. 18: Frequency distribution of raw material types in analysed layers .

Tab. 20: llam and ratio blank to CTE in Hummalian layers
*as defined by F.Bordes number of blades x100/total number of blades,
flakes and points

| layer | 6a | 6b | 6c2 | 7a | 7c | 6A1-2 | 6B | ah |
|---|-------|-------|-------|-------|-------|-------|-------|-------|
| N° of items with cortex and neocortex covers | 29 | 1213 | 49 | 4 | 68 | 16 | 25 | 618 |
| Items covered by neocortex | 5 | 253 | 14 | 2 | 12 | 13 | 17 | 185 |
| Percent of items with neocortex to all cortical items | 17.2% | 20.9% | 28.6% | 50.0% | 17.6% | 81.3% | 68.0% | 29.9% |

Table. 19: Frequency distribution of neocortex in all layers.

| | length (L) | | | width (W) | | | thickness (T) | | | WT platform | | | Volume (cm3) | | | mean | | | median | | | | | |
|-------|------------|-----|------|-----------|-----|-----|---------------|-----|-----|-------------|-----|-----|--------------|-----|------|------|------|------|--------|-----|-----|-----|------|--|
| | mean | max | min | mean | max | min | mean | max | min | mean | max | min | mean | max | min | LW | WT | LT | LW | WT | LT | | | |
| 6a | | | | | | | | | | | | | | | | | | | | | | | | |
| CTE | 4.0 | 3.9 | 7.4 | 3.0 | 2.7 | 3.0 | 3.5 | 1.0 | 0.6 | 0.5 | 1.0 | 0.5 | 2.8 | 2.7 | 4.0 | 1.4 | 6.6 | 5.6 | 8.0 | 4.2 | 1.3 | 6.0 | 6.7 | |
| Blank | 5.4 | 5.9 | 8.0 | 2.2 | 2.7 | 2.9 | 3.9 | 1.4 | 0.9 | 0.9 | 1.3 | 0.6 | 1.7 | 3.2 | 4.6 | 1.8 | 14.0 | 7.7 | 31.2 | 4.1 | 2.4 | 2.6 | 6.2 | |
| | | | | | | | | | | | | | | | | | | | | | | | | |
| 6c2 | | | | | | | | | | | | | | | | | | | | | | | | |
| CTE | 4.5 | 4.1 | 7.0 | 2.9 | 2.8 | 3.0 | 4.1 | 1.7 | 0.7 | 0.6 | 1.4 | 0.2 | 3.3 | 2.6 | 7.0 | 1.7 | 9.5 | 7.3 | 22.0 | 2.4 | 1.5 | 4.0 | 6.6 | |
| Blank | 7.3 | 7.0 | 12.8 | 2.9 | 2.8 | 2.8 | 6.3 | 1.6 | 0.7 | 0.7 | 1.3 | 0.3 | 3.4 | 3.1 | 8.3 | 1.3 | 17.1 | 12.8 | 55.8 | 3.3 | 2.7 | 4.1 | 10.5 | |
| | | | | | | | | | | | | | | | | | | | | | | | | |
| 6b | | | | | | | | | | | | | | | | | | | | | | | | |
| CTE | 6.0 | 5.7 | 14.0 | 3.0 | 3.4 | 3.2 | 8.9 | 1.2 | 1.2 | 1.1 | 3.2 | 0.3 | 2.6 | 2.3 | 8.0 | 0.9 | 28.1 | 20.1 | 221.8 | 1.3 | 1.8 | 2.9 | 5.1 | |
| Blank | 6.5 | 6.2 | 16.0 | 2.1 | 3.3 | 3.1 | 9.9 | 1.1 | 1.0 | 1.0 | 3.0 | 0.3 | 3.0 | 2.7 | 14.3 | 0.8 | 24.1 | 19.1 | 209.3 | 0.9 | 2.1 | 3.6 | 6.8 | |

Tab. 21 : Metrical data of blanks (without baldelets) and CTE in layers 6c, 6b and 6c.

| | length (L) | | | width (W) | | | thickness (T) | | | WT platform | | | Volume (cm3) | | | mean | | | median | | | | |
|-------|------------|--------|------|-----------|--------|-----|---------------|--------|-----|-------------|--------|-----|--------------|--------|-----|------|------|------|--------|-----|-----|-----|-----|
| | mean | median | min | mean | median | max | mean | median | max | mean | median | max | mean | median | max | LW | WT | LT | LW | WT | LT | | |
| 7c | | | | | | | | | | | | | | | | | | | | | | | |
| CTE | 6.3 | 5.7 | 11.2 | 3.7 | 3.5 | 3.4 | 4.7 | 2.3 | 1.0 | 1.0 | 0.4 | 1.7 | 3.6 | 3.7 | 5.5 | 1.5 | 23.3 | 23.2 | 3.4 | 3.8 | 1.8 | 3.9 | 8.1 |
| Blank | 6.5 | 6.2 | 10.6 | 3.0 | 3.2 | 3.1 | 6.1 | 1.6 | 0.8 | 0.8 | 1.6 | 0.4 | 3.8 | 3.3 | 9.0 | 0.5 | 18.3 | 16.1 | 46.4 | 2.7 | 2.2 | 4.1 | 8.3 |

| | length (L) | | | width (W) | | | thickness (T) | | | WT platform | | | Volume (cm3) | | | mean | | | median | | | | |
|-------|------------|--------|------|-----------|--------|-----|---------------|--------|-----|-------------|--------|-----|--------------|--------|------|------|------|------|--------|-----|-----|-----|-----|
| | mean | median | min | mean | median | max | mean | median | max | mean | median | max | mean | median | max | LW | WT | LT | LW | WT | LT | | |
| ah | | | | | | | | | | | | | | | | | | | | | | | |
| CTE | 7.1 | 6.6 | 3.7 | 13.7 | 3.5 | 3.3 | 7.2 | 1.5 | 1.2 | 1.1 | 3.6 | 0.3 | 2.9 | 2.6 | 10.0 | 0.4 | 384 | 26.2 | 213.8 | 5.0 | 2.1 | 4.2 | 6.5 |
| Blank | 7.2 | 7.3 | 14.4 | 1.7 | 3.1 | 3.0 | 10.7 | 0.8 | 0.8 | 0.8 | 3.4 | 0.3 | 3.0 | 2.8 | 21.0 | 0.1 | 21.0 | 16.7 | 170.1 | 1.6 | 2.5 | 4.1 | 9.2 |

Tab. 22: Metrical data of blanks (without baldelets) and CTE from layer 7c and ah .

| categories of CTE | 6a | | 6b | | 6c2 | | 7a | | 7c | | 6A1-2 | | 6B | | ah | |
|--------------------------------------|--------|--------|--------|--------|--------|--------|--------|--------|--------|--------|--------|--------|--------|--------|--------|--------|
| | counts | % |
| entames | | | 6 | 0.6% | | | | | | | | | | | 4 | 0.8% |
| cortical flakes (cx 51-99%) | 32 | 59.3% | 364 | 35.7% | 10 | 14.1% | 3 | 25.0% | 3 | 5.8% | | | 1 | 16.7% | 166 | 34.4% |
| crested | 1 | 1.9% | 5 | 0.5% | 2 | 2.8% | | | | | | | | | 3 | 0.6% |
| semi-crested | | | 37 | 3.6% | | | | | 1 | 1.9% | | | 1 | 16.7% | 7 | 1.4% |
| with plain back | 11 | 20.4% | 109 | 10.7% | 6 | 8.5% | 2 | 16.7% | 1 | 1.9% | 4 | 40.0% | 2 | 33.3% | 27 | 5.6% |
| with cortical back | 4 | | 76 | 7.4% | 2 | 2.8% | | | 5 | | 3 | 30.0% | | | 35 | 7.2% |
| <i>éclat débordant</i> prepared | | | 24 | 2.4% | | | | | | | | | | | 10 | 2.1% |
| cleaning | 3 | 5.6% | 55 | 5.4% | 5 | 7.0% | 1 | 8.3% | 1 | 1.9% | 2 | 20.0% | 2 | 33.3% | 31 | 6.4% |
| plunging | 2 | 3.7% | 43 | 4.2% | 2 | 2.8% | | | | | | | | | 13 | 2.7% |
| hinged | 1 | 1.9% | 38 | 3.7% | | | | | 3 | 5.8% | | | | | 28 | 5.8% |
| dorsal reduction flakes | | | 42 | 4.1% | 44 | 62.0% | 6 | 50.0% | 38 | 73.1% | | | | | 37 | 7.7% |
| preparation flakes <i>sensu lato</i> | | | 218 | 21.4% | | | | | | | | | | | 120 | 24.8% |
| rejuvenation flakes | | | 4 | 0.4% | | | | | | | | | | | 2 | 0.4% |
| Total | 54 | 100.0% | 1021 | 100.0% | 71 | 100.0% | 12 | 100.0% | 52 | 100.0% | 10 | 100.0% | 6 | 100.0% | 483 | 100.0% |

Tab. 23: Frequency of Core Trimming Element categories in all layers

| Layer | | 6a | 6b | 6c2 | 7c | 6A1-2 | ah |
|---------------------------------|--------|------|------|------|------|-------|-------|
| n of intact items | | 1 | 48 | 2 | 4 | 1 | 35 |
| Length (mm) | mean | 6.4 | 6.1 | 5.0 | 7.3 | 10.7 | 8.4 |
| | median | | 6.0 | 5.0 | 7.5 | | 8.2 |
| | sd | | 1.7 | 1.1 | 1.5 | | 1.8 |
| | max | | 9.9 | 5.7 | 8.8 | | 12.7 |
| | min | | 2.6 | 4.2 | 5.5 | | 5.5 |
| Width (mm) | mean | 3.9 | 3.1 | 2.7 | 3.9 | 2.5 | 3.5 |
| | median | | 3.0 | 2.7 | 3.9 | | 3.5 |
| | sd | | 1.0 | 0.6 | 0.7 | | 0.9 |
| | max | | 5.2 | 3.1 | 4.7 | | 5.1 |
| | min | | 1.5 | 2.2 | 3.3 | | 2.0 |
| Thickness | mean | 1.5 | 1.2 | 0.8 | 1.1 | 1.0 | 1.3 |
| | median | | 1.1 | 0.8 | 1.1 | | 1.2 |
| | sd | | 0.4 | 0.0 | 0.2 | | 0.6 |
| | max | | 2.3 | 0.8 | 1.3 | | 3.6 |
| | min | | 0.6 | 0.8 | 1.0 | | 0.7 |
| Surface area (mm ²) | mean | 25.0 | 19.5 | 13.5 | 28.9 | 26.8 | 28.7 |
| | median | | 16.6 | 13.5 | 29.1 | | 25.2 |
| | sd | | 9.6 | 6.0 | 8.1 | | 13.3 |
| | max | | 43.1 | 17.7 | 38.5 | | 58.4 |
| | min | | 3.8 | 9.2 | 18.7 | | 8.6 |
| Volume (mm ³) | mean | 37.4 | 24.5 | 10.8 | 32.0 | 26.8 | 42.5 |
| | median | | 19.5 | 10.8 | 33.5 | | 30.2 |
| | sd | | 16.1 | 4.8 | 7.7 | | 37.7 |
| | max | | 69.0 | 14.1 | 38.5 | | 179.9 |
| | min | | 2.8 | 7.4 | 22.4 | | 11.0 |
| Length/Width | mean | 1.6 | 2.1 | 1.9 | 1.9 | 4.3 | 2.5 |
| Width/Thickness | mean | 2.6 | 2.3 | 3.3 | 3.5 | 2.5 | 2.8 |
| Length/Thickness | mean | 4.3 | 5.7 | 6.2 | 6.7 | 10.7 | 6.8 |
| Talon W/T | mean | 0.8 | 2.4 | | 3.0 | 5.0 | 2.8 |
| | median | | 2.0 | | 3.7 | | 2.5 |
| | sd | | 1.0 | | 1.3 | | 1.8 |
| | max | | 4.5 | | 3.7 | | 10.0 |
| | min | | 0.9 | | 1.5 | | 1.0 |

Tab. 24: Metrical data of intact cortical backed elements.

| | | centripetal scars | uni/bidirectional scars |
|---------------------------------|--------|-------------------|-------------------------|
| n of intact items | | 9 | 39 |
| Length (mm) | mean | 5.6 | 6.3 |
| | median | 5.1 | 6.0 |
| | sd | 1.7 | 1.7 |
| | max | 8.1 | 9.9 |
| | min | 2.6 | 3.1 |
| Width (mm) | mean | 3.6 | 3.0 |
| | median | 3.5 | 3.0 |
| | sd | 1.1 | 0.9 |
| | max | 5.2 | 5.1 |
| | min | 1.5 | 1.5 |
| Thickness | mean | 1.3 | 1.1 |
| | median | 1.4 | 1.1 |
| | sd | 0.4 | 0.4 |
| | max | 1.9 | 2.3 |
| | min | 0.6 | 0.6 |
| Surface area (mm ²) | mean | 19.3 | 19.6 |
| | median | 21.9 | 16.3 |
| | sd | 9.9 | 9.7 |
| | max | 32.4 | 43.1 |
| | min | 3.8 | 4.7 |
| Volume (mm ³) | mean | 28.4 | 23.6 |
| | median | 30.7 | 19.5 |
| | sd | 16.6 | 16.1 |
| | max | 52.3 | 69.0 |
| | min | 4.1 | 2.8 |
| Length/Width | mean | 1.6 | 2.2 |
| Width/Thickness | mean | 3.3 | 2.9 |
| Length/Thickness | mean | 4.4 | 6.0 |
| Talon W/T | mean | 2.7 | 2.4 |
| | median | 3.0 | 2.0 |
| | sd | 0.8 | 1.0 |
| | max | 3.3 | 4.5 |
| | min | 1.7 | 0.9 |

Tab. 25: Metrical data of intact cortical edge flake with centripetal or uni/bidirectional former negatives on the upper surface in layer 6b..

| layers | 6a | | 6b | | 6c2 | | 7a | | 7c | | 6A1-2 | | ah | |
|-------------|----|--------|----|--------|-----|--------|----|--------|----|--------|-------|--------|----|--------|
| | n° | % | n° | % | n° | % | n° | % | n° | % | n° | % | n° | % |
| crushed | | | 7 | 9.2% | | | | | | | | | | |
| broken | 3 | 75.0% | 26 | 34.2% | | | 1 | 100.0% | | | 1 | 100.0% | | |
| cortical | | | 13 | 17.1% | | | | | 1 | 20.0% | | | 16 | 48.5% |
| plain | | | 13 | 17.1% | | | | | | | | | 7 | 21.2% |
| punctiforme | | | 9 | 11.8% | 2 | 100.0% | | | 2 | 40.0% | | | 4 | 12.1% |
| dihedral | | | | | | | | | 1 | 20.0% | | | | |
| faceted | 1 | 25.0% | 8 | 10.5% | | | | | 1 | 20.0% | | | 6 | 18.2% |
| total | 4 | 100.0% | 76 | 100.0% | 2 | 100.0% | 1 | 100.0% | 5 | 100.0% | 1 | 100.0% | 33 | 100.0% |

Tab. 26: Frequency of platform types in cortical backed elements.

| Layer | | 6b | ah |
|---------------------------------|--------|------|-------|
| n of intact cores | | 20 | 10 |
| Length (mm) | mean | 6.2 | 8.4 |
| | median | 5.4 | 8.2 |
| | sd | 2.0 | 1.5 |
| | max | 9.8 | 11.7 |
| | min | 3.2 | 6.5 |
| Width (mm) | mean | 4.4 | 4.1 |
| | median | 4.6 | 4.6 |
| | sd | 1.1 | 1.4 |
| | max | 6.4 | 5.4 |
| | min | 2.5 | 1.5 |
| Thickness | mean | 1.3 | 1.5 |
| | median | 1.3 | 1.4 |
| | sd | 0.5 | 0.5 |
| | max | 2.3 | 2.4 |
| | min | 0.7 | 0.8 |
| Surface area (mm ²) | mean | 26.4 | 34.8 |
| | median | 26.5 | 37.7 |
| | sd | 8.3 | 14.5 |
| | max | 43.0 | 53.8 |
| | min | 15.4 | 9.8 |
| Volume (mm ³) | mean | 35.9 | 55.3 |
| | median | 31.4 | 38.3 |
| | sd | 20.2 | 36.6 |
| | max | 88.0 | 129.2 |
| | min | 12.3 | 9.8 |
| Length/Width | mean | 1.5 | 2.3 |
| Width/Thickness | mean | 3.8 | 2.9 |
| Length/Thickness | mean | 5.2 | 6.0 |
| Talon W/T | mean | 2.2 | 2.9 |
| | median | 2.0 | 2.9 |
| | sd | 0.9 | 1.5 |
| | max | 4.5 | 4.7 |
| | min | 1.1 | 0.4 |

Tab. 27: Metrical data of intact backed element with prepared back.

| layers | 6b | | ah | |
|----------------|----|--------|----|--------|
| | n° | % | n° | % |
| unidirectional | 22 | 91.7% | 4 | 40.0% |
| bidirectional | 2 | 8.3% | 4 | 40.0% |
| indetermined | | | 2 | 20.0% |
| total | 24 | 100.0% | 10 | 100.0% |

Tab. 28: Dorsale scar pattern visible on éclats débordants.

| layers | 6b | | ah | |
|-------------|----|--------|----|--------|
| | n° | % | n° | % |
| crushed | 1 | 4.2% | | |
| broken | 4 | 16.7% | 1 | 10.0% |
| cortical | 4 | 16.7% | 1 | 10.0% |
| plain | 3 | 12.5% | 1 | 10.0% |
| punctiforme | 5 | 20.8% | 5 | 50.0% |
| dihedral | | | | |
| faceted | 7 | 29.2% | 2 | 20.0% |
| total | 24 | 100.0% | 10 | 100.0% |

Tab. 29: Frequency of platform types in éclat débordant

| Layer | | 6a | 6b | 6c2 | 7a | 7c | 6A1-2 | 6B | ah |
|--------------------|--------|-----|-------|------|------|------|-------|------|-------|
| n of intact cores | | 1 | 60 | 6 | 1 | 1 | 4 | 2 | 27 |
| Length (mm) | mean | 4.8 | 6.4 | 4.4 | 7.3 | 6.2 | 4.9 | 5.6 | 6.6 |
| | median | | 6.1 | 4.3 | | | 4.9 | 5.6 | 6.2 |
| | sd | | 1.9 | 1.0 | | | 0.5 | 1.8 | 2.0 |
| | max | | 12.2 | 5.8 | | | 5.4 | 6.8 | 11.9 |
| | min | | 3.4 | 3.1 | | | 4.3 | 4.3 | 3.8 |
| Width (mm) | mean | 1.1 | 3.0 | 2.3 | 3.4 | 3.1 | 2.7 | 2.7 | 3.4 |
| | median | | 2.8 | 2.1 | | | 2.7 | 2.7 | 3.1 |
| | sd | | 1.0 | 0.5 | | | 1.3 | 0.4 | 1.2 |
| | max | | 5.6 | 3.2 | | | 4.1 | 2.9 | 6.2 |
| | min | | 1.2 | 1.7 | | | 1.1 | 2.4 | 1.8 |
| Thickness | mean | 0.8 | 1.2 | 0.8 | 1.0 | 1.7 | 0.9 | 1.1 | 1.0 |
| | median | | 1.1 | 0.8 | | | 1.0 | 1.1 | 0.9 |
| | sd | | 0.5 | 0.2 | | | 0.2 | 0.3 | 0.4 |
| | max | | 3.2 | 1.0 | | | 1.0 | 1.3 | 2.1 |
| | min | | 0.7 | 0.5 | | | 0.5 | 0.9 | 0.5 |
| Surface area (cm2) | mean | 5.3 | 20.3 | 10.0 | 24.8 | 19.2 | 12.7 | 17.5 | 23.3 |
| | median | | 17.1 | 11.2 | | | 12.2 | 17.5 | 21.3 |
| | sd | | 11.2 | 2.7 | | | 6.1 | 11.6 | 13.8 |
| | max | | 53.7 | 12.2 | | | 20.5 | 25.6 | 73.8 |
| | min | | 6.8 | 5.3 | | | 5.9 | 9.3 | 8.4 |
| Volume (cm3) | mean | 4.2 | 27.9 | 8.2 | 24.8 | 32.7 | 11.4 | 15.0 | 26.3 |
| | median | | 20.1 | 9.4 | | | 12.2 | 15.0 | 17.8 |
| | sd | | 29.4 | 3.6 | | | 6.5 | 6.6 | 25.6 |
| | max | | 158.4 | 11.8 | | | 18.5 | 19.7 | 125.4 |
| | min | | 5.6 | 2.6 | | | 3.0 | 10.3 | 5.0 |
| Length/Width | mean | 4.4 | 2.3 | 2.0 | 2.1 | 2.0 | 2.4 | 2.1 | 2.1 |
| Width/Thickness | mean | 1.4 | 2.6 | 3.0 | 3.4 | 1.8 | 3.0 | 2.4 | 3.7 |
| Length/Thickness | mean | 6.0 | 5.6 | 5.9 | 7.3 | 3.6 | 6.4 | 5.0 | 7.1 |
| Talon W/T | mean | 1.4 | 2.4 | 2.1 | | | 2.0 | 2.4 | 2.9 |
| | median | | 2.2 | 2.1 | | | 2.3 | 2.4 | 2.5 |
| | sd | | 0.9 | 0.4 | | | 0.6 | 0.2 | 1.3 |
| | max | | 4.6 | 2.6 | | | 2.5 | 2.5 | 7.0 |
| | min | | 1.0 | 1.7 | | | 1.3 | 2.2 | 1.4 |

Tab. 30: Metrical data of intact backed element with plain back.

| layers | 6a | | 6b | | 6c2 | | 7a | | 7c | | 6A1-2 | | 6B | | dh | |
|----------------|----|--------|-----|--------|-----|--------|----|--------|----|--------|-------|--------|----|--------|----|--------|
| | n° | % | n° | % | n° | % | n° | % | n° | % | n° | % | n° | % | n° | % |
| unidirectional | 10 | 83.3% | 92 | 84.4% | 3 | 50.0% | 1 | 100.0% | 1 | 100.0% | 1 | 25.0% | 2 | 100.0% | 18 | 66.7% |
| bidirectional | 2 | 16.7% | 17 | 15.6% | 3 | 50.0% | 1 | 100.0% | | | 3 | 75.0% | | | 7 | 25.9% |
| indetermined | | | | 0.0% | | | | | | | | | | | 2 | 7.4% |
| total | 12 | 100.0% | 109 | 100.0% | 6 | 100.0% | 1 | 100.0% | 1 | 100.0% | 4 | 100.0% | 2 | 100.0% | 27 | 100.0% |

Tab. 31: Dorsale scar pattern visible on specimens with plain back.

| layers | 6a | | 6b | | 6c2 | | 7a | | 7c | | 6A1-2 | | 6B | | dh | |
|-------------|----|--------|-----|--------|-----|--------|----|--------|----|--------|-------|--------|----|--------|----|--------|
| | n° | % | n° | % | n° | % | n° | % | n° | % | n° | % | n° | % | n° | % |
| crushed | | | 10 | 9.2% | 1 | 16.7% | | | 1 | 100.0% | | | | | | |
| broken | 10 | 90.9% | 38 | 34.9% | | | | | | | | | | | | |
| cortical | | | 8 | 7.3% | 1 | 16.7% | | | | | | | | | | |
| plain | | | 19 | 17.4% | 2 | 33.3% | | | | | 2 | 50.0% | | | 16 | 59.3% |
| punctiforme | | | 8 | 7.3% | 2 | 33.3% | 1 | 100.0% | | | 1 | 25.0% | | | 6 | 22.2% |
| dihedral | | | 4 | 3.7% | | | | | | | | | | | | |
| faceted | 1 | 9.1% | 22 | 20.2% | | | | | | | 1 | 25.0% | 2 | 100.0% | 5 | 18.5% |
| total | 11 | 100.0% | 109 | 100.0% | 6 | 100.0% | 1 | 100.0% | 1 | 100.0% | 4 | 100.0% | 2 | 100.0% | 27 | 100.0% |

Tab. 32: Frequency of platform categories in plain backed specimens.

| Layer | | 6a | 6c2 | 6A1-2 | ah |
|---------------------------------|--------|-------------|------|-------|------|
| n of intact item | | 1 | 2 | 1 | 3 |
| Length (mm) | mean | 7.4 | 6.2 | 8.1 | 11.5 |
| | median | | 6.2 | | 10.4 |
| | sd | | 1.4 | | 1.9 |
| | max | | 7.2 | | 10.3 |
| | min | | 5.2 | | 13.7 |
| Width (mm) | mean | 3.5 | 2.5 | 2.6 | 2.9 |
| | median | | 2.5 | | 2.9 |
| | sd | | 0.1 | | 0.4 |
| | max | | 2.5 | | 2.5 |
| | min | | 2.4 | | 3.2 |
| Thickness | mean | 1.0 | 1.2 | 1.8 | 1.4 |
| | median | | 1.2 | | 1.4 |
| | sd | | 0.1 | | 0.1 |
| | max | | 1.3 | | 1.4 |
| | min | | 1.1 | | 1.3 |
| Surface area (mm ²) | mean | 25.9 | 14.7 | 21.1 | 32.9 |
| | median | | 14.7 | | 33.3 |
| | sd | | 3.0 | | 7.0 |
| | max | | 16.8 | | 25.8 |
| | min | | 12.5 | | 39.7 |
| Volume (mm ³) | mean | 25.9 | 17.2 | 37.9 | 45.2 |
| | median | | 17.2 | | 46.6 |
| | sd | | 6.6 | | 11.1 |
| | max | | 21.8 | | 33.5 |
| | min | | 12.5 | | 55.6 |
| Length/Width | mean | 2.1 | 2.5 | 3.1 | 4.0 |
| Width/Thickness | mean | 3.5 | 2.2 | 1.4 | 2.1 |
| Length/Thickness | mean | 7.4 | 5.2 | 4.5 | 8.4 |
| Talon W/T | mean | punctiforms | | | 3.1 |
| | median | | | | 3.1 |
| | sd | | | | 0.6 |
| | max | | | | 2.7 |
| | min | | | | 3.5 |

Tab. 33: Metrical data of intact crests.

| layers | 6a | | 6c2 | | 6A1-2 | | ah | |
|-------------|----|--------|-----|--------|-------|--------|----|--------|
| | n° | % | n° | % | n° | % | n° | % |
| crushed | | | 1 | 50.0% | | | 1 | 33.3% |
| broken | | | | | | | | |
| cortical | | | | | | | 2 | 66.7% |
| plain | | | | | | | | |
| punctiforme | 1 | 100.0% | 1 | 50.0% | 1 | 100.0% | | |
| faceted | | | | | | | | |
| total | 1 | 100.0% | 2 | 100.0% | 1 | 100.0% | 3 | 100.0% |

Tab. 34: Platforms visible in crests.

| Layer | | 6b | |
|---------------------------------|--------|------------------|-----------------|
| | | unilateral crest | secondary crest |
| n of intact item | | 6 | 22 |
| Length (mm) | mean | 7.6 | 6.3 |
| | median | 7.6 | 6.1 |
| | sd | 2.4 | 1.9 |
| | max | 11.0 | 11.6 |
| | min | 4.4 | 3.9 |
| Width (mm) | mean | 2.8 | 2.8 |
| | median | 2.4 | 2.6 |
| | sd | 1.0 | 0.8 |
| | max | 4.4 | 5.1 |
| | min | 2.0 | 1.4 |
| Thickness | mean | 1.7 | 1.4 |
| | median | 1.7 | 1.4 |
| | sd | 0.5 | 0.4 |
| | max | 2.3 | 2.4 |
| | min | 1.1 | 0.8 |
| Surface area (mm ²) | mean | 23.4 | 18.3 |
| | median | 17.4 | 14.6 |
| | sd | 15.1 | 11.6 |
| | max | 48.4 | 59.2 |
| | min | 8.8 | 3.4 |
| Volume (mm ³) | mean | 44.3 | 29.8 |
| | median | 26.0 | 20.5 |
| | sd | 39.5 | 28.4 |
| | max | 111.3 | 142.0 |
| | min | 10.6 | 9.7 |
| Length/Width | mean | 2.7 | 2.3 |
| Width/Thickness | mean | 1.7 | 2.0 |
| Length/Thickness | mean | 4.7 | 4.6 |
| Talon W/T | mean | 1.4 | 2.0 |
| | median | 1.4 | 2.0 |
| | sd | 0.2 | 0.5 |
| | max | 1.7 | 3.3 |
| | min | 1.1 | 1.6 |

Tab. 35: Metrical data of intact semi-crest versus secondary crests

| layers | 6b | | 6B | | ah | |
|-------------|----|--------|----|--------|----|--------|
| | n° | % | n° | % | n° | % |
| crushed | 3 | 8.1% | | | | |
| broken | 7 | 18.9% | | | | |
| cortical | 9 | 24.3% | | | 1 | 14.3% |
| plain | 6 | 16.2% | | | 3 | 42.9% |
| punctiforme | 5 | 13.5% | | | 1 | 14.3% |
| faceted | 7 | 18.9% | 1 | 100.0% | 2 | 28.6% |
| total | 37 | 100.0% | 1 | 100.0% | 7 | 100.0% |

Tab. 36: Platforms categories in semi-crest.

| Layer | | 6b | 6B | ah |
|---------------------------|--------|-------|------|------|
| n of intact item | | 28 | 1 | 7 |
| Length (mm) | mean | 6.6 | 11.3 | 7.9 |
| | median | 6.3 | | 9.3 |
| | sd | 2.1 | | 2.8 |
| | max | 11.6 | | 11.4 |
| | min | 3.9 | | 4.7 |
| Width (mm) | mean | 2.8 | 3.0 | 2.8 |
| | median | 2.5 | | 2.7 |
| | sd | 0.8 | | 0.6 |
| | max | 5.1 | | 3.8 |
| | min | 1.4 | | 2.2 |
| Thickness | mean | 1.5 | 1.1 | 1.1 |
| | median | 1.4 | | 1.0 |
| | sd | 0.4 | | 0.4 |
| | max | 2.4 | | 2.0 |
| | min | 0.8 | | 0.8 |
| Surface area (m | mean | 19.4 | 33.9 | 22.4 |
| | median | 15.6 | | 22.5 |
| | sd | 12.3 | | 10.7 |
| | max | 59.2 | | 37.6 |
| | min | 3.4 | | 11.7 |
| Volume (mm ³) | mean | 32.9 | 37.3 | 28.1 |
| | median | 20.7 | | 20.7 |
| | sd | 30.9 | | 23.0 |
| | max | 142.0 | | 70.7 |
| | min | 9.7 | | 10.2 |
| Length/Width | mean | 2.4 | 3.8 | 2.9 |
| Width/Thicknes | mean | 1.9 | 2.7 | 2.6 |
| Length/Thickne | mean | 4.6 | 10.3 | 7.3 |
| Talon W/T | mean | 1.8 | 3.3 | 2.4 |
| | median | 1.8 | | 2.4 |
| | sd | 0.5 | | 1.1 |
| | max | 3.3 | | 4.0 |
| | min | 1.1 | | 1.2 |

Tab. 37: Metrical data of intact semi-crest

| categories | 6a | | 6b | | 6c2 | | 7a | | 7c | | 6A1-2 | | 6B | | ah | |
|-------------------------|--------|--------|--------|--------|--------|--------|--------|---|--------|--------|--------|--------|--------|--------|--------|--------|
| | counts | % | counts | % | counts | % | counts | % | counts | % | counts | % | counts | % | counts | % |
| preparation (abrasion) | 18 | 60.0% | 346 | 47.5% | 24 | 36.9% | 2 | | 8 | 28.6% | 9 | 64.3% | 11 | 61.1% | 394 | 42.7% |
| series of tiny removals | | | 42 | 5.8% | 2 | 3.1% | | | 2 | 7.1% | | | | | 6 | 0.7% |
| hinge fracture | | | 94 | 12.9% | 10 | 15.4% | | | 4 | 14.3% | | | | | 122 | 13.2% |
| small triangle | | | | | | | | | | | | | | | | |
| dorsal removal | 12 | 40.0% | 246 | 33.8% | 29 | 44.6% | 2 | | 14 | 50.0% | 5 | 35.7% | 7 | 38.9% | 401 | 43.4% |
| Total | 30 | 100.0% | 728 | 100.0% | 65 | 100.0% | 4 | | 28 | 100.0% | 14 | 100.0% | 18 | 100.0% | 923 | 100.0% |
| Percent of blank blades | | | | | | | | | | | | | | | | |
| % preparation | | 43.9% | | 45.3% | | 58.1% | | | | 50.0% | | 64.3% | | 61.1% | | 66.0% |
| % dorsal reduction | | 22.6% | | 23.1% | | 46.8% | | | | 35.0% | | 33.3% | | 38.9% | | 50.7% |

Tab. 38: Frequency of preparations and dorsal reduction visible on the proximal part of retouched and unretouched blank blades in all layers.

| Layer | | 6a | 6b | 6c2 | 6A1-2 | ah |
|---------------------------|--------|-------------|------|------|-------|-------|
| n of intact cores | | 2 | 34 | 3 | 2 | 31 |
| Length (mm) | mean | 6.1 | 6.7 | 6.3 | 3.3 | 7.8 |
| | median | 6.1 | 6.4 | 6.7 | 3.3 | 7.4 |
| | sd | 2.6 | 1.8 | 0.8 | 0.6 | 2.3 |
| | max | 7.9 | 11.6 | 6.9 | 3.7 | 12.9 |
| | min | 4.2 | 4.0 | 5.4 | 2.8 | 3.7 |
| Width (mm) | mean | 3.1 | 3.3 | 3.6 | 5.6 | 3.1 |
| | median | 3.1 | 3.1 | 3.4 | 5.6 | 3.0 |
| | sd | 3.0 | 1.1 | 0.5 | 1.3 | 1.0 |
| | max | 5.2 | 6.5 | 4.1 | 6.5 | 6.0 |
| | min | 1.0 | 1.6 | 3.2 | 4.7 | 1.5 |
| Thickness | mean | 1.1 | 1.5 | 0.9 | 0.6 | 1.2 |
| | median | 1.1 | 1.5 | 0.7 | 0.6 | 1.2 |
| | sd | 0.1 | 0.4 | 0.3 | 0.1 | 0.5 |
| | max | 1.2 | 2.5 | 1.2 | 0.7 | 2.3 |
| | min | 1.0 | 0.5 | 0.7 | 0.5 | 0.3 |
| Surface area (n | mean | 22.6 | 22.7 | 22.6 | 18.6 | 24.9 |
| | median | 22.6 | 21.6 | 22.1 | 18.6 | 23.4 |
| | sd | 26.1 | 10.8 | 4.6 | 7.7 | 11.8 |
| | max | 41.1 | 48.8 | 27.5 | 24.1 | 46.6 |
| | min | 4.2 | 7.5 | 18.4 | 13.2 | 7.5 |
| Volume (mm ³) | mean | 26.7 | 35.6 | 18.9 | 10.6 | 33.2 |
| | median | 26.7 | 28.9 | 19.2 | 10.6 | 25.5 |
| | sd | 31.9 | 23.6 | 3.3 | 2.0 | 25.2 |
| | max | 49.3 | 87.8 | 22.0 | 12.0 | 107.2 |
| | min | 4.2 | 3.9 | 15.5 | 9.2 | 6.0 |
| Length/Width | mean | 2.9 | 2.1 | 1.8 | 0.6 | 2.7 |
| Width/Thickne | mean | 2.7 | 2.4 | 4.4 | 9.9 | 3.0 |
| Length/Thickn | mean | 5.4 | 4.8 | 8.0 | 5.7 | 7.5 |
| Talon W/T | mean | punctiforms | 2.4 | 5.2 | 3.3 | 2.9 |
| | median | | 2.2 | 5.2 | 3.3 | 2.7 |
| | sd | | 1.0 | 2.6 | 1.1 | 1.1 |
| | max | | 4.6 | 7.0 | 4.0 | 5.4 |
| | min | | 1.3 | 3.3 | 2.5 | 0.9 |

Tab. 39: Metrical data of intact cleaning flakes.

| layers | 6a | | 6b | | 6c2 | | 7a | | 7c | | 6A1-2 | | 6B | | dh | |
|----------------|----|--------|----|--------|-----|--------|----|--------|----|--------|-------|--------|----|--------|----|--------|
| | n° | % | n° | % | n° | % | n° | % | n° | % | n° | % | n° | % | n° | % |
| unidirectional | 1 | 33.3% | 42 | 76.4% | 3 | 60.0% | 1 | 100.0% | | | 2 | 100.0% | 2 | 100.0% | 11 | 35.5% |
| bidirectional | 2 | 66.7% | 12 | 21.8% | 2 | 40.0% | | | 1 | 100.0% | | | | | 18 | 58.1% |
| centripetal | | | | | | | | | | | | | | | 1 | 3.2% |
| indetermined | | | 1 | 1.8% | | | | | | | | | | | 1 | 3.2% |
| total | 3 | 100.0% | 55 | 100.0% | 5 | 100.0% | 1 | 100.0% | 1 | 100.0% | 2 | 100.0% | 2 | 100.0% | 31 | 100.0% |

Tab.40: Dorsale scar pattern visible on upper surface of cleaning flakes.

| layers | 6a | | 6b | | 6c2 | | 7a | | 7c | | 6A1-2 | | 6B | | dh | |
|-------------|----|--------|----|--------|-----|--------|----|--------|----|--------|-------|--------|----|--------|----|--------|
| | n° | % | n° | % | n° | % | n° | % | n° | % | n° | % | n° | % | n° | % |
| crushed | | | 5 | 9.1% | | | | | | | | | | | | |
| broken | | | 24 | 43.6% | 2 | 40.0% | | | 1 | 100.0% | | | 2 | 100.0% | | |
| cortical | | | | | | | | | | | | | | | 3 | 9.7% |
| plain | | | 11 | 20.0% | 1 | 20.0% | | | | | 1 | 50.0% | | | 12 | 38.7% |
| punctiforme | 3 | 100.0% | 6 | 10.9% | | | | | | | | | | | 2 | 6.5% |
| dihedral | | | | | 1 | 20.0% | | | | | | | | | 3 | 9.7% |
| faceted | | | 9 | 16.4% | 1 | 20.0% | 1 | 100.0% | | | 1 | 50.0% | | | 11 | 35.5% |
| total | 1 | 100.0% | 55 | 100.0% | 5 | 100.0% | 1 | 100.0% | 1 | 100.0% | 2 | 100.0% | 2 | 100.0% | 31 | 100.0% |

Tab. 41: Platforms aspect elements with cortical back

| Layer | | 6a | 6b | 7c | ah |
|-----------------------|--------|-----|------|------|------|
| n of intact specimens | | 1 | 32 | 3 | 26 |
| Length (cm) | mean | 2.5 | 4.9 | 4.5 | 7.1 |
| | median | | 4.4 | 4.3 | 7.1 |
| | sd | | 1.5 | 0.9 | 1.8 |
| | max | | 9.3 | 3.7 | 11.8 |
| | min | | 3.1 | 5.4 | 4.1 |
| Width (cm) | mean | 3.7 | 3.1 | 3.3 | 3.2 |
| | median | | 2.9 | 3.0 | 3.2 |
| | sd | | 1.0 | 1.1 | 0.7 |
| | max | | 5.7 | 2.3 | 5.0 |
| | min | | 1.2 | 4.5 | 2.4 |
| Thickness | mean | 0.5 | 0.8 | 0.7 | 0.9 |
| | median | | 0.8 | 0.6 | 0.9 |
| | sd | | 0.3 | 0.3 | 0.3 |
| | max | | 1.4 | 0.4 | 2.0 |
| | min | | 0.3 | 1.0 | 0.5 |
| Surface area (c | mean | 9.3 | 15.4 | 15.2 | 22.8 |
| | median | | 13.3 | 12.9 | 22.0 |
| | sd | | 9.4 | 8.2 | 7.3 |
| | max | | 53.0 | 8.5 | 38.9 |
| | min | | 0.8 | 24.3 | 11.1 |
| Volume (cm3) | mean | 4.6 | 13.3 | 11.8 | 22.7 |
| | median | | 10.9 | 7.7 | 19.5 |
| | sd | | 11.1 | 11.0 | 13.8 |
| | max | | 58.3 | 3.4 | 65.9 |
| | min | | 1.3 | 24.3 | 8.4 |
| Length/Width | mean | 0.7 | 1.6 | 1.4 | 2.3 |
| Width/Thickne | mean | 7.4 | 4.1 | 5.1 | 3.7 |
| Length/Thickn | mean | 5.0 | 6.4 | 7.3 | 8.1 |
| Talon W/T | mean | 2.8 | 3.4 | 5.2 | 3.6 |
| | median | | 2.8 | 5.2 | 2.6 |
| | sd | | 1.7 | 0.4 | 4.3 |
| | max | | 8.0 | 4.9 | 21.0 |
| | min | | 1.2 | 5.5 | 1.5 |

Tab. 42: Metrical data of intact hinges.

| layers | 6a | | 6b | | 7c | | ah | |
|----------------|----|---|----|--------|----|---|----|--------|
| | n° | % | n° | % | n° | % | n° | % |
| unidirectional | 1 | | 30 | 78.9% | 3 | | 18 | 66.7% |
| bidirectional | | | 8 | 21.1% | 1 | | 9 | 33.3% |
| centripetal | | | | | | | 1 | 3.7% |
| indetermined | | | | | | | 1 | 3.7% |
| total | 1 | | 38 | 100.0% | 4 | | 27 | 100.0% |

Tab.43 : Dorsale scar pattern visible on hinged flakes

| layers | 6a | | 6b | | 7c | | ah | |
|-------------|----|---|----|--------|----|---|----|--------|
| | n° | % | n° | % | n° | % | n° | % |
| crushed | | | 6 | 15.8% | | | 3 | |
| broken | | | 5 | 13.2% | | | 2 | |
| cortical | | | | | | | 1 | 3.6% |
| plain | | | 8 | 21.1% | 1 | | 3 | 10.7% |
| punctiforme | | | 7 | 18.4% | 1 | | 3 | 10.7% |
| dihedral | | | 1 | 2.6% | 1 | | 2 | |
| faceted | 1 | | 10 | 26.3% | 1 | | 14 | 50.0% |
| lipped | | | 1 | 2.6% | | | | |
| total | 1 | | 38 | 100.0% | 4 | | 28 | 100.0% |

Tab.44: Frequency of platform types in hinged flake.

Tab. 43, 44

| Layer | | 6a | 6b | 6c2 | ah |
|---------------------------|--------|-----|-------|------|------|
| n of intact cores | | 1 | 22 | 2 | 13 |
| Length (mm) | mean | 4.4 | 6.1 | 3.4 | 6.4 |
| | median | | 5.7 | 3.4 | 5.8 |
| | sd | | 2.3 | 0.7 | 1.5 |
| | max | | 14.0 | 3.9 | 9.7 |
| | min | | 3.6 | 2.9 | 4.3 |
| Width (mm) | mean | 2.2 | 3.6 | 2.8 | 2.6 |
| | median | | 3.4 | 2.8 | 2.0 |
| | sd | | 1.2 | 0.4 | 1.5 |
| | max | | 6.6 | 3.1 | 6.6 |
| | min | | 2.4 | 2.5 | 1.3 |
| Thickness | mean | 0.6 | 1.1 | 0.5 | 0.9 |
| | median | | 1.0 | 0.5 | 0.8 |
| | sd | | 0.4 | 0.1 | 0.2 |
| | max | | 2.4 | 0.6 | 1.3 |
| | min | | 0.6 | 0.4 | 0.6 |
| Surface area (n | mean | 9.7 | 23.7 | 9.7 | 17.9 |
| | median | | 17.0 | 9.7 | 12.8 |
| | sd | | 18.3 | 3.4 | 15.1 |
| | max | | 92.4 | 12.1 | 64.0 |
| | min | | 8.9 | 7.3 | 5.6 |
| Volume (mm ³) | mean | 5.8 | 30.6 | 4.6 | 15.2 |
| | median | | 19.5 | 4.6 | 9.0 |
| | sd | | 45.5 | 0.3 | 12.6 |
| | max | | 221.8 | 4.8 | 51.2 |
| | min | | 5.3 | 4.4 | 5.0 |
| Length/Width | mean | 2.0 | 1.8 | 1.2 | 2.8 |
| Width/Thickne | mean | 3.7 | 3.6 | 6.0 | 3.1 |
| Length/Thickn | mean | 7.3 | 6.0 | 7.3 | 7.8 |
| Talon W/T | mean | | 2.9 | 4.2 | 3.0 |
| | median | | 3.1 | 4.2 | 2.7 |
| | sd | | 0.9 | 1.7 | 1.3 |
| | max | | 4.3 | 5.4 | 6.3 |
| | min | | 1.5 | 3.0 | 1.8 |

Tab. 45: Metrical data of intact plungings.

Tab. 45

| layers | 6a | | 6b | | 6c2 | | ah | |
|----------------|----|---|----|--------|-----|---|----|--------|
| | n° | % | n° | % | n° | % | n° | % |
| unidirectional | 2 | | 31 | 72.1% | 2 | | 10 | 76.9% |
| bidirectional | | | 10 | 23.3% | | | 3 | 23.1% |
| indetermined | | | 2 | 4.7% | | | | |
| total | 2 | | 43 | 100.0% | 2 | | 13 | 100.0% |

Tab. 46: Dorsale scar pattern visible on plungings.

| layers | 6a | | 6b | | 6c2 | | ah | |
|-------------|----|---|----|--------|-----|---|----|--------|
| | n° | % | n° | % | n° | % | n° | % |
| crushed | | | 3 | 6.8% | | | | |
| broken | 1 | | 22 | 50.0% | | | | |
| cortical | | | 6 | 13.6% | | | 1 | 7.7% |
| plain | | | 2 | 4.5% | 2 | | 5 | 38.5% |
| punctiforme | 1 | | 3 | 6.8% | | | 2 | 15.4% |
| dihedral | | | | | | | 1 | 7.7% |
| faceted | | | 5 | 11.4% | | | 4 | 30.8% |
| lipped | | | 3 | 6.8% | | | | |
| total | 2 | | 44 | 100.0% | 2 | | 13 | 100.0% |

Tab. 47: Frequency of platform types in plungings.

| Layer | | 6a | 6b | 6c2 | 7a | 7c | 6A1-2 | 6B | dh |
|--------------------|-----------|------|-------|------|------|------|-------|------|-------|
| n of intact blanks | | 3 | 205 | 30 | 3 | 16 | 8 | 5 | 466 |
| Length (cm) | mean | 5.4 | 7.6 | 7.3 | 7.4 | 6.4 | 8.4 | 7.5 | 7.8 |
| | median | 5.9 | 7.2 | 6.9 | 7.0 | 6.3 | 8.8 | 7.4 | 7.7 |
| | sd | 0.9 | 1.9 | 2.0 | 1.0 | 1.8 | 2.0 | 1.6 | 2.0 |
| | max | 6.0 | 16.0 | 11.2 | 8.6 | 10.4 | 10.3 | 9.9 | 14.4 |
| | min | 4.4 | 4.0 | 4.3 | 6.7 | 4.2 | 5.0 | 6.1 | 3.4 |
| Width (cm) | mean | 2.1 | 2.9 | 2.6 | 3.1 | 2.6 | 3.2 | 2.4 | 2.7 |
| | median | 2.2 | 2.9 | 2.3 | 3.0 | 2.6 | 3.3 | 2.7 | 2.7 |
| | sd | 0.2 | 0.7 | 0.8 | 0.5 | 0.7 | 1.1 | 0.6 | 0.7 |
| | max | 2.2 | 6.5 | 4.6 | 3.7 | 4.1 | 4.6 | 2.8 | 5.5 |
| | min | 1.8 | 1.3 | 1.6 | 2.7 | 1.6 | 1.7 | 1.4 | 0.8 |
| Thickness | mean | 0.7 | 1.1 | 0.7 | 1.0 | 0.8 | 0.7 | 0.9 | 0.8 |
| | median | 0.7 | 1.0 | 0.6 | 0.9 | 0.7 | 0.8 | 0.9 | 0.8 |
| | sd | 0.2 | 0.4 | 0.2 | 0.2 | 0.3 | 0.4 | 0.2 | 0.3 |
| | max | 0.9 | 2.6 | 1.3 | 1.3 | 1.6 | 1.5 | 1.1 | 2.4 |
| | min | 0.6 | 0.4 | 0.3 | 0.9 | 0.4 | 0.3 | 0.6 | 0.3 |
| Surface area (cm2) | mean | 11.2 | 22.9 | 20.2 | 23.6 | 17.6 | 28.5 | 18.2 | 21.8 |
| | median | 10.6 | 21.1 | 16.9 | 21.0 | 17.4 | 25.1 | 20.7 | 20.8 |
| | sd | 1.8 | 10.5 | 12.1 | 7.2 | 8.6 | 14.5 | 7.4 | 10.3 |
| | max | 13.2 | 91.0 | 48.3 | 31.8 | 37.3 | 46.5 | 26.7 | 70.9 |
| | min | 9.7 | 6.6 | 8.2 | 18.1 | 6.7 | 10.5 | 8.5 | 4.1 |
| Volume (cm3) | mean | 8.4 | 25.9 | 15.3 | 24.1 | 14.3 | 24.2 | 17.0 | 20.0 |
| | median | 7.4 | 21.6 | 10.1 | 27.3 | 12.0 | 12.5 | 22.8 | 15.8 |
| | sd | 3.1 | 21.2 | 13.8 | 6.8 | 10.5 | 20.7 | 9.3 | 16.7 |
| | max | 11.9 | 209.3 | 55.8 | 28.6 | 41.0 | 61.2 | 24.3 | 170.1 |
| | min | 5.8 | 2.6 | 3.3 | 16.3 | 2.7 | 3.2 | 6.0 | 1.8 |
| Length/Width | mean | 2.7 | 2.7 | 2.9 | 2.4 | 2.4 | 2.8 | 3.3 | 3.0 |
| Width/Thickness | mean | 2.9 | 3.0 | 4.1 | 3.1 | 3.8 | 5.0 | 2.7 | 3.5 |
| Length/Thickness | mean | 7.5 | 7.7 | 11.6 | 7.5 | 9.2 | 12.7 | 8.8 | 10.1 |
| Talon (cm) mean | width | 1.5 | 1.7 | 1.5 | 1.9 | 2.0 | 1.5 | 1.8 | 1.6 |
| | thickness | 0.5 | 0.7 | 0.5 | 0.6 | 0.6 | 0.4 | 0.6 | 0.6 |
| Talon W/T | mean | 2.7 | 2.6 | 3.3 | 4.2 | 4.0 | 3.6 | 3.4 | 3.1 |
| | median | 2.7 | 2.3 | 2.9 | 4.2 | 3.5 | 2.7 | 3.2 | 2.8 |
| | sd | 0.9 | 1.2 | 1.2 | 3.0 | 2.3 | 2.1 | 2.0 | 1.8 |
| | max | 5.3 | 12.0 | 6.0 | 6.3 | 9.0 | 6.8 | 6.8 | 25.6 |
| | min | 1.6 | 0.8 | 1.3 | 2.1 | 1.2 | 1.6 | 1.8 | 0.6 |

Tab. 48: Metrical data of intact, unretouched blank blades

Tab. 48

| layers | CV length | CV width | CV thickness | CV butt ratioW/T |
|--------|-----------|----------|--------------|------------------|
| 6b | 0.3 | 0.2 | 0.4 | 0.5 |
| 6c2 | 0.3 | 0.3 | 0.3 | 0.4 |
| 7c | 0.3 | 0.3 | 0.4 | 0.6 |
| ah | 0.3 | 0.3 | 0.4 | 0.6 |

Tab. 49: The coefficient of variation (CV*) of mean length, width and thickness of intact and unretouched blank blades from layers 6b and ah.

*CV is calculated by dividing the standard deviation by the mean

| layers | 6b | | 6c2 | | ah | | |
|--------------------|--------|---------|-------|---------|-------|---------|-------|
| butt | plain | faceted | plain | faceted | plain | faceted | |
| n of intact blanks | 55 | 70 | 10 | 15 | 125 | 219 | |
| angle | mean | 97.5 | 93.1 | 104.2 | 98.3 | 97.5 | 93.3 |
| | median | 95.0 | 90.0 | 105.0 | 97.5 | 95.0 | 90.0 |
| | sd | 6.4 | 4.3 | 3.8 | 5.6 | 5.5 | 4.6 |
| | max | 110.0 | 105.0 | 110.0 | 105.0 | 115.0 | 105.0 |
| | min | 90.0 | 90.0 | 100.0 | 90.0 | 90.0 | 90.0 |

Tab. 51 :The flaking angles in layers 6b, 6c2 and ah.

| layers | 6a | | 6b | | 6c2 | | 7a | | 7c | | 6A1-2 | | 6B | | dh | |
|-------------|----|--------|------|--------|-----|--------|----|---|----|--------|-------|--------|----|--------|-----|--------|
| | n° | % | n° | % | n° | % | n° | % | n° | % | n° | % | n° | % | n° | % |
| crushed | 8 | 14.3% | 78 | 5.5% | 1 | 2.4% | | | | | | | 1 | 10.0% | 35 | 7.5% |
| broken | 26 | 46.4% | 670 | 47.5% | 15 | 35.7% | 2 | | 22 | 55.0% | 3 | 18.8% | 3 | 30.0% | | |
| cortical | 2 | 3.6% | 21 | 1.5% | 1 | 2.4% | | | | | | | 1 | 10.0% | 31 | 6.7% |
| plain | 6 | 10.7% | 290 | 20.6% | 7 | 16.7% | 1 | | 4 | 10.0% | 4 | 25.0% | 2 | 20.0% | 147 | 31.5% |
| punctiforme | 4 | 7.1% | 22 | 1.6% | 2 | 4.8% | | | 1 | 2.5% | | | | | 22 | 4.7% |
| dihedral | 1 | 1.8% | 34 | 2.4% | 2 | 4.8% | | | 2 | 5.0% | 3 | 18.8% | | | 29 | 6.2% |
| faceted | 9 | 16.1% | 290 | 20.6% | 14 | 33.3% | 3 | | 11 | 27.5% | 6 | 37.5% | 3 | 30.0% | 191 | 41.0% |
| lipped | | | 6 | 0.4% | | | | | | | | | | | 11 | 2.4% |
| total | 56 | 100.0% | 1411 | 100.0% | 42 | 100.0% | 6 | | 40 | 100.0% | 16 | 100.0% | 10 | 100.0% | 466 | 100.0% |

Tab. 50: Frequency of platform types in unretouched blank-blades.

| layers | | 6b | | 6c2 | | ah | |
|---------------------------------|--------|---------|------------|---------|-----------|---------|------------|
| | | with cx | without cx | with cx | withou cx | with cx | without cx |
| n of intact blanks | | 32 | 172 | 10 | 20 | 134 | 332 |
| Length (cm) | mean | 7.9 | 7.6 | 7.5 | 7.2 | 8.4 | 7.5 |
| | median | 7.5 | 7.2 | 7.0 | 6.9 | 8.1 | 7.5 |
| | sd | 2.0 | 1.9 | 2.3 | 1.9 | 1.9 | 2.1 |
| | max | 5.2 | 4.0 | 11.0 | 11.2 | 14.4 | 13.9 |
| | min | 13.2 | 16.0 | 4.3 | 4.4 | 4.8 | 3.4 |
| Width (cm) | mean | 3.0 | 2.9 | 3.0 | 2.4 | 2.9 | 2.6 |
| | median | 3.0 | 2.9 | 3.0 | 2.2 | 2.9 | 2.6 |
| | sd | 0.8 | 0.7 | 1.1 | 0.7 | 0.8 | 0.7 |
| | max | 1.4 | 1.3 | 4.6 | 4.1 | 5.6 | 5.0 |
| | min | 5.3 | 6.5 | 1.7 | 1.6 | 1.4 | 0.8 |
| Thickness | mean | 1.1 | 1.0 | 0.8 | 0.6 | 1.0 | 0.8 |
| | median | 1.1 | 1.0 | 0.8 | 0.6 | 0.9 | 0.7 |
| | sd | 0.3 | 0.4 | 0.3 | 0.2 | 0.4 | 0.3 |
| | max | 0.5 | 0.4 | 1.3 | 1.2 | 3.3 | 2.4 |
| | min | 2.0 | 2.6 | 0.4 | 0.3 | 0.3 | 0.3 |
| Surface area (cm ²) | mean | 24.7 | 22.5 | 24.0 | 18.3 | 25.1 | 20.5 |
| | median | 22.8 | 20.8 | 20.1 | 15.9 | 22.6 | 19.5 |
| | sd | 12.2 | 10.2 | 14.7 | 10.4 | 10.7 | 9.9 |
| | max | 8.8 | 6.6 | 48.3 | 44.8 | 70.9 | 62.7 |
| | min | 63.6 | 91.0 | 8.2 | 9.0 | 7.3 | 4.1 |
| Volume (cm ³) | mean | 30.3 | 25.1 | 20.9 | 12.4 | 27.2 | 17.4 |
| | median | 26.2 | 21.2 | 13.3 | 9.5 | 18.8 | 14.4 |
| | sd | 23.0 | 20.8 | 17.9 | 10.6 | 24.9 | 12.9 |
| | max | 5.5 | 2.6 | 55.8 | 40.3 | 170.1 | 78.3 |
| | min | 108.1 | 209.3 | 3.3 | 3.6 | 3.8 | 1.8 |
| Length/Width | mean | 2.7 | 2.7 | 2.7 | 3.0 | 3.0 | 3.0 |
| Width/Thickness | mean | 2.8 | 3.0 | 3.9 | 4.1 | 3.3 | 3.5 |
| Length/Thickness | mean | 7.3 | 7.8 | 10.0 | 12.4 | 9.6 | 10.3 |
| Talon W/T | mean | 2.4 | 2.7 | 3.2 | 3.3 | 2.9 | 3.2 |
| | median | 2.3 | 2.4 | 2.7 | 3.3 | 2.6 | 2.8 |
| | sd | 0.8 | 1.3 | 1.4 | 1.2 | 1.1 | 2.0 |
| | max | 1.5 | 0.8 | 5.4 | 6.0 | 7.5 | 25.6 |
| | min | 4.5 | 12.0 | 1.3 | 1.3 | 0.6 | 0.7 |

Tab. 52: Metrical data of intact, unretouched blank blades.

Tab. 52

| broadest part | proximal | | medial | | distal | | proximal-medial | | distal-medial | | whole | | total |
|---------------|----------|-------|--------|-------|--------|-------|-----------------|------|---------------|------|-------|------|-------|
| | n° | % | n° | % | n° | % | n° | % | n° | % | n° | % | |
| 6a | 8 | 29.6% | 14 | 51.9% | | | 2 | 7.4% | 1 | 3.7% | 2 | 7.4% | 27 |
| 6b | 79 | 23.7% | 175 | 52.6% | 27 | 8.1% | 27 | 8.1% | 14 | 4.2% | 11 | 3.3% | 333 |
| 6c2 | 5 | 15.6% | 16 | 50.0% | 9 | 28.1% | 2 | 6.3% | | | | | 32 |
| 7a | | | 2 | | | | | | | | | | 2 |
| 7c | 10 | 62.5% | 6 | 37.5% | | | | | | | | | 16 |
| 6A1-2 | 1 | 14.3% | 5 | 71.4% | 1 | 14.3% | | | | | | | 8 |
| 6B | 2 | 40.0% | 3 | 60.0% | | | | | | | | | 6 |
| ah | 120 | 31.7% | 164 | 43.4% | 44 | 11.6% | 19 | 5.0% | 20 | 5.3% | 11 | 2.9% | 378 |

Tab. 53: The broadest part of blade blanks in all layers.

Tab. 53

| layers | 6a | | 6b | | 6c2 | | 7a | | 7c | | 6A1-2 | | 6B | | ah | |
|------------|----|--------|-----|--------|-----|--------|----|---|----|--------|-------|--------|----|---|-----|--------|
| | n° | % | n° | % | n° | % | n° | % | n° | % | n° | % | n° | % | n° | % |
| converging | 15 | 40.5% | 107 | 52.2% | 20 | 60.6% | 1 | | 14 | 73.7% | 5 | 71.4% | 4 | | 264 | 59.3% |
| expanding | | | 19 | 9.3% | 6 | 18.2% | | | | 0.0% | 1 | 14.3% | | | 45 | 10.1% |
| parallel | 22 | 59.5% | 79 | 38.5% | 7 | 21.2% | 1 | | 5 | 26.3% | 1 | 14.3% | 1 | | 136 | 30.6% |
| total | 37 | 100.0% | 205 | 100.0% | 33 | 100.0% | 2 | | 19 | 100.0% | 7 | 100.0% | 5 | | 445 | 100.0% |

Tab. 54: Shape of lateral edges of blade blanks.

| layers | 6a | | 6b | | 6c2 | | 7a | | 7c | | 6A1-2 | | 6B | | ah | |
|---------------------------|----|--------|-----|--------|-----|--------|----|---|----|--------|-------|--------|----|---|-----|--------|
| | n° | % | n° | % | n° | % | n° | % | n° | % | n° | % | n° | % | n° | % |
| unidirectional parallel | 2 | 66.7% | 148 | 72.2% | 19 | 61.3% | 2 | | 14 | 87.5% | 3 | 37.5% | 4 | | 239 | 51.3% |
| unidirectional convergent | | | 6 | 2.9% | 1 | 3.2% | | | | | | | | | 13 | 2.8% |
| bidirectional | 1 | 33.3% | 45 | 22.0% | 11 | 35.5% | 1 | | 2 | 12.5% | 5 | 62.5% | 1 | | 209 | 44.8% |
| crossed | | | 1 | 0.5% | | | | | | | | | | | 4 | 0.9% |
| undetermined | | | 5 | 2.4% | | | | | | | | | | | 1 | 0.2% |
| total | 3 | 100.0% | 205 | 100.0% | 31 | 100.0% | 3 | | 16 | 100.0% | 8 | 100.0% | 5 | | 466 | 100.0% |

Tab. 55: Dorsale scar pattern visible on intact unretouched blank-blades.

| layers | 6a | | 6b | | 6c2 | | 7a | | 7c | | 6A1-2 | | 6B | | dh | |
|-----------------------------|----|--------|-----|--------|-----|--------|----|---|----|--------|-------|---|----|---|-----|--------|
| | n° | % | n° | % | n° | % | n° | % | n° | % | n° | % | n° | % | n° | % |
| two previous scars | 15 | 38.5% | 30 | 14.6% | 2 | 6.1% | | | 2 | 12.5% | 1 | | | | 61 | 13.9% |
| three previous scars | 17 | 43.6% | 95 | 46.3% | 20 | 60.6% | 2 | | 11 | 68.8% | 1 | | 2 | | 159 | 36.1% |
| four or five previous scars | 7 | 17.9% | 80 | 39.0% | 11 | 33.3% | | | 3 | 18.8% | 5 | | 3 | | 220 | 50.0% |
| total | 39 | 100.0% | 205 | 100.0% | 33 | 100.0% | 2 | | 16 | 100.0% | 7 | | 5 | | 440 | 100.0% |

Tab. 56: Numbers of scars visible on the dorsal face of blade blanks

| layers | serie of small removals | | one or two short hinge | | triangular removal | | total preparation | | longitudinal removal | | total | |
|--------|-------------------------|---|------------------------|---|--------------------|---|-------------------|-------|----------------------|-------|-------|---|
| | n° | % | n° | % | n° | % | n° | % | n° | % | n° | % |
| 6a | 17 | | | | | | 17 | 47.2% | 9 | 25.0% | | |
| 6b | 297 | | 23 | | 88 | | 408 | 70.7% | 102 | 17.7% | | |
| 6c2 | 10 | | 1 | | 7 | | 18 | 42.9% | 16 | 38.1% | | |
| 7a | 2 | | | | | | 2 | 66.7% | 2 | 66.7% | | |
| 7c | 7 | | 1 | | 3 | | 11 | 55.0% | 11 | 55.0% | | |
| 6A1-2 | 3 | | | | | | 3 | 37.5% | 6 | 75.0% | | |
| 6B | 3 | | | | | | 3 | 60.0% | 4 | 80.0% | | |
| dh | 239 | | 6 | | 73 | | 318 | 68.1% | 231 | 49.5% | | |

Tab. 57: Frequency of the preparations of the proximal end of unretouched blank blades.

| point of percussion | axial | | lateral | | punctiform | |
|---------------------|-------|---|---------|---|------------|---|
| | n° | % | n° | % | n° | % |
| 6a | 12 | | 3 | | 4 | |
| 6b | 213 | | 79 | | 144 | |
| 6c2 | | | 27 | | 23 | |
| 7a | | | | | | |
| 7c | 7 | | 8 | | 8 | |
| 6A1-2 | 6 | | 1 | | 2 | |
| 6B | 1 | | 2 | | 1 | |
| dh | 233 | | 63 | | 164 | |

Tab. 58: Location of point of percussion in blank blades.

| layers | | 6b | | |
|---------------------------------|--------|-----------|--------------|-----------|
| | | Prismatic | undetermined | Levallois |
| n of intact blanks | | 116 | 59 | 30 |
| Length (cm) | mean | 8.1 | 7.0 | 7.0 |
| | median | 7.7 | 6.9 | 6.8 |
| | sd | 2.2 | 1.3 | 1.2 |
| | max | 16.0 | 11.4 | 9.4 |
| | min | 4.0 | 5.2 | 4.3 |
| Width (cm) | mean | 2.9 | 2.8 | 3.0 |
| | median | 2.9 | 2.9 | 3.0 |
| | sd | 0.8 | 0.4 | 0.6 |
| | max | 6.5 | 3.9 | 4.1 |
| | min | 1.3 | 1.9 | 1.7 |
| Thickness | mean | 1.1 | 0.9 | 0.7 |
| | median | 1.1 | 0.9 | 0.7 |
| | sd | 0.4 | 0.1 | 0.2 |
| | max | 2.6 | 1.1 | 1.1 |
| | min | 0.6 | 0.5 | 0.4 |
| Surface area (cm ²) | mean | 24.7 | 20.0 | 17.4 |
| | median | 23.2 | 20.4 | 15.6 |
| | sd | 12.5 | 5.9 | 5.0 |
| | max | 91.0 | 35.3 | 34.0 |
| | min | 6.6 | 10.1 | 15.5 |
| Volume (cm ³) | mean | 32.5 | 17.6 | 16.1 |
| | median | 27.7 | 17.6 | 13.4 |
| | sd | 25.5 | 6.7 | 8.6 |
| | max | 209.3 | 31.8 | 42.4 |
| | min | 4.3 | 6.3 | 2.8 |
| Length/Width | mean | 2.9 | 2.5 | 2.5 |
| Width/Thickness | mean | 2.5 | 3.3 | 4.7 |
| Length/Thickness | mean | 6.9 | 8.2 | 12.3 |
| Talon W/T | mean | 2.4 | 2.2 | 4.1 |
| | median | 2.3 | 2.2 | 3.8 |
| | sd | 0.8 | 0.6 | 2.0 |
| | max | 4.7 | 4.5 | 12.0 |
| | min | 1.3 | 0.8 | 2.0 |

Tab. 59: Metrical data of intact, unretouched Prismatic, undetermined and Levallois blank blades in layer 6b.

Tab. 59

| layers | | 6c2 | | |
|--------------------|--------|-----------|--------------|-----------|
| | | Prismatic | undetermined | Levallois |
| n of intact blanks | | 21 | 3 | 6 |
| Length (cm) | mean | 7.8 | 6.1 | 5.9 |
| | median | 7.8 | 4.4 | 5.8 |
| | sd | 1.9 | 3.1 | 0.7 |
| | max | 11.2 | 9.7 | 6.7 |
| | min | 5.1 | 4.3 | 5.0 |
| Width (cm) | mean | 2.7 | 2.3 | 2.4 |
| | median | 2.3 | 2.2 | 2.2 |
| | sd | 0.9 | 0.5 | 0.6 |
| | max | 4.6 | 2.8 | 3.2 |
| | min | 1.6 | 1.9 | 1.9 |
| Thickness | mean | 0.7 | 0.5 | 0.6 |
| | median | 0.7 | 0.4 | 0.6 |
| | sd | 0.2 | 0.2 | 0.2 |
| | max | 1.3 | 0.7 | 0.8 |
| | min | 0.4 | 0.4 | 0.3 |
| Surface area (c | mean | 22.3 | 15.0 | 14.1 |
| | median | 18.6 | 9.7 | 12.7 |
| | sd | 13.0 | 10.6 | 4.2 |
| | max | 48.3 | 27.2 | 20.8 |
| | min | 9.0 | 8.2 | 10.5 |
| Volume (cm3) | mean | 17.6 | 8.7 | 8.8 |
| | median | 11.3 | 3.9 | 8.8 |
| | sd | 15.1 | 8.9 | 5.0 |
| | max | 55.8 | 19.0 | 16.6 |
| | min | 3.6 | 3.3 | 3.8 |
| Length/Width | mean | 3.0 | 2.6 | 2.6 |
| Width/Thickne | mean | 3.9 | 4.8 | 4.3 |
| Length/Thickn | mean | 11.6 | 11.9 | 11.5 |
| Talon W/T | mean | 3.1 | 3.1 | 4.2 |
| | median | 2.8 | 3.1 | 4.2 |
| | sd | 1.3 | 1.3 | 0.5 |
| | max | 6.0 | 4.0 | 4.8 |
| | min | 1.3 | 2.2 | 3.6 |

Tab. 60: Metrical data of intact, unretouched Prismatic, undetermined and Levallois blank blades in layer 6c2.

Tab. 60

| layers | | ah | | |
|---------------------------|--------|-----------|--------------|-----------|
| | | Prismatic | undetermined | Levallois |
| n of intact blanks | | 203 | 181 | 82 |
| Length (cm) | mean | 8.3 | 7.4 | 7.4 |
| | median | 8.1 | 7.4 | 7.4 |
| | sd | 2.2 | 1.9 | 1.9 |
| | max | 14.4 | 12.8 | 10.8 |
| | min | 3.9 | 3.4 | 4.0 |
| Width (cm) | mean | 2.8 | 2.6 | 2.8 |
| | median | 2.7 | 2.6 | 2.8 |
| | sd | 0.8 | 0.7 | 0.7 |
| | max | 5.5 | 4.9 | 4.6 |
| | min | 1.0 | 0.8 | 1.4 |
| Thickness | mean | 1.0 | 0.7 | 0.7 |
| | median | 1.0 | 0.7 | 0.7 |
| | sd | 0.3 | 0.2 | 0.2 |
| | max | 2.4 | 1.0 | 1.3 |
| | min | 0.4 | 0.3 | 0.4 |
| Surface area (c | mean | 23.8 | 19.7 | 21.3 |
| | median | 22.2 | 18.6 | 21.8 |
| | sd | 11.6 | 8.7 | 9.2 |
| | max | 70.9 | 62.7 | 46.0 |
| | min | 5.3 | 4.1 | 5.6 |
| Volume (cm ³) | mean | 26.8 | 14.4 | 15.3 |
| | median | 20.7 | 13.0 | 14.1 |
| | sd | 21.4 | 8.5 | 9.2 |
| | max | 170.1 | 56.4 | 44.7 |
| | min | 3.2 | 1.8 | 3.4 |
| Length/Width | mean | 3.1 | 3.0 | 2.7 |
| Width/Thickne | mean | 2.9 | 3.9 | 4.2 |
| Length/Thickn | mean | 8.7 | 11.1 | 11.3 |
| Talon W/T | mean | 2.8 | 2.8 | 3.9 |
| | median | 2.5 | 2.7 | 3.7 |
| | sd | 1.1 | 1.0 | 1.5 |
| | max | 8.7 | 6.5 | 7.7 |
| | min | 0.6 | 0.7 | 1.4 |

Tab. 61: Metrical data of intact, unretouched Prismatic, undetermined and Levallois blank blades in sand ah.

Tab. 61

| layers | 6b | | | | 6c2 | | | | 7c | | | | ah | | | |
|--------------|-----|-----|-----|---------|-----|-----|-----|---------|-----|-----|-----|---------|-----|-----|-----|---------|
| | CVL | CVW | CVT | CV butt | CVL | CVW | CVT | CV butt | CVL | CVW | CVT | CV butt | CVL | CVW | CVT | CV butt |
| Prismatic | 0.3 | 0.3 | 0.3 | 0.3 | 0.2 | 0.3 | 0.3 | 0.4 | | | | | 0.3 | 0.3 | 0.3 | 0.4 |
| Levallois | 0.2 | 0.2 | 0.2 | 0.5 | | | | | 0.3 | 0.2 | 0.2 | 0.5 | 0.3 | 0.3 | 0.3 | 0.4 |
| Indetermined | 0.2 | 0.1 | 0.2 | 0.3 | | | | | | | | | 0.3 | 0.3 | 0.3 | 0.4 |

Tab. 62: The coefficient of variation (CV) of mean length, width and thickness of intact and unretouched Prismatic, Levallois and indetermined blank blades from layers 6b, 6c2, 7c and ah.

| layers | 6b | | | | | | 6c2 | | | 7c | | | ah | | | | | |
|------------------|-----------|--------|----------|--------|-----------|--------|-----------|--------|----------|----|-----------|-------|-----------|--------|----------|--------|-----------|--------|
| | Prismatic | | Undeterm | | Levallois | | Prismatic | | Undeterm | | Levallois | | Prismatic | | Undeterm | | Levallois | |
| | n° | % | n° | % | n° | % | n° | % | n° | % | n° | % | n° | % | n° | % | n° | % |
| unid. parallel | 77 | 66.4% | 50 | 84.7% | 20 | 66.7% | 19 | 63.3% | 2 | 3 | 5 | 81.8% | 106 | 52.2% | 111 | 61.3% | 23 | 28.0% |
| unid. convergent | 5 | 4.3% | | | 2 | 6.7% | | | | | | | 1 | 0.5% | | 0.0% | 12 | 14.6% |
| bidirectional | 29 | 25.0% | 8 | 13.6% | 7 | 23.3% | 11 | 36.7% | 1 | 2 | | 18.2% | 95 | 46.8% | 69 | 38.1% | 42 | 51.2% |
| crossed | | | | | 1 | 3.3% | | | | | | | | | | | 4 | 4.9% |
| undetermined | 5 | 4.3% | 1 | 1.7% | | | | | | | | | 1 | 0.5% | 1 | 0.6% | 1 | 1.2% |
| total | 116 | 100.0% | 59 | 100.0% | 30 | 100.0% | 30 | 100.0% | 3 | 5 | 5 | 0.0% | 203 | 100.0% | 181 | 100.0% | 82 | 100.0% |

Tab. 63: Dorsale scar pattern visible on intact unretouched blank-blades.

| layers | 6b | | | 6c2 | | | 7c | | | ah | | | | | | | | | | |
|---------------|-----------|----------|-----------|-----------|----------|-----------|-----------|----------|-----------|-----------|----------|-----------|----|--------|-----|--------|-----|--------|----|--------|
| | Prismatic | Undeterm | Levallois | | | | | | | | |
| type of blade | n° | % | n° | % | n° | % | n° | % | n° | % | n° | % | n° | % | | | | | | |
| converging | 59 | 50.9% | 33 | 55.9% | 15 | 50.0% | 18 | 60.0% | 2 | 60.0% | 4 | 80.0% | 4 | 63.6% | 113 | 55.7% | 111 | 66.9% | 48 | 58.5% |
| expanding | 12 | 10.3% | 5 | 8.5% | 2 | 6.7% | 7 | 23.3% | 1 | 23.3% | | | | | 22 | 10.8% | 13 | 7.8% | 10 | 12.2% |
| parallel | 45 | 38.8% | 21 | 35.6% | 13 | 43.3% | 5 | 16.7% | | 16.7% | 1 | 20.0% | 1 | 36.4% | 68 | 33.5% | 42 | 25.3% | 24 | 29.3% |
| total | 116 | 100.0% | 59 | 100.0% | 30 | 100.0% | 30 | 100.0% | 3 | 100.0% | 5 | 100.0% | 5 | 100.0% | 203 | 100.0% | 166 | 100.0% | 82 | 100.0% |

Tab. 64: Shape of lateral edges of blank blades.

| broadest part | proximal | | medial | | distal | | proximal-medial | | distal-medial | | whole | | total | | |
|---------------|--------------|----|--------|-----|--------|----|-----------------|---|---------------|----|-------|----|-------|-----|-----|
| | n° | % | n° | % | n° | % | n° | % | n° | % | n° | % | | | |
| 6b | Prismatic | 28 | 24.1% | 58 | 50.0% | 16 | 13.8% | 4 | 3.4% | 3 | 2.6% | 7 | 6.0% | 116 | |
| | Undetermined | 8 | 14.8% | 33 | 61.1% | 4 | 7.4% | 5 | 9.3% | 1 | 1.9% | 3 | 5.6% | | 54 |
| | Levallois | 10 | 33.3% | 14 | 46.7% | 4 | 13.3% | 1 | 3.3% | 1 | 3.3% | 30 | | | |
| 6c2 | Prismatic | 5 | 16.7% | 14 | 46.7% | 9 | 30.0% | 2 | 6.7% | | | | | 30 | |
| | Undetermined | | | 1 | | 1 | | 1 | | | | | | | 3 |
| | Levallois | 2 | | 2 | | | | 1 | | | | | | | |
| 7c | Prismatic | 4 | | 1 | | | | | | | | | | 5 | |
| | Levallois | 6 | 54.5% | 5 | 45.5% | | | | | | | | | | 11 |
| | | | | | | | | | | | | | | | |
| dh | Prismatic | 47 | 23.2% | 107 | 52.7% | 23 | 11.3% | 8 | 3.9% | 12 | 5.9% | 6 | 3.0% | 203 | |
| | Undetermined | 62 | 37.6% | 71 | 43.0% | 16 | 9.7% | 9 | 5.5% | 4 | 2.4% | 3 | 1.8% | | 165 |
| | Levallois | 37 | 45.1% | 23 | 28.0% | 8 | 9.8% | 8 | 9.8% | 4 | 4.9% | 2 | 2.4% | | |

Tab. 65: The broadest part of blade blanks.

| layers | serie of small removals | one or two short hinge | triangular removal | total preparation | | longitudinal removal | | |
|--------|-------------------------|------------------------|--------------------|-------------------|-----|----------------------|----|-------|
| | | | | n° | % | n° | % | |
| 6b | Prismatic | 75 | 16 | 20 | 111 | 54.1% | 30 | 14.6% |
| | Undetermined | 28 | 15 | 4 | 47 | 74.6% | 16 | 25.4% |
| | Levallois | 8 | 3 | 2 | 13 | 43.3% | 7 | 26.9% |
| 6c2 | Prismatic | 10 | 1 | 7 | 18 | 60.0% | 14 | 46.7% |
| | Undetermined | 1 | | 1 | 2 | 66.7% | | |
| | Levallois | 2 | | 1 | 3 | 60.0% | 4 | 80.0% |
| 7c | Prismatic | 3 | | 2 | 5 | 100.0% | 2 | 40.0% |
| | Levallois | 4 | 1 | 1 | 6 | 54.5% | 8 | 72.7% |
| ah | Prismatic | 107 | 3 | 38 | 148 | 72.9% | 96 | 47.3% |
| | Undetermined | 107 | 3 | 24 | 134 | 74.0% | 89 | 49.2% |
| | Levallois | 25 | 1 | 11 | 37 | 45.1% | 47 | 57.3% |

Tab. 66: Frequency of the preparations of the proximal end of unretouched blank blades by blade category.

Tab. 66

| layers category | 6b | | | 6c2 | | | 7c | | αh | | |
|--------------------|-------------------|----------------------|-------------------|-------------------|----------------------|-------------------|-------------------|-------------------|-------------------|----------------------|-------------------|
| | Prismatic n° % | Undetermined n° % | Levallois n° % | Prismatic n° % | Undetermined n° % | Levallois n° % | Prismatic n° % | Levallois n° % | Prismatic n° % | Undetermined n° % | Levallois n° % |
| crushed | 42 36.2% | 11 18.6% | 4 13.3% | 6 20.0% | 1 | 1 9.1% | 22 10.8% | 21 11.6% | 2 2.4% | 2 2.4% | |
| cortical | 5 4.3% | 5 8.5% | 2 6.7% | 1 3.3% | | | 20 9.9% | 18 9.9% | 5 6.1% | 5 6.1% | |
| plain | 27 23.3% | 26 44.1% | 3 10.0% | 6 20.0% | 1 | 1 18.2% | 55 27.1% | 59 32.6% | 9 11.0% | 9 11.0% | |
| punctiforme | 4 3.4% | 5 8.5% | 2 6.7% | 2 6.7% | 1 | 1 | 12 5.9% | 7 3.9% | 3 3.7% | 3 3.7% | |
| dihedral | 5 4.3% | 1 1.7% | | 2 6.7% | 1 | | 13 6.4% | 17 9.4% | | | |
| faceted | 32 27.6% | 11 18.6% | 19 63.3% | 13 43.3% | 1 | 2 | 76 37.4% | 53 29.3% | 63 76.8% | 63 76.8% | |
| lipped | 1 0.9% | | | | | | 5 2.5% | 6 3.3% | | | |
| total | 116 100.0% | 59 100.0% | 30 100.0% | 30 100.0% | 3 | 5 | 203 100.0% | 181 100.0% | 82 100.0% | 82 100.0% | |

Tab. 67 : Frequency of platforms in unretouched blades by category.

| layers | 6b | | | αh | | |
|------------------|-------------------|----------------------|-------------------|-------------------|----------------------|-------------------|
| | Prismatic n° % | Undetermined n° % | Levallois n° % | Prismatic n° % | Undetermined n° % | Levallois n° % |
| rectiligne | 34 29.3% | 20 33.9% | 4 13.3% | 35 116.7% | 34 1133.3% | 9 180.0% |
| bowed | | | | | | |
| on whole length | 57 49.1% | 28 47.5% | 17 56.7% | 135 450.0% | 126 4200.0% | 54 1080.0% |
| on prox-med part | 10 8.6% | 2 3.4% | 2 6.7% | 28 93.3% | 14 466.7% | 1 20.0% |
| on dis-med part | 14 12.1% | 9 15.3% | 7 23.3% | 5 16.7% | 6 200.0% | 18 360.0% |
| twisted | 1 0.9% | | | | 1 33.3% | |
| total | 116 100.0% | 59 100.0% | 30 100.0% | 203 676.7% | 181 6033.3% | 82 1640.0% |

Tab. 68: Profile of blades in layers 6b and αh.

| Layer | | 6a | 6b | 6c2 | 7a | 7c | 6A1-2 | 6B | ah |
|--------------------|-----------|------|-------|------|------|------|-------|------|-------|
| n of intact blanks | | 47 | 182 | 8 | 4 | 12 | 5 | 4 | 153 |
| Length (cm) | mean | 3.3 | 5.1 | 4.9 | 5.5 | 5.2 | 4.3 | 5.4 | 6.1 |
| | median | 3.0 | 4.9 | 4.0 | 5.8 | 5.2 | 4.4 | 5.0 | 6.0 |
| | sd | 0.8 | 1.6 | 1.8 | 1.7 | 1.1 | 0.5 | 0.6 | 1.5 |
| | max | 7.3 | 11.4 | 8.9 | 7.0 | 6.8 | 4.9 | 6.1 | 11.0 |
| | min | 2.2 | 2.4 | 3.7 | 3.5 | 3.0 | 3.8 | 5.0 | 2.7 |
| Width (cm) | mean | 2.7 | 3.8 | 3.4 | 4.4 | 3.4 | 3.9 | 4.6 | 4.2 |
| | median | 3.0 | 3.6 | 2.8 | 4.3 | 3.4 | 3.2 | 4.2 | 4.0 |
| | sd | 0.5 | 1.3 | 1.5 | 2.2 | 0.8 | 2.7 | 1.4 | 1.2 |
| | max | 3.9 | 9.9 | 6.3 | 6.6 | 5.4 | 8.7 | 6.1 | 8.4 |
| | min | 2.0 | 1.8 | 2.2 | 2.5 | 2.2 | 2.2 | 3.4 | 2.2 |
| Thickness | mean | 0.7 | 0.9 | 0.7 | 0.9 | 0.8 | 0.5 | 0.9 | 0.8 |
| | median | 0.7 | 0.8 | 0.6 | 0.6 | 0.8 | 0.7 | 1.0 | 0.7 |
| | sd | 0.0 | 0.3 | 0.2 | 0.7 | 0.2 | 0.2 | 0.3 | 0.4 |
| | max | 1.0 | 2.3 | 1.0 | 2.0 | 1.2 | 0.7 | 1.1 | 3.3 |
| | min | 0.6 | 0.4 | 0.5 | 0.4 | 0.5 | 0.3 | 0.5 | 0.3 |
| Surface area (cm2) | mean | 8.9 | 20.0 | 17.8 | 26.9 | 17.5 | 17.7 | 25.1 | 26.6 |
| | median | 8.4 | 17.6 | 12.9 | 26.9 | 17.1 | 14.1 | 21.0 | 24.1 |
| | sd | 3.7 | 10.8 | 12.1 | 19.1 | 4.8 | 14.1 | 10.7 | 11.9 |
| | max | 25.6 | 66.7 | 40.1 | 44.9 | 25.2 | 42.6 | 37.2 | 80.0 |
| | min | 5.2 | 5.0 | 8.4 | 9.1 | 9.0 | 8.4 | 17.0 | 9.0 |
| Volume (cm3) | mean | 5.4 | 19.8 | 12.9 | 32.1 | 14.3 | 9.5 | 23.5 | 24.4 |
| | median | 4.2 | 16.1 | 9.0 | 17.1 | 14.2 | 9.9 | 21.0 | 19.2 |
| | sd | 3.8 | 17.0 | 12.1 | 40.2 | 6.3 | 7.1 | 16.4 | 22.7 |
| | max | 25.6 | 119.3 | 40.1 | 89.8 | 25.3 | 21.3 | 40.9 | 155.2 |
| | min | 2.6 | 2.8 | 4.2 | 4.6 | 5.4 | 2.5 | 8.5 | 4.1 |
| Length/Width | mean | 1.2 | 1.4 | 1.5 | 1.4 | 1.6 | 1.4 | 1.2 | 1.5 |
| Width/Thickness | mean | 4.7 | 4.5 | 5.2 | 5.8 | 4.5 | 7.8 | 5.5 | 5.8 |
| Length/Thickness | mean | 5.7 | 6.1 | 7.4 | 8.0 | 6.7 | 8.7 | 6.8 | 8.2 |
| Talon (cm) mean | width | 1.9 | 2.3 | 2.8 | 2.5 | 2.4 | 2.1 | 2.5 | 2.4 |
| | thickness | 0.6 | 0.7 | 0.7 | 0.6 | 0.7 | 0.6 | 0.7 | 0.7 |
| Talon W/T | mean | 3.2 | 3.6 | 4.8 | 4.6 | 4.0 | 3.9 | 4.7 | 3.8 |
| | median | 3.2 | 3.0 | 4.3 | 4.4 | 3.6 | 3.8 | 2.7 | 3.3 |
| | sd | 1.4 | 1.9 | 2.1 | 2.2 | 1.7 | 0.8 | 3.7 | 1.7 |
| | max | 4.6 | 14.3 | 8.3 | 7.3 | 6.6 | 5.0 | 9.0 | 9.0 |
| | min | 1.8 | 0.8 | 3.0 | 2.1 | 2.1 | 3.0 | 2.4 | 0.6 |

Tab. 69: Metrical data of intact, unretouched flakes.

Tab. 69

| layers | CV length | CV width | CV thickness | CV butt ratio W/T |
|--------|-----------|----------|--------------|-------------------|
| 6a | 0.2 | 0.2 | 0.0 | 0.4 |
| 6b | 0.3 | 0.3 | 0.3 | 0.5 |
| 7c | 0.2 | 0.2 | 0.3 | 0.4 |
| ah | 0.2 | 0.3 | 0.5 | 0.4 |

Tab. 70: The coefficient of variation (CV) of mean length, width and thickness of of intact flakes from layers 6a, 6b, 7c and ah.

Tab. 70

| layers | 6a | | 6b | | 6c2 | | 7a | | 7c | | 6A1-2 | | 6B | | ah | |
|-------------|----|--------|-----|--------|-----|--------|----|--------|----|--------|-------|--------|----|--------|-----|--------|
| | n° | % | n° | % | n° | % | n° | % | n° | % | n° | % | n° | % | n° | % |
| crushed | 9 | 14.3% | 15 | 6.1% | | | | | | | | | | | | |
| broken | 13 | 20.6% | 53 | 21.6% | | | | | | | 1 | | 1 | | | |
| cortical | 8 | 12.7% | 21 | 8.6% | | | 2 | | | | | | | | 16 | 10.5% |
| plain | 9 | 14.3% | 38 | 15.5% | | | 2 | | 1 | | 1 | | | | 39 | 25.5% |
| punctiforme | 9 | 14.3% | 25 | 10.2% | 2 | | | | 1 | | | | | | 20 | 13.1% |
| dihedral | 3 | 4.8% | 9 | 3.7% | | | | | 2 | | 2 | | 1 | | 13 | 8.5% |
| faceted | 12 | 19.0% | 84 | 34.3% | 6 | | | 2 | 5 | | 2 | | 3 | | 65 | 42.5% |
| lipped | | 0.0% | | 0.0% | | | | | | | | | | | | |
| total | 63 | 100.0% | 245 | 100.0% | 8 | 100.0% | 4 | 100.0% | 12 | 100.0% | 6 | 100.0% | 5 | 100.0% | 153 | 100.0% |

Tab. 71: Platforms aspect in unretouched blank-blades

| layers | | 6b | | ah | |
|--------------------|--------|-------|---------|-------|---------|
| butt | | plain | faceted | plain | faceted |
| n of intact blanks | | 38 | 30 | 30 | 30 |
| angle | mean | 101.0 | 94.2 | 99.1 | 94.6 |
| | median | 100.0 | 90.0 | 100.0 | 92.0 |
| | sd | 6.4 | 5.5 | 6.6 | 5.3 |
| | max | 115.0 | 110.0 | 115.0 | 105.0 |
| | min | 90.0 | 90.0 | 90.0 | 90.0 |
| Length (cm) | mean | 4.8 | 5.8 | 6.1 | 6.6 |
| Width | mean | 3.6 | 3.4 | 3.7 | 3.8 |
| Thickness | mean | 1.0 | 1.1 | 0.9 | 1.0 |

Tab.72: Flaking angle in layer 6b and ah.

Tab. 72

| layers | 6a | | 6b | | 6c2 | | 7a | | 7c | | 6A1-2 | | 6B | | ah | |
|---------------------------|----|--------|-----|--------|-----|--------|----|--------|----|--------|-------|--------|----|--------|-----|--------|
| | n° | % | n° | % | n° | % | n° | % | n° | % | n° | % | n° | % | n° | % |
| unidirectional parallel | 38 | 80.9% | 136 | 75.6% | 5 | | 2 | | 9 | | 5 | | 3 | | 105 | 68.6% |
| unidirectional convergent | | | 8 | 4.4% | | | 2 | | | | | | | | 7 | 4.6% |
| bidirectional | 5 | 10.6% | 21 | 11.7% | 3 | | | | 3 | | | | | | 35 | 22.9% |
| centrpetal | | | 11 | 6.1% | 1 | | | | | | | | 2 | | 5 | 3.3% |
| undetermined | 4 | 8.5% | 4 | 2.2% | | | | | | | | | | | 1 | 0.7% |
| total | 47 | 100.0% | 180 | 100.0% | 8 | 100.0% | 4 | 100.0% | 12 | 100.0% | 5 | 100.0% | 5 | 100.0% | 153 | 100.0% |

Tab. 73: Dorsale scar pattern visible on intact unretouched blank-blades

| point of percussion | axial | lateral | punctiform |
|---------------------|-------|---------|------------|
| | n° | n° | n° |
| 6a | 11 | 6 | 8 |
| 6b | 84 | 42 | 66 |
| 6c2 | 5 | 1 | 4 |
| 7a | 4 | | 3 |
| 7c | 6 | 6 | 3 |
| 6A1-2 | 2 | 3 | 1 |
| 6B | 3 | 1 | 1 |
| αh | 48 | 23 | 48 |

Tab. 74: Location of point of percussion to dorsal.

Tab. 74

| layers | serie of small removals | one or two short hinge | triangular removal | total preparation | |
|--------|-------------------------|------------------------|--------------------|-------------------|-------|
| | n° | n° | | n° | % |
| 6a | 7 | | 2 | 9 | 14.3% |
| 6b | 80 | 18 | 7 | 105 | 42.5% |
| 6c2 | 3 | | | 3 | 37.5% |
| 7a | | | | | 0.0% |
| 7c | 2 | 2 | 1 | 5 | 41.7% |
| 6A1-2 | 4 | | | 4 | 66.7% |
| 6B | 3 | | | 3 | 60.0% |
| ch | 43 | 1 | 7 | 51 | 33.3% |

Tab. 75: Frequency of the preparations of the proximal end of unretouched blank flakes.

| layers | | 6b | | ah | |
|----------------------|--------|-----------|---------|-----------|---------|
| | | Levallois | non-Lev | Levallois | non-Lev |
| n of blanks (intact) | | 99(93) | 153(95) | 58 | 93 |
| Length (cm) | mean | 5.0 | 5.2 | 5.2 | 6.3 |
| | median | 5.0 | 4.9 | 5.0 | 6.1 |
| | sd | 1.5 | 1.6 | 1.4 | 1.5 |
| | max | 9.4 | 11.4 | 10.0 | 11.0 |
| | min | 2.6 | 2.1 | 2.6 | 3.2 |
| Width (cm) | mean | 3.9 | 3.7 | 4.9 | 4.2 |
| | median | 3.8 | 3.5 | 5.0 | 4.0 |
| | sd | 1.1 | 1.5 | 1.3 | 1.2 |
| | max | 7.2 | 9.9 | 7.9 | 8.4 |
| | min | 1.8 | 1.1 | 2.4 | 2.2 |
| Thickness | mean | 0.8 | 1.0 | 0.7 | 0.9 |
| | median | 0.7 | 1.0 | 0.7 | 0.8 |
| | sd | 0.2 | 0.4 | 0.2 | 0.4 |
| | max | 1.7 | 2.3 | 1.3 | 3.3 |
| | min | 0.4 | 0.4 | 0.3 | 0.3 |
| Surface area (cm2) | mean | 20.1 | 19.8 | 16.7 | 27.3 |
| | median | 18.1 | 16.6 | 11.1 | 23.1 |
| | sd | 9.6 | 12.1 | 12.0 | 13.0 |
| | max | 48.9 | 66.7 | 63.0 | 80.0 |
| | min | 5.0 | 2.3 | 3.0 | 9.0 |
| Volume (cm3) | mean | 16.4 | 23.1 | 21.3 | 27.5 |
| | median | 14.3 | 18.4 | 19.2 | 19.7 |
| | sd | 11.0 | 20.9 | 11.1 | 24.0 |
| | max | 58.7 | 119.3 | 56.7 | 155.2 |
| | min | 2.8 | 0.9 | 4.1 | 4.5 |
| Length/Width | mean | 1.3 | 1.5 | 1.5 | 1.6 |
| Width/Thickness | mean | 5.3 | 3.7 | 3.8 | 5.1 |
| Length/Thickness | mean | 6.9 | 5.3 | 8.1 | 7.8 |
| Talon W/T | mean | 4.5 | 2.4 | 6.3 | 3.0 |
| | median | 4.3 | 2.3 | 5.7 | 2.7 |
| | sd | 2.1 | 0.7 | 6.2 | 1.3 |
| | max | 14.3 | 5.0 | 36.6 | 7.0 |
| | min | 1.9 | 0.8 | 1.3 | 0.6 |

Tab. 76: Metrical data of intact, unretouched blank flakes.

Tab. 76

| type of tool | 6a | % | 6b | % | 6c2 | % | 7a | % | 7c | % | 6A1-2 | % | 6B | % | dh | % |
|--------------|----|--------|-----|--------|-----|------|----|---|----|--------|-------|---|----|--------|-----|--------|
| on blade | 11 | 100.0% | 274 | 78.7% | 21 | 91% | 1 | | 9 | 69.2% | 6 | | 8 | 80.0% | 323 | 88.0% |
| on flake | | | 66 | 19.0% | 2 | 9% | 1 | | 4 | 30.8% | 3 | | 2 | 20.0% | 39 | 10.6% |
| on debris | | | 8 | 2.3% | | | | | | | | | | | 5 | 1.4% |
| total | 11 | 100% | 348 | 100.0% | 23 | 100% | 2 | | 13 | 100.0% | 9 | | 10 | 100.0% | 367 | 100.0% |

Tab. 77: Type of blank for retouched tools.

| type of tool | 6a | % | 6b | % | 6c2 | % | 7a | % | 7c | % | 6A1-2 | % | 6B | % | dh | % |
|--------------------------------|----|--------|-----|--------|-----|------|----|---|----|--------|-------|---|----|--------|-----|--------|
| retouched point on blade | 2 | 18.2% | 89 | 25.6% | 7 | 32% | | | 2 | 15.4% | 3 | | 3 | 30.0% | 104 | 28.3% |
| retouched point on flake | | | 3 | 0.9% | | | | | | | | | | | 7 | 1.9% |
| blade retouched on one bord | 6 | 54.5% | 118 | 33.9% | 11 | 50% | | | 3 | 23.1% | 2 | | 3 | 30.0% | 150 | 40.9% |
| blade retouched on two bords | 2 | 18.2% | 38 | 10.9% | | | | | 2 | 15.4% | | | | | 43 | 11.7% |
| single scraper (on flake) | | | 13 | 3.7% | 1 | 5% | 1 | | 2 | 15.4% | 1 | | 1 | 10.0% | 17 | 4.6% |
| double scraper (on flake) | | | | | | | | | 1 | 7.7% | | | 1 | 10.0% | 1 | 0.3% |
| transversal scraper (on flake) | | | 1 | 0.3% | | | | | | | | | | | | |
| face plane | | | 2 | 0.6% | | | | | | | | | | | 2 | 0.5% |
| notch/denticulate | | | 29 | 8.3% | | | | | 1 | 7.7% | | | 2 | 20.0% | 14 | 3.8% |
| perçoir | | | 4 | 1.1% | 1 | 5% | | | | | | | | | 2 | 0.5% |
| truncation | | | 10 | 2.9% | | | | | | | | | | | 4 | 1.1% |
| end-scraper | | | 14 | 4.0% | | | | | | | | | | | 3 | 0.8% |
| atypical end-scraper | | | 6 | 1.7% | | | | | | | | | | | 1 | 0.3% |
| thinning on proxima end | | | 3 | 0.9% | 1 | | | | | | | | | | 2 | 0.5% |
| tang | | | 4 | 1.1% | | | | | | | | | | | 6 | 1.6% |
| diverse | 1 | 9.1% | 14 | 4.0% | 1 | 5% | 1 | | 2 | 15.4% | | | | | 11 | 3.0% |
| Total | 11 | 100.0% | 348 | 100.0% | 22 | 100% | 2 | | 13 | 100.0% | 9 | | 10 | 100.0% | 367 | 100.0% |

Tab. 79: Types of retouched tools recognised in Hummalian layers.

| Layer | | 6a | 6b | 6c2 | 7a | 7c | 6A1-2 | 6B | ah |
|------------------------------|--------|---------|-------|------|------|------|-------|------|-------|
| n of intact retouched blanks | | 2 | 178 | 21 | 1 | 11 | 10 | 8 | 371 |
| Length (cm) | mean | 7.5 | 6.7 | 8.2 | 8.4 | 8.1 | 6.7 | 7.4 | 8.2 |
| | median | 7.5 | 6.4 | 8.2 | | 8.5 | 7.4 | 7.5 | 8.2 |
| | sd | 0.1 | 2.1 | 2.3 | | | | | 2.3 |
| | max | 8.0 | 14 | 12.8 | | 10.6 | 8.8 | 11.3 | 13.7 |
| | min | 6.9 | 2.8 | 2.9 | | 6.1 | 4.1 | 4.1 | 1.7 |
| Width (cm) | mean | 3.0 | 3.4 | 3.0 | 4.4 | 3.7 | 3.3 | 3.0 | 3.4 |
| | median | 3.0 | 3.2 | 3.0 | | 3.2 | 3.4 | 2.9 | 3.0 |
| | sd | 0.1 | 1.1 | 0.6 | | 1.2 | 0.7 | 0.4 | 1.5 |
| | max | 3.0 | 7.3 | 4.3 | | 6.1 | 4.3 | 3.6 | 10.7 |
| | min | 2.9 | 1.2 | 1.6 | | 2.4 | 2.2 | 2.5 | 0.9 |
| Thickness | mean | 1.3 | 1.2 | 0.8 | 0.6 | 1.0 | 0.9 | 1.1 | 0.9 |
| | median | 1.3 | 1.0 | 0.8 | | 1.0 | 0.8 | 1.0 | 0.9 |
| | sd | 0.0 | 0.5 | 0.2 | | 0.2 | 0.4 | 0.2 | 0.3 |
| | max | 1.3 | 3.0 | 1.3 | | 1.3 | 1.8 | 1.3 | 3.4 |
| | min | 1.3 | 0.2 | 0.5 | | 0.7 | 0.5 | 0.8 | 0.1 |
| Surface area (cm2) | mean | 22.1 | 23.0 | 24.5 | 37.0 | 29.9 | 22.3 | 22.1 | 26.7 |
| | median | 22.1 | 21.0 | 42.2 | | 28.2 | 21.1 | 21.0 | 24.6 |
| | sd | 2.8 | 10.9 | 8.7 | | 9.8 | 8.3 | 6.8 | 10.9 |
| | max | 2.4 | 77.0 | 44.8 | | 47.3 | 37.0 | 33.9 | 71.2 |
| | min | 2.0 | 5.3 | 10.4 | | 16.5 | 10.6 | 10.7 | 3.4 |
| Volume (cm3) | mean | 28.6 | 28.0 | 21.4 | 22.2 | 28.4 | 18.4 | 23.6 | 25.8 |
| | median | 28.6 | 21.3 | 20.2 | | 28.8 | 18.0 | 23.9 | 20.9 |
| | sd | 3.7 | 21.4 | 10.5 | | 9.9 | 8.7 | 9.4 | 18.5 |
| | max | 31.2 | 169.4 | 44.8 | | 46.4 | 37.9 | 40.7 | 154.7 |
| | min | 26.0 | 2.6 | 6.2 | | 17.9 | 10.6 | 9.6 | 2.6 |
| Length/Width | mean | 2.5 | 2.1 | 2.9 | 1.9 | 2.4 | 2.1 | 2.5 | 2.9 |
| Width/Thickness | mean | 2.7 | 3.3 | 3.7 | 7.3 | 4.2 | 4.4 | 2.9 | 3.7 |
| Length/Thickness | mean | 5.7 | 6.6 | 10.0 | 14.0 | 8.8 | 9.1 | 7.1 | 10.2 |
| Talon W/T | mean | punctif | 2.8 | 3.0 | 4.3 | 3.7 | 4.1 | 2.5 | 2.8 |
| | median | | 2.7 | 3.0 | | 2.8 | 3.6 | 2.6 | 2.7 |
| | sd | | 1.1 | 0.9 | | 2.2 | 1.2 | 0.5 | 1.0 |
| | max | | 6.3 | 5.3 | | 7.8 | 6.0 | 3.0 | 9.0 |
| | min | | 0.8 | 2.0 | | 1.8 | 3.0 | 1.8 | 0.1 |

Tab. 78: Metrical data of intact, retouched blank

Tab. 78

| Layer | | 6b | 6c2 | 7c | ah |
|--------------------|----------|-------|------|------|------|
| n of intact blanks | | 106 | 20 | 7 | 324 |
| Length (cm) | mean | 7.7 | 8.6 | 8.8 | 8.8 |
| | median | 7.8 | 8.7 | 9.0 | 8.4 |
| | sd | 1.8 | 2.0 | 1.3 | 1.8 |
| | max | 14.0 | 12.8 | 10.6 | 14.4 |
| | min | 4.3 | 6.1 | 6.6 | 1.7 |
| Width (cm) | mean | 3.0 | 2.9 | 3.1 | 3.0 |
| | median | 2.9 | 2.9 | 3.1 | 2.9 |
| | sd | 0.7 | 0.5 | 0.7 | 0.7 |
| | max | 5.5 | 3.8 | 4.3 | 5.8 |
| | min | 1.2 | 1.6 | 2.4 | 0.9 |
| Thickness | mean | 1.1 | 0.9 | 1.1 | 0.9 |
| | median | 1.0 | 0.8 | 1.1 | 0.9 |
| | sd | 0.4 | 0.2 | 0.2 | 0.3 |
| | max | 2.6 | 1.3 | 1.3 | 2.2 |
| | min | 0.2 | 0.5 | 0.8 | 0.1 |
| Surface area (cm2) | mean | 23.7 | 25.3 | 27.4 | 26.6 |
| | median | 21.8 | 25.4 | 28.2 | 24.2 |
| | sd | 10.3 | 8.7 | 7.2 | 10.7 |
| | max | 77.0 | 44.8 | 38.7 | 3.4 |
| | min | 5.3 | 10.4 | 16.5 | 71.2 |
| Volume (cm3) | mean | 26.6 | 22.2 | 28.7 | 25.3 |
| | median | 23.4 | 20.3 | 28.8 | 20.6 |
| | sd | 20.2 | 10.5 | 10.0 | 17.3 |
| | max | 169.4 | 44.8 | 46.4 | #### |
| | min | 2.6 | 6.2 | 17.9 | 2.6 |
| Length/Width | mean | 2.6 | 3.0 | 2.9 | 3.1 |
| Width/Thickness | mean | 3.1 | 3.5 | 3.1 | 3.6 |
| Length/Thickness | mean | 7.9 | 10.4 | 8.7 | 10.6 |
| Talon (cm) mean | width | 1.8 | 1.8 | 2.0 | 1.7 |
| | thicknes | 0.7 | 0.6 | 0.9 | 0.7 |
| Talon W/T | mean | 2.7 | 3.0 | 2.4 | 2.7 |
| | median | 2.6 | 3.0 | 2.2 | 2.6 |
| | sd | 1.0 | 0.9 | 0.7 | 1.0 |
| | max | 6.3 | 5.3 | 3.4 | 9.0 |
| | min | 0.8 | 2.0 | 1.8 | 0.1 |

Tab. 80: Metrical data of intact, retouched blades.

Tab. 80

| layers | 6b | | 6c2 | | 7c | | ah | |
|-------------|-----|--------|-----|--------|----|---|-----|--------|
| | n° | % | n° | % | n° | % | n° | % |
| crushed | | | 3 | 15.0% | 1 | | 25 | 7.7% |
| cortical | 8 | 7.5% | 1 | 5.0% | 2 | | 21 | 6.5% |
| plain | 54 | 50.9% | 7 | 35.0% | 2 | | 112 | 34.6% |
| punctiforme | 3 | 2.8% | 2 | 10.0% | 1 | | 22 | 6.8% |
| dihedral | 5 | 4.7% | 4 | 20.0% | | | 10 | 3.1% |
| faceted | 36 | 34.0% | 3 | 15.0% | 1 | | 130 | 40.1% |
| lipped | | | | | | | 4 | 1.2% |
| total | 106 | 100.0% | 20 | 100.0% | 7 | | 324 | 100.0% |

Tab. 81: Type of platforms in retouched blades.

| layers | 6b | | 6c2 | | 7c | | ah | |
|-------------------------|-----|--------|-----|--------|----|--------|-----|--------|
| | n° | % | n° | % | n° | % | n° | % |
| unidirectional parallel | 81 | 76.4% | 16 | 76.2% | 4 | | 206 | 63.6% |
| unidir. convergent | 1 | 0.9% | | | | | 2 | 0.6% |
| bidirectional | 22 | 20.8% | 5 | 23.8% | 3 | | 114 | 35.2% |
| undetermined | 2 | 1.9% | | | | | 2 | 0.6% |
| total | 106 | 100.0% | 21 | 100.0% | 7 | 100.0% | 324 | 100.0% |

Tab. 82 : Dorsale scar pattern visible on intact retouched blades.

| layers | 6b | | ah | |
|------------------|-----|--------|-----|--------|
| | n° | % | n° | % |
| rectiligne | 8 | 7.5% | 28 | 8.6% |
| bowed | | | | |
| on whole length | 56 | 52.8% | 225 | 69.4% |
| on prox-med part | 5 | 4.7% | 47 | 14.5% |
| on dis-med part | 33 | 31.1% | 22 | 6.8% |
| twisted | 2 | 1.9% | | |
| irregular | 2 | 1.9% | 2 | 0.6% |
| total | 106 | 100.0% | 324 | 100.0% |

Tab. 83: Profile of retouched blades.

| layers | serie of small removals | one or two short hinge | triangular removal | total preparation | | longitudinal removal | total |
|--------|-------------------------|------------------------|--------------------|-------------------|-------|----------------------|-------|
| | n° | n° | | n° | % | n° | % |
| 6b | 84 | 4 | 13 | 101 | 95.3% | 62 | 58.5% |
| 6c2 | 14 | 3 | 1 | 18 | 90.0% | 12 | 60.0% |
| 7c | 1 | 1 | 1 | 3 | | 4 | 57.1% |
| ah | 153 | | 58 | 211 | 65.1% | 170 | 52.5% |

Tab. 84: Frequency of the preparations of the proximal end on retouched blades

Tab. 84

| Layer | | 6b | 6c2 | ah |
|---------------------------------|----------|-------|------|-------|
| n of intact blanks | | 37 | 11 | 150 |
| Length (cm) | mean | 7.9 | 8.7 | 8.7 |
| | median | 7.9 | 8.7 | 8.3 |
| | sd | 2.0 | 2.4 | 1.6 |
| | max | 14.0 | 12.8 | 13.7 |
| | min | 4.3 | 6.1 | 4.5 |
| Width (cm) | mean | 3.1 | 2.9 | 3.0 |
| | median | 2.9 | 2.9 | 3.0 |
| | sd | 0.8 | 0.4 | 0.7 |
| | max | 5.5 | 3.7 | 5.2 |
| | min | 1.7 | 2.2 | 0.9 |
| Thickness | mean | 1.1 | 0.9 | 0.9 |
| | median | 1.0 | 0.8 | 0.8 |
| | sd | 0.4 | 0.2 | 0.3 |
| | max | 2.2 | 1.3 | 2.2 |
| | min | 0.3 | 0.5 | 0.1 |
| Surface area (cm ²) | mean | 25.3 | 25.8 | 26.9 |
| | median | 22.4 | 26.1 | 24.7 |
| | sd | 13.0 | 9.5 | 10.5 |
| | max | 77.0 | 44.8 | 71.2 |
| | min | 9.0 | 14.5 | 5.2 |
| Volume (cm ³) | mean | 29.9 | 23.0 | 25.4 |
| | median | 25.8 | 21.5 | 20.6 |
| | sd | 28.7 | 11.8 | 18.1 |
| | max | 169.4 | 44.8 | 128.2 |
| | min | 4.9 | 9.1 | 2.6 |
| Length/Width | mean | 2.6 | 3.0 | 3.0 |
| Width/Thickness | mean | 3.2 | 3.6 | 3.9 |
| Length/Thickness | mean | 7.9 | 10.5 | 11.0 |
| Talon (cm) mean | width | 1.8 | 1.8 | 1.7 |
| | thicknes | 0.7 | 0.6 | 0.7 |
| Talon W/T | mean | 2.6 | 2.7 | 2.8 |
| | median | 2.5 | 2.5 | 2.7 |
| | sd | 0.9 | 0.7 | 1.0 |
| | max | 6.3 | 4.1 | 7.0 |
| | min | 0.8 | 2.0 | 0.7 |

Tab. 85 Metrical data of intact, single scarpers on blades.

Tab. 85

| layers | 6b | | 6c2 | | ah | |
|---------------------------|----|--------|-----|--------|-----|--------|
| | n° | % | n° | % | n° | % |
| unidirectional parallel | 31 | 83.8% | 9 | 75.0% | 86 | 57.3% |
| unidirectional convergent | | | | | | |
| bidirectional | 6 | 16.2% | 3 | 25.0% | 60 | 40.0% |
| undetermined | | | | | 4 | 2.7% |
| total | 37 | 100.0% | 12 | 100.0% | 150 | 100.0% |

Tab. 86: Dorsale scar pattern visible on intact retouched blades

Tab. 86

| layers | 6b | | 6c2 | | ah | |
|-----------------------------|----|--------|-----|--------|-----|--------|
| | n° | % | n° | % | n° | % |
| two previous scars | 5 | 13.9% | 2 | 18.2% | 13 | 8.7% |
| three previous scars | 16 | 44.4% | 8 | 72.7% | 52 | 34.7% |
| four or five previous scars | 15 | 41.7% | 1 | 9.1% | 85 | 56.7% |
| total | 36 | 100.0% | 11 | 100.0% | 150 | 100.0% |

Tab. 87: Numbers of scars visible on the dorsal face of retouched blades.

| layers | 6b | | 6c2 | | ah | |
|------------|----|--------|-----|--------|-----|--------|
| | n° | % | n° | % | n° | % |
| converging | 25 | 67.6% | 9 | 81.8% | 97 | 64.7% |
| expanding | 1 | 2.7% | | | 17 | 11.3% |
| parallel | 11 | 29.7% | 2 | 18.2% | 36 | 24.0% |
| total | 37 | 100.0% | 11 | 100.0% | 150 | 100.0% |

Tab. 88: Shape of lateral edges of retouched blades .

Tab. 87, 88

| Layer | | 6b | 6c2 | ah |
|---------------------------------|----------|------|------|------|
| n of intact blanks | | 37 | 7 | 104 |
| Length (cm) | mean | 8.2 | 8.7 | 8.9 |
| | median | 8.3 | 9.1 | 8.4 |
| | sd | 1.4 | 1.2 | 1.7 |
| | max | 12.1 | 10.1 | 13.5 |
| | min | 4.5 | 7.2 | 5.2 |
| Width (cm) | mean | 3.0 | 3.0 | 2.8 |
| | median | 3.2 | 3.1 | 2.7 |
| | sd | 0.6 | 0.5 | 0.7 |
| | max | 4.4 | 3.8 | 5.1 |
| | min | 2.0 | 2.4 | 1.1 |
| Thickness | mean | 1.1 | 0.9 | 0.9 |
| | median | 1.1 | 0.8 | 0.8 |
| | sd | 0.3 | 0.1 | 0.2 |
| | max | 2.6 | 1.2 | 1.4 |
| | min | 0.6 | 0.8 | 0.4 |
| Surface area (cm ²) | mean | 25.0 | 26.5 | 25.3 |
| | median | 23.1 | 25.4 | 23.2 |
| | sd | 8.0 | 5.9 | 9.5 |
| | max | 44.9 | 34.6 | 68.9 |
| | min | 9.9 | 18.0 | 10.4 |
| Volume (cm ³) | mean | 27.0 | 23.3 | 23.5 |
| | median | 26.8 | 20.3 | 19.8 |
| | sd | 10.9 | 7.3 | 14.5 |
| | max | 58.3 | 34.6 | 96.4 |
| | min | 6.9 | 14.4 | 6.7 |
| Length/Width | mean | 2.8 | 2.9 | 3.3 |
| Width/Thickness | mean | 2.9 | 3.6 | 3.3 |
| Length/Thickness | mean | 8.0 | 10.1 | 10.6 |
| Talon (cm) mean | width | 2.0 | 1.9 | 1.7 |
| | thicknes | 0.7 | 0.6 | 0.7 |
| Talon W/T | mean | 2.8 | 3.3 | 2.7 |
| | median | 2.7 | 3.2 | 2.7 |
| | sd | 0.8 | 1.0 | 1.0 |
| | max | 4.8 | 5.3 | 9.0 |
| | min | 1.3 | 2.1 | 1.3 |

Tab. 89: Metrical data of intact, retouched pointed blades.

Tab. 89

| layers | 6b | | 6c2 | | ah | |
|---------------------------|----|--------|-----|---|-----|--------|
| | n° | % | n° | % | n° | % |
| unidirectional parallel | 29 | 78.4% | 6 | | 83 | 79.8% |
| unidirectional convergent | | | | | | |
| bidirectional | 7 | 18.9% | 1 | | 20 | 19.2% |
| undetermined | 1 | 2.7% | | | 1 | 1.0% |
| total | 37 | 100.0% | 7 | | 104 | 100.0% |

Tab.90: Dorsale scar pattern visible on intact retouched blades

| layers | 6b | | 6c2 | | ah | |
|-------------|----|--------|-----|--------|-----|--------|
| | n° | % | n° | % | n° | % |
| crushed | 6 | 16.2% | 1 | | 10 | 9.6% |
| cortical | 4 | 10.8% | | | 2 | 1.9% |
| plain | 11 | 29.7% | 3 | | 43 | 41.3% |
| punctiforme | 2 | 5.4% | | | 5 | 4.8% |
| dihedral | 1 | 2.7% | 3 | | 5 | 4.8% |
| faceted | 13 | 35.1% | | | 36 | 34.6% |
| lipped | | | | | 3 | 2.9% |
| total | 37 | 100.0% | 7 | 100.0% | 104 | 100.0% |

Tab. 91: Type of platforms in retouched pointed blades

Tab. 90, 91

| | | | |
|---------------------------------|----------|------|------|
| n of intact blanks | | 9 | 43 |
| Length (cm) | mean | 7.9 | 8.8 |
| | median | 7.9 | 8.7 |
| | sd | 1.9 | 2.1 |
| | max | 11.7 | 13.0 |
| | min | 5.3 | 1.7 |
| Width (cm) | mean | 2.9 | 3.1 |
| | median | 2.7 | 3.0 |
| | sd | 0.8 | 0.7 |
| | max | 4.2 | 4.9 |
| | min | 2.2 | 1.9 |
| Thickness | mean | 1.0 | 0.9 |
| | median | 1.0 | 0.8 |
| | sd | 0.2 | 0.3 |
| | max | 1.4 | 1.9 |
| | min | 0.6 | 0.5 |
| Surface area (cm ²) | mean | 23.4 | 27.8 |
| | median | 21.3 | 26.7 |
| | sd | 9.8 | 11.1 |
| | max | 39.5 | 59.3 |
| | min | 13.3 | 4.8 |
| Volume (cm ³) | mean | 24.2 | 26.5 |
| | median | 20.7 | 21.5 |
| | sd | 15.0 | 16.9 |
| | max | 55.3 | 83.0 |
| | min | 9.8 | 7.2 |
| Length/Width | mean | 2.8 | 3.0 |
| Width/Thickness | mean | 3.0 | 3.6 |
| Length/Thickness | mean | 8.3 | 10.4 |
| Talon (cm) mean | width | 1.7 | 1.7 |
| | thicknes | 0.6 | 0.6 |
| Talon W/T | mean | 3.3 | 2.7 |
| | median | 2.9 | 2.6 |
| | sd | 1.2 | 0.8 |
| | max | 5.3 | 4.8 |
| | min | 2.0 | 1.6 |

Tab. 92: Metrical data of intact double scrapers.

Tab. 92

| layers | 6b | | ah | |
|---------------------------|----|--------|----|--------|
| | n° | % | n° | % |
| unidirectional parallel | 32 | 88.9% | 17 | 38.6% |
| unidirectional convergent | | | 2 | 4.5% |
| bidirectional | 4 | 11.1% | 24 | 54.5% |
| undetermined | | | 1 | 2.3% |
| total | 36 | 100.0% | 44 | 100.0% |

Tab. 93: Dorsale scar pattern visible on intact double scrapers on blades.

| layers | 6b | | ah | |
|-------------|----|--------|----|--------|
| | n° | % | n° | % |
| crushed | 2 | 8.7% | | |
| cortical | 1 | 4.3% | 1 | 2.6% |
| plain | 12 | 52.2% | 11 | 28.2% |
| punctiforme | 2 | 8.7% | 2 | 5.1% |
| dihedral | | | | |
| faceted | 6 | 26.1% | 25 | 64.1% |
| lipped | | | | |
| total | 23 | 100.0% | 39 | 100.0% |

Tab. 94: Type of platforms in double scrapers on blades.

Tab. 93, 94

| Layer | | 6b | ah |
|--------------------|----------|-------|-------|
| n of intact blanks | | 66 | 43 |
| Length (cm) | mean | 5.2 | 6.6 |
| | median | 4.9 | 6.5 |
| | sd | 1.4 | 1.6 |
| | max | 9.3 | 10.7 |
| | min | 2.8 | 2.8 |
| Width (cm) | mean | 4.1 | 4.1 |
| | median | 3.8 | 3.9 |
| | sd | 1.3 | 1.0 |
| | max | 7.3 | 6.7 |
| | min | 2.1 | 2.4 |
| Thickness | mean | 1.2 | 1.0 |
| | median | 1.1 | 0.9 |
| | sd | 0.6 | 0.5 |
| | max | 3.0 | 3.4 |
| | min | 0.5 | 0.4 |
| Surface area (cm2) | mean | 22.4 | 27.9 |
| | median | 18.0 | 25.0 |
| | sd | 12.0 | 12.9 |
| | max | 58.6 | 65.0 |
| | min | 7.3 | 8.7 |
| Volume (cm3) | mean | 29.7 | 30.9 |
| | median | 20.0 | 22.8 |
| | sd | 23.4 | 26.7 |
| | max | 109.0 | 154.7 |
| | min | 4.3 | 4.1 |
| Length/Width | mean | 1.3 | 1.6 |
| Width/Thickness | mean | 3.8 | 4.4 |
| Length/Thickness | mean | 4.9 | 7.4 |
| Talon (cm) mean | width | 2.4 | 2.4 |
| | thicknes | 0.8 | 0.8 |
| Talon W/T | mean | 3.2 | 3.2 |
| | median | 3.0 | 3.0 |
| | sd | 1.3 | 1.2 |
| | max | 6.3 | 7.0 |
| | min | 1.0 | 0.8 |

Tab. 95 Metrical data of intact retouched flakes.

Tab. 95

| layers | 6b | | ah | |
|-------------------------|-----------|---------------|-----------|---------------|
| | n° | % | n° | % |
| unidirectional parallel | 57 | 86.4% | 24 | 55.8% |
| unidir. convergent | 1 | 1.5% | 1 | 2.3% |
| bidirectional | 6 | 9.1% | 15 | 34.9% |
| centripetal | 1 | 1.5% | 1 | 2.3% |
| undetermined | 1 | 1.5% | 2 | 4.7% |
| total | 66 | 100.0% | 43 | 100.0% |

Tab. 96: Dorsale scar pattern visible on intact retouched flakes.

| layers | 6b | | ah | |
|--------------|-----------|---------------|-----------|---------------|
| | n° | % | n° | % |
| crushed | 2 | 4.9% | 2 | 4.7% |
| cortical | 1 | 2.4% | 6 | 14.0% |
| plain | 9 | 22.0% | 10 | 23.3% |
| punctiforme | 5 | 12.2% | 3 | 7.0% |
| dihedral | | | 3 | 7.0% |
| faceted | 24 | 58.5% | 19 | 44.2% |
| lipped | | | | |
| total | 41 | 100.0% | 43 | 100.0% |

Tab. 97: Type of platforms in retouched flakes.

| Layer | on block | | on flake | | badelets cores | | burins-cores | | summa |
|--------------|----------|-----|----------|-----|----------------|-----|--------------|------|------------|
| | n | % | n | % | n | % | n | % | |
| 6a | | | 3 | 75% | | | 1 | 25% | 4 |
| 6b | 94 | 48% | 53 | 27% | 13 | 7% | 36 | 18% | 196 |
| 6c-2 | 2 | 29% | 2 | 29% | 2 | 29% | 2 | 29% | 7 |
| 7a | | | | | | | 2 | 100% | 2 |
| 7c | 5 | 71% | 2 | 29% | | | | | 7 |
| 6A1-2 | 2 | 40% | 2 | 40% | | | 1 | 20% | 5 |
| 6B | 1 | 14% | 5 | 71% | | | 1 | 14% | 7 |
| <i>Total</i> | 104 | 46% | 67 | 29% | 15 | 7% | 43 | 19% | 228 |
| ah | 33 | 40% | 35 | 43% | 3 | 4% | 11 | 13% | 82 |
| <i>Total</i> | | | | | | | | | <i>310</i> |

| Layer | Bladelets cores | Burins-cores |
|-------|-----------------|--------------|
| 6a | 1 | |
| 6b | 13 | 36 |
| 6c2 | 2 | 2 |
| 7a | | 2 |
| 7c | | |
| ah | 3 | 11 |
| 6A1-2 | | 1 |
| 6B2 | | 1 |

Tab. 98: Frequency of cores in Hummalian layers.

| Layer intact cores/blanks Length (cm) | 6a | | 6b | | 6c2 | | 7c | | 6A1-2 | | 6B | | ah | |
|---|-------|--------|-------|--------|-------|--------|-------|--------|-------|--------|-------|--------|-------|--------|
| | cores | blanks |
| mean | 4.3 | 5.4 | 5.5 | 6.4 | 7.0 | 7.3 | 5.5 | 6.5 | 5.0 | 6.6 | 5.0 | 7.1 | 5.8 | 7.2 |
| median | 4.4 | 5.9 | 5.2 | 6.2 | 7.0 | 7.0 | 5.5 | 6.2 | 4.6 | 6.3 | 4.4 | 7.3 | 5.4 | 7.3 |
| sd | 1.3 | 1.9 | 1.5 | 2.2 | 3.5 | 2.3 | 1.1 | 1.9 | 0.8 | 2.2 | 1.8 | 1.9 | 1.6 | 2.4 |
| max | 5.6 | 8.0 | 11.6 | 16.0 | 9.4 | 12.8 | 7.2 | 10.6 | 5.9 | 10.3 | 8.3 | 11.3 | 12.8 | 14.4 |
| min | 4.0 | 2.2 | 2.9 | 2.1 | 4.5 | 2.9 | 4.2 | 3.0 | 4.6 | 3.8 | 3.5 | 4.1 | 3.5 | 1.7 |

Tab. 99: Cores length (without core-burin) versus blank length (without bladelets)

| layer | 6a | | 6b | | 6c2 | | 6A1-2 | | 6B | | 7a | | 7c | | ah | |
|----------------|----|---|-----|--------|-----|---|-------|---|----|---|----|---|----|---|----|--------|
| | n° | % | n° | % | n° | % | n° | % | n° | % | n° | % | n° | % | n° | % |
| Laminar | 1 | | 126 | 64.6% | 3 | | 2 | | 4 | | | | 2 | | 46 | 56.1% |
| Levallois | | | 3 | 1.5% | | | | | | | | | | | 1 | 1.2% |
| Bladelet core | 1 | | 50 | 25.6% | 3 | | 1 | | 1 | | 2 | | | | 14 | 17.1% |
| Nahr Ibrahim | 2 | | 15 | 7.7% | 1 | | 2 | | 2 | | | | 1 | | 19 | 23.2% |
| indeterminable | | | 1 | 0.5% | | | | | | | | | | | 2 | 2.4% |
| Total | 4 | | 195 | 100.0% | 7 | | 5 | | 7 | | 2 | | 5 | | 82 | 100.0% |

Tab. 100: Frequency of core categories in analysed layers.

| cores types | 6b | | 6A1-2 | | 6B | | 6c2 | | 7c | | ah | |
|----------------|----------|----------|----------|----------|----------|----------|----------|----------|----------|----------|----------|----------|
| | on block | on flake |
| Laminar | 82 | 38 | 1 | | 1 | | 2 | 2 | 1 | | 41 | 15 |
| Semi-rotating | 3 | 3 | | | | | | | 1 | | 2 | 2 |
| Frontal | 85 | 41 | 1 | | 1 | | 4 | | 2 | | 41 | 17 |
| Total | | | | | | | | | | | | |
| % of all cores | | 64.3% | | 40.0% | | 28.6% | | 57.1% | | 28.6% | | 70.7% |

Tab. 101: Frequency of Laminar cores in analysed layers.

| Layer | | 6b | 6A1-2 | 6B | ah |
|---------------------------------|--------|-------|-------|------|-------|
| n of intact cores | | 105 | 1 | 1 | 58 |
| Length (mm) | mean | 5.4 | 4.6 | 5.5 | 5.5 |
| | median | 5.1 | | | 5.1 |
| | sd | 1.5 | | | 1.6 |
| | max | 11.6 | | | 12.8 |
| | min | 2.9 | | | 3.8 |
| Width (mm) | mean | 4.2 | 5.5 | 4.0 | 4.5 |
| | median | 3.9 | | | 4.4 |
| | sd | 1.2 | | | 1.4 |
| | max | 7.8 | | | 7.9 |
| | min | 1.9 | | | 1.9 |
| Thickness | mean | 1.9 | 3.7 | 2.1 | 2.2 |
| | median | 1.8 | | | 1.9 |
| | sd | 0.6 | | | 1.0 |
| | max | 5.0 | | | 5.8 |
| | min | 0.9 | | | 1.0 |
| Surface area (mm ²) | mean | 22.8 | 25.3 | 22.0 | 26.0 |
| | median | 19.1 | | | 21.1 |
| | sd | 11.1 | | | 15.3 |
| | max | 59.2 | | | 101.1 |
| | min | 8.6 | | | 8.2 |
| Volume (mm ³) | mean | 46.6 | 93.6 | 46.2 | 66.1 |
| | median | 36.7 | | | 39.9 |
| | sd | 37.0 | | | 86.2 |
| | max | 261.3 | | | 586.5 |
| | min | 7.6 | | | 11.9 |
| Length/Width | | 1.4 | 0.9 | 1.4 | 1.3 |
| Width/Thickness | | 2.4 | 1.5 | 1.9 | 2.4 |

Tab. 102: Metrical data of intact semi-rotating cores.

| Layer | | 6b | | ah | |
|---------------------------------|--------|----------|----------|----------|----------|
| | | on block | on flake | on block | on flake |
| intact cores | | | | | |
| number | | 70 | 35 | 41 | 17 |
| Length (cm) | mean | 5.4 | 5.4 | 5.8 | 4.8 |
| | median | 5.2 | 4.9 | 5.3 | 4.5 |
| | sd | 1.3 | 1.9 | 1.7 | 0.9 |
| | max | 9.2 | 11.6 | 12.8 | 6.9 |
| | min | 3.0 | 2.9 | 4.0 | 3.8 |
| Width (cm) | mean | 4.4 | 3.9 | 4.7 | 4.2 |
| | median | 4.2 | 3.6 | 4.4 | 4.3 |
| | sd | 1.2 | 1.2 | 1.4 | 1.3 |
| | max | 7.8 | 6.9 | 7.9 | 6.7 |
| | min | 2.2 | 1.9 | 2.0 | 1.9 |
| Thickness | mean | 2.0 | 1.6 | 2.4 | 1.6 |
| | median | 2.0 | 1.5 | 2.0 | 1.4 |
| | sd | 0.7 | 0.4 | 1.0 | 0.5 |
| | max | 5.0 | 2.7 | 5.8 | 2.5 |
| | min | 1.0 | 0.9 | 1.1 | 1.0 |
| Surface area (cm ²) | mean | 23.7 | 21.4 | 28.3 | 20.3 |
| | median | 20.7 | 16.7 | 23.0 | 20.0 |
| | sd | 10.0 | 13.1 | 17.2 | 7.0 |
| | max | 52.3 | 59.2 | 101.1 | 35.9 |
| | min | 8.9 | 8.6 | 8.2 | 8.2 |
| Volume (cm ³) | mean | 51.6 | 37.3 | 80.3 | 31.8 |
| | median | 41.6 | 21.9 | 44.5 | 29.2 |
| | sd | 38.2 | 33.4 | 98.7 | 18.0 |
| | max | 261.3 | 142.6 | 586.5 | 89.7 |
| | min | 11.4 | 7.6 | 11.9 | 12.2 |
| Length/Width | | 1.3 | 1.6 | 1.3 | 1.3 |
| Width/Thickness | | 2.3 | 2.5 | 2.1 | 3.0 |
| scars on upper face | mean | 3.4 | 3.5 | 3.6 | 3.0 |
| | max | 9.0 | 10.0 | 10.0 | 5.0 |
| | min | 2.0 | 2.0 | 2.0 | 2.0 |

Tab. 103: Metrical data of intact semi-rotating cores on block and flake.

Tab. 102, 103

| layers | 6b | | 6A1-2 | | 6B | | ch | |
|---------------------------|-----|--------|-------|---|----|---|----|--------|
| | n° | % | n° | % | n° | % | n° | % |
| unidirectional | 59 | 49.6% | 1 | | | | 27 | 46.6% |
| unidirectional convergent | 15 | 12.6% | | | | | 2 | |
| bidirectional | 13 | | | | | | 22 | |
| bidirectional off axis | 32 | 26.9% | | | 1 | | 7 | 12.1% |
| total | 119 | 100.0% | 1 | | 1 | | 58 | 100.0% |

Tab. 104: Dorsale scar pattern visible on semi-rotating cores.

| layers | 6b | | 6A1-2 | | 6B | | ch | |
|----------|-----|--------|-------|---|----|---|----|--------|
| | n° | % | n° | % | n° | % | n° | % |
| crushed | 15 | 9.5% | | | | | 3 | 3.5% |
| cortical | 11 | 7.0% | | | | | 6 | 7.1% |
| plain | 40 | 25.3% | 1 | | 2 | | 21 | 24.7% |
| prepared | 71 | 44.9% | | | | | 52 | 61.2% |
| faceted | 21 | 13.3% | | | | | 3 | 3.5% |
| total | 158 | 100.0% | 1 | | 2 | | 85 | 100.0% |

Tab. 105: Platforms aspect in semi-rotating cores.

| Layer | | 6b | 7c | ah |
|---------------------------------|--------|------|------|------|
| n of intact cores | | 5 | 1 | 2 |
| Length (mm) | mean | 6.9 | 5.0 | 6.8 |
| | median | 6.8 | | 6.8 |
| | sd | 0.8 | | 0.8 |
| | max | 8.1 | | 7.4 |
| | min | 6.0 | | 6.2 |
| Width (mm) | mean | 3.9 | 2.0 | 4.1 |
| | median | 4.0 | | 4.1 |
| | sd | 1.1 | | 1.0 |
| | max | 5.3 | | 4.7 |
| | min | 2.6 | | 3.4 |
| Thickness | mean | 2.6 | 2.6 | 1.6 |
| | median | 2.6 | | 1.6 |
| | sd | 0.8 | | 0.5 |
| | max | 3.7 | | 1.9 |
| | min | 1.4 | | 1.2 |
| Surface area (mm ²) | mean | 26.3 | 10.0 | 27.9 |
| | median | 25.1 | | 27.9 |
| | sd | 6.4 | | 9.7 |
| | max | 34.5 | | 34.8 |
| | min | 17.7 | | 21.1 |
| Volume (mm ³) | mean | 65.5 | 26.0 | 45.7 |
| | median | 65.4 | | 45.7 |
| | sd | 17.6 | | 28.8 |
| | max | 89.6 | | 66.1 |
| | min | 42.1 | | 25.3 |
| Length/Width | | 1.9 | 2.6 | 1.7 |
| Width/Thickness | | 1.7 | 0.8 | 2.7 |

Tab. 106: Metrical data of intact frontal cores

| layers | 6b | | 7c | | ah | |
|---------------------------|----|--------|----|------|----|--------|
| | n° | % | n° | % | n° | % |
| unidirectional | 5 | 83.3% | | | 2 | 100.0% |
| unidirectional convergent | | | | | | |
| bidirectional | 1 | 16.7% | 1 | 100% | | |
| total | 6 | 100.0% | 1 | 100% | 2 | 100.0% |

Tab. 107: Dorsale scar pattern visible on frontal cores.

| layers | 6b | | 7c | | ah | |
|----------|----|--------|----|---|----|---|
| | n° | % | n° | % | n° | % |
| crushed | 1 | 14.3% | | | | |
| cortical | 1 | 14.3% | | | 1 | |
| plain | 2 | 28.6% | 1 | | | |
| faceted | 3 | 42.9% | 2 | | 1 | |
| total | 7 | 100.0% | 3 | | 2 | |

Tab. 108: Platforms aspect in frontal cores.

Tab. 107, 108

| cores types | 6b | 7c | ah |
|---------------------------|------|-------|------|
| Lineal | 2 | 1 | |
| Recurrent | | | |
| unidirectional parallel | 1 | | 1 |
| unidirectional converging | | | |
| bidirectional | | | |
| subcentripetal | | 1 | |
| Total | 3 | 2 | 1 |
| percent of all cores | 1.5% | 40.0% | 1.2% |

Tab. 109: Dorsal scar patterns as visible on the Levallois cores

| Layer | | 6b | | 7c | | ah | |
|---------------------------------|--------|--------|-----------|--------|-----------|--------|-----------|
| | | lineal | recurrent | lineal | recurrent | lineal | recurrent |
| intact cores | number | 2 | 1 | | 2 | | 1 |
| Length (cm) | mean | 5.4 | 5.9 | | 4.8 | | 5.1 |
| | median | 5.4 | | | | | |
| | sd | 2.5 | | | | | |
| | max | 7.1 | | | | | |
| | min | 3.6 | | | | | |
| Width (cm) | mean | 5.6 | 3.7 | | 4.2 | | 4.3 |
| | median | 5.6 | | | | | |
| | sd | 0.6 | | | | | |
| | max | 6.0 | | | | | |
| | min | 5.1 | | | | | |
| Thickness | mean | 1.8 | 2.2 | | 1.7 | | 0.8 |
| | median | 1.8 | | | | | |
| | sd | 0.8 | | | | | |
| | max | 2.3 | | | | | |
| | min | 1.2 | | | | | |
| Surface area (cm ²) | mean | 30.5 | 21.8 | | 20.2 | | 21.7 |
| | median | 30.5 | | | | | |
| | sd | 17.1 | | | | | |
| | max | 42.6 | | | | | |
| | min | 18.4 | | | | | |
| Volume (cm ³) | mean | 60.0 | 48.0 | | 34.0 | | 17.5 |
| | median | 60.0 | | | | | |
| | sd | 53.7 | | | | | |
| | max | 98.0 | | | | | |
| | min | 22.0 | | | | | |
| Length/Width | mean | 0.9 | 1.6 | | 1.1 | | 1.2 |
| Width/Thickness | mean | 3.4 | 1.7 | | 2.5 | | 5.4 |
| scars on upper face | mean | 2.0 | 3.0 | | 3.0 | | 3.0 |

Tab. 110 Metrical data of intact Levallois cores.

Tab. 109, 110

| Layer | | 6a | 6b | 6c-2 | 7c | 6A1-2 | 6B | ah |
|----------------------|--------|------|------|------|------|-------|------|------|
| n of intact NI cores | | 2 | 11 | 1 | 1 | 2 | 2 | 19 |
| Length (mm) | mean | 4.3 | 5.9 | 6.0 | 5.9 | 5.3 | 6.1 | 6.5 |
| | median | 4.3 | 5.8 | | | 5.3 | 6.1 | 6.6 |
| | sd | 1.8 | 1.4 | | | 0.9 | 3.2 | 1.3 |
| | max | 5.6 | 8.1 | | | 5.9 | 8.3 | 8.4 |
| | min | 3.0 | 3.4 | | | 4.6 | 3.8 | 4.0 |
| Width (mm) | mean | 4.9 | 4.3 | 4.7 | 4.3 | 3.2 | 5.9 | 3.5 |
| | median | 4.9 | 4.3 | | | 3.2 | 5.9 | 3.6 |
| | sd | 0.7 | 0.8 | | | 0.4 | 2.7 | 0.8 |
| | max | 5.4 | 5.9 | | | 3.4 | 7.8 | 6.0 |
| | min | 4.4 | 3.3 | | | 2.9 | 4.0 | 2.4 |
| Thickness | mean | 1.4 | 1.4 | 1.0 | 1.1 | 1.3 | 1.1 | 1.2 |
| | median | 1.4 | 1.4 | | | 1.3 | 1.1 | 1.0 |
| | sd | 0.4 | 0.3 | | | 0.4 | 0.1 | 0.4 |
| | max | 1.6 | 1.9 | | | 1.6 | 1.2 | 1.9 |
| | min | 1.1 | 1.1 | | | 1.0 | 1.0 | 1.0 |
| Surface area (cm2) | mean | 20.4 | 25.8 | | 25.4 | 16.4 | 40.0 | 22.5 |
| | median | 20.4 | 25.5 | | | 16.4 | 40.0 | 20.7 |
| | sd | 6.0 | 8.1 | | | 1.0 | 35.0 | 6.5 |
| | max | 24.6 | 38.3 | | | 17.1 | 64.7 | 40.8 |
| | min | 16.2 | 15.0 | | | 15.6 | 15.2 | 15.2 |
| Volume (cm3) | mean | 26.5 | 36.9 | | 27.9 | 21.1 | 46.4 | 26.7 |
| | median | 26.5 | 35.7 | | | 21.1 | 46.6 | 22.9 |
| | sd | 0.8 | 17.4 | | | 5.6 | 44.2 | 13.7 |
| | max | 27.1 | 72.8 | | | 25.0 | 77.7 | 69.4 |
| | min | 25.9 | 16.5 | | | 17.2 | 15.2 | 13.7 |
| Length/Width | | 0.9 | 1.4 | 1.3 | 1.4 | 1.4 | 1.0 | 1.9 |
| Width/Thickness | | 3.7 | 4.1 | 4.7 | 3.9 | 2.2 | 5.3 | 3.2 |
| scars on upper face | mean | 2.5 | 3.2 | | 2.0 | 1.5 | 2.0 | 2.7 |
| | max | 3.0 | 5.0 | | | 2.0 | 2.0 | 6 |
| | min | 2.0 | 1.0 | | | 1.0 | 2.0 | 1 |

Tab. 111: Metrical data of unbroken NI cores.

Tab. 111

| layers | 6a | | 6b | | 6c2 | | 7c | | 6A1-2 | | 6B | | ah | |
|--------------------|----|---|----|--------|-----|---|----|---|-------|---|----|---|----|--------|
| | n° | % | n° | % | n° | % | n° | % | n° | % | n° | % | n° | % |
| unidirectional | 1 | | 6 | 40.0% | 1 | | | | | | | | 9 | 47.4% |
| unidir. convergent | | | 1 | 6.7% | | | | | | | | | 2 | 10.5% |
| bidirectional | 1 | | 8 | 53.3% | | | 1 | | 2 | | 2 | | 8 | 42.1% |
| total | 2 | | 15 | 100.0% | 1 | | 1 | | 2 | | 2 | | 19 | 100.0% |

Tab. 112: Dorsale scar pattern visible on NI cores.

| Layer | | 6a | 6b | 6c2 | 7a | 6B | ah |
|---------------------|--------|-----|-----|-----|-----|-----|------|
| cores-burin | | 1 | 49 | 3 | 2 | 1 | 14 |
| Length (mm) | mean | 3.0 | 4.6 | 3.6 | 5.9 | 5.0 | 6.3 |
| | median | | 4.4 | 3.6 | 5.9 | | 5.6 |
| | sd | | 1.4 | 1.4 | 0.4 | | 2.0 |
| | max | | 8.6 | 5.1 | 6.2 | | 10.2 |
| | min | | 2.0 | 2.3 | 5.6 | | 3.5 |
| Width (mm) | mean | 1.9 | 3.6 | 2.3 | 5.1 | 5.0 | 3.2 |
| | | | 3.0 | 2.4 | 5.1 | | 3.4 |
| | sd | | 1.6 | 0.2 | 3.1 | | 0.7 |
| | max | | 7.6 | 2.5 | 7.3 | | 4.1 |
| | min | | 1.3 | 2.1 | 2.9 | | 2.2 |
| Thickness | mean | 1.5 | 1.6 | 1.0 | 2.0 | 1.0 | 1.3 |
| | median | | 1.6 | 1.0 | 2.0 | | 1.2 |
| | sd | | 0.7 | 0.1 | 1.1 | | 0.5 |
| | max | | 4.0 | 1.0 | 2.8 | | 2.7 |
| | min | | 0.6 | 0.9 | 1.2 | | 0.7 |
| Last scars length | mean | 1.1 | 2.5 | 2.6 | 2.8 | 3.1 | 3.2 |
| | median | 1.1 | 2.4 | 2.6 | 2.8 | 3.1 | 3.0 |
| | sd | 0.4 | 1.0 | 1.3 | 0.9 | 1.0 | 0.8 |
| | max | 1.5 | 5.0 | 5.0 | 4.0 | 3.7 | 5.0 |
| | min | 0.7 | 1.2 | 1.0 | 1.7 | 2.0 | 2.0 |
| Last scars width | mean | 0.4 | 0.6 | 0.8 | 0.9 | 0.9 | 0.8 |
| | median | 0.4 | 0.6 | 0.8 | 0.9 | 0.9 | 0.8 |
| | sd | 0.1 | 0.2 | 0.2 | 0.1 | 0.2 | 0.1 |
| | max | 0.5 | 1.1 | 1.1 | 1.0 | 0.9 | 1.1 |
| | min | 0.4 | 0.3 | 0.5 | 0.7 | 0.7 | 0.7 |
| scars on upper face | mean | 3.0 | 2.6 | 4.3 | 2.5 | 3.0 | 2.6 |
| | max | | 6.0 | 6.0 | 3.0 | | 5.0 |
| | min | | 1.0 | 3.0 | 2.0 | | 1.0 |

Tab. 113: Metrical data of cores-burin.

Tab. 112, 113

| Layer | | 6a | 6b | | 6c2 | 7a | | 6B | | ah | |
|---------------------|--------|-----------|-----------|----------|-----------|-----------|----------|-----------|----------|-----------|----------|
| | | on debris | on debris | on flake | on debris | on debris | on flake | on debris | on flake | on debris | on flake |
| number | | 1 | 24 | 25 | 3 | 1 | 1 | 1 | | 1 | 13 |
| Length (cm) | mean | 3.0 | 4.2 | 5.1 | 3.6 | 6.2 | 5.6 | 5.0 | | 4.4 | 6.5 |
| | median | | 3.9 | 4.8 | 3.6 | | | | | | 5.7 |
| | sd | | 1.5 | 8.6 | 1.4 | | | | | | 2.0 |
| | max | | 7.9 | 2.7 | 5.1 | | | | | | 10.2 |
| | min | | 2.0 | 1.2 | 2.3 | | | | | | 3.5 |
| Width (cm) | mean | 1.9 | 3.7 | 3.5 | 2.3 | 7.3 | 2.9 | 5.0 | | 3.1 | 3.2 |
| | median | | 3.2 | 3.0 | 2.4 | | | | | | 3.4 |
| | sd | | 1.6 | 7.2 | 0.2 | | | | | | 0.7 |
| | max | | 7.6 | 1.3 | 2.5 | | | | | | 4.1 |
| | min | | 1.4 | 1.6 | 2.1 | | | | | | 2.2 |
| Thickness | mean | 1.5 | 1.7 | 1.7 | 1.0 | 1.2 | 2.8 | 1.0 | | 1.0 | 1.3 |
| | median | | 1.7 | 1.4 | 1.0 | | | | | | 1.2 |
| | sd | | 0.5 | 4.5 | 0.1 | | | | | | 0.6 |
| | max | | 2.8 | 0.6 | 1.0 | | | | | | 2.7 |
| | min | | 1.0 | 0.9 | 0.9 | | | | | | 0.7 |
| Surface area (cm2) | mean | 5.7 | 15.9 | 17.7 | 8.2 | 45.3 | 16.2 | 25.0 | | 13.6 | 27.1 |
| | median | | 12.8 | 16.0 | 8.2 | | | | | | 25.3 |
| | sd | | 11.2 | 42.5 | 3.1 | | | | | | 15.1 |
| | max | | 47.4 | 5.5 | 11.7 | | | | | | 70.8 |
| | min | | 5.9 | 8.5 | 5.8 | | | | | | 12.2 |
| Volume (cm3) | mean | 8.6 | 28.7 | 31.8 | 8.0 | 54.3 | 45.5 | 25.0 | | 13.6 | 20.6 |
| | median | | 19.9 | 21.3 | 8.0 | | | | | | 19.5 |
| | sd | | 24.6 | 6.6 | 3.4 | | | | | | 6.7 |
| | max | | 88.2 | 131.6 | 11.7 | | | | | | 33.7 |
| | min | | 7.5 | 27.8 | 2.1 | | | | | | 12.2 |
| Length/Width | | 1.6 | 1.3 | 1.8 | 1.6 | 0.9 | 1.9 | 1.0 | | 1.4 | 2.1 |
| Width/Thickness | | 1.3 | 2.4 | 2.4 | 2.4 | 6.0 | 1.0 | 5.0 | | 3.1 | 2.7 |
| scars on upper face | mean | 3.0 | 2.8 | 2.3 | 4.3 | 2.0 | 2.0 | 3.0 | | 2.0 | 2.6 |
| | max | | 7.0 | 4.0 | 6.0 | | | | | | 7.0 |
| | min | | 1.0 | 1.0 | 3.0 | | | | | | 1.0 |

Tab. 114: Metrical data of cores-burin on block and o flake.

Tab. 114

| layers | 6a | | 6b | | 6c2 | | 7a | | 6B | | ah | |
|--------------------|----|---|----|------|-----|---|----|---|----|---|----|--------|
| | n° | % | n° | % | n° | % | n° | % | n° | % | n° | % |
| unidirectional | 2 | | 43 | 86% | 1 | | 2 | | 1 | | 11 | 78.6% |
| unidir. convergent | | | 1 | 2% | | | | | | | | |
| bidirectional | | | 6 | 12% | 2 | | | | | | 3 | 21.4% |
| total | 2 | | 50 | 100% | 3 | | 2 | | 1 | | 14 | 100.0% |

Tab. 115: Dorsale scar pattern visible on semi-rotating cores.

| layers | 6a | | 6b | | 6c2 | | 7a | | 6B | | ah | |
|----------|----|---|----|------|-----|---|----|---|----|---|----|--------|
| | n° | % | n° | % | n° | % | n° | % | n° | % | n° | % |
| crushed | | | 2 | 4% | | | | | | | | |
| cortical | | | | | | | | | | | | |
| plain | 2 | | 22 | 39% | 4 | | 1 | | 1 | | 4 | 26.7% |
| faceted | | | 25 | 45% | 1 | | 1 | | | | 9 | 60.0% |
| on break | | | 7 | 13% | | | | | | | 2 | 13.3% |
| total | 2 | | 56 | 100% | 5 | | 2 | | 1 | | 15 | 100.0% |

Tab. 116: Platforms aspect in semi-rotating cores.

| Layer | | 6a | 6b | 6c2 | 7a | 7c | 6A1-2 | ah |
|---------------------------------|-----------|-------|---------|-------|-----|-------|-------|---------|
| n of blanks (Intact) | | 22(2) | 153(14) | 11(2) | 1 | 10(1) | (2) | 100(10) |
| Length (cm) | mean | 4.2 | 3.4 | 3.5 | 3.0 | 3.0 | | 4.0 |
| | median | 4.2 | 3.4 | 2.6 | | | | 3.9 |
| | sd | 0.8 | 0.7 | 1.2 | | | | 0.5 |
| | max | 4.8 | 4.6 | 4.3 | | | | 3.2 |
| | min | 3.6 | 2.3 | 2.6 | | | | 4.7 |
| Width (cm) | mean | 1.0 | 1.0 | 1.0 | 1.0 | 0.9 | 1.1 | 0.9 |
| | median | 1.0 | 1.0 | 1.0 | | 1.0 | 1.1 | 0.9 |
| | sd | 0.1 | 0.2 | 0.1 | | 0.2 | 0.1 | 0.1 |
| | max | 1.4 | 1.4 | 1.2 | | 1.3 | 1.1 | 0.7 |
| | min | 0.7 | 0.6 | 0.8 | | 0.6 | 1.0 | 1.2 |
| Thickness | mean | 0.5 | 0.4 | 1.9 | 0.4 | 0.5 | 0.4 | 0.3 |
| | median | 0.5 | 0.4 | 1.2 | | 0.5 | 0.4 | 0.3 |
| | sd | 0.1 | 0.2 | 1.4 | | 0.1 | 0.1 | 0.1 |
| | max | 1.0 | 0.2 | 4.3 | | 0.8 | 0.4 | 0.2 |
| | min | 0.4 | 1.2 | 0.1 | | 0.3 | 0.3 | 0.6 |
| Surface area (cm ²) | mean | 5.2 | 4.0 | 4.0 | 3.0 | 3.9 | | 4.4 |
| | median | 5.2 | 3.9 | 2.9 | | | | 4.2 |
| | sd | 2.2 | 1.5 | 1.6 | | | | 0.9 |
| | max | 6.7 | 6.4 | 5.2 | | | | 3.2 |
| | min | 3.6 | 1.8 | 2.9 | | | | 5.6 |
| Volume (cm ³) | mean | 4.1 | 2.8 | 1.1 | 1.2 | 3.1 | | 1.8 |
| | median | 4.1 | 1.7 | 0.6 | | | | 1.8 |
| | sd | 3.7 | 2.3 | 0.7 | | | | 0.8 |
| | max | 6.7 | 7.2 | 1.5 | | | | 0.6 |
| | min | 1.4 | 0.5 | 0.6 | | | | 2.8 |
| Length/Width | mean | 3.5 | 3.0 | 3.0 | 3.0 | 2.3 | | 3.6 |
| Width/Thickness | mean | 2.0 | 2.3 | 4.8 | 2.5 | 1.8 | | 3.1 |
| Length/Thickness | mean | 6.9 | 6.4 | 13.7 | 7.5 | 3.8 | | 11.3 |
| Butt (cm) mean | width | 0.3 | 0.3 | 0.2 | 0.2 | 0.7 | | 0.5 |
| | thickness | 0.6 | 0.8 | 0.1 | 0.1 | 0.8 | | 0.9 |
| Butt W/T | mean | 1.9 | 1.8 | 5.0 | 2.0 | 1.1 | | 2.1 |
| | median | 1.8 | 1.2 | 4.5 | | 1.1 | | 2.1 |
| | sd | 0.5 | 1.8 | 2.3 | | 0.2 | | 0.8 |
| | max | 2.5 | 5.5 | 7.5 | | 1.3 | | 1.5 |
| | min | 1.5 | 0.1 | 3.0 | | 1.0 | | 2.7 |

Tab. 117: Metrical data of bladelets.

| layers | CV length | CV width | CV thickness | CV butt ratio W/T |
|--------|-----------|----------|--------------|-------------------|
| 6a | 0.2 | 0.1 | 0.2 | 0.3 |
| 6b | 0.2 | 0.2 | 0.1 | 1.0 |
| 6c2 | 0.3 | 0.1 | 1.6 | 0.5 |
| 7c | 0.3 | 0.2 | 0.2 | 0.2 |
| ah | 0.1 | 0.1 | 0.3 | 0.4 |

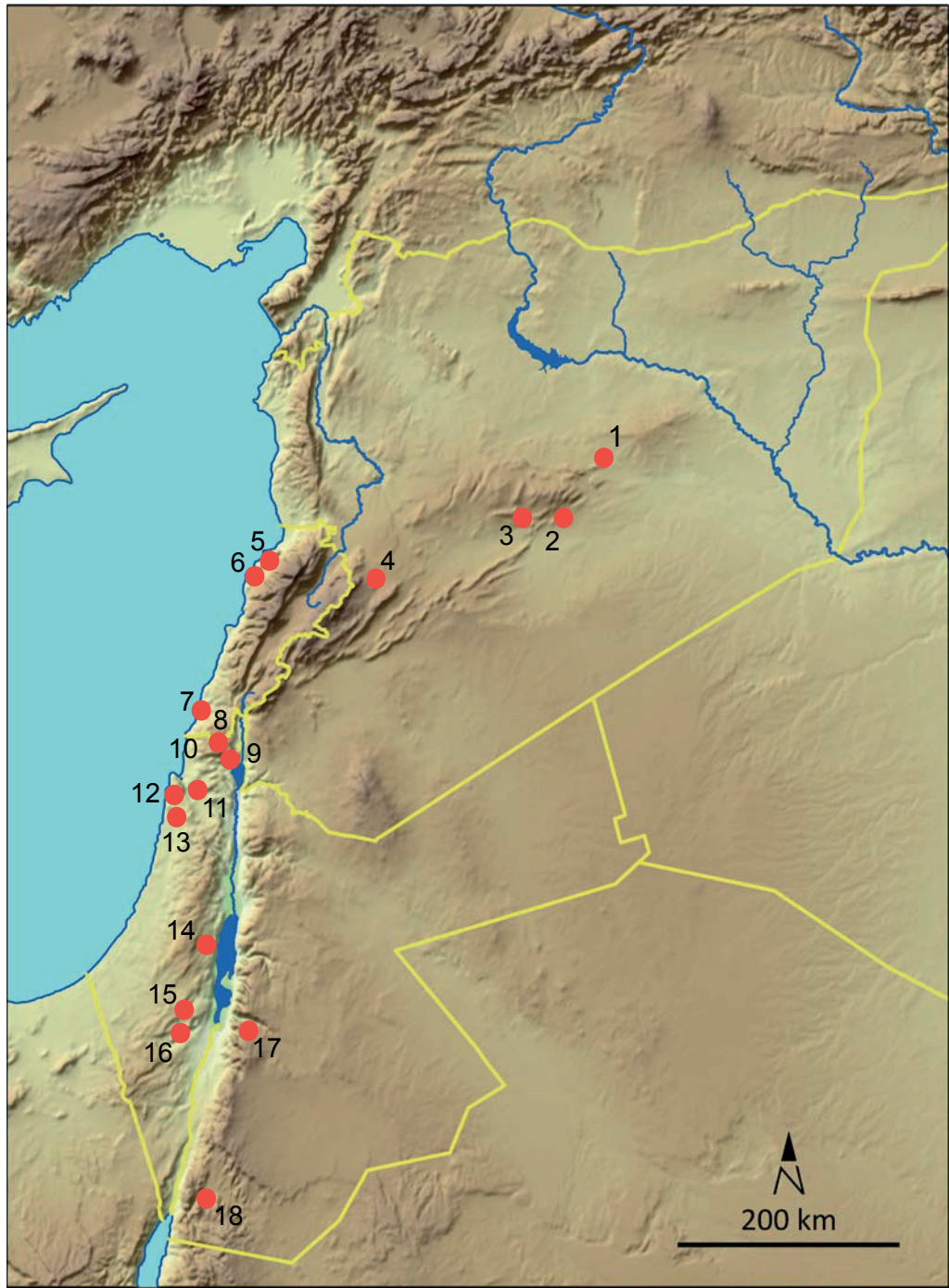
Tab. 118: The coefficient of variation (CV) of mean length, width, thickness and WT butts of bladelets.

CV is calculated by dividing the standard deviation by the mean

Tab. 117, 118

| Type Groupe | count | % |
|----------------|-------|------|
| Cores | 7 | 2% |
| CTE | 43 | 14% |
| Flakes | 46 | 15% |
| Tools on flake | 23 | 7% |
| Blades | 104 | 33% |
| Tools on blade | 89 | 29% |
| Total | 312 | 100% |

Tab. 119: Artefacts frequencies by type in Nadaouiyeh.



il. R. Jagher

Fig. 1: Map showing sites mentioned in text.

1 El Kowm, 2 Jerf Ajla, 3 Duara, 4 Yabrud, 5 Masloukh, 6 Nahr Ibrahim, 7 Adlun, 8 Qafzeh, 9 Amud, 10 Hayonim, 11 Qesem, 12 Tabun, 13, Kebara, 14 Abu Sif, 15 Boker Tachtit, 16 Rosh Ein Mor, 17 Ain Difla, 18 Tor Faraj

Fig. 1



Fig. 2: The well of Hummal (Tell Hassan Unozi) in 1967. The photo shows the northern half of the funnel (Suzuki et al. 1970).

Fig. 2

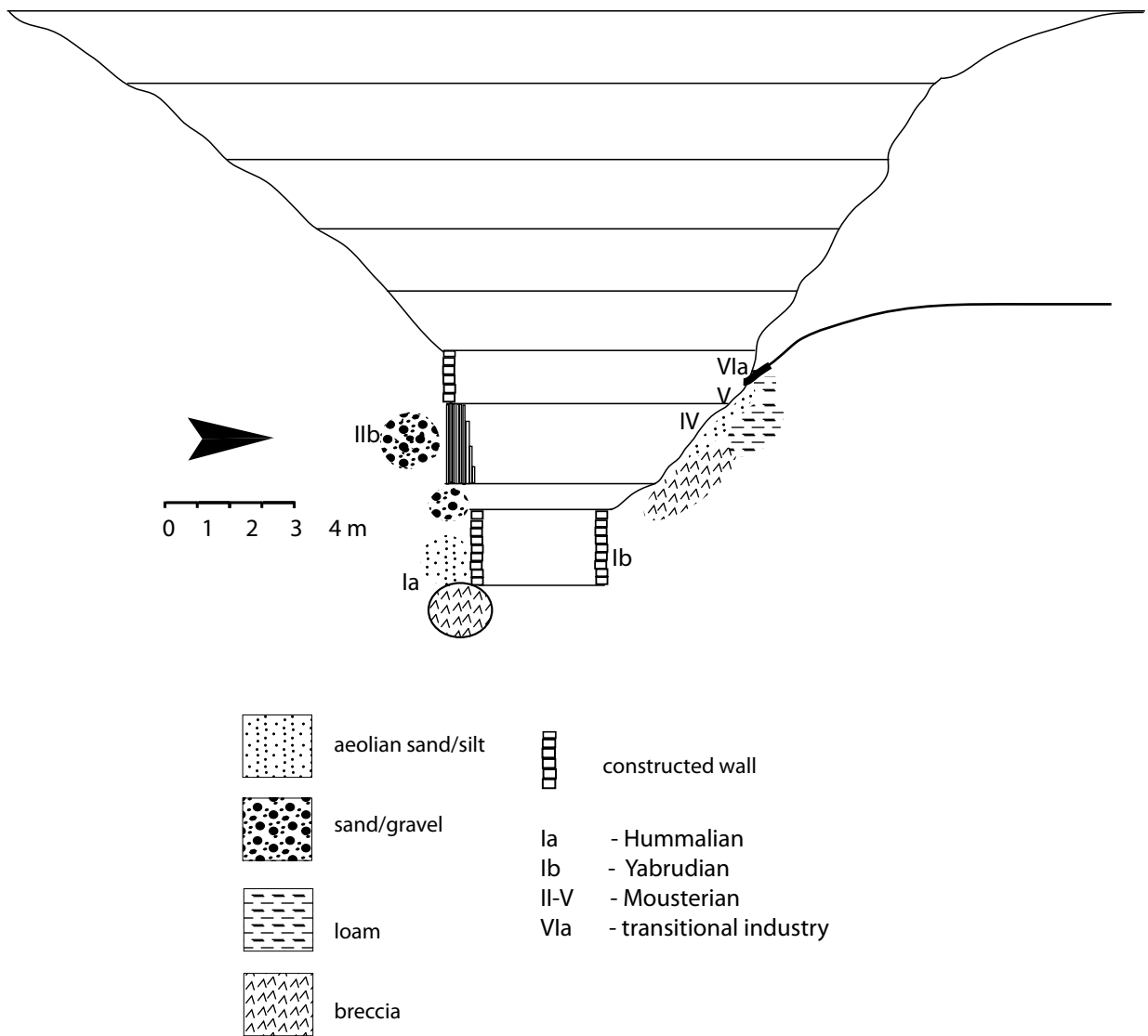


Fig. 3: Hummal well in 1980, modified after Besançon and Sanlaville (1991).

Fig. 3

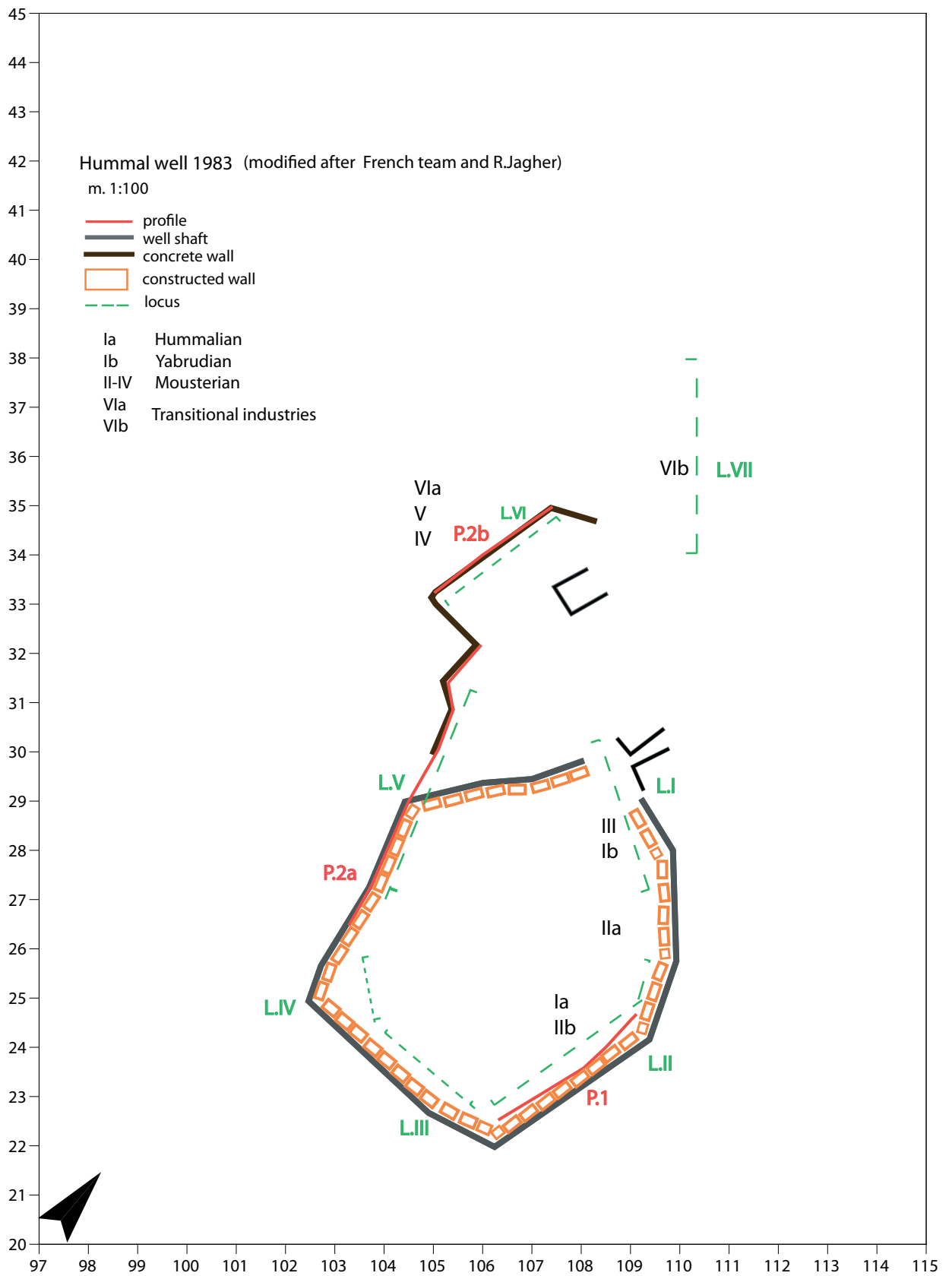


Fig. 4

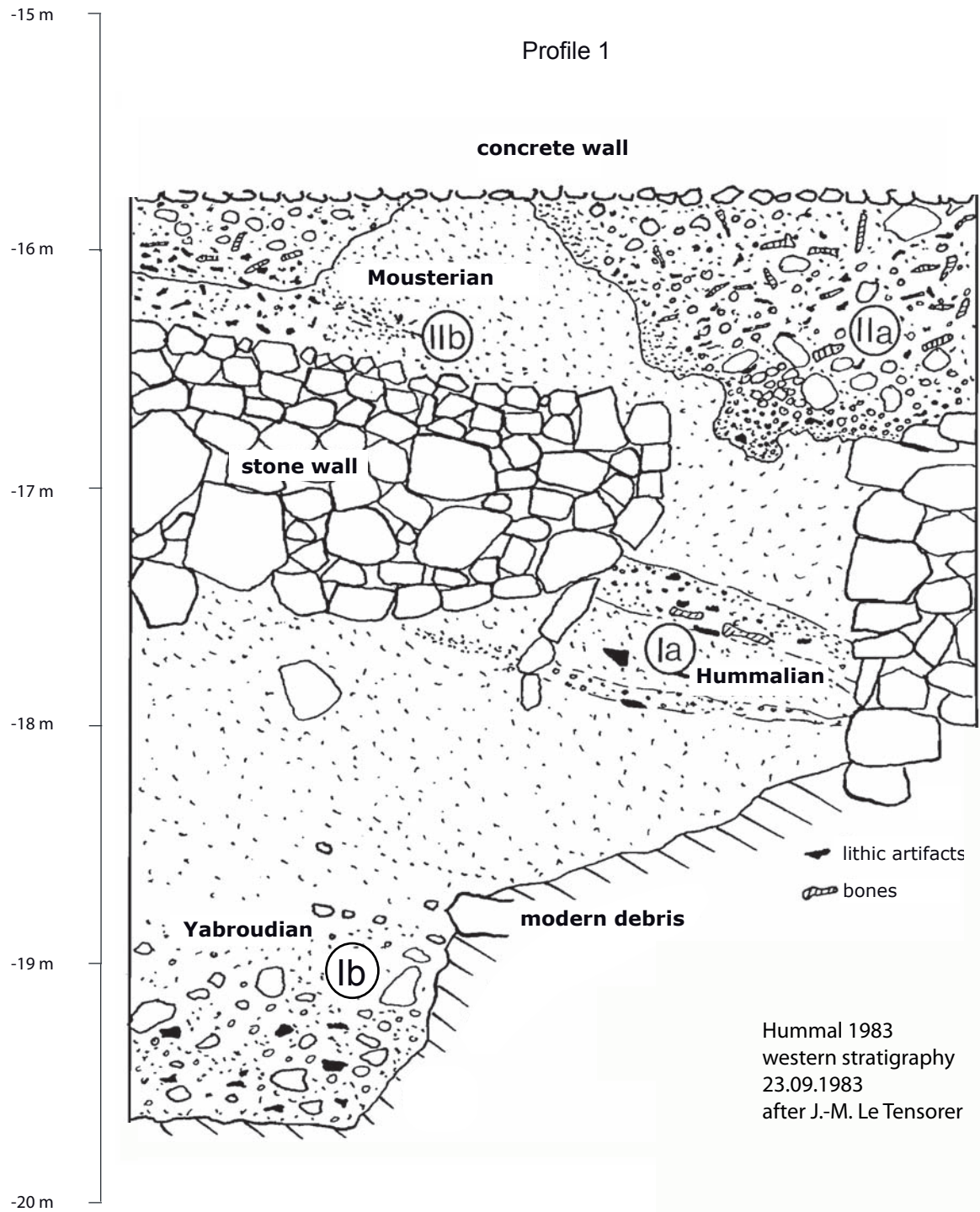


Fig. 5

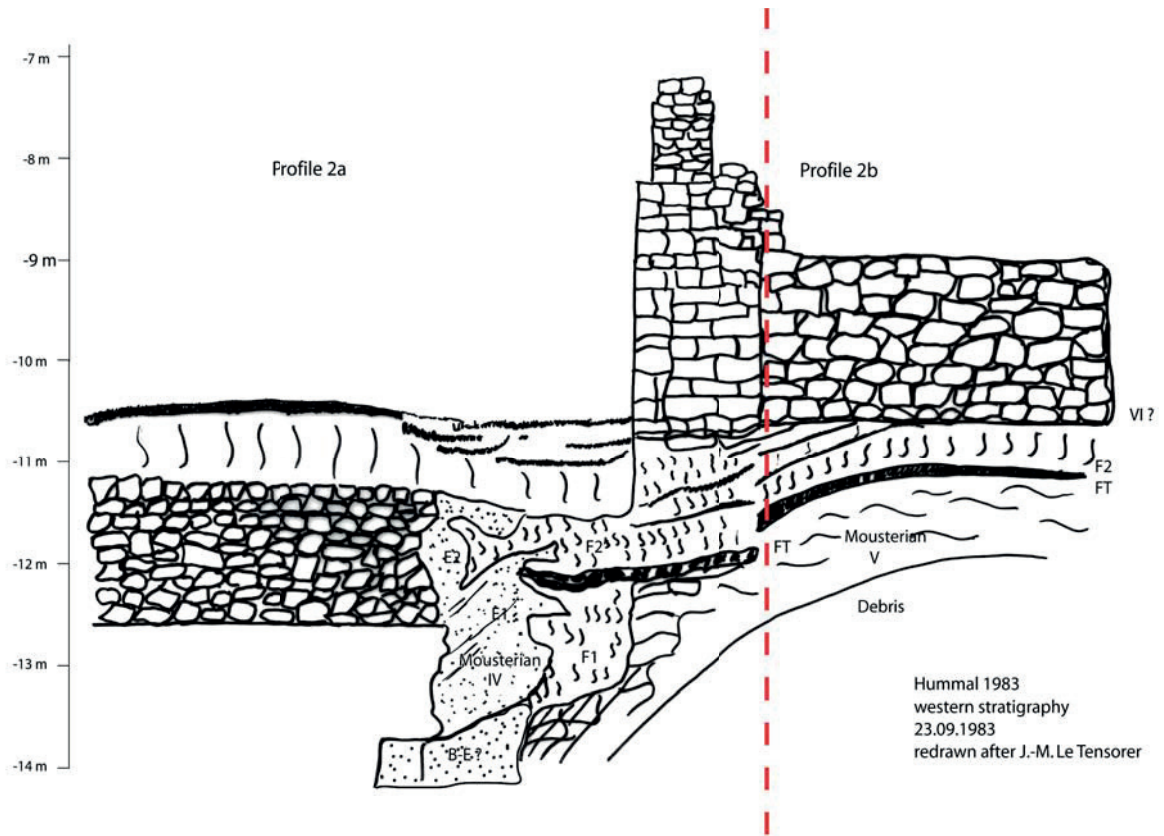
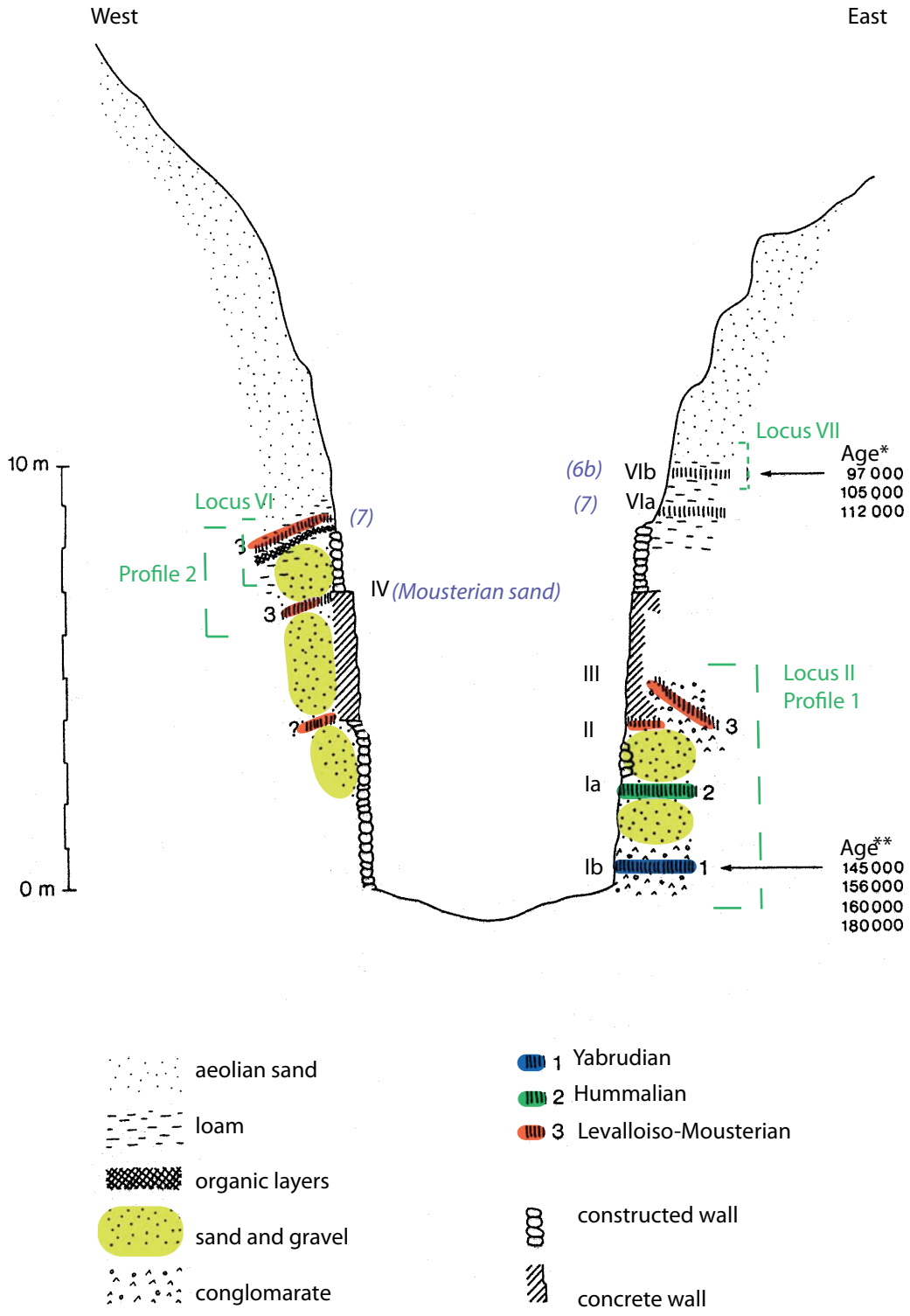


Fig. 6 : The well of Hummal . Drawing of western stratigraphy and its photo were made in 1983 by J.- M. Le Tensorer.

Fig. 6



* Ancient TL supplement, Oxford, 1988
 ** Henning & Hours, 1982

*label in violet corresponding to current research
 6b, 7-Hummalian*

Fig. 7: Schematic profile of Hummal, modified after Jagher (1991).

Fig. 7

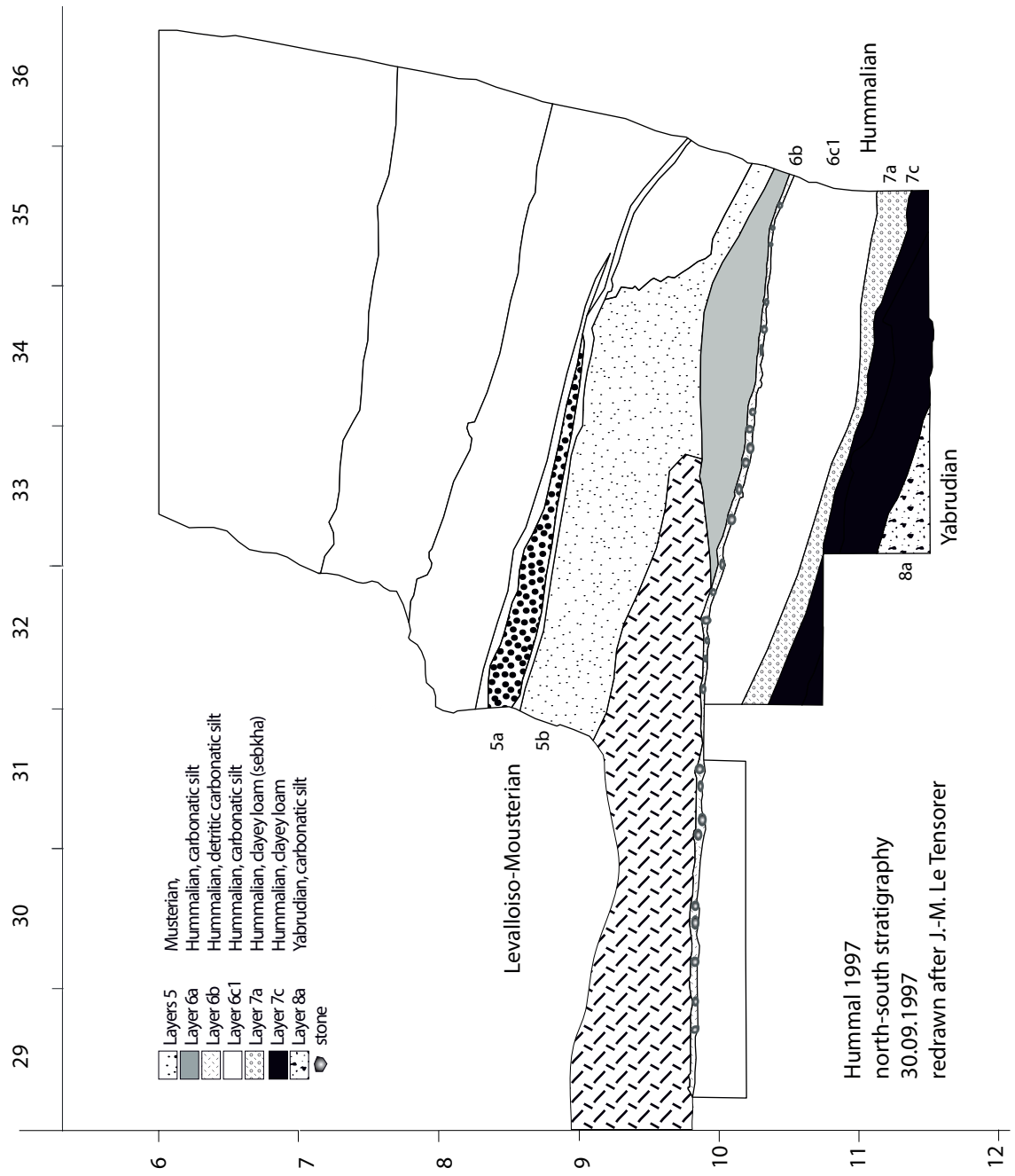


Fig. 8: Profile 3

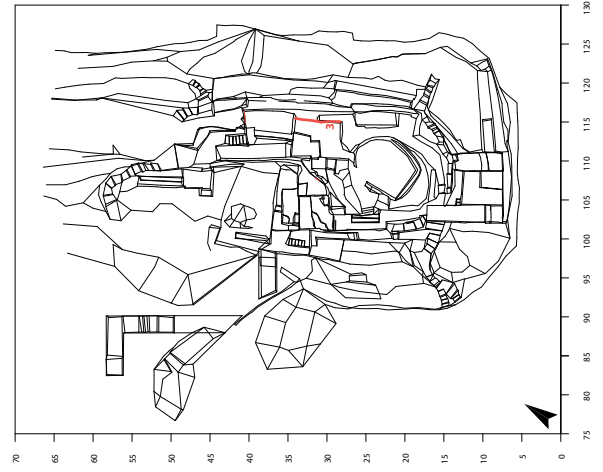


Fig. 8

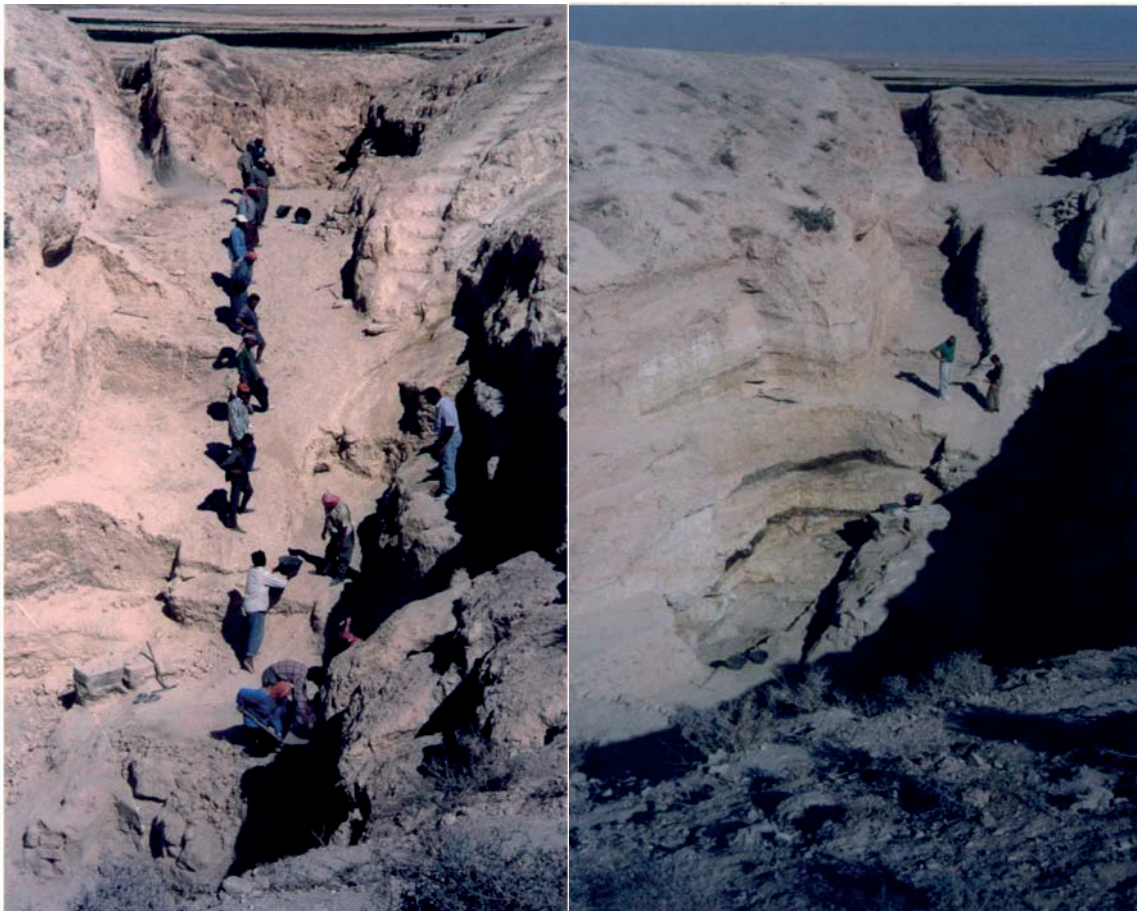
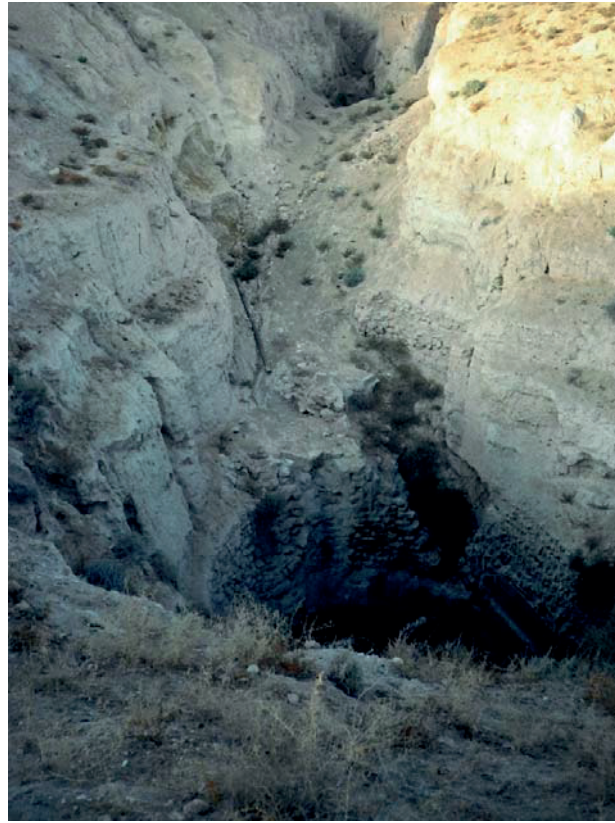


Fig. 9: The well of Hummal in 1997 (top), at the beginning (bottom left) and at the end (bottom right) of field season in 1999 (photos J.-M. Le Tensorer and V. von Falkenstein).

Fig. 9



Fig. 10 : The well of Hummal in 2001(photo J.-M. Le Tensorer). Photo shows the north-east part of excavation.

Fig. 10

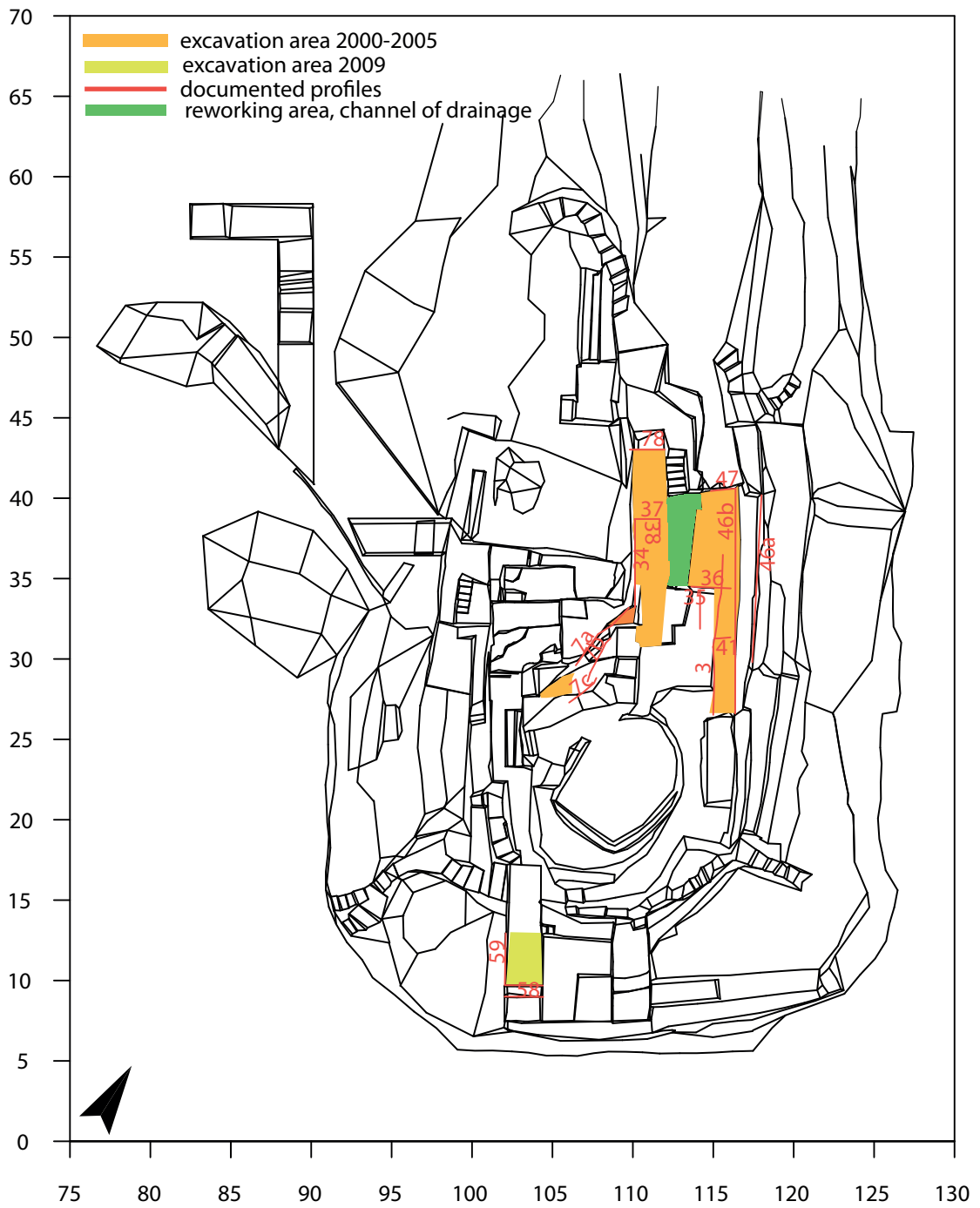
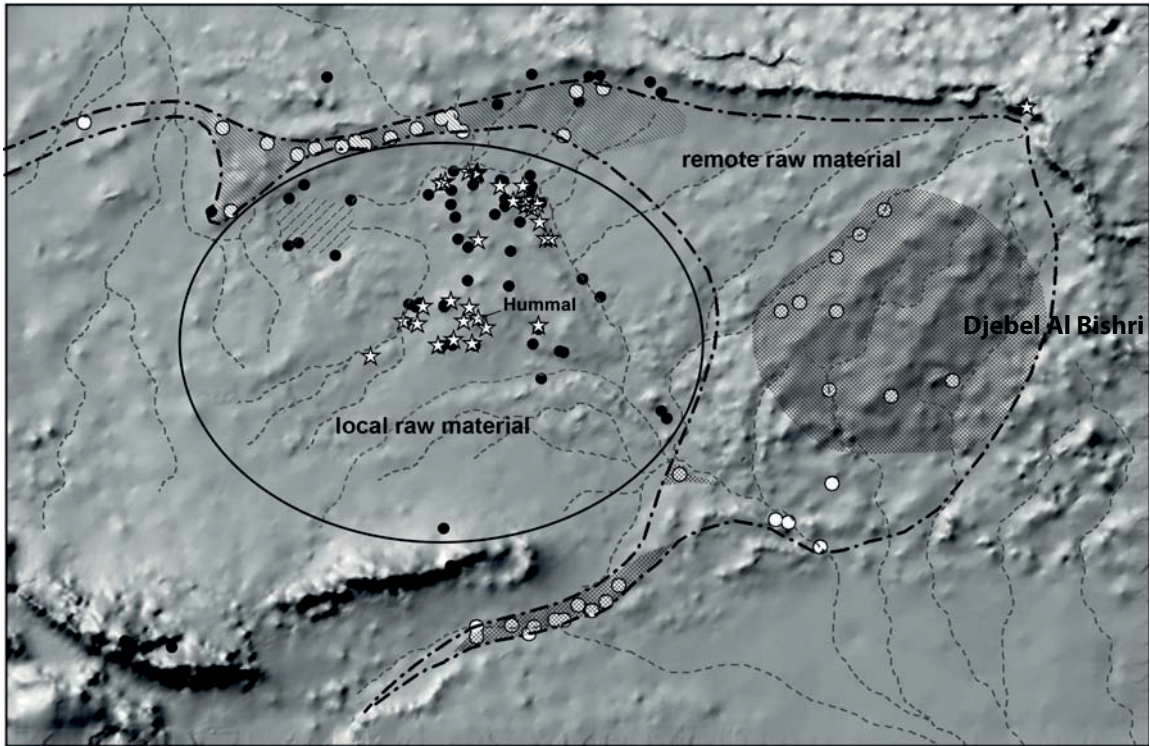


Fig. 11: Location of excavation surfaces (2000-2005 and 2009) covering the Hummalian deposits of Hummal.

Fig. 11



modified after Le Tensorer et al. 2001



0 km 10 km 20 km 30 km

flint raw material and site distribution in the El Kowm area

-  local raw material in secondary position
-  potential spread of primary raw material
-  rich flint outcrops
-  scarce flint outcrops
-  sites related to raw material source
-  spring sites
-  open air sites



Fig. 12: Availability of flint raw material and site distribution in the region of El-Kowm.

Fig. 12

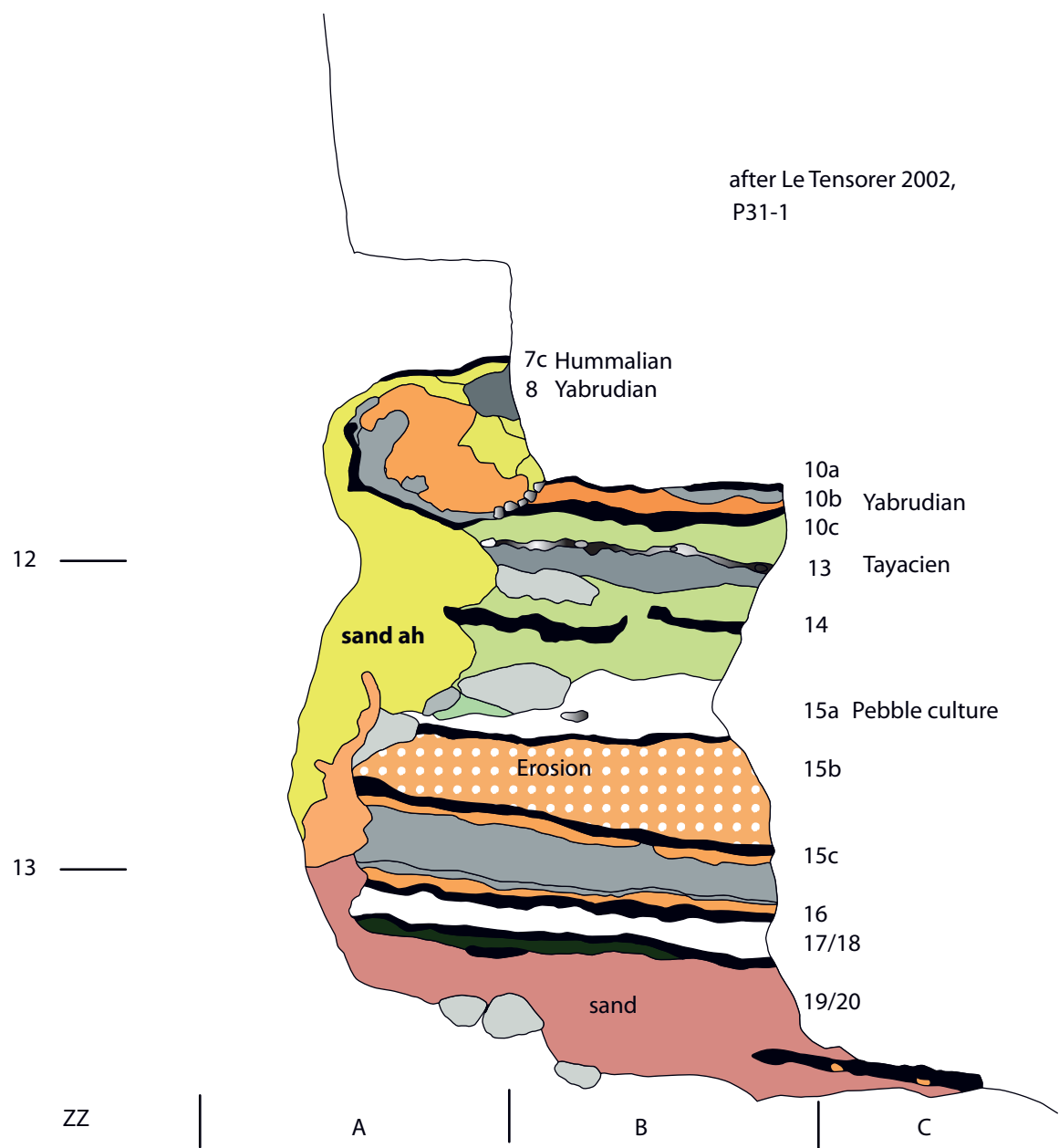


Fig. 13: Profiles documenting stratigraphical position of sand ah between layers 8 and 7c.

Fig. 13

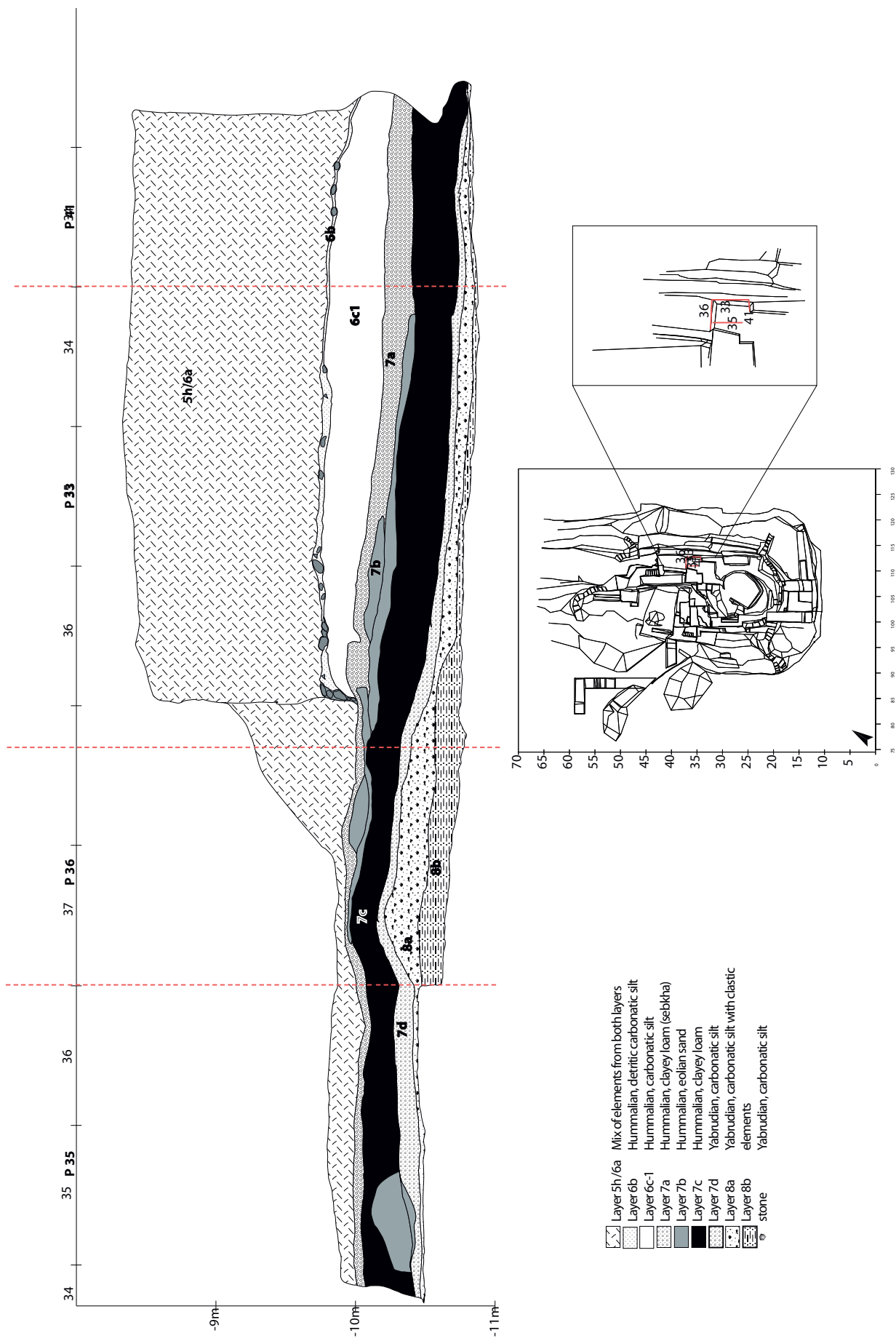


Fig. 14: Compilation of profiles 33, 35, 36 and 41 documenting the part of Hummlian sequence in the Western section of Hummal.

Fig. 14

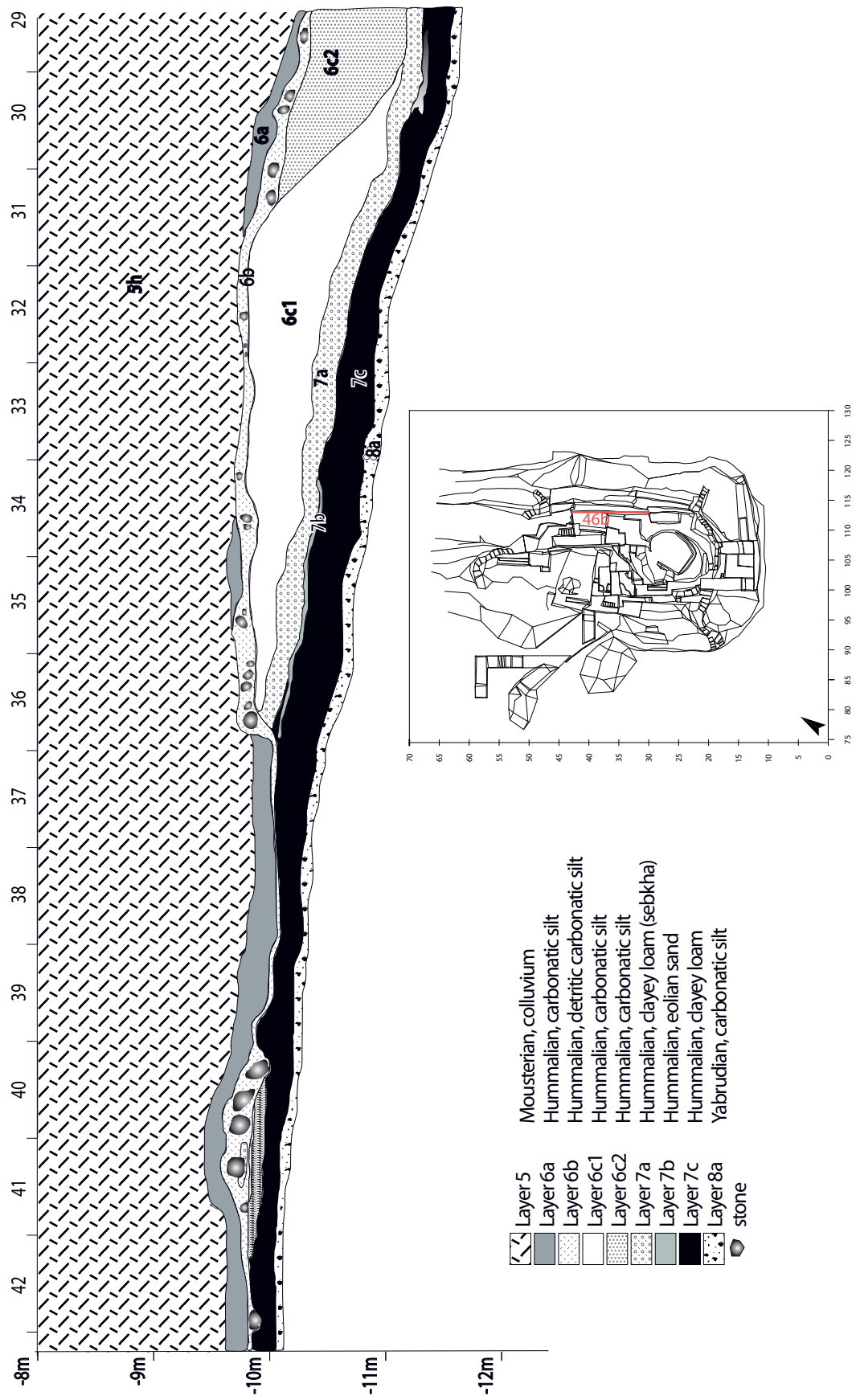


Fig.15

Fig. 15: Profile 46b documenting the part of Hummalian sequence in the Eastern section of Hummal.

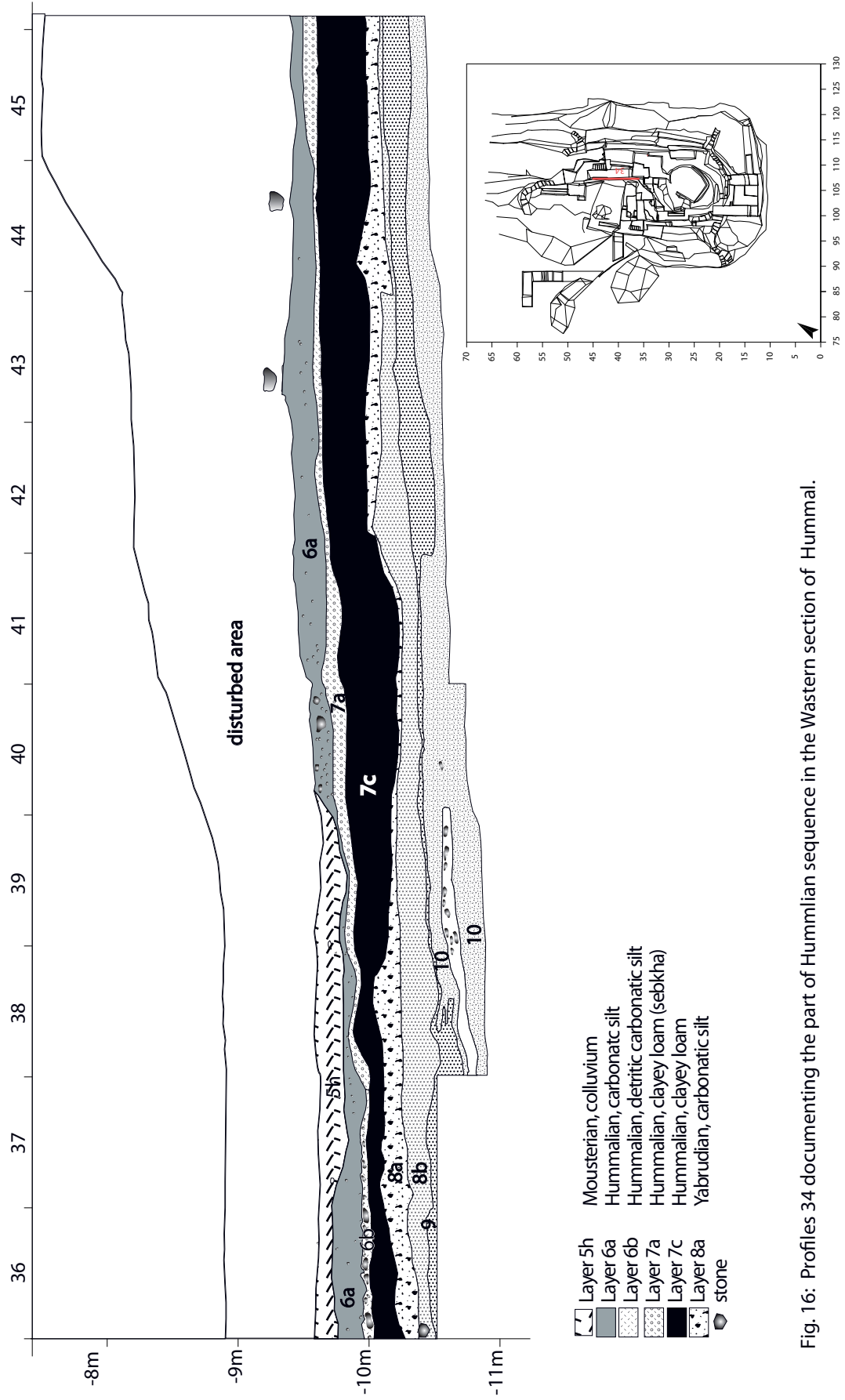


Fig.16

Fig. 16: Profiles 34 documenting the part of Hummalian sequence in the Western section of Hummal.

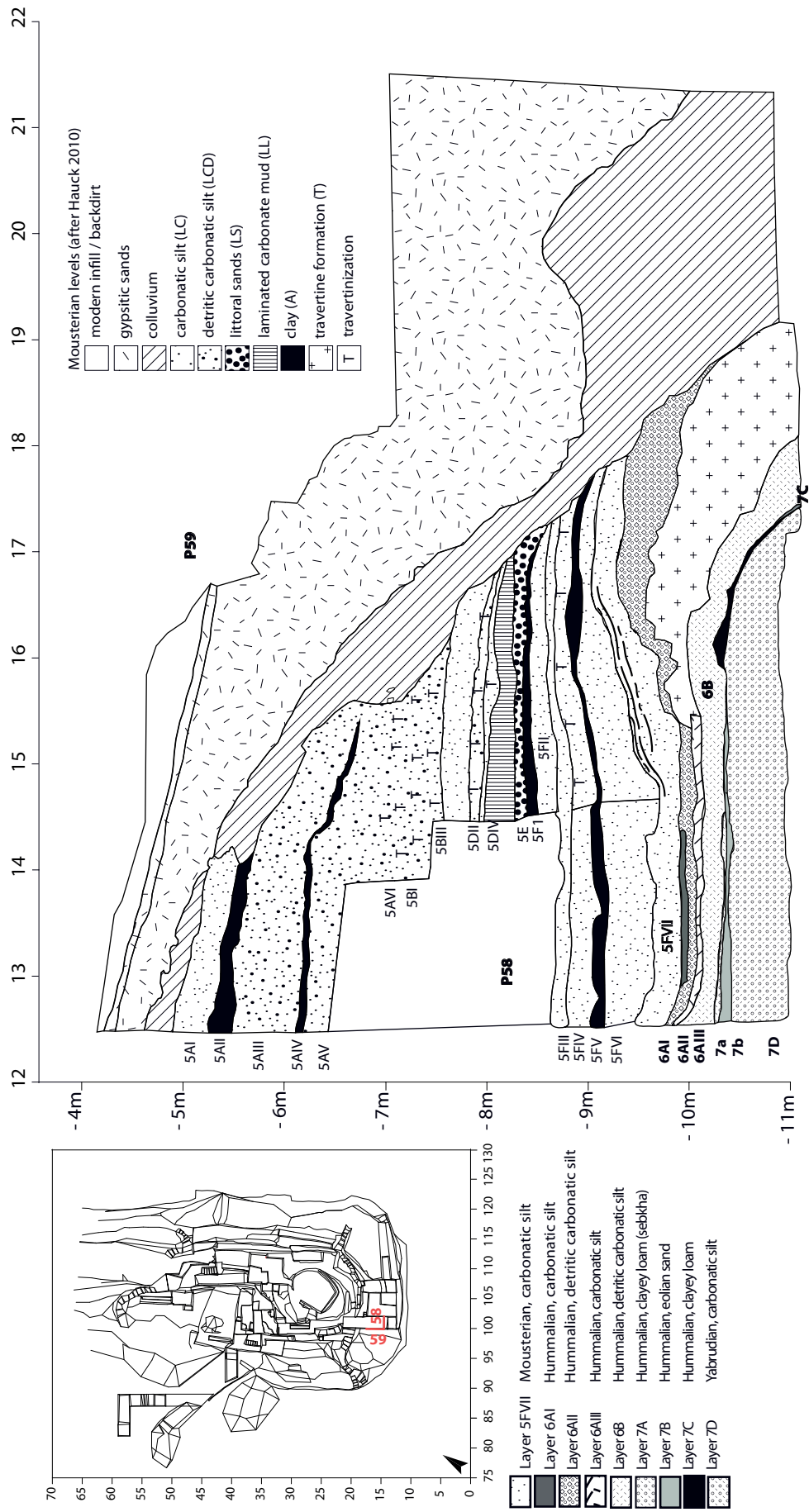
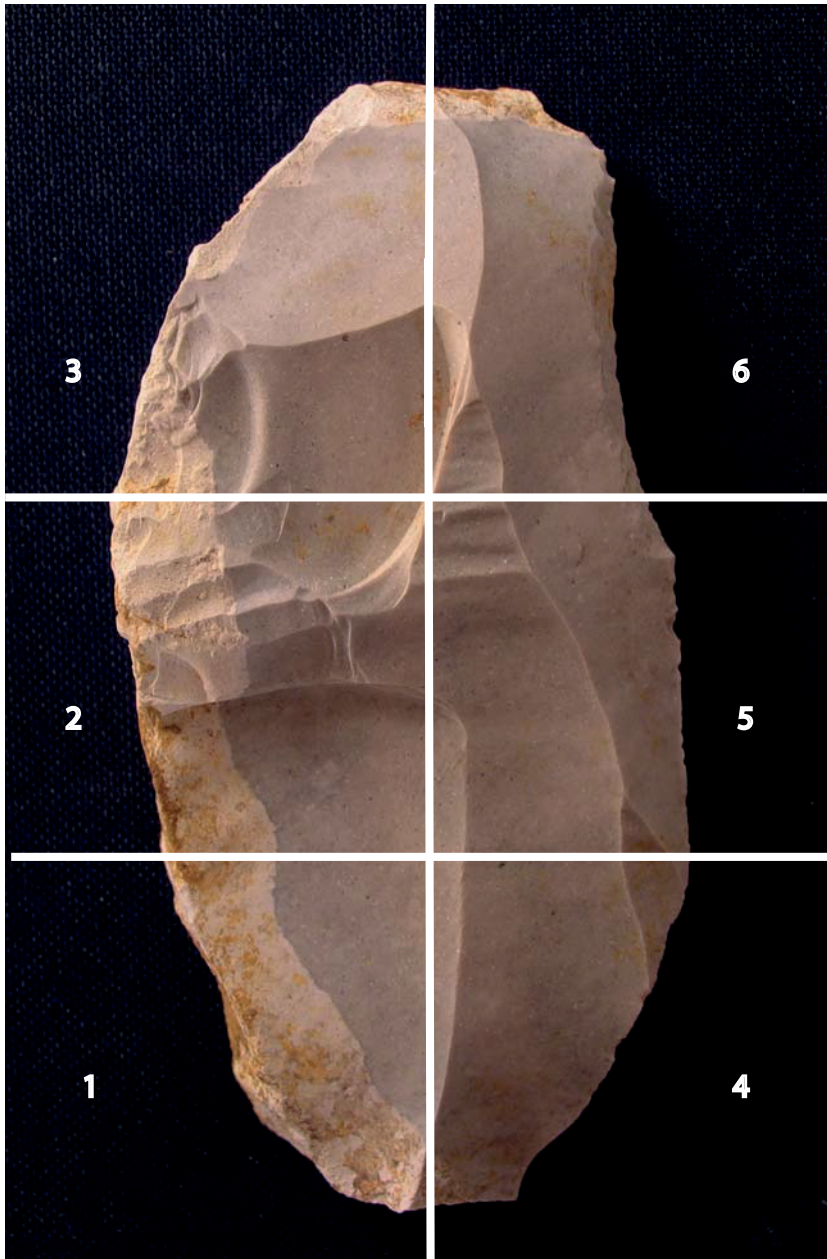


Fig. 17: Profiles 58 and 59 documenting the Hummalian South sequence.

Fig.17



1. Proximal left
2. Medial left
3. Distal left

4. Proximal right
5. Medial right
6. Distal right

Fig. 18: Partition on sectors for determining the location -of cortex and edge damage.

Fig. 18

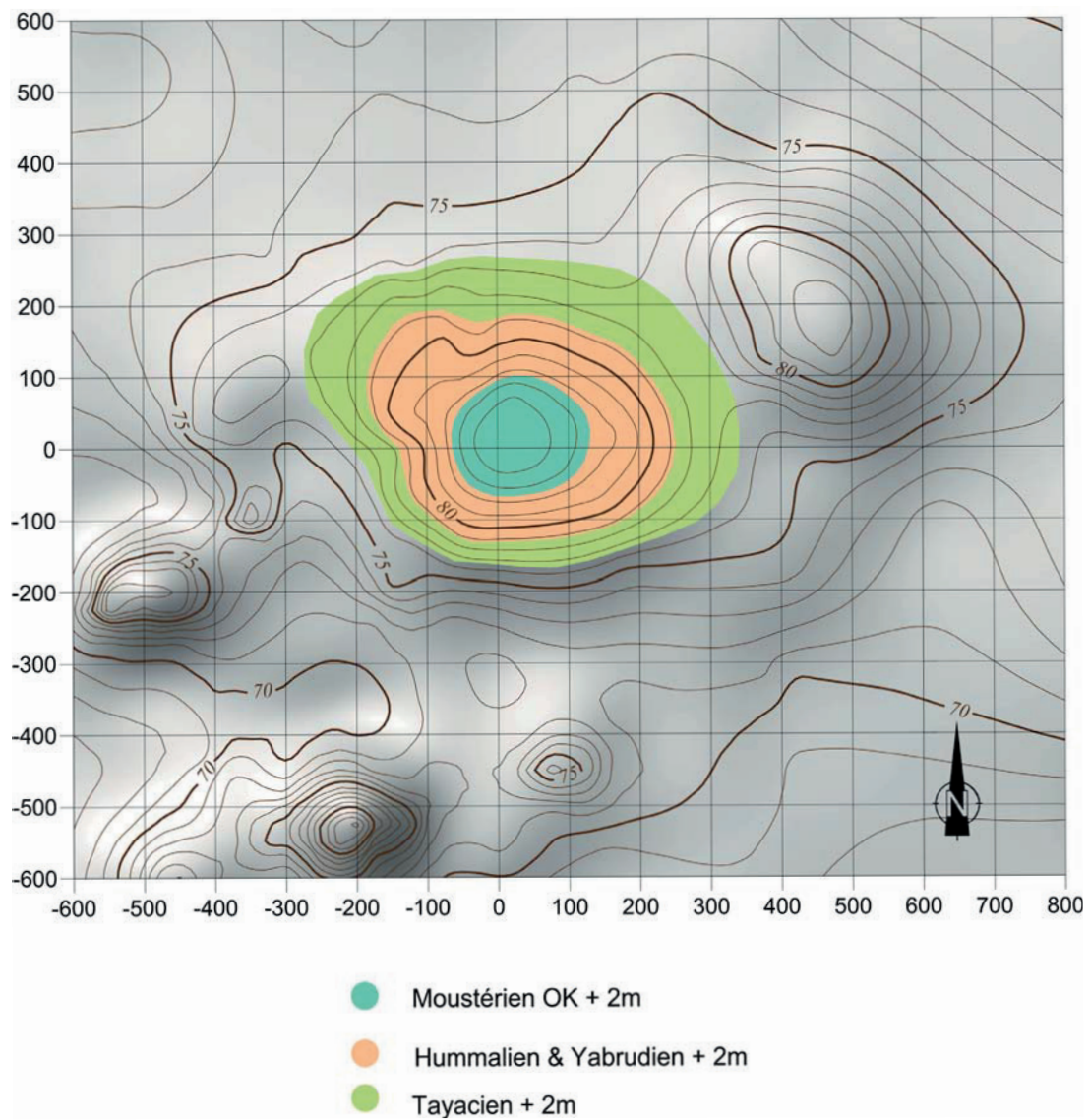


Fig. 19: Estimation of Moustérien, Hummalien-Yabrudien and Tayacien surface occupations in Hummal (after Jagher 2003/2004).

Fig.19

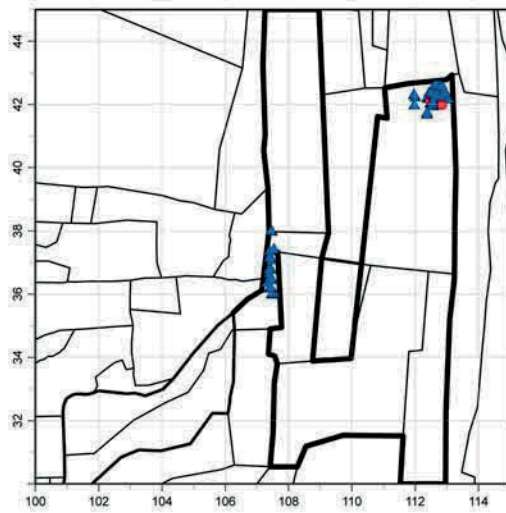
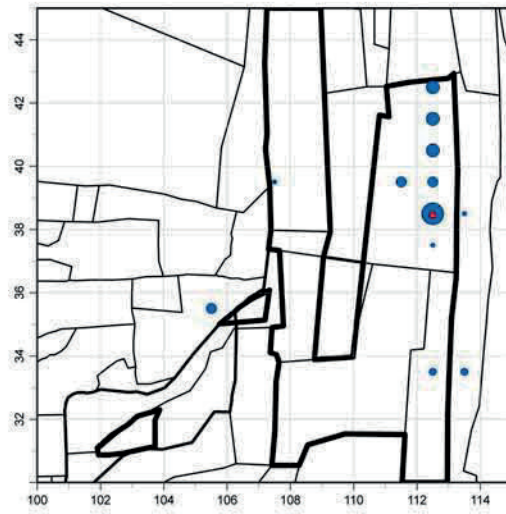


Fig. 20: Horizontal distribution of artefacts in Layer 6a.

Fig. 20

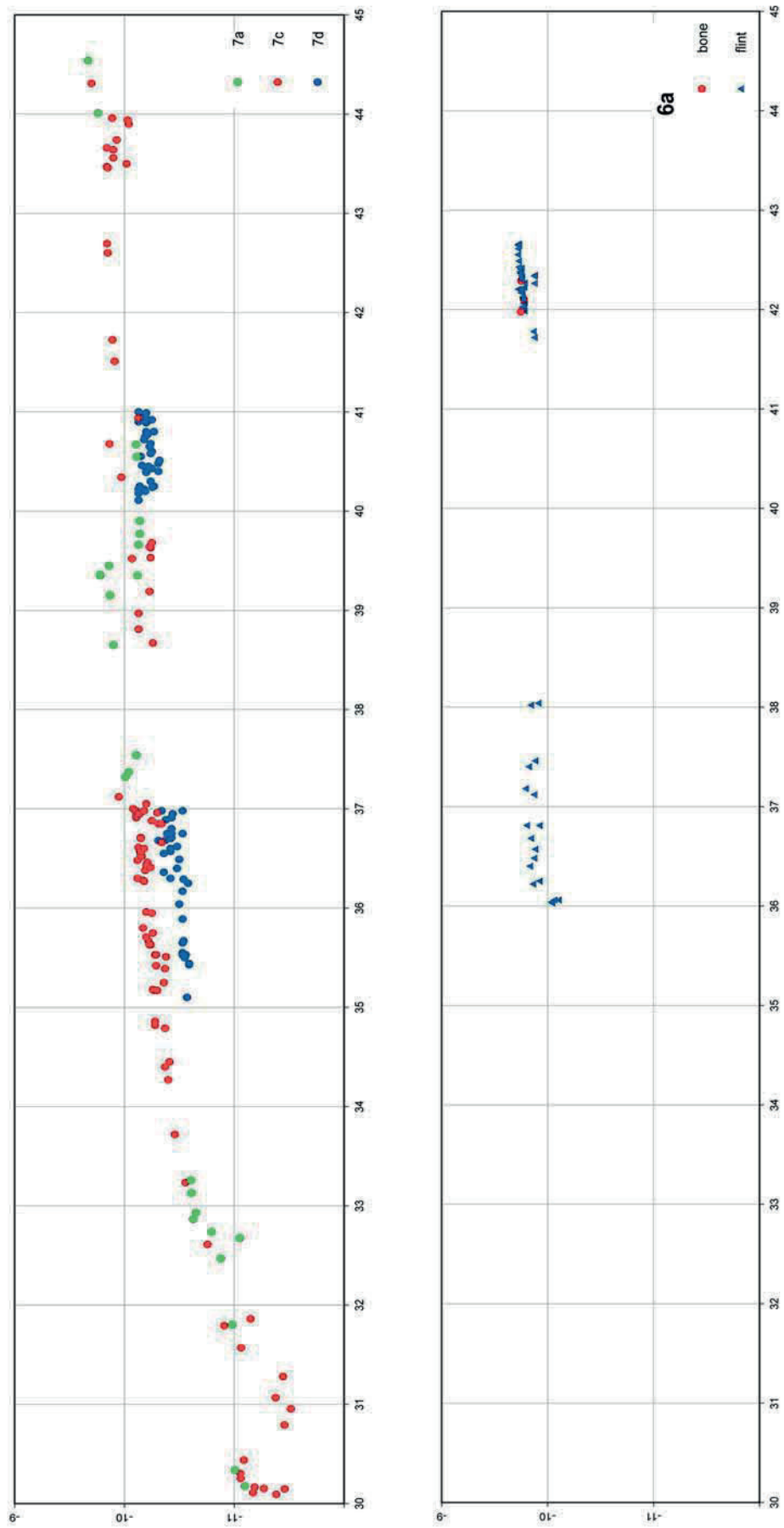


Fig. 21: Vertical distribution of artefacts in Layer 6a and 7a, 7c, 7d.

Fig.21

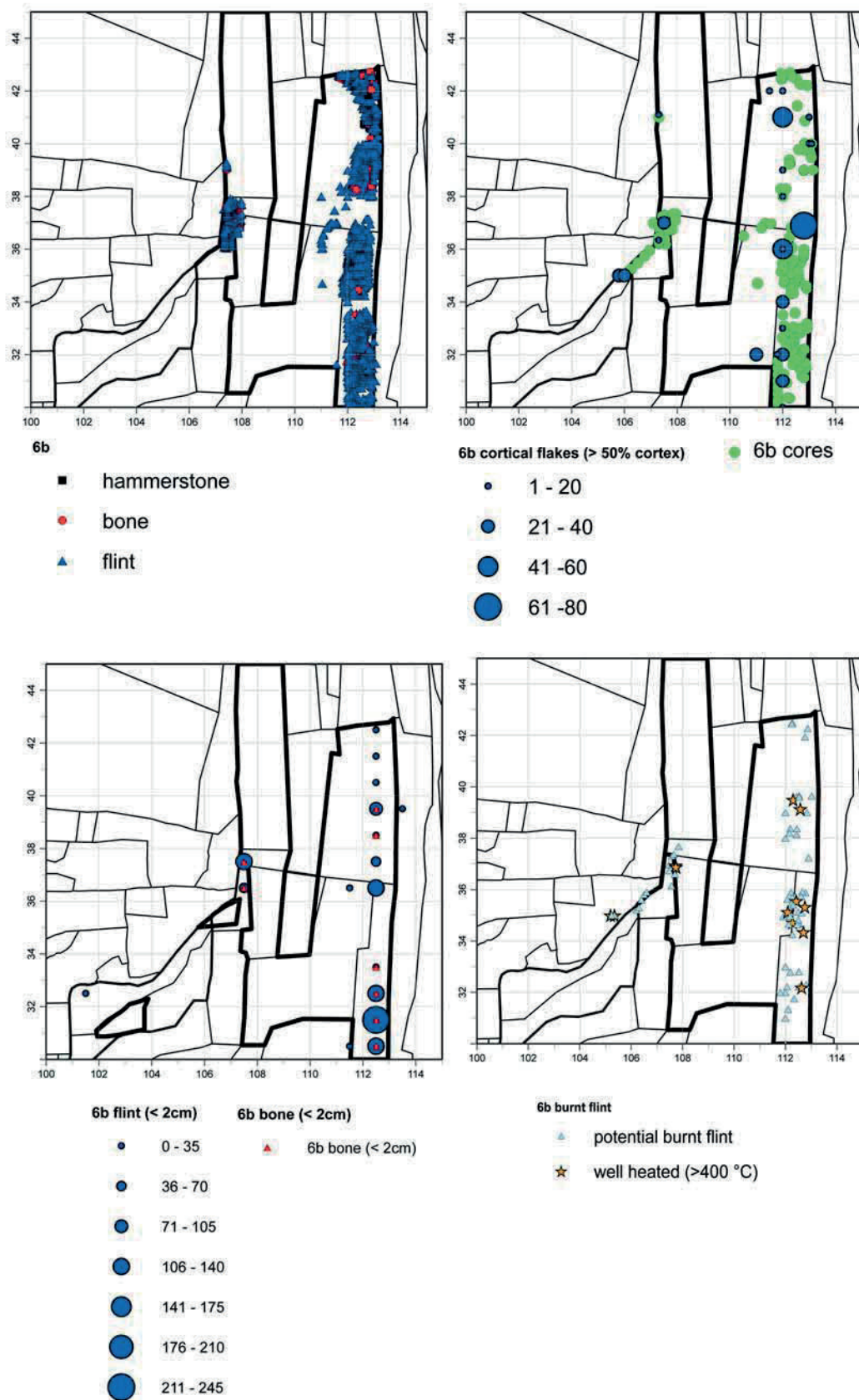


Fig. 22: Horizontal distribution of artefacts in Layer 6b.

Fig. 22

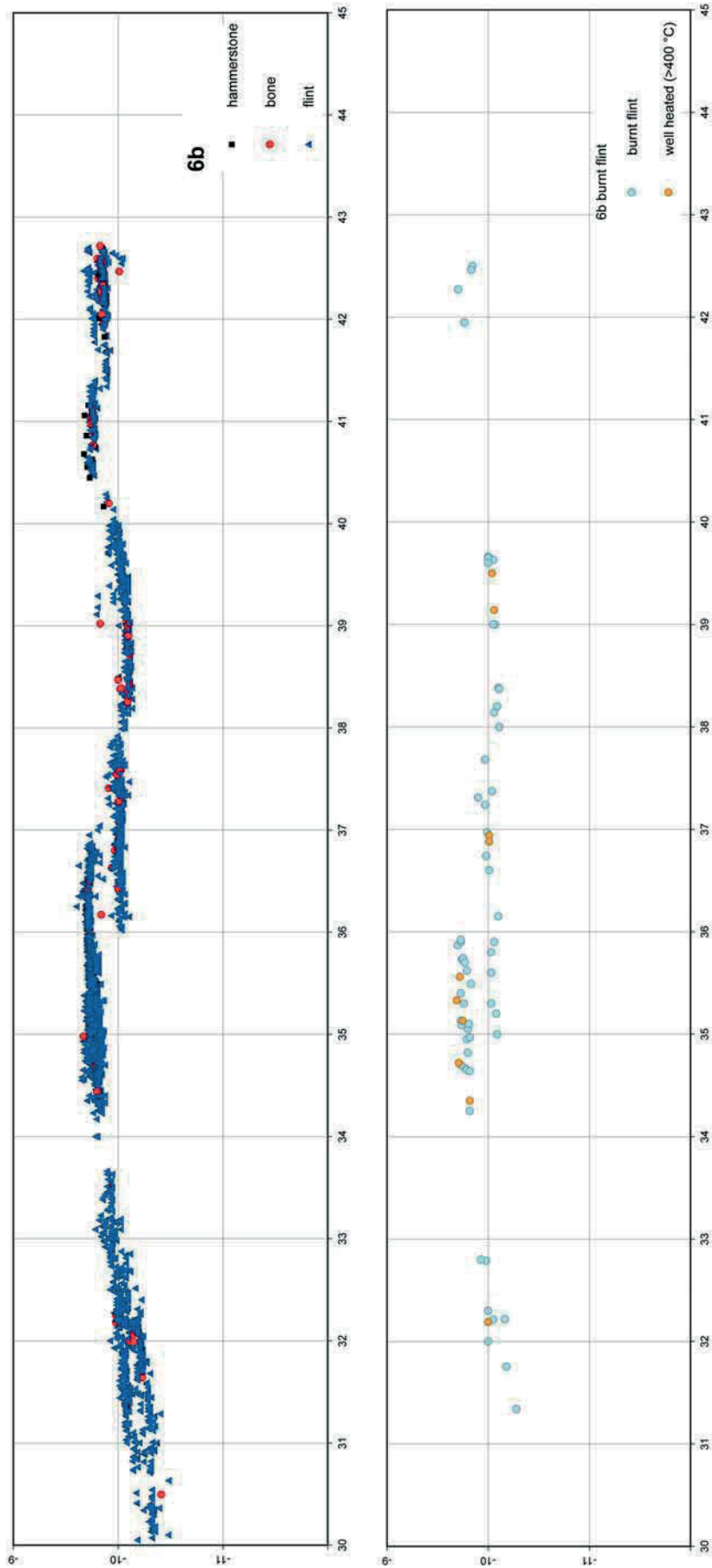


Fig. 23: Vertical distribution of artefacts in Layer 6b.

Fig.23



Fig. 24: Artefacts from layer 6b showing crushing.

Fig. 24

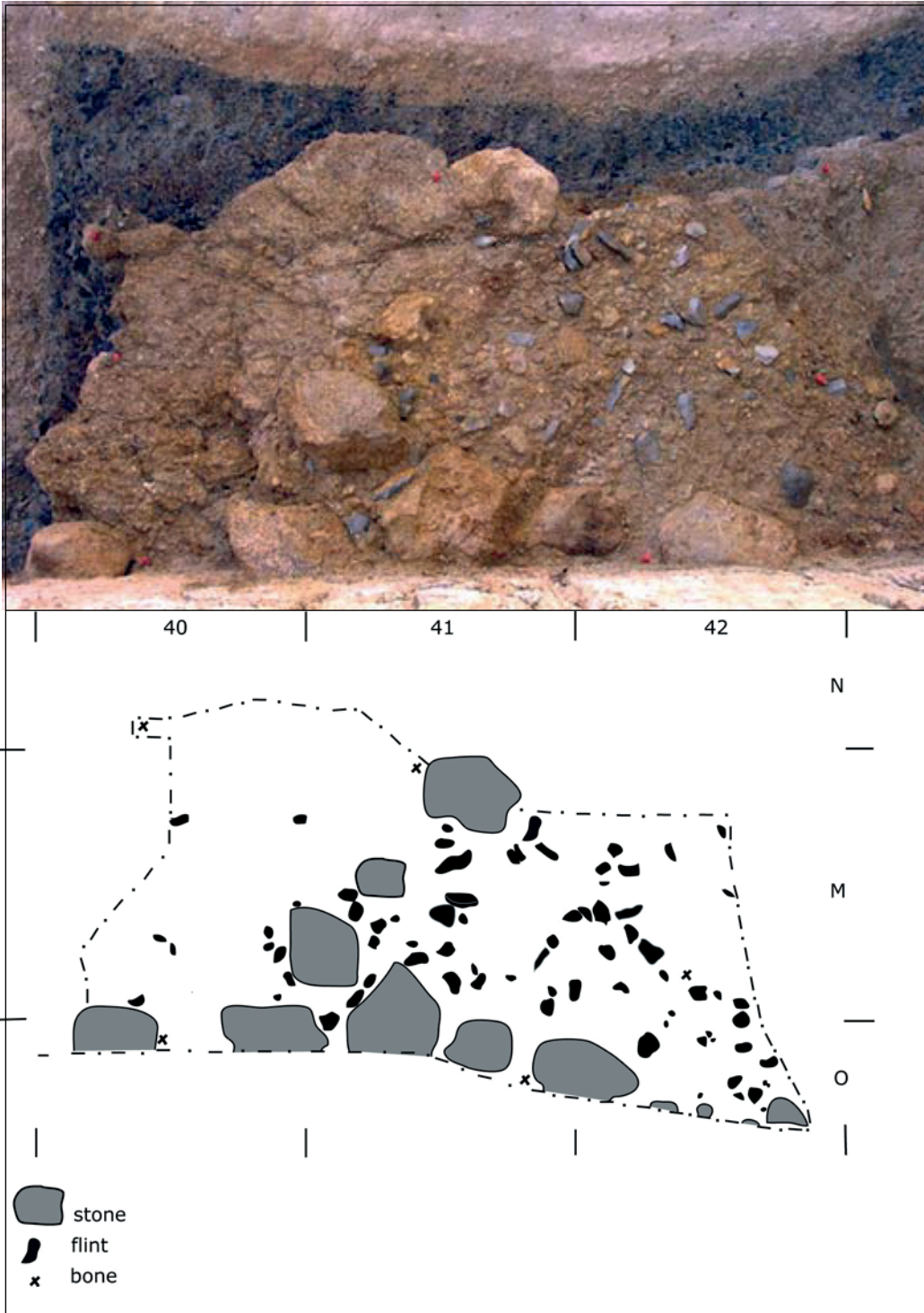


Fig. 25: Layer 6b, Manuport living floor.

Fig. 25

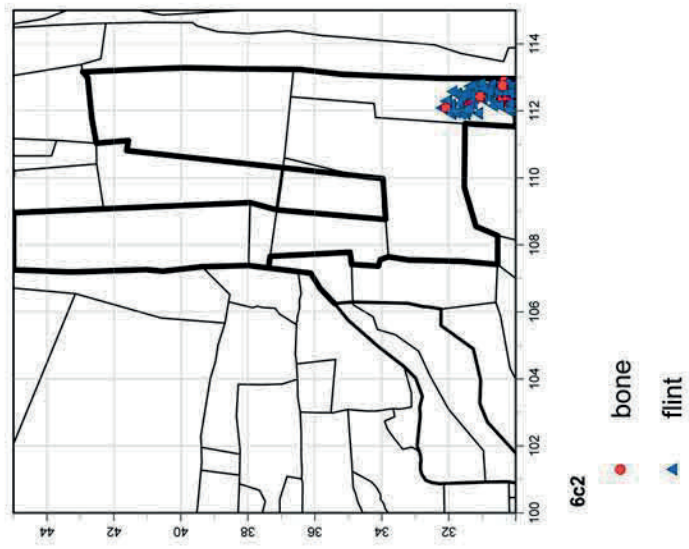


Fig. 26: Horizontal and vertical distribution of artefacts in Layer 6c2.

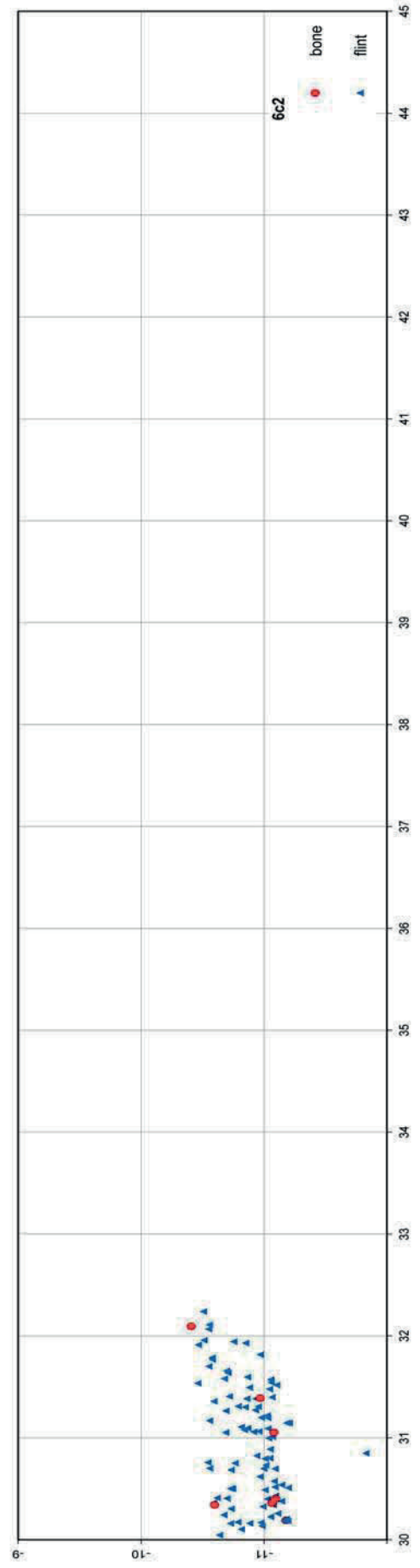
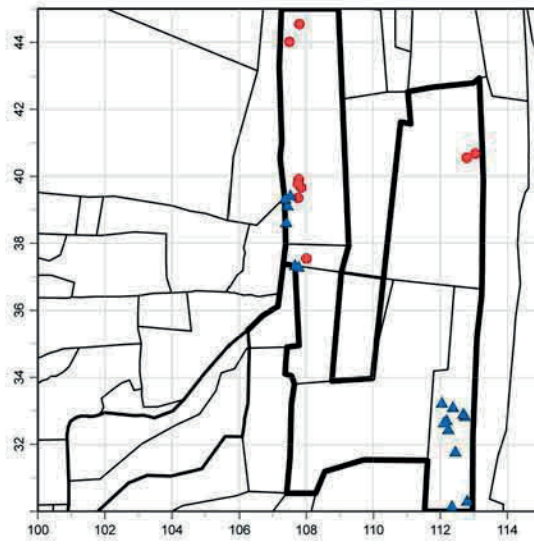
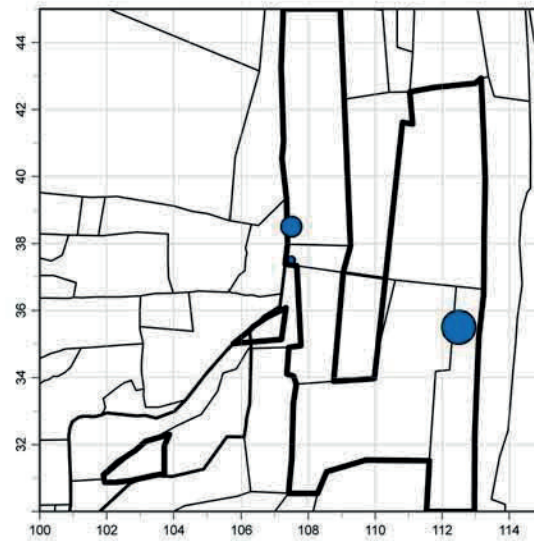


Fig. 26



7a (>2cm)

- bone
- ▲ flint

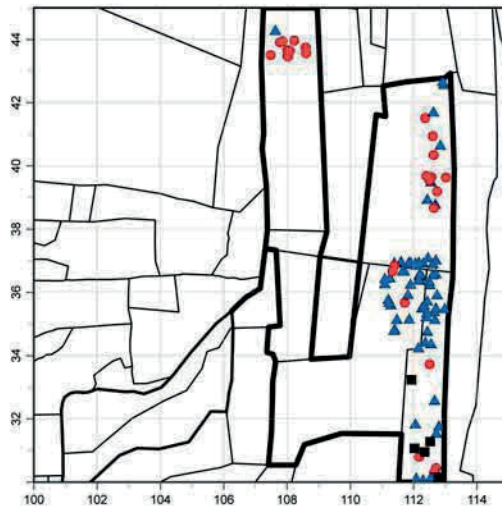


7a flint (< 2cm)

- 0-10
- 11-15
- 16-25

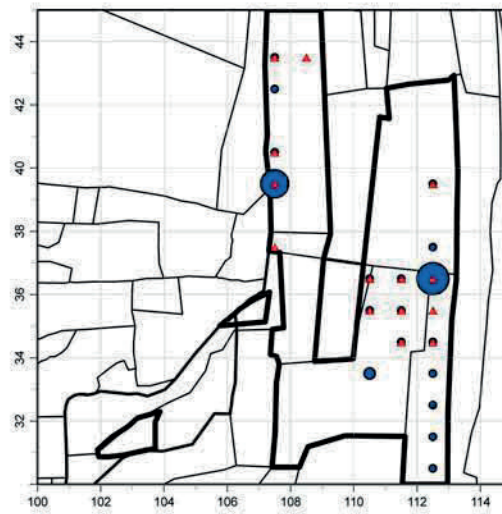
Fig. 27: Horizontal distribution of artefacts in Layer 7a.

Fig. 27



7c (>2cm)

- hammerstone
- bone
- ▲ flint



7c flint (<2cm)

▲ 7c bone (<2cm)

- 0 - 25
- 26 - 50
- 51 - 75
- 76 - 100
- 101 - 125
- 126 - 150
- 151 - 175

Fig. 28: Horizontal distribution of artefacts in Layer 7c.

Fig. 28



Fig. 29: Debitage workshop discovered in layer 7c.

Fig. 29



Fig. 30: Glossy flint from sand layer h.

Fig. 30

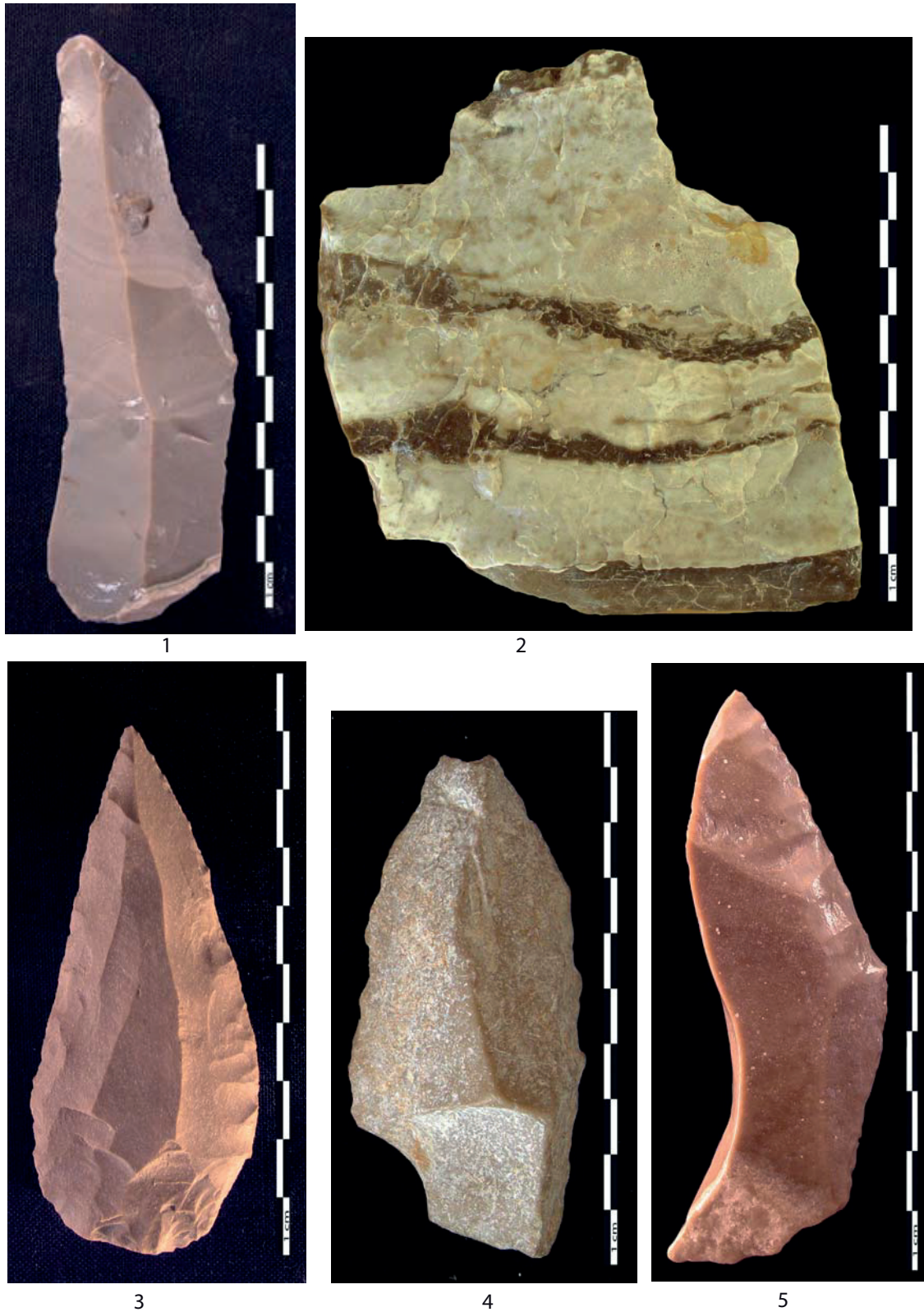


Fig. 31: Artefacts from layers 6b and sand h made on Cretaceous flint and on limestone.
1- blade made on Cretaceous flint ; 2-bloc of Cretaceous flint
3, 4, 5- blades made on limestone .

Fig. 31

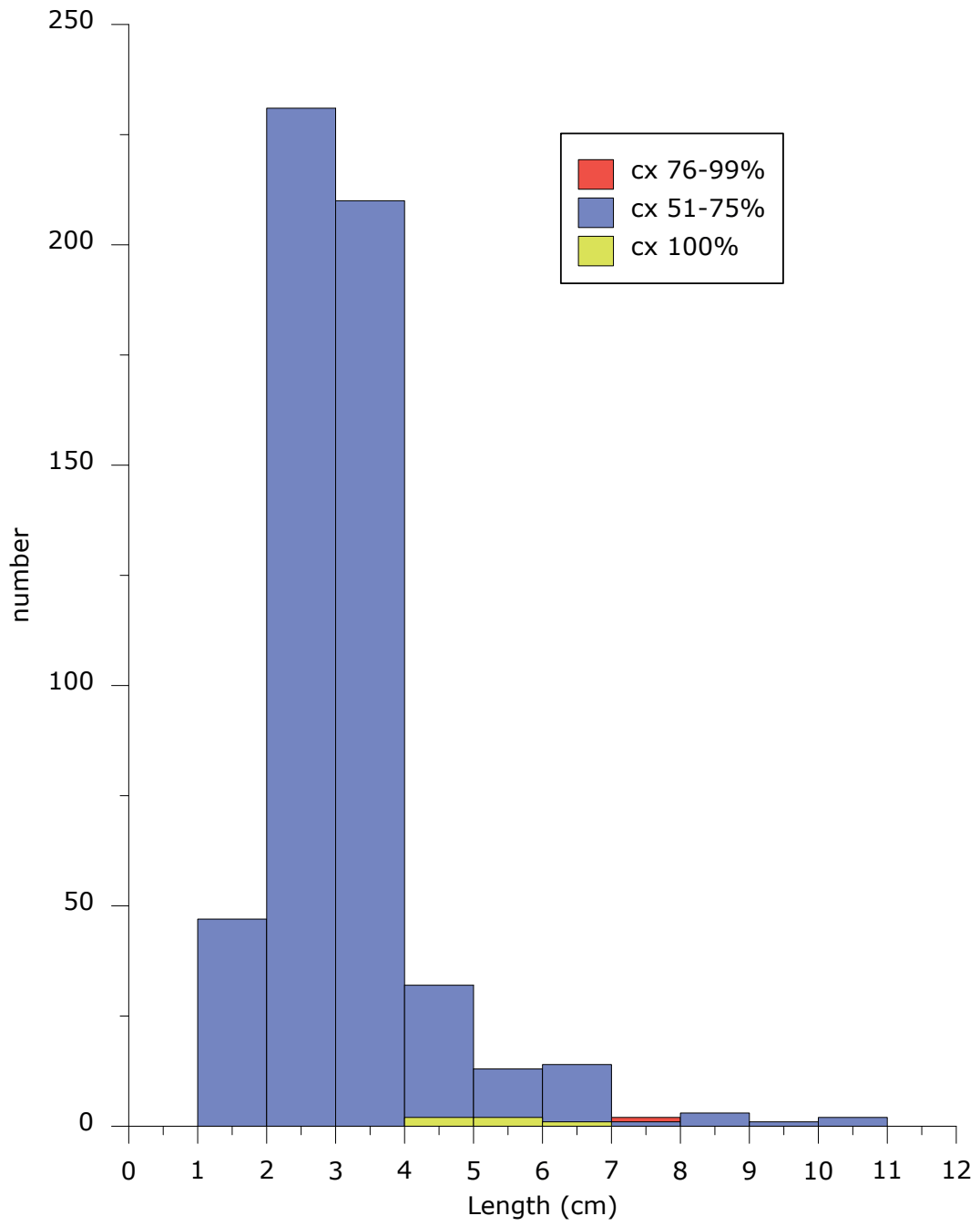


Fig. 32: Length of cortical elements in layer 6b.

Fig. 32

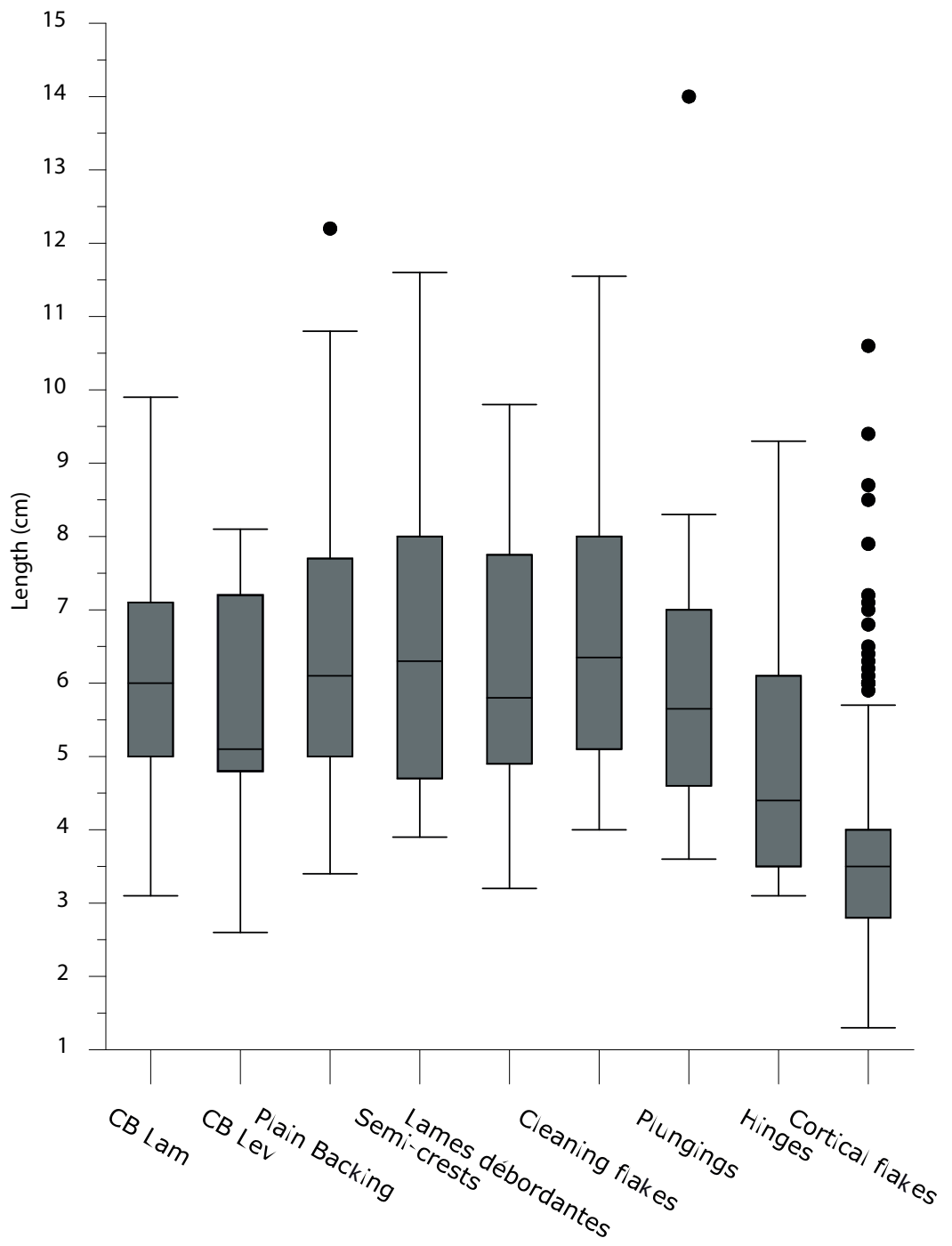


Fig. 33: Length of CTE from layer 6b.

Fig. 33

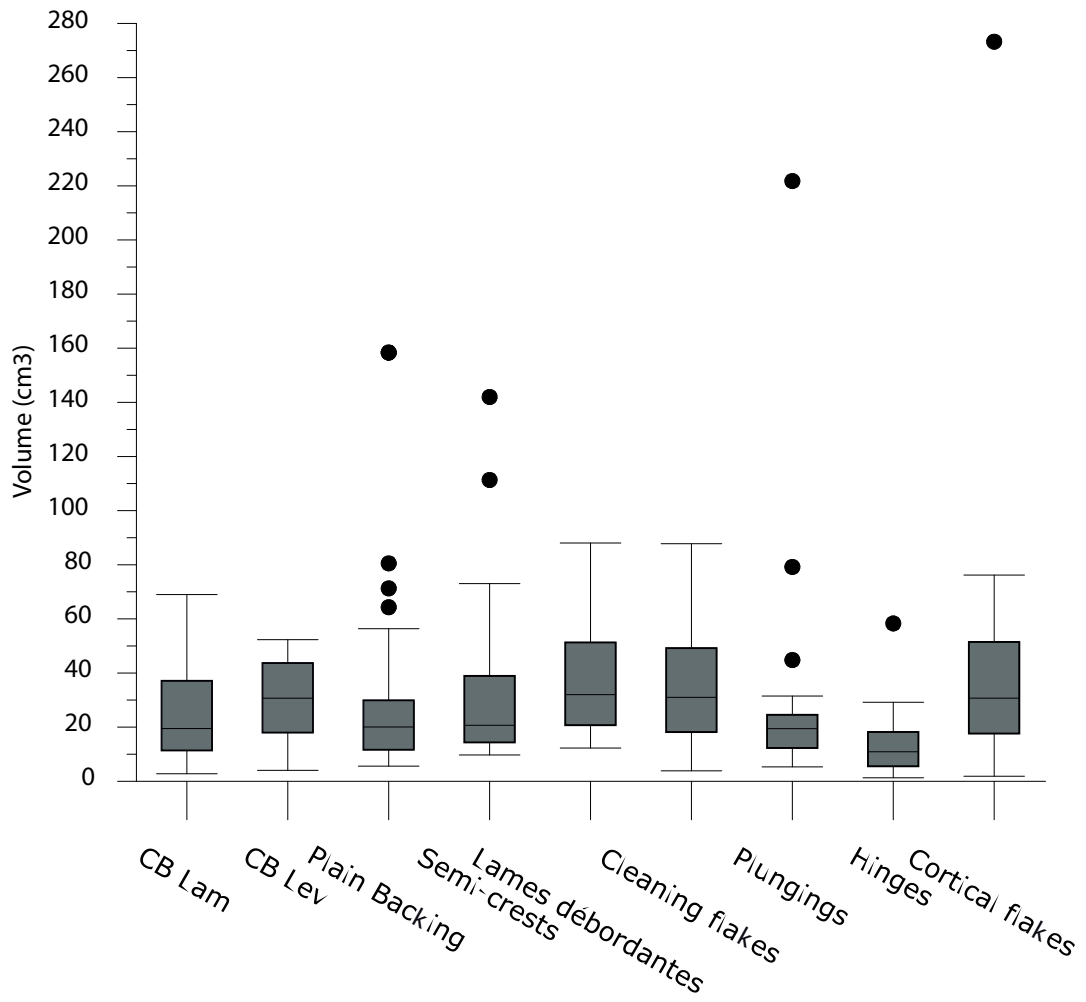


Fig. 34: Volume of CTE from layer 6b.

Fig. 34

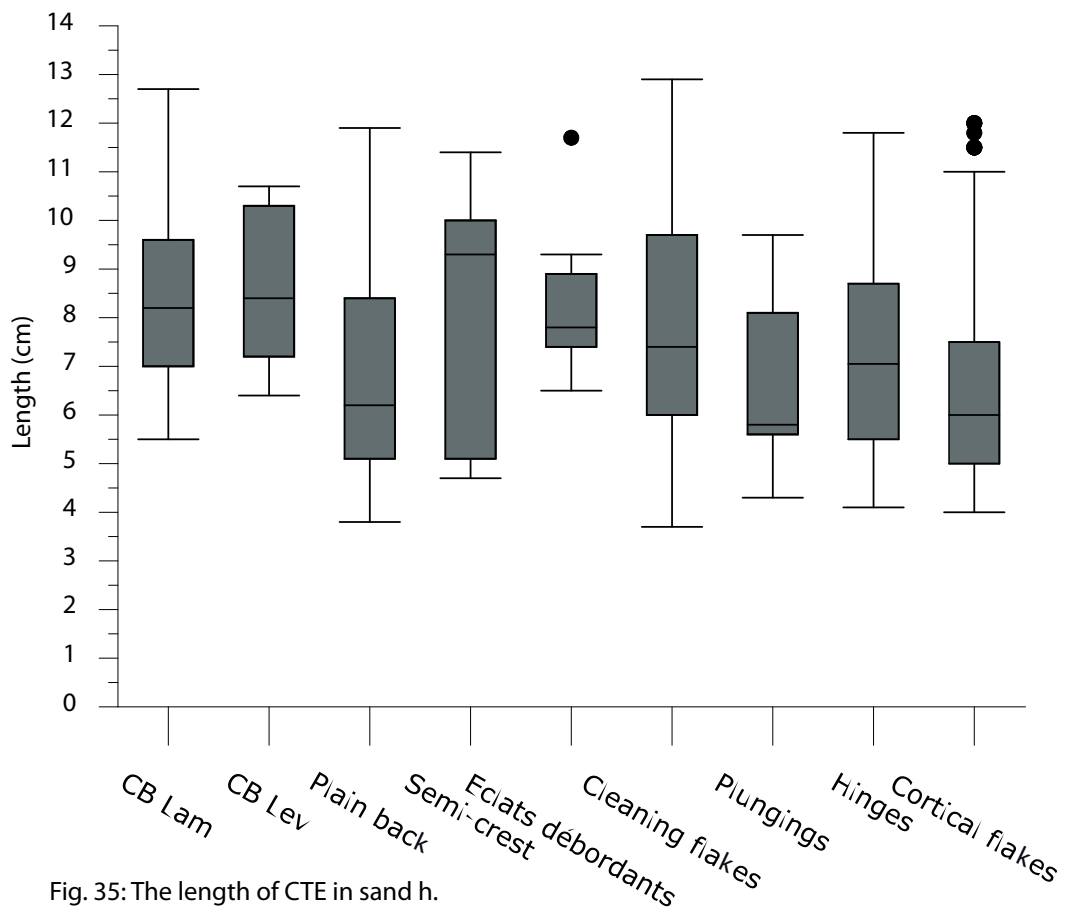


Fig. 35: The length of CTE in sand h.

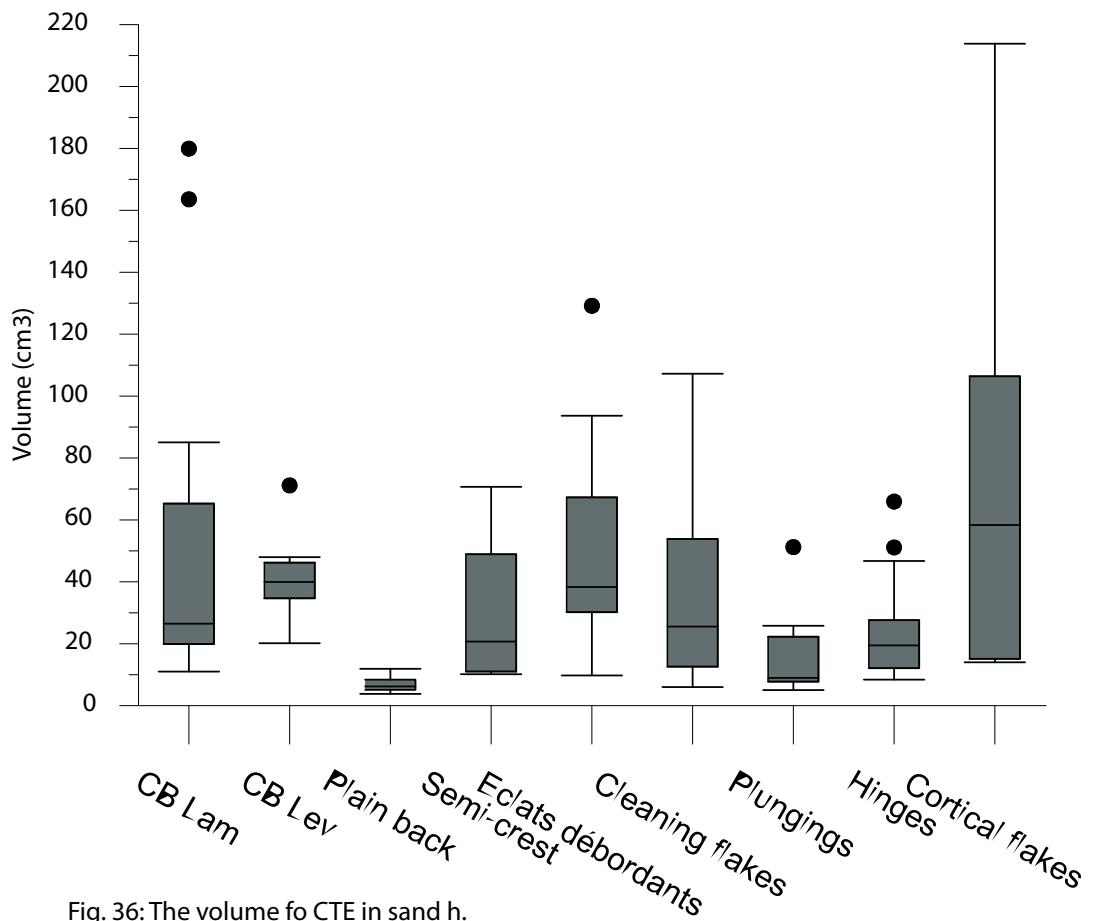


Fig. 36: The volume fo CTE in sand h.

Fig. 35, 36

Plot Group Means with 95% Confidence Intervals

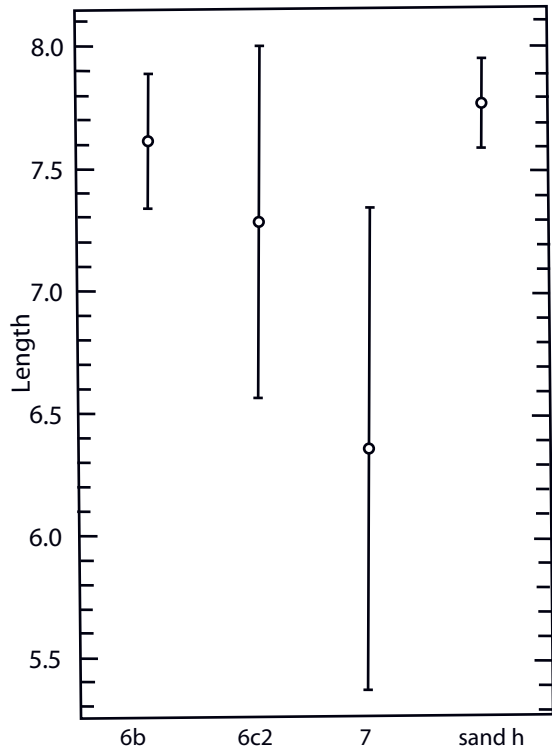


Fig. 37: Central tendency in length of blank blades.

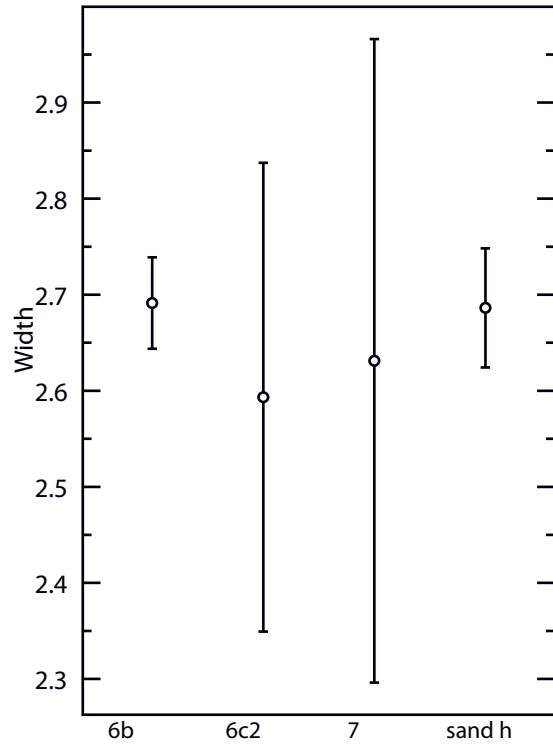


Fig. 40: Central tendency in width of blank blades.

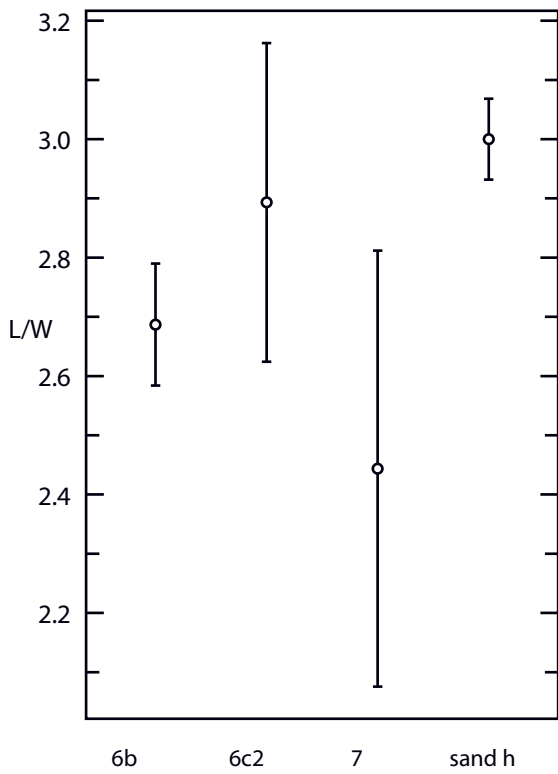


Fig. 42: Central tendency in ratio L/W of blank blades

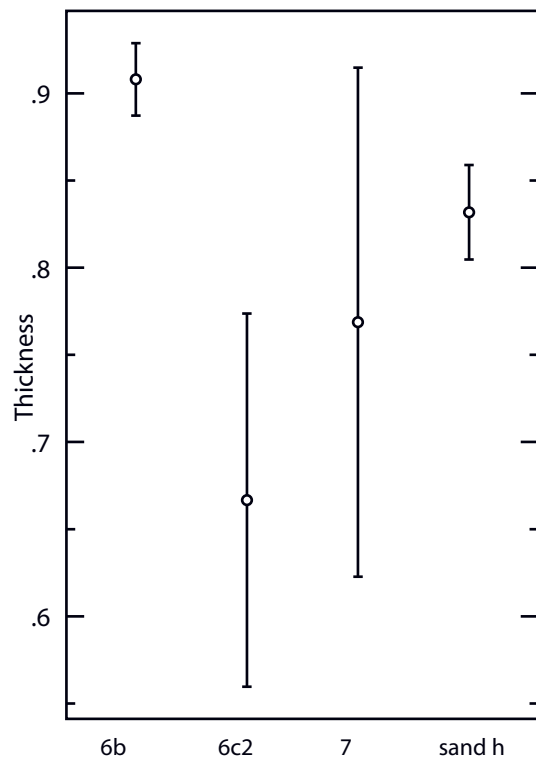


Fig. 44: Central tendency in thickness of blank blades.

Fig. 37, 40, 42, 44

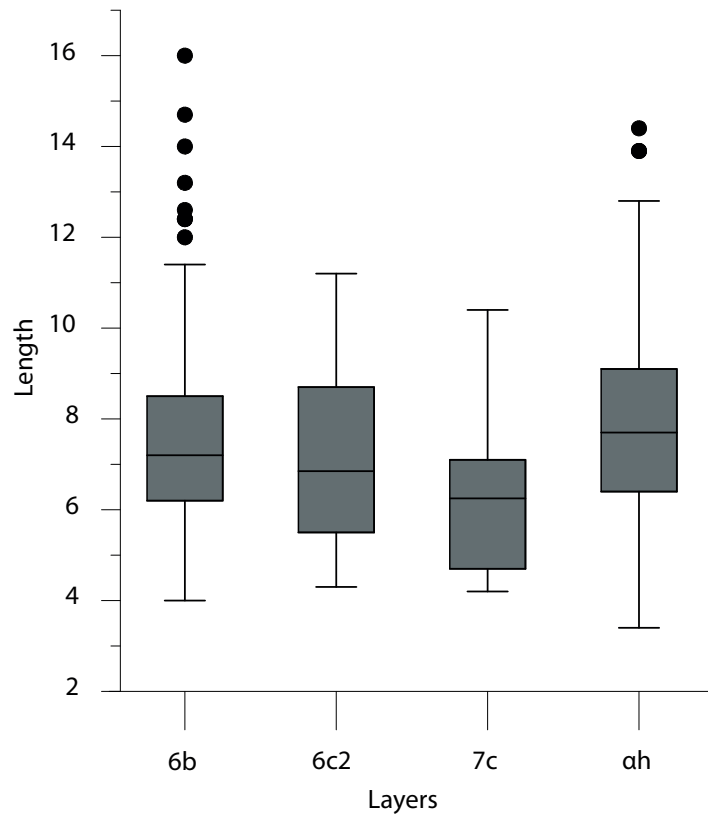


Fig.38: Length of intact, unretouched blank-blades in layers 6b, 6c2, 7c and sand ah.

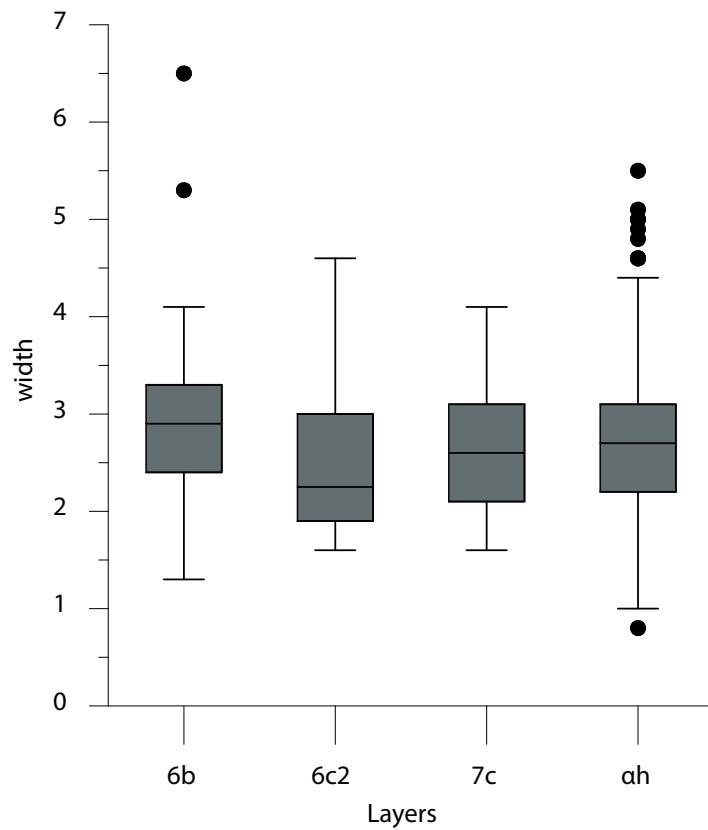


Fig. 39: Width of intact, unretouched blank-blades in layers 6b, 6c2, 7c and sand ah.

Fig. 38, 39

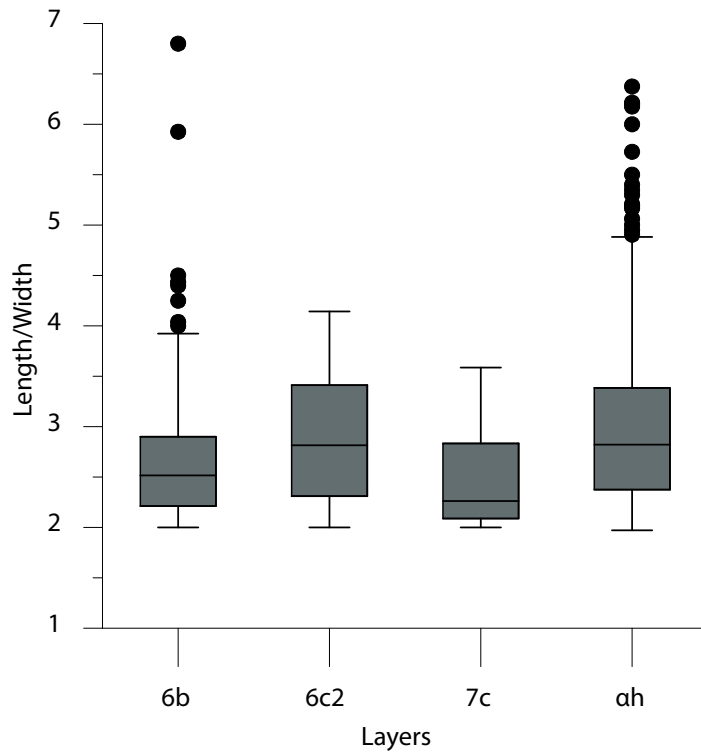


Fig. 41: Ratio L/W of intact, unretouched blank-blades from layers 6b, 6c2, 7c and sand ah.

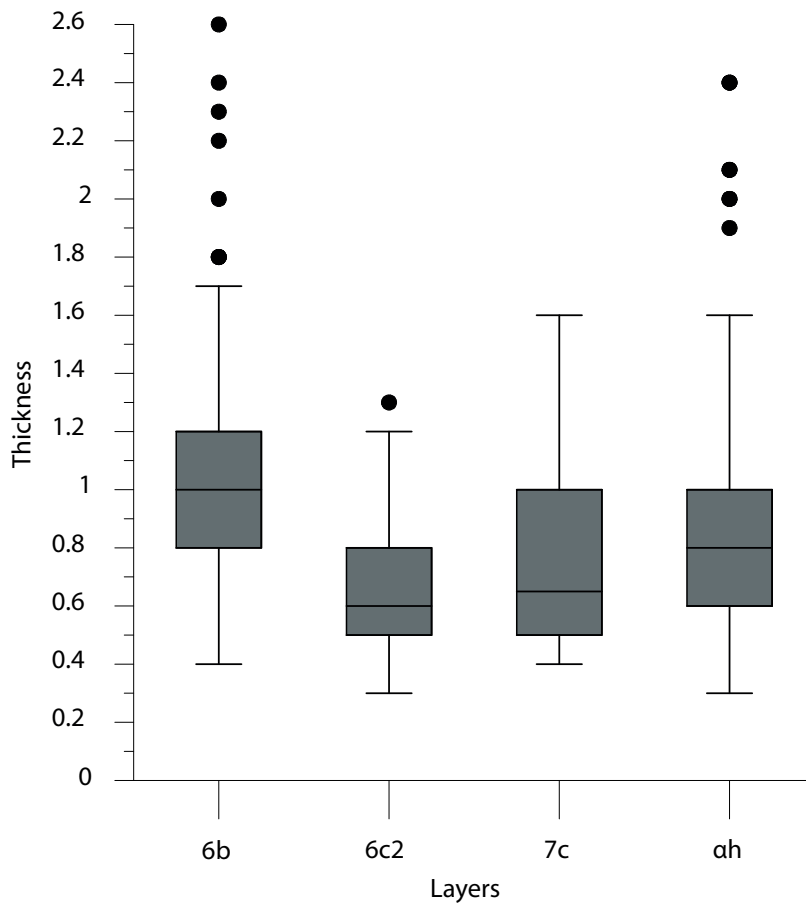


Fig. 43: Thickness of intact, unretouched blank-blades in layers 6b, 6c2, 7c and sand ah.

Fig. 41, 43

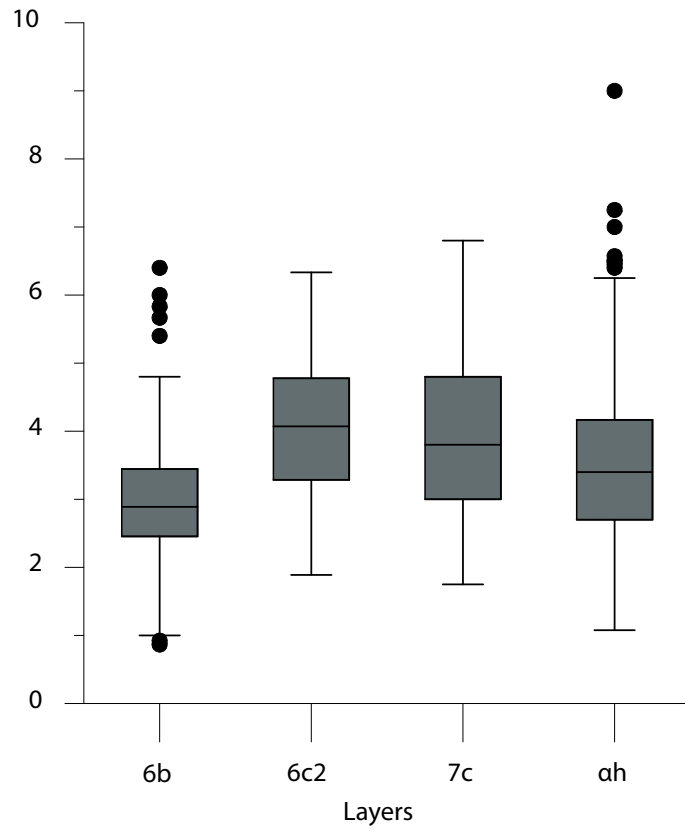


Fig. 45: Ratio W/T of intact, unretouched blank-blades in layers 6b, 6c2, 7c and sand ah.

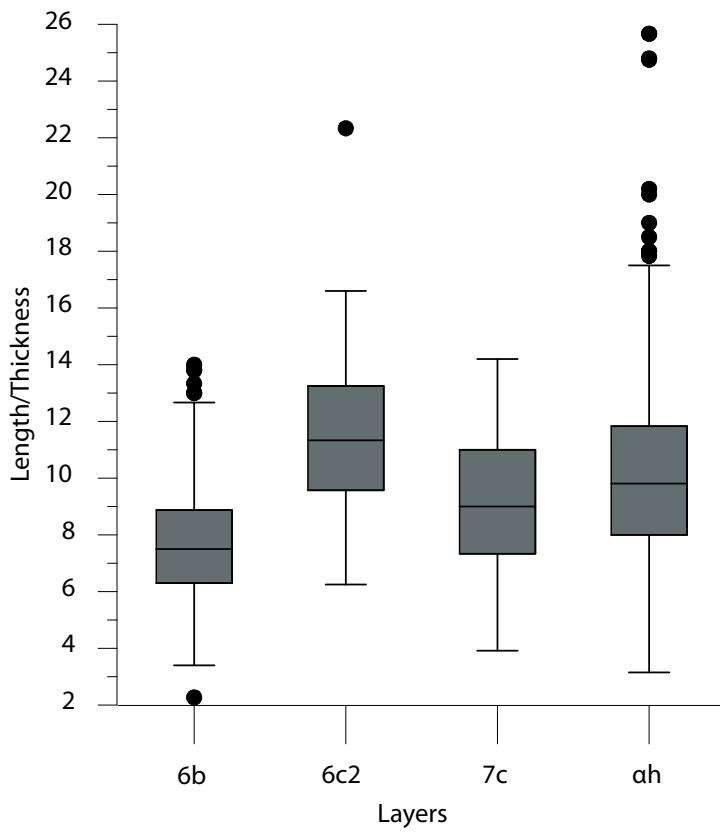


Fig. 47: Ratio Length/Thickness of intact, unretouched blank-blades from layers 6b, 6c2, 7c and sand ah.

Fig. 45, 47

Plot Group Means with 95% Confidence Intervals

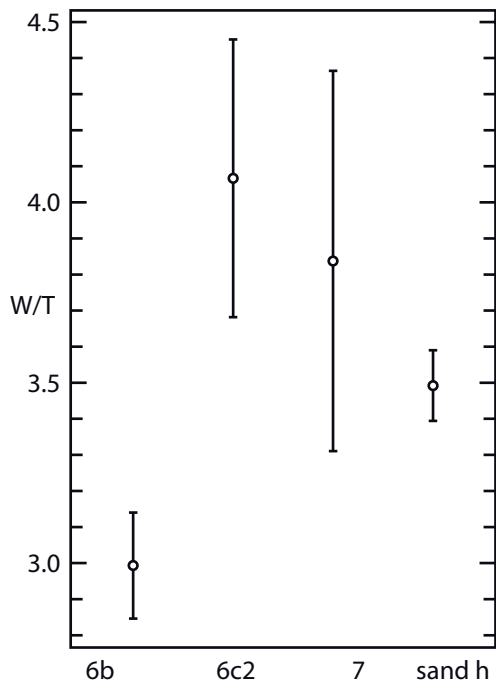


Fig. 46: Central tendency in ratio W/T of blank blades.

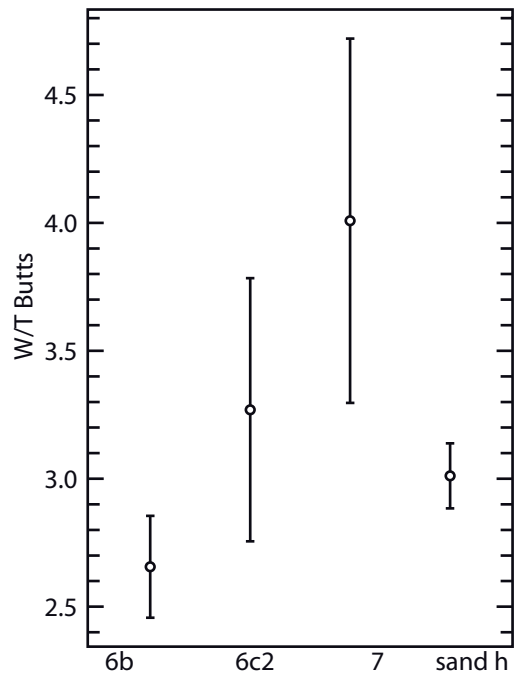


Fig. 49: Central tendency in ratio W/T of butts of blank blades.

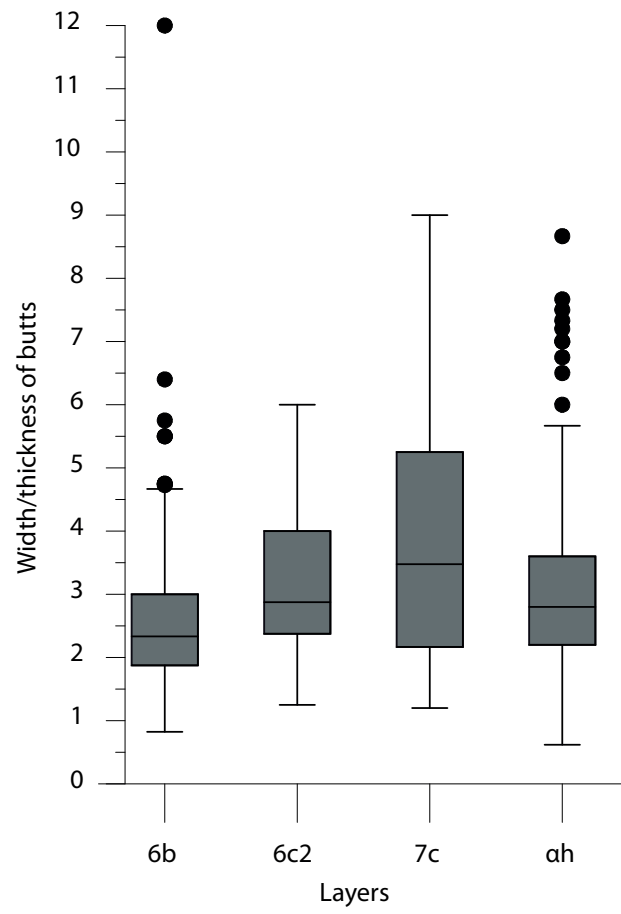


Fig. 48: Ratio W/T of butts of intact, unretouched blank-blades from layers 6b, 6c2, 7c and sand ah.

Fig. 48

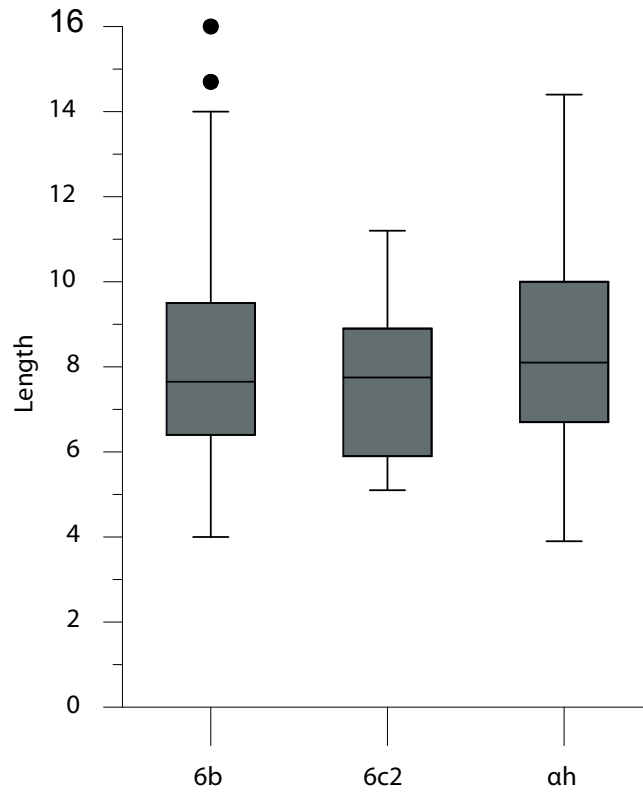


Fig. 50: Length of Laminar blanks from layers 6b, 6c2 and sand ah.

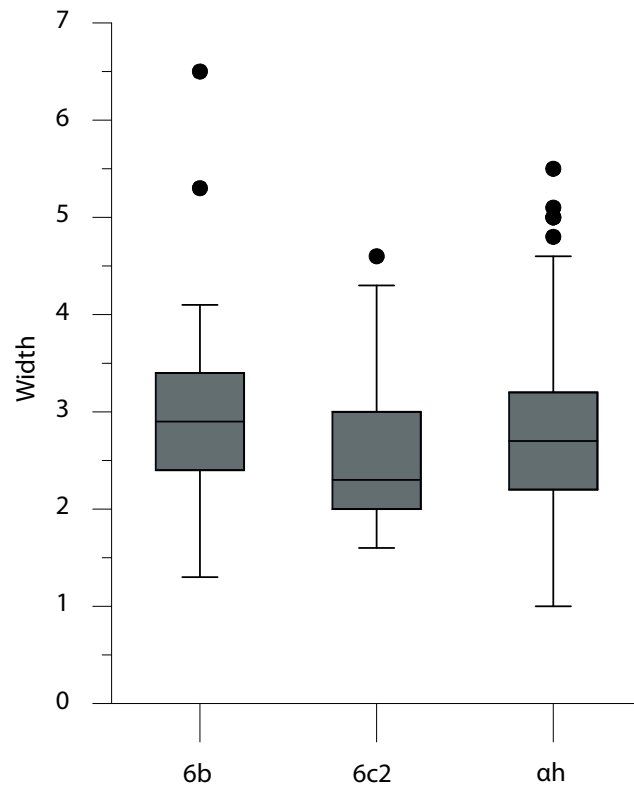


Fig. 52: Width of Laminar blank from layers 6b, 6c2 and sand ah.

Fig. 50, 52

Plot Group Means with 95% Confidence Intervals

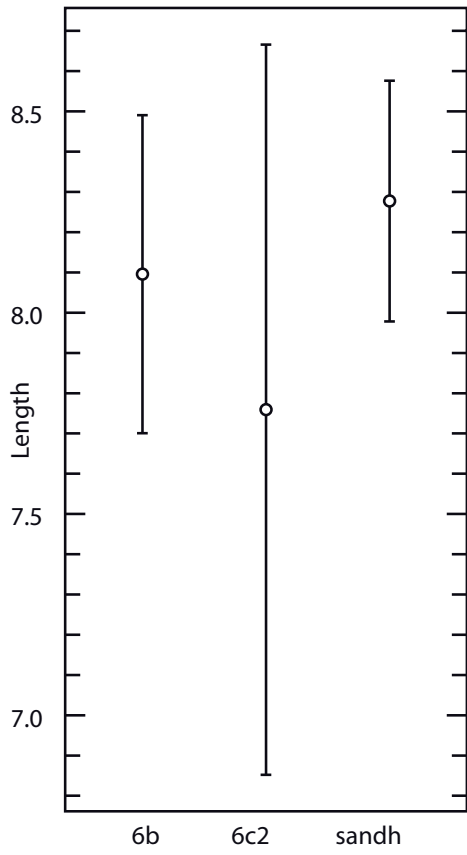


Fig. 51a: Central tendency in length of prismatic blades.

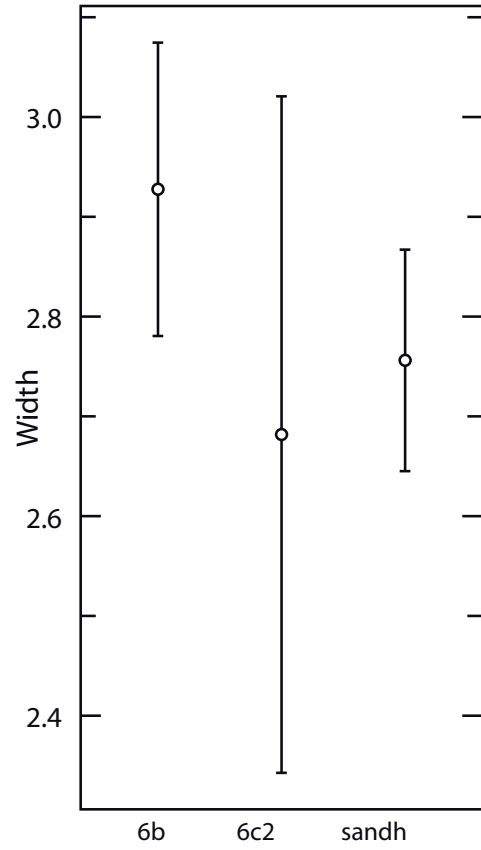


Fig. 51b: Central tendency in width of prismatic blades.

Fig. 51

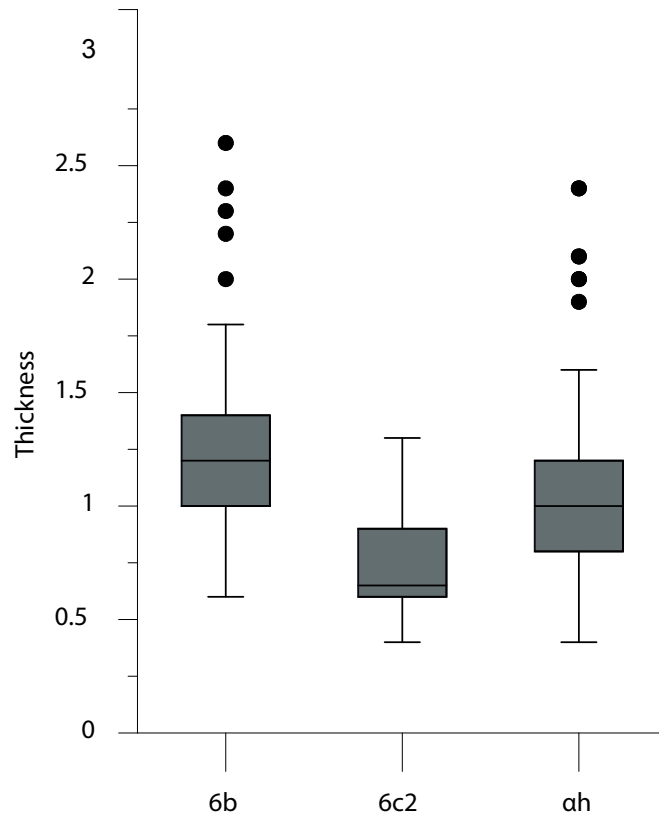


Fig.53: Thickness of Prismatic blades from layers 6b, 6c2 and sand ah.

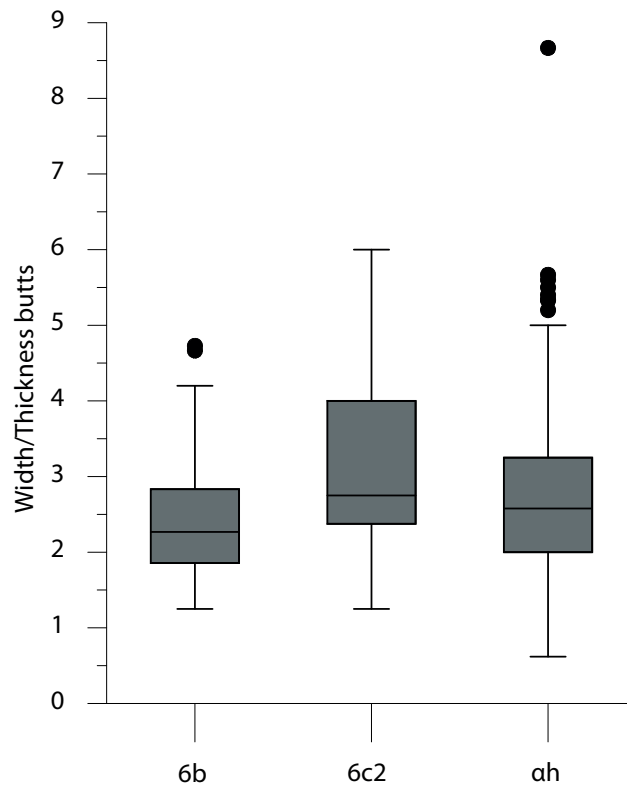


Fig.55: Ratio W/T butts of Prismatic blades from layers 6b, 6c2 and sand ah.

Fig. 53, 55

Plot Group Means with 95% Confidence Intervals

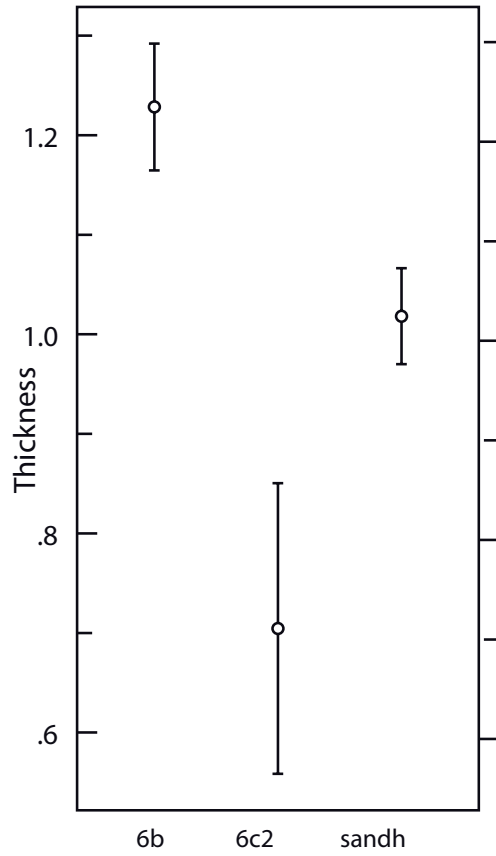


Fig. 54: Central tendency in Thickness of prismatic blades.

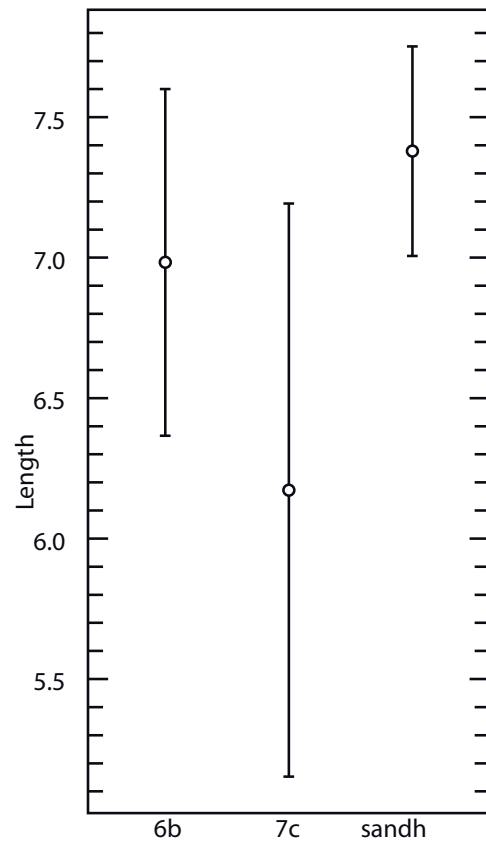


Fig. 58: Central tendency in Length of Levallois blades.

Fig. 54, 58

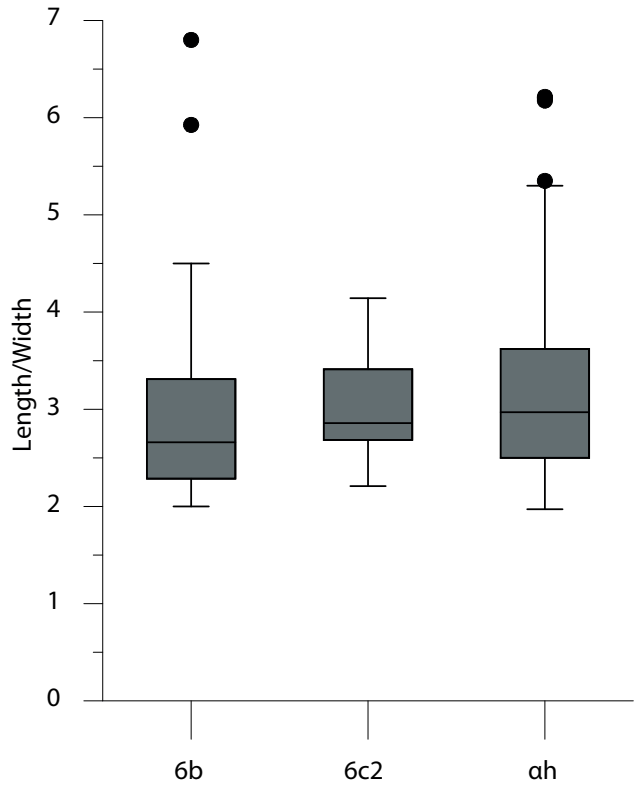


Fig. 56: Ratio L/W of Laminae from layers 6b, 6c2 and sand ah.

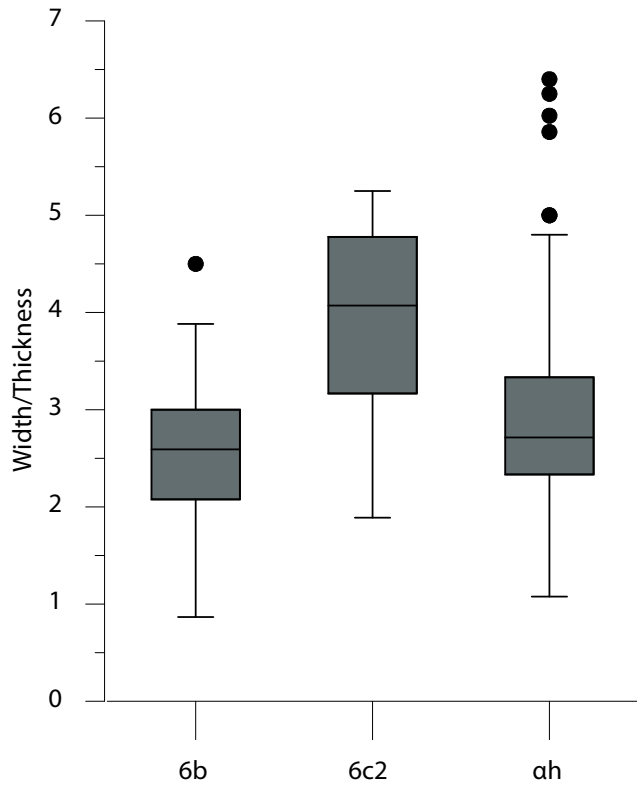


Fig. 57: Ratio W/T of Laminae from layers 6b, 6c2 and sand ah.

Fig. 56, 57

Plot Group Means with 95% Confidence Intervals

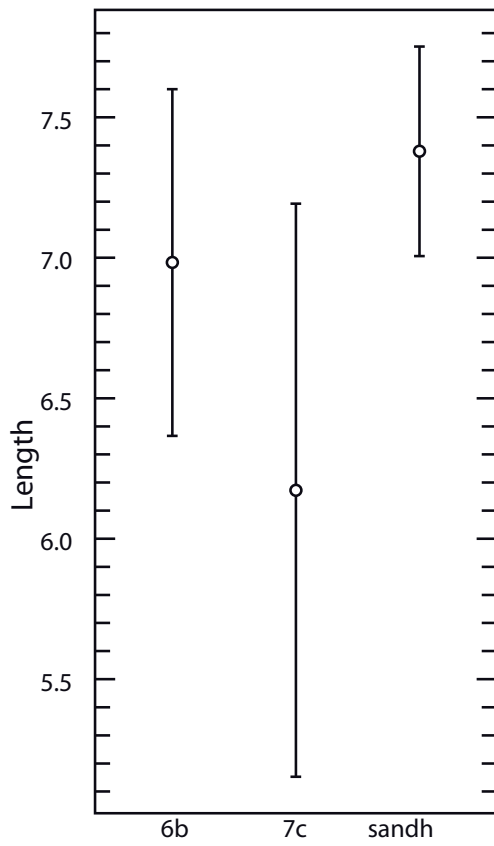


Fig. 58: Central tendency in Length of Levallois blades.

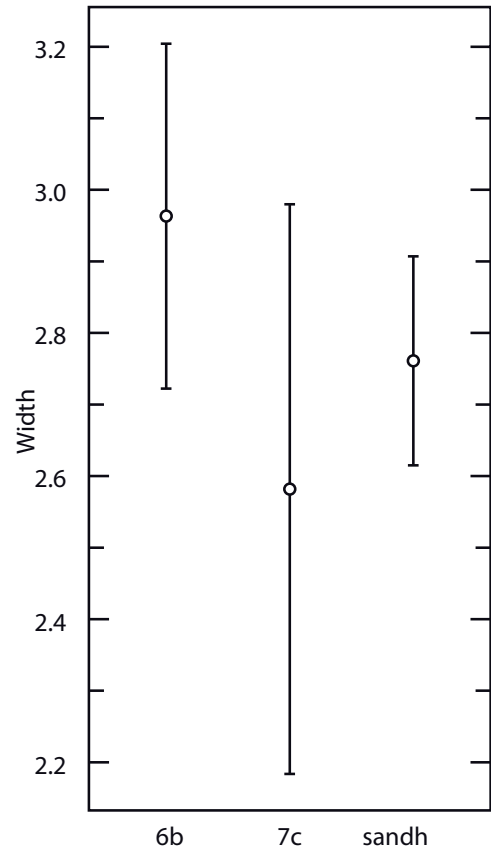


Fig. 61: Central tendency in Width of Levallois blades.

Fig. 58, 61

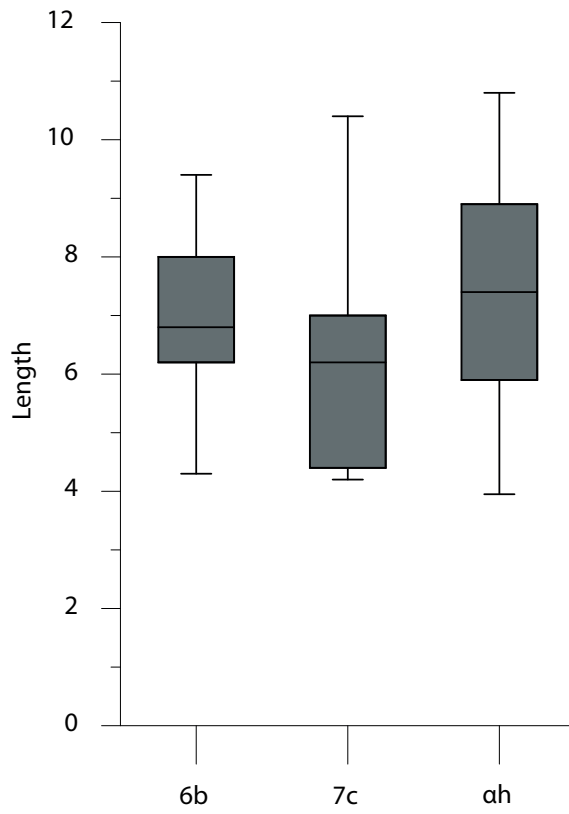


Fig.59: Length of Levallois blank from layers 6b, 7c and sand ah.

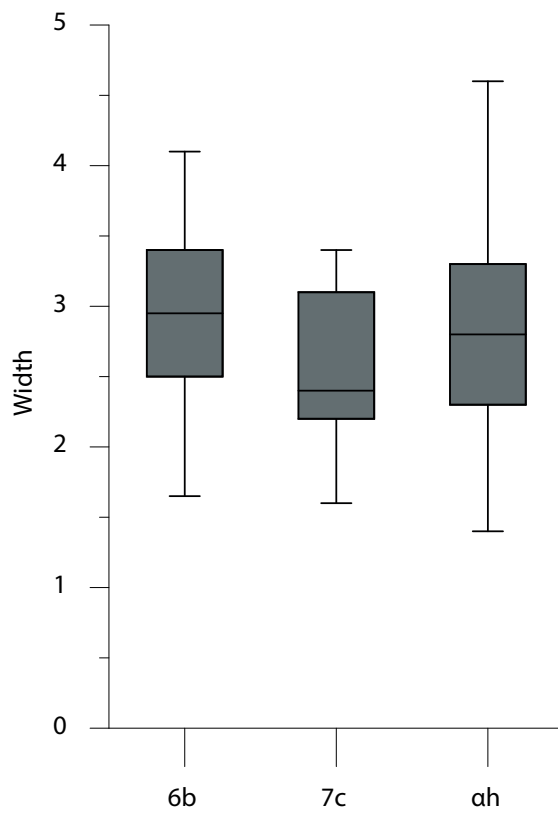


Fig. 60: Width of Levallois blank from layers 6b, 7c and sand ah.

Fig. 59, 60

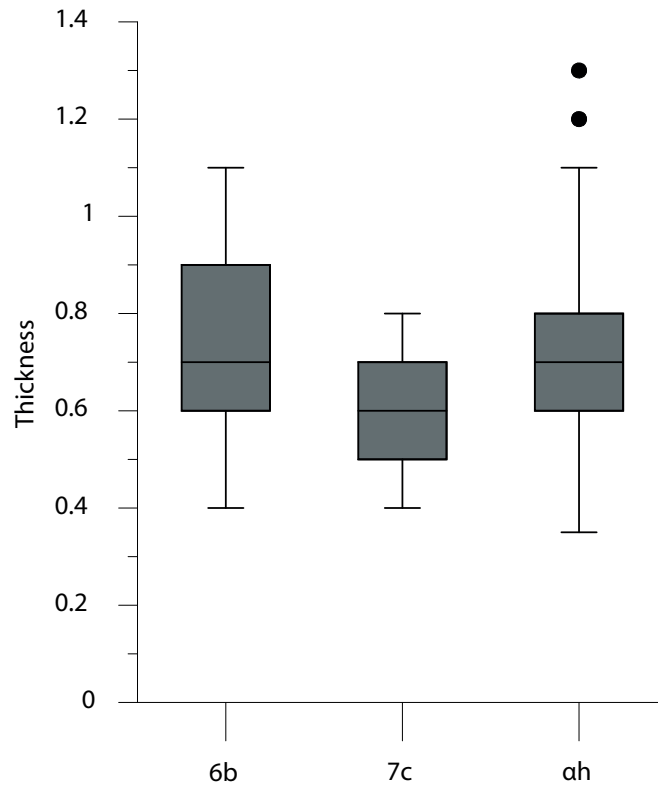


Fig. 62: Thickness of Lavallois blank from layers 6b, 7c and sand ah.

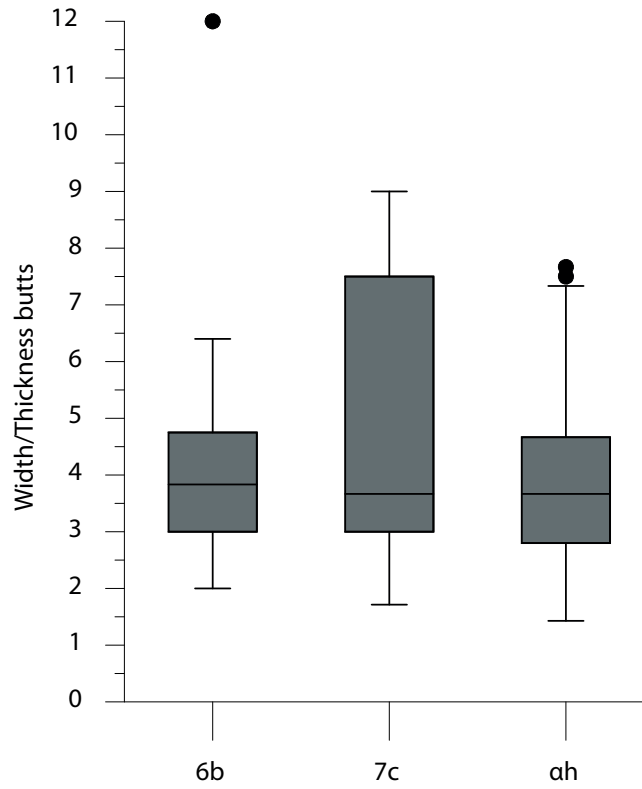


Fig. 64: Ratio W/T butts of Lavallois blank from layers 6b, 7c and sand h.

Fig. 62, 64

Plot Group Means with 95% Confidence Intervals

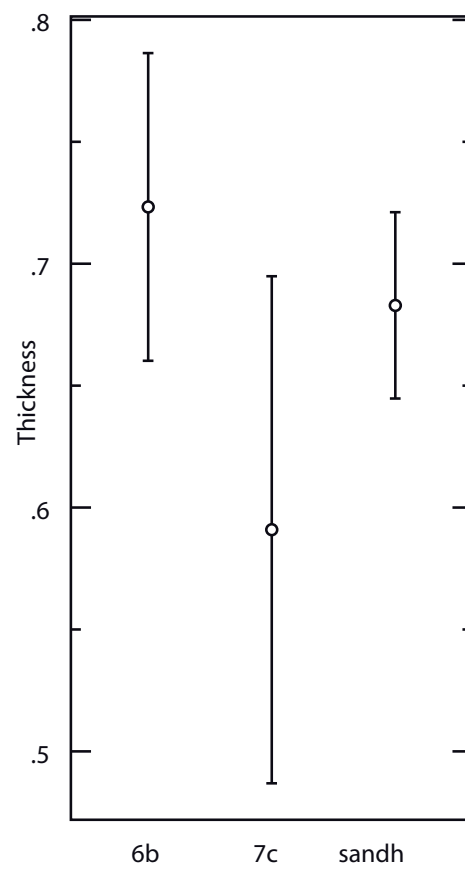


Fig. 63: Central tendency in Thickness of Levallois blades.

Fig. 63

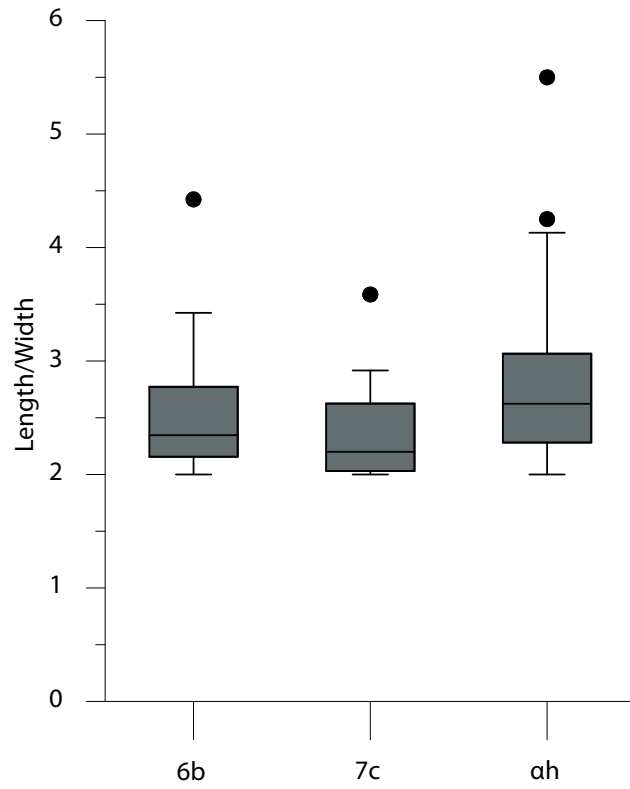


Fig. 65: Ratio L/W of Levallois blank from layers 6b, 7c ad sand ah.

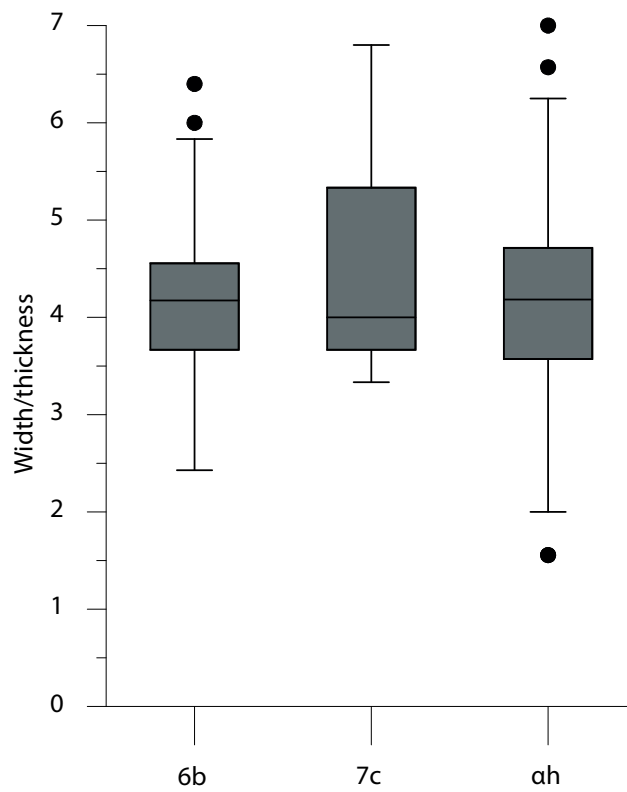


Fig. 66: Ratio W/T of Lavllois blank from layers 6b, 7c and sand ah.

Fig. 65, 66

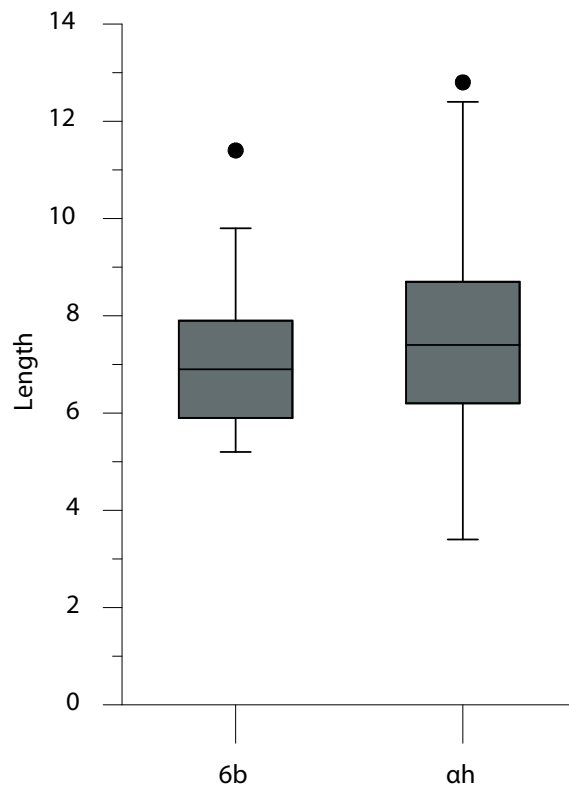


Fig. 67: Length of Indetermined blank blades from layers 6b and sand ah.

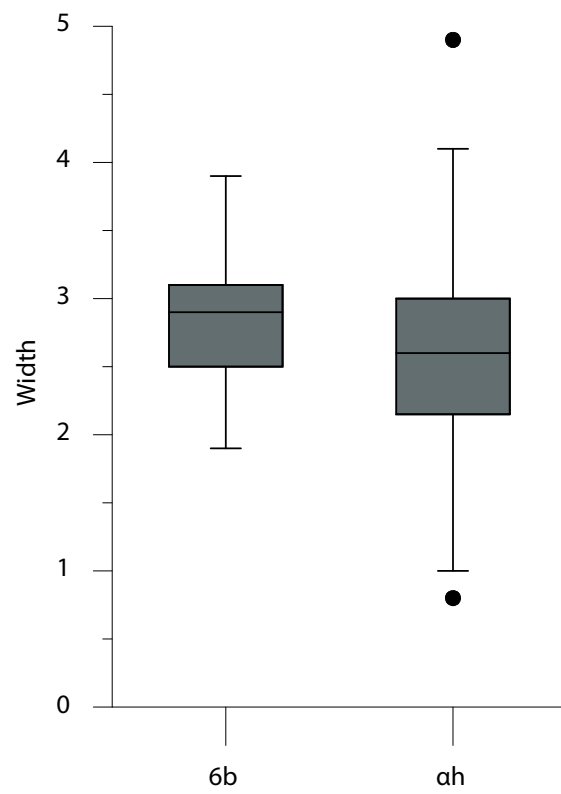


Fig. 68: Width of Indetermined blank blades from layers 6b and sand ah.

Fig. 67, 68

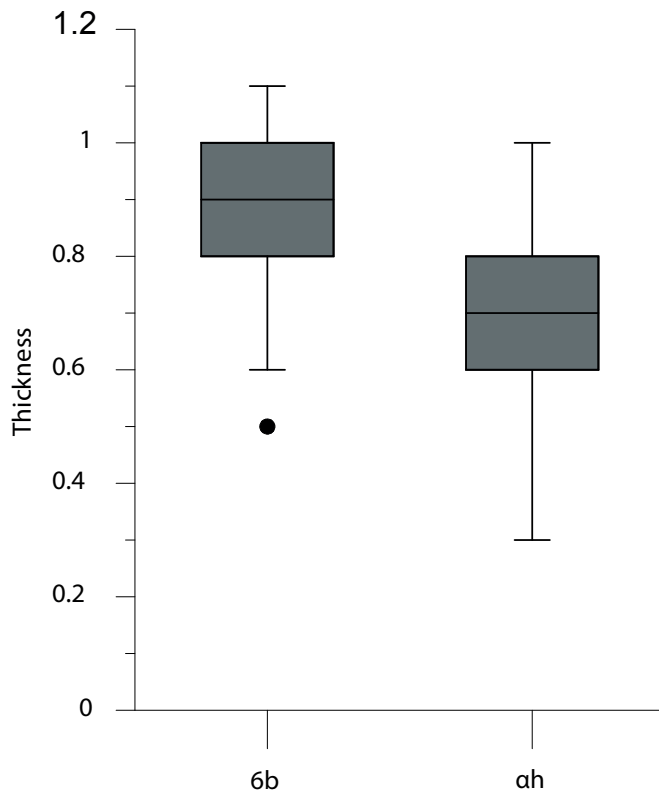


Fig. 69: Thickness of Indetermined blank blades from layers 6b and sand ah.

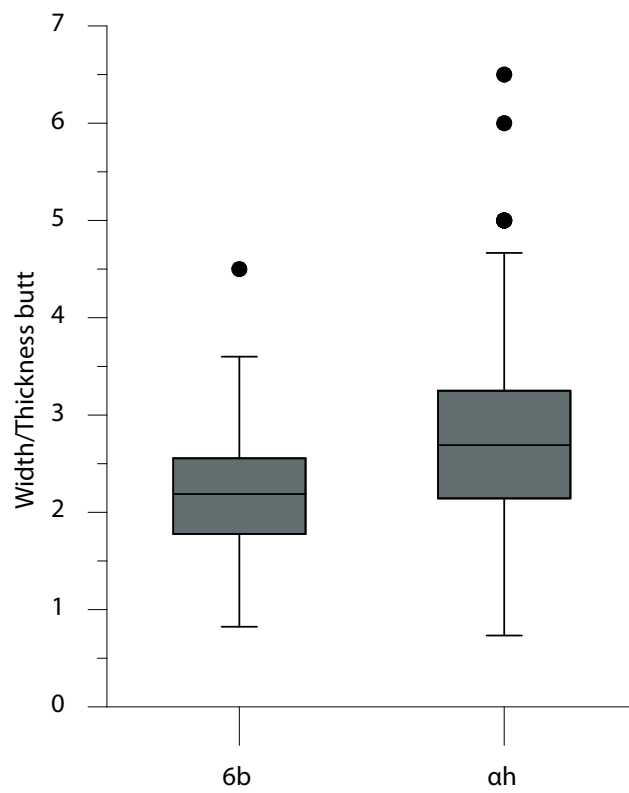


Fig. 70: Ratio W/T butts of Indetermined blank blades from layers 6b and sand ah.

Fig. 69, 70

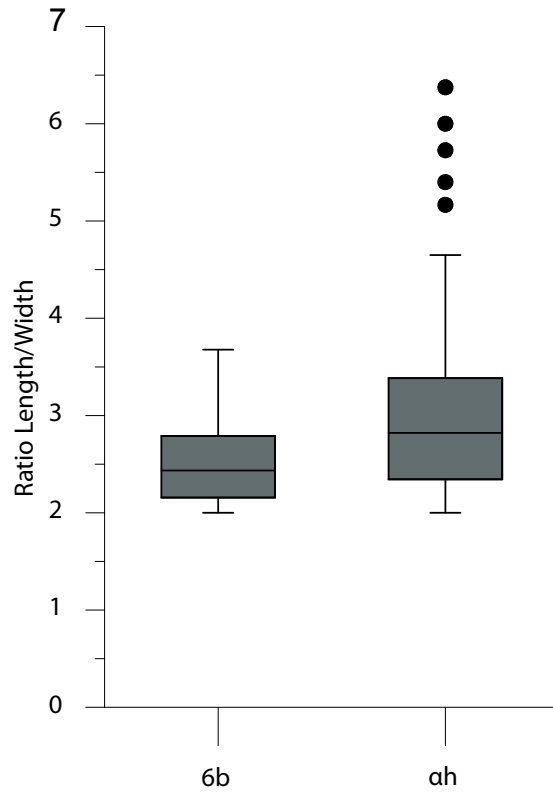


Fig. 71: Ratio L/W of Indetermined blank blades from layers 6b and sand ah.

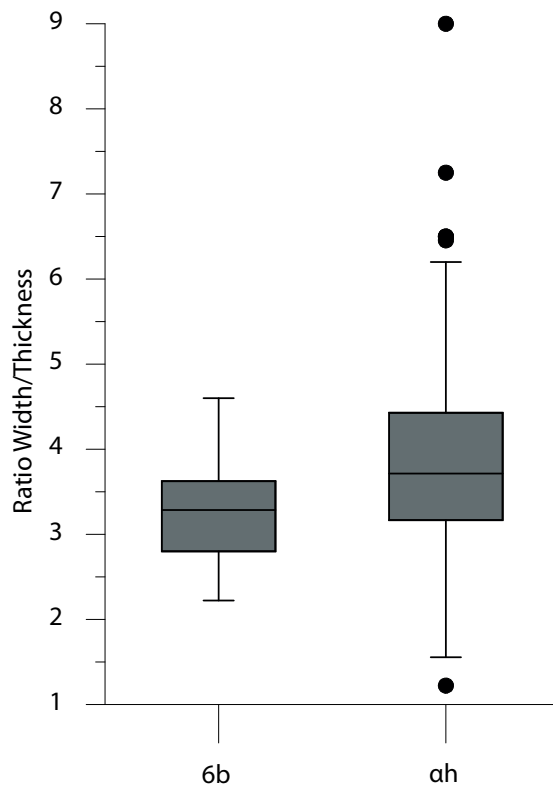


Fig. 72: Ratio W/T of Indetermined blank blades from layers 6b and sand ah.

Fig. 71, 72

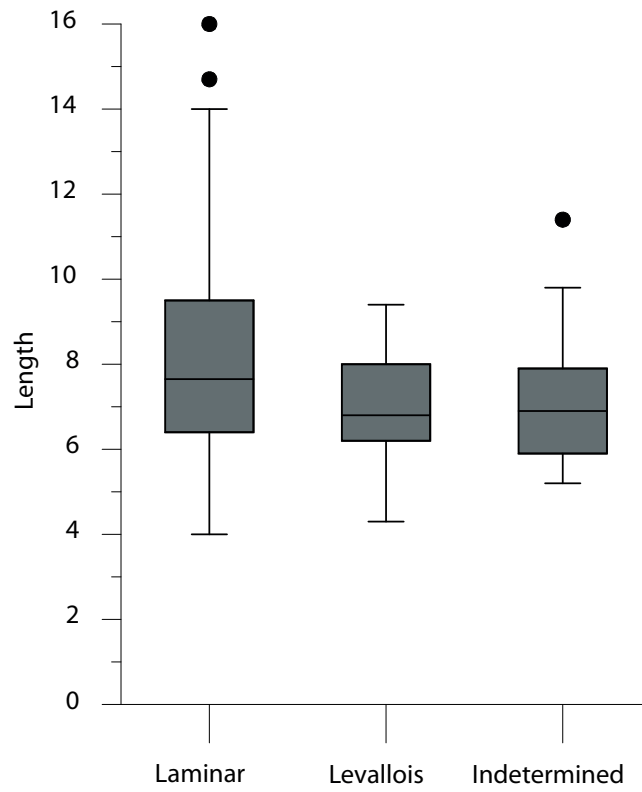


Fig. 73: Length of intact, unretouched blank blades categories from layer 6b.

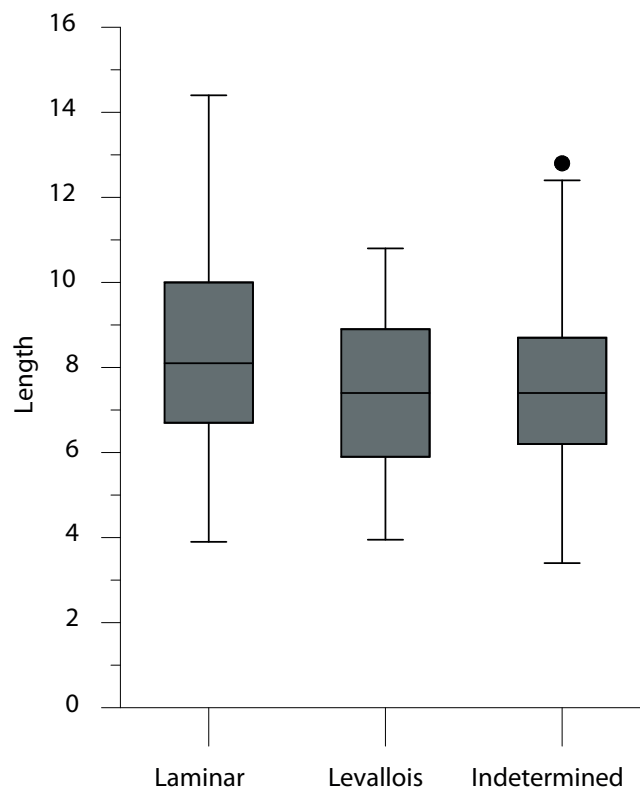


Fig. 74: Length of intact, unretouched blank blades categories from sand ah.

Fig. 73, 74

Plot Group Means with 95% Confidence Intervals

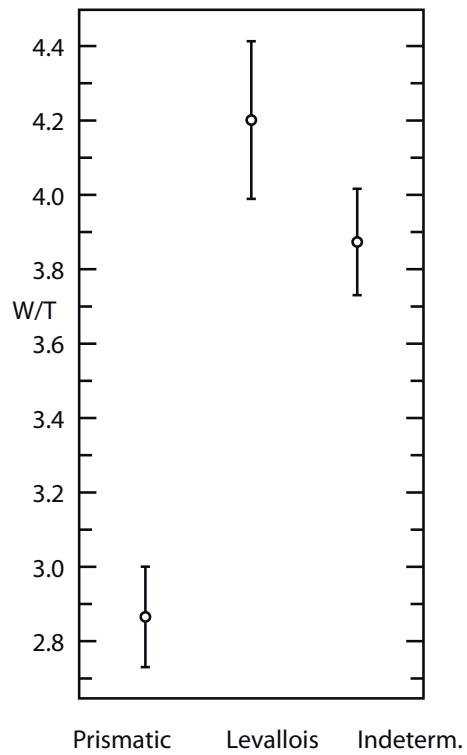
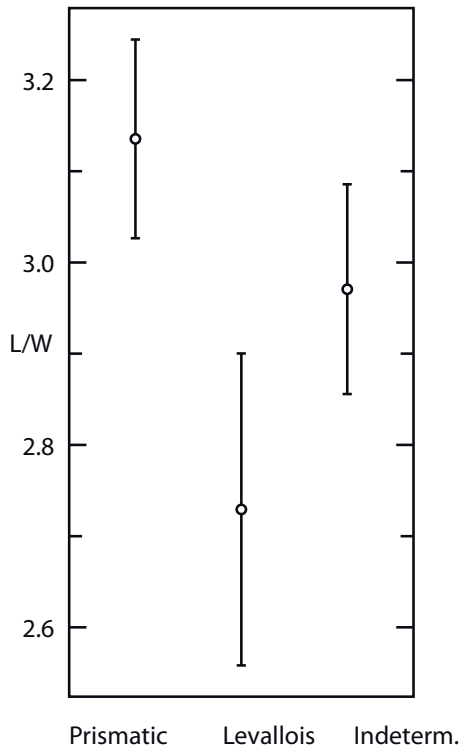


Fig. 75a: Central tendency in ratio L/W of Prismatic, Levallois and Indetermined blades in sand h.

Fig. 75b: Central tendency in ratio W/T of Prismatic, Levallois and Indetermined blades in sand h.

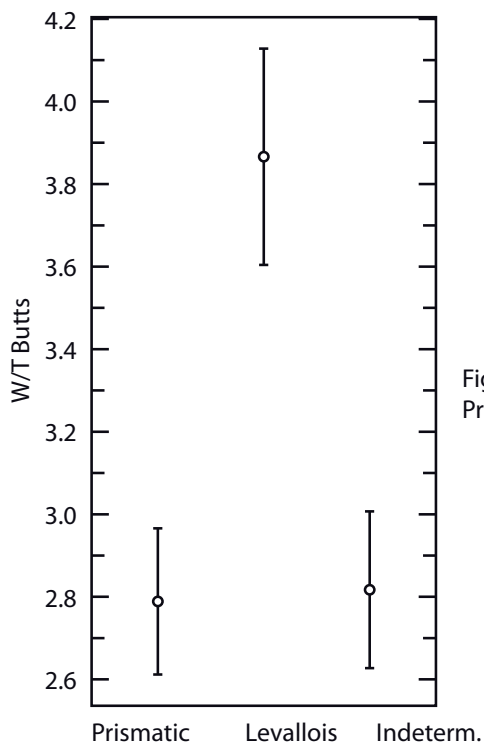


Fig. 75c: Central tendency in ratio W/T of butts of Prismatic, Levallois and Indetermined blades in sand h.

Fig. 75

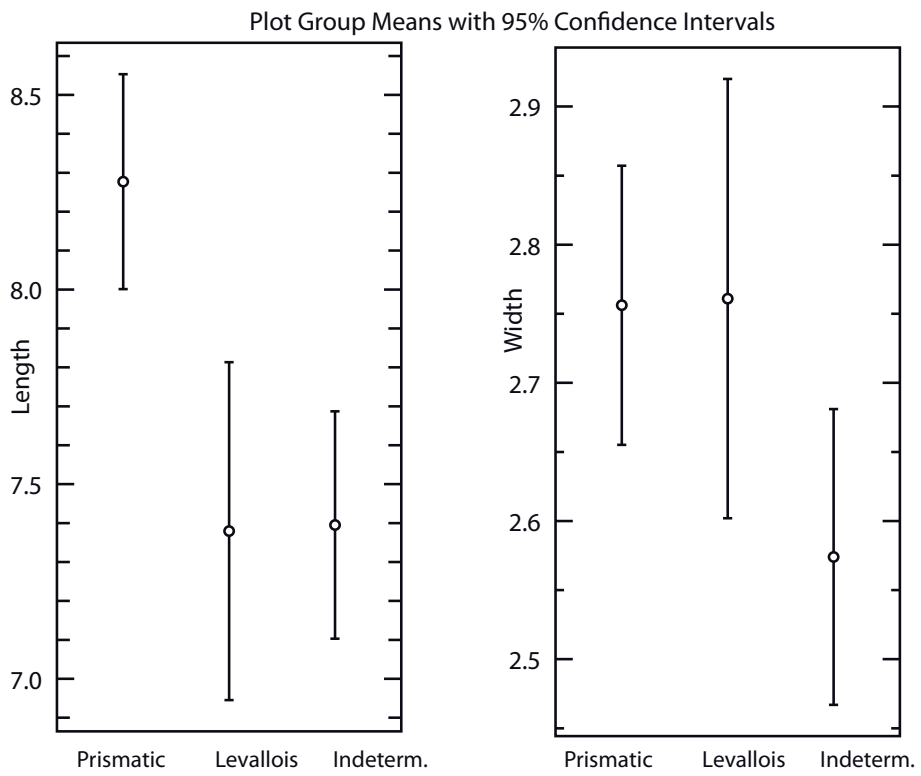


Fig. 76a : Central tendency in length of Prismatic, Levallois and Indetermined blades in sand h.

Fig. 76b: Central tendency in width of Prismatic, Levallois and Indetermined blades in sand h.

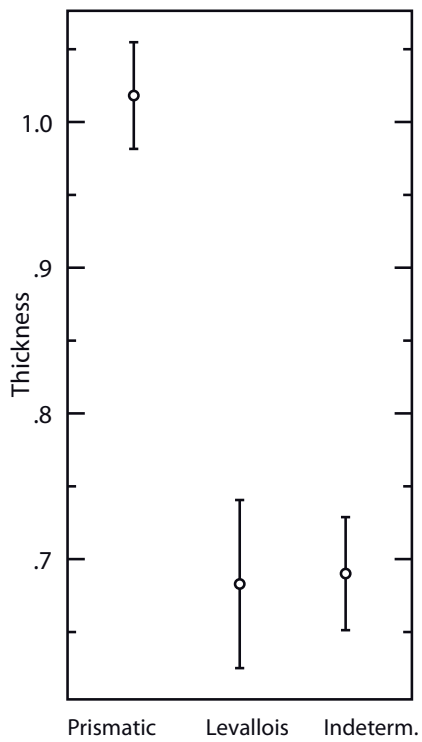


Fig. 76c: Central tendency in thickness of Prismatic, Levallois and Indetermined blades in sand h.

Fig. 76

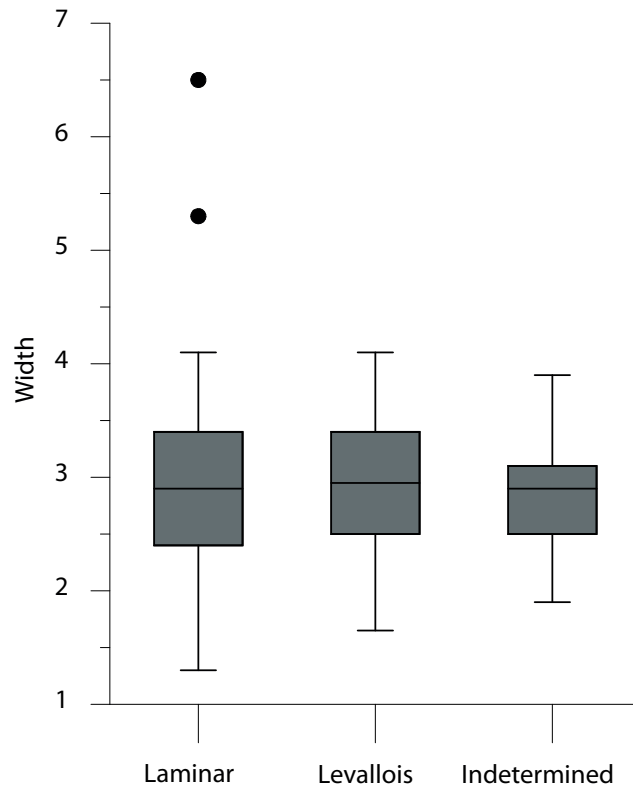


Fig. 77: Width of intact, unretouched blank blades from layer 6b.

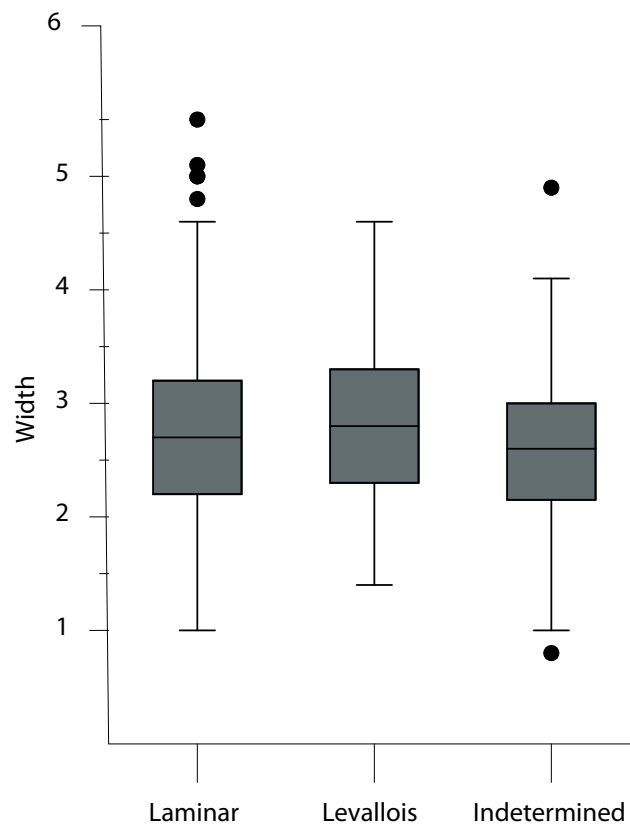


Fig. 78: Width of intact, unretouched blank blades from sand ah.

Fig. 77, 78

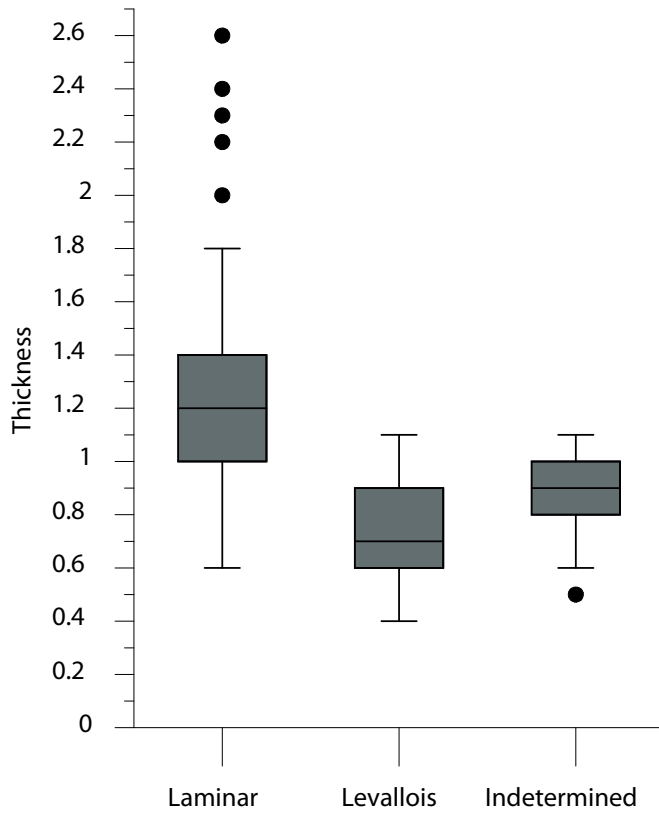


Fig. 79: Thickness of different categories of inactive, unretouched blades from layer 6b.

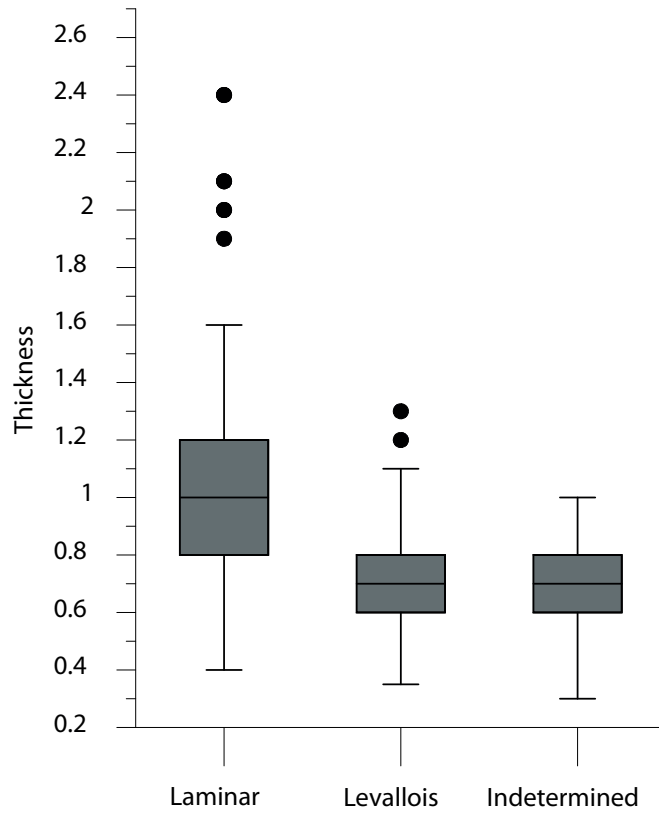


Fig. 80: Thickness of different categories of intact, unretouched blades from sand ah.

Fig. 79, 80

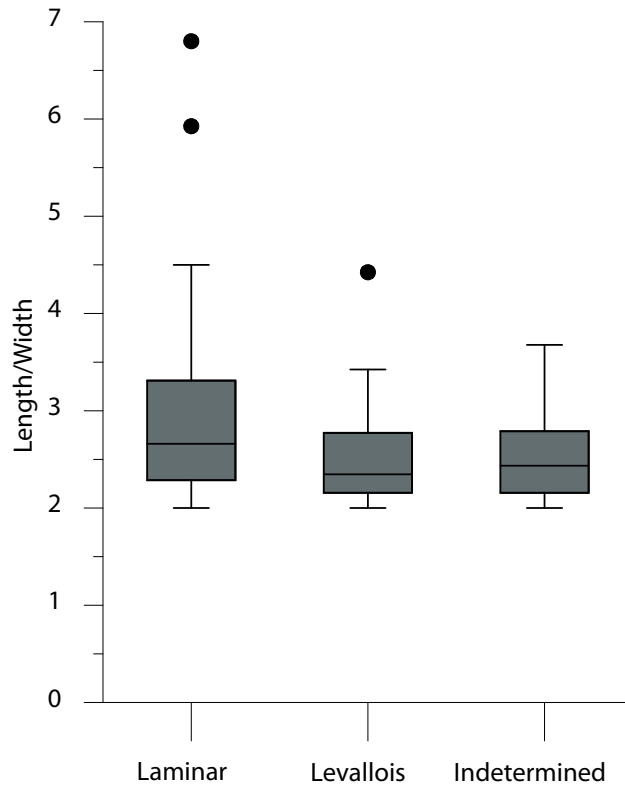


Fig. 81: Ratio L/W of different types of intact, unretouched blades from layer 6b.

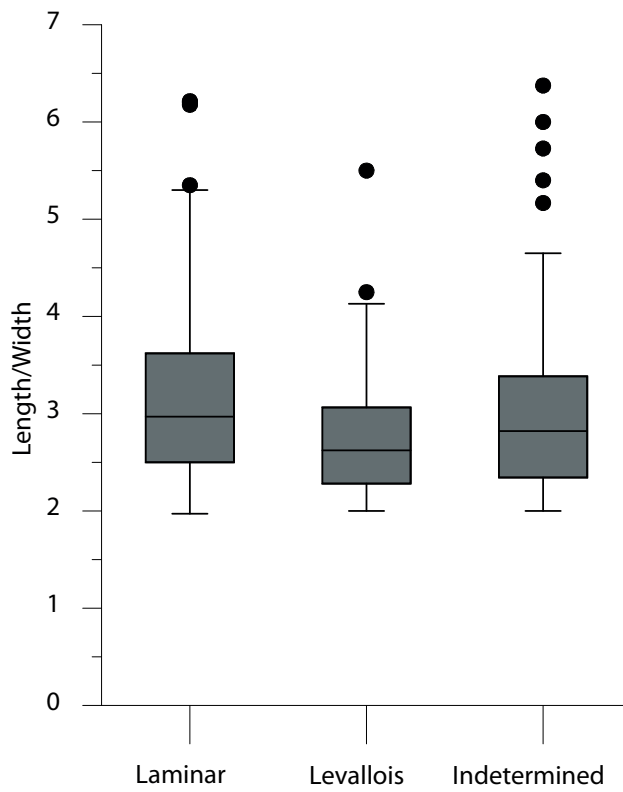


Fig. 82: Ratio L/W of intact, unretouched blade categories from sand ah.

Fig. 81, 82

Plot Group Means with 95% Confidence Intervals

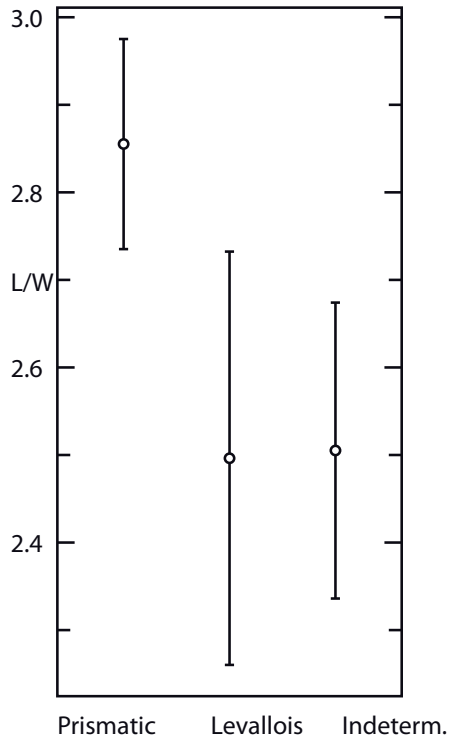


Fig. 83 Central tendency in ratio L/W of Prismatic, Levallois and Indetermined blades in layer 6b.

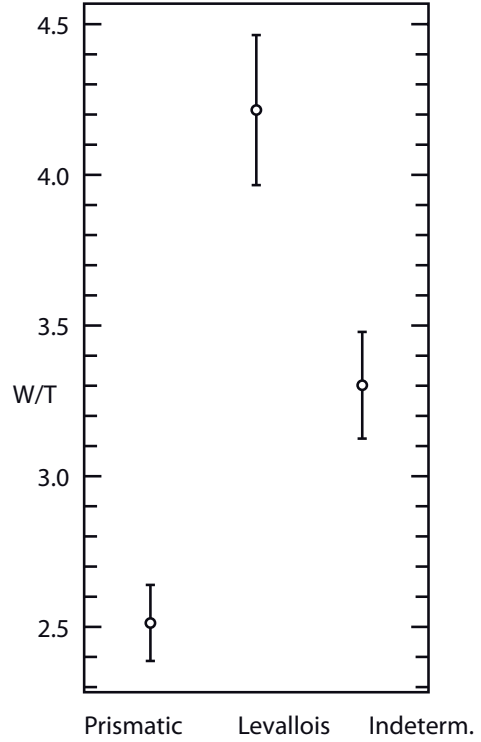


Fig. 87: Central tendency in ratio W/T of Prismatic, Levallois and Indetermined blades in layer 6b.

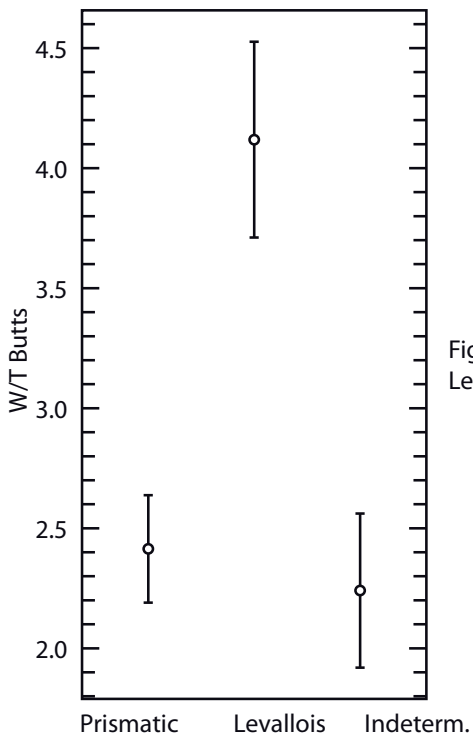


Fig. 91: Central tendency in ratio W/T of butts of Prismatic, Levallois and Indetermined blades in layer 6b.

Fig. 83, 87, 91

Plot Group Means with 95% Confidence Intervals

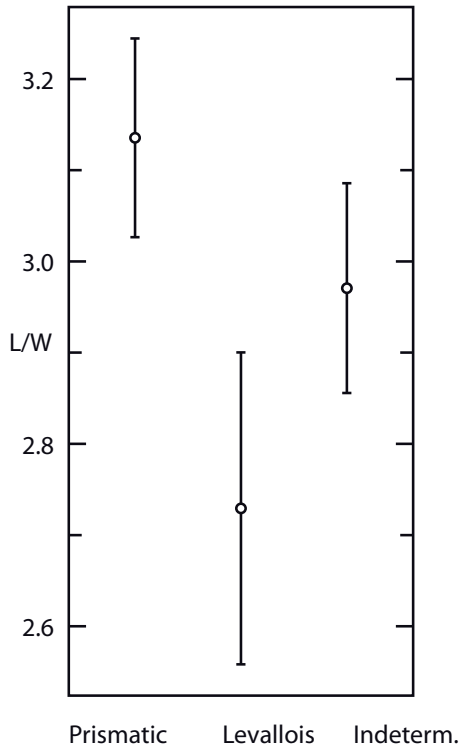


Fig. 84: Central tendency in ratio L/W of Prismatic, Levallois and Indetermined blades in sand h.

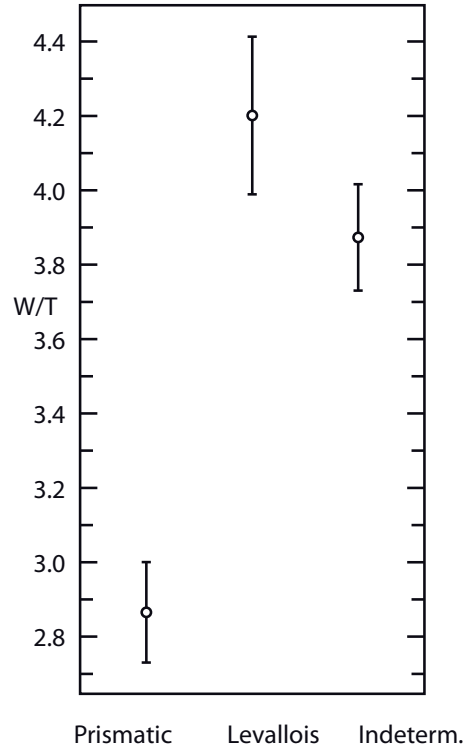


Fig. 88: Central tendency in ratio W/T of Prismatic, Levallois and Indetermined blades in sand h.

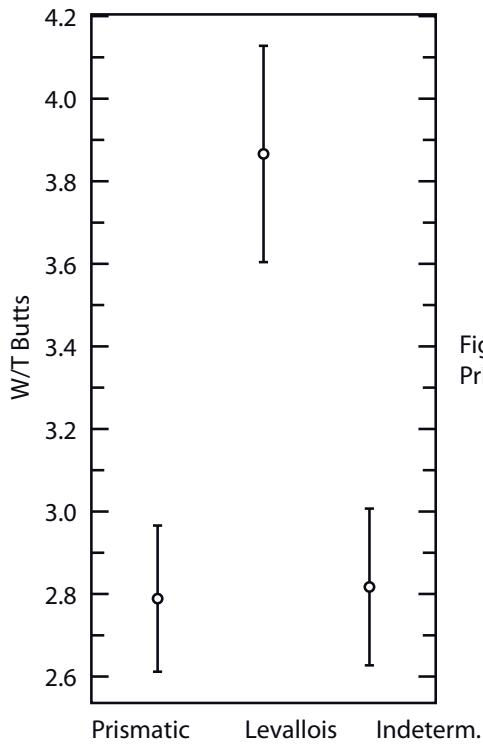


Fig. 92: Central tendency in ratio W/T of butts of Prismatic, Levallois and Indetermined blades in sand h.

Fig. 84, 88, 92

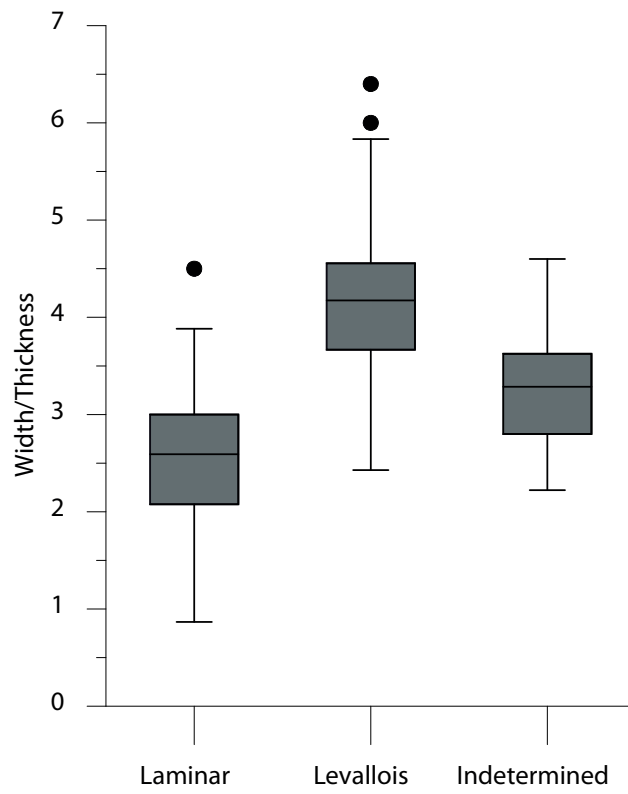


Fig. 85: Ratio W/T of blade categories in layer 6b.

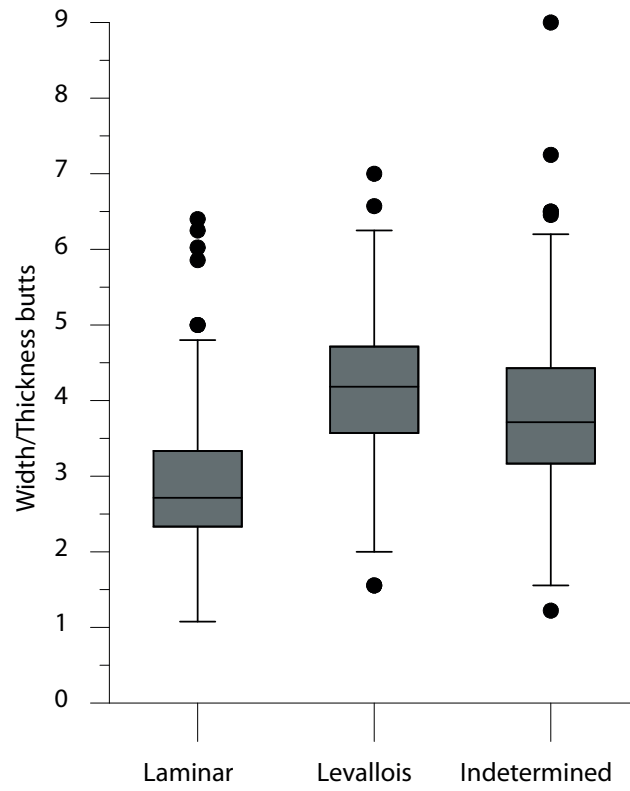


Fig. 86: Ratio W/T butts of blade categories in sand ch.

Fig. 85, 86

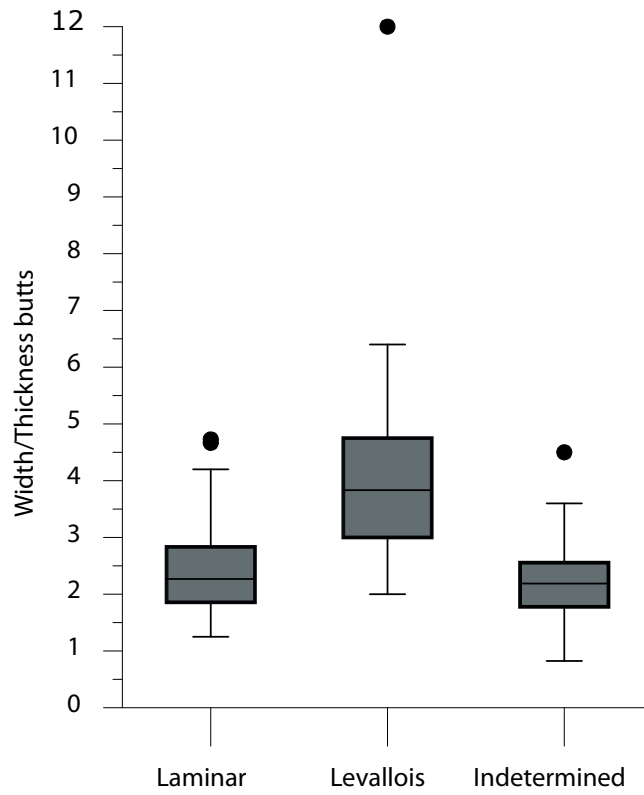


Fig. 89: Ratio W/T of butts of inactive blade categories from layer 6b.

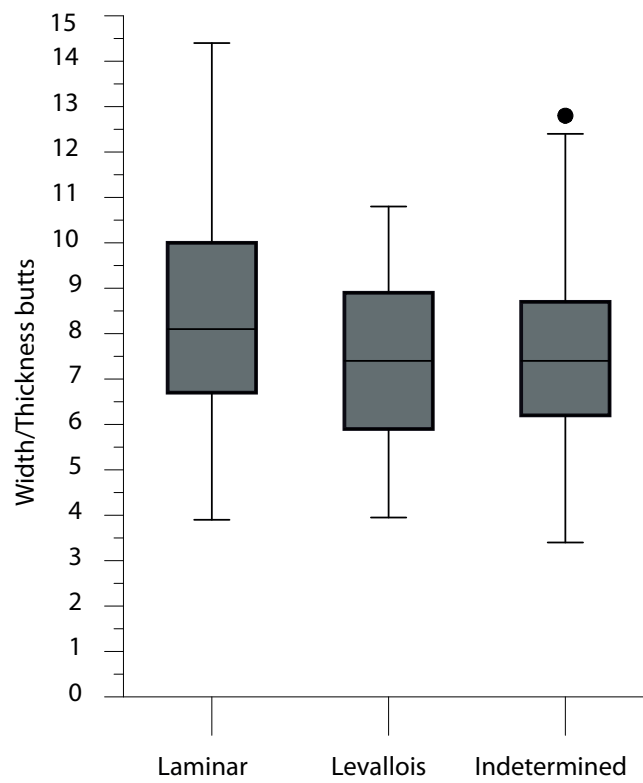


Fig. 90: Ratio W/T butts of inactive blade categories from sand oh.

Fig. 89, 90

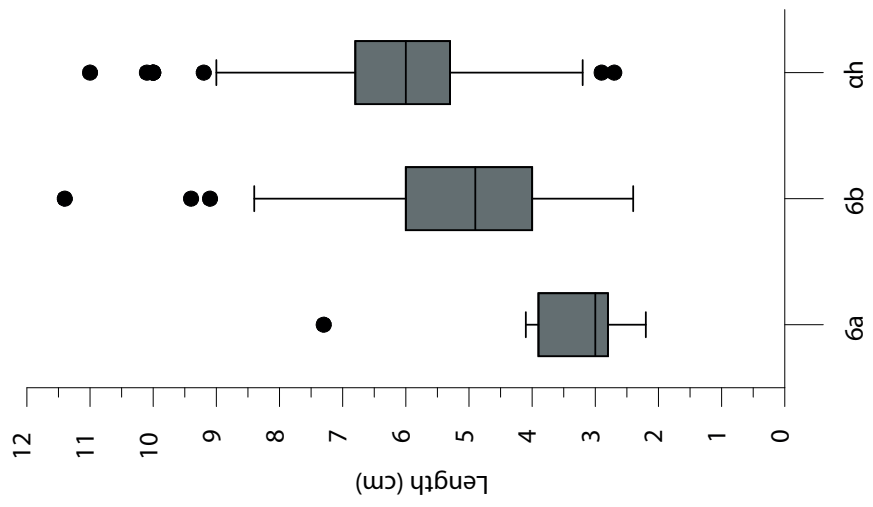


Fig. 93: Length of intact, unretouched flakes.

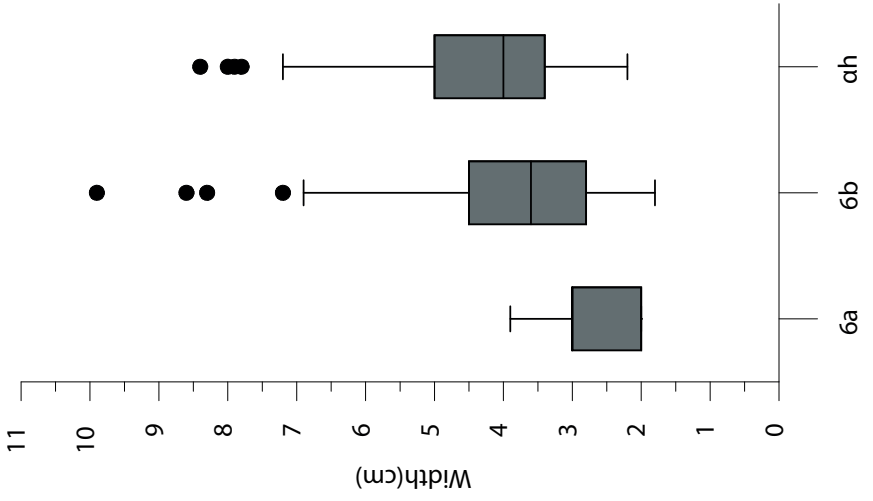


Fig. 96: Width of intact, unretouched flakes.

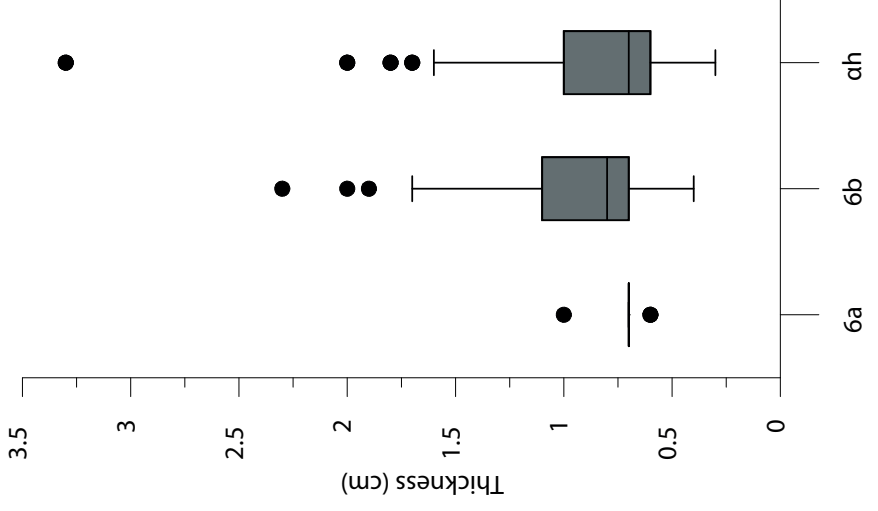


Fig. 99: Thickness of intact, unretouched blank flakes.

Fig. 93, 96, 99

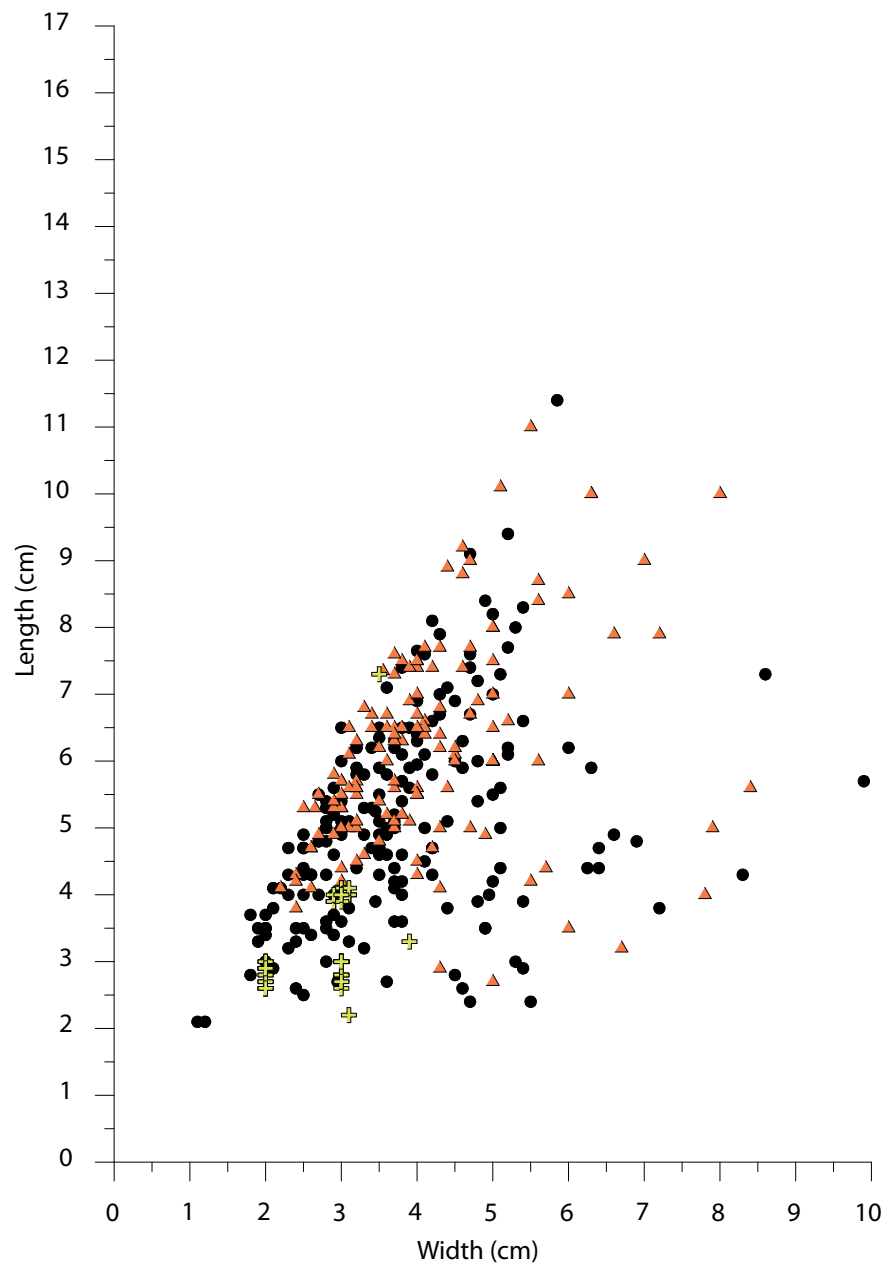


Fig. 94

Plot Group Means with 95% Confidence Intervals

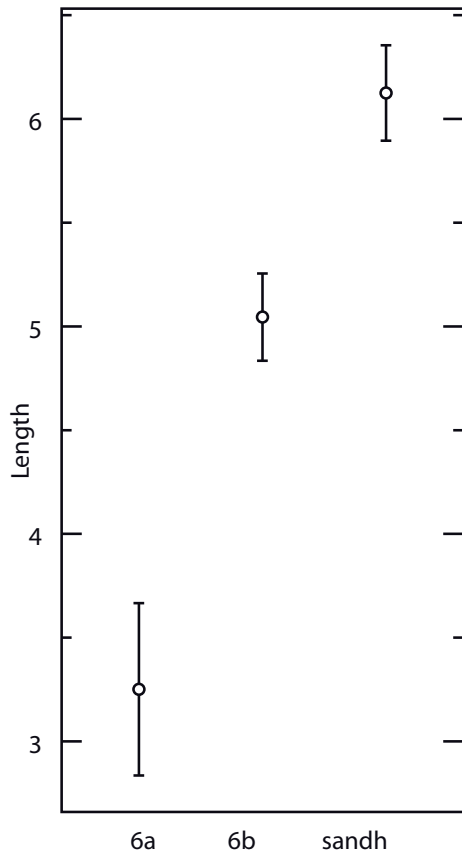


Fig. 95: Central tendency in Length of blank-flakes.

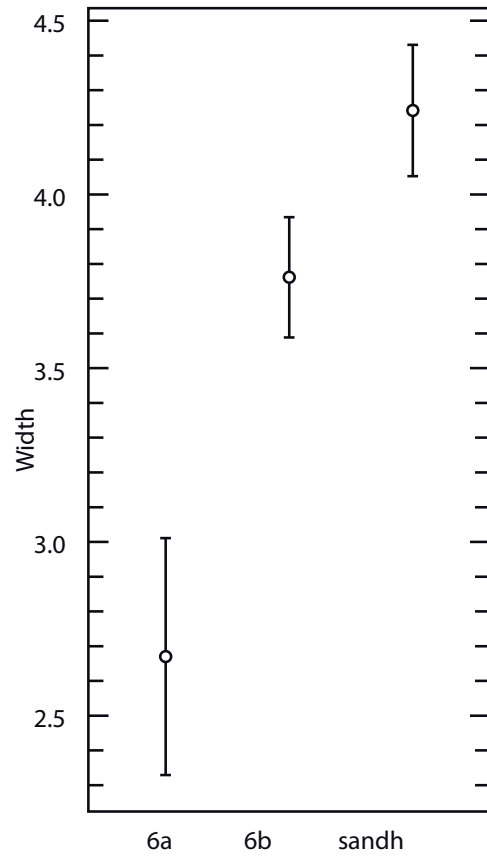


Fig. 97: Central tendency in Width of blank-flakes.

Fig. 95, 97

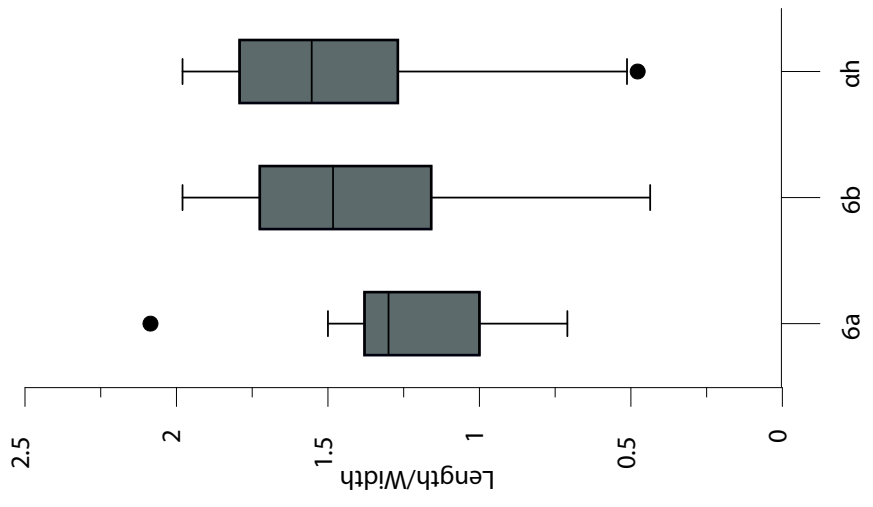


Fig. 98: Ratio LW of unretouched blank flakes.

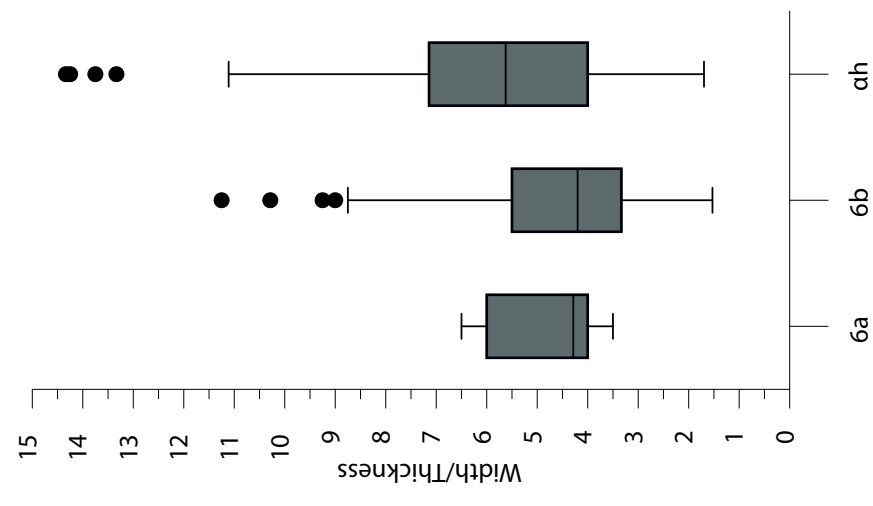


Fig. 101: Ratio WT of unretouched blank flakes.

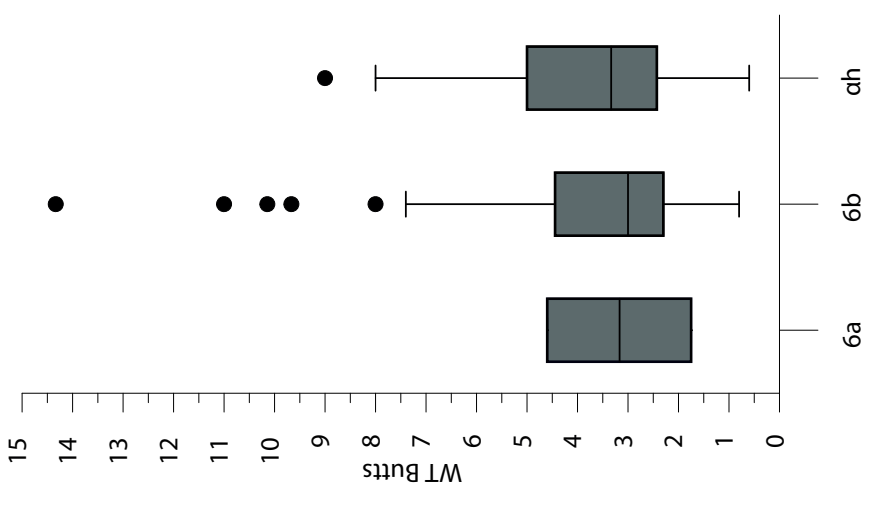


Fig. 102: WT of butts of unretouched blank flakes.

Fig. 98, 101, 102

Plot Group Means with 95% Confidence Intervals

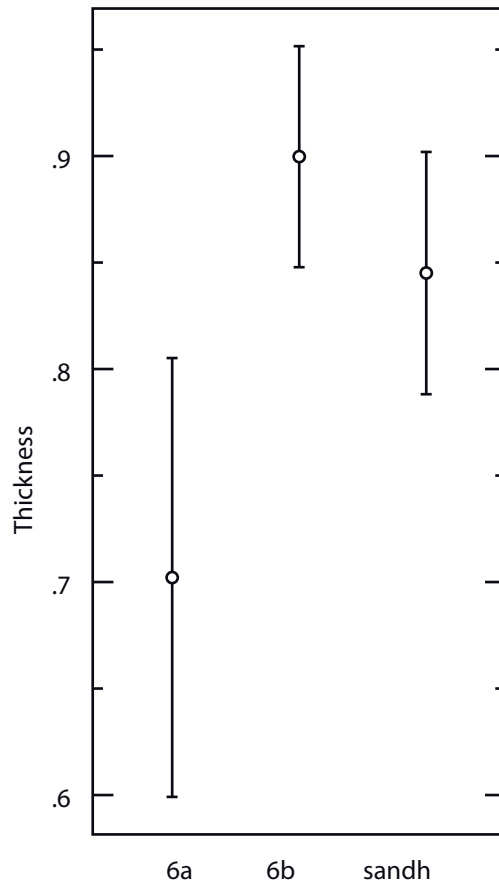


Fig. 100: Central tendency in Thickness of blank-flakes.

Fig. 100

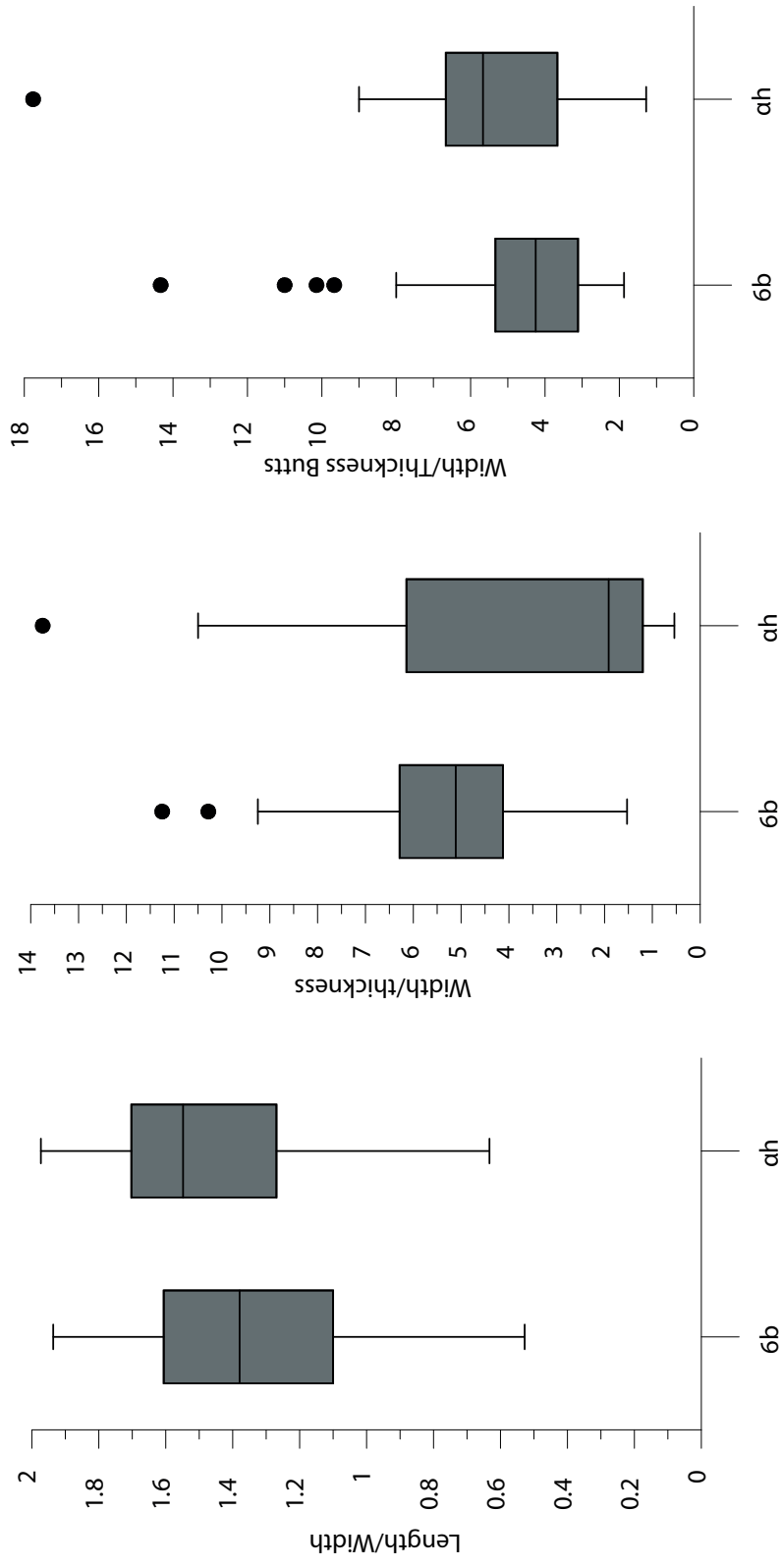


Fig. 105: Ratio L/W of Levallois blank flakes. Fig. 108: Ratio W/T of Levallois blank flakes. Fig. 109: W/T of butts of Levallois blank flakes.

Fig. 105, 108, 109

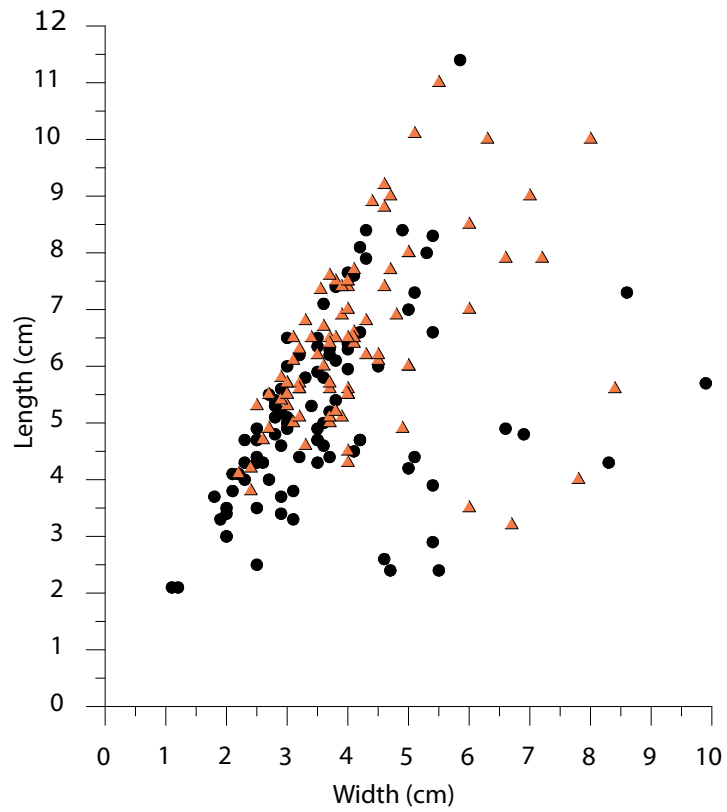


Fig. 110: The scatter plot of non-Levallois blank flakes from layer 6b (circles) and sand ch (triangles).

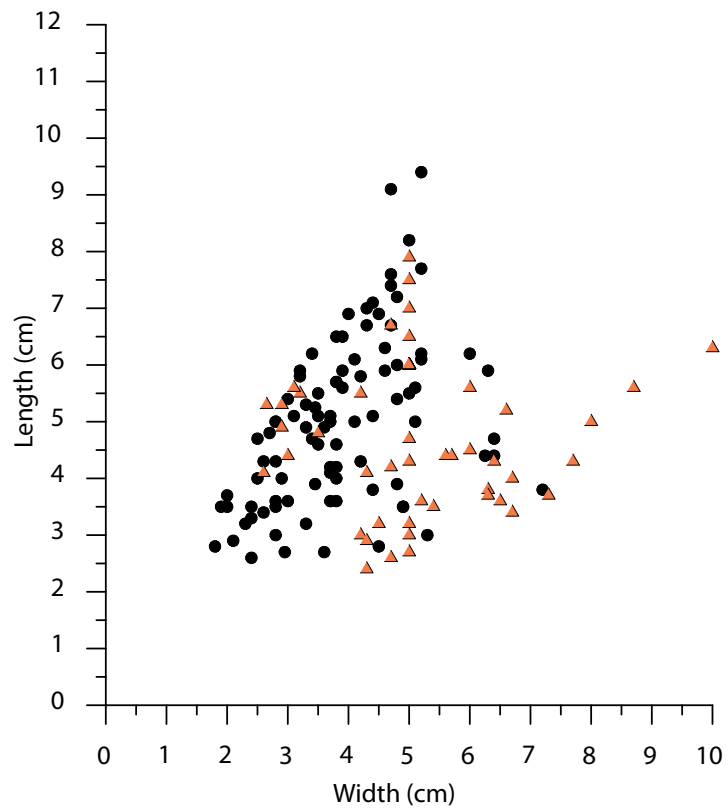


Fig. 106: The scatter plot of Levallois blank flakes from layer 6b (circle) and sand ch (triangle).

Fig. 106, 110

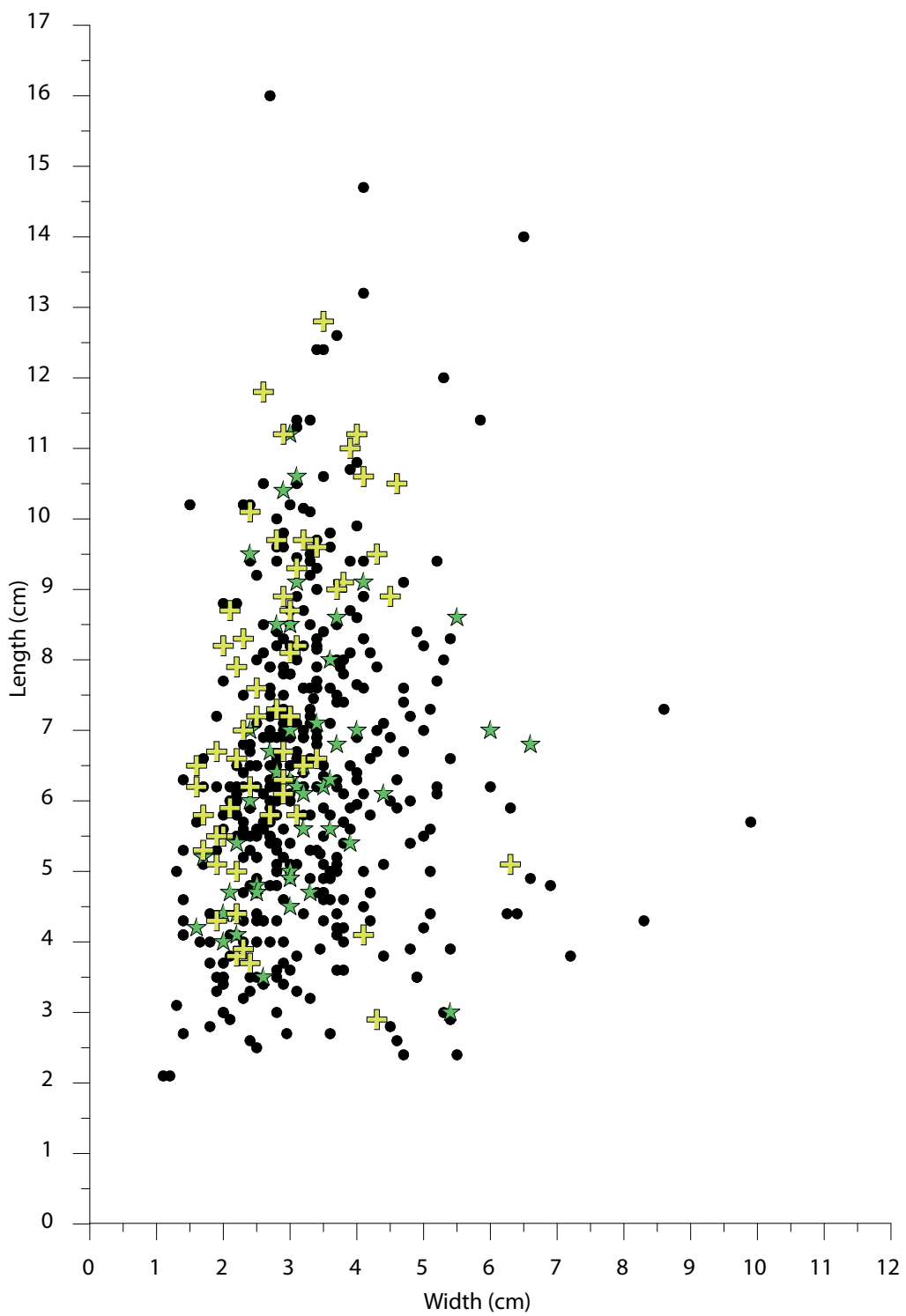


Fig. 111: Unretouched blanks from layer 6b (circle), 6c2 (cross) and 7c (star).

Fig. 111

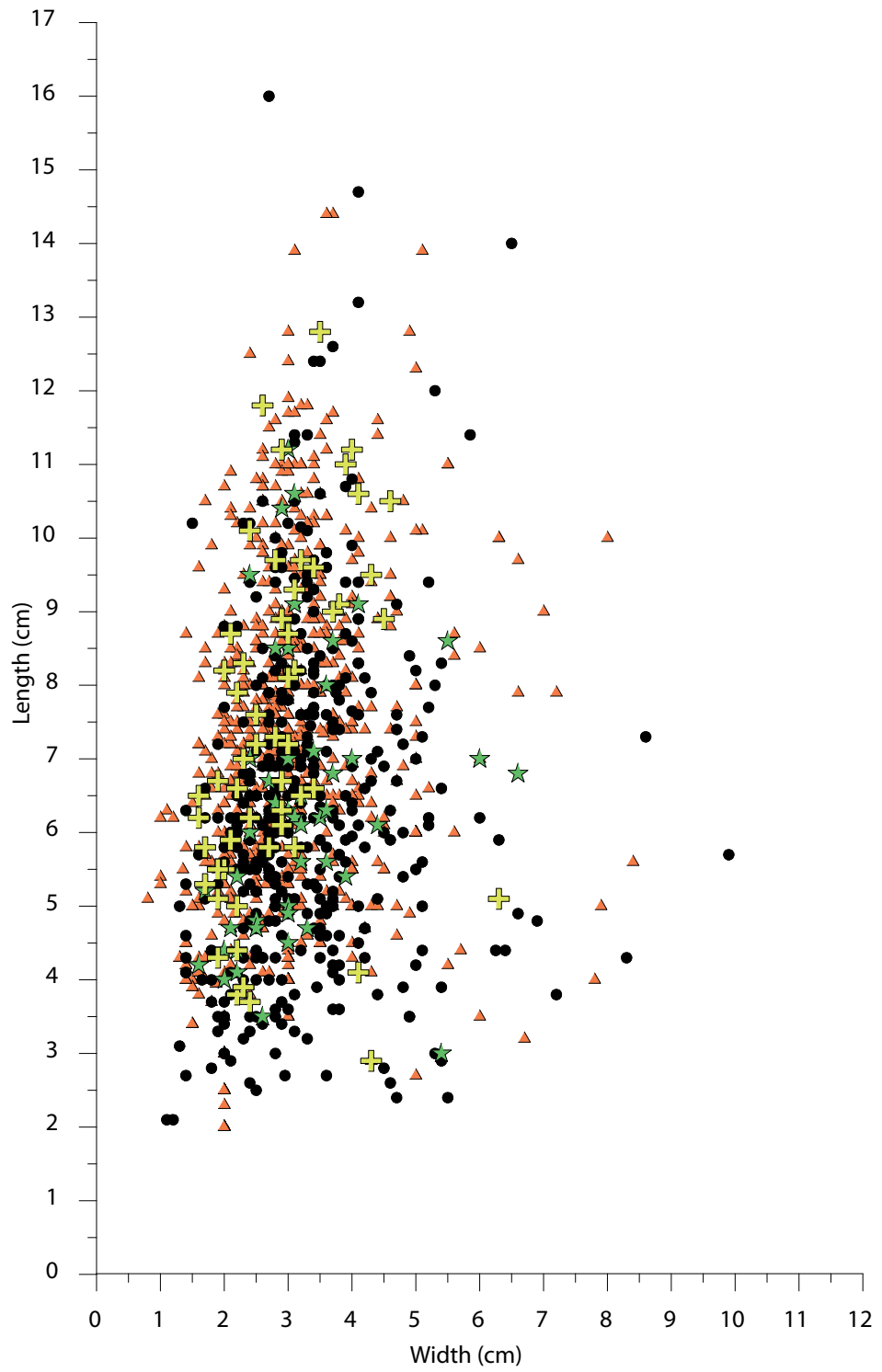


Fig. 112: The scatter plot of unretouched blanks from layer 6b (circle), sand ah (triangle), 6c2 (cross) and 7c (star).

Fig. 112

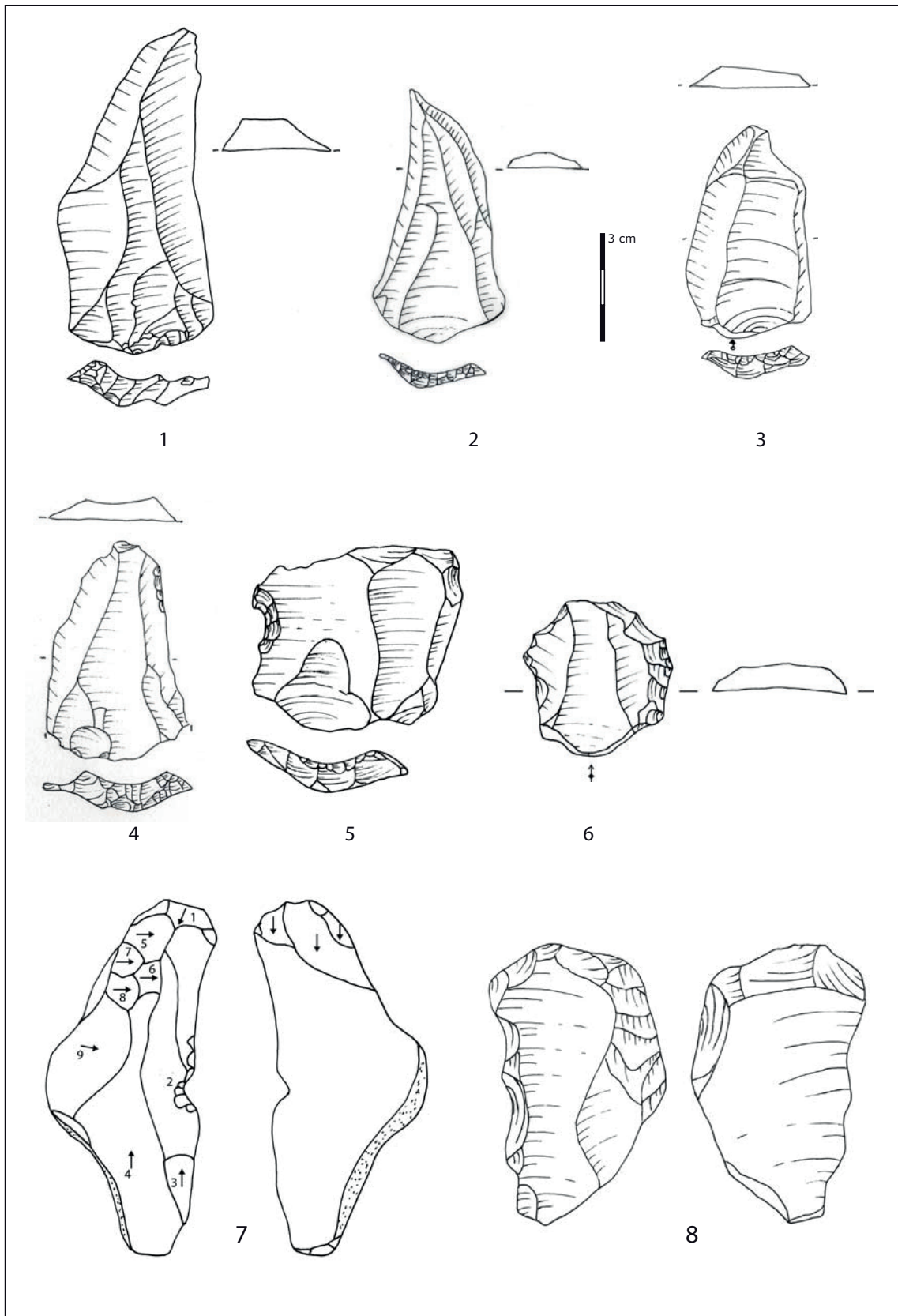


Fig. 113: Selected artefacts from assemblages 6b, 7c and sand h .
 1, 2 3, 4: unretouched Levallois blanks; 5: notch made on Levallois flake;
 6: denticulate made on Levallois flake; 7, 8: *lames débordantes*.

Fig. 113

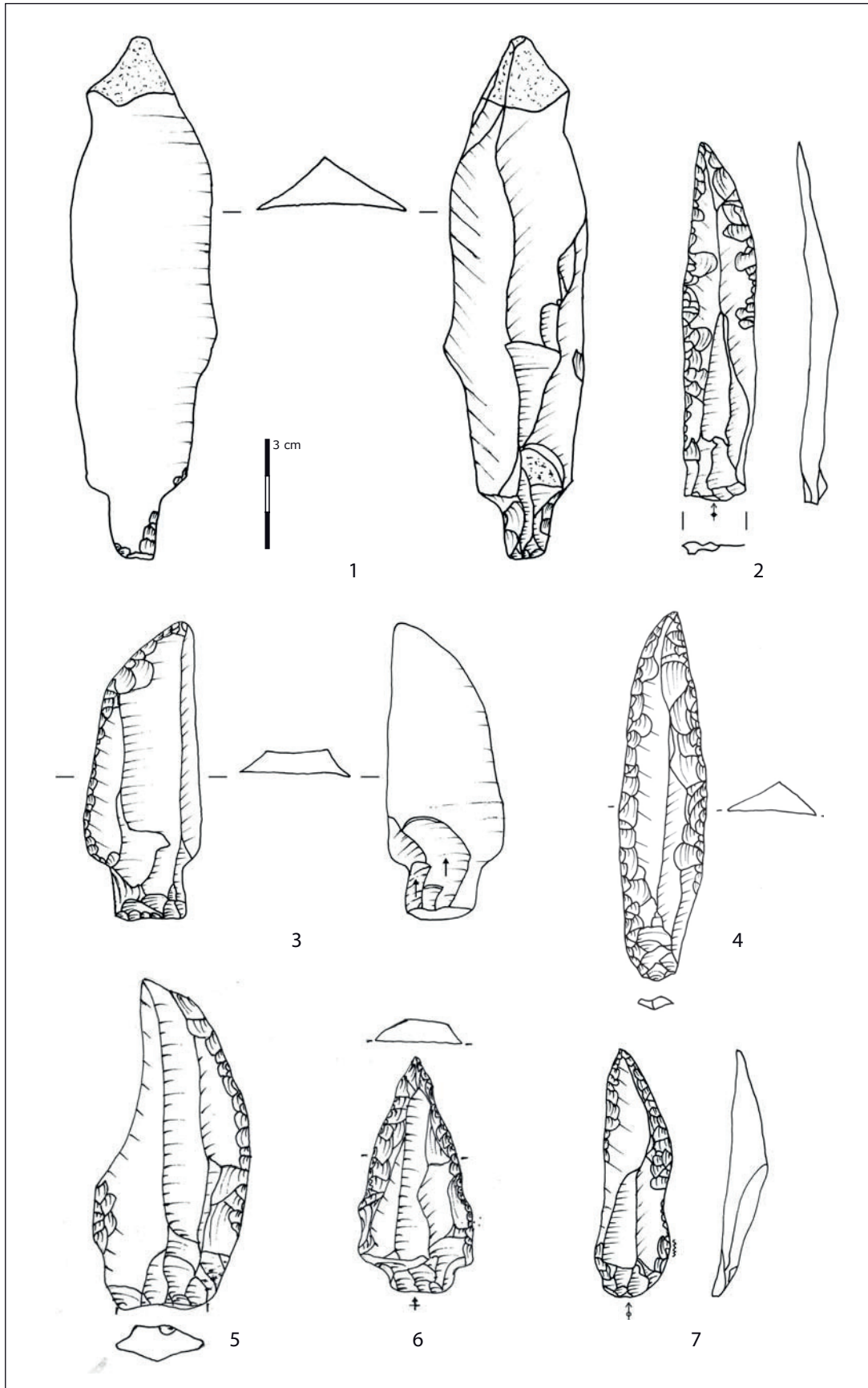


Fig. 114: Selected artefacts from assemblages 6b, 6c2 and sand h.

- 1: blade with tang; 2, 4, 5, 6, 7: retouched points with well prepared proximal part
- 3: single scarper with tang;

Fig. 114

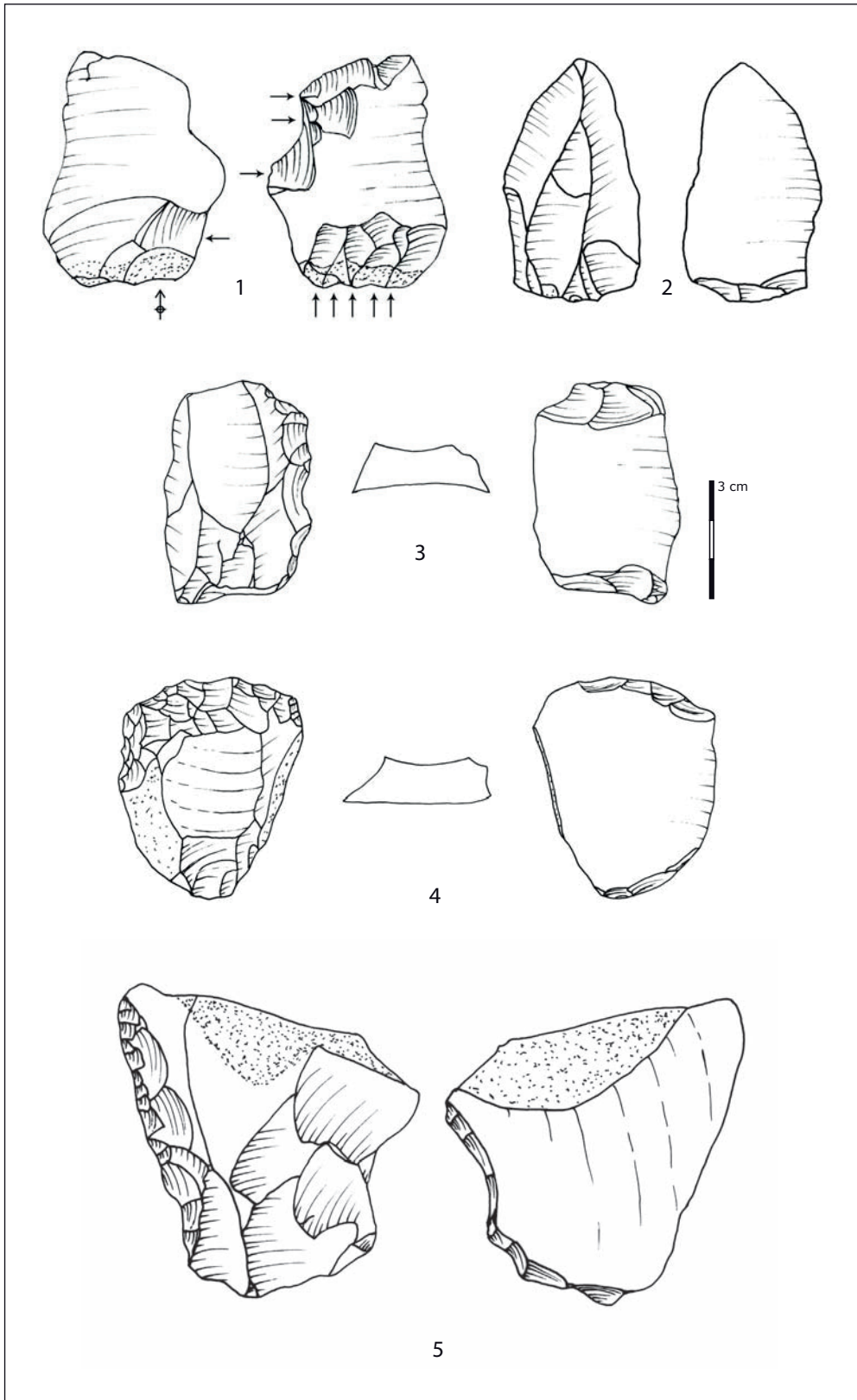


Fig. 115: Nahr Ibrahim items from Layers 6a, 6b and 6c2.

Fig. 115

Plot Group Means with 95% Confidence Intervals

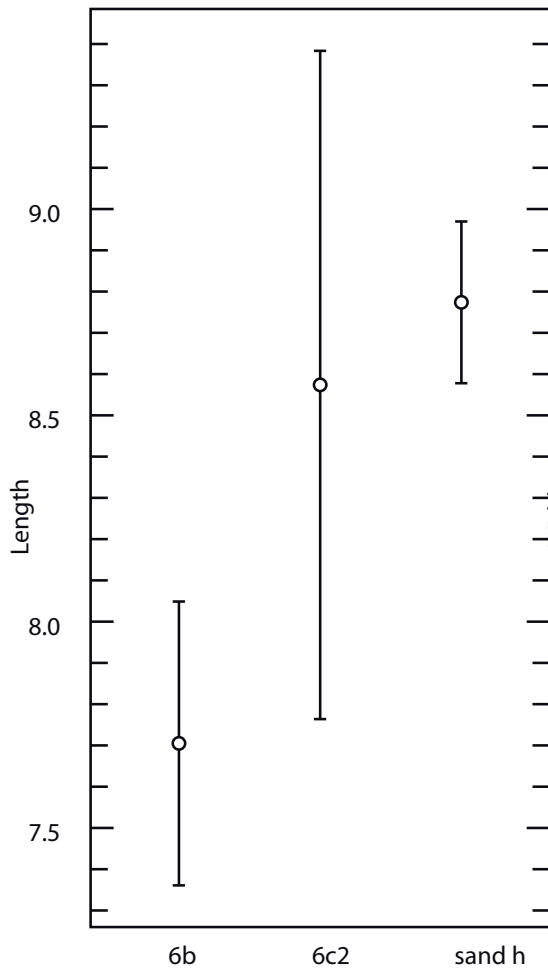


Fig. 116: Central tendency in Length of retouched tools on blades.

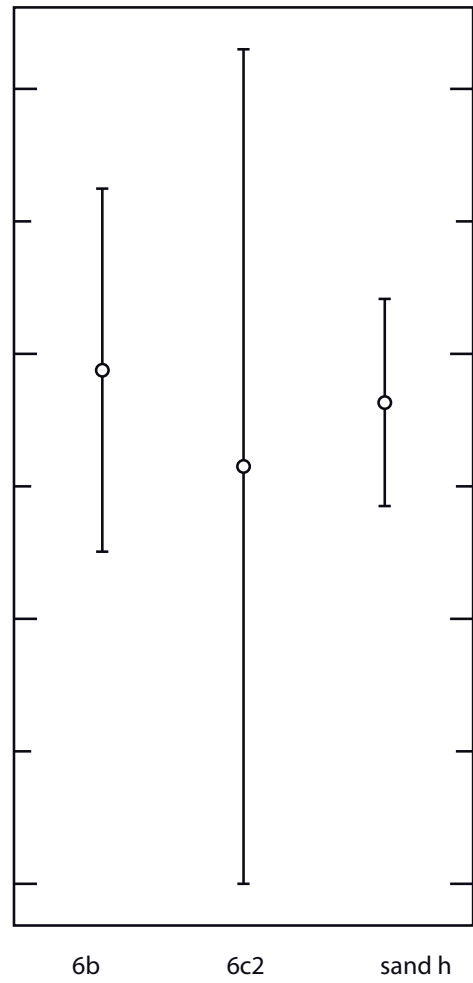


Fig. 119: Central tendency in Width of retouched tools on blades.

Fig. 116, 119

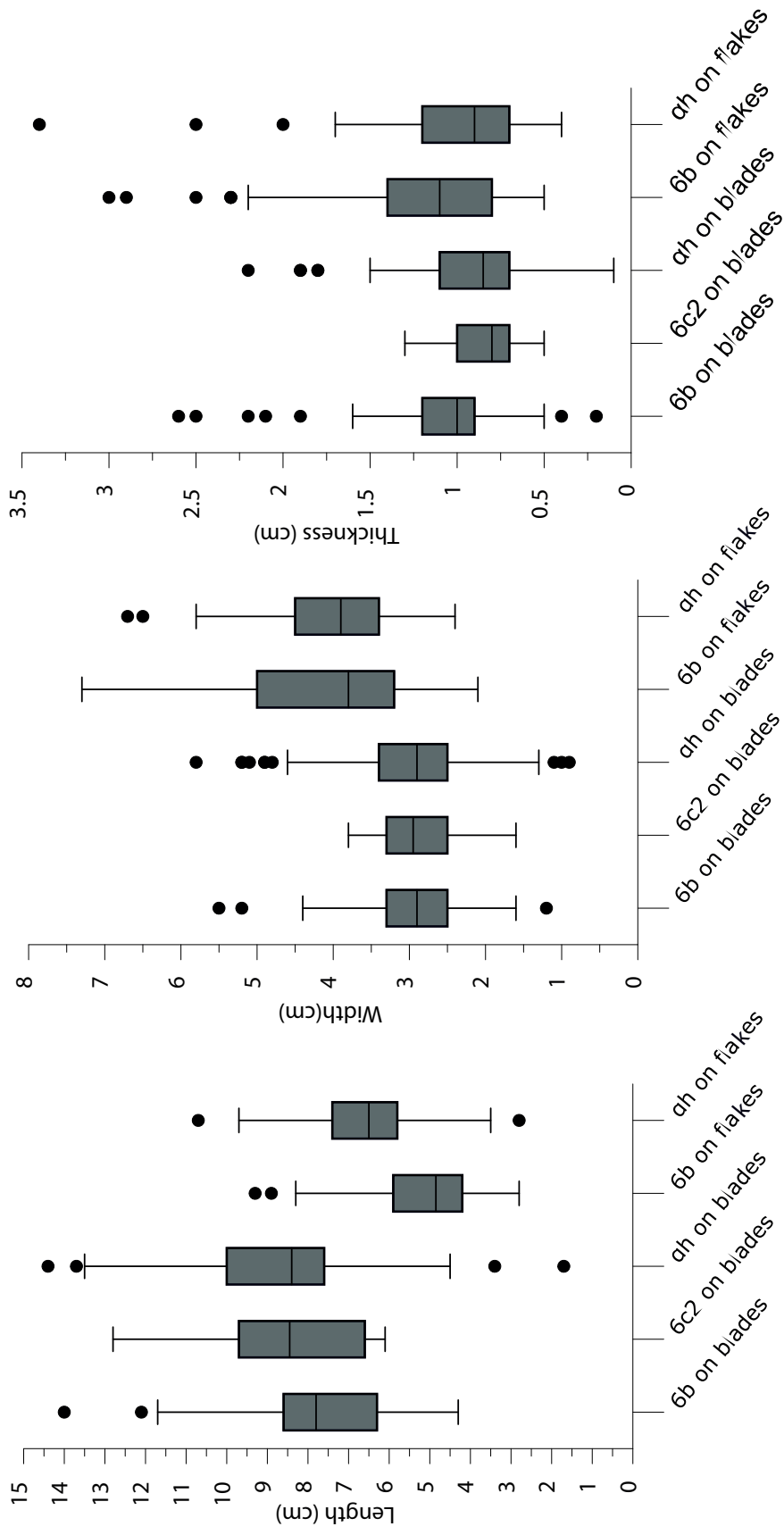


Fig. 117, 118, 122

Fig. 117: Length of retouched tools.

Fig. 118: Width of retouched tools.

Fig. 122: Thickness of retouched blades.

Plot Group Means with 95% Confidence Intervals

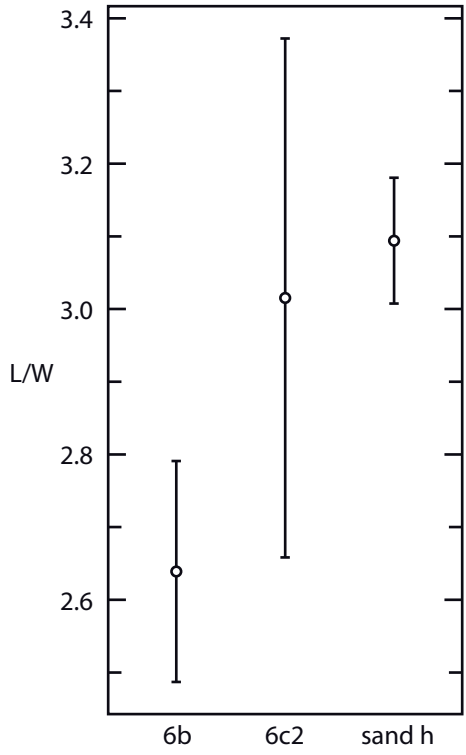


Fig. 120a: Central tendency in ratio L/W of retouched tools on blades.

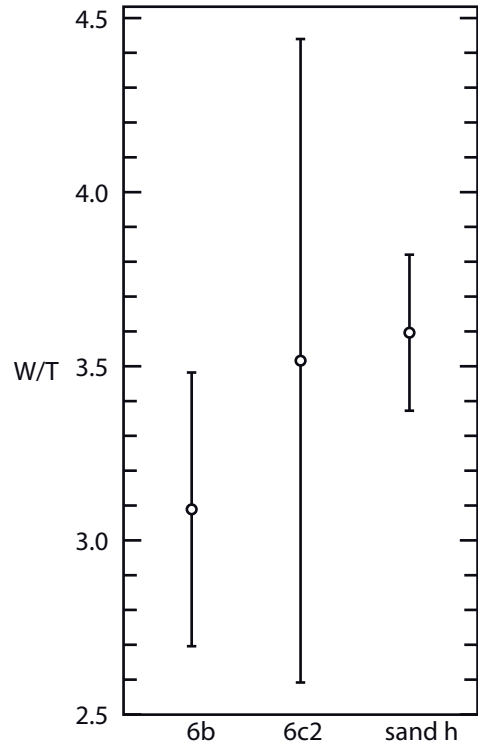


Fig. 120b: Central tendency in ratio W/T of retouched tools on blades.

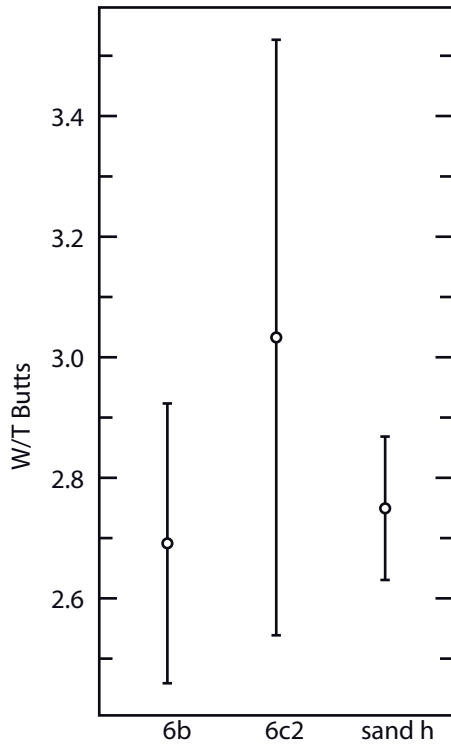


Fig. 120c: Central tendency in ratio W/T of butts of retouched tools on blades.

Fig. 120

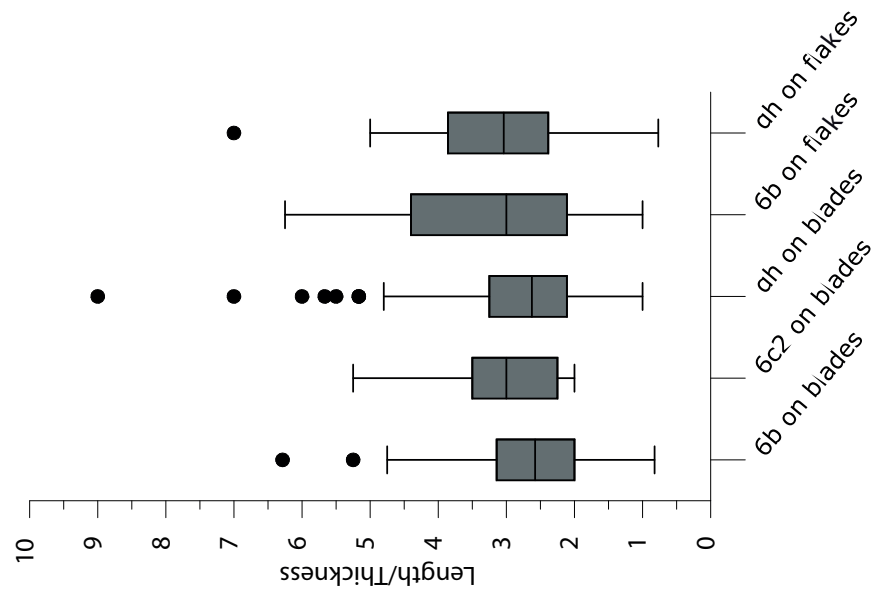


Fig.121c: Ratio W/T of butts of retouched tools.

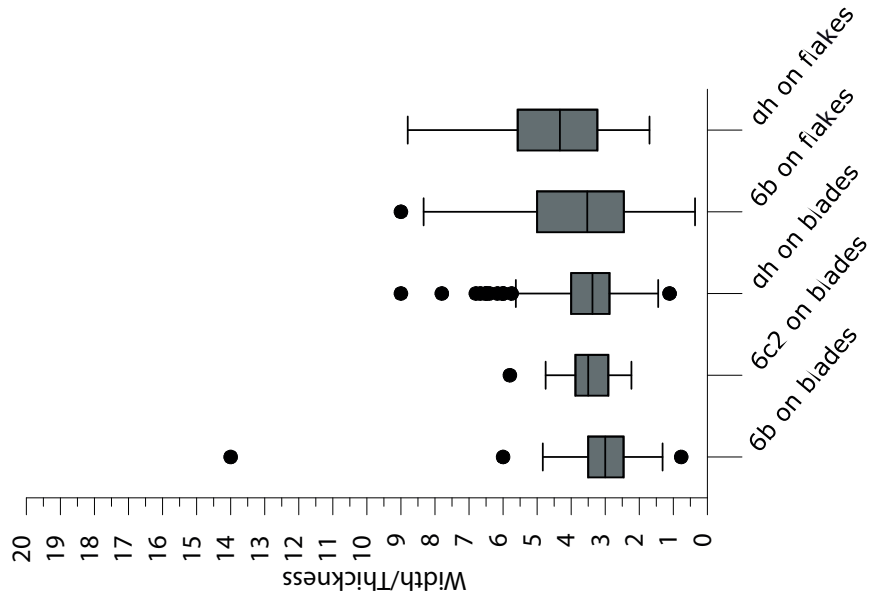


Fig.121b: Ratio W/T of retouched blades.

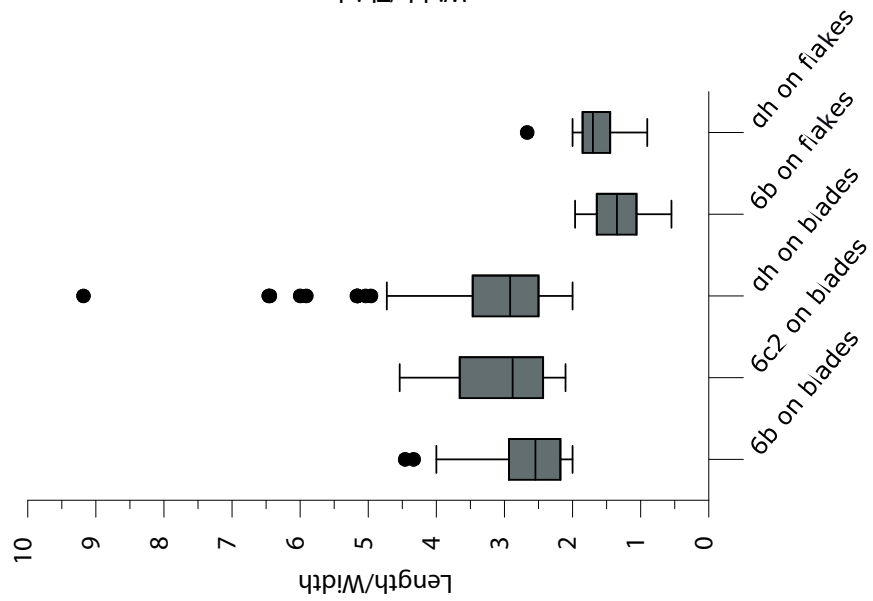


Fig.121a: Ratio L/W of retouched tools.

Fig. 121

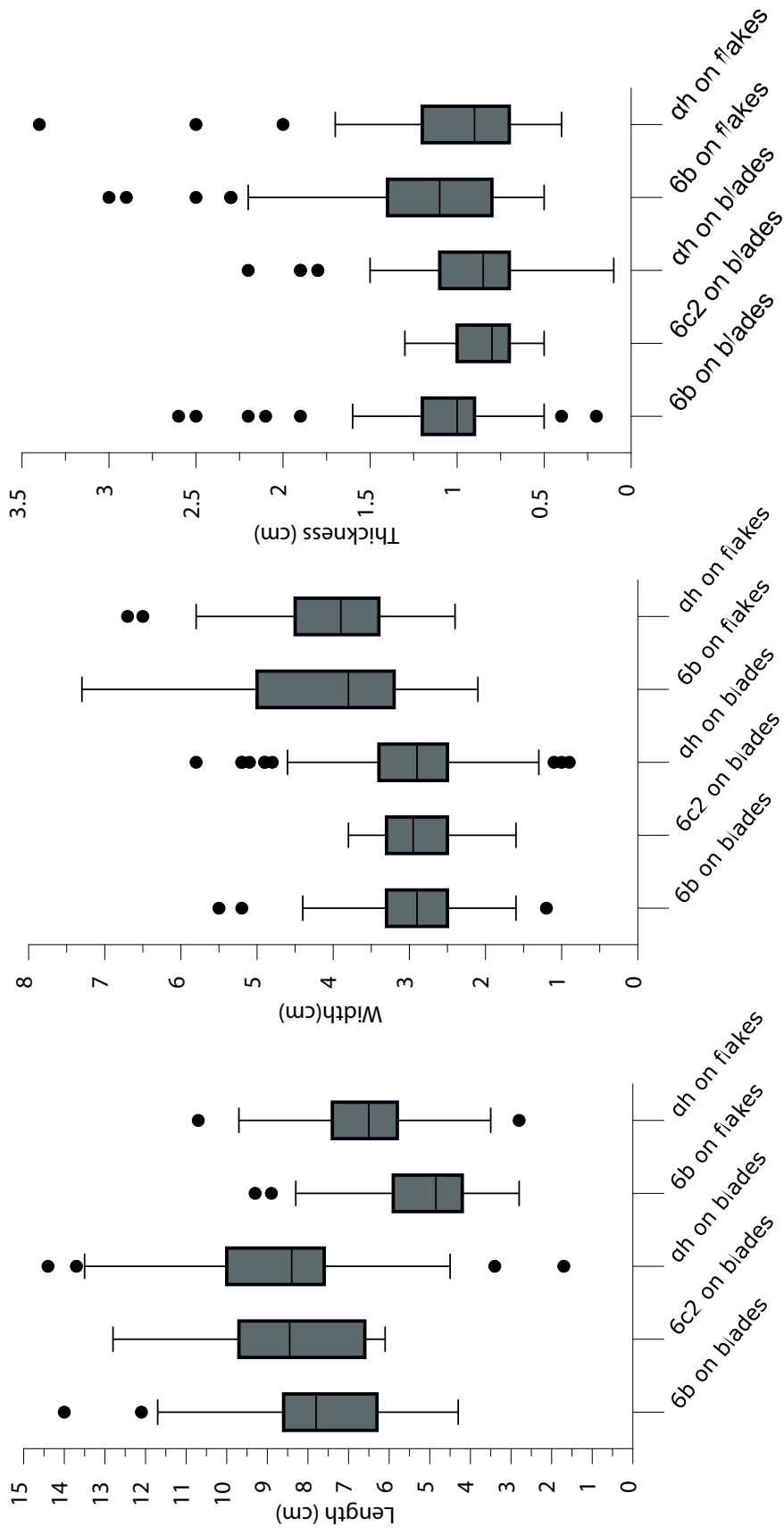


Fig. 117, 118, 122

Fig. 117: Length of retouched tools.

Fig. 118: Width of retouched tools.

Fig. 122: Thickness of retouched blades.

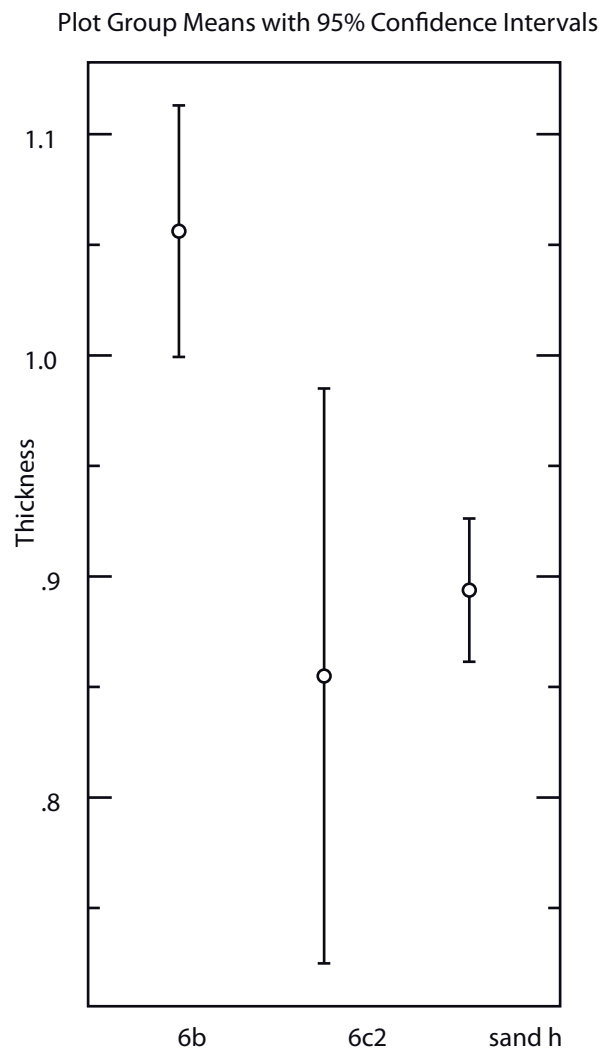


Fig. 123: Central tendency in thickness of retouched tools.

Fig. 123

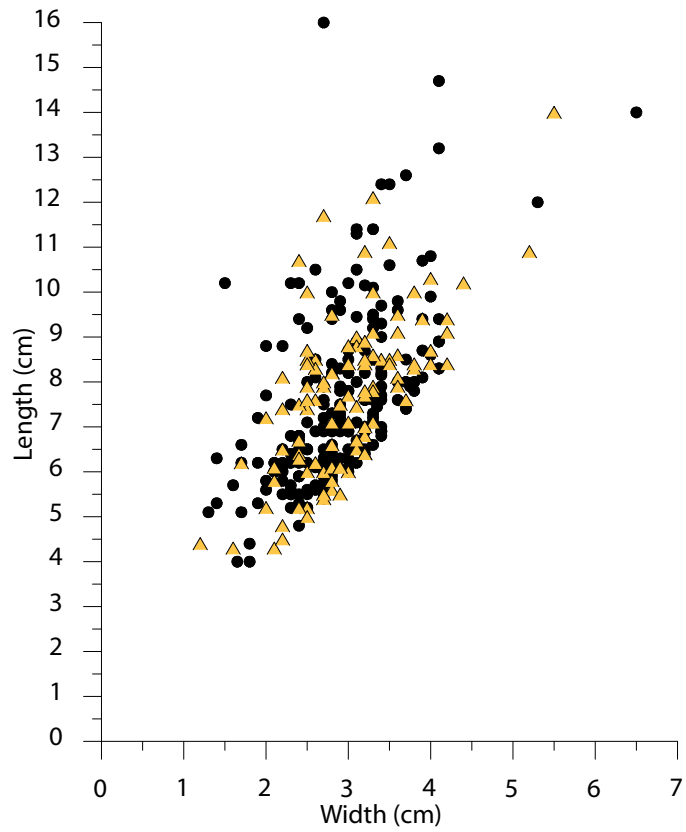


Fig. 124: The length and width of retouched (triangle) and unretouched (circle) blades from layer 6b.

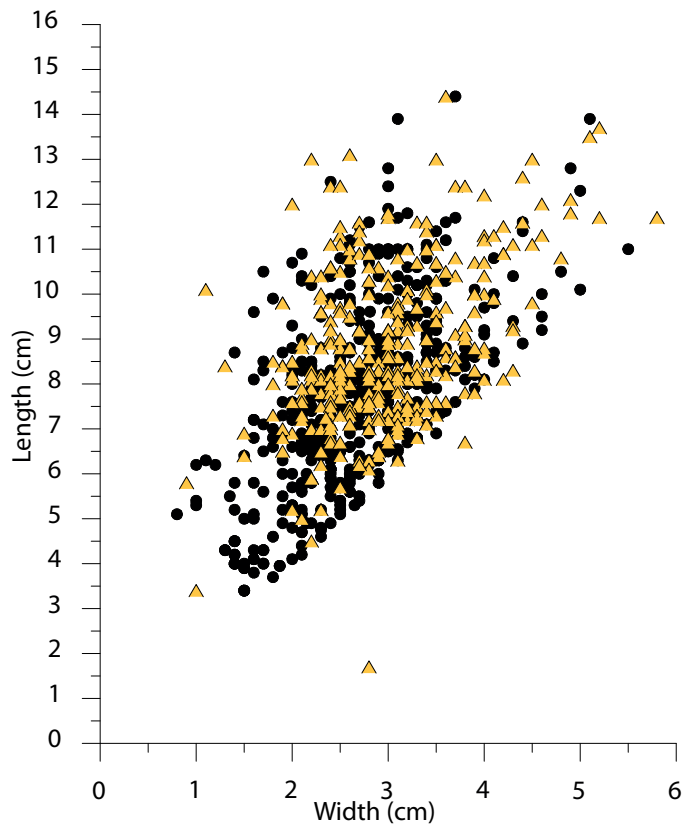


Fig. 125: The length and width of retouched (triangle) and unretouched (circle) blades from sand ah.

Fig. 124, 125

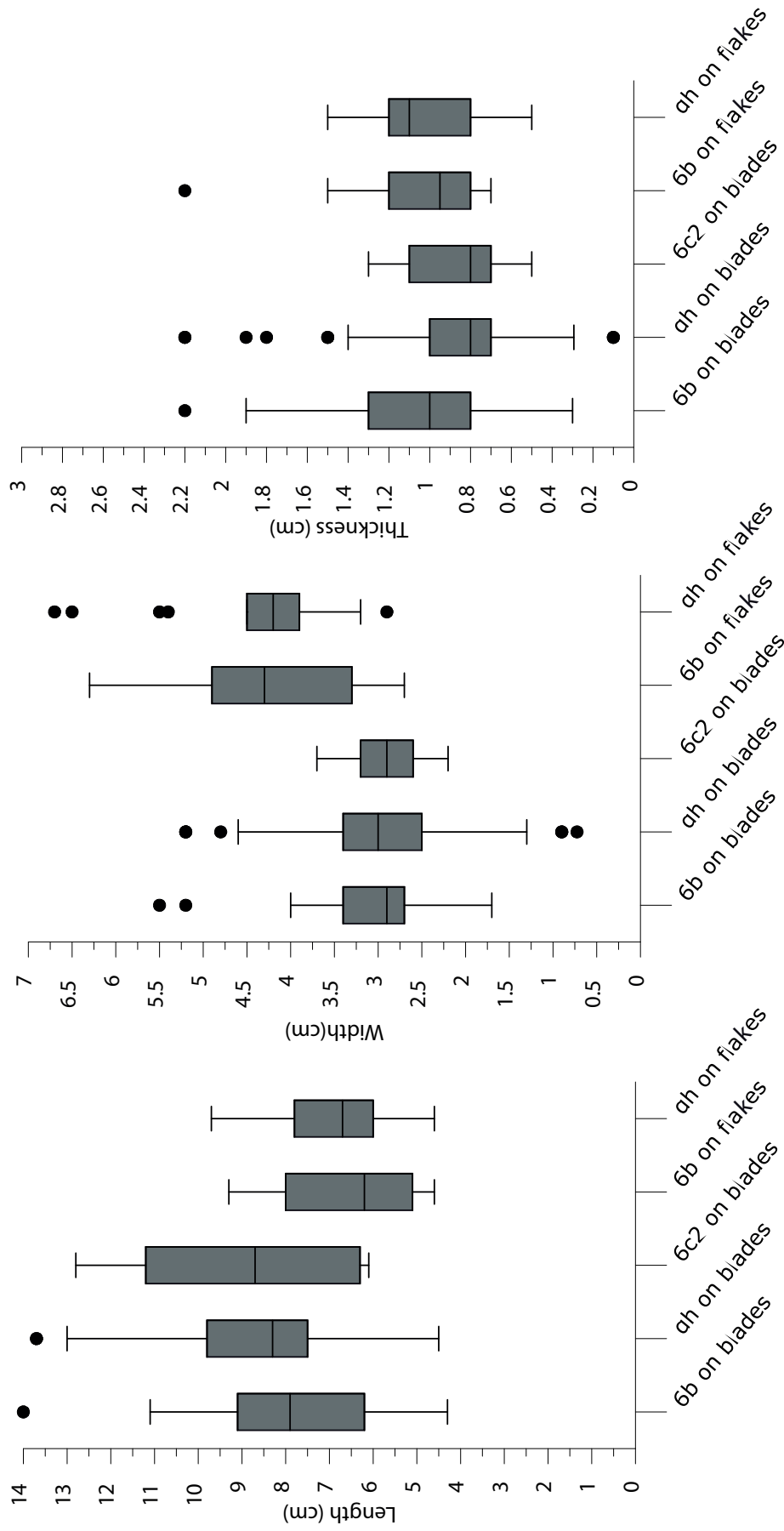


Fig. 126

Fig. 126a: Length of single scrapers.

Fig. 126b: Width of single scrapers.

Fig. 126c: Thickness of single scrapers.

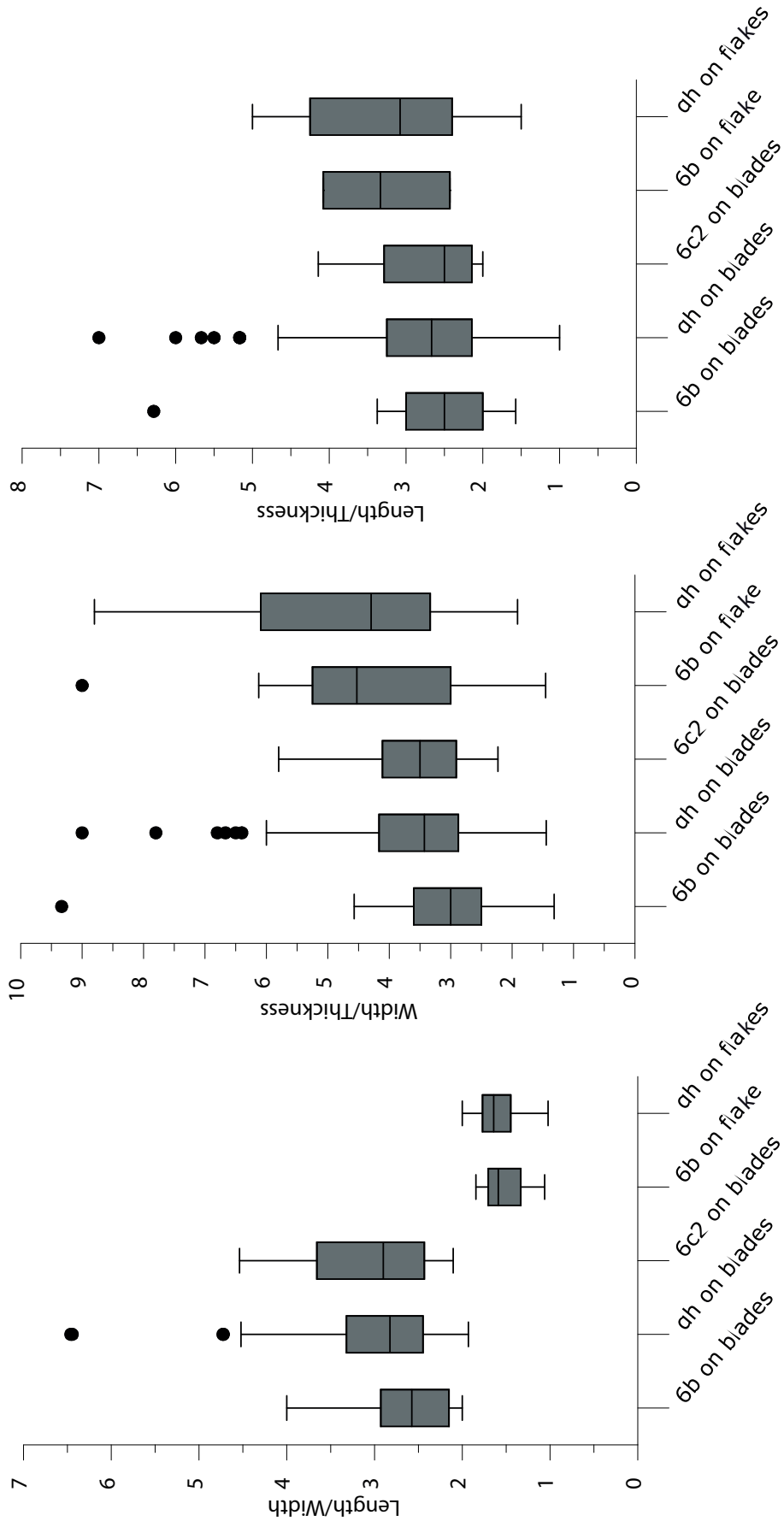


Fig. 127

Fig. 127a: Ratio L/W of single scrapers.

Fig. 127b: Ratio W/T of single scrapers.

Fig. 127c: Ratio W/T of butts of single scrapers.

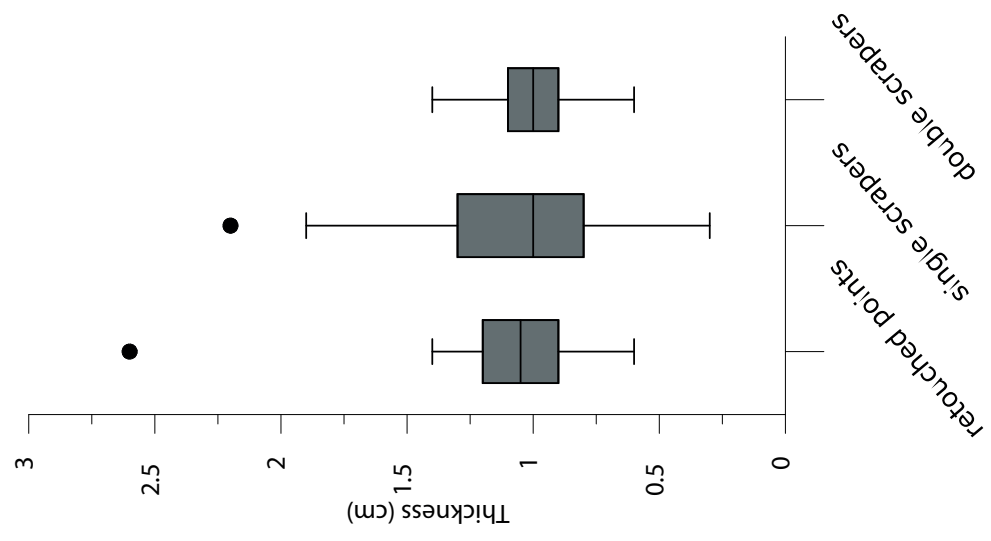


Fig. 128c: Thickness of retouched tools on blades in layer 6b.

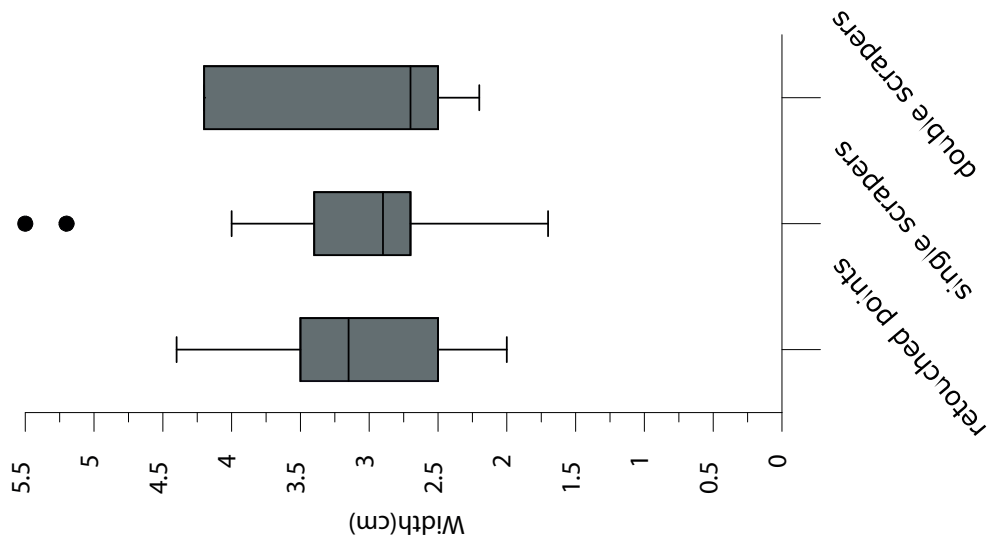


Fig. 128b: Width of retouched tools on blades in layer 6b.

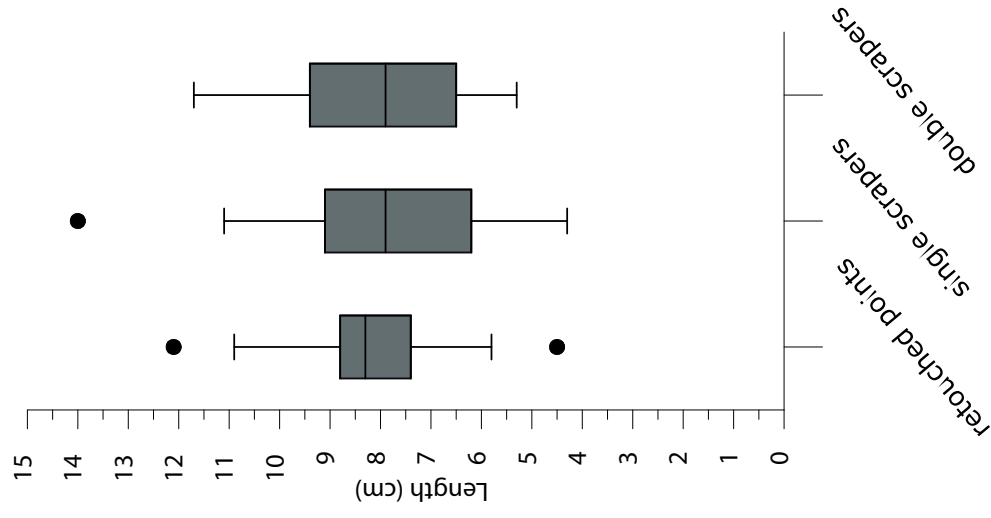


Fig. 128a: Length of retouched tools on blades in layer 6b.

Fig. 128

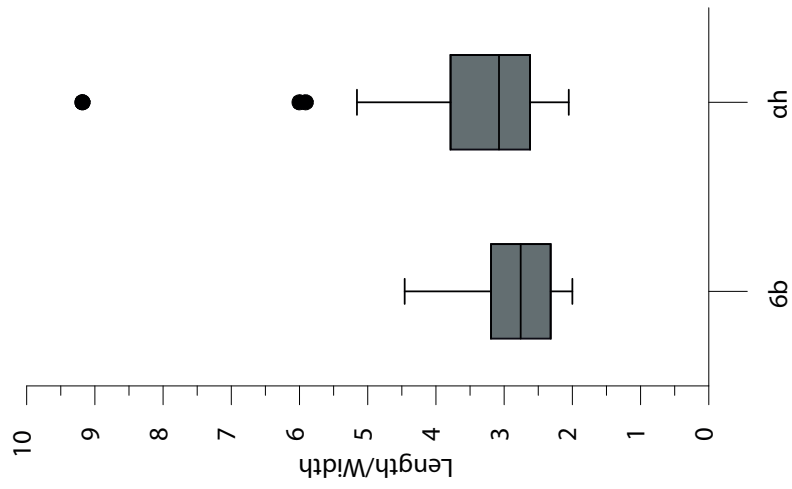


Fig. 129a: Ratio L/W of retouched points on blades.

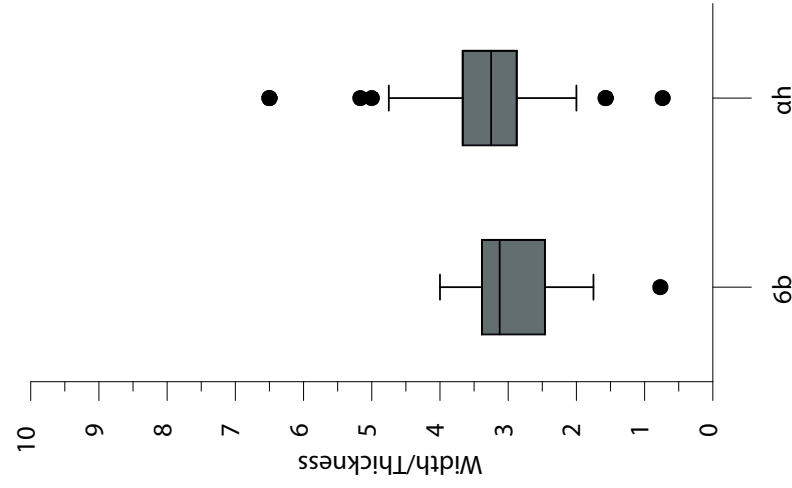


Fig. 129b: Ratio W/T of retouched points on blades.

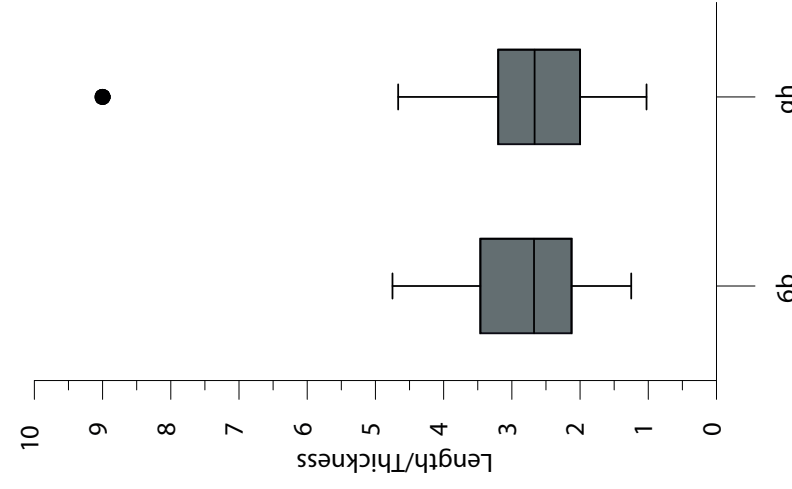


Fig. 129c: Ratio W/T of butts of retouched points on blades.

Fig. 129

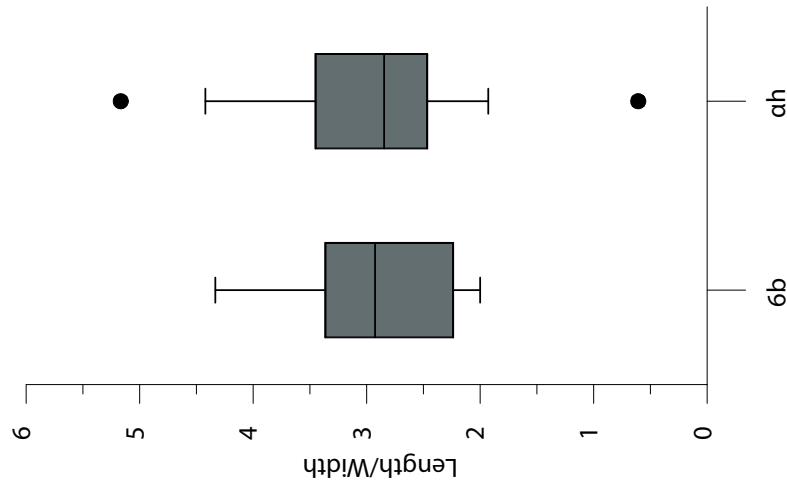


Fig. 130a: Ratio L/W of double scrapers on blades.

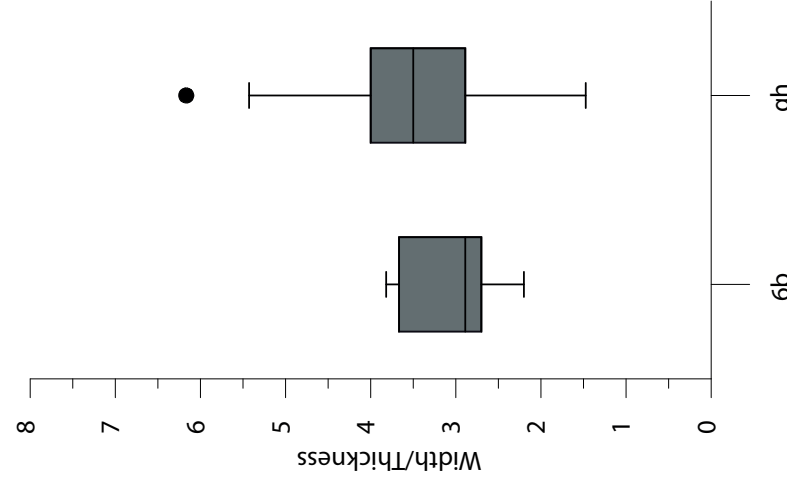


Fig. 130b: Ratio W/T of double scrapers on blades.

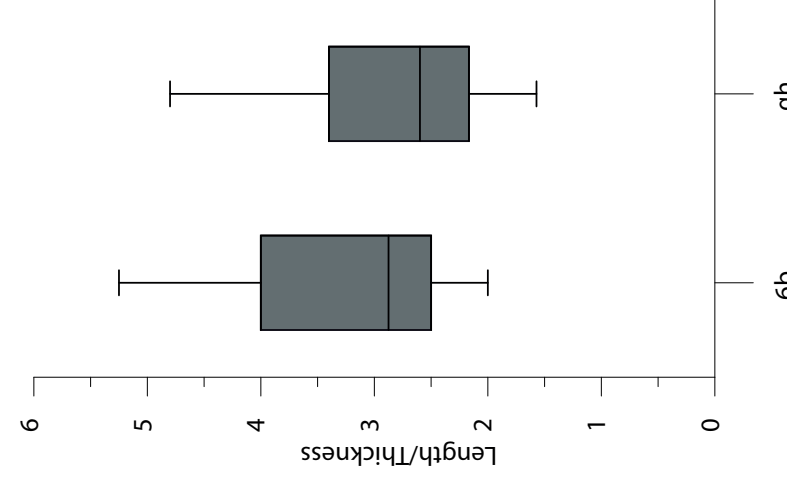


Fig. 130c: Ratio W/T of butts of double scrapers on blades.

Fig. 130

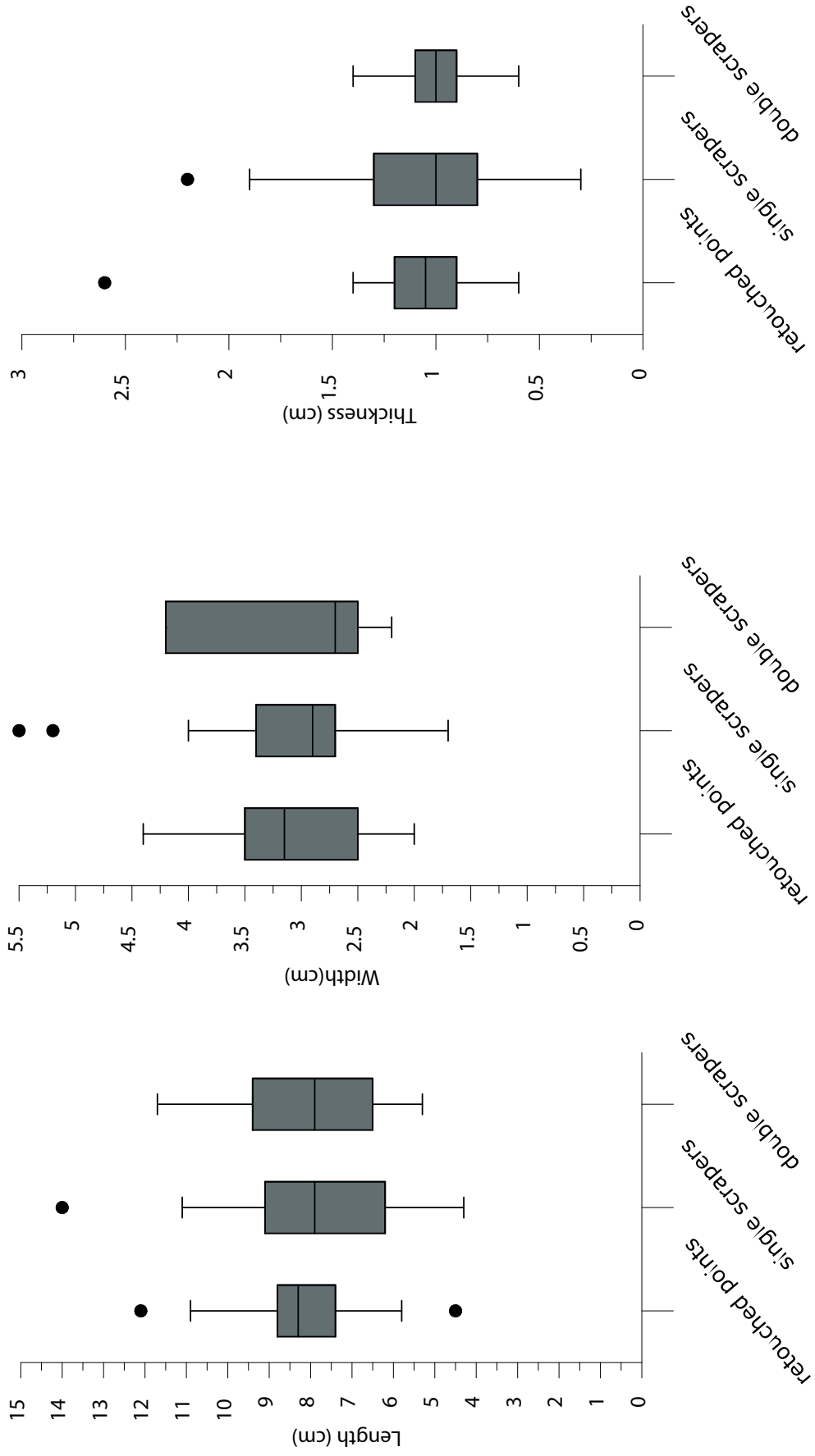


Fig. 131

Fig.131a: Length of retouched tools on blades in layer 6b.

Fig. 131b: Width of retouched tools on blades in layer 6b.

Fig. 131c: Thickness of retouched tools on blades in layer 6b.

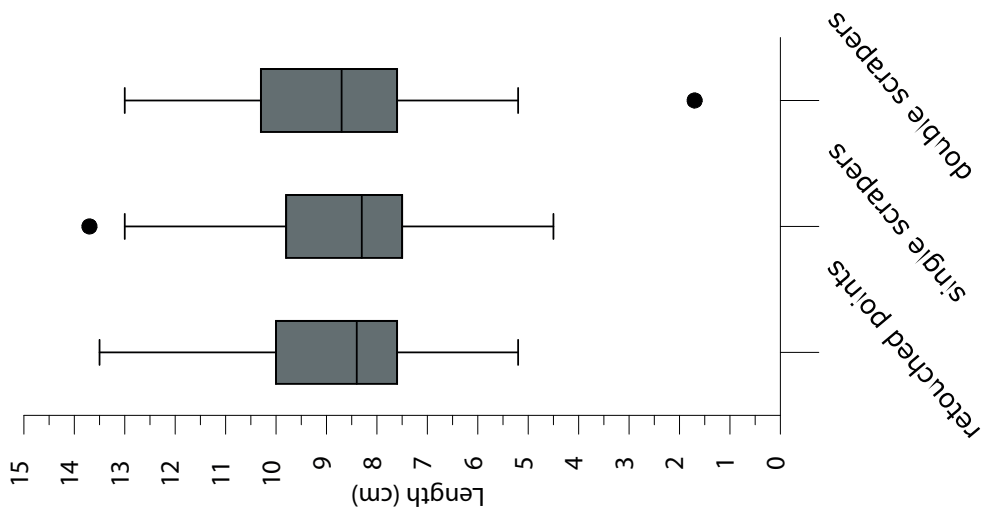


Fig. 132a: Length of retouched tools on blades in sand ah.

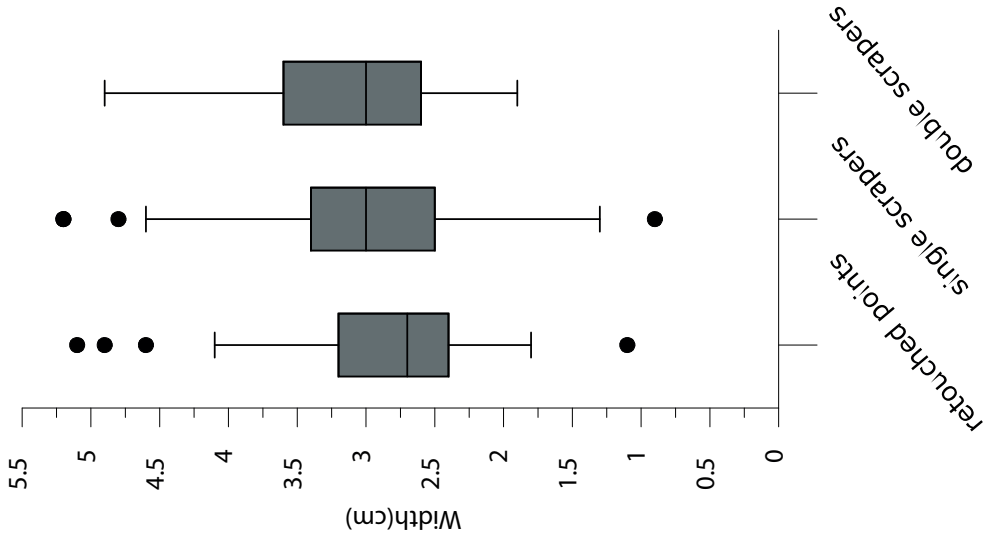


Fig. 132b: Width of retouched tools on blades in sand ah.

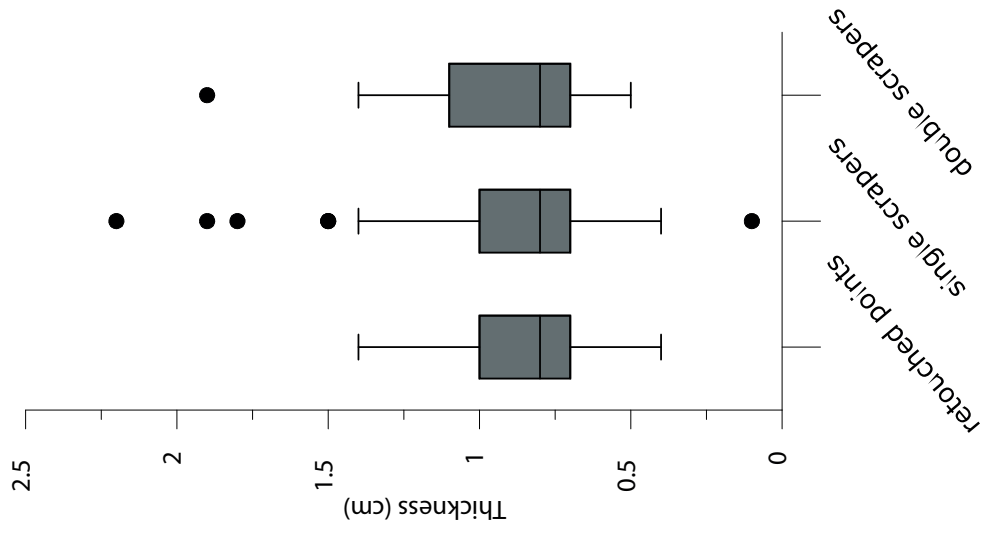


Fig. 132c: Thickness of retouched tools on blades in sand ah.

Fig. 132

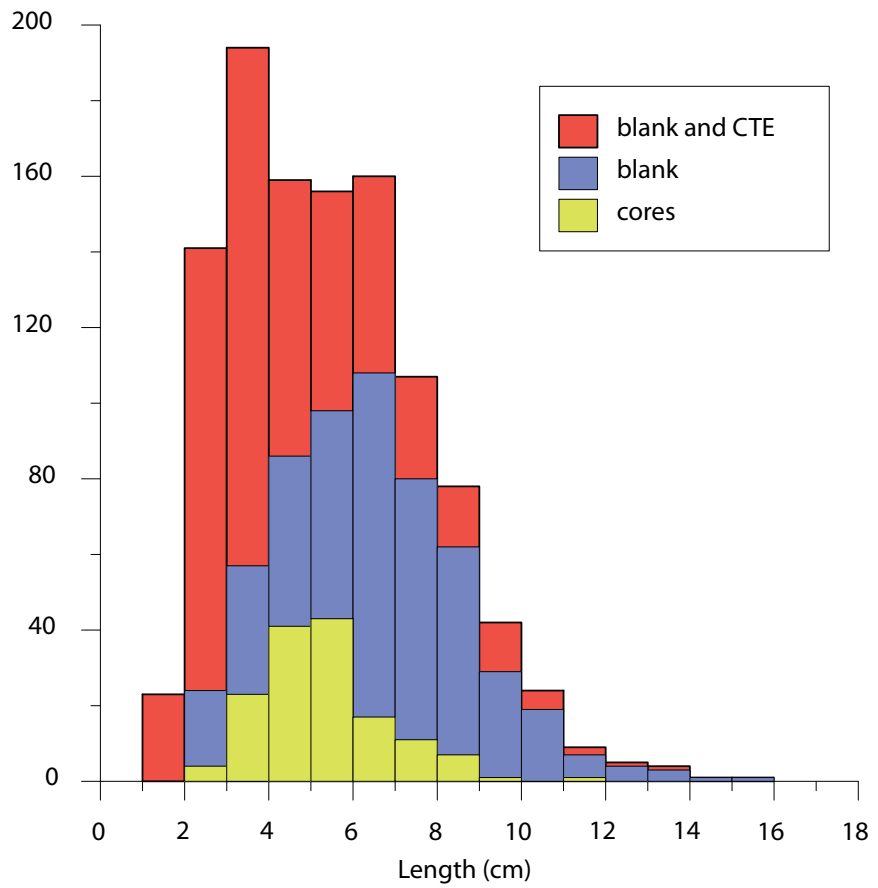


Fig. 133: Layer 6b: length of cores, blanks and CTE.

Fig. 133

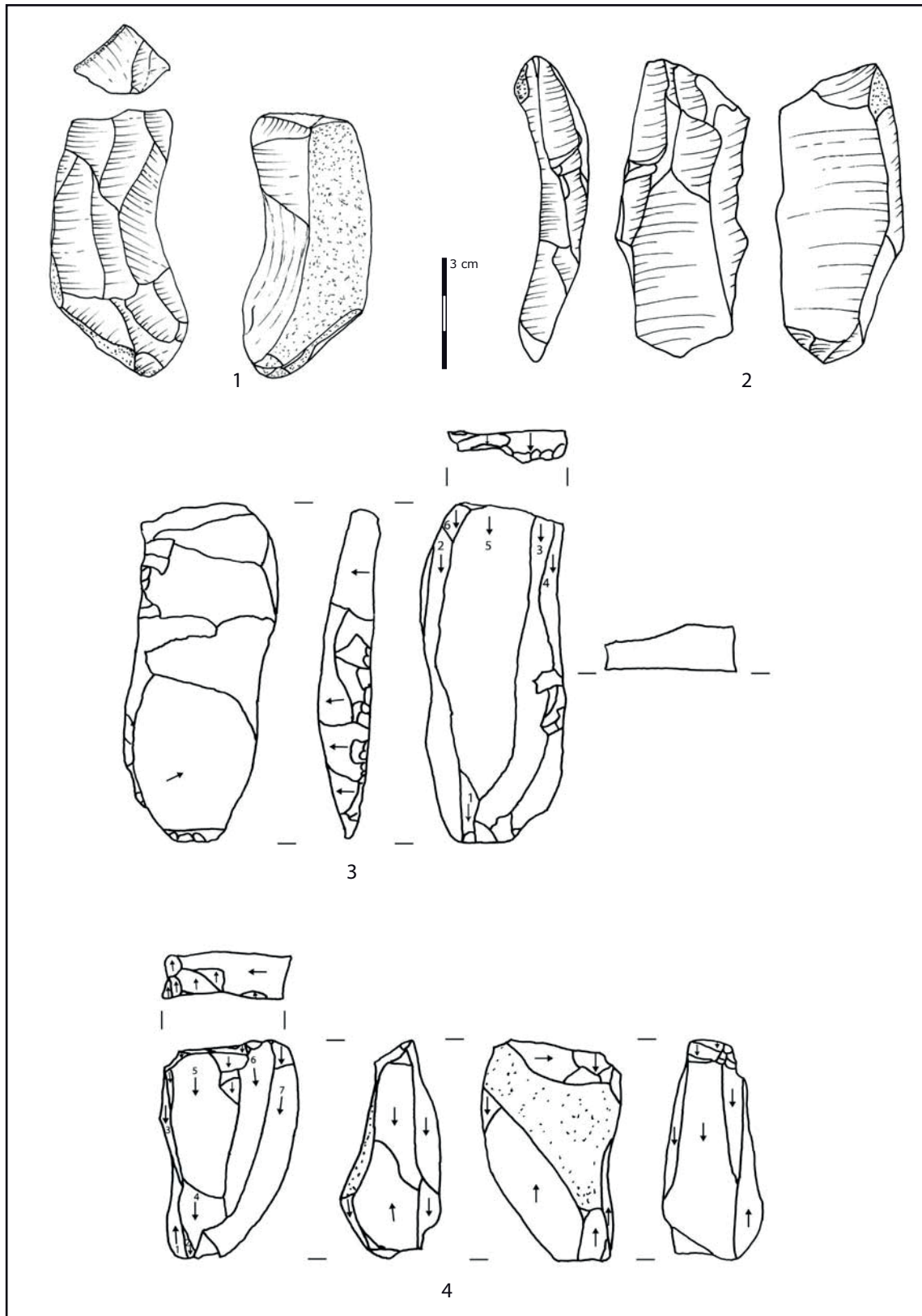
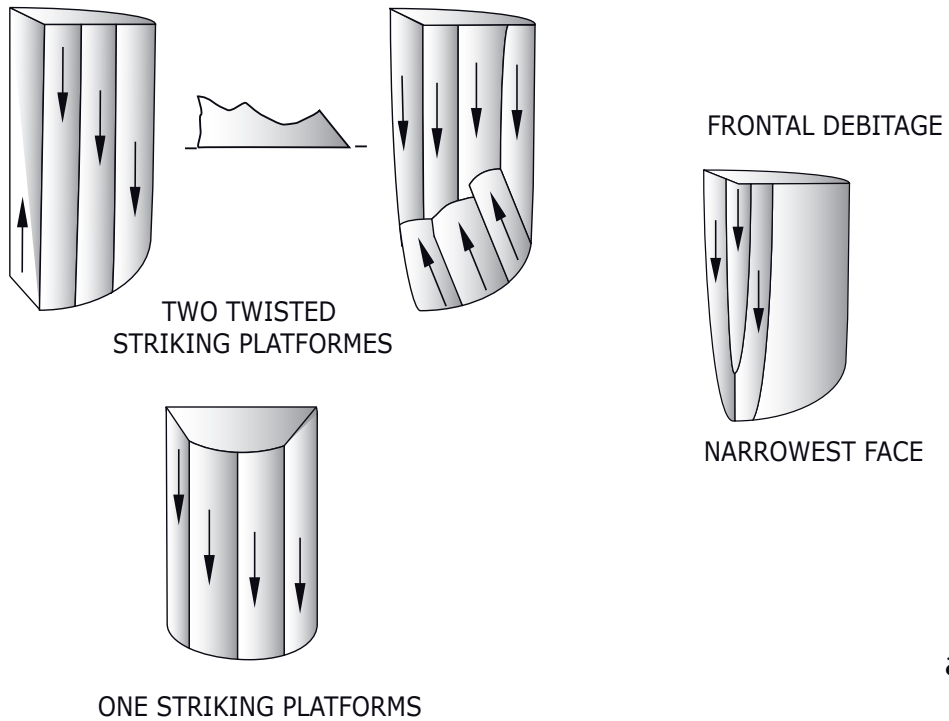


Fig. 134 : Laminar cores from Layer 6b.
 1: bidirectional cores on block; 2: bidirectional core on flake; 3: unidirectional core on flake;
 4: core on block.

Fig. 134

REDUCTION STRATEGY IN LAMINAR METHOD
SEMI-ROTATING DEBITAGE



CROSS SECTION OF LAMINAR CORES

side allowing the extension of flaking surface

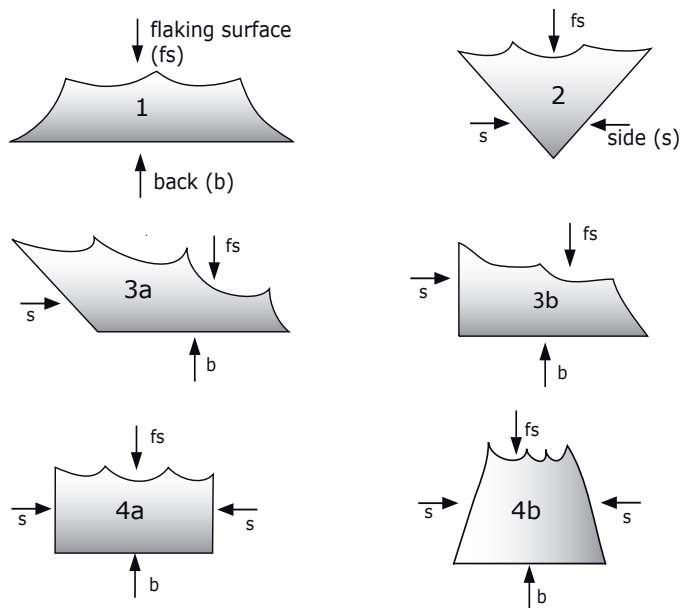


Fig. 135

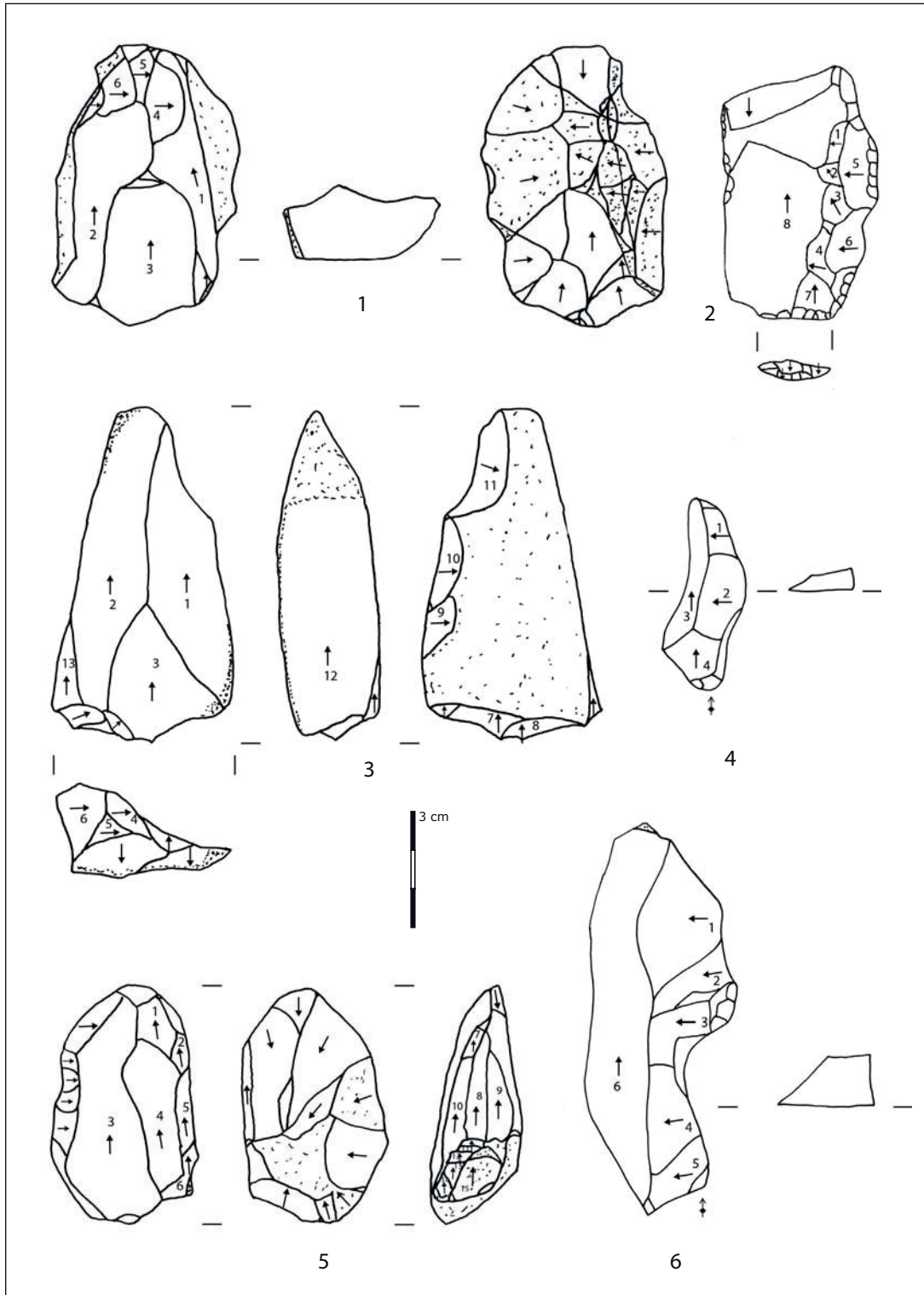


Fig. 136 : Levallois cores and products from Layer 6b.

1: core showing recurrent method;

2: *enlèvement II*

3, 5: cores showing recurrent method, reused for bladelets production:
frontal debitage on its side;

4, 6: *lames débordantes*.

Fig. 136

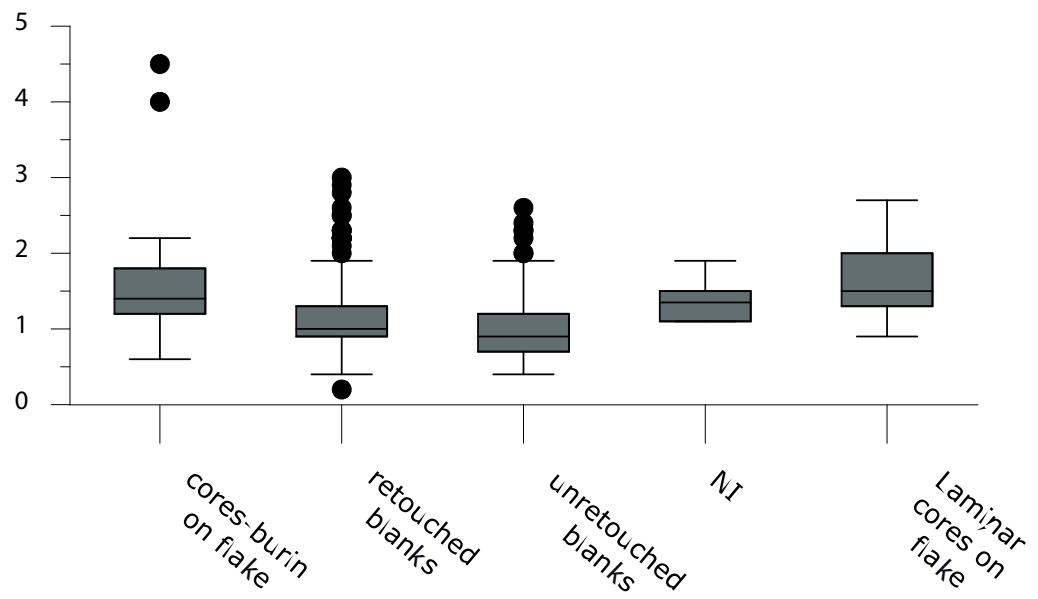


Fig. 137: Thickness of cores-burin, cores NI, cores on flake and blanks in layer 6b.

Fig. 137

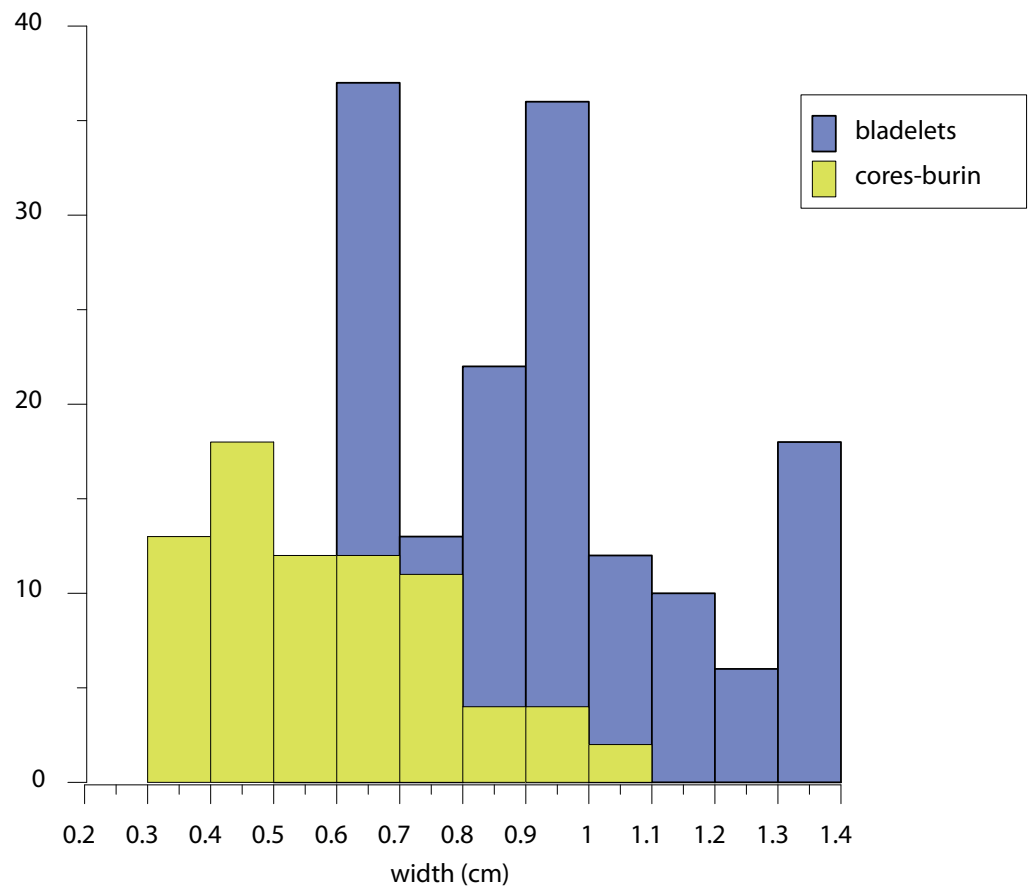


Fig.138: Layer 6b-width of bladelets and last negatives visible on the core-burins.

Fig. 138

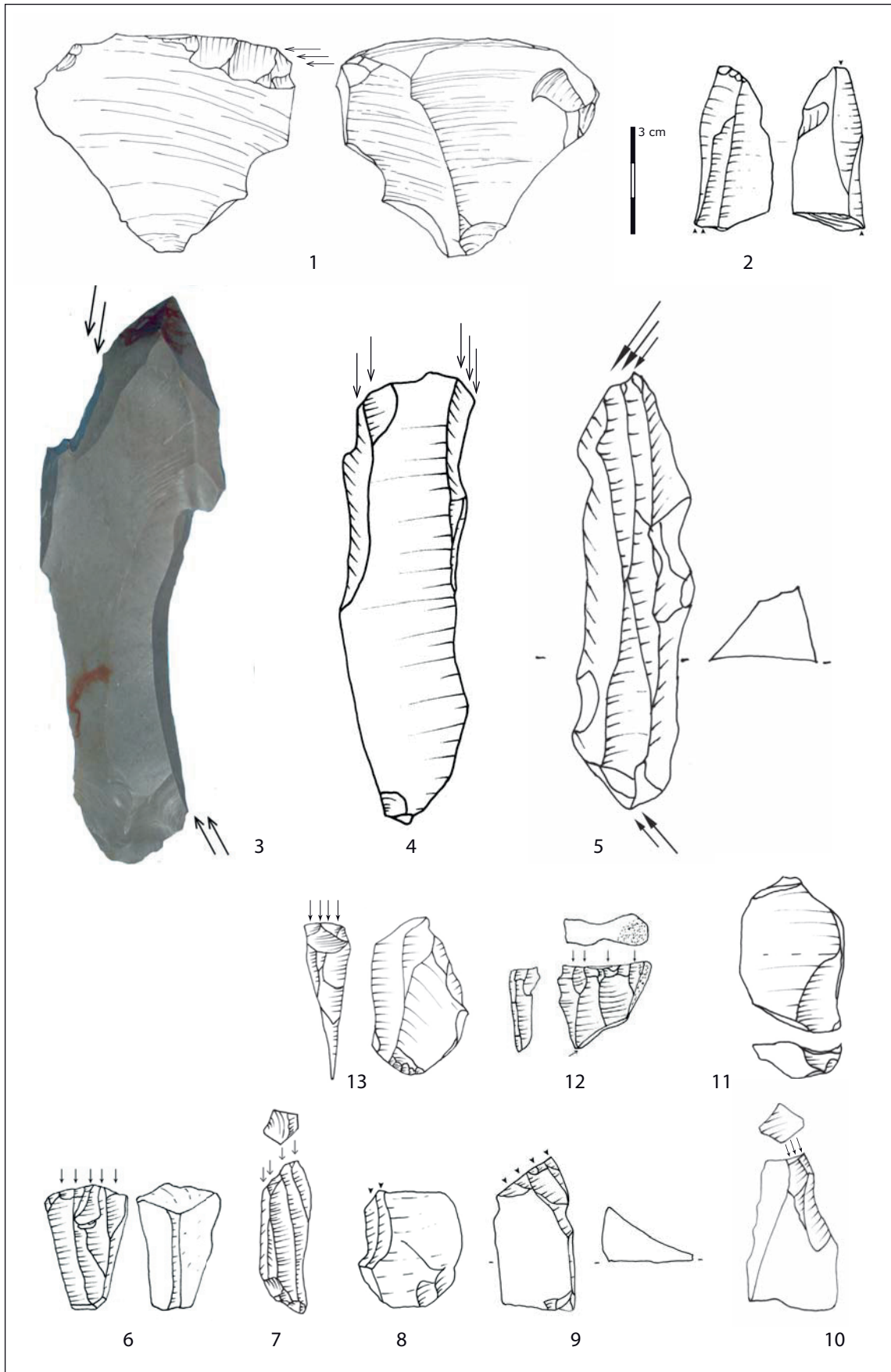


Fig. 139: Core-burins and bladelets cores from assemblages 6b, 6c2 and sand h.

1: core-burin made on distal part of overpassed flake; 2: core-burin made on débris;

3, 4, 5: cores-burins made on blades; 6, 12: bladelets cores;

7: core-burin made on blade; 8, 9: cores-burins made on débris; 10, 11, 13: cores- burin made on flake.

Fig. 139

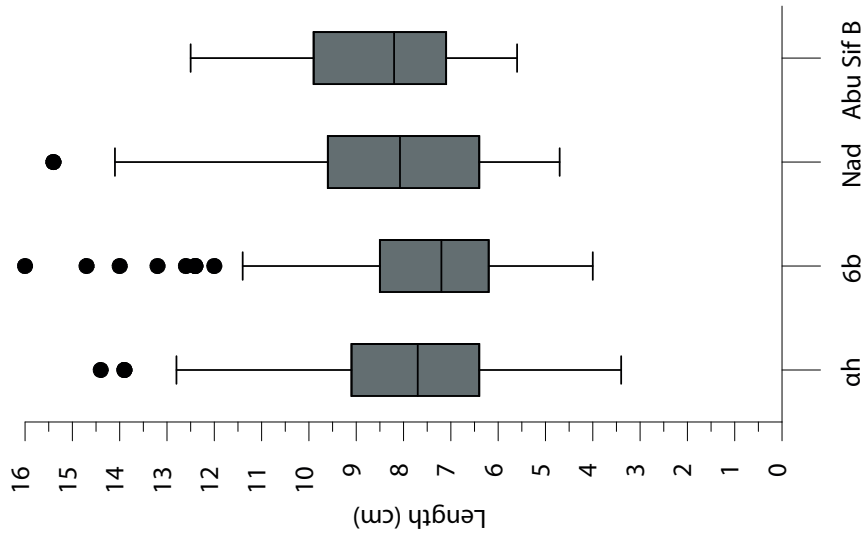


Fig. 140a: Length of unretouched blades in industries from Hummal, Nad. and Abu Sif.

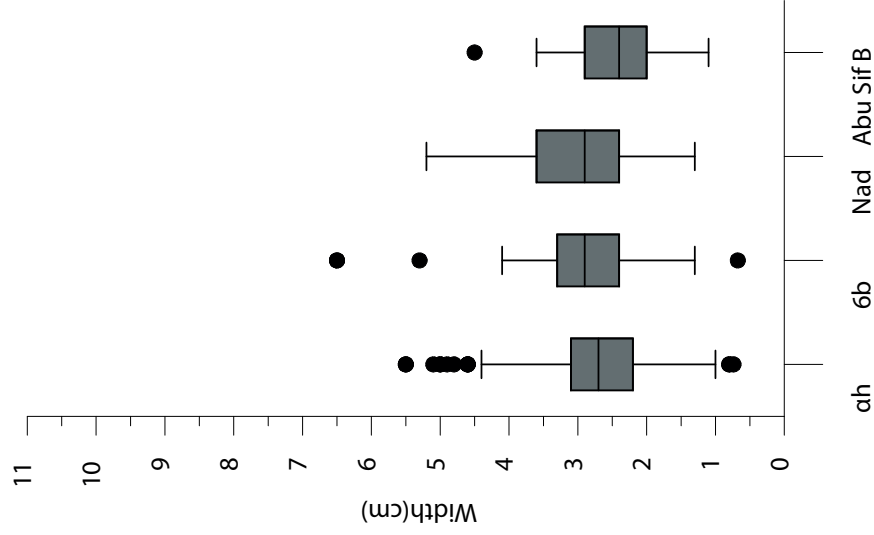


Fig.140 b:Width of unretouched blades in industries from Hummal, Nad. and Abu Sif.

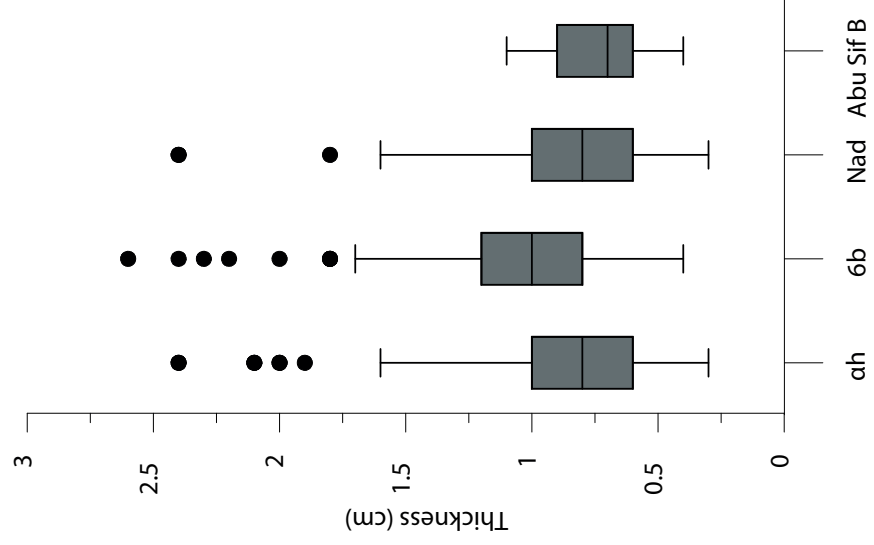


Fig. 140 c:Thickness of unretouched blades in industries from Hummal, Nad. and Abu Sif.

Fig. 140

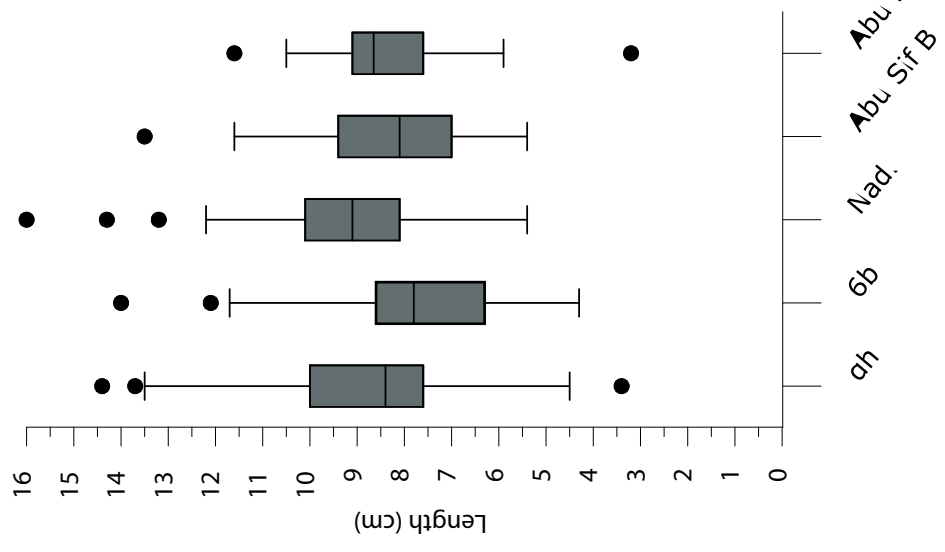


Fig.142a: Length of retouched blades in industries from Hummal, Nad. and Abu Sif.

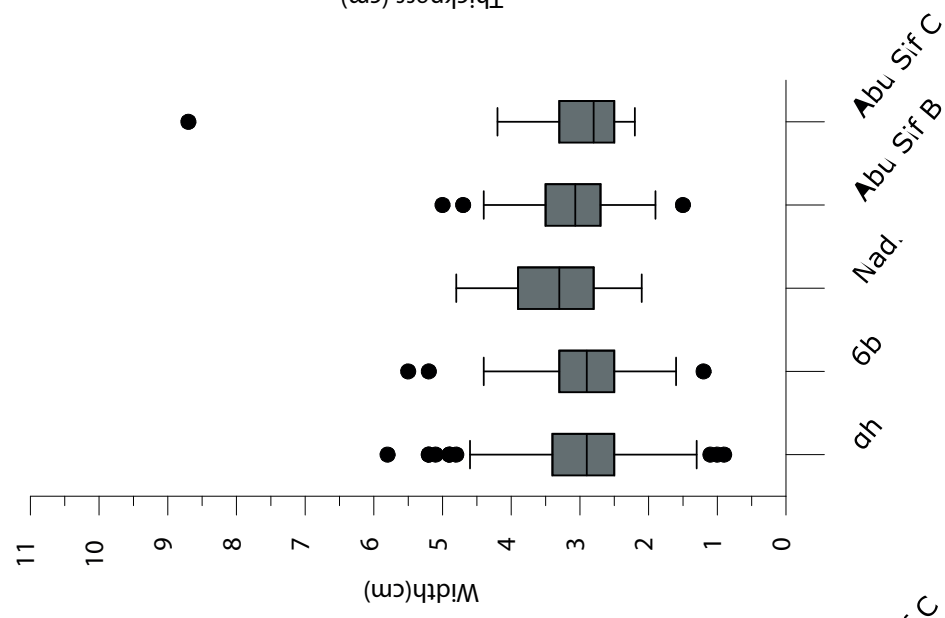


Fig.142b: Width of retouched blades in industries from Hummal, Nad. and Abu Sif.

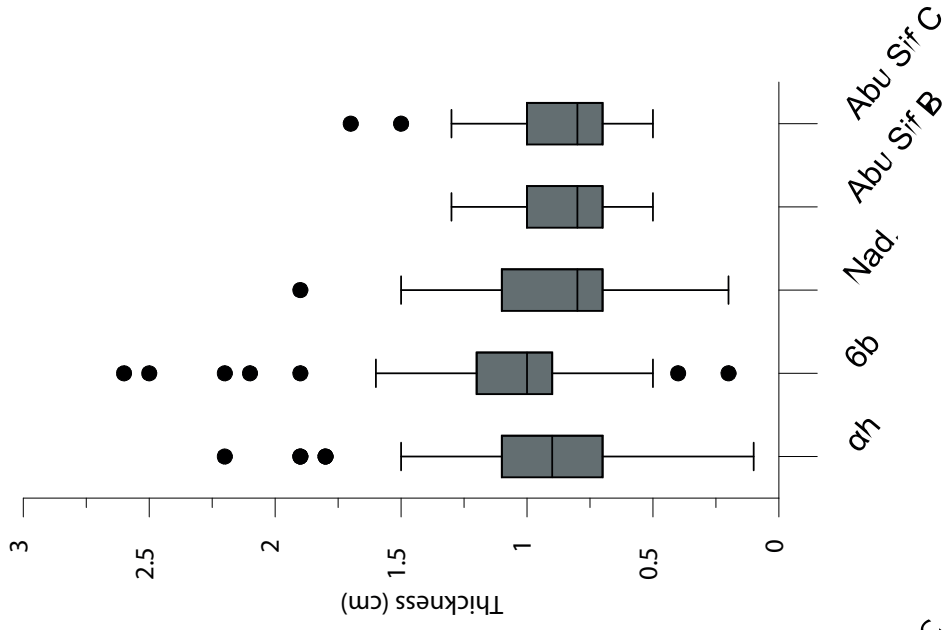


Fig.142c: Thickness of retouched blades in industries from Hummal, Nad. and Abu Sif.

Fig. 142

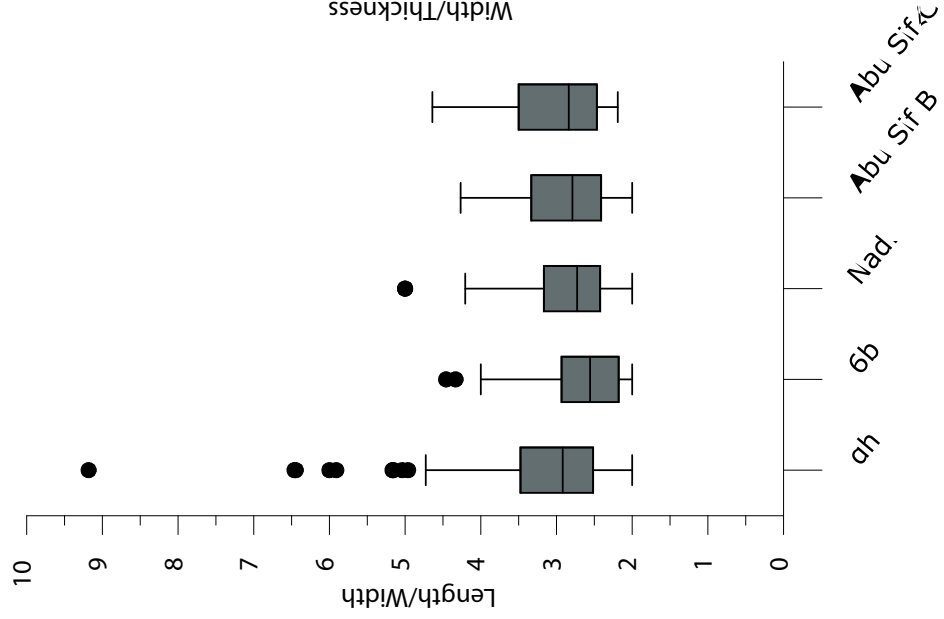


Fig. 143a: Ratio LW of retouched blades in assemblages from Hummal, Nad and Abu Sif.

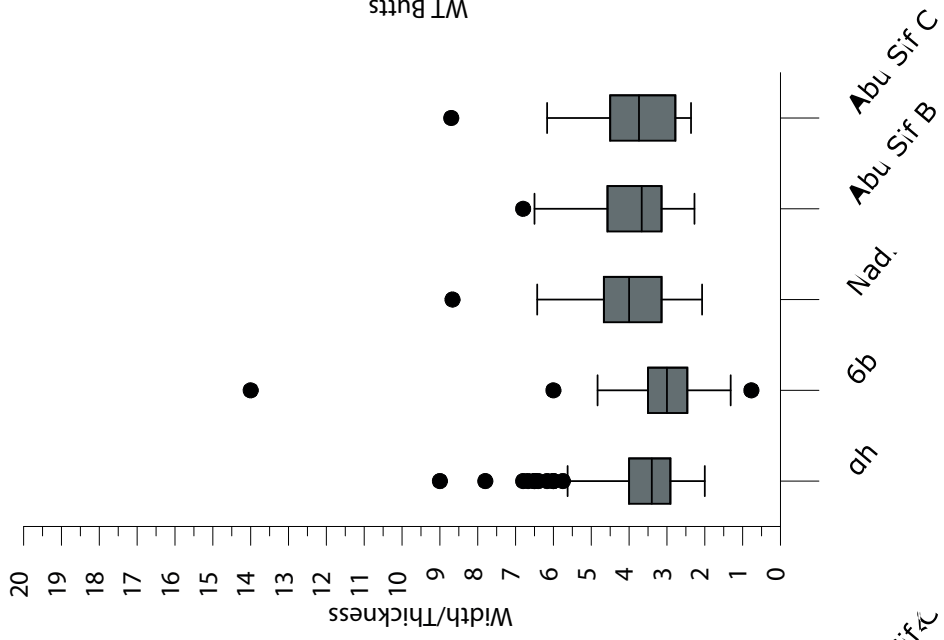


Fig. 143b: Ratio WT of retouched blades in assemblages from Hummal, Nad, and Abu Sif.

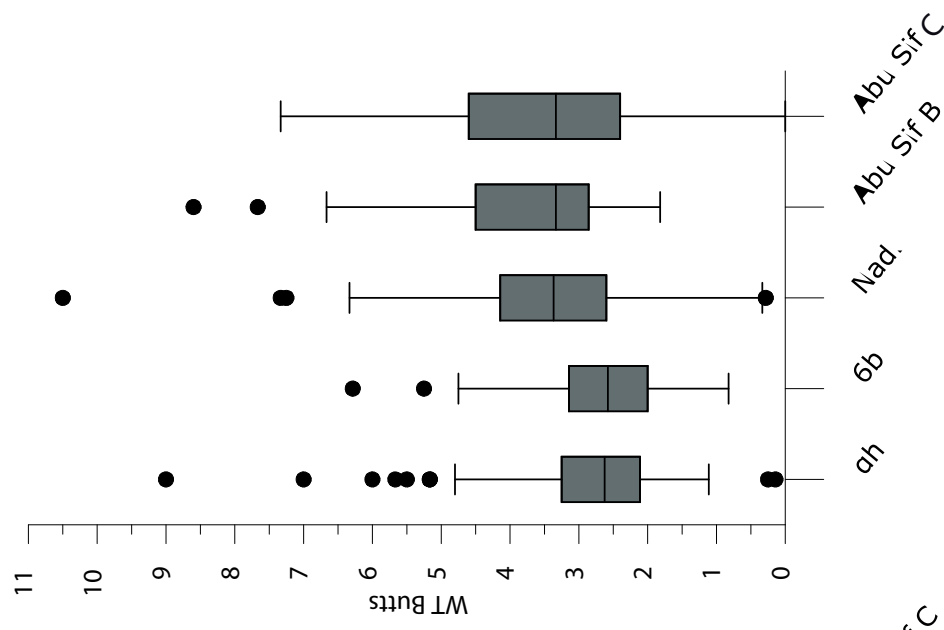


Fig. 143c: WT of butts of retouched blades in assemblages from Hummal, Nad, and Abu Sif.

Fig. 143

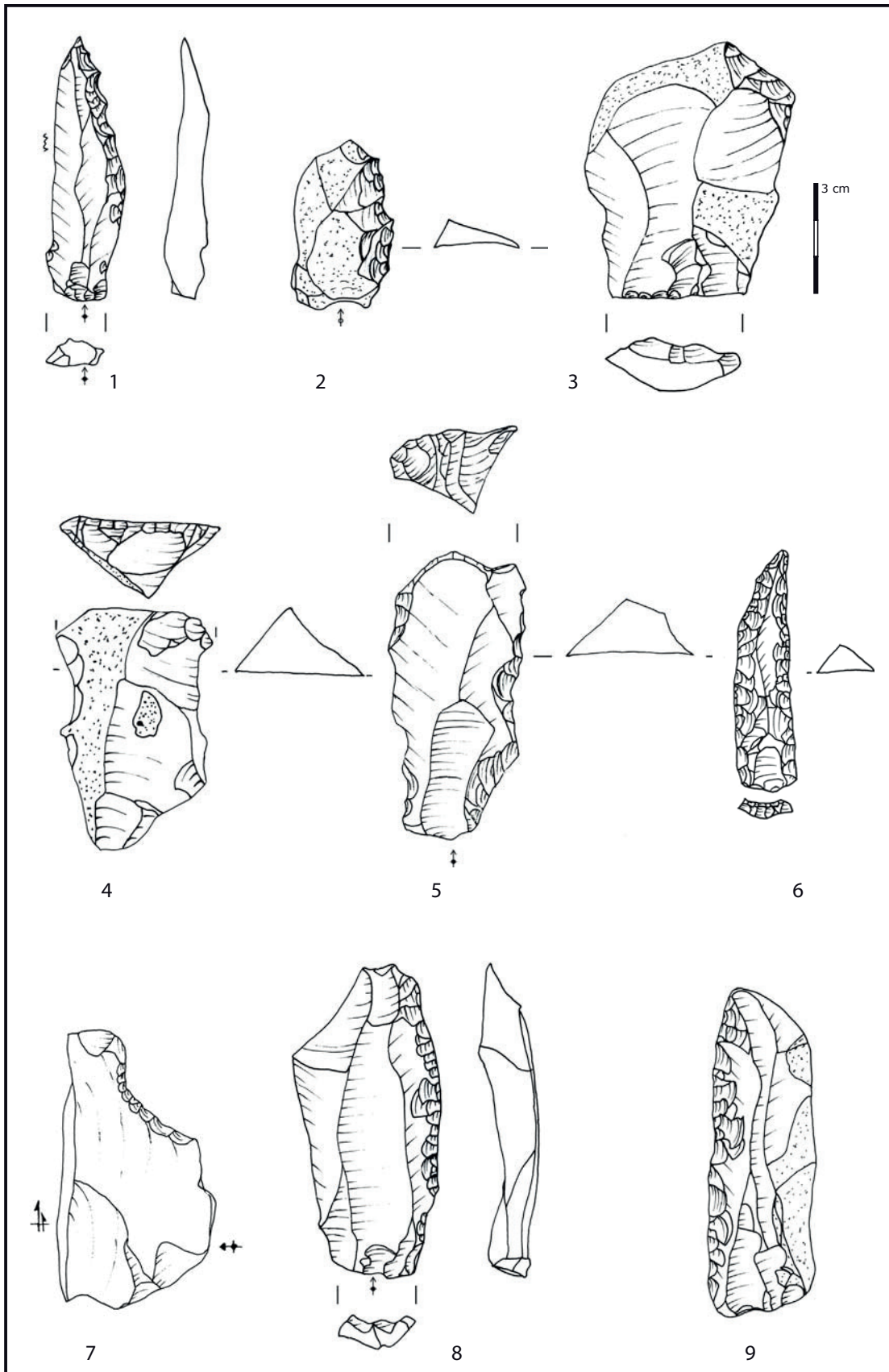


Fig. 144: Selected artefacts from assemblages 6b and sand h.
 1: single scrapper, denticulate; 2: denticulate on cortical flak; 3: retouched cortical flake;
 4, 5: end-scrape; 6: pointed, retouched blade (perforator); 7: notch made on broken flake;
 8: single scraper on large blade; 9: single scraper with cortical back;

Fig. 144

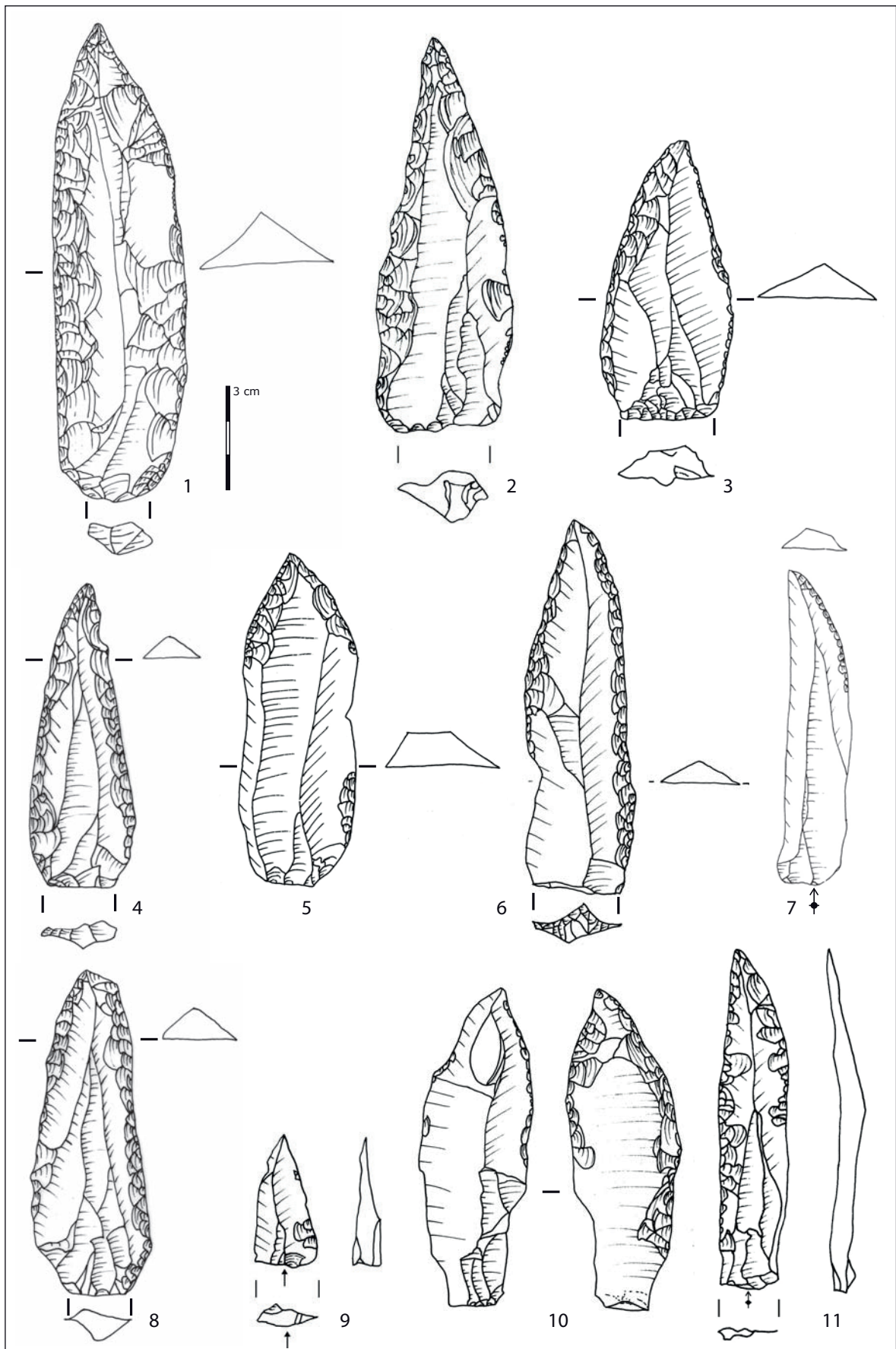


Fig. 145: Selected artefacts from assemblages 6b and sand h.
 1, 2, 3, 4, 5, 6, 7, 8, 11: retouched pointed blades; 9: unretouched point;
 10: pointed blade with ventral retouch.

Fig. 145

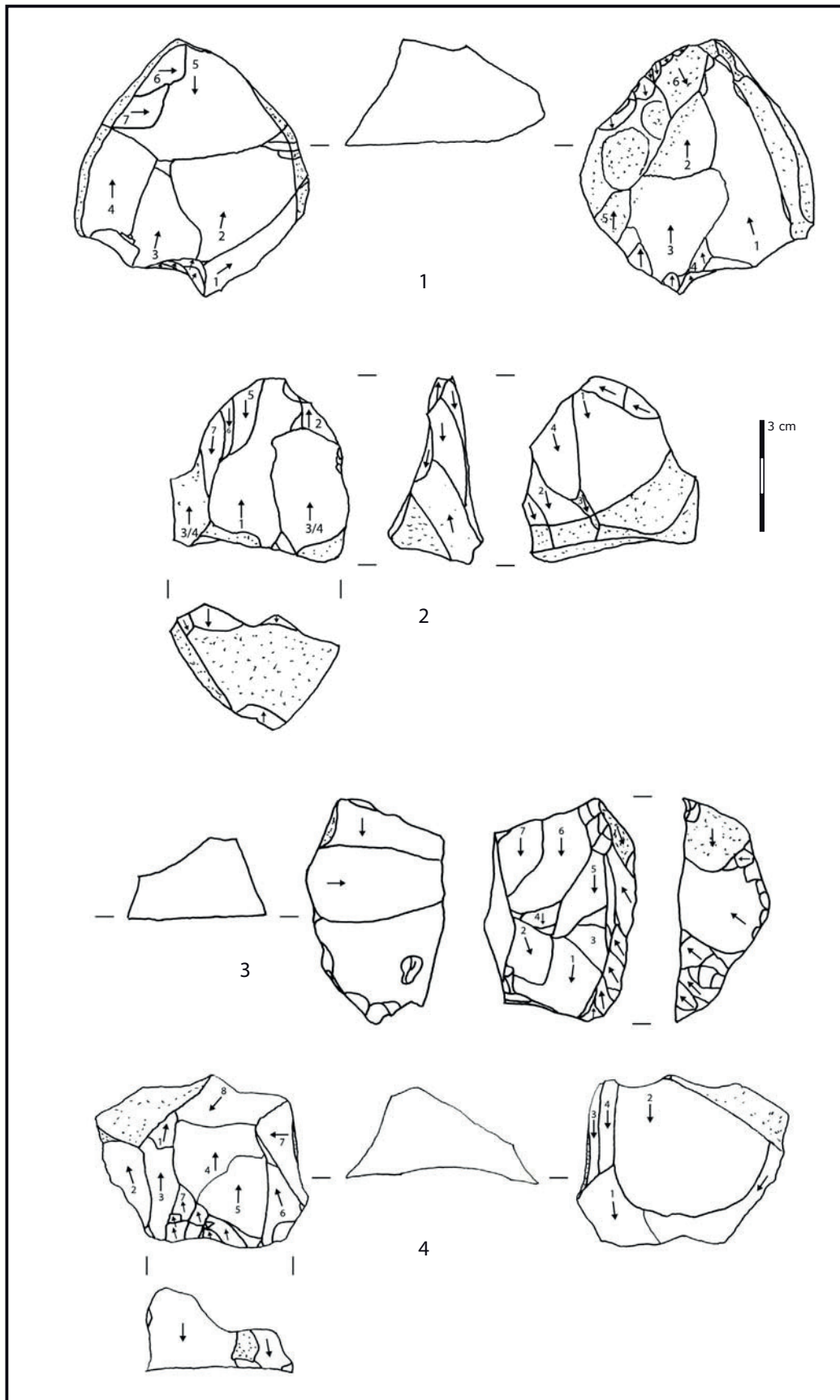


Fig. 146 : Laminar cores from Layer 6b.

1, 2, 3, 4: cores on block exploited on ventral and dorsal surfaces.

Fig. 146

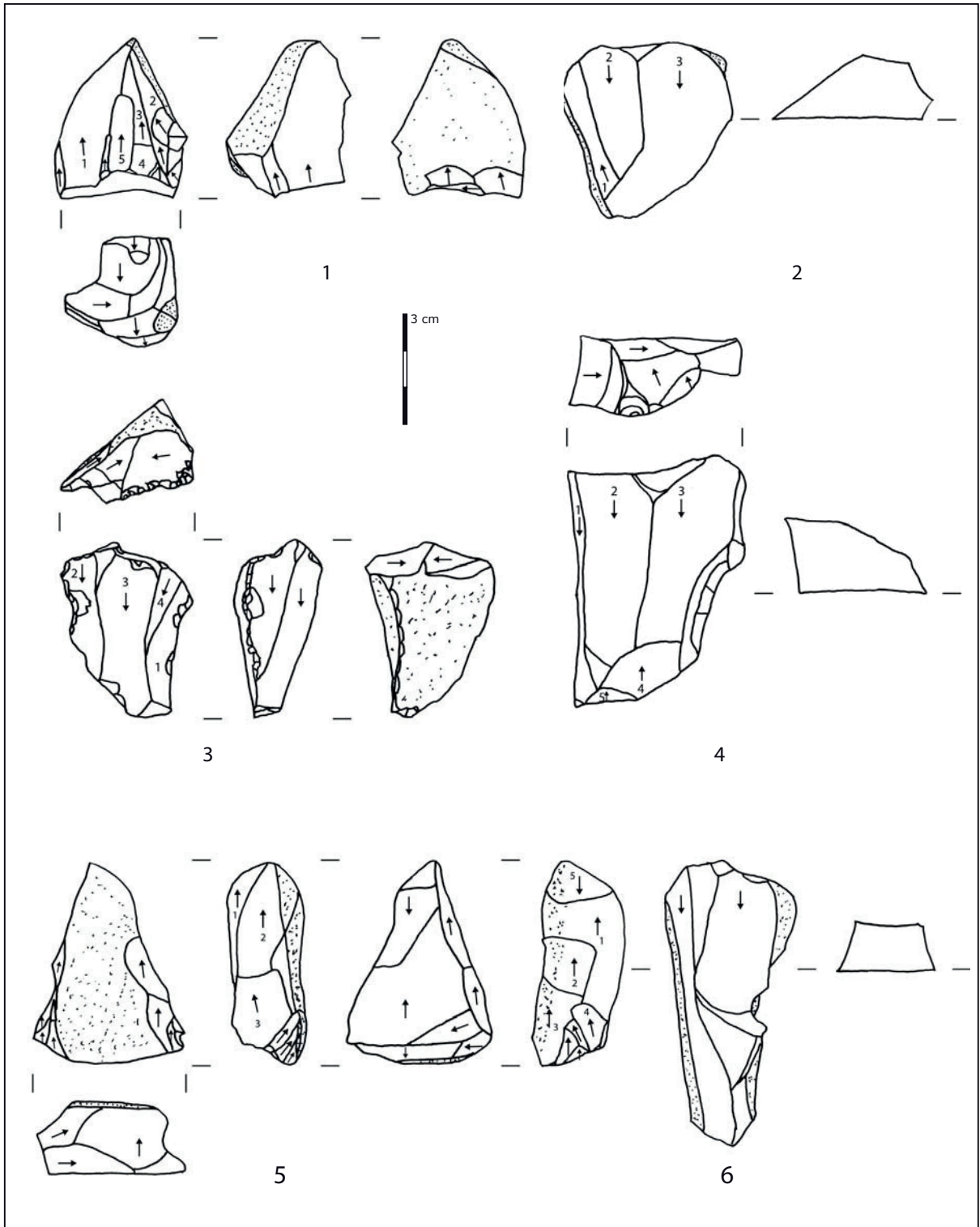


Fig. 147 : Laminar cores from Layers 6b.
 1, 3, 6: unidirectional cores on block; 4: fragment of bidirectional core;
 2: core on block showing bidirectional debitage ;
 5: core on block showing frontal debitage on both sides.

Fig. 147

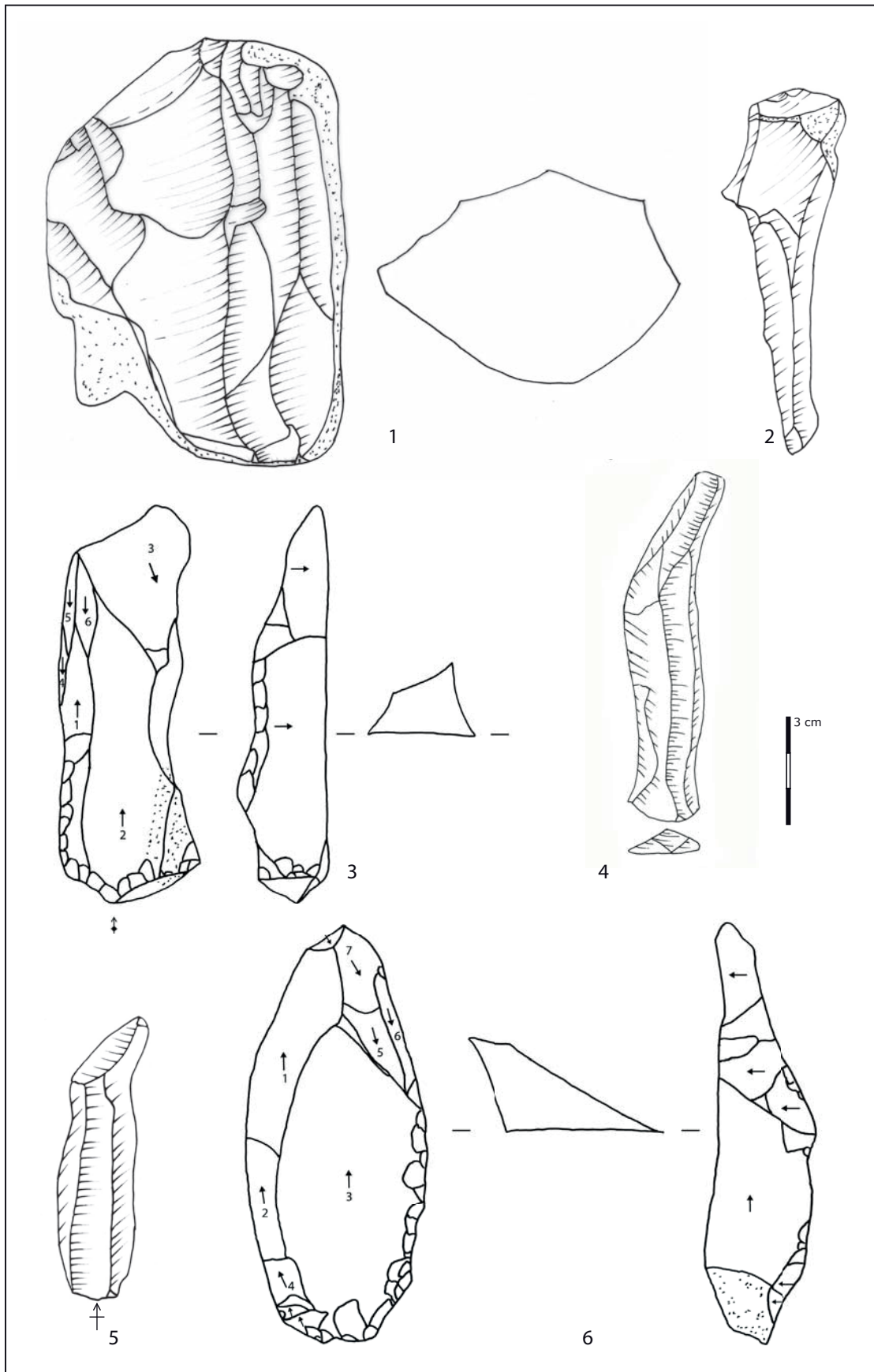


Fig. 148 : Selected artefacts from Layer 6b.

1: bidirectional core made on block; 2: plunging blade showing the bidirectional -off set scar pattern; 3, 6: backed items; 4, 5: blades showing bidirectional -off set scar pattern .

Fig. 148

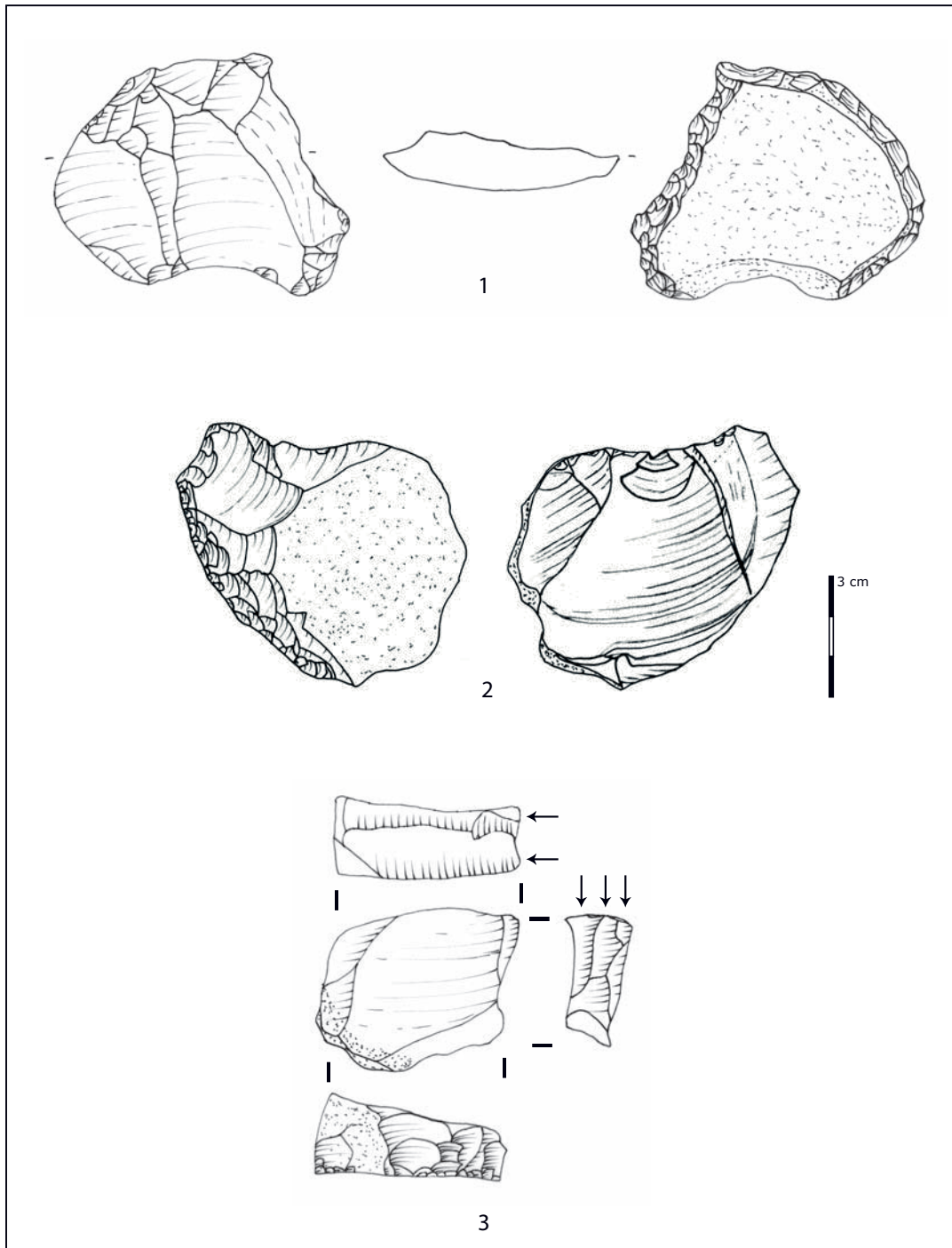


Fig. 149 : Selected artefacts from layers 6b.
 1: exhausted bidirectional core transformed into tool (core-tool);
 2: core made on Yabrudian scraper;
 3: core-tool, scraper made on exhausted bladelet core.

Fig. 149

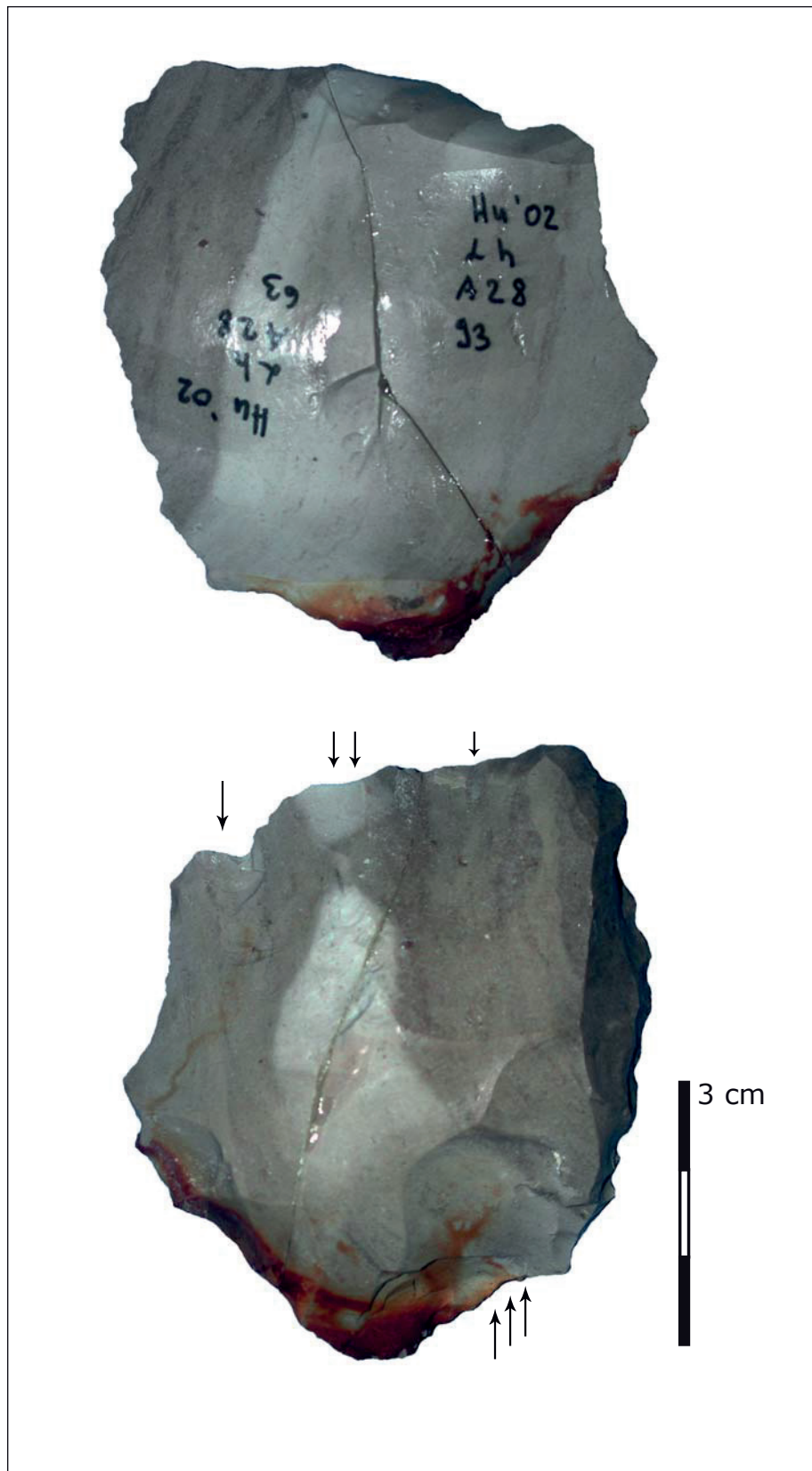


Fig. 150: Nahr Ibrahim made on flakes from sand h.

Fig. 150

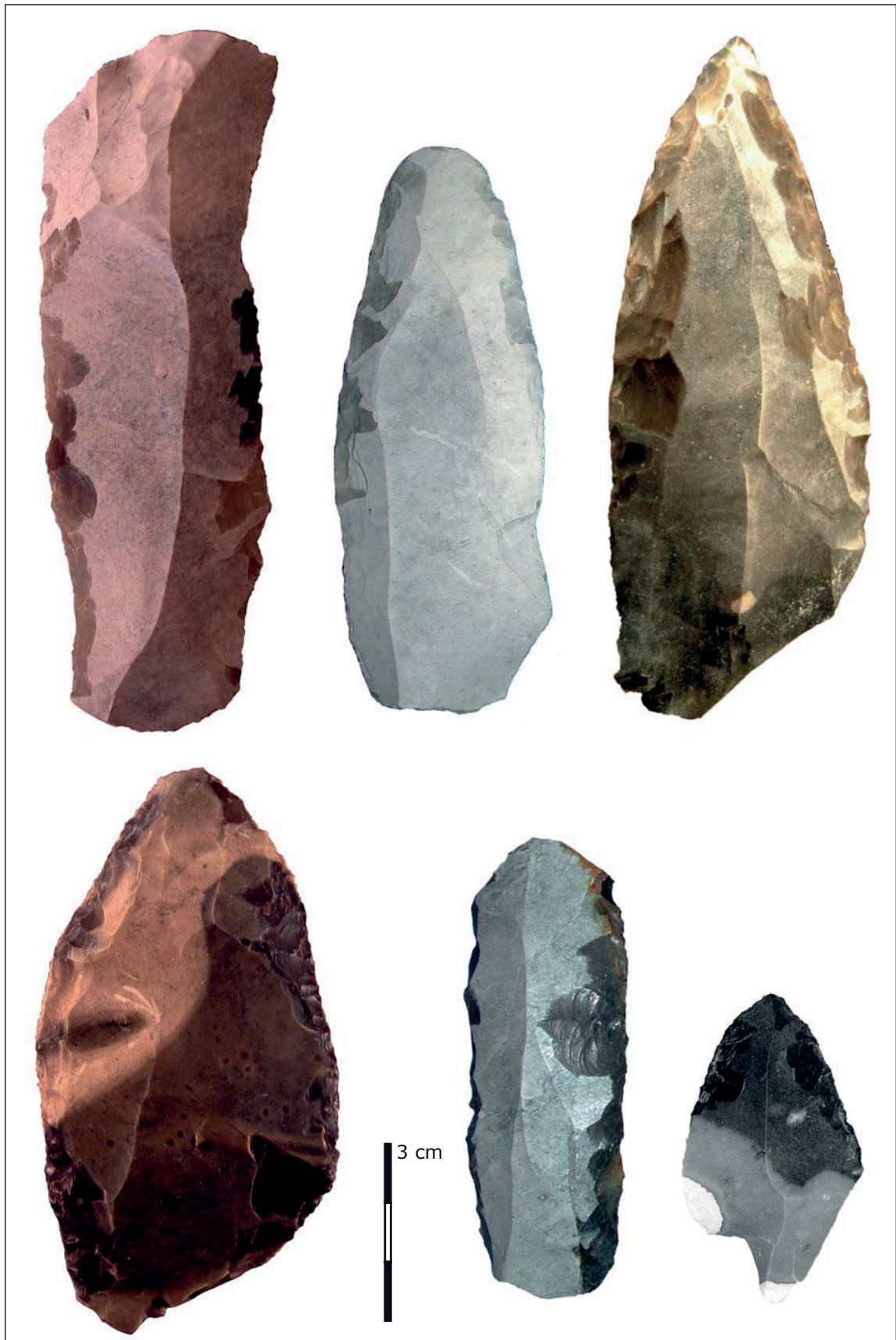


Fig. 151: Selected recycled artefacts made on patinated items from sand h.

Fig. 151

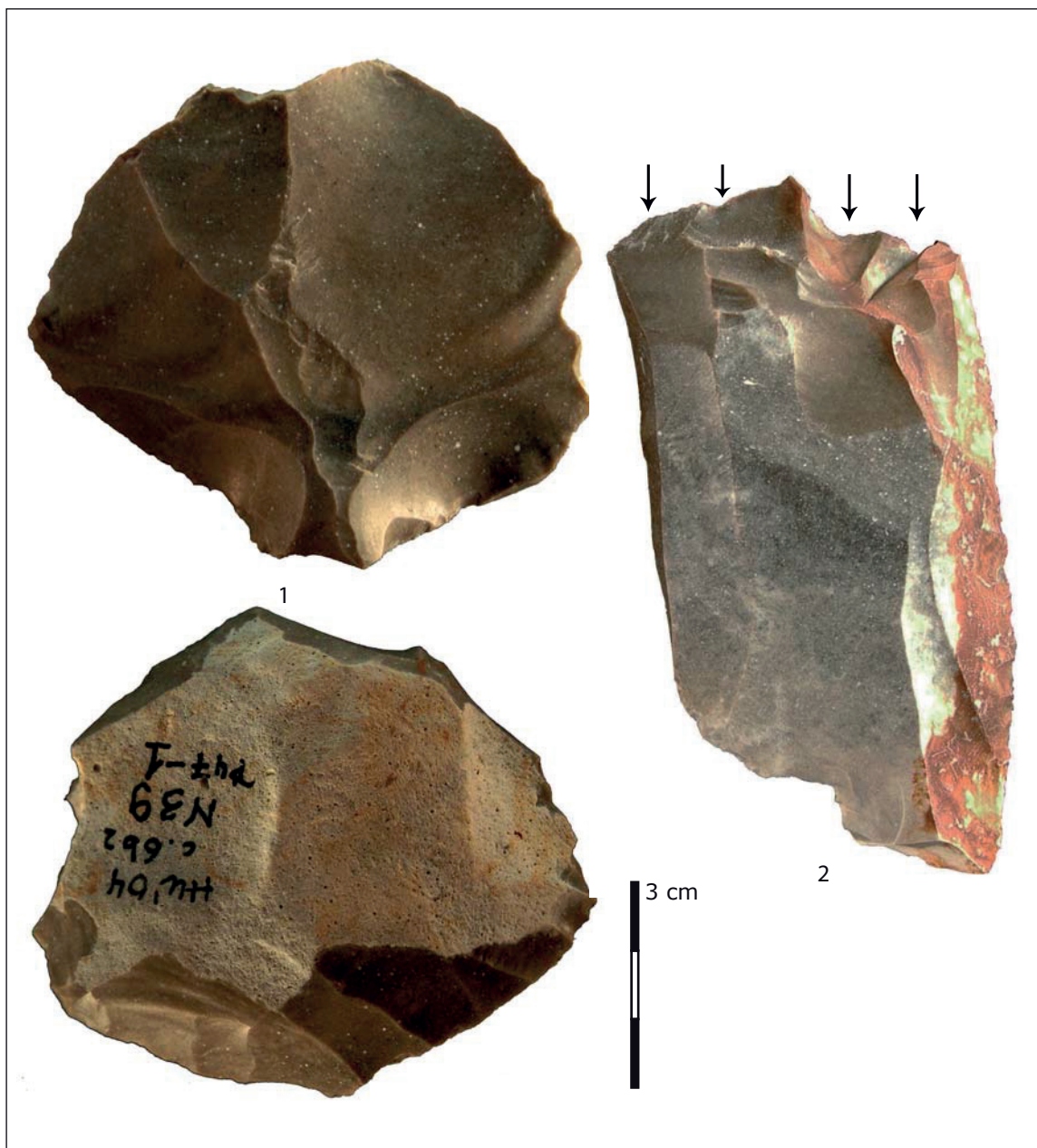


Fig. 152: Selected recycled artefacts made on patinated items from Layers 6b and sand h.
1: core made on patinated flake;
2: unidirectional NI made on blades fragment.

Fig. 152

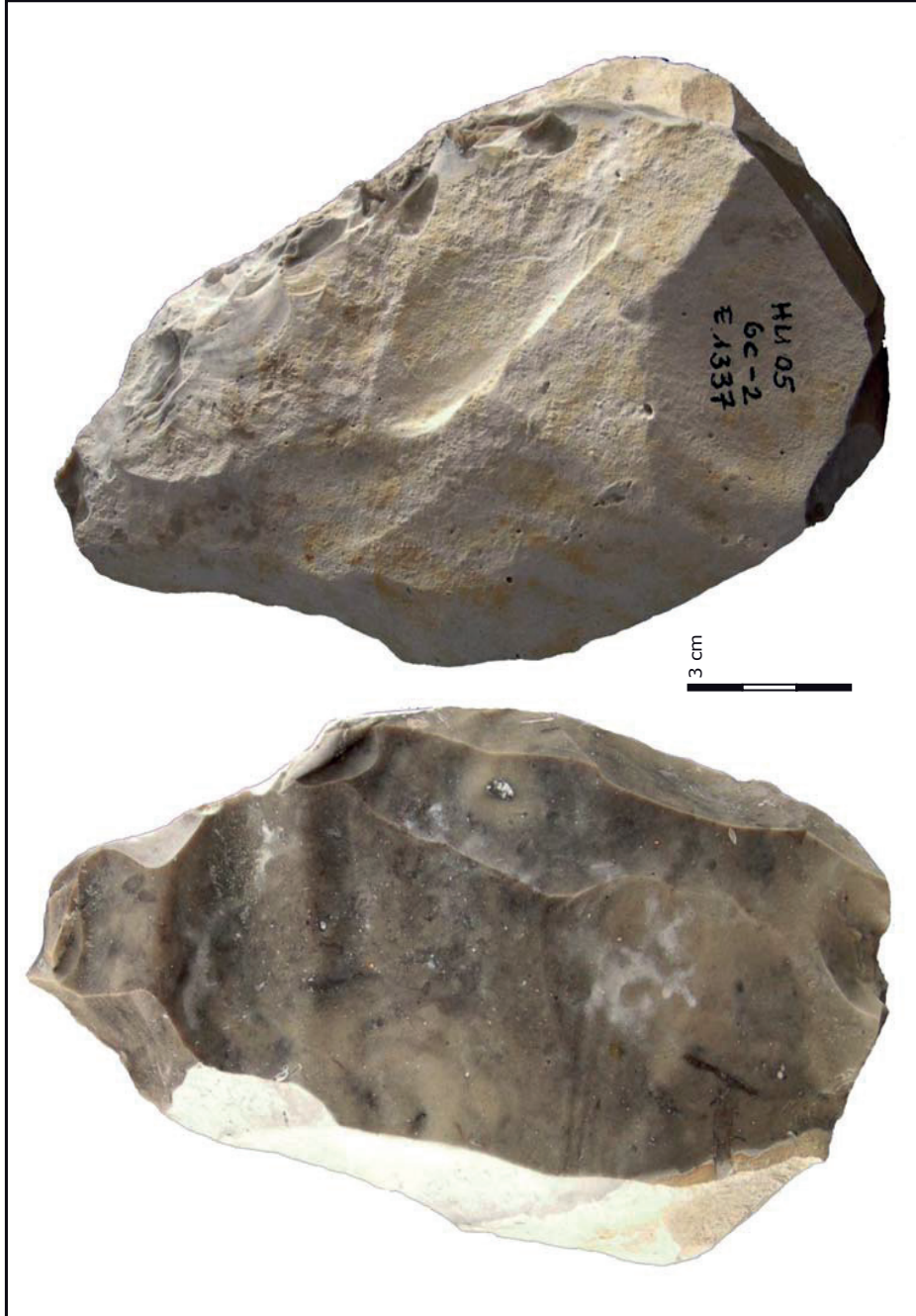


Fig. 153: core made on Yabrudian patinated scraper from Layer 6c2.

Fig. 153

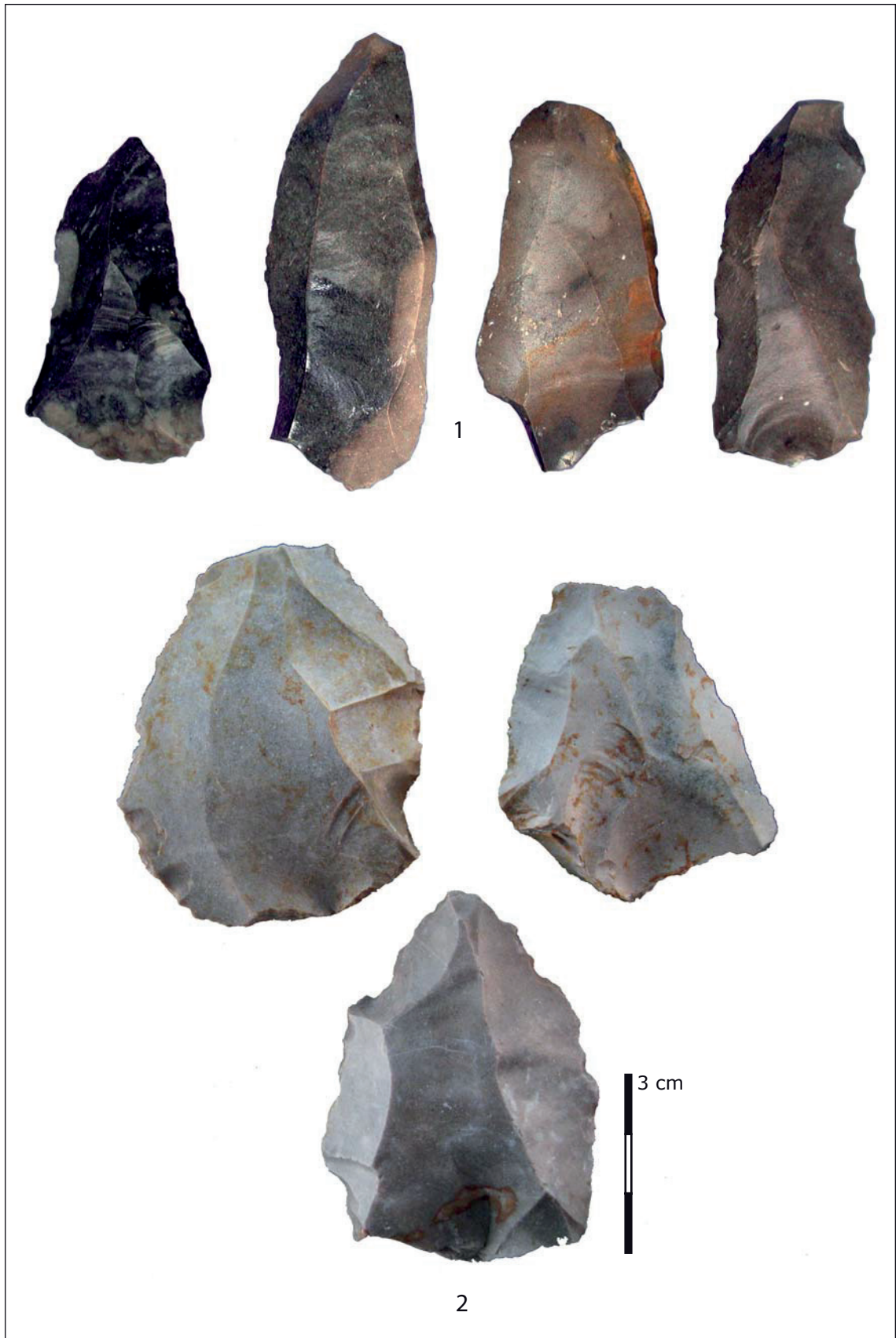


Fig. 154: Levallois-like artefacts from Layer 6b (2) and sand h (1).

Fig. 154



Fig. 155: Levallois flakes from Layer 6b (2) and sand h (1).

Fig. 155



Fig. 156: Crests from sand h and Layer 6b.

Fig. 156



Fig. 157: Selected artefacts from sand h. 1: notch made on cortical blade; 2, 3, 6, 7, 8: retouched blades; 4, 5: bipolar blades.

Fig. 157

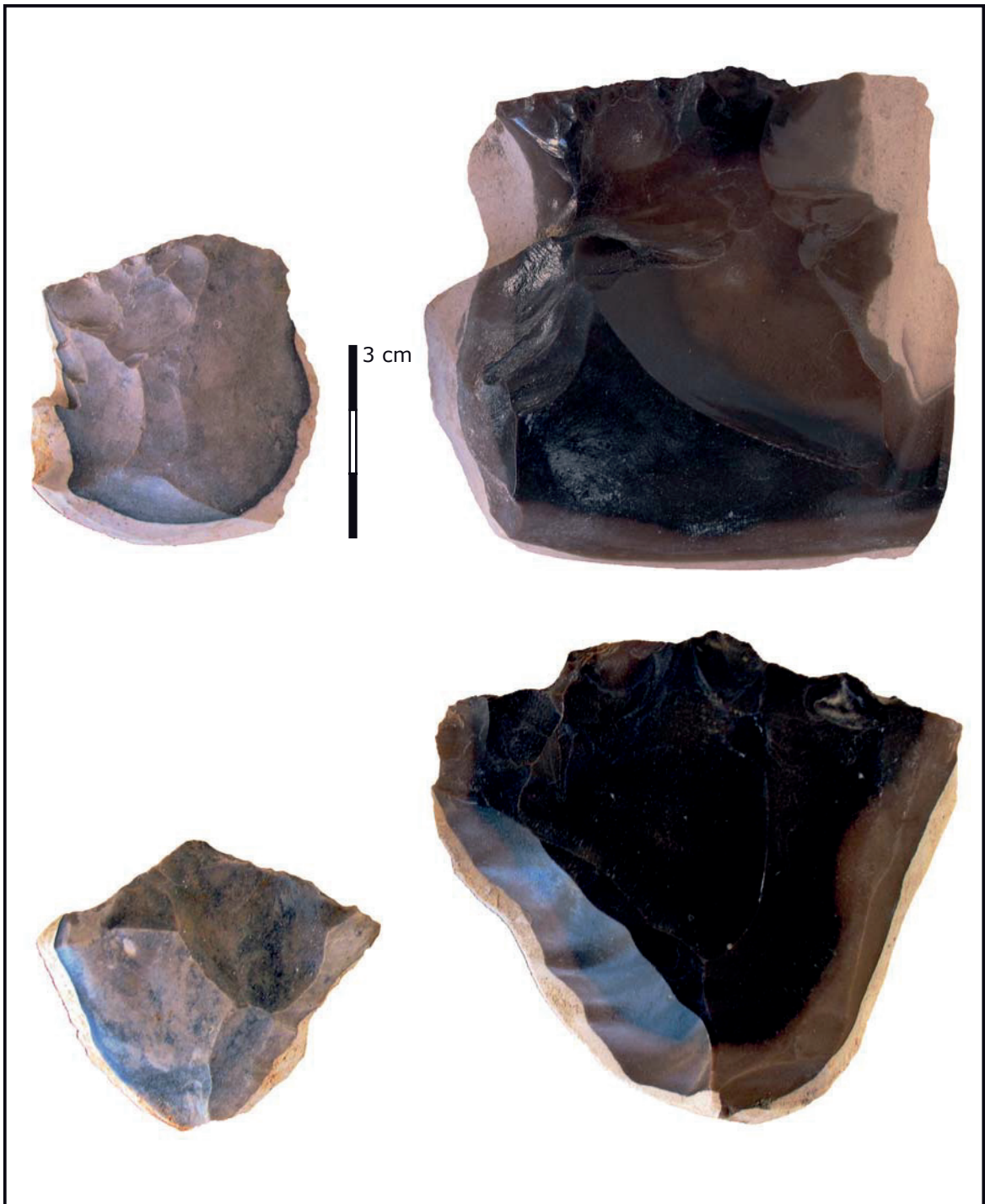


Fig. 158: Cores coming from Layers 6b (left) and sand h (right) showing the same morphology despite their dimension.

Fig. 158



Fig. 159: Bladelets from Layers 6a (middle), 6b (bottom) and sand h (top).

Fig. 159

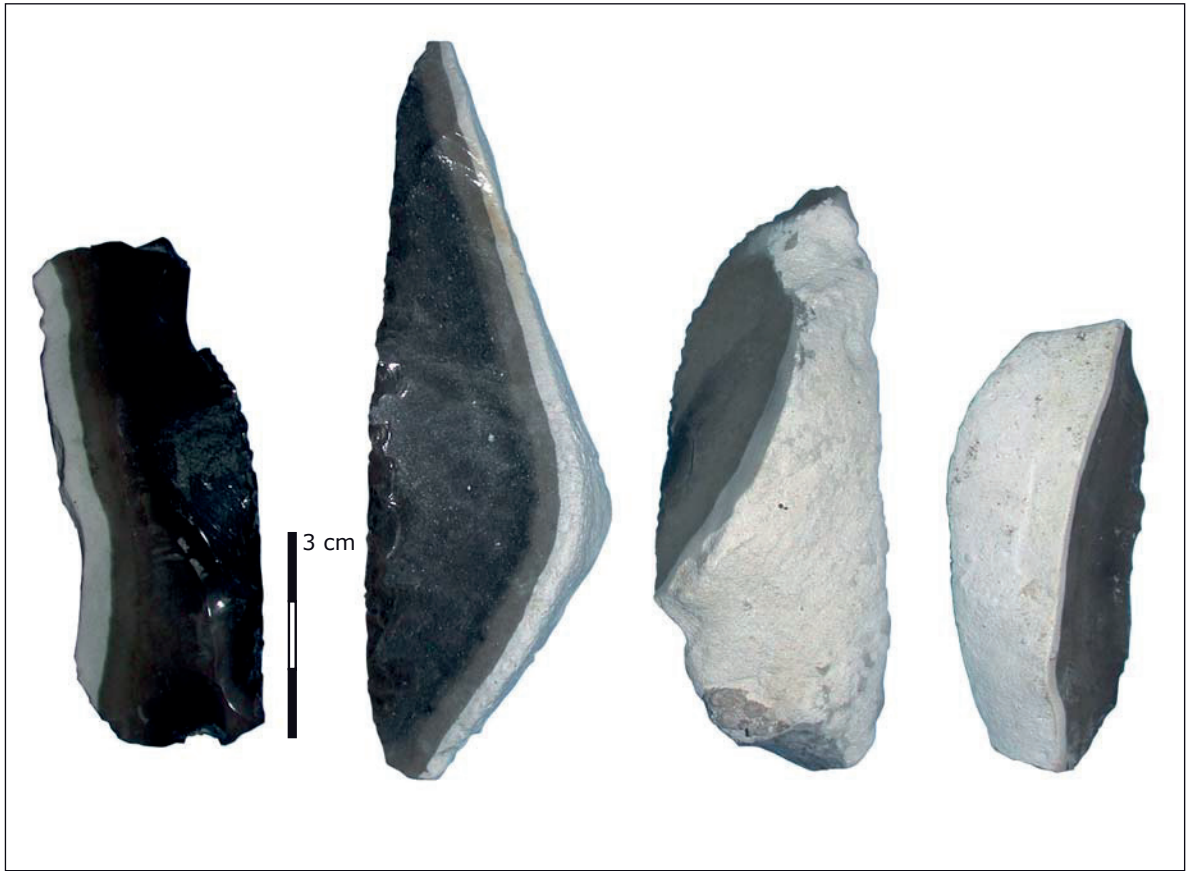


Fig. 160: Cortical backed items: *couteaux à dos* from sand h.

Fig. 160

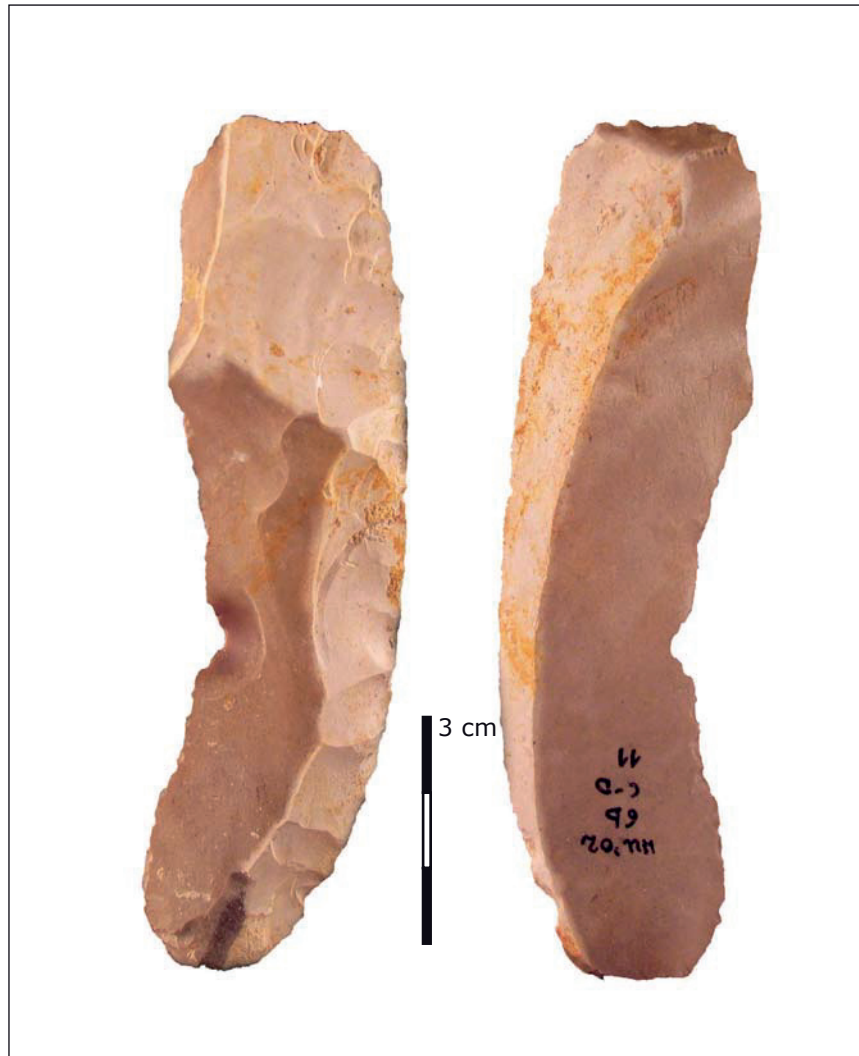


Fig. 161: Edge blade knapped from Yabrudian scraper from Laye 6b.

Fig. 161



Fig. 162: Accumulation of sand in Layer 7.

Fig. 162



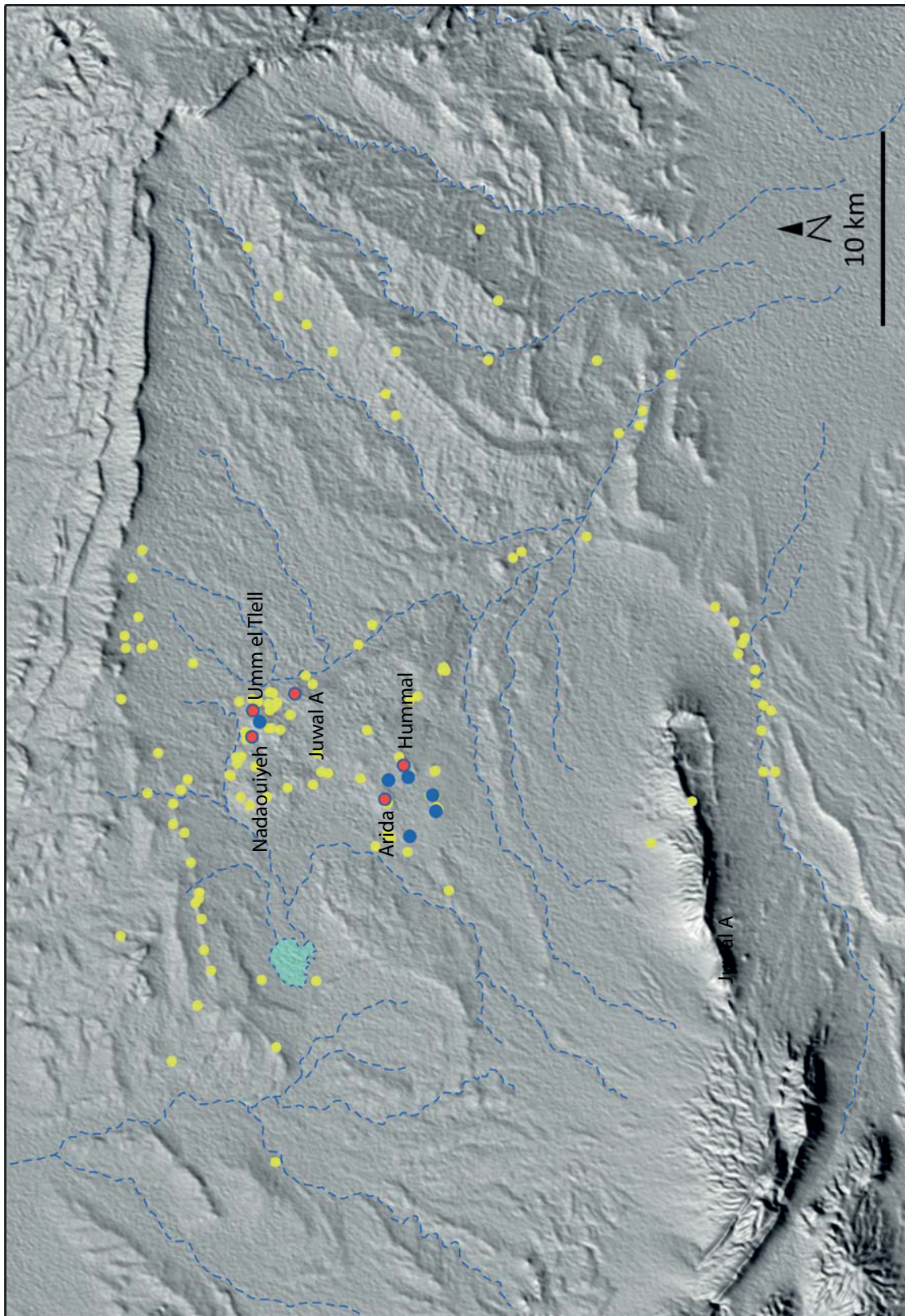
Fig. 163 : The well of Hummal in 2005 field season (photos J.-M. Le Tensorer and D. Wojtczak).

Fig. 163



Fig. 164 : View over the Research Centre of Tell Arida (photo J.-M. Le Tensorer).

Fig. 164



R. Jagher

Fig. 165: Distribution of Paleolithic sites in the area of El-Kowm.

- Hummalian sites
- Yabrudian sites

Fig. 165

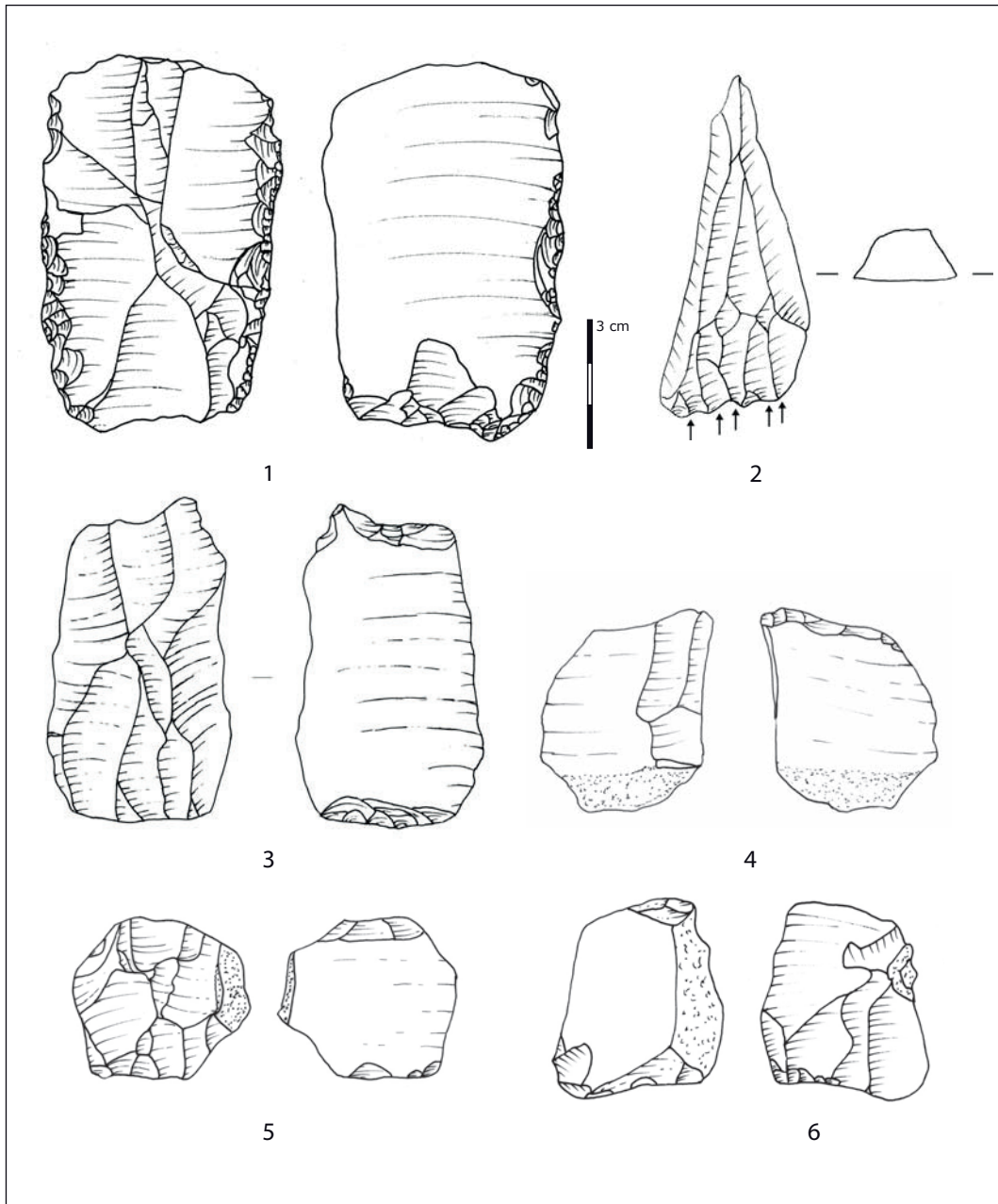


Fig. 166: Nahr Ibrahim made on flakes from Layers 6a, 6b and 7c.

1: bidirectional NI and tool: double scraper; 2: unidirectional NI made on thick blade;
 3, 5, 7: bidirectional NI made on flakes; 4, 6: unidirectional NI made on cortical flakes.

Fig. 166

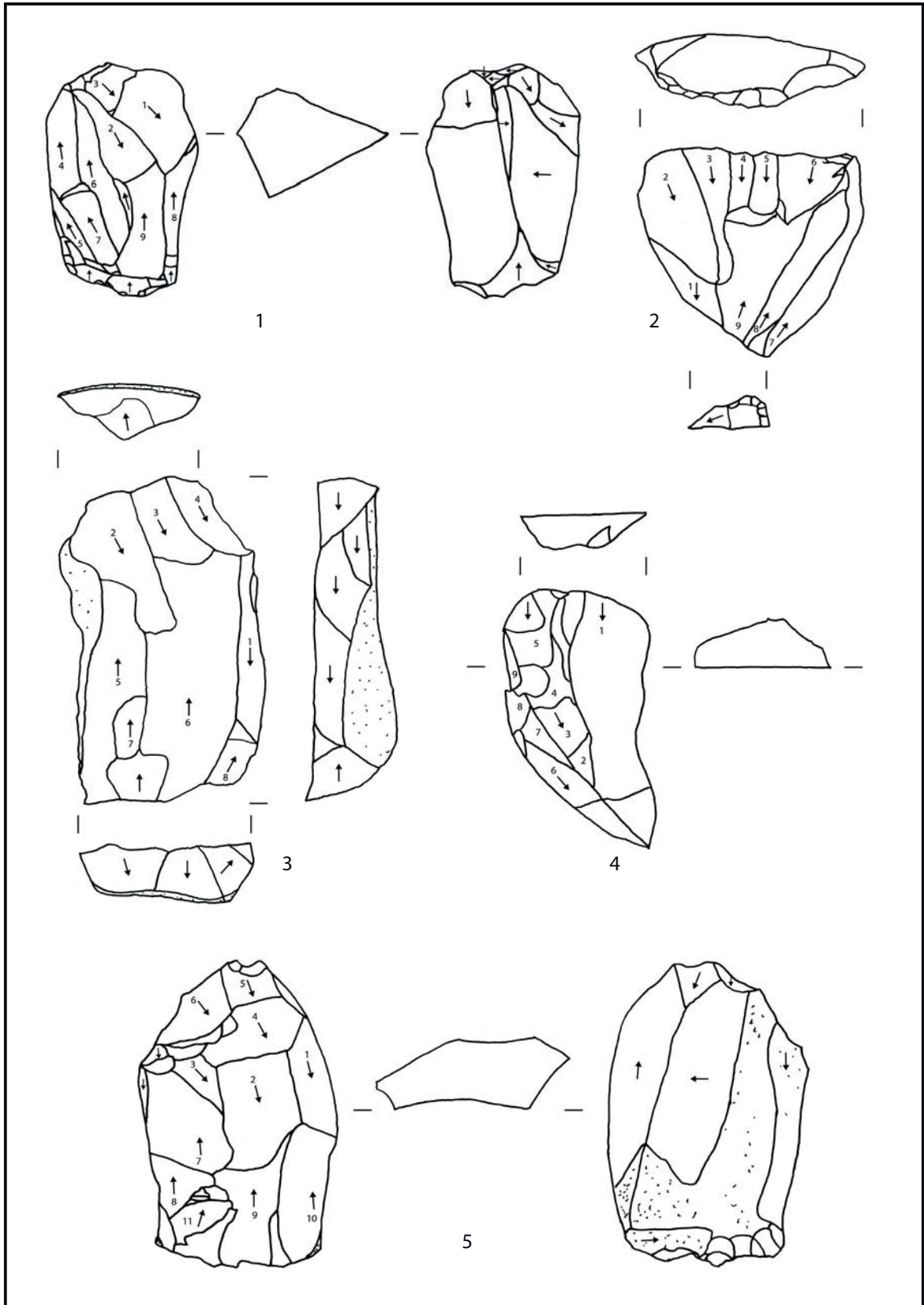


Fig. 167: Laminar cores from Layers 6b.
 1, 3, 5: Bidirectional cores with off set platform.
 4: unidirectional core made on thick blade;

Fig. 167